Design and Development of Stereoselective Methods for *C*-, *O*-, and *S*-Glycoside Synthesis Utilizing Sterically Strained Nitrogen Bases and Cyclic Sulfonium Salts

A Dissertation Submitted to the
Indian Institute of Technology Guwahati
As Partial Fulfillment for the Degree of

Doctor of Philosophy in Chemistry

Submitted by

Priyanka Pradhan

Roll No. 206122112

Department of Chemistry
Indian Institute of Technology Guwahati
Guwahati, Assam-781039, India

Dedicated

To

My Family

INDIAN INSTITUTE OF TECHNOLOGY GUWAHATI

Department of Chemistry

STATEMENT

I do hereby declare that the matter embodied in this thesis entitled "***Design and Development of Stereoselective Methods for C-, O-, and S-Glycoside Synthesis Utilizing Sterically Strained Nitrogen Bases and Cyclic Sulfonium Salts***" is the result of experiments carried out by me in the Department of Chemistry, Indian Institute of Technology Guwahati, India, under the supervision of Dr. Pavan Kumar Kancharla.

In keeping with the general practice of reporting scientific observations, due acknowledgements have been made wherever the work described is based on the findings of other investigators.

Priyanka Pradhan

Date: 26.03.2026
Place: IIT Guwahati

Priyanka Pradhan

Indian Institute of Technology Guwahati
Department of Chemistry
North Guwahati, Guwahati-781039, India
Phone: +91 (361) 258 3480 (O); Fax: +91 (361) 258 2349
e-mail: **pavankancharla@iitg.ac.in**

CERTIFICATE

This is to certify that **Ms. Priyanka Pradhan** (Roll No. 206122112) has been working under my supervision since January 2021 as a regular registered Ph.D. student. I am forwarding her thesis entitled "***Design and Development of Stereoselective Methods for C-, O-, and S-Glycoside Synthesis Utilizing Sterically Strained Nitrogen Bases and Cyclic Sulfonium Salts***" to be submitted for the Ph.D. (Science) Degree of this Institute. I certify that she has fulfilled all the requirements according to the rules of this institute regarding the investigations embodied in her thesis and this work has not been submitted elsewhere for a degree.

Date: 26.03.2026
Place: IIT Guwahati

Dr. Pavan Kumar Kancharla
Thesis Supervisor
Department of Chemistry

Acknowledgements

A Ph.D. journey is not always smooth; however, I had the honor of meeting many individuals who helped me and made it enjoyable. My heartfelt thanks to everyone who helped me, directly or indirectly, along the way and inspired me to keep going toward success.

It is always a great privilege to express sincere gratitude to my thesis supervisor, Dr. Pavan Kumar Kancharla, for his invaluable guidance, encouragement, and inspiration throughout my PhD journey. Many of my research achievements would not have been possible without his support. His dominance and leadership in carbohydrate chemistry have always inspired me, and working with him has greatly enhanced my research knowledge and skills, helping me to become an independent researcher. I am also thankful to him for giving me the freedom to pursue my research interests within his lab.

I am very happy to express my sincere gratitude to my doctoral committee members, Prof. Bhubaneswar Mandal, Prof. Chandan Kumar Jana, and Dr. Krishna Pada Bhabak, for their valuable suggestions and advice in the progress of my PhD thesis.

I want to express my sincere gratitude to all the faculty members and non-teaching staff of the Department of Chemistry, as well as the staff of the Central Instruments Facility, for their support and guidance throughout my research.

It is an obvious pleasure to acknowledge the Ministry of Education, Government of India, for awarding me the Prime Minister's Research Fellowship (PMRF), which encouraged and enabled me to pursue my research activities more actively. I also thank the Department of Chemistry, the Central Instruments Facility (CIF), and the NECBH (R&D section) at IIT Guwahati for providing essential research infrastructure and instrumental support.

Furthermore, I am grateful to all my past and present group members for their unwavering support and invaluable friendship. My special thanks to my seniors, Dr. Ananya Mukherji and Sangay Moktan, for their invaluable guidance during my early learning period. I am also grateful to my colleagues, Kohin Mahendra and Ashish Biswas, for their willingness to share ideas, engage in discussions, and provide invaluable support throughout my Ph.D. journey. I am indeed very happy to express my heartfelt gratitude to my juniors, Sriram, Rajesh, Mousumi, and Swagatam, for their support with my research; without their help, it would have been much more difficult for me to complete this Ph.D. thesis. I always remember the cheerful and enjoyable environment they fostered in the lab. It was a great pleasure to work with and spend time with such lovely human beings, and I will always remember their jokes, laughter, and infectious humor that made each day brighter.

I am extremely grateful to my respected teachers, Prof. Niranjan Panda, Dr. Anil Kumar Barik, Dr. Nabakumar Bera, Saraj Kumar Giri, and Pratul Kumar De, for their invaluable guidance and significant contributions in shaping me as a chemist. I am also thankful to Dr. Kanchanbala Sahoo, who introduced me to the fundamentals and laboratory techniques of organic chemistry during my M.Sc. project at NIT Rourkela, which inspired me to pursue a Ph.D. in this field.

It is a great blessing to have a best friend like Dr. Sayanta Roy, who has graciously shared every moment with me. His unwavering support, infinite love, and constant motivation and encouragement since my MSc days have been crucial to my life. He has stood with me in every struggle in my life. I am profoundly grateful to him for his invaluable guidance, especially for his help in securing the prestigious Prime Minister's Research Fellowship (PMRF) during my Ph.D. career. I wish him continued success, happiness, and fulfillment in his future endeavors.

Finally, I would like to express my deepest gratitude to my family members, who have been my greatest strength in life. I would also like to express my immense respect to my grandfather, the late Ramchandra Pradhan, who is my source of inspiration even today. My deepest gratitude and eternal love for my beloved parents, Tapas Kumar Pradhan and Sanghamaitri Pradhan, who have showered me with unwavering support, love, and constant encouragement throughout my life. I would also like to express my gratitude towards my brothers (Subhankar and Supriya), sisters (Sukanya and Prativa), uncles (Manas Pradhan, Animesh Pradhan, and Siladitya Dey), and aunts. It is because of their blessings that my Ph.D. endeavors were possible. It is my great honor to dedicate this thesis to my family members. I am truly grateful for their belief in me and for giving me the freedom to pursue my dreams.

Above all, I bow to the Supreme Goddess Maa Bipodtarini, who blesses me in every aspect of my life.

Priyanka Pradhan

List of abbreviations

Å	Angstrom
Ac	Acetyl
ACN	Acetonitrile
AcOH	Acetic Acid
α	Alpha
β	Beta
BAr^F_4	Tetrakis(3,5-bis(trifluoromethyl)phenyl)borate
BF_3	Boron Trifluoride
BF_4	Tetrafluoroborate
Bn	Benzyl
Bz	Benzoyl
°C	Degree Celsius
cat.	Catalytic/Catalyst
$CDCl_3$	Deuterated Chloroform
CH_3	Methyl
$CHCl_3$	Chloroform
$(COCl)_2$	Oxalyl Chloride
DCE	1,2-Dichloroethane
DCM	Dichloromethane
deg	Degree
DIPEA	N,N-Diisopropylethylamine
DMF	N,N-Dimethylformamide
DMSO	Dimethylsulfoxide
DTBMP	2,6-Di-*tert*-butyl-4-methylpyridine

DTBP	2,6-Di-*tert*-butylpyridine
δ	Delta
Eq.	Equation
Equiv	Equivalent
ESI-MS	Electrospray Ionization Mass Spectrometry
Et	Ethyl
EtOAc	Ethyl Acetate
Et_3SiH	Triethylsilane
Fmoc	9-Fluorenylmethoxycarbonyl
FT-IR	Fourier Transformation Infrared
g	Gram
h	Hour
HCl	Hydrochloric Acid
HBr	Hydrobromic Acid
HRMS	High-resolution Mass Spectrometry
IPA	Isopropyl Alcohol
K_2CO_3	Potassium Carbonate
KOAc	Potassium Acetate
LiBr	Lithium Bromide
LiOH	Lithium Hydroxide
Me	Methyl
MeI	Methyl Iodide
MeOH	Methanol
mg	Milligram
MHz	Megahertz

min	Minute
mL	Millilitre
mM	Millimolar
µM	Micromolar
µl	Microlitre
NaH	Sodium Hydride
$NaHCO_3$	Sodium Bicarbonate
Na_2SO_4	Sodium Sulfate
NEt_3	Triethylamine
NIS	N-Iodosuccinimide
nm	Nanometer
NMR	Nuclear Magnetic Resonance
NOESY	Nuclear Overhauser Effect Spectroscopy
NSAIDs	Nonsteroidal Anti-Inflammatory Drugs
Nu	Nucleophile
o-NosylOXY	Ethyl 2-cyano-2-(2-nitrophenylsulfonyloxyimino)
ORTEP	Oak Ridge Thermal Ellipsoid Plot
PCy_3	Tricyclohexylphosphine
$PdCl_2$	Palladium(II) Chloride
$PdCl_2(PPh_3)_2$	Bis(triphenylphosphine)palladium(II) Dichloride
$Pd(COOCF_3)_2$	Palladium(II) Trifluoroacetate
$Pd_2(dba)_3$	Tris(dibenzylideneacetone)dipalladium(0)
$Pd(OAc)_2$	Palladium(II) Acetate
$Pd(PPh_3)_4$	Tetrakis(triphenylphosphine)palladium(0)
Ph	Phenyl

PPh_3	Triphenylphosphine
ppm	Parts Per Million
PS	Proton Sponge (1,8-Bis(dimethylamino)naphthalene)
rt	Room Temperature
SC-XRD	Single Crystal X-Ray Diffraction
$SOCl_2$	Thionyl Chloride
TBDMS	*tert*-Butyldimethylsilyl
TBDPS	*tert*-Butyldiphenylsilyl
*t*Bu	*tert*-Butyl
TES	Triethylsilyl
Tf	Triflate
TFA	Trifluoroacetic Acid
TfOH	Triflic Acid
THF	Tetrahydrofuran
TIPS	Triisopropylsilane
TIPDS	Tetraisopropyl disiloxane
TLC	Thin-layer Chromatography
TMS	Trimethylsilane
TMSOTf	Trimethyltrifluoromethanesulfonate
Ts	Tosylate
TTBP	2,4,6-Tri- *tert*-butylpyrimidine
TTBPy	2,4,6-Tri-*tert*-butylpyridine
UV	Ultraviolet

Abstract

The contents of the thesis entitled **"*Design and Development of Stereoselective Methods for C-, O-, and S-Glycoside Synthesis Utilizing Sterically Strained Nitrogen Bases and Cyclic Sulfonium Salts*"** are divided into five chapters based on the experimental results obtained during my research period.

Chapter I: This chapter describes a general introduction and literature review on glycosides, sterically strained nitrogen bases, and phenolic salts, as well as their utility in various organic transformations and glycosylation reactions.

Chapter II: This chapter discusses the first organocatalytic synthesis of 2-deoxy N-O-linked glycosides directly facilitated by strained 2,4,6-tri-*tert*-butylpyridinium salts.

Chapter III: This chapter shows an electrostatically tuned phenolic sulfonium salt-catalyzed stereoselective synthesis of *O*- and *S*-septanosides via ring-opening of 1,2-cyclopropanated sugar donors.

Chapter IV: This chapter presents a Pd-catalyzed stereo and regioselective synthesis of biologically significant aryl *C*-glycosides utilizing 1,8-bis(dimethylamino)naphthalene.

Chapter V: This chapter demonstrates the influence of sterics vs inductive vs through-space stabilization effects on the basicity and reactivity of the pyridinium cation.

Chapter-wise summaries of the mentioned research works are presented below.

Chapter I. *Introduction*

Glycosylation, the linkage of sugar moieties to other sugars, lipids, proteins, natural products, or drugs, forms the cornerstone of glycochemistry and glycobiology. In the past century, significant advancements in carbohydrate chemistry have enabled the efficient construction of *O*-, *C*-, *N*-, and *S*-linked glycosidic bonds with outstanding stereo and regioselectivity. Despite progress, stereocontrol in glycosylation reactions remains a key challenge, as the α/β-anomeric selectivity critically impacts carbohydrate bioactivity. Conventional glycosylation requires stoichiometric Lewis acids and excess acid scavengers, while modern approaches rely on complex donors; in contrast, catalytic methods using simple donors offer a more practical and ideal alternative. Among *C*-glycosides, aryl *C*-glycosides are notable for their diverse bioactivities and synthetic utility, while *O*-and *S*-glycosylation enhances bioavailability and pharmacological properties. Therefore, stereocontrolled synthesis of *C*-, *O*-, and *S*-glycosides is arguably a key focus in carbohydrate chemistry.

Sterically hindered 2,4,6-tri-*tert*-butylpyridine (TTBPy) and other pyridine derivatives, 2,6-di-*tert*-butyl-4-methylpyridine (DTBMP), 2,4,6-tri-*tert*-butylpyrimidine (TTBP), and 2,6-di-*tert*-butylpyridine (DTBP) are known for their utility as proton trapping agents and have been used as a traditional acid scavenger for a long time. However, due to its steric bulk around the cationic site, the hydrogen bond is prevented in the sterically strained 2,4,6-tri-*tert*-butylpyridinium salts, resulting in poor electrostatic interactions within the ion-pair. In this thesis, we exploit these unique, poor electrostatic/strained interactions toward achieving a biologically significant class of N-O-linked glycosides in a highly diastereoselective manner.

Building on this, recent advances highlight the utility of noncovalent interactions such as hydrogen bonding as versatile platforms to tackle stereoselectivity challenges and enable access to synthetically difficult septanosides. Additionally, designing small-molecule catalysts capable of concerted activation of both reaction partners remains a cornerstone in advancing stereoselective glycosylation. In this thesis, we present a robust catalytic strategy using a simple, electrostatically tuned phenolic sulfonium salt that leverages hydrogen bonding networks to enable α-selective strain-release *O*- and *S*-glycosylation toward biologically significant seven-membered oxepane frameworks.

In parallel, we explore the underutilized potential of 1,8-bis-dimethylaminonaphthalene (DMAN), commonly known as proton sponge, which is widely recognized for its exceptional proton affinity. The release in the electronic strain between the lone pairs of the two peri-nitrogens has been attributed to its behavior as a strong base relative to other anilines. Despite significant development in bidentate ligands, proton sponge (DMAN) with a bidentate character has never been explored in palladium catalysis. In this thesis, we showcase the triple role of DMAN, as a two-electron reductant, as a stabilizing ligand of Pd(0) and as an organic base replacing the traditional inorganic bases in the palladium-catalyzed coupling of glycals with aryl iodides.

Chapter II. *Strained Ion-Pair Interactions Driven Anion Assisted Concerted Addition of Ketoximes/Aldoximes and Hydroxamic Acids to Glycals*

Sterically encumbered 2,4,6-tri-*tert*-butylpyridine (TTBPy) is widely recognized for its utility as a proton-trapping agent and has long served as a traditional acid scavenger. In glycosylation reactions, it is commonly employed to trap in situ-generated triflic acid. The resulting pyridinium salt is not expected to exhibit Brønsted acidity, as the $[N\text{-}H]^+$ moiety is effectively shielded by the bulky ortho *tert*-butyl groups. In typical pyridinium salts, the $[N\text{-}H]^+$ is stabilized via hydrogen bonding with the counterion. However, due to its steric bulk around the cationic site, such hydrogen bonding is impeded between the cation and anion in the case of 2,4,6-tri-*tert*-butylpyridinium salts, resulting in poor electrostatic interactions within the ion-pair.

In this chapter, we present unique poor electrostatic/strained interactions in the pyridinium chloride salt to achieve the glycosylation of aldoximes, ketoximes, and hydroxamic acids, thereby accessing a biologically significant class of N-O-linked glycosides with high diastereoselectivity. The unique reactivity of the sterically bulky pyridinium salt has been studied by ^{1}H-NMR, IR, UV, and fluorescence spectroscopic studies. We demonstrate that the pyridinium salt activates the oxime via a unique anion-assisted lone-pair-π interaction between the oxime and pyridinium cation. The resulting intermediate undergoes a concerted addition to the glycal, forming the observed products with excellent selectivity. The concerted nature of the addition has been confirmed through a deuterium-labeling experiment, which provides conclusive evidence supporting the proposed mechanism. The method exhibits a vast substrate scope and enables the construction of diverse N-O-linked glycosides in excellent yields and with high selectivity. Its scalability has been demonstrated at the gram-scale. The method has been extended to glycosylation as a late-stage modification of some N-O bond-containing drug molecules.

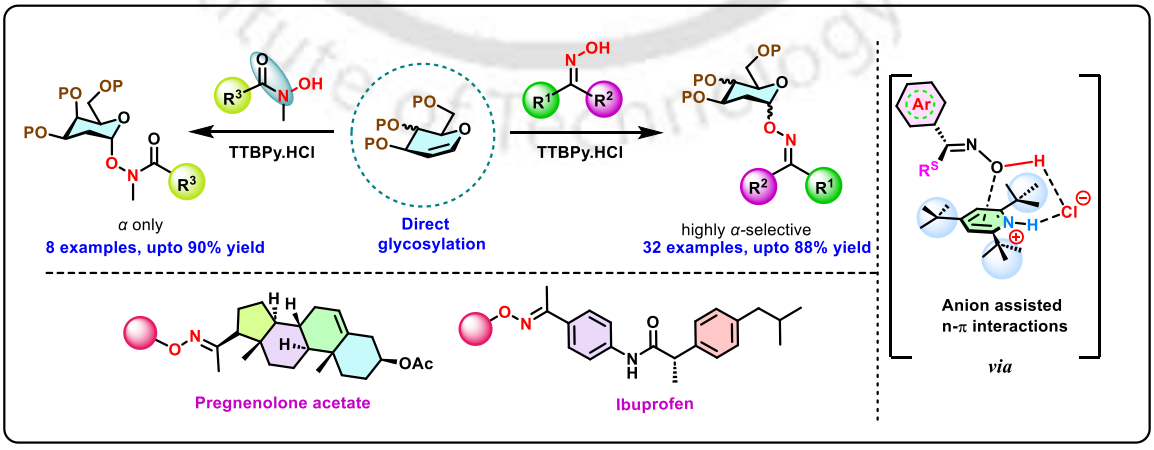

(*Org. Lett.* **2024**, *26*, 10382−10387)

Figure 1. Synthesis of 2-deoxy N-O-linked glycosides.

Chapter III. *Sulfonium Stabilized Phenols as Hydrogen Bonding Catalysts toward Diastereoselective Glycosylation of Cyclopropanated Sugars*

Imitating natural glycans is a sophisticated strategy for evading recognition by microorganisms and disease-associated enzymes. A prominent approach to carbohydrate mimicry involves modifying the ring size by expanding or contracting it. Ring-expanded hexose analogs, known as septanoses or carbohydrate-based oxepanes, have emerged as potent mimics of natural carbohydrates. Notably, research by Peczuh and colleagues on protein-carbohydrate interactions, particularly those involving concanavalin A and methyl septanosides, has provided compelling evidence that septanosides can effectively mimic pyranosides. This advancement has inspired many researchers to develop methods for synthesizing carbohydrate-based oxepanes and septanose-containing glycoconjugates.

In parallel, recent advances in small-molecule catalyst design have offered compelling solutions to persistent glycosylation challenges, unlocking new possibilities for achieving high levels of selectivity in coupling reactions. In our pursuit of a simple and modular catalytic system, we found phenols, cost-effective compounds known for their catalytic efficiency, particularly appealing as dual-function Brønsted acids and hydrogen bond donors. To this end, we designed a phenol-based catalyst incorporating a sulfonium moiety as a charged arm to modulate the catalytic properties of the phenol core, collectively referred to as electrostatically tuned phenols (ETPs). In this chapter, we present a robust catalytic strategy using a simple, electrostatically tuned phenolic sulfonium salt that leverages hydrogen bonding networks to enable α-selective strain-release *O*- and *S*-glycosylation toward biologically significant seven-membered oxepane frameworks. The unique reactivity of the phenolic cyclic sulfonium salt has been studied by ^{1}H-NMR, IR, UV, and fluorescence spectroscopy. This strategy offers excellent functional group tolerance and synthetic versatility, enabling the septanosylation of a diverse array of structurally intricate alcohols and carboxylic acids. The efficacy of this methodology is highlighted by its ability to achieve site-selective transformations on glycosylated scaffolds, facilitate late-stage diversification of bioactive drug molecules, and enable streamlined disaccharide assembly.

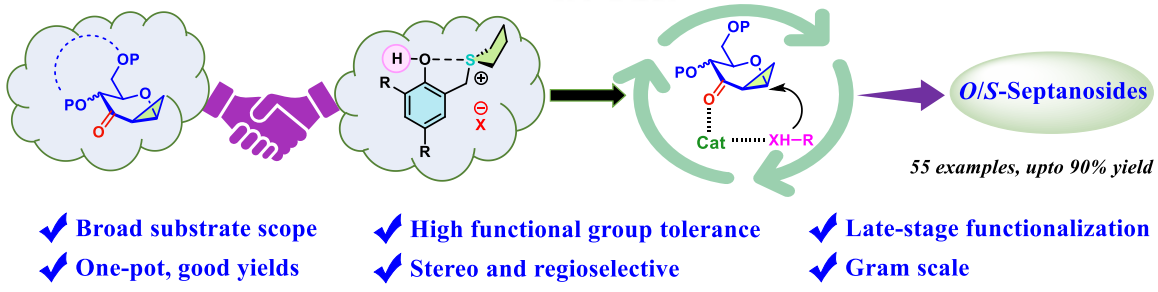

(*Org. Lett.* **2025**, *27*, 11650−11655)

Figure 2. Sulfonium salt-catalyzed strain-release *O*- and *S*-septanosylation.

Chapter IV. *Triple Role of Proton Sponge (DMAN) in the Palladium-Catalyzed Direct Stereoselective Synthesis of C-Aryl Glycosides from Glycals*

C-glycosides are carbohydrate analogs with a carbon-carbon bond at the anomeric position. Among *C*-glycosides, aryl *C*-glycosides are notable for their diverse bioactivities and synthetic utility. Few methods enable *C*-aryl glycoside synthesis from glycals with C-3 oxygen retention, but they often require prefunctionalized substrates, directing groups, and exogenous ligands, and show limited substrate scope. Therefore, developing straightforward methods for the stereo- and regioselective synthesis of aryl *C*-glycosides with broad substrate compatibility is highly desirable. In this chapter, we have displayed the utility of the 1,8-bis-dimethylaminonaphthalene in the palladium-catalyzed *C*-glycosylation of glycals.

1,8-bis-dimethylaminonaphthalene, known as proton sponge, is widely used as a strong organic base due to the release of electronic strain between the lone pairs of its peri-nitrogens. Despite its bidentate nature, steric congestion around the nitrogen sites renders the proton sponge weakly nucleophilic, suggesting it is unsuitable as a ligand for metal complexes. However, in 2004, Okeya and colleagues synthesized and characterized the first proton sponge palladium(II) complex using X-ray crystallography, demonstrating its robust coordination ability. Despite its commercial availability and affordability, the utilization of this proton sponge in metal catalysis has seen limited progress. In our study, we unveil the triple role of the proton sponge: it acts as a reductant, serves as a ligand precursor to stabilize in situ formed zero-valent palladium, and functions as an organic base. We demonstrate its application in the Heck-type coupling of glycals with aryl iodides, leading to the synthesis of biologically significant aryl *C*-glycosides. Remarkably, this study reports the first use of a palladium proton sponge complex in coupling reactions. Additionally, a few β-aryl glycosides were synthesized using our tri-*tert*-butyl pyridinium salt catalysis.

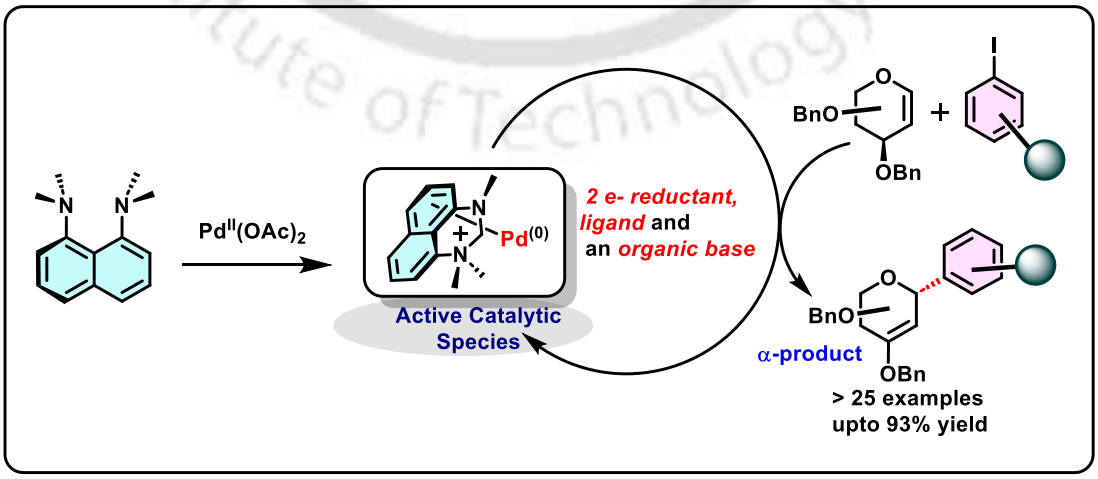

(*Org. Lett.* **2024**, *26*, 3563−3568)

Figure 3. Palladium-catalyzed *C*-glycosylation of glycals.

Chapter V. *Influence of Sterics vs Inductive vs Through Space Stabilization Effects on the Basicity and Reactivity of the Pyridinium Cation*

Organic bases are essential reagents in synthetic organic chemistry, playing a pivotal role in many reactions where deprotonation is crucial for forming new structures. The specific base required varies with different applications and reaction conditions. Consequently, a diverse range of organic bases has been developed and is widely used. These bases are categorized based on their strength, nucleophilicity, steric hindrance, or solubility. Significant efforts have been invested in enhancing their basicity while minimizing their nucleophilic properties. Sterically hindered aliphatic amines, anilines, and N-heterocycles have emerged as effective non-nucleophilic bases, functioning as organocatalysts with numerous practical applications, including Dieckmann cyclization, polymerizations, and metalation reactions.

It is well-known that 2,6-di-*tert*-butylpyridine (DTBP), 2,6-di-*tert*-butyl-4-methylpyridine (DTBMP), and 2,4,6-tri-*tert*-butylpyridine (TTBPy) are non-nucleophilic bases, albeit at a relatively high cost. Drawing inspiration from the unique reactivity of these strained pyridinium salts, we focused on developing a structurally similar, sterically hindered non-nucleophilic base that can be synthesized more affordably. We aim to evaluate their effectiveness as alternatives to the established non-nucleophilic bases such as TTBPy, DTBP, and DTBMP. Notably, TTBPy features ortho-*tert*-butyl groups on both sides, which are integral to the substrate. We propose that substituting one of the methyl groups of the *tert*-butyl moiety with various alkoxy groups could significantly impact the molecule's properties. After synthesizing these heteroatom-containing molecules, we have investigated the resulting structural modifications, their associated physical and chemical properties, and their potential applications in stereoselective glycosylation reactions.

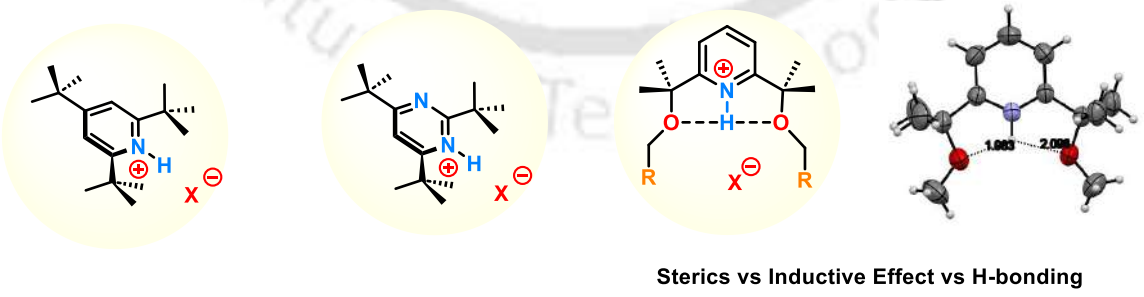

Figure 4. Heteroatom-containing sterically hindered salts.

Table of contents

Chapter 3. Sulfonium Stabilized Phenols as Hydrogen Bonding Catalysts toward Diastereoselective Glycosylation of Cyclopropanated Sugars

Chapter 1

An Introduction to the Reactivity and Synthetic Utility of Sterically Strained Nitrogen Bases and Electrostatically Tuned Phenols

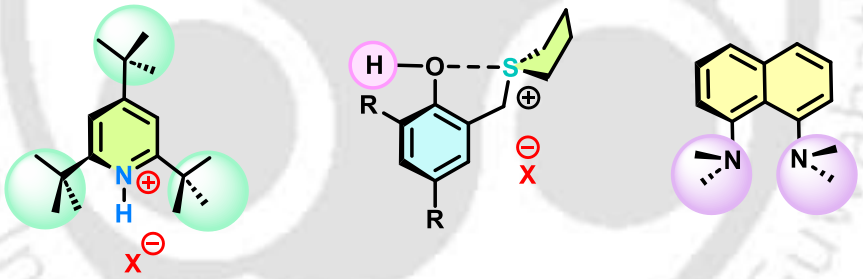

1.1. Introduction

1.1.1. Carbohydrates

Carbohydrates, mainly as glycoconjugates or polysaccharides, are abundant natural compounds that are essential to bioactive molecules[1] and traditionally recognized for their roles in energy storage, structure, and metabolism.[2] Carbohydrates are now known to play pivotal roles in essential biological processes, including cell growth, metastasis, immune defense, signal transduction, intercellular adhesion, and fertilization.[3, 4] A wide range of clinically important drugs, including Streptomycin,[5] Landomycin F,[6] Jadomycin,[6] Acarbose,[7] Tamiflu,[8] Zanamivir,[8] Topiramate,[9] Miglitol,[7] and Voglibose,[7] are carbohydrate-based therapeutics used to treat bacterial infections, breast cancer, diabetes, influenza, migraines, and epilepsy (Figure 1.1). Unraveling the roles of carbohydrates in cell biology would significantly advance the field of glycoscience.[10]

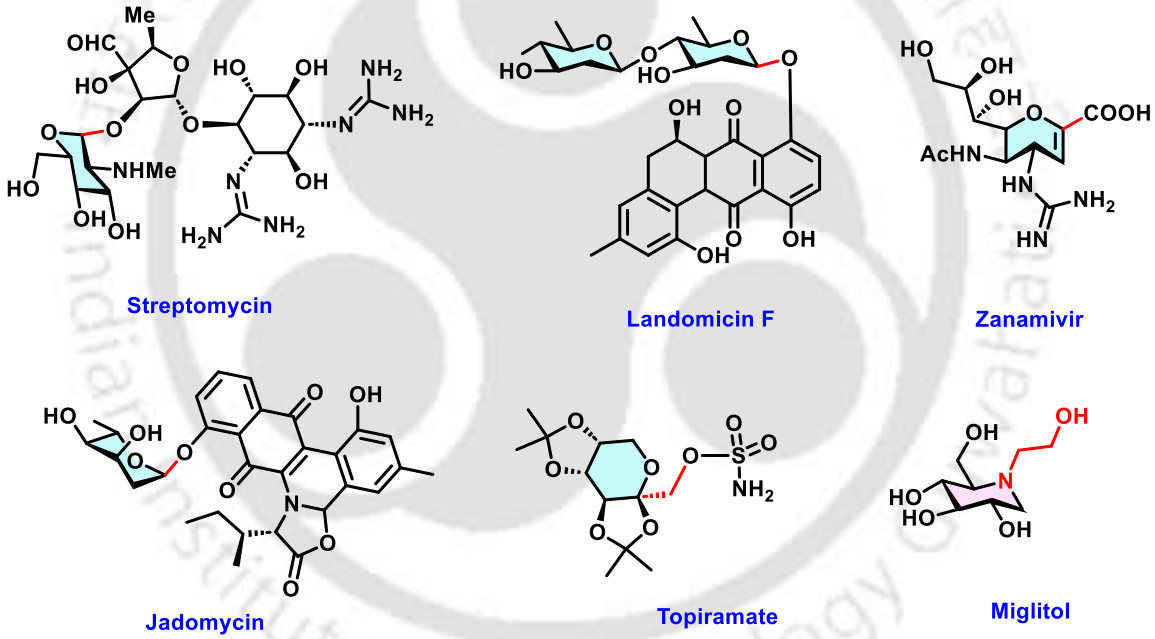

Figure 1.1. Carbohydrate-based therapeutics in medicinal chemistry.

1.1.2. Glycosylation

Glycosylation refers to the covalent attachment of carbohydrate units to other saccharides, lipids, proteins, natural products, or drugs, and forms the cornerstone of glycochemistry and glycobiology. Over the past century, significant advances in carbohydrate chemistry have enabled the efficient synthesis of *S*-, *N*-, *C*-, and *O*-linked glycosides with outstanding stereo- and regioselectivity.[11] Glycosides exhibit diverse biological activities[12] and serve as essential scaffolds in drugs such as remogliflozin, heparin, and lactitol.[13] Consequently, the stereoselective synthesis of *O*-glycosides remains a central goal in carbohydrate

chemistry.[14] Despite significant advances, achieving precise control over α/β-anomeric selectivity remains a major challenge due to its crucial role in determining biological function. Conventional glycosylation requires stoichiometric Lewis acids and excess acid scavengers, with stereoselectivity dependent on saturated donors with anomeric leaving groups and their activation; in contrast, catalytic methods using simple donors offer a more practical and ideal alternative (Scheme 1.1).[11]

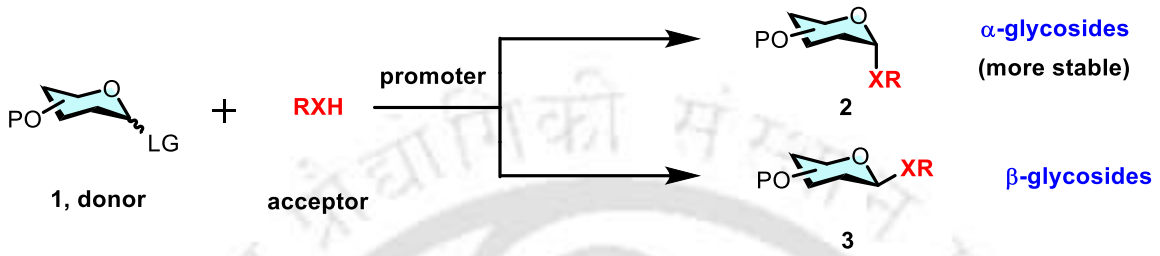

Scheme 1.1. General outline of glycosylation.

Scheme 1.2 illustrates a generalized pathway in which donor **1**, pre-activated with an anomeric leaving group, forms complex **4** upon addition of a promoter, leading to the generation of oxocarbenium intermediate **5** in a flattened half-chair conformation, followed by nucleophilic attack by alcohol to afford glycoside **6**. Due to the oxocarbenium ion's structure, acceptor attack can proceed via two pathways: bottom-face attack forms α (1,2-cis) glycoside **6a**, while top-face attack produces β (1,2-trans) glycoside **6b** (Scheme 1.2).[15]

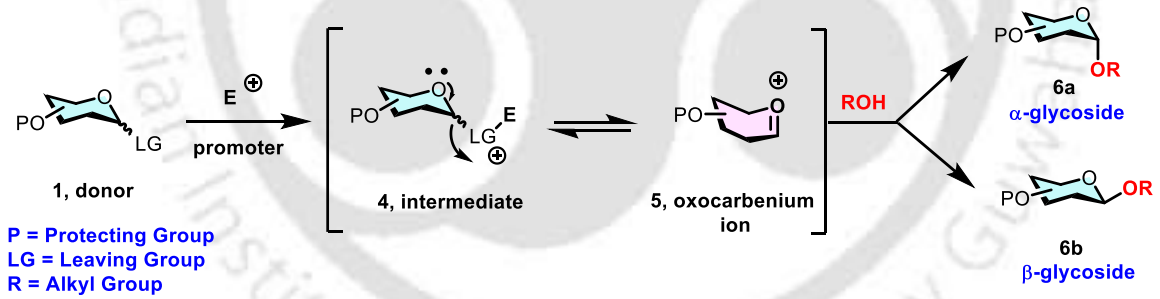

Scheme 1.2. Mechanistic insights into glycosylation.

1.1.3. Key factors influencing glycosylation reactions

Beyond the intrinsic complexity of glycosylation, several competing processes must be carefully considered. Side reactions, including elimination, substitution (cleavage of the glycosidic linkage at the anomeric position or formation of unintended substitution products), cyclization through intra- and intermolecular orthoesterification, redox reactions, and migration, can frequently disrupt stereocontrol and reduce glycosylation yields. The stereoselectivity and efficiency of glycosylation are influenced by various parameters, including the anomeric effect, neighbouring group participation, reaction

temperature, solvent system, nature of the glycosyl acceptor and donor, type and quantity of promoter, and the arrangement of protecting groups (Figure 1.2).[11]

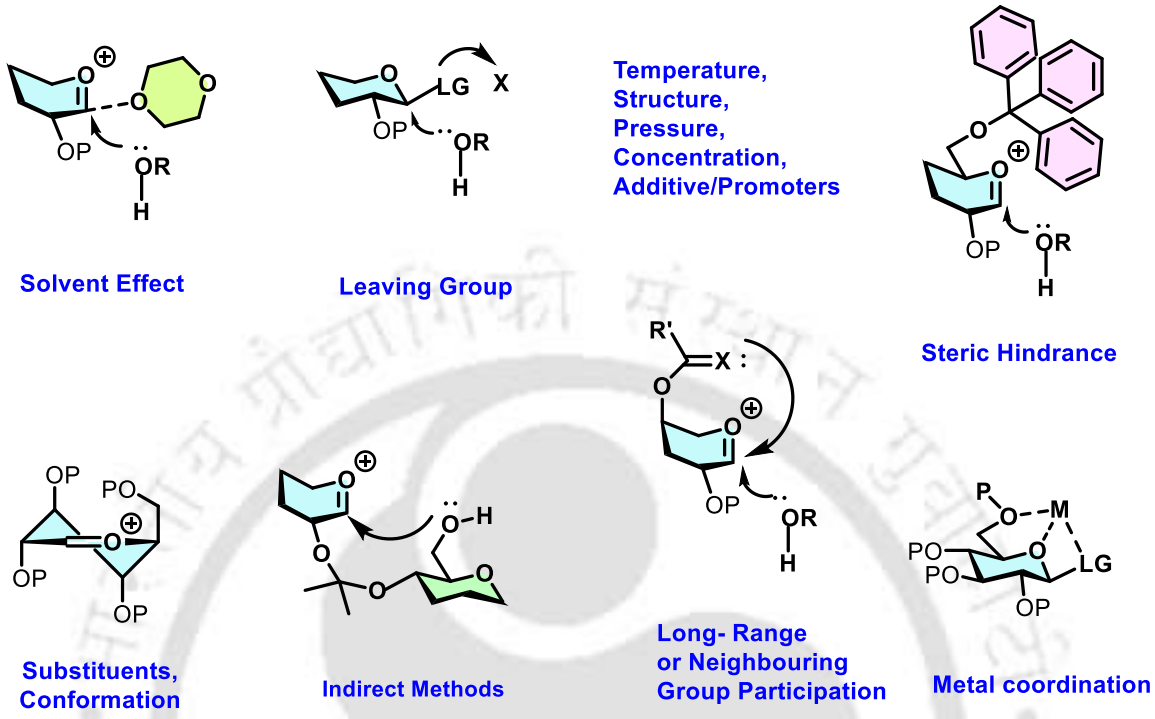

Figure 1.2. Factors influencing stereoselectivity.

1.2. Reactivity and synthetic utility of sterically strained Brønsted salts

1.2.1. Emphasis on bulky pyridine bases

Pyridine, an isostere of benzene, is a versatile precursor in the synthesis of agrochemicals and pharmaceuticals, and functions as a reagent and solvent. In 1846, Anderson first isolated pyridine from picoline, and Dewar and Körner later elucidated its structure in 1871.[16] The six-membered heteroaromatic pyridine ring is prevalent in bioactive compounds, including alkaloids (e.g., nicotine), niacin (vitamin B_3), pyridoxine (vitamin B_6), and coenzymes (Figure 1.3).[17]

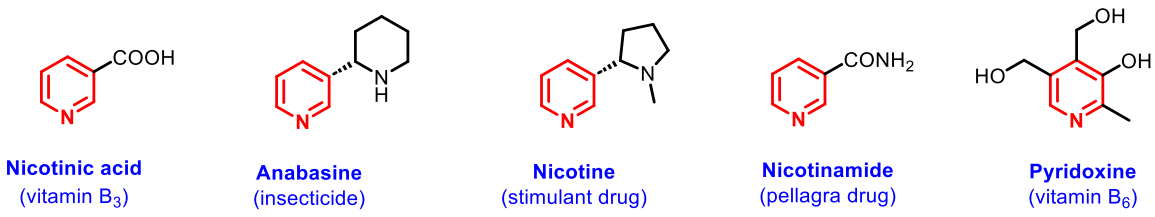

Figure 1.3. Natural pyridine-based compounds.

Pyridine-based compounds are known for their wide-ranging biological activities, including antiviral, antimicrobial, antioxidant, antidiabetic, anti-inflammatory, and anticancer activities. They serve as widely used scaffolds in drug design and synthesis, attracting significant interest across various research fields.[18] Key pyridine-based drugs include montelukast, isoniazid, lansoprazole, esomeprazole, and pioglitazone, along with antibacterial agents such as ethionamide and ozenoxacin (Figure 1.4).[18, 19]

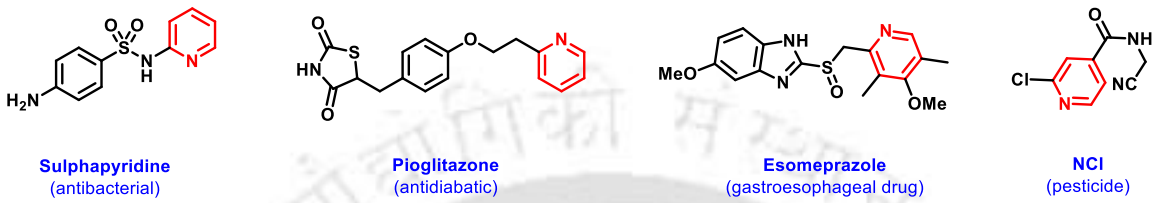

Figure 1.4. Pyridine scaffolds in drug development and therapeutics.

Several well-studied bulky pyridine derivatives, such as 2,6-lutidine, 2,4,6-trimethylpyridine (collidine), 2,6-di-*tert*-butylpyridine (DTBP), 2,6-di-*tert*-butyl-4-methylpyridine (DTBMP), 2,4,6-tri-*tert*-butylpyridine (TTBPy), and 2,4,6-tri-*tert*-butylpyrimidine (TTBP) are widely recognized for their utility as proton-trapping agents and have long been employed as traditional acid scavengers (Figure 1.5).[20, 21]

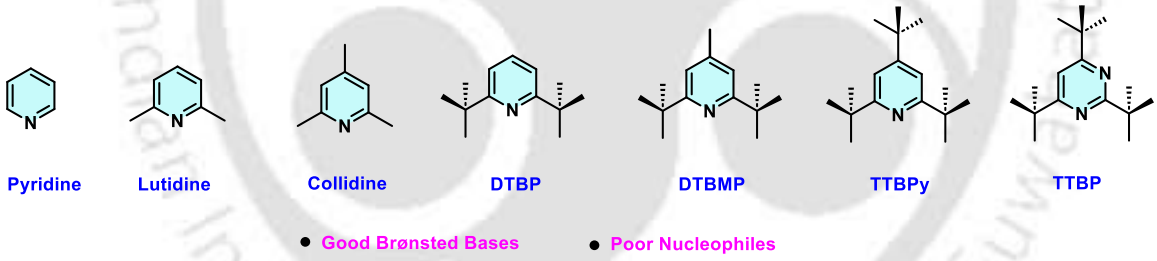

Figure 1.5. Sterically hindered pyridine derivatives.

1.2.2. Significance of bulky pyridine derivatives in organic reactions

TTBPy, a sterically bulky pyridine analog, was first prepared by Dimroth and Mach in 1968[22] via oxonium salt intermediates. Alongside its analogue DTBP,[23] it is distinguished by its inability to coordinate with small Lewis acids such as BF_3 or CH_3^+, except H^+.[24] Owing to its pronounced non-nucleophilic basicity, TTBPy has proven useful in a range of organic reactions, especially for neutralizing acidic byproducts and maintaining pH balance in metal-ion-mediated processes conducted in aqueous environments.[25] Effenberger utilized TTBPy to quantify acylium ion concentrations during aromatic acylation reactions by trapping the released triflic acid (Scheme 1.3).[26] Furthermore, its influence on k_H/k_D isotope effects has provided mechanistic insight into proton transfer pathways within these systems.

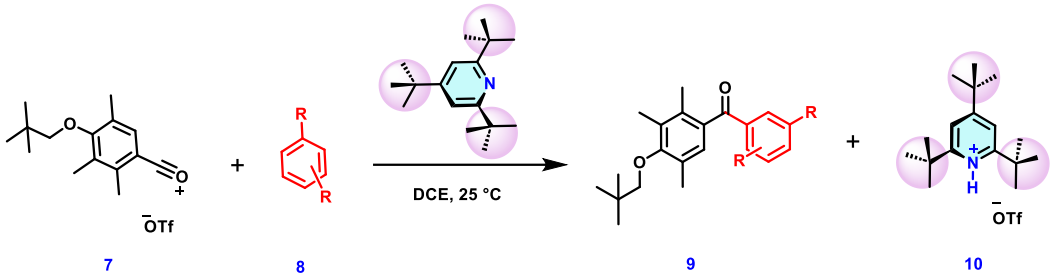

Scheme 1.3. Influence of TTBPy on aromatic acylation reactions.

Shibata and coworkers synthesized indole triflones using a TTBPy/Tf_2O system. Biindolyl triflones were obtained via base-mediated dimerization through a deprotonation-addition-elimination sequence, with the SO_2CF_3 group playing a crucial role. The use of weak base TTBPy was essential to suppress undesired byproducts, unlike conventional Lewis acid-mediated methods that yielded complex mixtures (Scheme 1.4).[21]

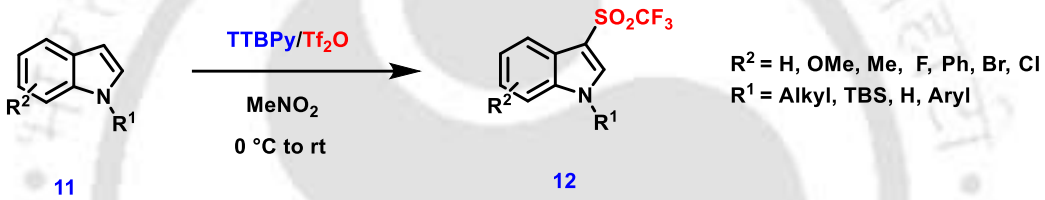

Scheme 1.4. Synthesis of indole triflones using TTBPy and triflic anhydride.

Berke and colleagues demonstrated that hindered TTBPy, when combined with $B(C_6F_5)_3$ or $[(acridine)BCl_2]^-[AlCl_4]$, forms a stable FLP (frustrated Lewis pair) capable of heterolytically cleaving H_2 (Scheme 1.5).[27]

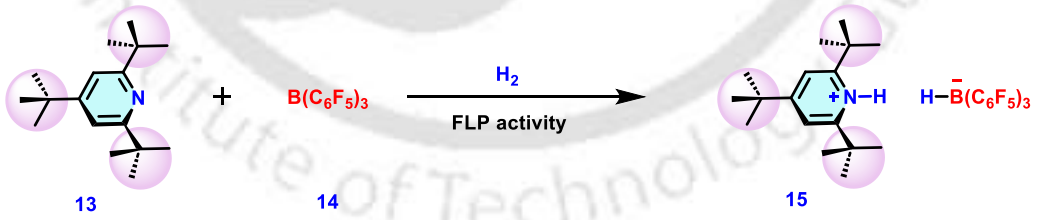

Scheme 1.5. H_2 activation via frustrated Lewis pair.

1.2.3. Utility of bulky pyridine derivatives in glycosylation reactions

TTBPy, along with other sterically bulky bases such as DTBP, TTBP, and DTBMP, is commonly utilized in glycosylation reactions to trap protons and neutralize strongly acidic byproducts generated during the process.[28] Gin and coworkers displayed a method for synthesizing glycosyl-1-phosphates from hemiacetal donors using dialkyl phosphates, diphenyl sulfoxide (2 equiv), and triflic anhydride. This protocol employed an excess of

TTBPy (5 equiv) to efficiently neutralize the undesired acidic byproducts generated during activation (Scheme 1.6).[28]

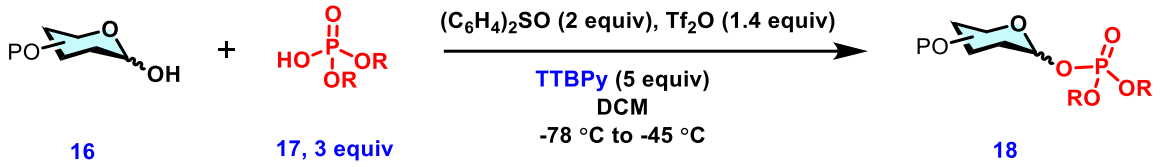

Scheme 1.6. Dehydrative glycosylation strategy for glycosyl-1-phosphate synthesis.

The steric bulk of TTBPy effectively suppresses its nucleophilicity, a feature deliberately exploited in a range of organic transformations. In 2000, the Crich group introduced a stereoselective method for synthesizing β-mannopyranosides using 2,6-di-*tert*-butyl-4-methylpyridine (DTBMP). Upon activation of mannopyranosyl sulfoxide donors with Tf_2O in DCM at –78 °C, DTBMP facilitated the selective glycosylation of secondary alcohols, yielding β-mannosides with excellent stereoselectivity (Scheme 1.7).[20]

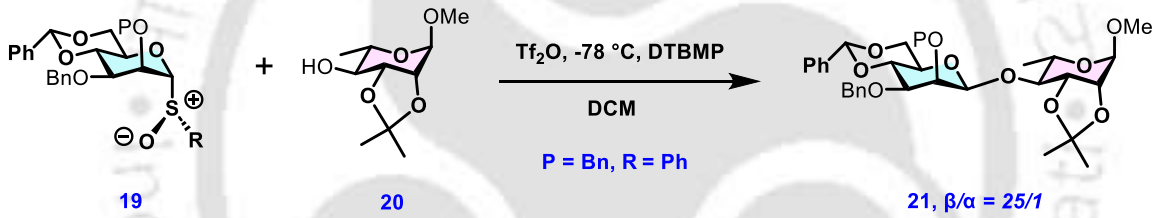

Scheme 1.7. DTBMP-mediated glycosylation approach to β-mannopyranosides.

1.2.4. Design and synthesis of sterically hindered Brønsted salts

Inspired by the distinctive reactivity of sterically encumbered pyrimidine and pyridine derivatives, our efforts focused on designing structurally strained Brønsted salts as organocatalysts and selective hydrogen bond donors in stereocontrolled glycosylation processes.

The pK_a of DTBP in water is approximately two units lower than predicted, even though its gas-phase pK_a aligns with theoretical data. This discrepancy, also observed in TTBPy and TTBP, arises from poor solvation of their protonated forms due to steric hindrance, resulting in weak basicity (e.g., $TTBPyH^+$, pK_a = 3.54) (Figure 1.6). The effect is more pronounced in DMSO, where DTBP shows a pK_{DMSO} of 0.81, indicating minimal hydrogen bonding with the bulky solvent. Consequently, the behavior of $TTBPyH^+$ is strongly influenced by the strong hydrogen bonding capacity of the solvent (Figure 1.7).[24]

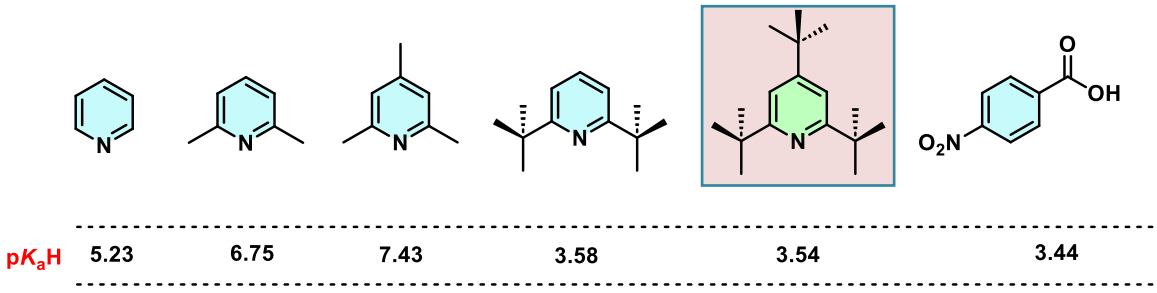

Figure 1.6. Substituent effects on pyridine basicity.

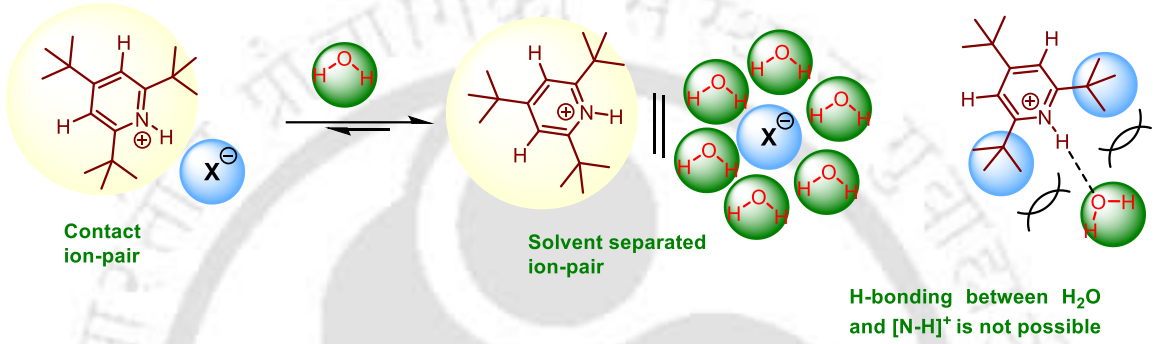

Figure 1.7. Reasons for the weak basicity in aqueous solution.

Our investigation focused on the reactivity of $TTBPyH^+$ in commonly used solvents, such as DCM and DCE, where it acts effectively as a proton scavenger. Notably, the reactivity of cationic and neutral Brønsted acids may differ significantly in such nonpolar media.[29] A key question is whether the protonated TTBPy acts as a true cationic acid capable of protonating sterically hindered glycals or instead forms a strong ion pair with its counter anion, exhibiting neutral character due to limited solvation (Figure 1.8).

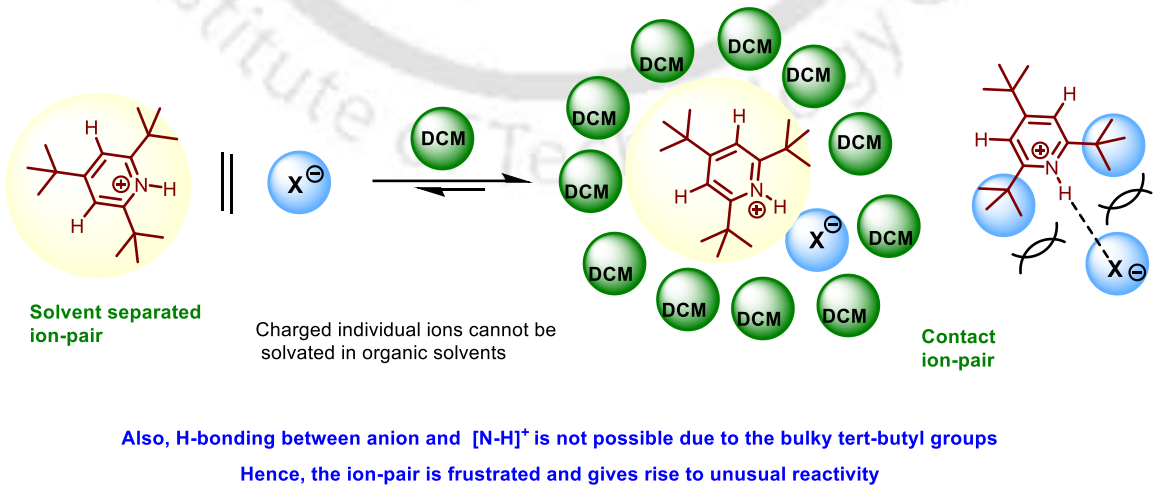

Figure 1.8. Behaviour of the bulky pyridinium salts in nonpolar organic solvents.

Our findings provide insight into the reaction mechanism, indicating that $TTBPyH^+$ promotes the reaction through hydrogen-bonding-assisted activation rather than a classical Brønsted acid pathway. Moreover, its catalytic efficiency appears to depend on the identity of the counterion. TTBPy salts bearing various counter anions, including chloride, bromide, triflate, tetrafluoroborate, and $BAr^F{}_4$ were synthesized as presented in the scheme 1.8.[24]

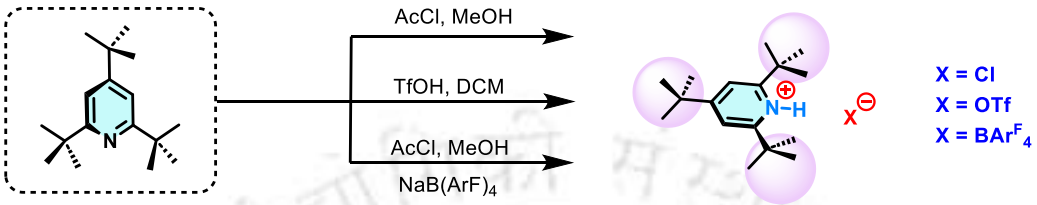

Scheme 1.8. Synthesis of pyridinium salts.

1.2.5. Utility of sterically bulky Brønsted salts in glycosylation reactions

In 2019, our group introduced the use of the chloride salt of TTBPy as an organocatalyst for stereoselective glycosylation. In this system, the protonated TTBPy cation serves as a strong hydrogen bond donor to activate the acceptor, which then reacts with the donor to yield 2-deoxy glycosides (Scheme 1.9).[24]

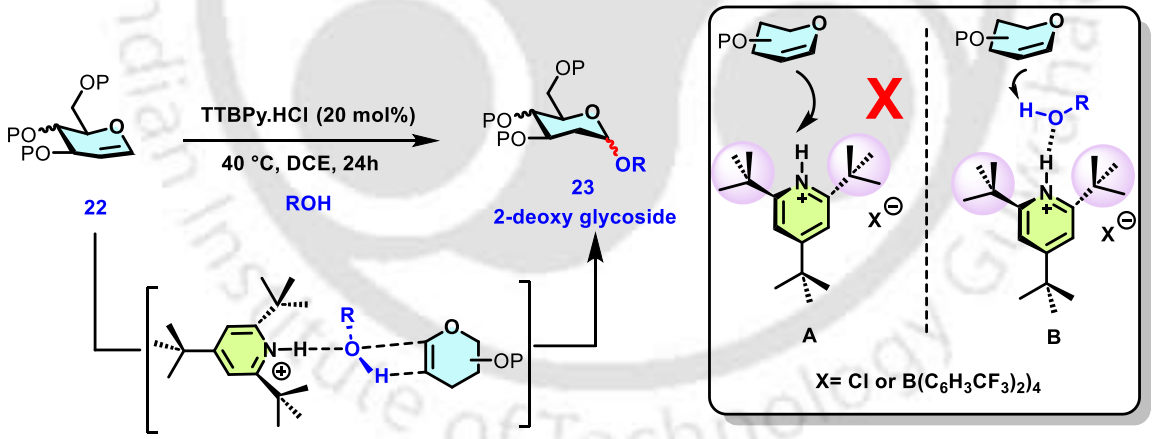

Scheme 1.9. *O*-glycosylation via TTBPy·HCl salt.

In 2020, our group demonstrated that bulky TTBPy·HCl serves as an efficient organocatalyst for converting acid-labile silyl-protected donors into hemiacetals with excellent yields via C-H···Cl^- interaction-assisted hydration. The catalyst's activity was found to be dependent on water concentration, which influenced the product outcome (Scheme 1.10).[30]

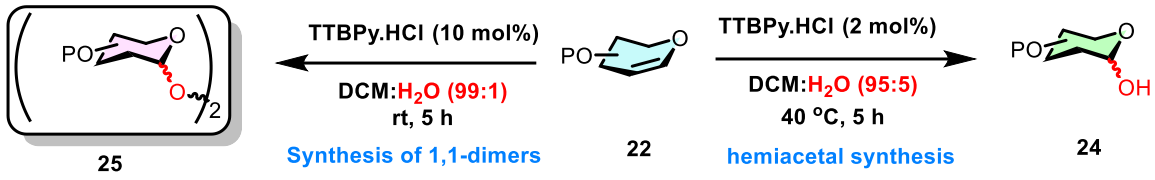

Scheme 1.10. Synthesis of hemiacetals via TTBPy·HCl salt.

In 2022, our group demonstrated that the protonated pyridinium triflate salt is a stable, efficient catalyst for selective *C*-glycosylation of glycal donors. Its capacity to activate silylenolethers and allylsilanes through TfO⁻···H-O-H interactions, facilitating silicon cation generation, highlights its broader potential in organic transformations (Scheme 1.11).[31]

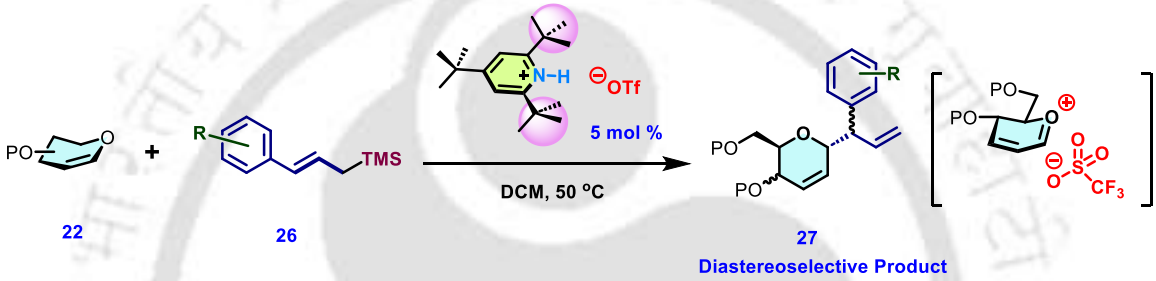

Scheme 1.11. *C*-Ferrier glycosylation via pyridinium triflate salt.

In 2025, our group developed the hindered and frustrated pyrimidinium BArF salt as an efficient, metal-free catalyst for the silylation of various sugar and non-sugar alcohols using silanes as the silicon source. Its distinctive π-Lewis acidic character enabled the mild and selective protection of acid-sensitive sugar and non-carbohydrate alcohols (Scheme 1.12).[32]

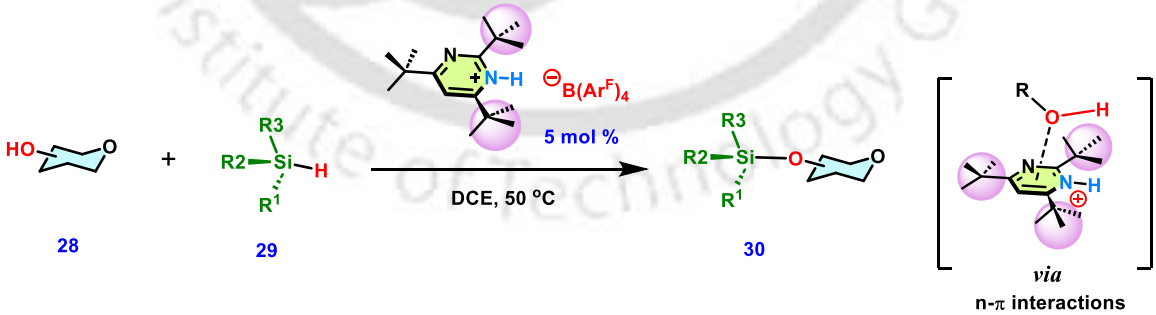

Scheme 1.12. Silylation of sugar alcohols via pyrimidinium BArF salt.

Due to its steric bulk around the cationic site, the hydrogen bond is prevented in the sterically strained 2,4,6-tri-*tert*-butylpyridinium salts, resulting in poor electrostatic interactions within the ion-pair. In this thesis, we exploit these unique, poor electrostatic/strained interactions to achieve a biologically significant class of N-O-linked glycosides in a highly diastereoselective manner.

1.3. Design and reactivity profiles of phenolic salts in organocatalysis

1.3.1. Emphasis on phenol-based catalysts

After successfully utilizing sterically frustrated Brønsted ion pairs as organocatalysts in multiple glycosylation reactions to achieve glycosides with excellent yields and selectivity, we focused on developing a simpler and more modular catalytic system. Phenols, being inexpensive and well-established for their catalytic roles as Brønsted acids and hydrogen bond donors, emerged as attractive candidates. Motivated by this dual functionality, we designed a phenol-based catalyst incorporating a cyclic sulfonium moiety as a charged arm to modulate the electronic and catalytic properties of the phenol core.

Recent advances in small-molecule catalyst design have provided compelling solutions to longstanding glycosylation challenges, enabling high levels of selectivity in coupling reactions. The advent of small-molecule catalysts that engage in hydrogen bonding[33] or covalent interactions[34] with either the glycosyl donor or acceptor has ushered in new possibilities for stereoselective glycosylation by enabling simultaneous activation of both reaction partners. This innovative approach was spearheaded by the pioneering contributions of Schmidt,[35] Fairbanks,[36] Toshima,[37] Jacobsen,[38] Taylor,[39] and us[24] (strained pyridinium salt). In simple, modular catalytic systems, phenols emerge as cost-effective compounds with notable catalytic efficiency, particularly attractive due to their dual functionality as Brønsted acids and hydrogen bond donors.[40] To date, numerous strategies have been introduced to improve the catalytic efficiency of phenolic scaffolds (Figure 1.9).[41-43]

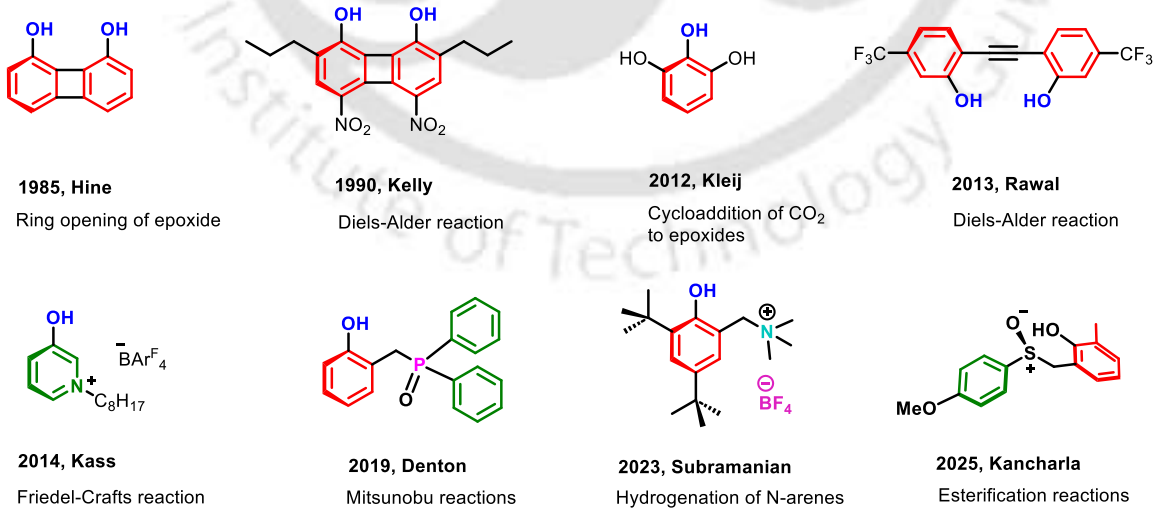

Figure 1.9. Phenol-based organocatalyst.

Wassermann's early observation in 1942 that phenol modestly accelerates the Diels-Alder reaction between benzoquinone and cyclopentadiene has since inspired the design of a wide range of phenol-based catalytic systems.[44] In 1985, Hine and colleagues demonstrated that 1,8-biphenylenediol (BPD), acting as a dual hydrogen bond donor, effectively promotes the ring-opening of phenyl glycidyl ether and enhances activation of oxygen-containing substrates like pyrones and epoxides, though its limited solubility in nonpolar (chlorinated) solvents remains a drawback (Figure 1.10).[40]

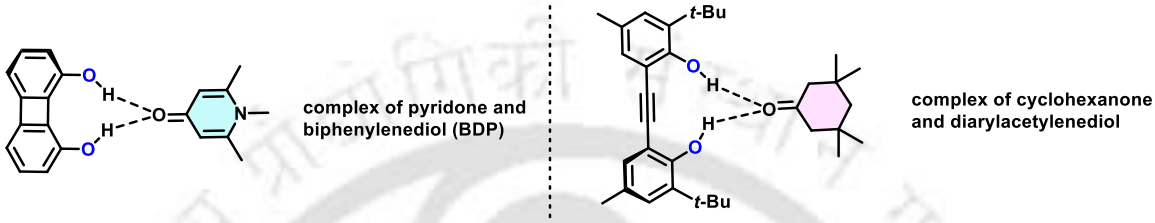

Figure 1.10. Hydrogen-bonding interactions in diol complexes.

In 1990, Kelly *et al.* introduced a nitro-substituted, soluble biphenylenediol analog that significantly enhanced the efficiency of the Diels-Alder reaction, achieving up to a 30-fold increase in conversion compared to the uncatalyzed process and exhibiting superior catalytic performance relative to p-nitrophenol (Scheme 1.13).[45]

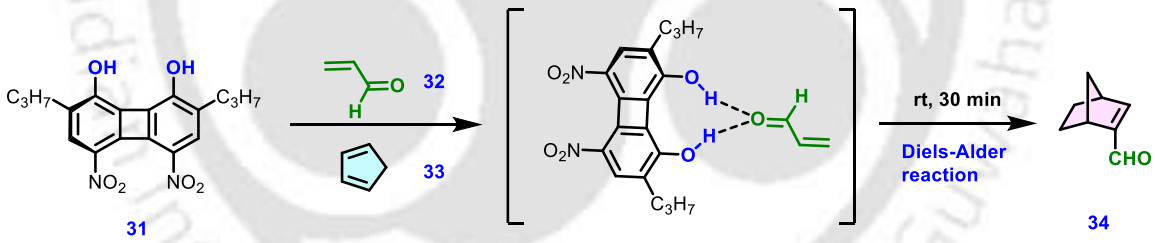

Scheme 1.13. Hydrogen-bond-assisted Diels-Alder reaction.

In 2012, Kleij and coworkers introduced a binary catalytic system comprising substituted phenols and nBu_4NI salt, where the multiphenolic derivative, stabilized by intramolecular

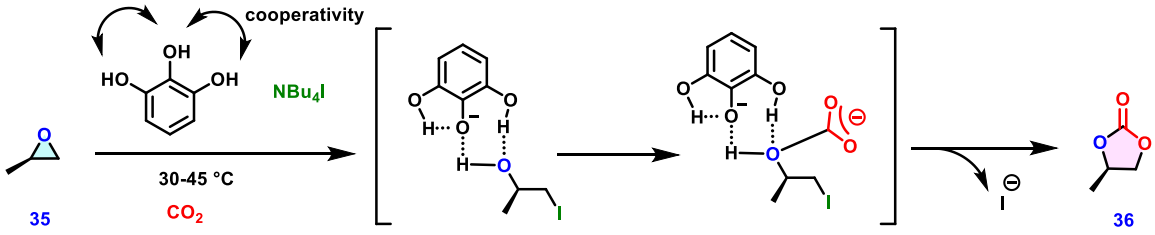

Scheme 1.14. Cycloaddition reaction via epoxide activation.

hydrogen bonding, enhanced epoxide activation through synergistic interactions, and promoted efficient cycloaddition with carbon dioxide to form organic carbonates (Scheme 1.14).[46]

1.3.2. Applications of phenolic salts in organic synthesis

Interestingly, charged systems have shown remarkable rate enhancements and improved performance in various organic transformations. Notably, the catalytic effect is especially pronounced when the charge is localized on complex aromatic frameworks or heteroatoms within such units.[43] These insights have motivated researchers to explore simpler, modular scaffolds that are synthetically accessible and capable of delivering efficient organocatalytic activity.

In 2019, the Denton group developed a redox-neutral Mitsunobu protocol using a catalytic amount of organophosphine oxide. In this strategy, the phenolic hydroxyl moiety is pivotal in generating the reactive oxyphosphonium intermediate, facilitating nucleophilic substitution via an S_N2 mechanism (Scheme 1.15).[41]

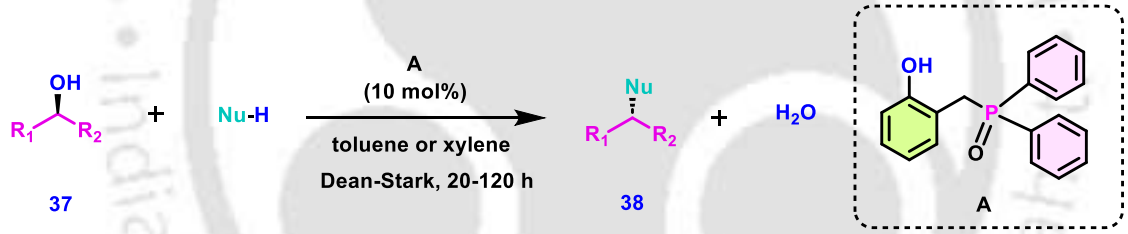

Scheme 1.15. Organophosphine oxide-catalyzed Mitsunobu reaction.

We anticipated that a sulfoxide-based catalyst bearing a phenolic tether could generate a cyclic intermediate via an intramolecular interrupted Pummerer-type pathway under mildly acidic conditions. Given the increased polarity of sulfoxides, we further hypothesized a mechanistic shift in their behaviour during esterification. Guided by this rationale, in 2025, our group introduced a phenolic sulfoxide-derived organocatalyst that promotes direct esterification of carboxylic acids with alcohols through redox-neutral sulfur(IV) catalysis (Scheme 1.16).[42]

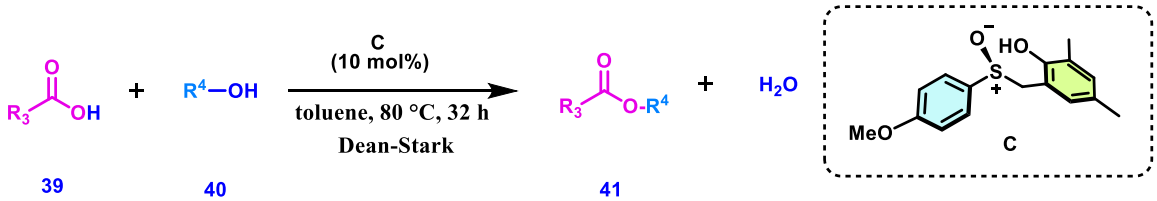

Scheme 1.16. Organocatalytic esterification.

1.3.3. Structural design of phenolic cyclic sulfonium salts

Building on previous studies and our ongoing interest in developing organocatalytic scaffolds from readily available sources for glycosylation reactions, we designed a catalyst featuring a phenol core with a cyclic sulfonium side arm to modulate its electronic and catalytic properties. This phenolic sulfonium salt harnesses hydrogen-bonding networks to promote α-selective, strain-release *O*- and *S*-septanosylation, enabling access to biologically relevant seven-membered oxepane frameworks (Figure 1.11).

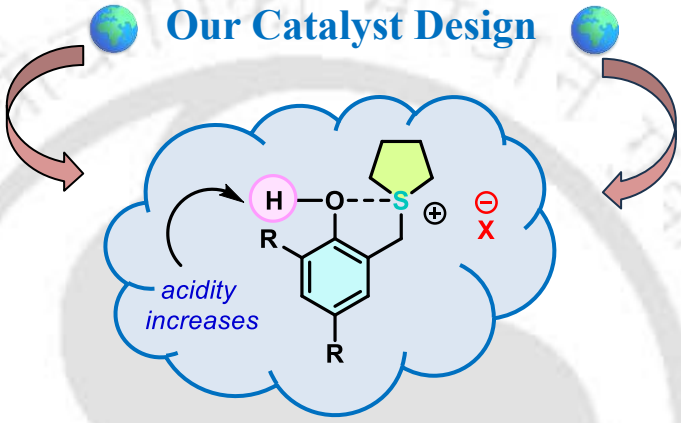

Figure 1.11. Phenolic cyclic sulfonium salt.

1.4. Reactivity and synthetic utility of sterically strained proton sponge

1.4.1. Emphasis on bulky proton sponge

1,8-bis(dimethylamino)naphthalene, commonly known as *proton sponge*,[47] features two closely positioned dimethylamino groups. It is widely used as a strong organic base, attributed to the release of electronic strain between the lone pairs of its peri-nitrogens.[48, 49] This compound was first reported by Alder *et al.* in 1968.[50] Despite its bidentate nature, steric congestion around the nitrogen sites renders the proton sponge weakly nucleophilic, leading to the assumption that it is unsuitable as a ligand for metal complexes.[51] However, in 2004, Okeya and colleagues synthesized and characterized the first proton sponge palladium(II) complex using X-ray crystallography, demonstrating its robust coordination ability.[52] In addition, DMAN serves as a reducing agent, effecting the transformation of Rh(III) to Rh(I) via a two-electron process (Scheme 1.17).[53] The exceptional basicity of proton sponge has rendered it a valuable reagent in synthetic organic chemistry, alongside other superbases.

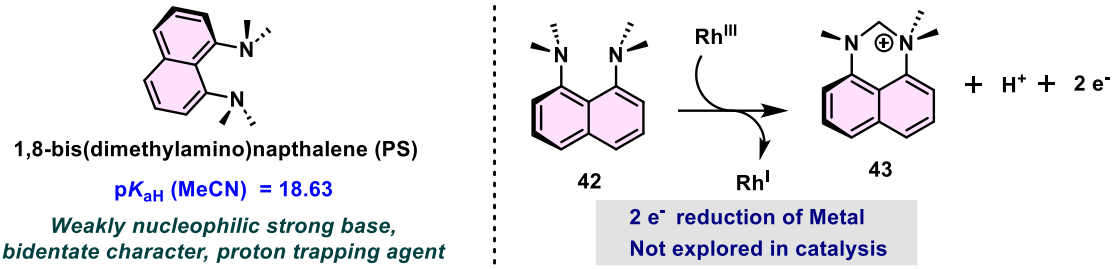

Scheme 1.17. DMAN-induced reduction of Rh(III) to Rh(I).

1.4.2. Synthetic utility of proton sponge

Several well-established methods are employed to synthesize proton sponge derivatives, typically involving N-H bond ionization using strong bases such as KH or NaH in dry THF, or KOH in DMSO. These conditions generate N-anions from the parent and partially alkylated amines, which act as key reactive intermediates. The high NH-acidity of compound **44** (p*K*a 24.5 in DMSO at 25 °C) facilitates efficient deprotonation, with the resulting anion **45** stabilized through intramolecular hydrogen bonding (IHB) (Scheme 1.18).[54]

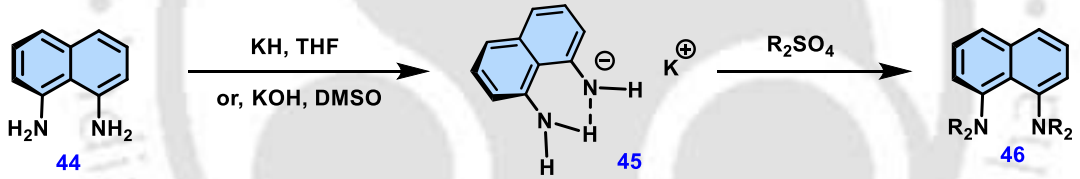

Scheme 1.18. Synthetic route of proton sponge.

Though proton sponges are unsuitable for E2 eliminations due to low kinetic basicity, their low nucleophilicity makes them ideal for scavenging acids without disturbing base-sensitive groups. Using DMAN to convert imidazoles **47** into 2-sila-3H-imidazo[2,1-b]thiazoles **48** yields over 80% of the target products (Scheme 1.19). In contrast, substituting DMAN with conventional bases results in S-Si bond cleavage.[55]

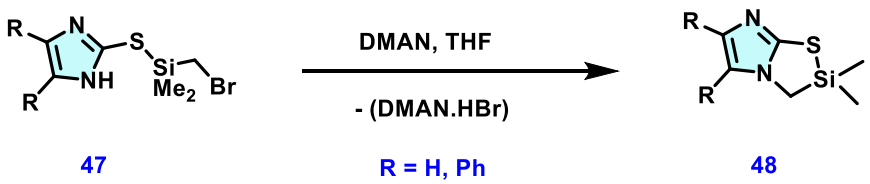

Scheme 1.19. Silyl-linked mercaptoazole cyclization via condensation and dehydrohalogenation.

The cis-trans isomerization of pyrazolines (**49→51**), via an open-chain anionic intermediate, occurs efficiently with DMAN, whereas typical bases interfere with electrophilic substituents (Scheme 1.20).[56]

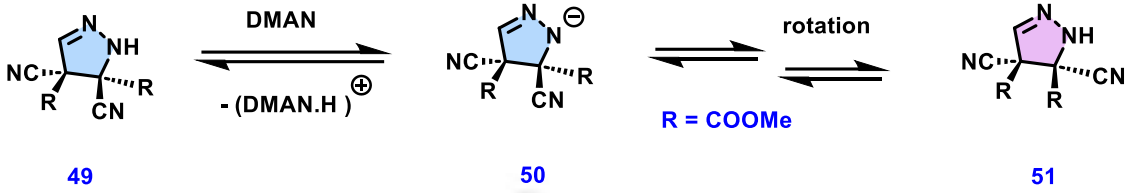

Scheme 1.20. Cis-trans isomerization of pyrazolines.

In base-mediated reactions of chiral compounds, proton sponges effectively suppress racemization and maintain high optical purity. A notable example is the transformation of optically active alcohols into ethers using trialkyloxonium tetrafluoroborates (Scheme 1.21).[57]

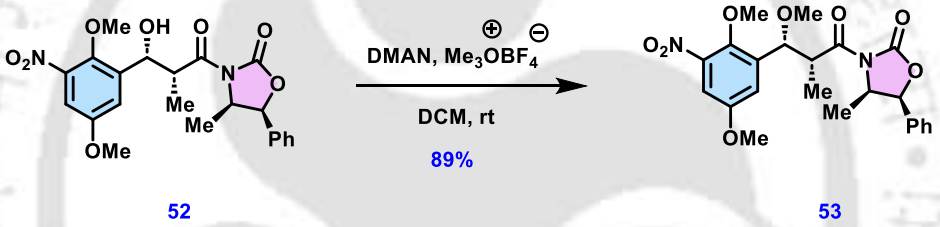

Scheme 1.21. Alkylation of optically active alcohols.

Activated phosphate **56**, in combination with a proton sponge, efficiently promotes peptide and amide synthesis from carboxylic acids. DMAN outperformed conventional bases such as 2,6-lutidine, N,N-dimethylaniline, Hünig's base, and triethylamine (Scheme 1.22).[58]

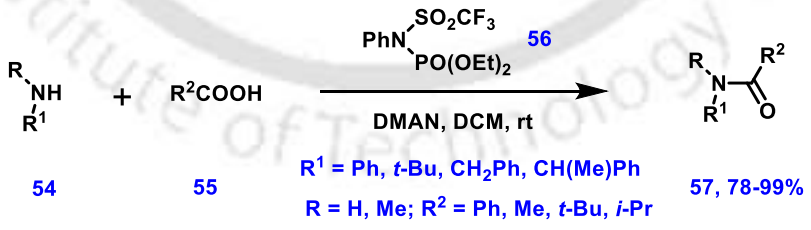

Scheme 1.22. Activated phosphate enables efficient amide and peptide coupling.

DMAN significantly improves enantioselectivity in Pd-catalyzed alkenylation and arylation of olefins with alkenyl (aryl) triflates. In contrast, the use of aliphatic amines (*i*-Pr_2NEt, Et_3N), substituted pyridines (2,6-di-*tert*-butyl-4-methyl-, 2,6-dimethyl-), or inorganic salts (Na_2CO_3, AcONa) leads to diminished yields and lower optical purity (Scheme 1.23).[59, 60]

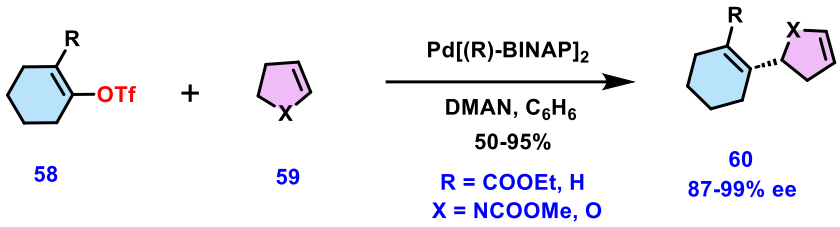

Scheme 1.23. Pd-catalyzed alkenylation of cyclic olefins.

DMAN was effectively used to deprotect the 2-(allyloxy)phenylacetyl ester (APAC) in carbohydrates. Heating compound **61** with a Pd catalyst and proton sponge gave compound **63** in near-quantitative yield via a relay mechanism involving allyl ether cleavage followed by intramolecular ester hydrolysis (Scheme 1.24).

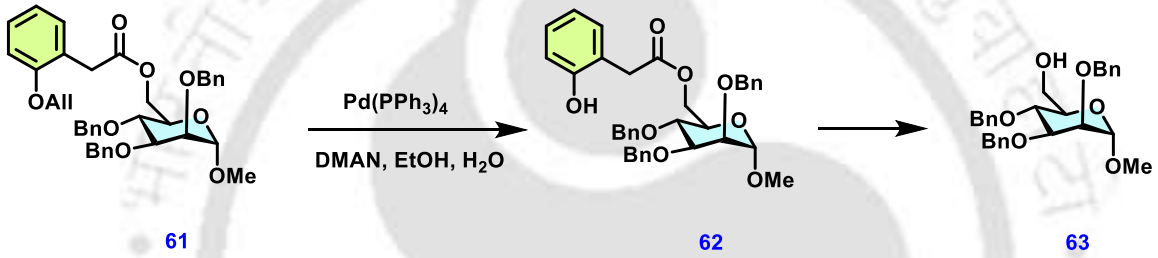

Scheme 1.24. Pd-catalyzed cleavage of 2-(allyloxy)phenylacetyl ester group.

The reaction conditions leave benzoyl, acetyl, and levulinoyl esters intact, crucial for oligosaccharide synthesis. In contrast, Et_3N leads to incomplete conversion, yielding a mixture of **63** and intermediate **62**. The high basicity and poor metal coordination of DMAN ensure efficient deprotection.[61]

DMAN reacts rapidly with bromomaleic anhydride at rt to yield 4-maleicanhydridoproton sponge (MAPS). This compound is isolated as a purple solid and displays pronounced solvatochromism in solution. Although MAPS is a weaker base than DMAN, it exhibits reversible colorimetric behavior upon protonation: the characteristic purple hue fades upon protonation and is restored upon treatment with a stronger base. This reversible chromogenic response enables MAPS to function as a colorimetric analogue of proton sponge (Scheme 1.25).[62] The reaction of DMAN with BMA represents more than a synthetic novelty; it offers a promising strategy for efficiently functionalizing proton sponge frameworks.

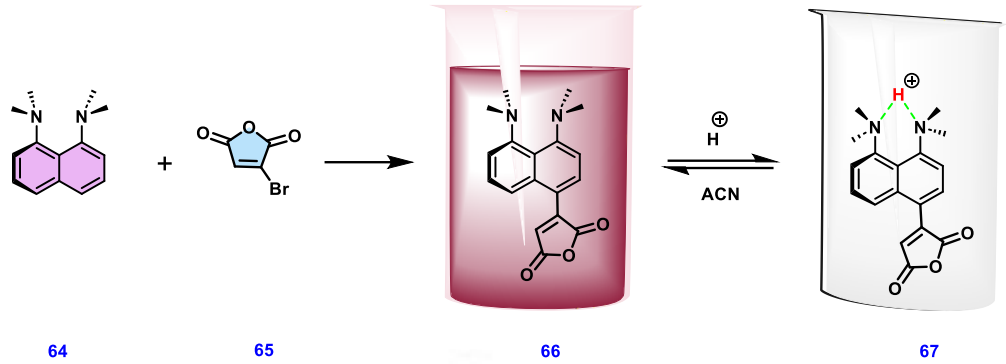

Scheme 1.25. Acid–base modulated colorimetric switching in ACN.

Despite significant development in bidentate ligands, proton sponge (DMAN) with a bidentate character has never been explored in palladium catalysis. In this thesis, we showcase the triple role of DMAN, as a two-electron reductant, as a stabilizing ligand of Pd(0) and as an organic base replacing the traditional inorganic bases in the palladium-catalyzed coupling of glycals with aryl iodides.

1.5. Conclusion and summary

Chapter I provides an overview of the significance of carbohydrates, emphasizing their roles as natural products, biologically active molecules, and therapeutic agents in medicinal chemistry. The general discussion on glycosylation chemistry highlights that numerous factors influence the stereochemical course of glycosylation reactions.

Also, this chapter summarizes the synthetic applications of proton sponge, a well-known organic superbase. Although not a dominant reagent, it enables mild and selective transformations within organic synthesis. Beyond its practical utility, proton sponge has contributed substantially to the development of acid-base theory, hydrogen bonding interactions, general structural principles, and preparative methodologies. Nevertheless, despite its distinctive properties, the broader utilization of superbases remains relatively underexplored. Sterically hindered pyridine derivatives such as TTBPy, DTBMP, DTBP, and TTBP are well known as non-nucleophilic proton scavengers, with their utility in diverse organic transformations extensively documented. In 2019, Kancharla and coworkers first demonstrated using bulky TTBPy salts as organocatalysts for stereoselective glycosylation of glycals. Their broader applicability under varied reaction conditions was revealed by harnessing ion-pair frustration and the unique reactivity of these Brønsted salts.

The upcoming chapters of this thesis focus on: (i) first organocatalytic synthesis of 2-deoxy N-O-linked glycosides facilitated by strained pyridinium salts (ii) an

electrostatically tuned phenolic sulfonium salt-catalyzed stereoselective synthesis of *O*- and *S*-septanosides (iii) Pd-catalyzed stereo- and regioselective synthesis of biologically significant aryl *C*-glycosides using DMAN, and (iv) influence of sterics vs inductive vs through space stabilization effects on the basicity and reactivity of the pyridinium cation.

1.6. References

1. Wali, J. A.; Milner, A. J.; Luk, A. W. S.; Pulpitel, T. J.; Dodgson, T.; Facey, H. J. W.; Wahl, D.; Kebede, M. A.; Senior, A. M.; Sullivan, M. A.; Brandon, A. E.; Yau, B.; Lockwood, G. P.; Koay, Y. C.; Ribeiro, R.; Solon-Biet, S. M.; Bell-Anderson, K. S.; O'Sullivan, J. F.; Macia, L.; Forbes, J. M.; Cooney, G. J.; Cogger, V. C.; Holmes, A.; Raubenheimer, D.; Le Couteur, D. G.; Simpson, S. J., Impact of dietary carbohydrate type and protein–carbohydrate interaction on metabolic health. *Nat. Metab.* **2021,** *3* (6), 810-828.
2. Montreuil, J., Primary structure of glycoprotein glycans: basis for the molecular biology of glycoproteins. *Adv. Carbohydr. Chem. Biochem.* **1980,** *37*, 157-223.
3. Ritchie, G. E.; Moffatt, B. E.; Sim, R. B.; Morgan, B. P.; Dwek, R. A.; Rudd, P. M., Glycosylation and the Complement System. *Chem. Rev.* **2002,** *102* (2), 305-319.
4. Davis, B. G., Synthesis of Glycoproteins. *Chem. Rev.* **2002,** *102* (2), 579-601.
5. Qian, H.; Li, J.; Pan, X.; Sun, Z.; Ye, C.; Jin, G.; Fu, Z., Effects of streptomycin on growth of algae Chlorella vulgaris and Microcystis aeruginosa. *Environmental toxicology* **2012,** *27* (4), 229-237.
6. Kharel, M. K.; Rohr, J., Delineation of gilvocarcin, jadomycin, and landomycin pathways through combinatorial biosynthetic enzymology. *Curr. Opin. Chem. Biol.* **2012,** *16* (1), 150-161.
7. Ernst, B.; Magnani, J. L., From carbohydrate leads to glycomimetic drugs. *Nat. Rev. Drug Discov.* **2009,** *8* (8), 661-677.
8. Dreitlein, W. B.; Maratos, J.; Brocavich, J., Zanamivir and oseltamivir: two new options for the treatment and prevention of influenza. *Clin. Ther.* **2001,** *23* (3), 327-355.
9. Maryanoff, B. E.; Nortey, S. O.; Gardocki, J. F.; Shank, R. P.; Dodgson, S. P., Anticonvulsant O-alkyl sulfamates. 2,3:4,5-Bis-O-(1-methylethylidene)-.beta.-D-fructopyranose sulfamate and related compounds. *J. Med. Chem.* **1987,** *30* (5), 880-887.
10. Flitsch, S. L., Introduction: Glycosciences. *Chem. Rev.* **2022,** *122* (20), 15501-15502.
11. Nigudkar, S. S.; Demchenko, A. V., Stereocontrolled 1,2-cis glycosylation as the driving force of progress in synthetic carbohydrate chemistry. *Chem. Sci.* **2015,** *6* (5), 2687-2704.
12. Reddy, D.; Kumavath, R.; Barh, D.; Azevedo, V.; Ghosh, P., Anticancer and Antiviral Properties of Cardiac Glycosides: A Review to Explore the Mechanism of Actions. *Molecules* **2020,** *25* (16), 3596.
13. Mohan, V.; Mithal, A.; Joshi, S. R.; Aravind, S. R.; Chowdhury, S., Remogliflozin Etabonate in the Treatment of Type 2 Diabetes: Design, Development, and Place in Therapy. *Drug Des. Dev. Ther.* **2020,** *14*, 2487-2501.
14. Nielsen, M. M.; Holmstrøm, T.; Pedersen, C. M., Stereoselective O-Glycosylations by Pyrylium Salt Organocatalysis. *Angew. Chem. Int. Ed.* **2022,** *61* (6), e202115394.
15. Das, R.; Mukhopadhyay, B., Chemical O-Glycosylations: An Overview. *ChemistryOpen* **2016,** *5* (5), 401-433.
16. De, S.; Kumar S K, A.; Shah, S. K.; Kazi, S.; Sarkar, N.; Banerjee, S.; Dey, S., Pyridine: the scaffolds with significant clinical diversity. *RSC Adv.* **2022,** *12* (24), 15385-15406.
17. Ling, Y.; Hao, Z. Y.; Liang, D.; Zhang, C. L.; Liu, Y. F.; Wang, Y., The Expanding Role of Pyridine and Dihydropyridine Scaffolds in Drug Design. *Drug Des. Dev. Ther.* **2021,** *15*, 4289-4338.
18. Alrooqi, M.; Khan, S.; Alhumaydhi, F. A.; Asiri, S. A.; Alshamrani, M.; Mashraqi, M. M.; Alzamami, A.; Alshahrani, A. M.; Aldahish, A. A., A Therapeutic Journey of Pyridine-based Heterocyclic

Compounds as Potent Anticancer Agents: A Review (From 2017 to 2021). *Anticancer Agents Med. Chem.* **2022,** *22* (15), 2775-2787.
19. Heravi, M. M.; Zadsirjan, V., Prescribed drugs containing nitrogen heterocycles: an overview. *RSC Adv.* **2020,** *10* (72), 44247-44311.
20. Crich, D.; Dudkin, V., An unusual example of steric buttressing in glycosylation. *Tetrahedron Lett.* **2000,** *41* (30), 5643-5646.
21. Xu, X.-H.; Liu, G.-K.; Azuma, A.; Tokunaga, E.; Shibata, N., Synthesis of Indole and Biindolyl Triflones: Trifluoromethanesulfonylation of Indoles with Tf2O/TTBP (2,4,6-tri-tert-butylpyridine) System. *Org. Lett.* **2011,** *13* (18), 4854-4857.
22. Dimroth, K.; Mach, W., Preparation of 2,4,6-Tri-tert-butylpyrylium Tetrafluoroborate, 2,4,6-Tri-tert-butylpyridine, and 2,4,6-Tri-tert-butylphosphorin. *Angew. Chem. Int. Ed. Engl.* **1968,** *7* (6), 460-461.
23. Brown, H. C.; Kanner, B., Preparation and Reactions of 2,6-Di-t-butylpyridine and Related Hindered Bases. A Case of Steric Hindrance toward the Proton1,2. *J. Am. Chem. Soc.* **1966,** *88* (5), 986-992.
24. Ghosh, T.; Mukherji, A.; Kancharla, P. K., Sterically Hindered 2,4,6-Tri-tert-butylpyridinium Salts as Single Hydrogen Bond Donors for Highly Stereoselective Glycosylation Reactions of Glycals. *Org. Lett.* **2019,** *21* (10), 3490-3495.
25. Deutsch, E.; Cheung, N. K. V., Noncoordinating buffers. I. Synthesis and characterization of water soluble derivatives of 2,6-di-tert-butylpyridine. *J. Org. Chem.* **1973,** *38* (6), 1123-1126.
26. Effenberger, F.; Eberhard, J. K.; Maier, A. H., The First Unequivocal Evidence of the Reacting Electrophile in Aromatic Acylation Reactions1. *J. Am. Chem. Soc.* **1996,** *118* (50), 12572-12579.
27. Clark, E. R.; Ingleson, M. J., [(acridine)BCl2]+: A Borenium Cation That Is a Strong Boron- and Carbon-Based Lewis Acid. *Organometallics* **2013,** *32* (22), 6712-6717.
28. Garcia, B. A.; Gin, D. Y., Synthesis of Glycosyl-1-phosphates via Dehydrative Glycosylation. *Org. Lett.* **2000,** *2* (14), 2135-2138.
29. Paenurk, E.; Kaupmees, K.; Himmel, D.; Kütt, A.; Kaljurand, I.; Koppel, I. A.; Krossing, I.; Leito, I., A unified view to Brønsted acidity scales: do we need solvated protons? *Chem. Sci.* **2017,** *8* (10), 6964-6973.
30. Mukherji, A.; Kancharla, P. K., C–H···Anion Interactions Assisted Addition of Water to Glycals by Sterically Hindered 2,4,6-Tri-tert-butylpyridinium Hydrochloride. *Org. Lett.* **2020,** *22* (6), 2191-2195.
31. Addanki, R. B.; Halder, S.; Kancharla, P. K., TfO–···H–O–H Interaction-Assisted Generation of a Silicon Cation from Allylsilanes: Access to Phenylallyl Ferrier Glycosides from Glycals. *Org. Lett.* **2022,** *24* (7), 1465-1470.
32. Rotta, M. K. V.; Addanki, R. B.; Kancharla, P. K., Sterically Hindered and Electron-Deficient 2,4,6-Tri-tert-butylpyrimidinium as a π-Lewis Acid Toward Organocatalytic Silyl Protection of Carbohydrates Using Trialkyl/aryl Silanes. *Org. Lett.* **2025,** *27* (24), 6409-6414.
33. Balmond, E. I.; Coe, D. M.; Galan, M. C.; McGarrigle, E. M., α-Selective organocatalytic synthesis of 2-deoxygalactosides. *Angew. Chem. Int. Ed. Engl.* **2012,** *51* (36), 9152-5.
34. Yu, F.; Li, J.; DeMent, P. M.; Tu, Y. J.; Schlegel, H. B.; Nguyen, H. M., Phenanthroline-Catalyzed Stereoretentive Glycosylations. *Angew. Chem. Int. Ed. Engl.* **2019,** *58* (21), 6957-6961.
35. Geng, Y.; Kumar, A.; Faidallah, H. M.; Albar, H. A.; Mhkalid, I. A.; Schmidt, R. R., Cooperative Catalysis in Glycosidation Reactions with O-Glycosyl Trichloroacetimidates as Glycosyl Donors. *Angew. Chem. Int. Ed.* **2013,** *52* (38), 10089-10092.
36. Cox, D. J.; Smith, M. D.; Fairbanks, A. J., Glycosylation Catalyzed by a Chiral Brønsted Acid. *Org. Lett.* **2010,** *12* (7), 1452-1455.
37. Kimura, T.; Sekine, M.; Takahashi, D.; Toshima, K., Chiral Brønsted Acid Mediated Glycosylation with Recognition of Alcohol Chirality. *Angew. Chem. Int. Ed.* **2013,** *52* (46), 12131-12134.
38. Park, Y.; Harper, K. C.; Kuhl, N.; Kwan, E. E.; Liu, R. Y.; Jacobsen, E. N., Macrocyclic bis-thioureas catalyze stereospecific glycosylation reactions. *Science* **2017,** *355* (6321), 162-166.

39. Desai, S. P.; Yatzoglou, G.; Turner, J. A.; Taylor, M. S., Boronic Acid-Catalyzed Regio- and Stereoselective N-Glycosylations of Purines and Other Azole Heterocycles: Access to Nucleoside Analogues. *J. Am. Chem. Soc.* **2024,** *146* (7), 4973-4984.
40. Hine, J.; Linden, S. M.; Kanagasabapathy, V. M., 1,8-biphenylenediol is a double-hydrogen-bonding catalyst for reaction of an epoxide with a nucleophile. *J. Am. Chem. Soc.* **1985,** *107* (4), 1082-1083.
41. Beddoe, R. H.; Andrews, K. G.; Magné, V.; Cuthbertson, J. D.; Saska, J.; Shannon-Little, A. L.; Shanahan, S. E.; Sneddon, H. F.; Denton, R. M., Redox-neutral organocatalytic Mitsunobu reactions. *Science* **2019,** *365* (6456), 910-914.
42. Biswas, A.; Pradhan, P.; Wakpanjar, S. A.; Kancharla, P. K., Direct organocatalytic esterification of carboxylic acids and alcohols by redox neutral sulfur(iv) catalysis via intramolecularly interrupted Pummerrer intermediates. *Chem. Commun.* **2025,** *61* (31), 5746-5749.
43. Patel, B.; Dabas, S.; Patel, P.; Subramanian, S., Electrostatically tuned phenols: a scalable organocatalyst for transfer hydrogenation and tandem reductive alkylation of N-heteroarenes. *Chem. Sci.* **2023,** *14* (3), 540-549.
44. Wassermann, A., 126. The mechanism of additions to double bonds. Part XIV. The nature of the activated complex in bimolecular diene syntheses. *J. Chem. Soc.* **1942,** (0), 612-617.
45. Kelly, T. R.; Meghani, P.; Ekkundi, V. S., Diels-alder reactions: Rate acceleration promoted by a biphenylenediol. *Tetrahedron Lett.* **1990,** *31* (24), 3381-3384.
46. Whiteoak, C. J.; Nova, A.; Maseras, F.; Kleij, A. W., Merging Sustainability with Organocatalysis in the Formation of Organic Carbonates by Using CO2 as a Feedstock. *ChemSusChem* **2012,** *5* (10), 2032-2038.
47. Brzezinski, B.; Głowiak, T.; Grech, E.; Malarski, Z.; Sobczyk, L., 1,8-Bis(dimethylaminomethyl)naphthaiene: a new proton sponge. *J. Chem. Soc. Perkin Trans. 2* **1991,** (10), 1643-1647.
48. Llamas-Saiz, A. L.; Foces-Foces, C.; Elguero, J., Proton sponges. *J. Mol. Struct.* **1994,** *328*, 297-323.
49. Pozharskii, A. F.; Ozeryanskii, V. A., Proton Sponges and Hydrogen Transfer Phenomena. *Mendeleev Commun.* **2012,** *22* (3), 117-124.
50. Alder, R. W.; Bowman, P. S.; Steele, W. R. S.; Winterman, D. R., The remarkable basicity of 1,8-bis(dimethylamino)naphthalene. *Chem. Commun.* **1968,** (13), 723-724.
51. Wüstefeld, H.-U.; Kaska, W. C.; Schüth, F.; Stucky, G. D.; Bu, X.; Krebs, B., Transition Metal Complexes with the Proton Sponge 4,9-Dichloroquino[7,8-h]quinoline: Highly Twisted Aromatic Systems and an Extreme "Out-of-Plane" Position of the Coordinated Transition Metal Atom. *Angew. Chem. Int. Ed.* **2001,** *40* (17), 3182-3184.
52. Yamasaki, T.; Ozaki, N.; Saika, Y.; Ohta, K.; Goboh, K.; Nakamura, F.; Hashimoto, M.; Okeya, S., First Transition Metal Complex of 1,8-Bis(dimethylamino)naphthalene (proton sponge). *Chem. Lett.* **2004,** *33* (7), 928-929.
53. Gamage, S. N.; Morris, R. H.; Rettig, S. J.; Thackray, D. C.; Thorburn, I. S.; James, B. R., Formation of a trimethyldihydroperimidinium cation from proton sponge [1,8-bis(dimethylamino)naphthalene] during base-promoted reactions of rhodium and ruthenium complexes. *J. Chem. Soc., Chem. Commun.* **1987,** (12), 894-895.
54. Pozharskii, A. F.; Ozeryanskii, V. A., Proton Sponges. In *The Chemistry of Anilines*, 2007; pp 931-1026.
55. Alper, H.; Wolin, M. S., Azole chemistry. X. Silaazoles. *J. Org. Chem.* **1975,** *40* (4), 437-438.
56. Huisgen, R.; Mitra, A.; Moran, J. R., 1,3-Dipolare Cycloadditionen, 93 Überraschungen bei der Umsetzung des 2,3-Dicyanfumarsäure-dimethylesters mit Diazomethan. *Chem. Ber.* **1987,** *120* (2), 159-169.
57. Diem, M. J.; Burow, D. F.; Fry, J. L., Oxonium salt alkylation of structurally and optically labile alcohols. *J. Org. Chem.* **1977,** *42* (10), 1801-1802.

58. Yasuhara, T.; Nagaoka, Y.; Tomioka, K., An activated phosphate for an efficient amide and peptide coupling reagent. *J. Chem. Soc., Perkin Trans. 1* **2000,** (17), 2901-2902.
59. Ozawa, F.; Kubo, A.; Hayashi, T., Palladium-catalyzed asymmetric arylation of 2,3-dihydrofuran: 1,8-Bis(dimethylamino)naphthalene as an efficient base. *Tetrahedron Lett.* **1992,** *33* (11), 1485-1488.
60. Ozawa, F.; Kobatake, Y.; Hayashi, T., Palladium-catalyzed asymmetric alkenylation of cyclic olefins. *Tetrahedron Lett.* **1993,** *34* (15), 2505-2508.
61. Arranz, E.; Boons, G.-J., The 2-(allyloxy) phenyl acetyl ester as a new relay protecting group for oligosaccharide synthesis. *Tetrahedron Lett.* **2001,** *42* (37), 6469-6471.
62. Swor, C. D.; Zakharov, L. N.; Tyler, D. R., A Colorimetric Proton Sponge. *J. Org. Chem.* **2010,** *75* (20), 6977-6979.

Chapter 2

Strained Ion-Pair Interactions Driven Anion Assisted Concerted Addition of Ketoximes/Aldoximes and Hydroxamic Acids to Glycals

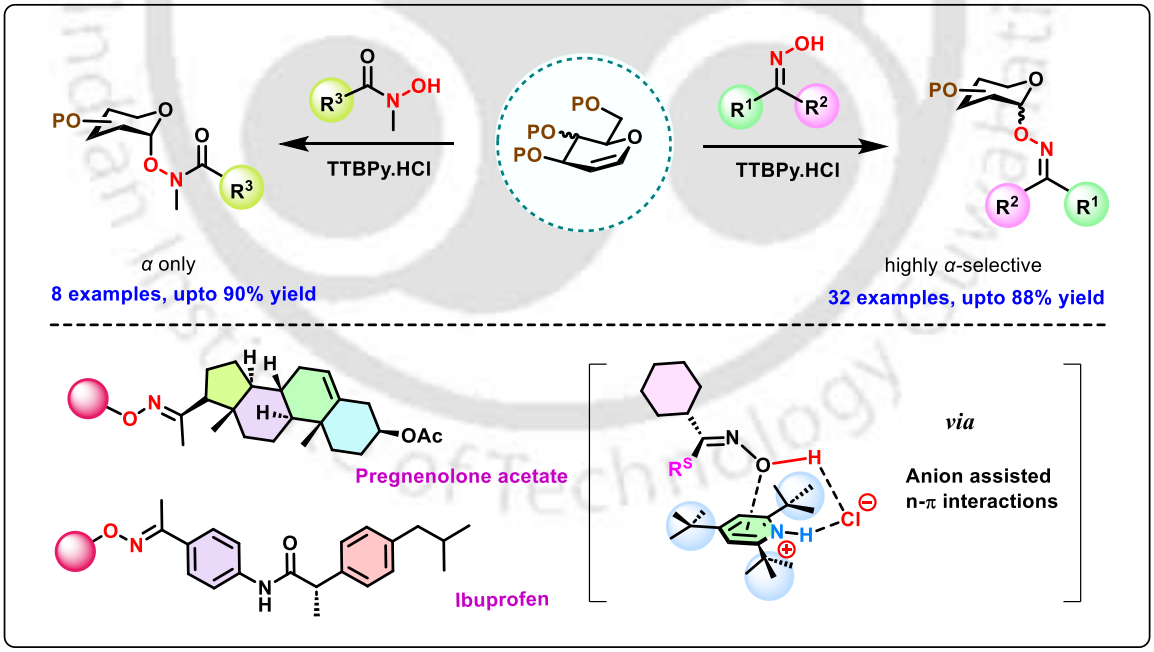

(*Org. Lett.* **2024**, *26*, 10382−10387)

2.1. Introduction

2.1.1. Importance of N-O-linked glycosides

N-O-linked glycosides are known for exhibiting a broad spectrum of bioactivities, including anticancer, antimicrobial, and antitumor properties, and hold promise for therapeutic applications in cardiovascular disorders.[1] Their superior enzymatic stability makes them notable structural analogs of natural glycosides, drawing the research community's attention.[2] In recent years, aminooxylated carbohydrates have become key components for these purposes.[1] Notably, antitumor antibiotics like esperamicins A and calicheamicins contain N-O-linked oligosaccharides.[3, 4] These unique linkages are crucial in determining molecular conformation, essential for sequence-selective DNA binding (Figure 2.1).[5] Additionally, glycosidic linkages involving N-O bonds have been identified as metabolically stable analogues of conventional *O*-glycosidic bonds, enabling the design and synthesis of various multivalent constructs, such as glycoclusters and glycodendrimers.[6-8] For example, the inclusion of aminooxy glycosides has increased the significance of drosocin, leading to renewed efforts in synthetic methods (Figure 2.1).[9]

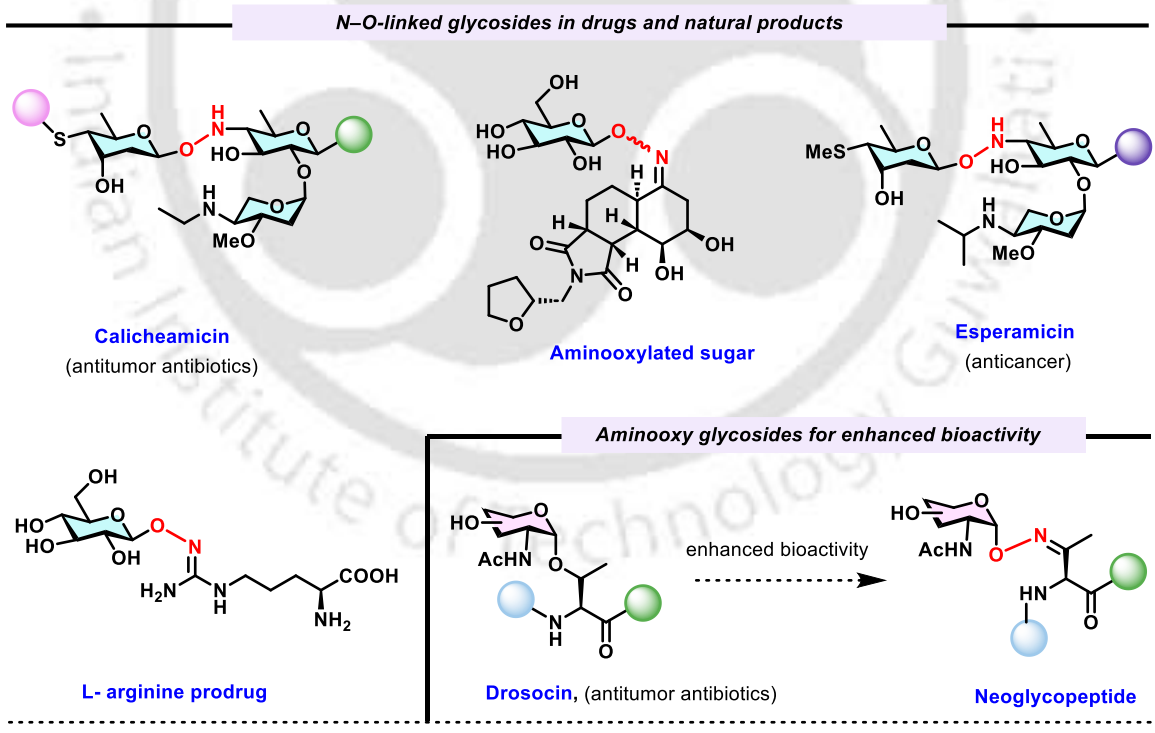

Figure 2.1. Biologically active N-O-linked glycosides.

Moreover, the straightforward synthesis and inherent stability of oximes have contributed to the widespread use of the aminooxy functional group as a versatile linker for conjugating diverse biomolecules (Scheme 2.1).[10] Owing to the exceptional

nucleophilicity of hydroxylamides and oximes and the distinctive conformational features of N-oxyamide and N-O linkages, this molecular combination has proven to be a valuable and versatile tool across a broad spectrum of applications.[2, 11]

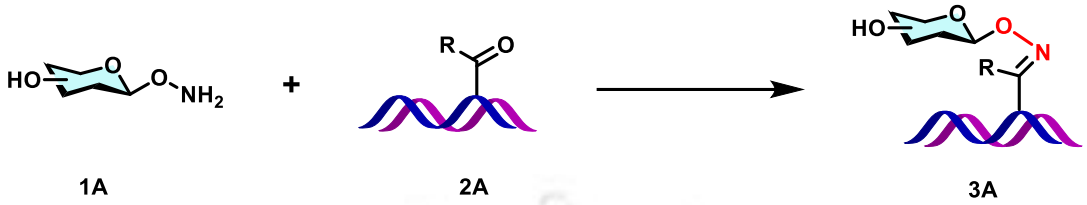

Scheme 2.1. Aminooxy glycosides for ligation.

2.1.2. Existing methods for synthesizing N-O-linked glycosides

Several methods have been reported to synthesize N-O-linked glycosides. These approaches include (1) condensation of sugar ketones with glycosyloxyamines[12] (2) S_N2 displacement on sugar trifluoromethanesulfonates[13] (3) glycosylation of glycosyl trichloroimidates or bromides with sugar nitrones (Scheme 2.2).[14]

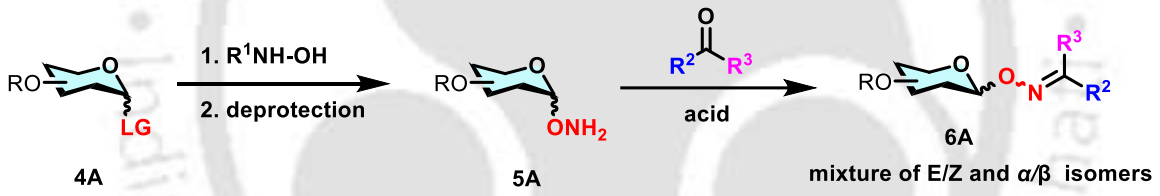

Scheme 2.2. Indirect synthetic route to oximoglycosides.

Direct glycosylation of oximes offers a more straightforward approach to bond formation; however, it remains challenging due to oximes' vulnerability to strong Lewis acids usually employed in traditional glycosylation methods (Scheme 2.3).[15] Additionally, oximes' remarkable capacity to coordinate with metals, making them effective directing groups in C-H activation, can occasionally result in unexpected reaction pathways (Scheme 2.3).[16]

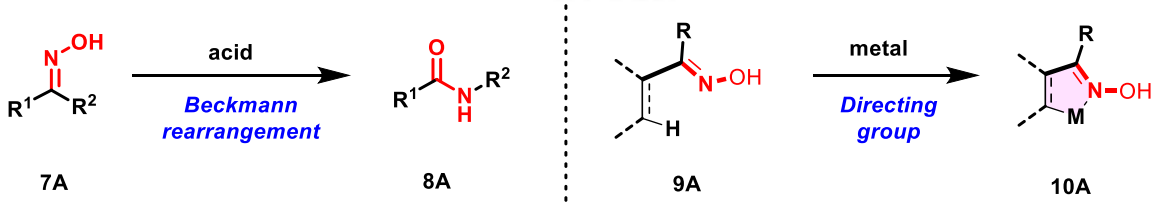

Scheme 2.3. Challenges in direct glycosylation with oximes.

Until now, only a handful of methods have been invented for synthesizing N-O-linked glycosides. In 2012, Yu and co-workers disclosed a pioneering direct glycosylation

strategy involving glycosyl ortho-hexynylbenzoate donors and sugar oximes, facilitated by the mild PPh_3AuOTf catalyst (Scheme 2.4).[17]

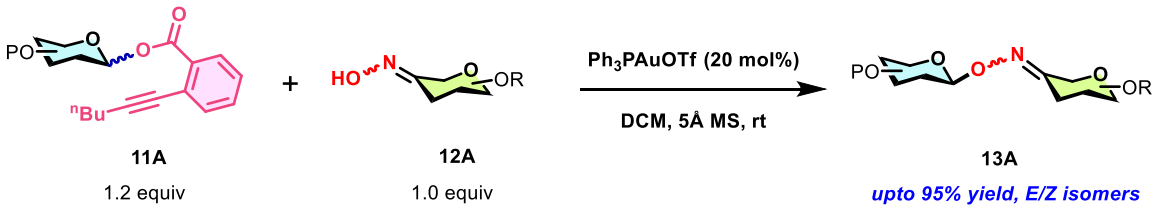

Scheme 2.4. Gold (Au)-catalyzed direct glycosylation.

In 2023, Dai and colleagues presented a palladium-catalyzed method for stereospecific glycosylation using 3,4-*O*-carbonate glycal donors and oximes, forming N-O-linked Ferrier glycosides (Scheme 2.5). This versatile approach enables scalable synthesis, broad substrate applicability, excellent functional group tolerance, and late-stage glycoside diversification of bioactive compounds.[18]

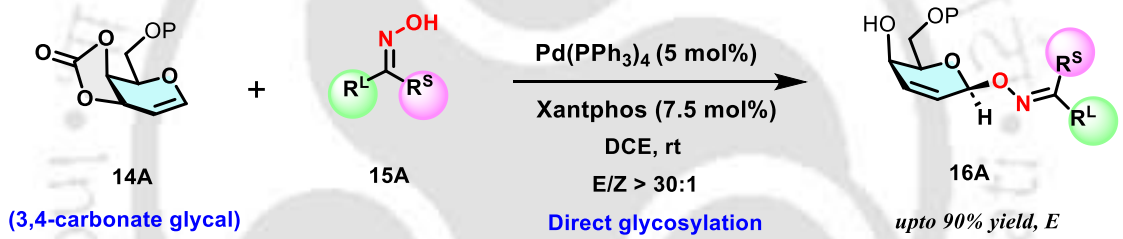

Scheme 2.5. Palladium (Pd)-catalyzed direct glycosylation.

In 2025, the same group introduced a Pd-catalyzed stereodivergent glycosylation strategy for coupling N-O nucleophiles with pyranone donors, employing $Pd_2(dba)_3{\cdot}CHCl_3$ (0.5 mol%) and DPPF (0.75 mol%) in DCM. This method enables the efficient synthesis of diverse glycosides bearing N-O linkages with high stereo-, regio-, and chemoselectivity, selectively favouring N-O nucleophiles over competing hydroxyl groups (Scheme 2.6).[19]

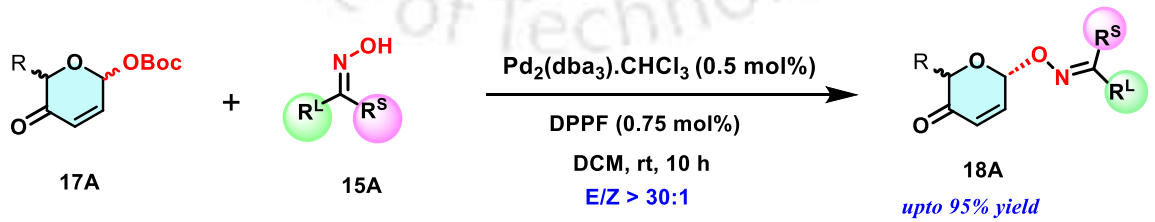

Scheme 2.6. Pd-catalyzed stereodivergent glycosylation.

In 2025, the Xu group introduced a mild and practical method for oxime *O*-glycosylation using unprotected glycosyl fluoride donors with alkyl/aryl oximes and modified steroid/sugar oximes in basic aqueous media. This strategy enabled efficient synthesis of

structurally diverse N-O-linked glycosides and oligosaccharides with high 1,2-trans-selectivity. The approach features broad substrate compatibility, gram-scale applicability, and straightforward glycoside diversification, facilitating scalable production for biomedical research (Scheme 2.7).[20]

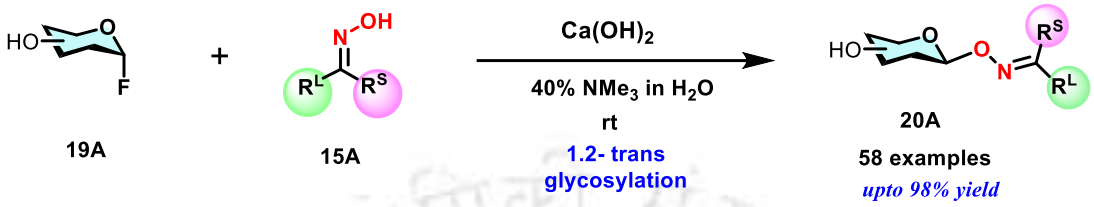

Scheme 2.7. Pd-catalyzed direct late-stage oxime glycosylation.

2.1.3. Knowledge gap

Most previously discussed methods for synthesizing 2-deoxy N-O-linked glycosides have relied on noble metal catalysts, with no organocatalytic glycosylation strategy currently available for this transformation. Therefore, developing an efficient synthetic platform for these medically significant glycosides is crucial, ensuring precise anomeric configurations and excellent control over Z/E geometry. In recent years, organocatalyzed glycosylations have emerged as powerful and versatile approaches for constructing diverse glycosides and glycoconjugates, owing to their operational simplicity and stereochemical fidelity. We propose that the mild activation imparted by organocatalysts offers a promising strategy for the direct coupling of oximes to synthesize aminooxy glycosides.

2.1.4. Purpose and objectives of the chapter

In Chapter 1, we have discussed the properties of sterically hindered pyridine derivatives such as TTBPy, DTBMP, DTBP, and TTBP, which are well known as non-nucleophilic proton scavengers and have demonstrated utility in diverse organic transformations driven by sterically strained ion-pair interactions.[21, 22]

In this chapter, we present the ability of these unique poor electrostatic/strained interactions in pyridinium chloride salt to achieve the glycosylation of aldoximes, ketoximes, and hydroxamic acids to access a biologically significant class of N-O-linked glycosides with high diastereoselectivity. The unique reactivity of the sterically bulky pyridinium salt has been studied by ^{1}H-NMR, IR, UV, and fluorescence spectroscopic studies. We demonstrate that the pyridinium salt activates the oxime via a unique anion-assisted lone-pair-π interaction between the oxime and pyridinium cation. The resulting intermediate undergoes a concerted addition to the glycal, forming the observed products with excellent selectivity. The concerted nature of the addition has been confirmed through a deuterium-labeling experiment, which provides conclusive evidence supporting

the proposed mechanism. The method exhibits a vast substrate scope and enables the construction of diverse N-O-linked glycosides in excellent yields and with high selectivity.

2.2. Results and discussion

2.2.1. Optimization study

We started our research by investigating the reaction between donor D-glucal (**1a**) and acceptor (E)-1-phenylethan-1-one oxime (**1aa**), utilizing different catalysts, solvents, and temperatures (Table 2.1). Initially, we attempted the reaction between **1a** and **1aa** using 20 mol% TTBPy.HCl salt (**3a**) in DCE at rt; however, no reaction was observed (Table 2.1, entry 1). Gratifyingly, elevating the temperature to 60 °C led to the formation of oxime glycoside **21** in 85% yield with 6:1 α/β selectivity within 5 hours (Table 2.1, entry 2). The stereochemistry (anomeric and E/Z ratio) of oxime glycoside **21** was elucidated through comprehensive 2D NMR analysis (^{1}H NMR, NOE experiments, and coupling constants) (see experimental section for details). When the catalyst **3a** was reduced to 5 mol% and 10 mol%, the yield of compound **21** decreased to 52% and 65%, respectively (Table 2.1, entries 3 and 4). Lowering the temperature to 40 °C also resulted in a further yield reduction to 72% (Table 2.1, entry 5). Building on prior insights into the role of counterions in glycosylation,[23] we explored the reactivity of a sterically demanding pyridinium-based catalyst by employing various TTBPy salts bearing chloride, triflate (OTf), and BArF counterions. Interestingly, using the catalysts **3b** and **3c**, which include weakly coordinating[24] OTf and BArF ions in DCE at 60 °C, led to the formation of Ferrier-type N-O-linked glucoside **21ab**. The reaction afforded a 75% yield after 5 hours and 24% after 24 hours, with an α/β selectivity ratio of 2:1 (Table 2.1, entries 6 and 7). The alteration in anion underscores the significant role of cation-anion interactions in modulating glycosylation reactivity and selectivity. Catalyst **3d**, the chloride salt of DTBP (2,6-di-*tert*-butylpyridine), promoted the reaction with moderately lower yield and selectivity (Table 2.1, entry 8). Interestingly, the less hindered 2,6-lutidine hydrochloride salt (**3e**) fails to catalyze the glycosylation reaction (Table 2.1, entry 9). This experiment highlights the unique role of sterically bulky pyridinium salts in the current organocatalytic process. Furthermore, various solvents were screened to assess their compatibility with catalyst **3a** (Table 2.1, entries 10-14). Compound **21** was obtained in moderate yields ranging from 45% to 63% when toluene, acetonitrile (ACN), and chloroform ($CHCl_3$) were used as solvents. In contrast, no product formation was observed in 1,4-dioxane or dimethylformamide (DMF). Additionally, the use of the conventional Lewis acid $BF_3{\cdot}OEt_2$ resulted in a modest 52%yield of the Ferrier product **21ab** (Table 2.1, entry 15), while no product formation was observed with the hydrogen-bonding catalyst **3f** (Table 2.1, entry 16). However, extending the reaction time to 24 hours under these conditions resulted in no change in yield or stereoselectivity, indicating

Table 2.1. Optimization of the reaction conditions[a]

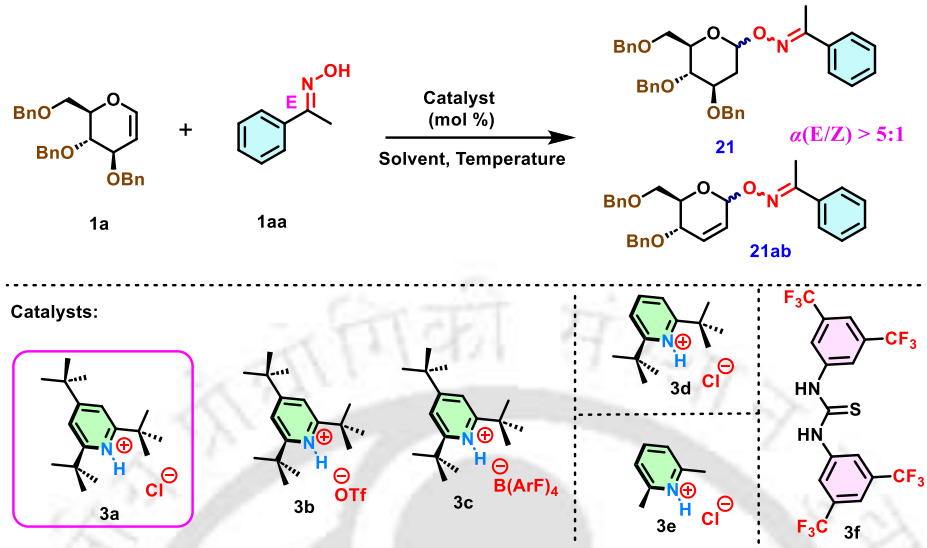

Entry	Catalyst	Solvent	Temp (°C)	Time	(21) (%)[b] (α/β)[c]	(21ab) (%)[b] (α/β)[c]
1	**3a**	DCE	rt	24 h	---	---
2	**3a**	DCE	60	5 h	85 (6:1)	---
3[d]	**3a**	DCE	60	24 h	52 (3:1)	---
4[e]	**3a**	DCE	60	24 h	65 (4:1)	---
5	**3a**	DCE	40	24 h	72 (4:1)	---
6	**3b**	DCE	60	5 h	---	75 (2:1)
7	**3c**	DCE	60	24h	---	24 (2:1)
8	**3d**	DCE	60	12h	72 (2:1)	----
9	**3e**	DCE	60	24h	---	----
10	**3a**	Toluene	60	24 h	45 (4:1)	---
11	**3a**	1,4-dioxane	60	24 h	----	----
12	**3a**	ACN	60	24 h	45 (3:1)	41 (1:1)
13	**3a**	DMF	60	24 h	----	----
14	**3a**	$CHCl_3$	60	24 h	63 (3:1)	22 (2:1)
15[f]	$BF_3.Et_2O$	DCM	RT	10 h	---	52 (2:1)
16[g]	**3f**	DCE	60	24 h	---	---
17	**3a**	DCE	60	24 h	84 (6:1)	---

[a]Reaction conditions: **1a** and **1aa** (0.17 mmol), **3a-3e** (20 mol%), solvent (1 mL). [b]Isolated yield. [c]determined from crude ^{1}H NMR. [d]5 mol%, [e]10 mol%, [f]15 mol%, [g]6 mol% catalysts were used.

that the reaction is kinetically rather than thermodynamically controlled (Table 2.1, entry 17). Consequently, the optimal condition was 20 mol% of chloride salt **3a** in dry DCE at 60 °C.

2.2.2. Substrate scope

A wide range of alkyl and aryl oximes served as suitable substrates, affording the desired 2-deoxy N-O-linked galactosides with exclusive α-selectivity and complete retention of E/Z geometry. Both electron-donating (Me, Et, OMe, SMe) and electron-withdrawing (F, Cl) substituents on the phenyl moiety reacted efficiently under the optimized conditions, affording the corresponding N-O-linked galactosides (Table 2.2, entries **1**-**6**, **8**-**9**) with excellent yields (78-89%). Notably, the biphenyl acetone-derived oxime (Table 2.2, **7**) also demonstrated excellent compatibility with the current protocol, providing the product with an impressive 86% yield as an exclusively α-isomer. Symmetric oximes (Table 2.2, **10**, **15**, and **17**), bicyclic ring-fused oximes (Table 2.2, **16**, **18**, and **19**) and aromatic ketoximes bearing ethyl, cyclopropyl, and isopropyl groups (Table 2.2, **11**-**14**) were well tolerated, producing the target products in excellent yields (80-88%) with exclusive α-selectivity and complete retention of E/Z configuration. Aromatic heterocycles, such as thiophene-derived oximes, also furnished the desired galactoside with good yield and exclusive α-selectivity (Table 2.2, **20**). Selected ketoximes were also evaluated with glucal donor, furnishing the corresponding glucosides with good to excellent yields and selectivities (Table 2.2, **21**-**26**). However, the selectivities observed with glucal are slightly lower compared to galactal. This disparity is likely due to a more favorable α-face preference in the transition-state conformations ($^4H_5$ or $^5H_4$) of galactal, attributed to the stereochemistry at the O4 position, which facilitates enhanced selectivity. Additionally, various substituted aromatic aldoximes (Ph, Me, NO_2, and Cl) were successfully coupled, affording N-O-linked 2-deoxy galactosides (Table 2.2, **27**-**30**) in excellent yields (82-85%) with high selectivity. To further establish the robustness of the methodology, oximes derived from biologically relevant compounds were employed as coupling partners. The reaction with pregnenolone acetate, a synthetic pregnane steroid, delivered N-O-linked 2-deoxy galactoside **31** as a single α-isomer with 82% yield (Table 2.2). Similarly, coupling with ibuprofen, a widely used anti-inflammatory drug, furnished galactoside **32** in 81% yield (Table 2.2). As expected, sugar-derived oxime **29aa** efficiently furnished the corresponding disaccharide **33** with 85% yield (Table 2.2). The protocol's applicability was further demonstrated using glucal substrates bearing armed or disarmed protecting groups, including *p*-methylbenzyl (PMB), methyl (Me), ethyl, and galactal derivatives containing TBS and OMe protecting groups. All substrates underwent successful transformation, delivering the corresponding glycosides (Table 2.3, **34**-**38**) in good yields and selectivity, favoring the α-anomer.

Table 2.2. Substrate scope of 2-Deoxy N-O-linked glycosides[a]

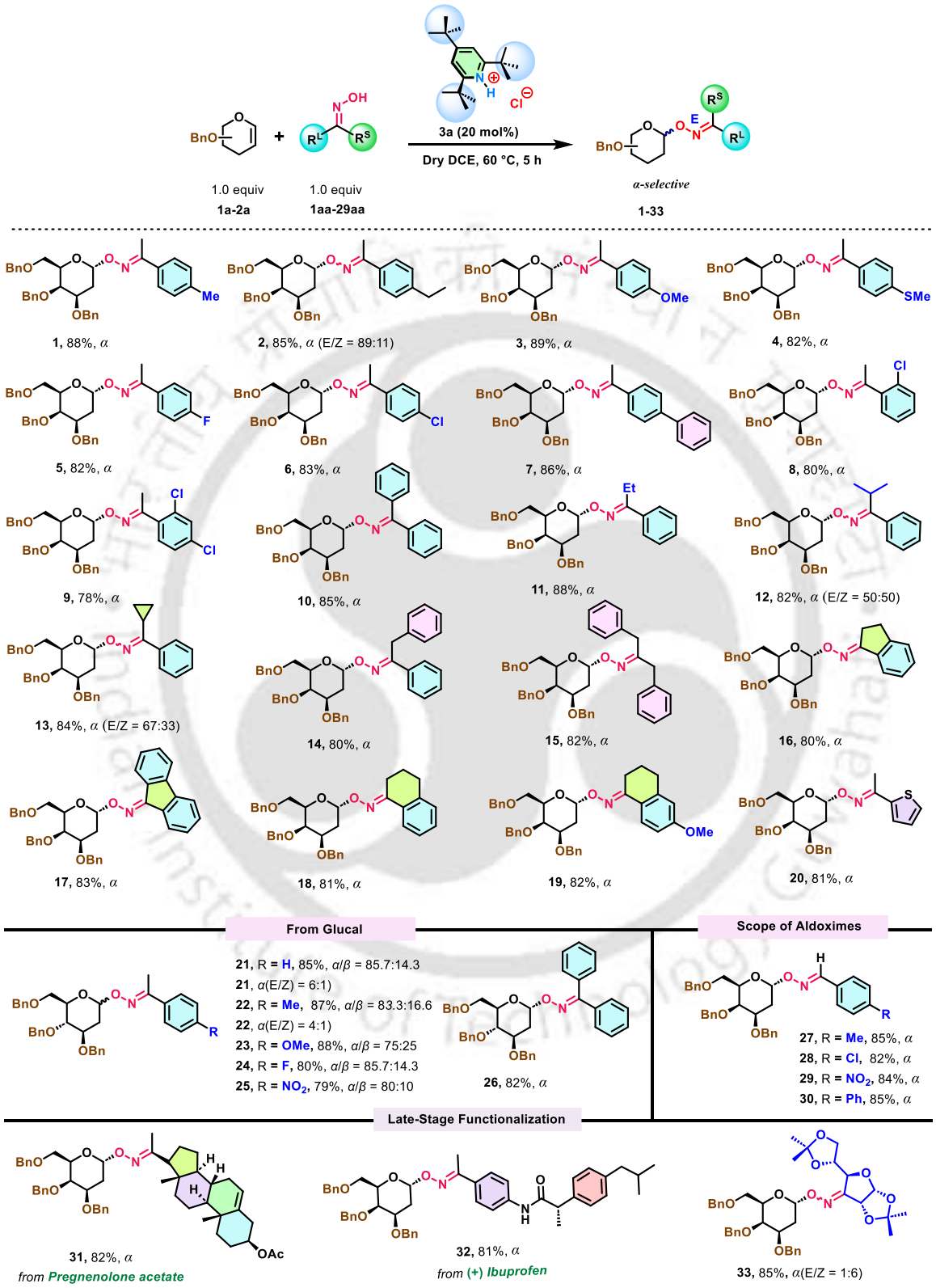

[a]Reaction conditions: **1a-7a** (0.17 mmol, 1.0 equiv), **1aa-29aa** (0.17 mmol, 1.0 equiv), **3a** (20 mol %), Dry DCE (1.0 mL), 60 °C, 5 h. Isolated yield. *α*/*β* and E/Z ratios were determined using ^{1}H NMR analysis.

Table 2.3. Variation in protecting groups[a]

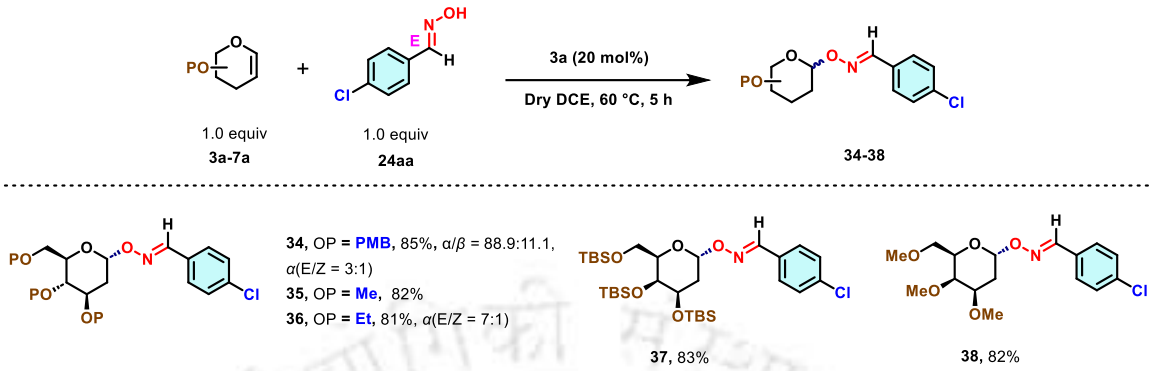

[a]Reaction conditions: **3a**-**7a** (0.17 mmol, 1.0 equiv), **24aa** (0.17 mmol, 1.0 equiv), **3a** (20 mol %), Dry DCE (1.0 mL), 60 °C, 5 h. Isolated yield. α/β ratios were determined using ^{1}H NMR analysis. PMB = *p*-methylbenzyl.

Table 2.4. Scope of glycosyloxyamines[a]

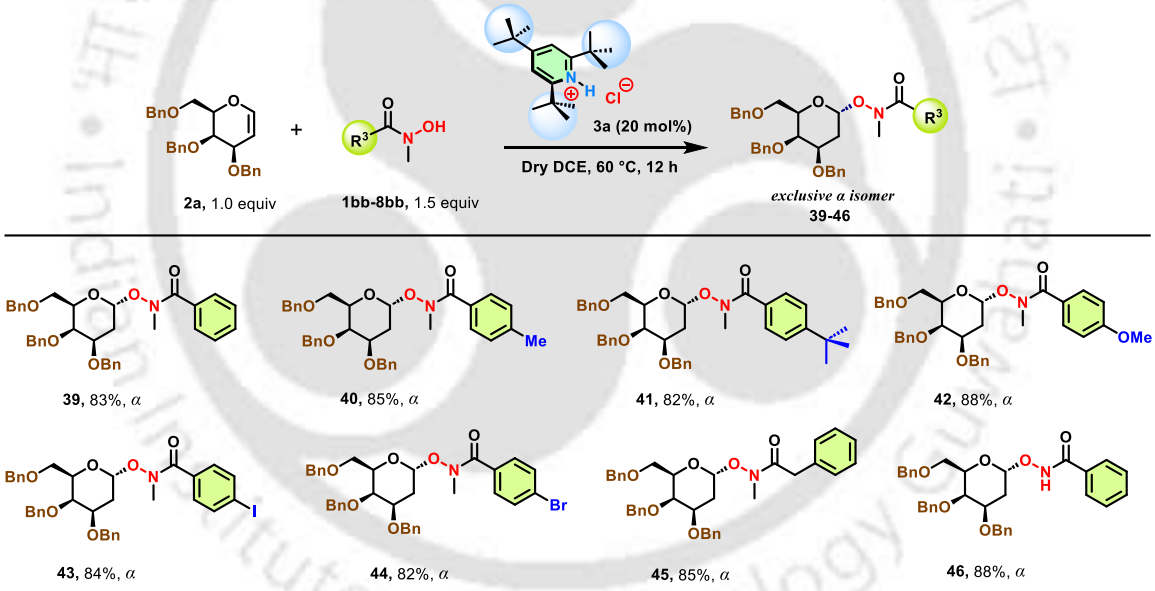

[a]Reaction conditions: **2a** (0.17 mmol, 1.0 equiv), **1bb-8bb** (0.26 mmol, 1.5 equiv), **3a** (20 mol %), Dry DCE (1.0 mL), 60 °C, 12 h. Isolated yield.

Moreover, glycosyloxyamines have successfully attached glycans to proteins or lipids containing a ketone or aldehyde moiety under bioorthogonal conditions.[8, 10] Aminooxy glycosides are generally synthesized from N-hydroxy-succinimide,[25] N-pentenoyl hydroxamate,[8] and HONPhth,[26] then deprotection of the N-protecting groups. After successfully coupling diverse oxime acceptors, the investigation was extended to hydroxamic acids as nucleophiles (Table 2.4). A range of substituted aromatic hydroxamic acids, with electron-donating groups like methyl, *tert*-butyl, and methoxy (**39-42**), as well as electron-withdrawing halogens (I, Br; **43-44**) at the para-position, reacted efficiently, yielding the corresponding galactosides in excellent yields (82-88%)

with α-stereoselectivity (Table 2.4). An aliphatic hydroxamic acid, **7bb**, similarly provided the desired α-galactoside **45** with 85% yield (Table 2.4). Commercially available benzohydroxamic acid, **8bb**, was also effective, producing **46** with 88% yield and high selectivity (Table 2.4).

2.2.3. Investigation of the mechanism

2.2.3.1. Control experiments

Some control experiments, as shown in Scheme 2.8, were performed to establish the mechanism of the current transformation. As expected, the coupling reaction does not proceed in the absence of the TTBPyHCl salt. In addition, the presence of just the neutral TTBPy also could not catalyze the reaction, indicating that the reaction is not base-catalyzed (Scheme 2.8). It has been established that the initiation step does not involve proton transfer from $TTBPyH^+$ to the glycal, excluding the possibility of $TTBPyH^+$ behaving as a typical Brønsted acid (BA).

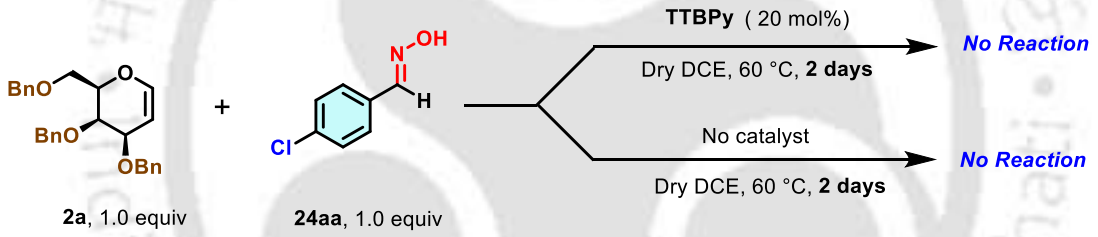

Scheme 2.8. Control experiments.

2.2.3.2. Deuterium labeling experiment

Interestingly, when we reacted with the deuterated oxime **24aa**, we observed almost 72% deuterium incorporation into the product. More significantly, all the deuterium was incorporated cis to the oxime, suggesting the concerted addition of the O-D bond to the glycal (Scheme 2.9). Equatorial deuterium incorporation was confirmed by NOE experiments (see experimental section for details).

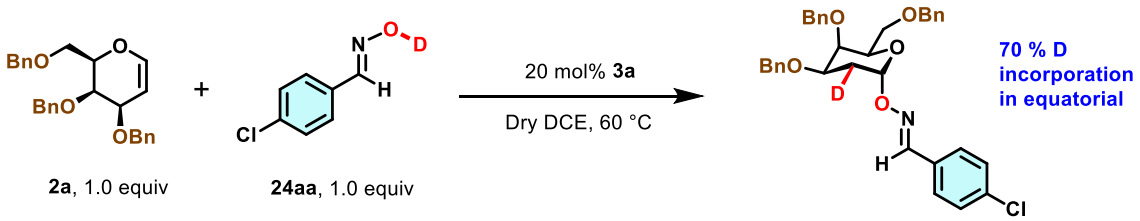

Scheme 2.9. Deuterium labeling experiment.

2.2.3.3. ^{1}H NMR titration experiments

To investigate the mechanism of the transformation, ^{1}H NMR experiments were conducted in $CDCl_3$ (Figure 2.2). Upon mixing catalyst **3a** and oxime **24aa** in a 1:1 ratio, a notable downfield shift was observed for the OH proton of **24aa** (H_D), from δ 7.72 to 8.36 ppm. A slight shift was also detected for the imine proton (H_C), from δ 8.08 to 8.18 ppm. Concurrently, the OH signal of **24aa** shifted downfield, while the NH proton (H_A) of catalyst **3a** shifted upfield, from δ 14.28 to 14.08 ppm. When **24aa** was used in six equivalents relative to catalyst **3a**, the shift in the imine proton (H_C) was less pronounced, changing from δ 8.08 to 8.11 ppm. These observations indicate the presence of a strong interaction between the catalyst and the oxime.

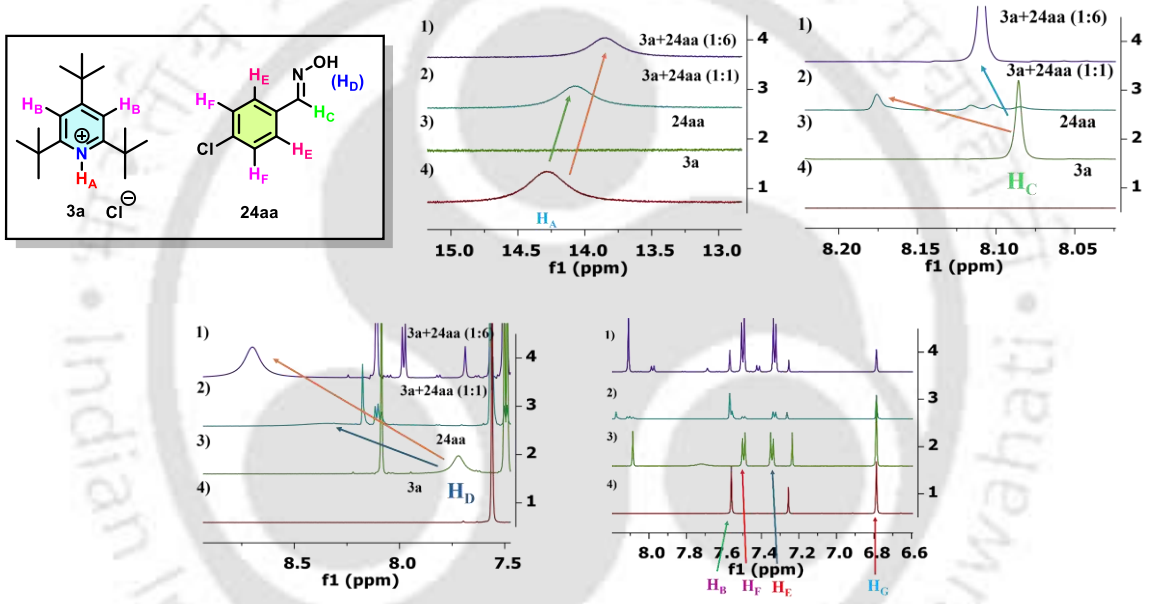

Figure 2.2. ^{1}H NMR titration of **3a** with **24aa** in 0.5 ml solution of $CDCl_3$: (1) 0.032 mmol of **3a** and 0.192 mmol **24aa** (2) 0.032 mmol of **3a** and 0.032 mmol of **24aa** (3) 0.032 mmol of **24aa** (4) 0.032 mmol of **3a**. 0.032 mmol of mesitylene is used as an internal standard in all the experiments for calibration.

2.2.3.4. The UV-Vis titration experiments in ACN

Four experimental groups were designed for UV-Vis analysis in acetonitrile (ACN). Group I consisted of three measurements for **24aa** solutions at concentrations of 0.06, 0.12, and 0.24 mM. Group II involved three measurements of mixtures containing **3a** (fixed at 0.12 mM) with varying concentrations of **24aa**. Group III included three measurements for **3a** solutions at concentrations of 0.06, 0.12, and 0.24 mM, and group IV consisted of three measurements of mixtures containing **24aa** (fixed at 0.36 mM) with varying concentrations of **3a** (Figure 2.3). These experiments revealed the formation of a

distinct species with a new λmax, indicating the presence of an activated complex between the catalyst and oxime (Scheme 2.10).

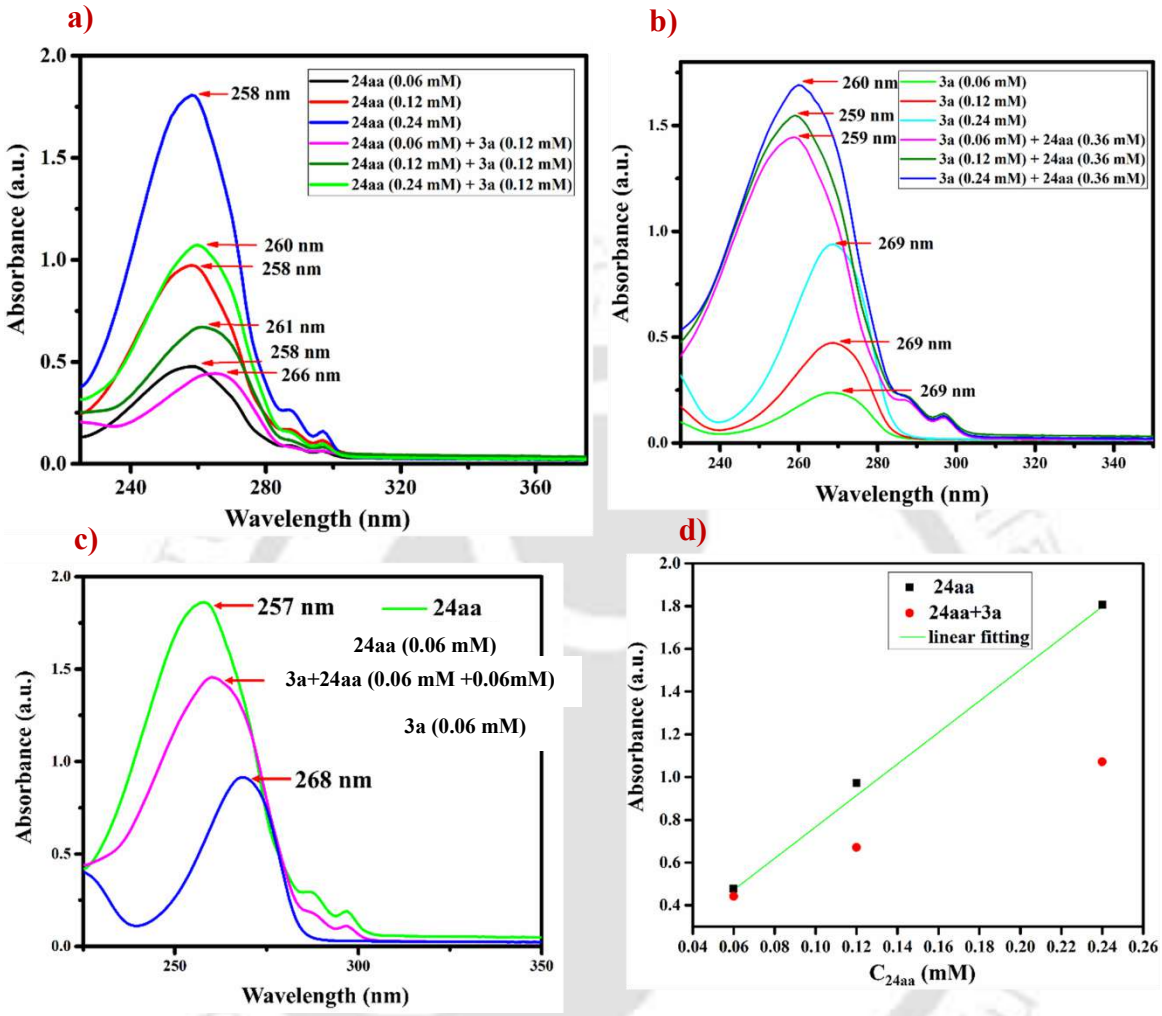

Figure 2.3. a) Concentration-dependent UV-Vis spectra of **24aa** and mixture of **24aa** and **3a**; b) Concentration-dependent UV-Vis spectra of **3a** and mixture of **3a** and **24aa**; c) Concentration-dependent UV-Vis spectra of **3a**, **24aa** and mixture of **3a** and **24aa**; d) Concentration-dependent absorbance plot of **24aa** and mixture of **24aa** and **3a** in ACN.

2.2.3.5. Fluorescence titration experiments in ACN

Two experimental groups were designed for fluorescence titration in acetonitrile (ACN). Group I consisted of two measurements of **3a** solutions at concentrations of 0.06 and 0.24 mM. Group II involved two measurements of mixtures containing **24aa** (fixed at 0.36 mM) with varying concentrations of **3a** (Figure 2.4). Interestingly, the fluorescence emission of the TTBPy salt is completely quenched in the presence of the oxime. These experiments revealed the formation of a distinct species with a new λmax, indicating the presence of an activated complex between the catalyst and oxime (Scheme 2.10).

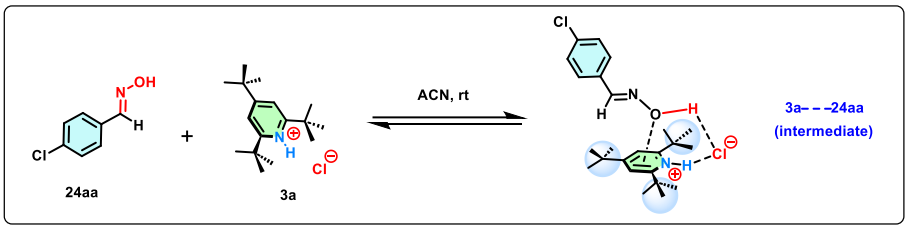

Scheme 2.10. Evidence for activated complex formation.

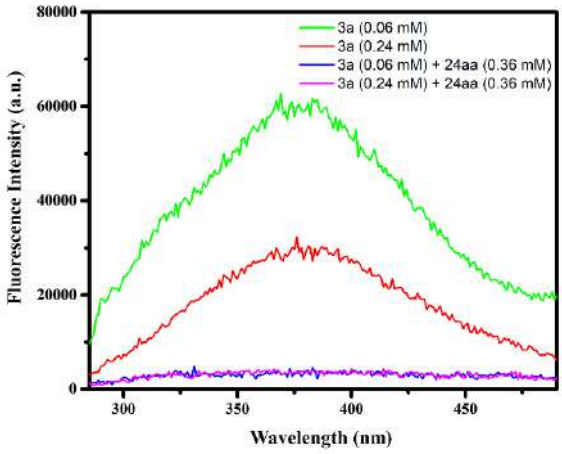

Figure 2.4. Concentration dependent fluorescence spectra of **3a** and mixture of **24aa** and **3a**.

2.2.3.6. Analysis of N-H stretching in TTBPy·HCl via IR spectroscopy

IR spectra were recorded for the catalyst (**3a**), the oxime (**24aa**), and their mixture. The overlaid spectrum is presented below. Notably, the N-H stretching frequency of the catalyst remained unchanged upon addition of oxime (**24aa**), indicating that no direct hydrogen bonding occurs between the protonated nitrogen ($[N\text{-}H]^+$) and the oxime oxygen (Figure 2.5).

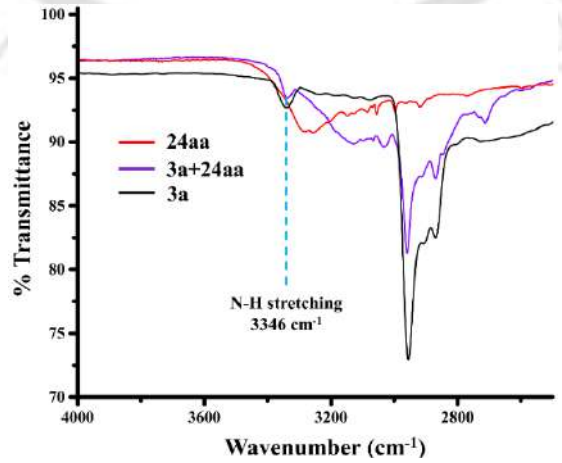

Figure 2.5. IR studies.

2.2.4. Synthetic applications

2.2.4.1. Gram-scale synthesis

To demonstrate the protocol's scalability, the coupling reaction between **2a** and **2aa** was performed on a 2.40 mmol scale, affording the product with 86% yield. Notably, product **1** was exclusively obtained as an α-isomer without any loss in selectivity, even at gram-scale synthesis (Scheme 2.11).

Procedure: In a screw-capped vial equipped with a magnetic stir bar, donor **2a** (1.00 g, 2.40 mmol), oxime **2aa** (358 mg, 2.40 mmol), and the catalyst **3a** (136 mg, 0.48 mmol, 20 mol%) were introduced under a nitrogen atmosphere. Dry DCE (10 mL) was then added, and the reaction mixture was stirred at 60 °C for 8-10 hours. Upon completion, the reaction was quenched with triethylamine (NEt_3, 6 mL), and the solvent was removed under reduced pressure. The crude product was purified by column chromatography (hexane/ethyl acetate = 95:5), affording the desired compound **1** as a colorless oil (1.17 g, 86% yield).

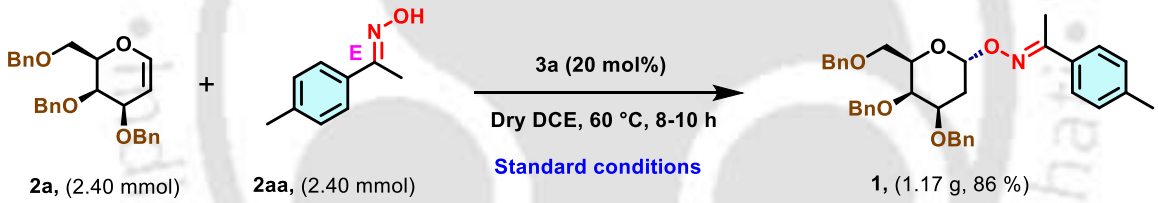

Scheme 2.11. Gram-scale synthesis of compound **1**.

2.2.4.2. Synthesis of N-O-linked *C*-aryl glycoside

The dependability and practical utility of this glycosylation were demonstrated through a series of synthetic transformations. Galactoside **43**, containing an aryl iodide moiety, underwent our newly developed C-H activation method.[27] This led to the formation of an intriguing pseudodisaccharide **47**, yielding it in 90% yield as a single isomer via stereospecific *C*-glycosylation (Scheme 2.12).

Procedure: In a screw-capped vial equipped with a magnetic stir bar, $Pd(OAc)_2$ (1.6 mg, 0.007 mmol, 6.0 mol%) was suspended in anhydrous DMF (0.5 mL). Under an argon atmosphere, DMAN (PS) (52 mg, 0.24 mmol, 2.0 equiv), aryl iodide **43** (99 mg, 0.14 mmol, 1.2 equiv), donor (glucal, 1a) (50 mg, 0.12 mmol, 1.0 equiv), and Bu_4NCl (66 mg, 0.24 mmol, 2.0 equiv) were added sequentially. The reaction mixture was stirred at 80 °C in an oil bath for 20-24 hours. Upon completion, the solvent was removed under

reduced pressure, and the crude product was purified by column chromatography (hexane/ethyl acetate = 80:20), affording compound **47** as a colorless oil (106 mg, 90% yield).

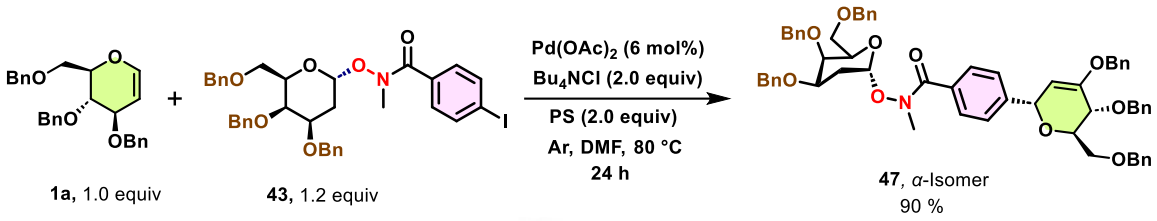

Scheme 2.12. Synthesis of N-O-linked pseudodisaccharide **47**.

2.2.4.3. Synthesis of N-O-linked propargyl alcohol

Glycoside **43** was further transformed into the N-O-linked propargyl alcohol analog **48** via Sonogashira coupling and its structure was unequivocally confirmed by X-ray crystallographic analysis (Scheme 2.13).[27]

Procedure: In a 5 mL dry flask equipped with a magnetic stir bar, iodoarene **43** (148 mg, 0.21 mmol), $Pd(PPh_3)_2Cl_2$ (1.3 mg, 0.0018 mmol, 1 mol%), CuI (1.0 mg, 0.0036 mmol, 2 mol%), and triethylamine (Et_3N, 4 mL) were added under an inert atmosphere and stirred at room temperature for 5-10 minutes. Propargyl alcohol (10 mg, 0.18 mmol) was then introduced, and the reaction mixture was stirred for 18-20 hours. Upon completion, the solvent was removed under reduced pressure, and the crude product was purified by column chromatography (hexane/ethyl acetate = 50:50), affording compound **48** as a colorless oil (106 mg, 95% yield).

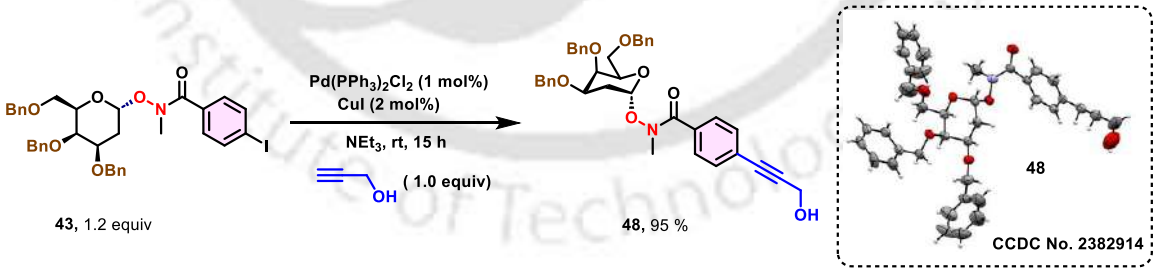

Scheme 2.13. Synthesis of N-O-linked propargyl alcohol **48**.

2.3. Proposed mechanism

Based on the above observations, we propose a concerted mechanism for this transformation, illustrated in Scheme 2.14. Initially, an anion-bridged activated complex forms between the oxime and the 2,4,6-tri-*tert*-butylpyridinium cation, stabilized by lone

pair-π interactions. This complex then interacts with glycal concertedly, resulting in the highly stereoselective formation of the glycosidic bond.

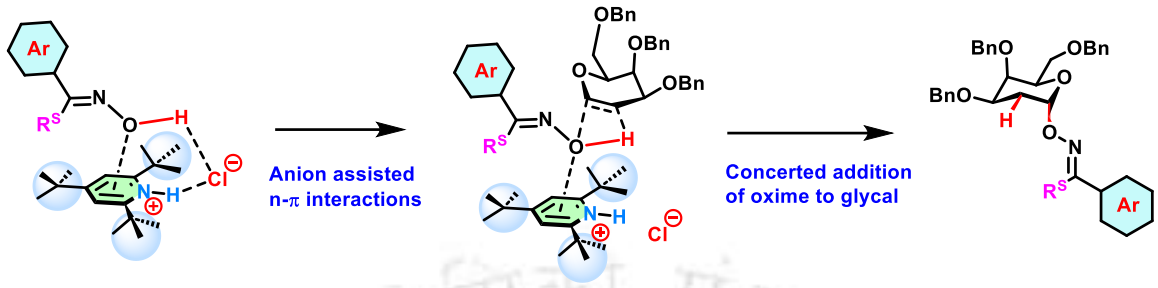

Scheme 2.14. Plausible reaction mechanism.

2.4. Conclusion

In conclusion, we have developed the first organocatalytic strategy for the synthesis of 2-deoxy N-O-linked glycosides. The 2,4,6-tri-*tert*-butylpyridinium hydrochloride salt was shown to function as a mild, electronically neutral, and stable organocatalyst, efficiently promoting the glycosylation of a diverse array of aldoximes, ketoximes, and hydroxamic acids. This method provides access to a relatively underexplored class of glycosides, yielding them in excellent yields and high diastereoselectivity. The utility of the protocol is further underscored by its successful application in the late-stage modification of bioactive and drug-like molecules, as well as its extension to pseudodisaccharide synthesis.

2.5. Experimental section

2.5.1. Donors and acceptors used in the present study

Following donors (**1a-7a**), oxime acceptors (**1aa-29aa**), and hydroxylamide acceptors (**1bb-8bb**) were used in this method.

Donors **1a**–**7a** were synthesized according to reported procedures.[27-30] Oxime acceptors **1aa**–**29aa** were prepared following literature methods.[18] Hydroxylamides (**1bb-7bb**) were prepared according to the literature procedures.[31, 32] Hydroxylamide **8bb** is commercially available.

Donors:

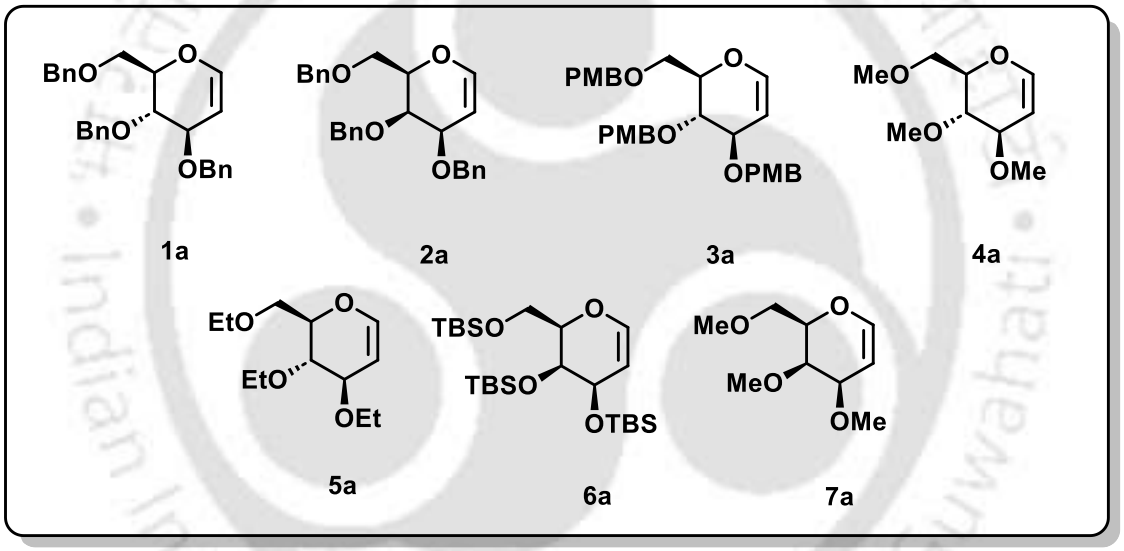

Hydroxylamide acceptors:

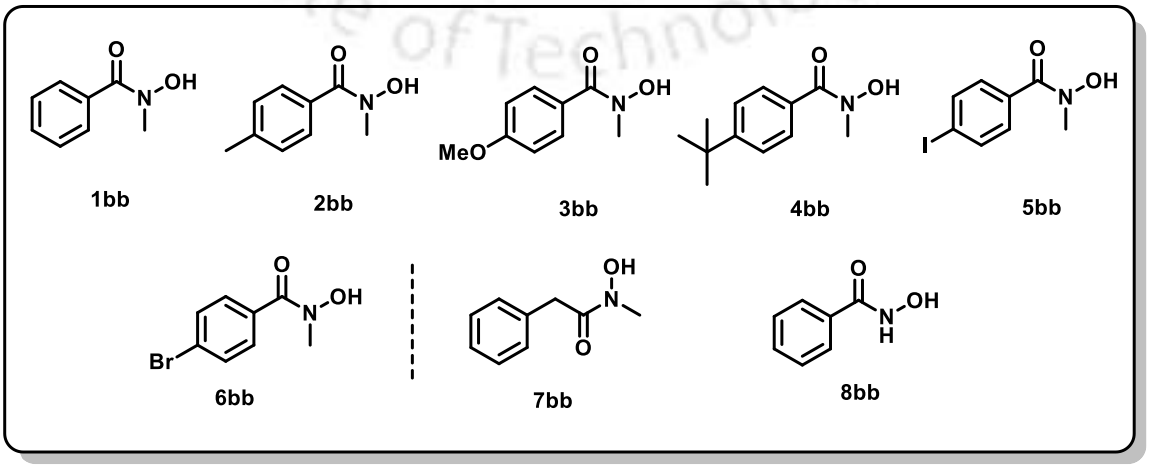

Oxime acceptors:

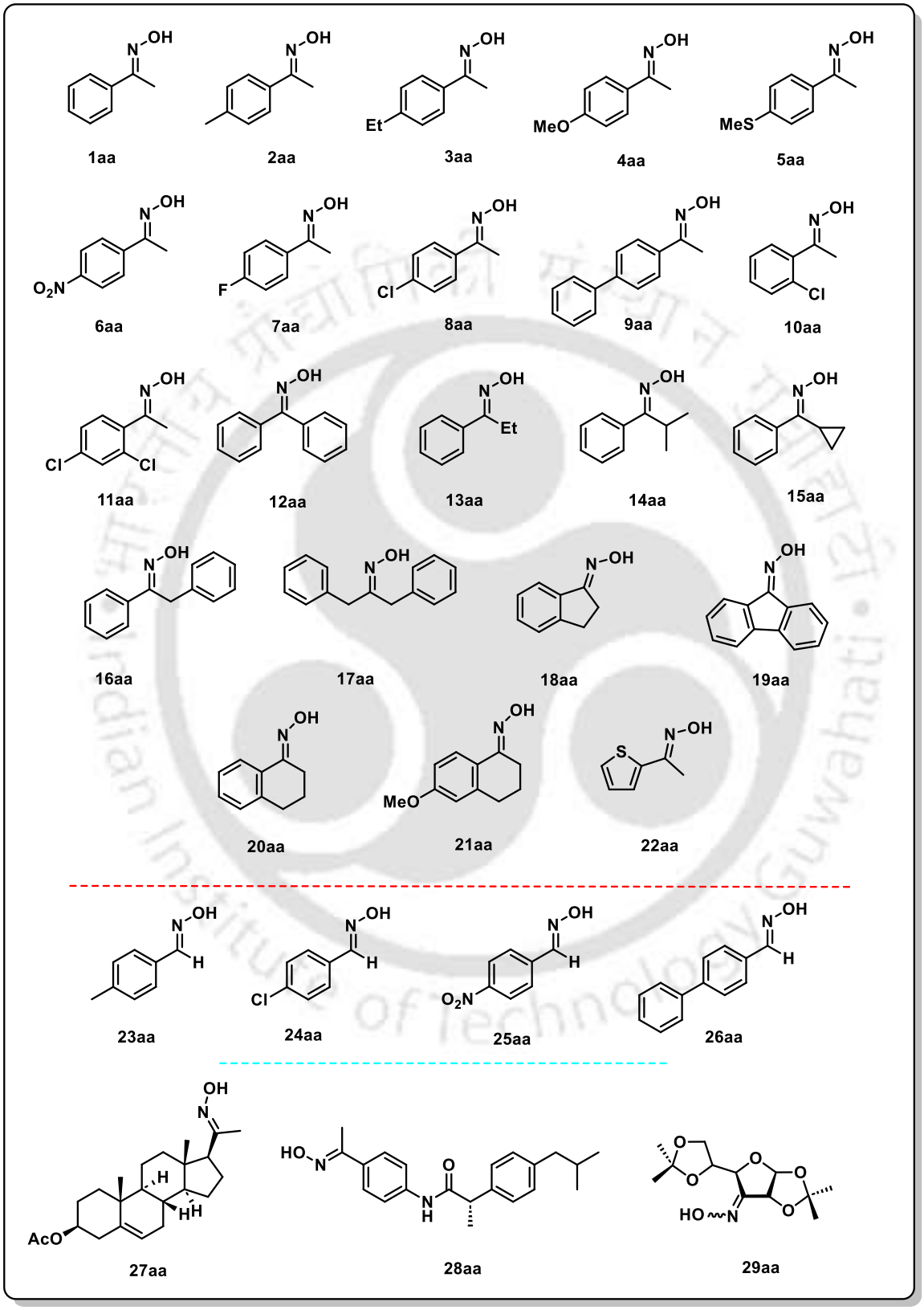

2.5.2. NMR titration experiments

^{1}H NMR titration of **3a** with **24aa** in 0.5 mL solution of $CDCl_3$.

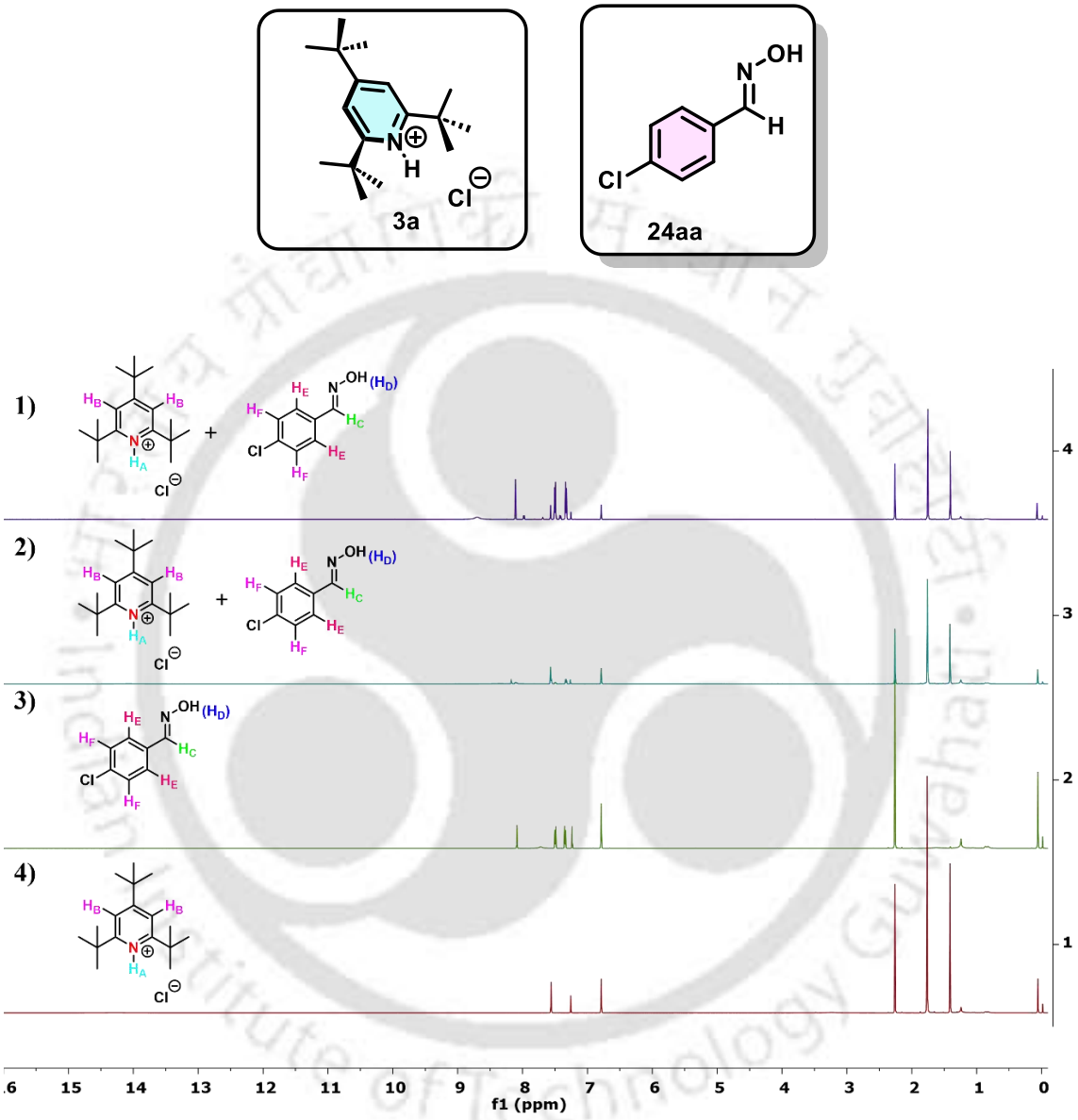

1) 0.032 mmol of **3a** and 0.192 mmol **24aa** (1:6 ratio) 2) 0.032 mmol of **3a** and 0.032 mmol of **24aa** (1:1 ratio) 3) 0.032 mmol of **24aa** and 4) 0.032 mmol of **3a**.

In all experiments for calibration, 0.032 mmol of mesitylene is used as an internal standard.

1:1 mixture of **3a** and mesitylene (0.032 mmol of each component in 0.5 mL of $CDCl_3$).

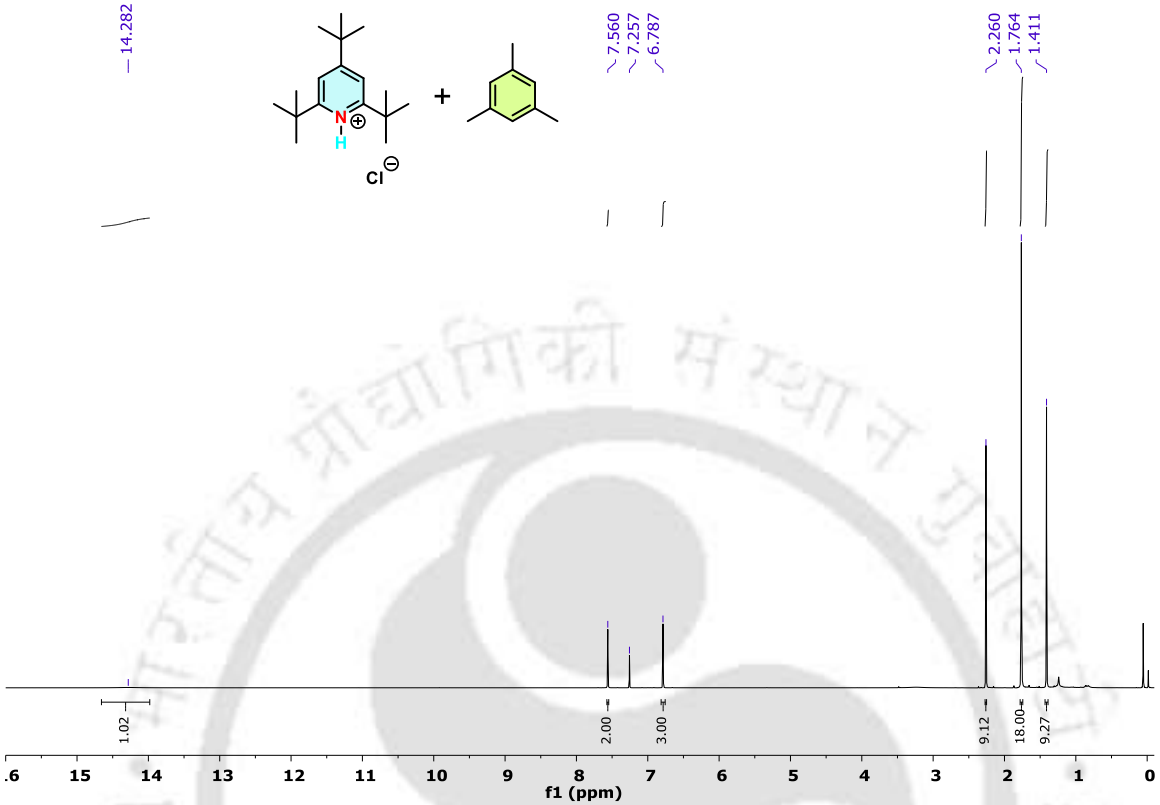

1:1 mixture of **24aa** and mesitylene (0.032 mmol of each component in 0.5 mL of $CDCl_3$)

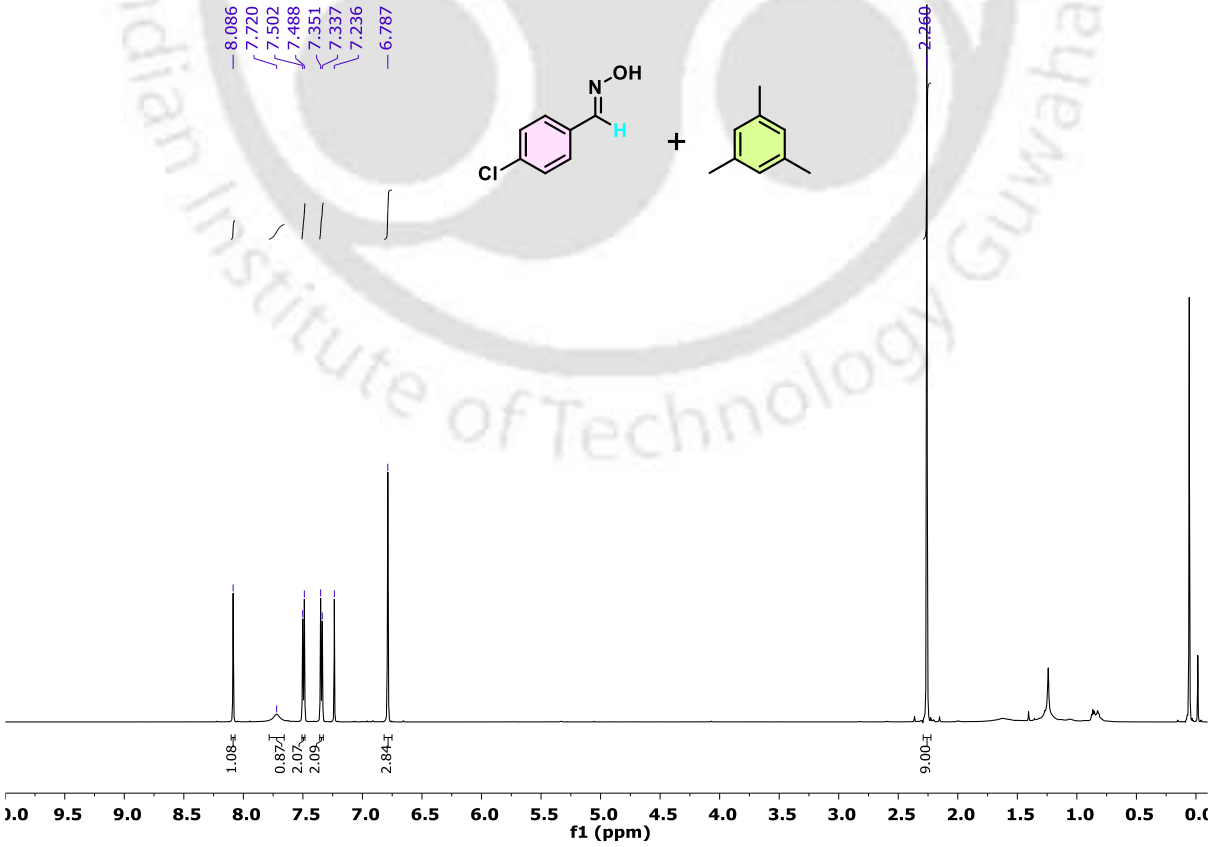

1:1:1 mixture of **3a**, **24aa** and mesitylene (0.032 mmol of each component).

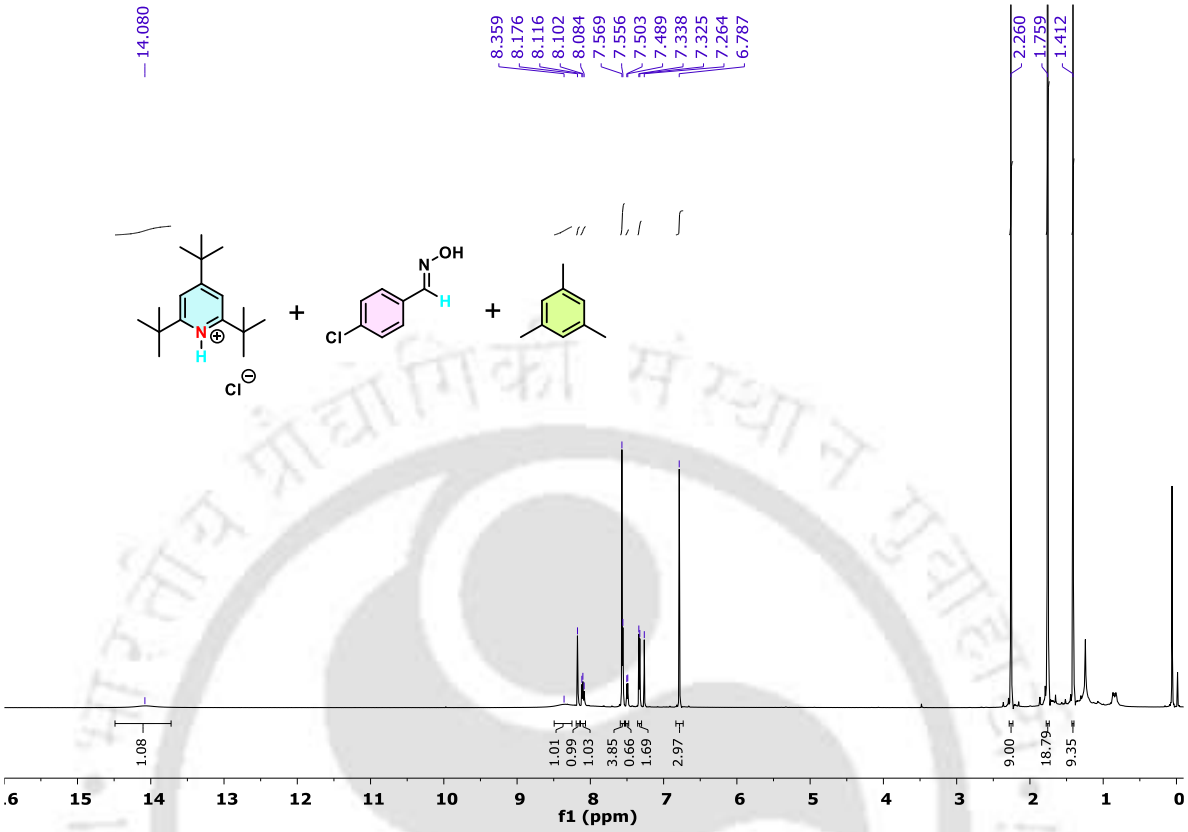

1:6:1 mixture of **3a**, **24aa** and mesitylene (0.032 mmol of each component)

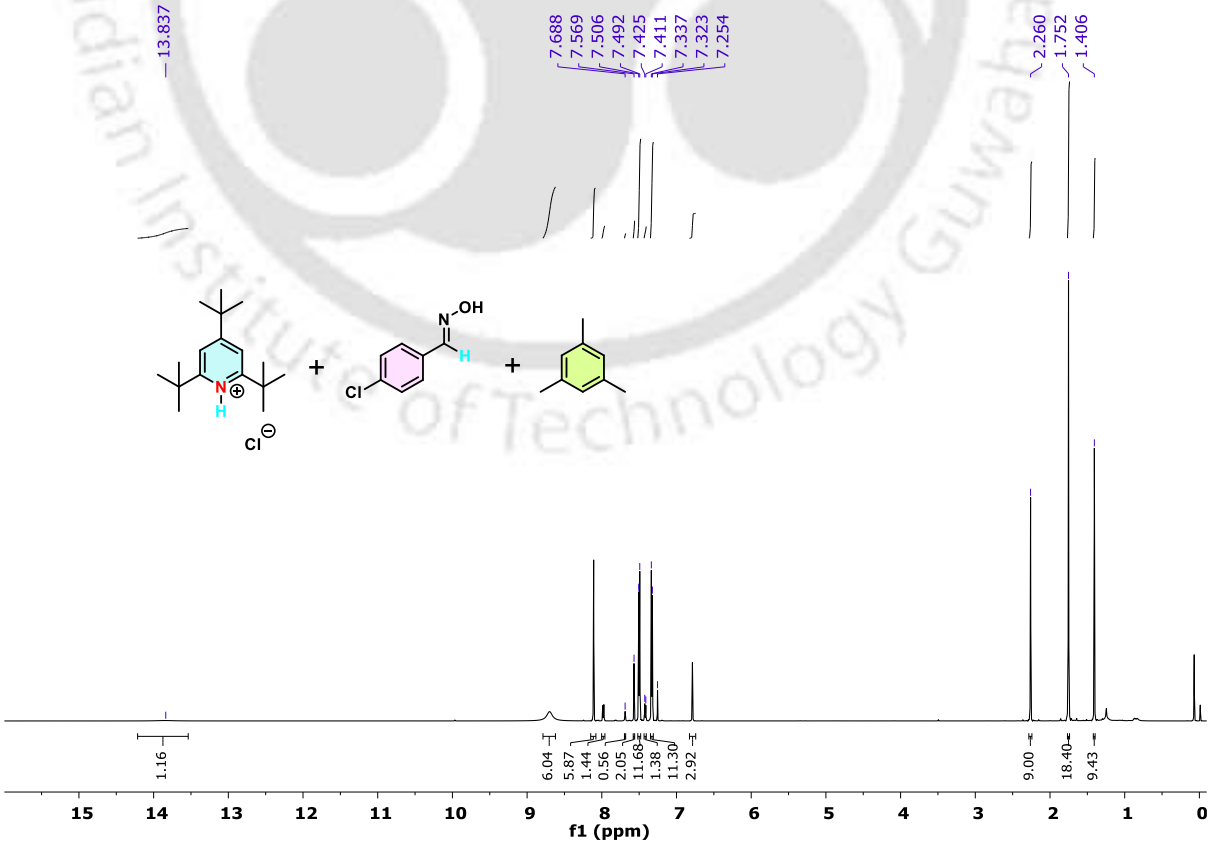

2.5.3. nOe experiments

nOe experiments of 28-D

^{1}H NMR of compound 28-D (600 MHz, $CDCl_3$)

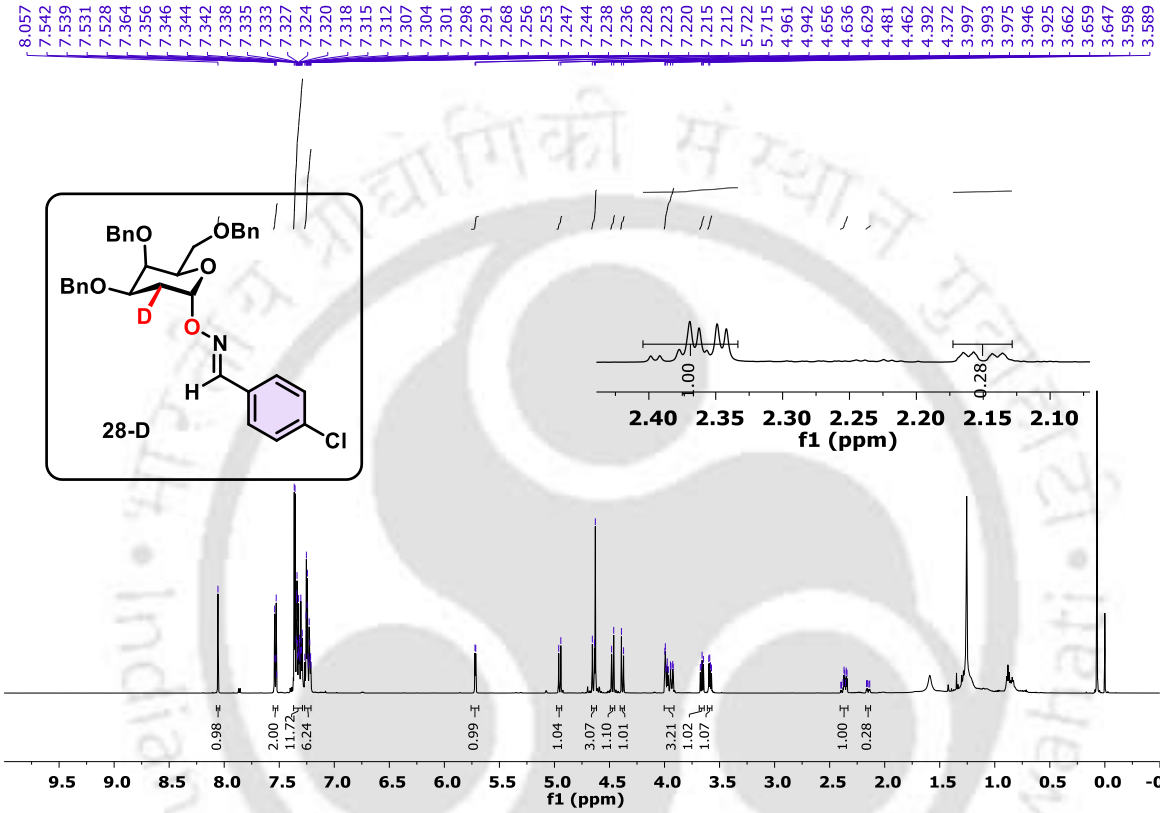

Irradiation of H_1: Upon irradiation of **H_1**, the enhancement on the **H_{axial}** proton (appearing at 2.370 ppm) is found 2.41%. In addition, there is no enhancement on the **$H_{equatorial}$** proton (appearing at 2.15 ppm) (Figure 2.6).

Irradiation of H_{axial}: Upon irradiation of **H_{axial}**, the enhancement of the **H_1** proton (appearing at 5.75 ppm) is found 3.13% (Figure 2.7). In addition, there is no enhancement on the **$H_{equatorial}$** proton (appearing at 2.15 ppm).

Irradiation of $H_{equatorial}$: Upon irradiation of **$H_{equatorial}$**, the enhancement of the **H_{axial}** proton (appearing at 2.370 ppm) is found 12.56%. In addition, there is no enhancement on the **H_1** proton (appearing at 5.75 ppm) (Figure 2.8).

The nOe experiments indicate that deuterium was exclusively incorporated at the equatorial position, i.e., cis to oxime functionality in the substrate.

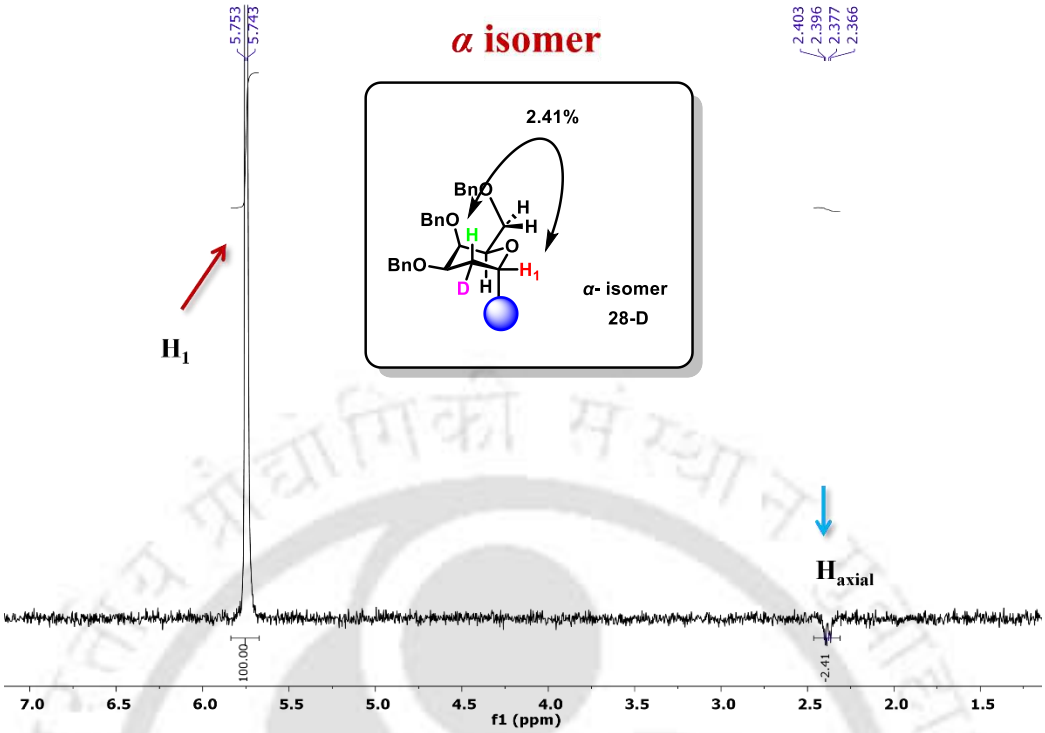

Figure 2.6. *nOe experiment of **28-D** (upon irradiation of **H**$_1$).*

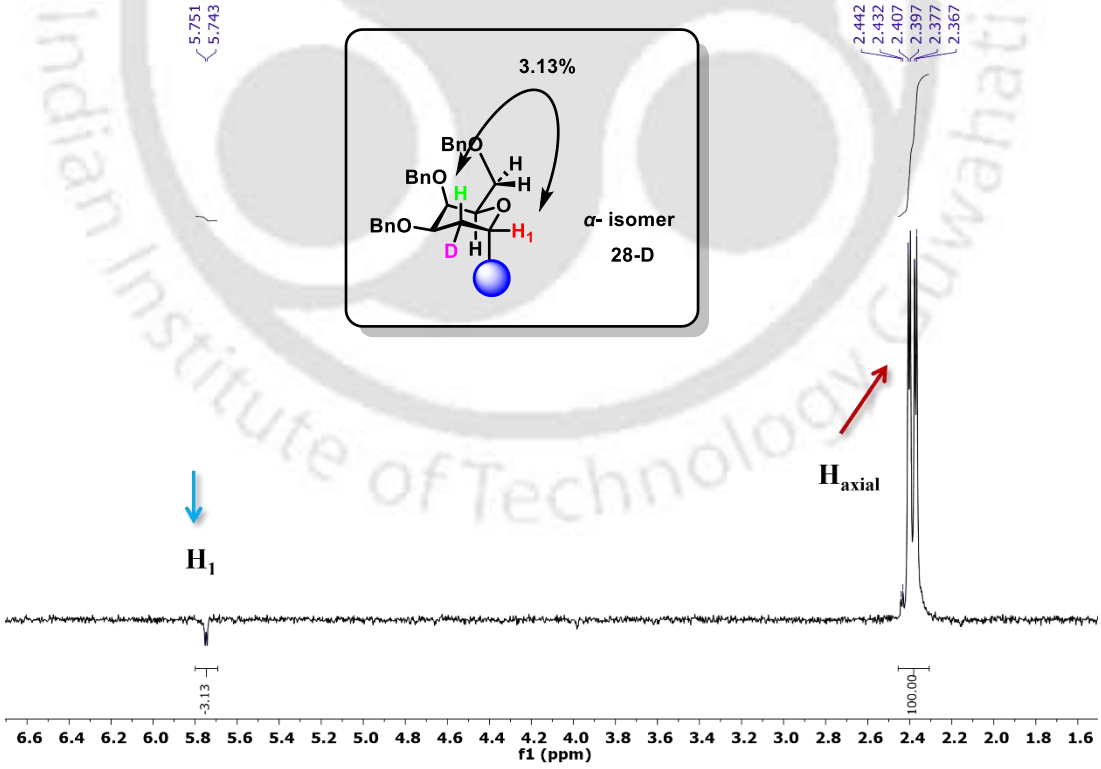

Figure 2.7. *nOe experiment of **28-D** (upon irradiation of **H**$_{axial}$).*

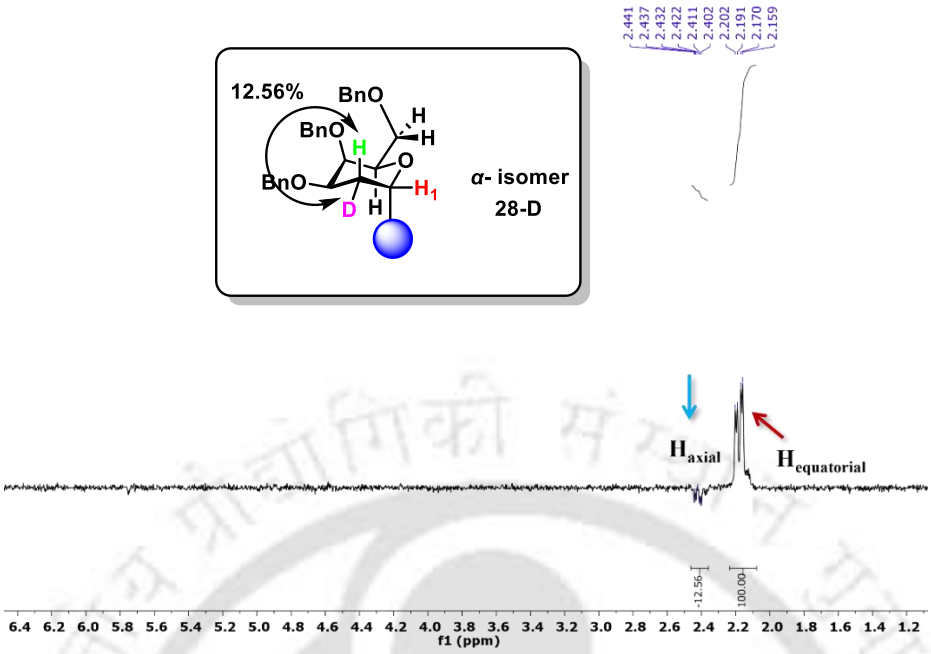

Figure 2.8. *nOe experiment of **28-D** (upon irradiation of **H**equatorial).*

nOe experiment of 26

Irradiation of H_1: Upon irradiation of **H_1**, the enhancement on the **H_6** proton (appearing at 3.691 ppm) is found 0.50% and the enhancement on the **H_2** protons (appearing at 2.320 and 1.866 ppm) are found 1.50% and 2.23%. In addition, there is no enhancement on the **H_5** proton (appearing at 3.817 ppm). Hence, **H_1** is trans to **H_5**. Thus, the compound is in **alpha** configuration (Figure 2.9).

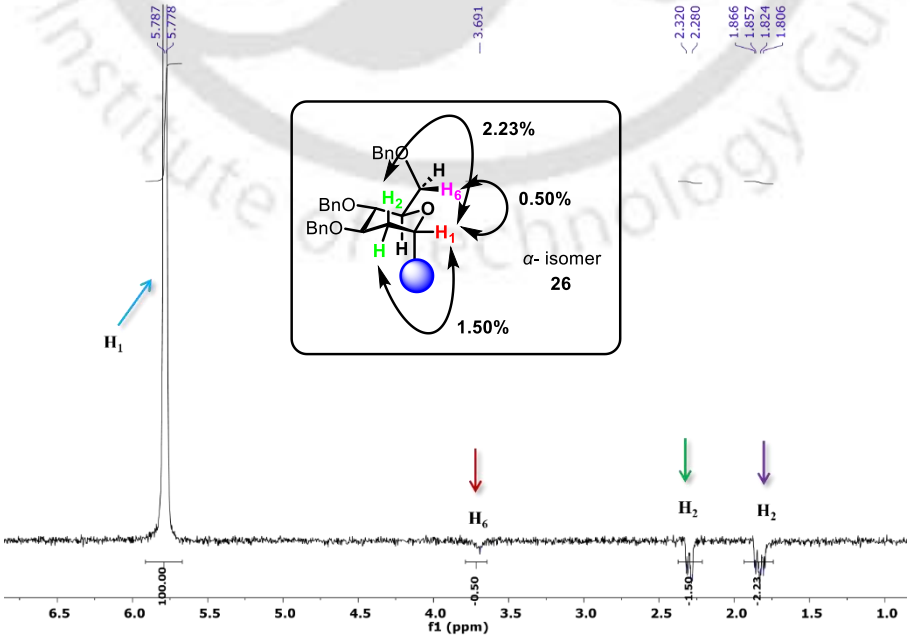

Figure 2.9. *nOe experiment of **26**.*

nOe experiment of 21 (α-isomer (E))

Irradiation of H_1: Upon irradiation of H_1, the enhancement on the H_2 protons (appearing at 2.513 and 1.935 ppm) are found 1.61% and 2.33%. In addition, there is no enhancement on the H_5 proton. Hence, H_1 is trans to H_5. Thus, the compound is in **alpha** configuration (Figure 2.10).

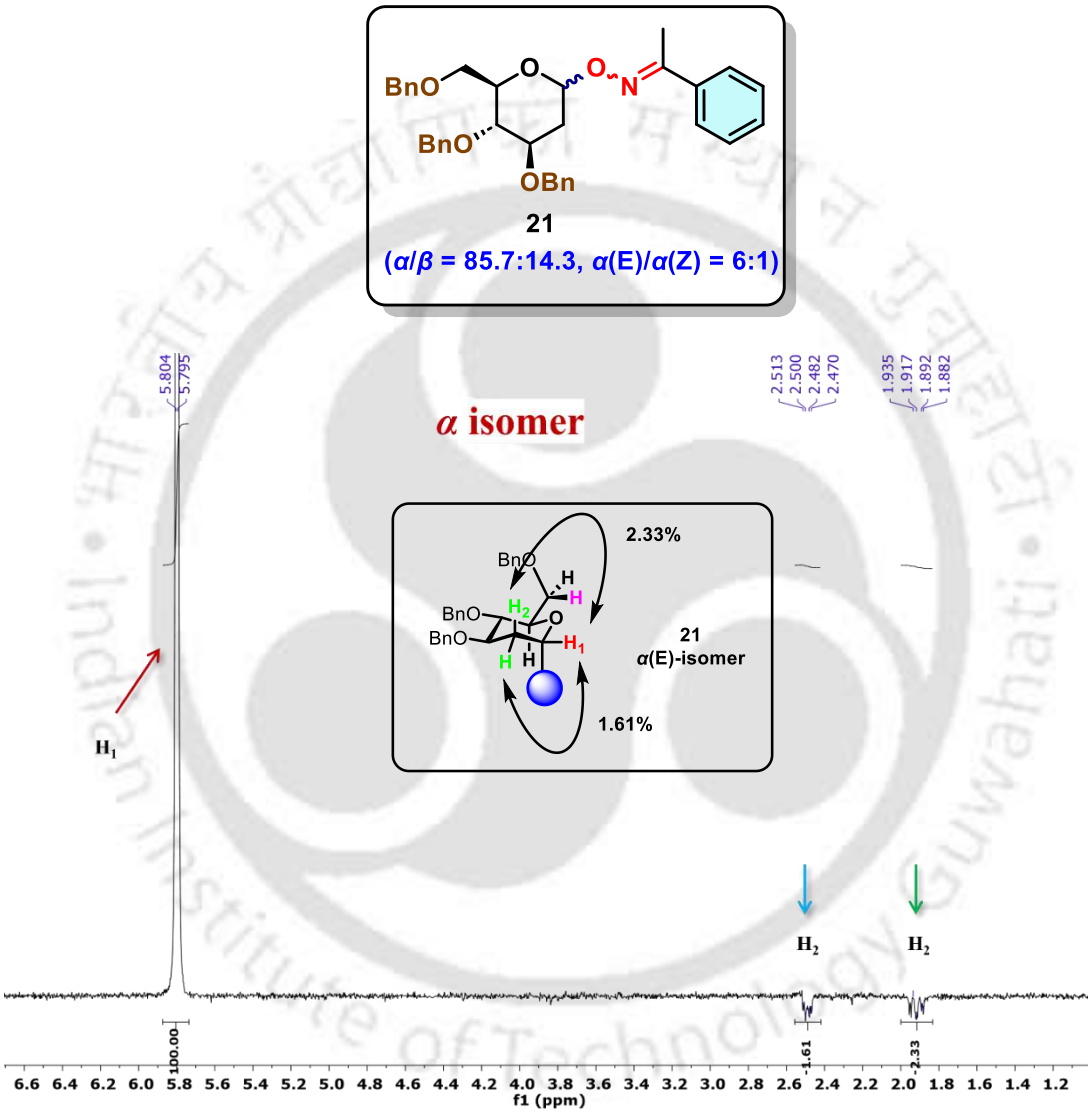

Figure 2.10. *nOe experiment of **21** (α-isomer (E)).*

nOe experiment of 21 (β-isomer)

Irradiation of H_1: Upon irradiation of H_1, the enhancement on the H_5 proton (appearing at 3.577 ppm) is found 3.57% and the enhancement on the H_2 proton (appearing at 2.517 ppm) is found 2.54%. Hence, H_1 is cis to H_5. Thus, the compound is in **beta** configuration (Figure 2.11).

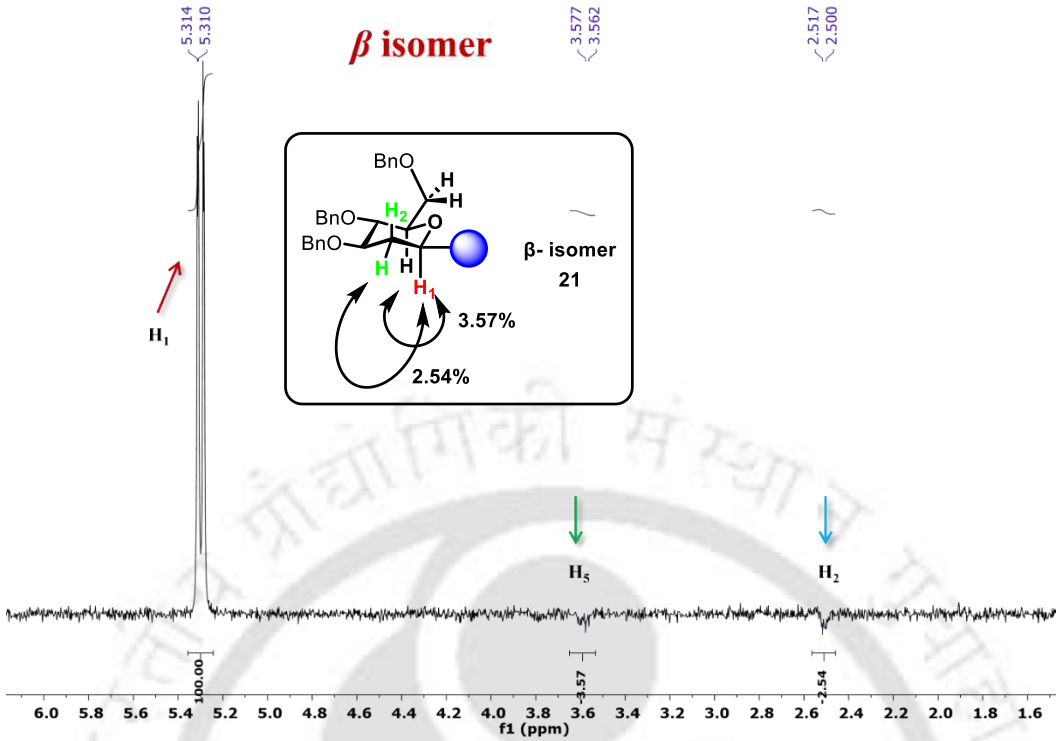

Figure 2.11. *nOe experiment of **21** (β-isomer).*

nOe experiment of 21 (α-isomer (Z))

Irradiation of H_1: Upon irradiation of **H_1**, the enhancement on the **H_2** protons (appearing at 2.357 and 1.783 ppm) are found 2.30% and 1.80%. In addition, there is no enhancement on the **H_5** proton. Hence, **H_1** is trans to **H_5**. Thus, the compound is in **alpha(Z)** configuration (Figure 2.12).

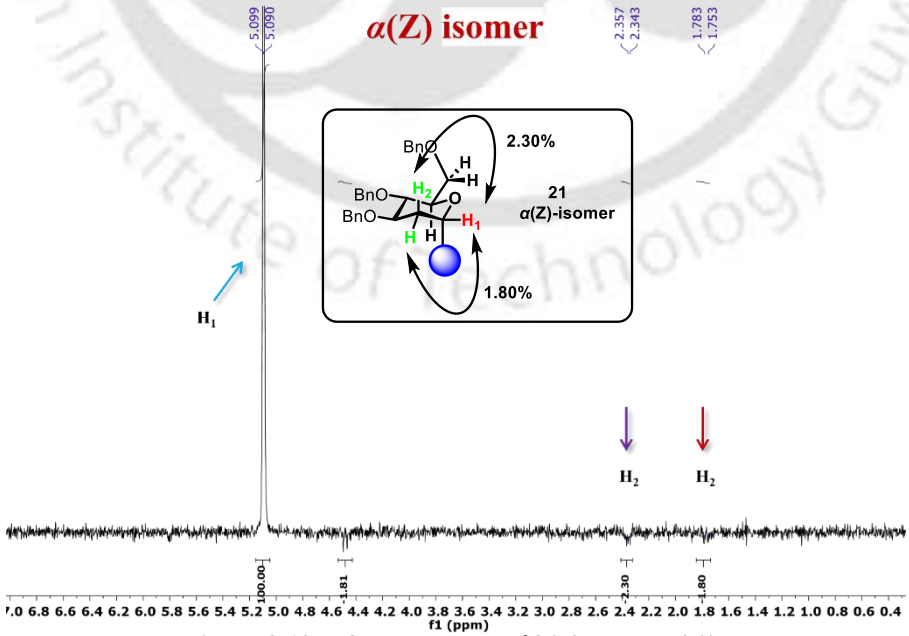

Figure 2.12. *nOe experiment of **21** (α-isomer (Z)).*

2.5.4. General procedure 1.1: synthesis of N-O-linked glycosides

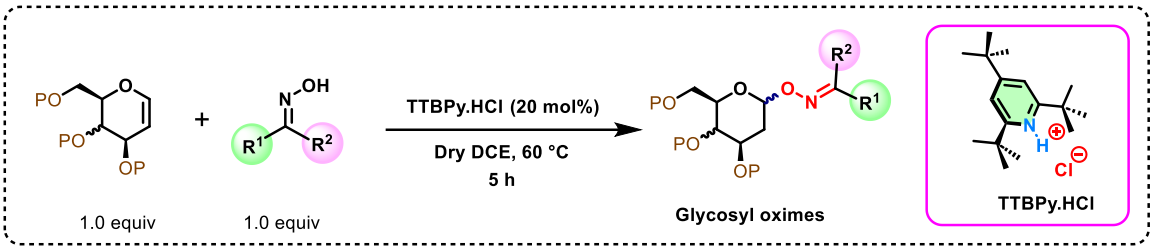

In a screw-capped reaction vial equipped with a magnetic stir bar, the glycal donor (0.17 mmol, 1.0 equiv), aryl or alkyl oxime (0.17 mmol, 1.0 equiv), and catalyst **3a** (2,4,6-tri-*tert*-butylpyridinium hydrochloride salt, 10.0 mg, 0.034 mmol, 20 mol%) were introduced under an inert atmosphere. Dry 1,2-dichloroethane (DCE, 1.0 mL) was added, and the reaction mixture was stirred at 60 °C for 4-5 hours. Upon completion, the reaction was quenched with triethylamine (NEt_3, 0.5 mL). The solvent was removed under reduced pressure, and the crude residue was purified by column chromatography on silica gel using ethyl acetate/hexane as the eluent to afford the corresponding glycosyl oximes. The anomeric configuration of the glycosides was determined by **^{1}H NMR** and **^{13}C NMR** data. **NOE** experiments further confirmed the **α**-configuration.

2.5.5. General procedure 1.2: synthesis of glycosyloxyamines

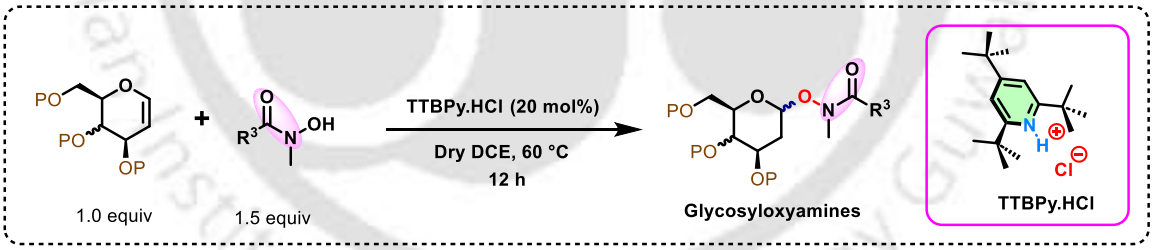

In a screw-capped reaction vial equipped with a magnetic stir bar, the glycal donor (0.17 mmol, 1.0 equiv), hydroxylamide acceptor (0.255 mmol, 1.5 equiv), and catalyst **3a** (10.0 mg, 0.034 mmol, 20 mol%) were introduced under an inert atmosphere. Dry 1,2-dichloroethane (DCE, 1.0 mL) was added, and the reaction mixture was stirred at 60 °C for 10-12 hours. Upon completion, the reaction was quenched with triethylamine (NEt_3, 0.5 mL). The solvent was removed under reduced pressure, and the crude residue was purified by column chromatography on silica gel using ethyl acetate/hexane as the eluent to afford the corresponding glycosyloxyamines. The anomeric configuration of the glycosides was determined by **^{1}H NMR** and **^{13}C NMR** data. **XRD** data further confirmed the **α**-configuration of glycoside **48**.

2.5.6. Spectroscopic data of N-O-linked glycosides (1-48)

(E)-1-(p-tolyl)ethan-1-one O-((2R,4R,5R,6R)-4,5-bis(benzyloxy)-6-((benzyloxy)methyl)tetrahydro-2H-pyran-2-yl) oxime (1)

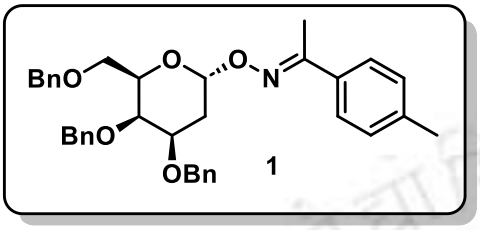

1 was obtained in 88% yield (84.6 mg), as a colorless oil, R_f = 0.4 (Hexane/EtOAc, 9:1, v/v), **[α]^{25}D** = +50.0 (*c* 0.05, $CHCl_3$). **^{1}H NMR** (600 MHz, $CDCl_3$) *δ* 7.55 (d, *J* = 8.0 Hz, 2H), 7.37 – 7.23 (m, 15H), 7.15 (d, *J* = 7.9 Hz, 2H), 5.75 (d, *J* = 3.7 Hz, 1H), 4.96 (d, *J* = 11.6 Hz, 1H), 4.67 – 4.63 (m, 3H), 4.47 (d, *J* = 11.6 Hz, 1H), 4.39 (d, *J* = 11.5 Hz, 1H), 4.00 (s, 1H), 3.98 – 3.92 (m, 2H), 3.68 (dd, *J* = 9.3, 7.8 Hz, 1H), 3.59 (dd, *J* = 9.2, 5.3 Hz, 1H), 2.35 (s, 4H), 2.17 (s, 4H). **^{13}C NMR** (151 MHz, $CDCl_3$) *δ* 156.2, 139.5, 139.1, 138.5, 138.1, 133.5, 129.1, 128.6, 128.6, 128.5, 128.4, 128.4, 128.3, 128.1, 127.8, 127.7, 127.6, 127.6, 126.3, 100.3, 74.6, 74.5, 73.6, 73.0, 70.9, 70.4, 69.2, 29.9, 21.4, 12.9. **HRMS** (ESI) m/z: $[M+H]^+$ calcd for $C_{36}H_{40}NO_5$ 566.2901; found 566.2875.

1-(4-ethylphenyl)ethan-1-one O-((2R,4R,5R,6R)-4,5-bis(benzyloxy)-6-((benzyloxy)methyl)tetrahydro-2H-pyran-2-yl) oxime (E/Z = 89:11) (2)

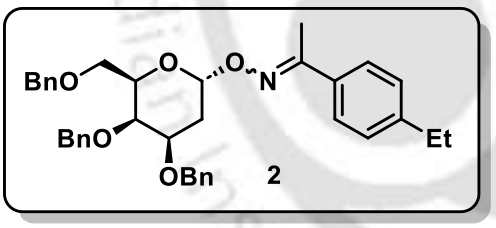

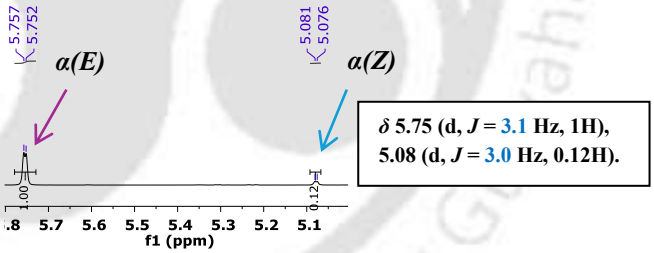

2 was obtained in 85% yield (83.8 mg), as a colorless oil, R_f = 0.5 (Hexane/EtOAc, 9:1, v/v), **[α]^{25}D** = +51.1 (*c* 0.18, $CHCl_3$), (E/Z = 89:11, from *α*-isomer, which is confirmed from coupling constants and NOE experiments). **^{1}H NMR** (600 MHz, $CDCl_3$) *δ* 7.57 (d, *J* = 8.2 Hz, 2H), 7.38 – 7.22 (m, 17H), 7.17 (d, *J* = 8.1 Hz, 2H), 5.75 (d, *J* = 3.1 Hz, 1H), 4.96 (d, *J* = 11.6 Hz, 1H), 4.68 – 4.62 (m, 3H), 4.47 (d, *J* = 11.5 Hz, 1H), 4.38 (d, *J* = 11.6 Hz, 1H), 4.00 (s, 1H), 3.98 – 3.93 (m, 2H), 3.68 (t, *J* = 8.5 Hz, 1H), 3.59 (dd, *J* = 9.2, 5.4 Hz, 1H), 2.65 (q, *J* = 7.6 Hz, 2H), 2.37 (td, *J* = 12.6, 3.8 Hz, 1H), 2.18 (s, 4H), 1.23 (t, *J* = 7.6 Hz, 3H). **^{13}C NMR** (151 MHz, $CDCl_3$) *δ* 156.3, 145.8, 139.0, 138.6, 138.4, 138.2, 138.1, 137.9, 133.8, 128.6, 128.5 (128.53, 128.52, 128.50, 128.46), 128.4, 128.3, 128.3, 128.1, 128.0, 127.9, 127.8 (127.81, 127.78), 127.7, 127.6 (127.64, 127.60), 127.5, 126.4, 100.3, 97.2, 74.9, 74.6, 74.5, 74.4, 73.6, 73.1, 73.0, 70.9, 70.6, 70.4, 70.2, 69.7, 69.2, 69.0, 31.3, 29.9, 29.8, 28.8, 15.7, 14.2, 12.9. **HRMS** (ESI) m/z: $[M+H]^+$ calcd for $C_{37}H_{42}NO_5$ 580.3057; found 580.3057.

(E)-1-(4-methoxyphenyl)ethan-1-one O-((2R,4R,5R,6R)-4,5-bis(benzyloxy)-6-((benzyloxy)methyl)tetrahydro-2H-pyran-2-yl) oxime (3)

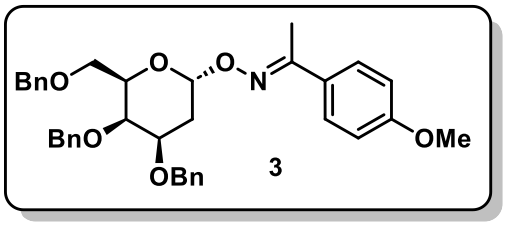

3 was obtained in 89% yield (88 mg), as a colorless oil, R_f = 0.5 (Hexane/EtOAc, 8:2, v/v), **[α]$^{25}_{D}$** = +57.1 (*c* 0.08, $CHCl_3$). **^{1}H NMR** (600 MHz, $CDCl_3$) δ 7.60 (d, *J* = 8.4 Hz, 2H), 7.39 – 7.21 (m, 15H), 6.86 (d, *J* = 8.4 Hz, 2H), 5.75 (d, *J* = 3.7 Hz, 1H), 4.96 (d, *J* = 11.6 Hz, 1H), 4.65 (d, *J* = 17.2 Hz, 3H), 4.47 (d, *J* = 11.5 Hz, 1H), 4.39 (d, *J* = 11.5 Hz, 1H), 4.00 (s, 1H), 3.98 – 3.93 (m, 2H), 3.81 (s, 3H), 3.68 (t, *J* = 8.5 Hz, 1H), 3.59 (dd, *J* = 9.3, 5.4 Hz, 1H), 2.37 (td, *J* = 12.5, 3.9 Hz, 1H), 2.17 (s, 4H). **^{13}C NMR** (151 MHz, $CDCl_3$) δ 160.7, 155.8, 139.0, 138.5, 138.1, 128.9, 128.5 (128.54, 128.46), 128.3, 128.3, 128.1, 127.8, 127.7, 127.6 (127.64, 127.59), 113.8, 100.2, 74.6, 74.5, 73.6, 73.0, 70.9, 70.4, 69.3, 55.4, 29.9, 29.8, 12.8. **HRMS** (ESI) m/z: $[M+H]^+$ calcd for $C_{36}H_{40}NO_6$ 582.2850; found 582.2855.

(E)-1-(4-(methylthio)phenyl)ethan-1-one O-((2R,4R,5R,6R)-4,5-bis(benzyloxy)-6-((benzyloxy)methyl)tetrahydro-2H-pyran-2-yl) oxime (4)

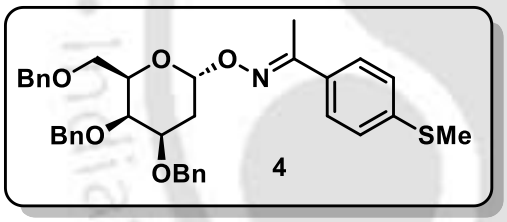

4 was obtained in 82% yield (83 mg), as a colorless oil, R_f = 0.6 (Hexane/EtOAc, 8:2, v/v), **[α]$^{25}_{D}$** = +68.3 (*c* 0.24, $CHCl_3$). **^{1}H NMR** (600 MHz, $CDCl_3$) δ 7.58 (d, *J* = 8.6 Hz, 2H), 7.39 – 7.18 (m, 17H), 5.75 (d, *J* = 3.7 Hz, 1H), 4.96 (d, *J* = 11.5 Hz, 1H), 4.69 – 4.61 (m, 3H), 4.47 (d, *J* = 11.5 Hz, 1H), 4.39 (d, *J* = 11.5 Hz, 1H), 4.00 (s, 1H), 3.98 – 3.92 (m, 2H), 3.71 – 3.65 (m, 1H), 3.59 (dd, *J* = 9.3, 5.4 Hz, 1H), 2.48 (s, 3H), 2.38 (td, *J* = 12.6, 3.9 Hz, 1H), 2.16 (s, 4H). **^{13}C NMR** (151 MHz, $CDCl_3$) δ 155.7, 140.3, 139.0, 138.4, 138.1, 132.9, 128.9, 128.6, 128.5, 128.4, 128.3, 128.1, 127.8, 127.7 (127.74, 127.65), 127.6, 126.7, 126.0, 125.1, 100.3, 74.5, 74.5, 73.6, 72.9, 70.9, 70.4, 69.3, 29.9, 15.6, 12.7. **HRMS** (ESI) m/z: $[M+H]^+$ calcd for $C_{36}H_{40}NO_5S$ 598.2622; found 598.2622.

(E)-1-(4-fluorophenyl)ethan-1-one O-((2R,4R,5R,6R)-4,5-bis(benzyloxy)-6-((benzyloxy)methyl)tetrahydro-2H-pyran-2-yl) oxime (5)

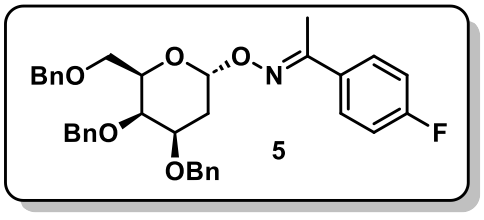

5 was obtained in 82% yield (79 mg), as a colorless oil, R_f = 0.4 (Hexane/EtOAc, 9:1, v/v), **[α]$^{25}_{D}$** = +68.0 (*c* 0.07, $CHCl_3$). **^{1}H NMR** (600 MHz, $CDCl_3$) δ 7.66 – 7.60 (m, 2H), 7.39 – 7.21 (m, 15H), 7.02 (t, *J* = 8.7 Hz, 2H), 5.75 (d, *J* = 3.7 Hz, 1H), 4.96 (d, *J* = 11.6 Hz, 1H), 4.68 – 4.60 (m, 3H), 4.47 (d, *J* = 11.6 Hz, 1H), 4.39

(d, *J* = 11.5 Hz, 1H), 4.00 (s, 1H), 3.97 – 3.92 (m, 2H), 3.70 – 3.65 (m, 1H), 3.59 (dd, *J* = 9.3, 5.5 Hz, 1H), 2.38 (td, *J* = 12.6, 3.9 Hz, 1H), 2.17 (s, 4H). **^{13}C NMR** (151 MHz, $CDCl_3$) *δ* 164.4, 162.8, 155.2, 138.9, 138.4, 138.1, 132.5, 132.4, 128.6, 128.5, 128.4, 128.3 (128.32, 128.26), 128.1, 128.0, 127.8 (127.81, 127.75), 127.7, 127.6, 115.5, 115.4, 100.4, 74.5 (74.53, 74.49), 73.6, 72.9, 70.9, 70.4, 69.2, 29.9, 12.9. **HRMS** (ESI) m/z: $[M+H]^+$ calcd for $C_{35}H_{37}FNO_5$ 570.2650; found 570.2652.

(E)-1-(4-chlorophenyl)ethan-1-one O-((2R,4R,5R,6R)-4,5-bis(benzyloxy)-6-((benzyloxy)methyl)tetrahydro-2H-pyran-2-yl) oxime (6)

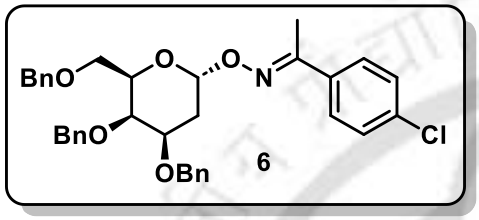

6 was obtained in 83% yield (83 mg), as a white foam, R_f = 0.6 (Hexane/EtOAc, 9:1, v/v), **$[\alpha]^{25}_D$** = +87.5 (*c* 0.04, $CHCl_3$). **^{1}H NMR** (600 MHz, $CDCl_3$) *δ* 7.59 (d, J = 8.4 Hz, 2H), 7.39 – 7.22 (m, 17H), 5.74 (d, *J* = 3.8 Hz, 1H), 4.96 (d, *J* = 11.6 Hz, 1H), 4.67 – 4.61 (m, 3H), 4.47 (d, *J* = 11.5 Hz, 1H), 4.39 (d, *J* = 11.5 Hz, 1H), 4.00 (s, 1H), 3.97 – 3.91 (m, 2H), 3.70 – 3.65 (m, 1H), 3.59 (dd, *J* = 9.3, 5.4 Hz, 1H), 2.38 (td, *J* = 12.6, 3.9 Hz, 1H), 2.16 (s, 4H). **^{13}C NMR** (151 MHz, $CDCl_3$) *δ* 155.2, 138.9, 138.4, 138.1, 135.4, 134.8, 128.7, 128.6 (128.59, 128.57), 128.5 (128.52, 128.49), 128.4, 128.3, 128.1, 127.8 (127.84, 127.77), 127.7 (127.71, 127.68), 127.6, 100.5, 74.5 (74.54, 74.46), 73.6, 72.9, 71.0, 70.4, 69.2, 29.9, 12.8. **HRMS** (ESI) m/z: $[M+H]^+$ calcd for $C_{35}H_{37}ClNO_5$ 586.2355; found 586.2351.

(E)-1-([1,1'-biphenyl]-4-yl)ethan-1-one O-((2R,4R,5R,6R)-4,5-bis(benzyloxy)-6-((benzyloxy)methyl)tetrahydro-2H-pyran-2-yl) oxime (7)

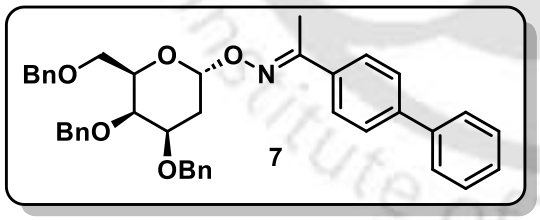

7 was obtained in 86% yield (91 mg), as a white foam, R_f = 0.4 (Hexane/EtOAc, 9:1, v/v), **$[\alpha]^{25}_D$** = +75.0 (*c* 0.04, $CHCl_3$). **^{1}H NMR** (600 MHz, $CDCl_3$) *δ* 7.74 (d, *J* = 7.9 Hz, 2H), 7.59 (dd, *J* = 12.3, 7.8 Hz, 4H), 7.45 (t, *J* = 7.5 Hz, 2H), 7.39 – 7.22 (m, 16H), 5.79 (d, *J* = 3.7 Hz, 1H), 4.97 (d, *J* = 11.5 Hz, 1H), 4.66 (d, *J* = 14.2 Hz, 3H), 4.48 (d, *J* = 11.6 Hz, 1H), 4.39 (d, *J* = 11.5 Hz, 1H), 4.03 – 3.95 (m, 3H), 3.69 (t, *J* = 8.5 Hz, 1H), 3.60 (dd, *J* = 9.5, 5.5 Hz, 1H), 2.40 (td, *J* = 12.5, 3.8 Hz, 1H), 2.25 – 2.17 (m, 4H). **^{13}C NMR** (151 MHz, $CDCl_3$) *δ* 155.9, 142.2, 140.6, 139.0, 138.5, 138.1, 135.2, 128.9, 128.6, 128.5 (128.52, 128.47), 128.4, 128.3, 128.1, 127.8, 127.8, 127.7 (127.72, 127.66), 127.6, 127.2 (127.18, 127.16), 126.9, 100.4, 74.5, 73.6, 72.9, 70.9, 70.5, 69.3, 29.9, 12.9. **HRMS** (ESI) m/z: $[M+H]^+$ calcd for $C_{41}H_{42}NO_5$ 628.3057; found 628.3047.

(E)-1-(2-chlorophenyl)ethan-1-one O-((2R,4R,5R,6R)-4,5-bis(benzyloxy)-6-((benzyloxy)methyl)tetrahydro-2H-pyran-2-yl) oxime (8)

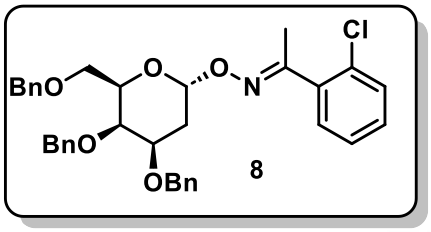

8 was obtained in 80% yield (79.7 mg), as a white foam, R_f = 0.5 (Hexane/EtOAc, 9:1, v/v), **[α]^{25}D** = +35.7 (*c* 0.084, $CHCl_3$). **^{1}H NMR** (600 MHz, $CDCl_3$) δ 7.40 – 7.34 (m, 7H), 7.34 – 7.24 (m, 11H), 7.19 (t, *J* = 7.5 Hz, 1H), 5.72 (d, *J* = 3.7 Hz, 1H), 4.96 (d, *J* = 11.5 Hz, 1H), 4.66 (d, *J* = 20.2 Hz, 3H), 4.50 (d, *J* = 11.7 Hz, 1H), 4.44 (s, 1H), 4.05 – 3.93 (m, 3H), 3.69 (t, *J* = 8.4 Hz, 1H), 3.61 (dd, *J* = 9.3, 5.4 Hz, 1H), 2.37 (td, *J* = 12.6, 3.8 Hz, 1H), 2.18 (s, 4H). **^{13}C NMR** (151 MHz, $CDCl_3$) δ 157.9, 139.0, 138.4, 136.7, 132.7, 130.5, 130.1, 129.9, 128.6, 128.5, 128.4 (128.39, 128.37), 128.0, 127.8 (127.81, 127.77), 127.7, 127.6, 126.9, 100.1, 74.57, 74.5, 73.6, 72.9, 70.9, 70.5, 69.3, 29.8, 16.6. **HRMS** (ESI) m/z: $[M+H]^+$ calcd for $C_{35}H_{37}ClNO_5$ 586.2355; found 586.2360.

(E)-1-(2,4-dichlorophenyl)ethan-1-one O-((2R,4R,5R,6R)-4,5-bis(benzyloxy)-6-((benzyloxy)methyl)tetrahydro-2H-pyran-2-yl) oxime (9)

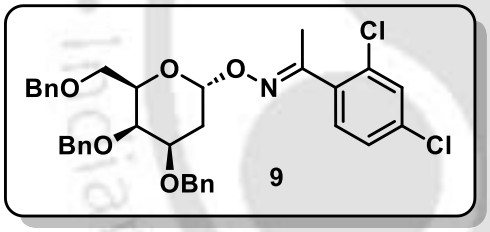

9 was obtained in 78% yield (82 mg), as a colorless oil, R_f = 0.6 (Hexane/EtOAc, 9:1, v/v), **[α]^{25}D** = +29.0 (*c* 0.1, $CHCl_3$). **^{1}H NMR** (600 MHz, $CDCl_3$) δ 7.39 – 7.24 (m, 16H), 7.20 (d, *J* = 8.2 Hz, 1H), 7.16 (dd, *J* = 8.2, 2.0 Hz, 1H), 5.71 (d, *J* = 3.7 Hz, 1H), 4.96 (d, *J* = 11.6 Hz, 1H), 4.69 – 4.62 (m, 3H), 4.49 (d, *J* = 11.7 Hz, 1H), 4.42 (d, *J* = 11.6 Hz, 1H), 4.01 (s, 1H), 3.98 – 3.91 (m, 2H), 3.71 – 3.64 (m, 1H), 3.60 (dd, *J* = 9.3, 5.5 Hz, 1H), 2.37 (td, *J* = 12.6, 3.9 Hz, 1H), 2.16 (s, 4H). **^{13}C NMR** (151 MHz, $CDCl_3$) δ 156.9, 138.9, 138.4, 138.2, 135.4, 135.2, 133.5, 131.4, 129.8, 128.6, 128.5, 128.4, 128.3, 128.0, 127.8 (127.84, 127.79), 127.7, 127.6 (127.64, 127.61), 127.3, 100.3, 74.6, 74.4, 73.6, 72.9, 70.9, 70.5, 69.3, 29.7, 16.5. **HRMS** (ESI) m/z: $[M+H]^+$ calcd for $C_{35}H_{36}Cl_2NO_5$ 620.1965; found 620.1952.

diphenylmethanone O-((2R,4R,5R,6R)-4,5-bis(benzyloxy)-6-((benzyloxy)methyl)tetrahydro-2H-pyran-2-yl) oxime (10)

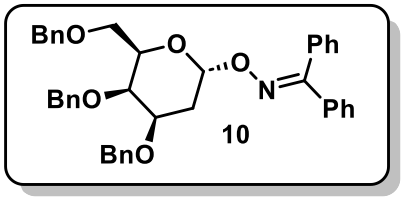

10 was obtained in 85% yield (88 mg), as a colorless oil, R_f = 0.4 (Hexane/EtOAc, 9:1, v/v), **[α]^{25}D** = +27.5 (*c* 0.04, $CHCl_3$). **^{1}H NMR** (600 MHz, $CDCl_3$) δ 7.50 (d, *J* = 7.7 Hz, 2H), 7.40 – 7.22 (m, 23H), 5.76 (d, *J* = 3.7 Hz, 1H), 4.91 (d, *J* = 11.6 Hz, 1H), 4.61 (d, *J* = 11.6 Hz,

1H), 4.52 – 4.43 (m, 3H), 4.39 (d, *J* = 11.6 Hz, 1H), 3.84 (s, 1H), 3.77 (t, *J* = 6.5 Hz, 1H), 3.66 – 3.57 (m, 2H), 3.52 (d, *J* = 12.2 Hz, 1H), 2.29 (td, *J* = 12.5, 3.9 Hz, 1H), 2.01 (dd, *J* = 12.8, 4.4 Hz, 1H). **^{13}C NMR** (151 MHz, $CDCl_3$) *δ* 158.8, 138.9, 138.5, 138.2, 136.1, 133.3, 129.7, 129.1, 128.9, 128.5 (128.54, 128.48), 128.4, 128.3 (128.33, 128.31), 128.1, 128.0, 127.8, 127.7, 127.6, 127.5, 100.7, 74.4, 74.3, 73.6, 72.9, 71.2, 70.3, 69.4, 29.8. **HRMS** (ESI) m/z: $[M+H]^+$ calcd for $C_{40}H_{40}NO_5$ 614.2901; found 614.2914.

(E)-1-phenylpropan-1-one O-((2R,4R,5R,6R)-4,5-bis(benzyloxy)-6-((benzyloxy)methyl)tetrahydro-2H-pyran-2-yl) oxime (11)

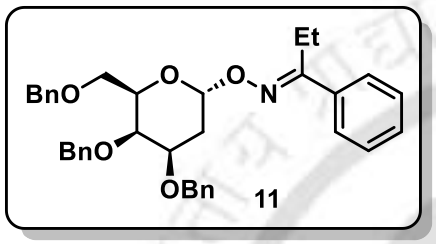

11 was obtained in 88% yield (84 mg), as a colorless oil, R_f = 0.5 (Hexane/EtOAc, 9:1, v/v), **[α]^{25}D** = +60.8 (*c* 0.09, $CHCl_3$). **^{1}H NMR** (600 MHz, $CDCl_3$) *δ* 7.66 – 7.60 (m, 2H), 7.39 – 7.21 (m, 18H), 5.74 (d, *J* = 3.7 Hz, 1H), 4.96 (d, *J* = 11.6 Hz, 1H), 4.69 – 4.63 (m, 3H), 4.48 (d, *J* = 11.5 Hz, 1H), 4.40 (d, *J* = 11.5 Hz, 1H), 4.02 – 3.92 (m, 3H), 3.71 – 3.65 (m, 1H), 3.60 (dd, *J* = 9.4, 5.3 Hz, 1H), 2.74 – 2.63 (m, 2H), 2.38 (td, *J* = 12.6, 3.9 Hz, 1H), 2.16 (dd, *J* = 13.4, 4.0 Hz, 1H), 1.09 (t, *J* = 7.6 Hz, 3H). **^{13}C NMR** (151 MHz, $CDCl_3$) *δ* 161.2, 139.0, 138.4, 138.1, 135.3, 129.4, 128.6, 128.5 (128.54, 128.47), 128.4, 128.3, 128.1, 127.8 (127.79, 127.77), 127.7, 126.7, 100.4, 74.5, 74.3, 73.6, 73.1, 72.9, 71.1, 70.6, 70.3, 69.3, 29.9, 20.6, 11.5. **HRMS** (ESI) m/z: $[M+H]^+$ calcd for $C_{36}H_{40}NO_5$ 566.2901; found 566.2875.

2-methyl-1-phenylpropan-1-one O-((2R,4R,5R,6R)-4,5-bis(benzyloxy)-6-((benzyloxy)methyl)tetrahydro-2H-pyran-2-yl) oxime (E/Z = 50:50) (12)

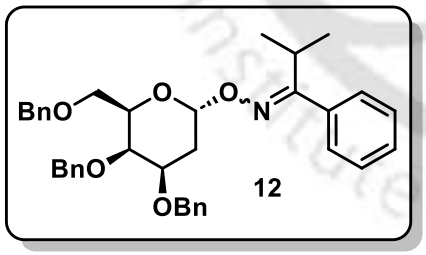

12 was obtained in 82% yield (80 mg), as a colorless oil, R_f = 0.5 (Hexane/EtOAc, 9:1, v/v), **[α]^{25}D** = +17.8 (*c* 0.05, $CHCl_3$). E/Z = 1:1 (14aa exists as an E/Z isomer in a 1:1 ratio). **^{1}H NMR** (600 MHz, $CDCl_3$) *δ* 7.30 (ddt, *J* = 39.5, 30.6, 11.7 Hz, 38H), 7.11 (q, *J* = 3.7, 3.0 Hz, 2H), 5.66 (d, *J* = 3.7 Hz, 1H), 5.60 (d, *J* = 3.8 Hz, 1H), 4.96 (d, *J* = 11.5 Hz, 1H), 4.87 (d, *J* = 11.6 Hz, 1H), 4.68 – 4.56 (m, 4H), 4.50 (d, *J* = 10.5 Hz, 2H), 4.45 – 4.37 (m, 4H), 4.00 (s, 1H), 3.97 (t, *J* = 6.4 Hz, 1H), 3.93 (d, *J* = 14.4 Hz, 1H), 3.74 (s, 1H), 3.68 (t, *J* = 8.4 Hz, 1H), 3.62 (t, *J* = 5.3 Hz, 2H), 3.57 (d, *J* = 6.3 Hz, 2H), 3.34 (dt, *J* = 15.8, 8.0 Hz, 2H), 2.82 (p, *J* = 6.8 Hz, 1H), 2.37 (td, *J* = 12.5, 3.5 Hz, 1H), 2.20 (td, *J* = 12.6, 3.6 Hz, 1H), 2.13 (dd, *J* = 12.8, 3.8 Hz, 1H), 1.89 (dd, *J* = 12.6, 3.8 Hz, 1H), 1.14 (t, *J* = 6.6 Hz, 6H), 1.10 (d, *J* = 6.8 Hz, 3H), 1.05 (d, *J* = 6.9 Hz, 3H). **^{13}C NMR** (151 MHz, $CDCl_3$) *δ* 165.6, 165.4, 139.0, 138.9, 138.5, 138.4, 138.3, 138.2, 135.8, 134.1, 128.7, 128.6, 128.5 (128.49, 128.48), 128.4 (128.38, 128.37), 128.3, 128.2, 128.2, 128.0, 127.9 (127.95, 127.89), 127.8 (127.80, 127.78), 127.7

(127.69, 127.67), 127.6 (127.62, 127.60), 127.5, 127.4, 100.4, 99.8, 74.5, 74.4, 74.3, 74.2, 73.7, 73.4, 72.9 (72.99, 72.91), 71.2, 70.9, 70.3 (70.29, 70.27), 69.5, 69.3, 34.4, 29.9, 29.8 (29.84, 29.78), 29.3, 20.4, 20.2, 19.8 (19.82, 19.77). **HRMS** (ESI) m/z: $[M+H]^+$ calcd for $C_{37}H_{42}NO_5$ 580.3057; found 580.3059.

cyclopropyl(phenyl)methanone O-((2R,4R,5R,6R)-4,5-bis(benzyloxy)-6-((benzyloxy)methyl)tetrahydro-2H-pyran-2-yl) oxime (E/Z = 66.7:33.3) (13)

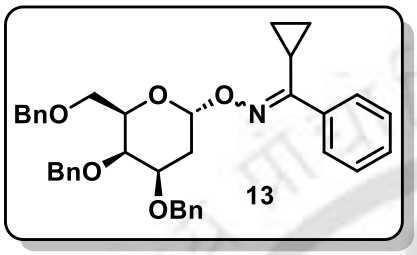

13 was obtained in 84% yield (82 mg), as a colorless oil, R_f = 0.5 (Hexane/EtOAc, 9:1, v/v), **$[\alpha]^{25}_D$** = +29.5 (*c* 0.13, $CHCl_3$). E/Z = 2:1 (15aa exists as an E/Z isomer in a 2:1 ratio). **^{1}H NMR** (600 MHz, $CDCl_3$) δ 7.34 (dddd, *J* = 32.2, 28.2, 16.8, 6.4 Hz, 60H), 5.74 (d, *J* = 3.6 Hz, 2H), 5.61 (d, *J* = 3.8 Hz, 1H), 5.00 (d, *J* = 11.6 Hz, 2H), 4.91 (d, *J* = 11.6 Hz, 1H), 4.73 – 4.67 (m, 6H), 4.62 (d, *J* = 11.7 Hz, 1H), 4.55 (d, *J* = 11.5 Hz, 3H), 4.46 (d, *J* = 12.6 Hz, 5H), 4.05 (d, *J* = 7.2 Hz, 4H), 4.00 (d, *J* = 11.3 Hz, 2H), 3.81 (s, 1H), 3.73 (t, *J* = 8.4 Hz, 2H), 3.69 – 3.61 (m, 5H), 3.45 (d, *J* = 11.2 Hz, 1H), 2.41 (td, *J* = 12.5, 3.8 Hz, 2H), 2.24 (qd, *J* = 12.5, 4.1 Hz, 3H), 2.14 (ddd, *J* = 14.1, 8.6, 5.4 Hz, 2H), 1.94 (dd, *J* = 12.8, 4.4 Hz, 1H), 1.81 (dt, *J* = 10.1, 6.0 Hz, 1H), 0.85 (ddd, *J* = 35.8, 15.1, 7.3 Hz, 8H), 0.61 (d, *J* = 5.2 Hz, 4H). **^{13}C NMR** (151 MHz, $CDCl_3$) δ 162.7, 161.5, 138.9, 138.5, 138.4, 138.3, 138.2, 133.9, 133.5, 128.9, 128.6, 128.5 (128.53, 128.50, 128.47), 128.4 (128.39, 128.37), 128.3, 128.1, 128.0, 127.9, 127.8 (127.80, 127.77), 127.7 (127.72, 127.67), 127.6 (127.64, 127.61), 127.5, 100.2, 99.9, 74.5, 74.4 (74.41, 74.37), 74.3, 73.6 (73.60, 73.58), 73.5, 72.9 (72.98, 72.89), 71.0, 70.8, 70.3, 70.2, 69.4 (69.39, 69.35), 29.9, 29.8, 29.7, 15.5, 9.9, 5.9, 5.80 (5.83, 5.80, 5.76). **HRMS** (ESI) m/z: $[M+H]^+$ calcd for $C_{37}H_{40}NO_5$ 578.2901; found 578.2904.

(E)-1,2-diphenylethan-1-one O-((2R,4R,5R,6R)-4,5-bis(benzyloxy)-6-((benzyloxy)methyl)tetrahydro-2H-pyran-2-yl) oxime (14)

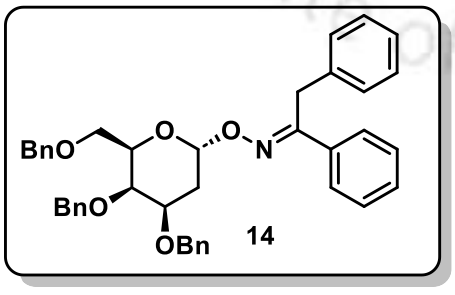

14 was obtained in 80% yield (85 mg), as a colorless oil, R_f = 0.4 (Hexane/EtOAc, 9:1, v/v), **$[\alpha]^{25}_D$** = +23.3 (*c* 0.06, $CHCl_3$). **^{1}H NMR** (600 MHz, $CDCl_3$) δ 7.69 – 7.66 (m, 2H), 7.36 – 7.22 (m, 18H), 7.19 – 7.09 (m, 5H), 5.78 (d, *J* = 3.8 Hz, 1H), 4.91 (d, *J* = 11.6 Hz, 1H), 4.61 (d, *J* = 11.6 Hz, 1H), 4.58 – 4.53 (m, 2H), 4.45 (d, *J* = 11.6 Hz, 1H), 4.36 (d, *J* = 11.6 Hz, 1H), 4.06 (q, *J* = 14.7 Hz, 2H), 3.83 (d, *J* = 2.5 Hz, 1H), 3.73 (ddd, *J* = 12.3, 4.6, 2.4 Hz, 1H), 3.61 – 3.56 (m, 2H), 3.55 – 3.49 (m, 1H), 2.34 (td, *J* = 12.6, 3.9 Hz, 1H), 2.10 (dd, *J* = 12.9, 4.5 Hz, 1H). **^{13}C NMR** (151 MHz, $CDCl_3$) δ 157.7, 139.0, 138.5, 138.3, 137.1, 135.7, 129.5, 128.7, 128.6 (128.59, 128.57), 128.4, 128.3, 128.3,

127.9, 127.8, 127.7, 127.6, 127.5, 126.9, 126.5, 100.7, 74.5, 74.2, 73.4, 72.9, 70.9, 70.3, 69.2, 33.4, 29.9. **HRMS** (ESI) m/z: $[M+H]^+$ calcd for $C_{41}H_{42}NO_5$ 628.3057; found 628.3034.

1,3-diphenylpropan-2-one O-((2R,4R,5R,6R)-4,5-bis(benzyloxy)-6-((benzyloxy)methyl)tetrahydro-2H-pyran-2-yl) oxime (15)

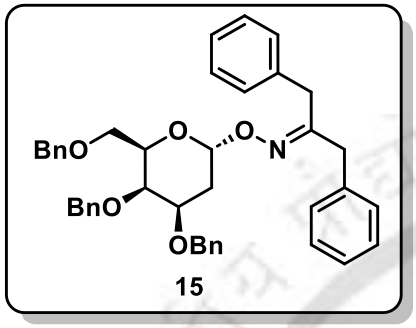

15

15 was obtained in 82% yield (89 mg), as a colorless oil, R_f = 0.4 (Hexane/EtOAc, 9:1, v/v). **^{1}H NMR** (600 MHz, $CDCl_3$) δ 7.26 (dddd, J = 49.8, 37.9, 20.4, 7.6 Hz, 23H), 7.01 (d, J = 6.9 Hz, 2H), 5.72 (d, J = 3.8 Hz, 1H), 4.93 (d, J = 11.6 Hz, 1H), 4.63 (d, J = 11.6 Hz, 1H), 4.60 – 4.48 (m, 3H), 4.42 (d, J = 11.8 Hz, 1H), 3.89 (s, 1H), 3.76 (q, J = 9.1, 6.7 Hz, 2H), 3.67 – 3.59 (m, 2H), 3.53 – 3.42 (m, 4H), 2.34 (td, J = 12.8, 4.1 Hz, 1H), 2.09 (dd, J = 12.9, 4.4 Hz, 1H). **^{13}C NMR** (151 MHz, $CDCl_3$) δ 159.8, 139.0, 138.4, 138.3, 136.7, 136.5, 129.3, 129.0, 128.7, 128.6, 128.5, 128.4 (128.38, 128.36), 128.0, 127.8 (127.81, 127.75), 127.7, 127.5, 126.9, 126.6, 100.0, 74.5, 74.3, 73.6, 72.9, 70.8, 70.3, 69.3, 40.0, 33.5, 29.8. **HRMS** (ESI) m/z: $[M+H]^+$ calcd for $C_{42}H_{44}NO_5$ 642.3214; found 642.3192.

(E)-2,3-dihydro-1H-inden-1-one O-((2R,4R,5R,6R)-4,5-bis(benzyloxy)-6-((benzyloxy)methyl)tetrahydro-2H-pyran-2-yl) oxime (16)

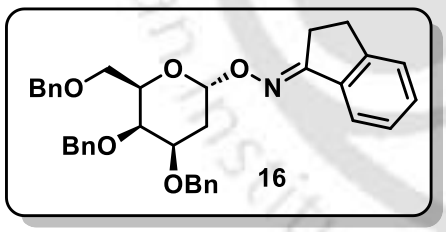

16

16 was obtained in 80% yield (76 mg), as a colorless oil, R_f = 0.4 (Hexane/EtOAc, 9:1, v/v), **$[\alpha]^{25}$D** = +21.7 (*c* 0.09, $CHCl_3$). **^{1}H NMR** (600 MHz, $CDCl_3$) δ 7.74 (d, J = 7.8 Hz, 1H), 7.39 – 7.21 (m, 18H), 5.74 (d, J = 3.2 Hz, 1H), 4.95 (d, J = 11.6 Hz, 1H), 4.65 (d, J = 18.2 Hz, 3H), 4.46 (d, J = 11.5 Hz, 1H), 4.38 (d, J = 11.5 Hz, 1H), 4.02 – 3.92 (m, 3H), 3.68 (t, J = 8.5 Hz, 1H), 3.59 (dd, J = 9.2, 5.4 Hz, 1H), 3.02 (t, J = 6.5 Hz, 2H), 2.84 (qt, J = 13.0, 6.4 Hz, 2H), 2.38 (td, J = 12.6, 3.9 Hz, 1H), 2.17 (dd, J = 12.8, 4.4 Hz, 1H). **^{13}C NMR** (151 MHz, $CDCl_3$) δ 164.6, 148.5, 139.0, 138.5, 138.1, 135.9, 130.7, 128.6, 128.5, 128.4, 128.3, 128.1, 127.8, 127.7 (127.73, 127.65), 127.6, 127.1, 125.6, 122.3, 100.3, 74.6, 73.6, 73.0, 70.9, 70.5, 69.2, 29.9, 28.6, 26.5. **HRMS** (ESI) m/z: $[M+H]^+$ calcd for $C_{36}H_{38}NO_5$ 564.2744; found 564.2736.

9H-fluoren-9-one O-((2R,4R,5R,6R)-4,5-bis(benzyloxy)-6-((benzyloxy)methyl)tetrahydro-2H-pyran-2-yl) oxime (17)

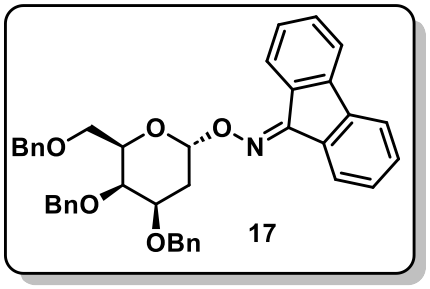

17 was obtained in 83% yield (86 mg), as a colorless oil, R_f = 0.4 (Hexane/EtOAc, 9:1, v/v), **[α]^{25}D** = +32.5 (*c* 0.04, $CHCl_3$). **^{1}H NMR** (600 MHz, $CDCl_3$) δ 7.85 (d, *J* = 7.6 Hz, 1H), 7.79 (d, *J* = 7.5 Hz, 1H), 7.63 (d, *J* = 7.5 Hz, 1H), 7.59 (d, *J* = 7.5 Hz, 1H), 7.45 – 7.16 (m, 19H), 7.10 (t, *J* = 7.5 Hz, 1H), 5.89 (d, *J* = 2.9 Hz, 1H), 4.99 (d, *J* = 11.5 Hz, 1H), 4.70 (d, *J* = 10.9 Hz, 3H), 4.42 (d, *J* = 11.5 Hz, 1H), 4.35 (d, *J* = 11.5 Hz, 1H), 4.06 – 3.96 (m, 3H), 3.68 (t, *J* = 8.5 Hz, 1H), 3.58 (dd, *J* = 9.0, 5.5 Hz, 1H), 2.53 – 2.46 (m, 1H), 2.34 – 2.29 (m, 1H). **^{13}C NMR** (151 MHz, $CDCl_3$) δ 153.6, 141.8, 140.4, 138.9, 138.3, 137.9, 135.4, 131.3, 130.5, 130.3, 128.9, 128.7, 128.4 (128.44, 128.41, 128.39), 128.2, 128.1, 127.9, 127.8, 127.7, 127.6, 122.4, 120.1, 119.9, 101.9, 74.6, 73.6, 73.5, 72.6, 71.0, 69.9, 68.9, 29.8. **HRMS** (ESI) m/z: $[M+H]^+$ calcd for $C_{40}H_{38}NO_5$ 612.2744; found 612.2744.

(E)-3,4-dihydronaphthalen-1(2H)-one O-((2R,4R,5R,6R)-4,5-bis(benzyloxy)-6-((benzyloxy)methyl)tetrahydro-2H-pyran-2-yl) oxime (18)

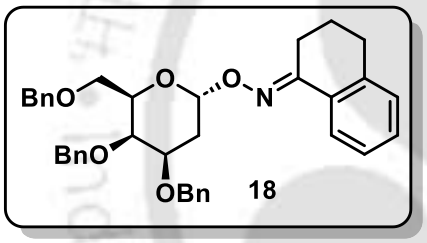

18 was obtained in 81% yield (79 mg), as a colorless oil, R_f = 0.4 (Hexane/EtOAc, 9:1, v/v), **[α]^{25}D** = +40.3 (*c* 0.05, $CHCl_3$). **^{1}H NMR** (600 MHz, $CDCl_3$) δ 8.01 (d, *J* = 7.9 Hz, 1H), 7.39 – 7.21 (m, 16H), 7.17 (t, *J* = 7.5 Hz, 1H), 7.13 (d, *J* = 7.5 Hz, 1H), 5.76 (d, *J* = 3.0 Hz, 1H), 4.96 (d, *J* = 11.6 Hz, 1H), 4.68 – 4.61 (m, 3H), 4.47 (d, *J* = 11.5 Hz, 1H), 4.39 (d, *J* = 11.5 Hz, 1H), 4.00 (s, 1H), 3.98 – 3.92 (m, 2H), 3.71 – 3.65 (m, 1H), 3.59 (dd, *J* = 9.3, 5.4 Hz, 1H), 2.69 (ddd, *J* = 24.0, 18.8, 8.1 Hz, 4H), 2.38 (td, *J* = 12.6, 3.8 Hz, 1H), 2.17 (dd, *J* = 12.7, 4.3 Hz, 1H), 1.82 (p, *J* = 6.3 Hz, 2H). **^{13}C NMR** (151 MHz, $CDCl_3$) δ 155.7, 139.8, 139.0, 138.5, 138.1, 130.5, 129.4, 128.6 (128.62, 128.55), 128.5, 128.4, 128.3, 128.1, 127.8, 127.7 (127.72, 127.65), 127.6, 126.5, 124.9, 100.4, 74.5, 73.6, 73.0, 70.9, 70.5, 69.3, 29.8, 24.5, 21.5. **HRMS** (ESI) m/z: $[M+H]^+$ calcd for $C_{37}H_{40}NO_5$ 578.2901; found 578.2882.

(E)-6-methoxy-3,4-dihydronaphthalen-1(2H)-one O-((2R,4R,5R,6R)-4,5-bis(benzyloxy)-6-((benzyloxy)methyl)tetrahydro-2H-pyran-2-yl) oxime (19)

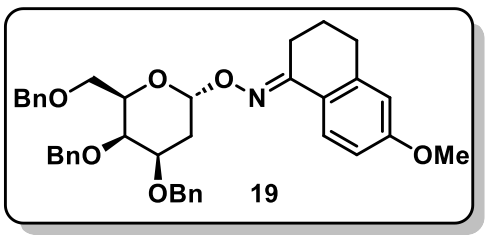

19 was obtained in 82% yield (84 mg), as a colorless oil, R_f = 0.4 (Hexane/EtOAc, 8:2, v/v), **[α]^{25}D** = +89.0 (*c* 0.1, $CHCl_3$). **^{1}H NMR** (600 MHz, $CDCl_3$) δ 7.88 (d, *J* = 8.6 Hz, 1H), 7.31 – 7.16 (m, 15H), 6.65 (d, *J* = 8.6 Hz, 1H), 6.56 (s, 1H), 5.66 (s, 1H), 4.88 (d, *J* = 11.6 Hz, 1H), 4.58 (d, *J* = 12.5 Hz, 3H), 4.40 (d, *J* = 11.6 Hz, 1H), 4.32 (d, *J* = 11.6 Hz, 1H), 3.94 – 3.85 (m,

3H), 3.73 (s, 3H), 3.64 – 3.59 (m, 1H), 3.53 (d, J = 5.2 Hz, 1H), 2.60 (dd, J = 12.7, 5.8 Hz, 4H), 2.30 (s, 1H), 2.10 (s, 1H), 1.77 – 1.72 (m, 2H). **^{13}C NMR** (151 MHz, $CDCl_3$) δ 160.5, 155.5, 141.6, 139.1, 138.5, 138.2, 128.6, 128.5, 128.4, 128.3, 128.1, 127.8, 127.7, 127.6 (127.64, 127.61, 126.60), 123.3, 112.9 (112.94, 112.91), 100.3, 74.6, 74.5, 73.6, 73.1, 70.9, 70.4, 69.3, 55.4, 30.1, 29.8, 24.4, 21.6. **HRMS** (ESI) m/z: $[M+H]^+$ calcd for $C_{38}H_{42}NO_6$ 608.3007; found 608.2987.

(E)-1-(thiophen-2-yl)ethan-1-one O-((2R,4R,5R,6R)-4,5-bis(benzyloxy)-6-((benzyloxy)methyl)tetrahydro-2H-pyran-2-yl) oxime (20)

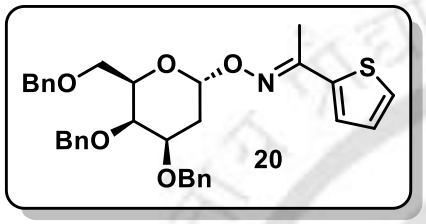

20 was obtained in 81% yield (76 mg), as a colorless oil, R_f = 0.4 (Hexane/EtOAc, 8:2, v/v), **[α]^{25}D** = +31.44 (c 0.26, $CHCl_3$). **^{1}H NMR** (600 MHz, $CDCl_3$) δ 7.39 – 7.22 (m, 17H), 7.01 (dd, J = 5.1, 3.7 Hz, 1H), 5.72 (d, J = 3.7 Hz, 1H), 4.95 (d, J = 11.6 Hz, 1H), 4.67 – 4.60 (m, 3H), 4.48 (d, J = 11.5 Hz, 1H), 4.39 (d, J = 11.5 Hz, 1H), 3.99 (d, J = 2.5 Hz, 1H), 3.97 – 3.91 (m, 2H), 3.68 (dd, J = 9.3, 7.6 Hz, 1H), 3.59 (dd, J = 9.3, 5.4 Hz, 1H), 2.36 (td, J = 12.6, 3.9 Hz, 1H), 2.20 (s, 4H). **^{13}C NMR** (151 MHz, $CDCl_3$) δ 152.1, 140.1, 139.0, 138.4, 138.1, 128.5 (128.54, 128.46), 128.4, 128.3, 128.1, 127.8, 127.7, 127.6 (127.64, 127.59), 127.4, 127.0, 126.8, 100.5, 74.5 (74.50, 74.46), 73.6, 72.9, 71.2, 70.4, 69.2, 29.8, 13.2. **HRMS** (ESI) m/z: $[M+H]^+$ calcd for $C_{33}H_{36}NO_5S$ 558.2309; found 558.2303.

1-phenylethan-1-one O-((4R,5S,6R)-4,5-bis(benzyloxy)-6-((benzyloxy)methyl)tetrahydro-2H-pyran-2-yl) oxime (α/β = 85.7:14.3, α(E/Z) = 6:1) (21)

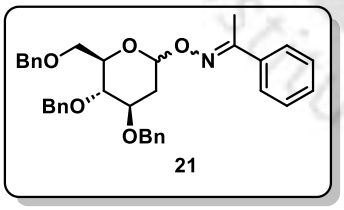

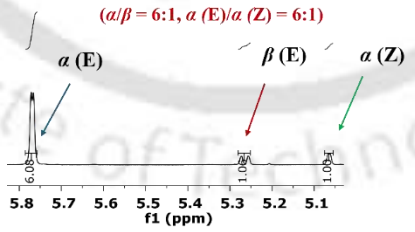

δ 5.77 (d, J = 3.6 Hz, 1H),
5.26 (dd, J = 10.3, 2.0 Hz, 0.16H),
5.06 (d, J = 3.5 Hz, 0.16H).

21 was obtained in 85% yield (80 mg), as a colorless oil, R_f = 0.4 (Hexane/EtOAc, 9:1, v/v), **[α]^{25}D** = +50.0 (c 0.08, $CHCl_3$), (α/β = 85.7:14.3, α(E/Z) = 6:1, anomeric ratio and E and Z ratio are confirmed by the ^{1}H NMR and NOE experiments**). ^{1}H NMR** (600 MHz, $CDCl_3$) δ 7.70 – 7.63 (m, 15H), 7.39 – 7.24 (m, 130H), 7.21 – 7.16 (m, 16H), 5.77 (d, J = 3.6 Hz, 6H), 5.26 (dd, J = 10.3, 2.0 Hz, 1H), 5.06 (d, J = 3.5 Hz, 1H), 4.90 (t, J = 11.2 Hz, 8H), 4.73 – 4.63 (m, 24H), 4.56 (d, J = 10.7 Hz, 8H), 4.51 – 4.43 (m, 8H), 4.07 – 3.98 (m, 8H), 3.84 – 3.73 (m, 24H), 3.68 (td, J = 10.6, 10.0, 3.2 Hz, 8H), 3.56 (ddd, J = 9.7, 4.3, 2.3 Hz, 1H), 2.50 – 2.44 (m, 7H), 2.35 – 2.32 (m, 1H), 2.28 (s, 3H), 2.22 (s,

19H), 1.92 – 1.86 (m, 7H), 1.77 (dd, *J* = 12.3, 3.5 Hz, 1H). **^{13}C NMR** (151 MHz, $CDCl_3$) *δ* 157.1, 156.5, 155.6, 138.8, 138.7, 138.6, 138.5 (138.54, 138.50, 138.45), 138.4, 138.3 (138.30, 138.26), 137.8, 136.4, 136.3, 129.5, 128.7, 128.6 (128.59, 128.55), 128.5 (128.51, 128.49), 128.4, 128.3, 128.2 (128.19, 128.15), 128.1 (128.10, 128.06), 128.0, 127.9, 127.8 (127.83, 127.81, 127.77, 127.75), 127.7, 127.1, 126.5, 126.4, 101.8, 99.9 (99.95, 96.92), 79.6, 78.4, 78.3, 77.9 (77.93, 77.85), 77.7, 75.5, 75.3, 75.2, 75.1, 73.6 (73.61, 73.58), 71.9 (71.96, 71.89), 71.7, 71.1, 68.9 (68.99, 68.95), 68.8, 65.5, 35.6, 35.2, 34.3, 13.8, 13.0. **HRMS** (ESI) m/z: $[M+H]^+$ calcd for $C_{35}H_{38}NO_5$ 552.2745; found 552.2742.

1-(p-tolyl)ethan-1-one O-((4R,5S,6R)-4,5-bis(benzyloxy)-6-((benzyloxy)methyl)tetrahydro-2H-pyran-2-yl) oxime (*α*/*β* = 83.3:16.6, *α*(E/Z) = 4:1) (22)

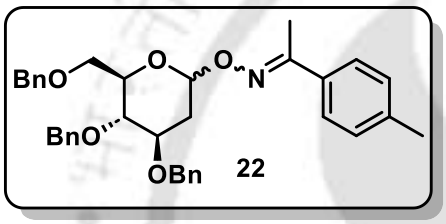

22 was obtained in 87% yield (84 mg), as a colorless oil, R_f = 0.5 (Hexane/EtOAc, 9:1, v/v), **$[\alpha]^{25}_D$** = +71.3 (*c* 0.10, $CHCl_3$), (*α*/*β* = 83.3:16.6, *α*(E/Z) = 4:1). **^{1}H NMR** (600 MHz, $CDCl_3$) *δ* 7.55 (dd, *J* = 13.7, 8.0 Hz, 11H), 7.40 – 7.21 (m, 96H), 7.21 – 7.13 (m, 25H), 5.75 (d, *J* = 3.6 Hz, 5H), 5.25 (dd, *J* = 10.3, 2.0 Hz, 1H), 5.06 (d, *J* = 3.5 Hz, 1H), 4.90 (t, *J* = 10.2 Hz, 7H), 4.74 – 4.63 (m, 21H), 4.57 – 4.43 (m, 14H), 4.02 (dddd, *J* = 16.7, 11.5, 8.9, 5.0 Hz, 6H), 3.85 – 3.71 (m, 20H), 3.70 – 3.62 (m, 8H), 3.56 (ddd, *J* = 9.7, 4.3, 2.1 Hz, 1H), 2.50 – 2.42 (m, 6H), 2.35 (s, 18H), 2.26 (s, 3H), 2.20 (s, 14H), 1.92 – 1.82 (m, 6H), 1.78 – 1.74 (m, 1H). **^{13}C NMR** (151 MHz, $CDCl_3$) *δ* 157.0, 156.5, 139.6, 138.8, 138.7, 138.6, 138.5 (138.54, 138.49), 138.4 (138.44, 138.36), 138.3 (138.30, 138.25), 137.8, 133.5, 133.4, 129.2 (129.21, 129.17), 128.6, 128.5 (128.53, 128.50, 128.48, 128.46), 128.4, 128.2 (128.24, 128.15), 128.1 (128.11, 128.05), 128.0, 127.9, 127.8 (127.81, 127.80, 127.75), 127.7 (127.67, 127.65), 126.4, 126.3, 101.7, 99.9, 96.9, 79.6, 78.4, 78.3, 77.9 (77.94, 77.84), 77.7, 75.4, 75.3, 75.2, 75.1, 73.6 (73.60, 73.56), 73.5, 71.9 (71.96, 71.93), 71.8, 71.7, 71.1, 35.6, 35.2, 34.3, 22.8, 21.4, 14.3, 13.7, 12.9. **HRMS** (ESI) m/z: $[M+H]^+$ calcd for $C_{36}H_{40}NO_5$ 566.2901; found 566.2900.

(E)-1-(4-methoxyphenyl)ethan-1-one O-((4R,5S,6R)-4,5-bis(benzyloxy)-6-((benzyloxy)methyl)tetrahydro-2H-pyran-2-yl) oxime (*α*/*β* = 3:1) (23)

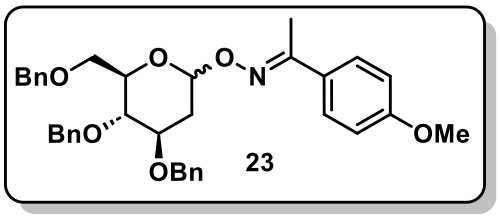

23 was obtained in 88% yield (87 mg), as a colorless oil, R_f = 0.5 (Hexane/EtOAc, 8:2, v/v), **$[\alpha]^{25}_D$** = +77.0 (*c* 0.10, $CHCl_3$), (*α*/*β* = 3:1). **^{1}H NMR** (600 MHz, $CDCl_3$) *δ* 7.61 (dd, *J* = 12.3, 8.5 Hz, 8H), 7.39 – 7.24 (m, 53H), 7.19 (d, *J* = 7.1 Hz, 8H), 6.87 (dd, *J* = 8.9, 2.6 Hz, 8H), 5.75 (d, *J* = 3.6 Hz, 3H), 5.24 (dd, *J* = 10.4,

2.0 Hz, 1H), 4.91 (d, *J* = 10.7 Hz, 4H), 4.70 (q, *J* = 11.5 Hz, 7H), 4.64 (d, *J* = 12.3 Hz, 5H), 4.55 (dd, *J* = 12.0, 5.2 Hz, 5H), 4.49 (d, *J* = 12.1 Hz, 3H), 4.01 (ddd, *J* = 11.7, 8.7, 5.0 Hz, 3H), 3.84 – 3.72 (m, 25H), 3.70 – 3.62 (m, 5H), 3.58 – 3.54 (m, 1H), 2.46 (td, *J* = 13.2, 12.4, 4.6 Hz, 4H), 2.25 (s, 3H), 2.19 (s, 9H), 1.88 (td, *J* = 12.4, 3.6 Hz, 5H). **^{13}C NMR** (151 MHz, $CDCl_3$) *δ* 160.7, 156.6, 156.1, 138.7, 138.6, 138.5 (138.50, 138.45), 138.4, 138.3, 128.8, 128.6, 128.5 (128.54, 128.51, 128.49), 128.4, 128.3, 128.2, 128.1, 127.9 (127.90, 127.87), 127.8 (127.84, 127.81, 127.76), 127.7 (127.68, 127.67), 113.9, 113.8, 101.7, 99.8, 79.6, 78.3, 77.9, 77.7, 75.4, 75.3, 75.1, 73.6 (73.57, 73.55), 71.9, 71.8, 71.7, 69.0, 68.8, 55.5, 35.2, 34.3, 13.6, 12.9. **HRMS** (ESI) m/z: $[M+H]^+$ calcd for $C_{36}H_{40}NO_6$ 582.2850; found 582.2846.

(E)-1-(4-fluorophenyl)ethan-1-one O-((4R,5S,6R)-4,5-bis(benzyloxy)-6-((benzyloxy)methyl)tetrahydro-2H-pyran-2-yl) oxime (*α*/*β* = 85.7:14.3) (24)

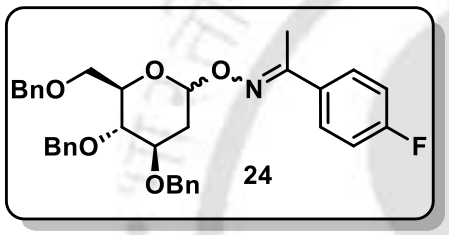

24 was obtained in 80% yield (77 mg), as a colorless oil, R_f = 0.5 (Hexane/EtOAc, 9:1, v/v), **$[\alpha]^{25}_D$** = +63.4 (*c* 0.05, $CHCl_3$), (*α*/*β* = 85.7:14.3). **^{1}H NMR** (600 MHz, $CDCl_3$) *δ* 7.65 (dd, *J* = 8.7, 5.4 Hz, 13H), 7.39 – 7.25 (m, 93H), 7.21 – 7.16 (m, 14H), 7.03 (td, *J* = 8.7, 3.0 Hz, 13H), 5.75 (d, *J* = 3.7 Hz, 6H), 5.24 (dd, *J* = 10.2, 2.0 Hz, 1H), 4.91 (d, *J* = 10.6 Hz, 7H), 4.73 – 4.62 (m, 21H), 4.56 (d, *J* = 10.4 Hz, 7H), 4.49 (d, *J* = 12.1 Hz, 7H), 4.00 (ddd, *J* = 11.6, 8.6, 5.0 Hz, 6H), 3.83 – 3.72 (m, 21H), 3.70 – 3.63 (m, 7H), 3.58 – 3.53 (m, 1H), 2.45 (dd, *J* = 13.2, 5.0 Hz, 7H), 2.26 (s, 3H), 2.20 (s, 18H), 1.89 (td, *J* = 12.4, 3.7 Hz, 7H).**^{13}C NMR** (151 MHz, $CDCl_3$) *δ* 164.5, 162.8, 156.0, 155.5, 138.7, 138.5, 138.4, 138.3 (138.32, 138.25), 132.4, 132.3, 128.7, 128.6 (128.59, 128.55), 128.5, 128.4 (128.43, 128.37), 128.3 (128.34, 128.28, 128.25), 128.2, 128.1 (128.09, 128.06), 128.0, 127.9, 127.8 (127.83, 127.79, 127.75), 127.7 (127.72, 127.70), 127.1, 115.6, 115.5, 115.4 (115.42, 115.38), 101.7, 99.9, 79.6, 78.2, 77.9, 77.6, 75.4, 75.3, 73.6 (73.58, 73.55), 71.9 (71.96, 71.89), 68.9, 68.8, 35.1, 34.3, 13.7, 13.0. **HRMS** (ESI) m/z: $[M+H]^+$ calcd for $C_{35}H_{37}FNO_5$ 570.2650; found 570.2630.

(E)-1-(4-nitrophenyl)ethan-1-one O-((4R,5S,6R)-4,5-bis(benzyloxy)-6-((benzyloxy)methyl)tetrahydro-2H-pyran-2-yl) oxime (*α*/*β* = 80:10) (25)

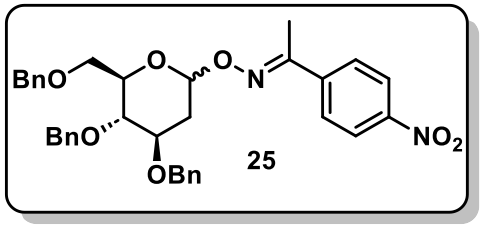

25 was obtained in 79% yield (80 mg), as a colorless oil, R_f = 0.5 (Hexane/EtOAc, 8:2, v/v), **$[\alpha]^{25}_D$** = +95.0 (*c* 0.04, $CHCl_3$), (*α*/*β* = 80:10). **^{1}H NMR** (600 MHz, $CDCl_3$) *δ* 8.24 – 8.16 (m, 18H), 7.86 – 7.79 (m, 18H), 7.40 – 7.23 (m, 118H), 7.19 (d, *J* = 7.0 Hz, 17H), 5.81 – 5.76 (m, 8H), 5.29 (d,

J = 10.3 Hz, 1H), 4.91 (d, *J* = 10.6 Hz, 9H), 4.75 – 4.68 (m, 17H), 4.63 (d, *J* = 12.0 Hz, 10H), 4.56 (d, *J* = 10.7 Hz, 10H), 4.50 (d, *J* = 12.1 Hz, 8H), 4.00 (dt, *J* = 12.4, 6.6 Hz, 8H), 3.83 – 3.72 (m, 26H), 3.68 (d, *J* = 10.0 Hz, 10H), 3.59 – 3.55 (m, 1H), 2.46 (dd, *J* = 13.3, 5.0 Hz, 9H), 2.31 (dd, *J* = 4.5, 1.6 Hz, 3H), 2.25 (d, *J* = 1.7 Hz, 24H), 1.92 (td, *J* = 12.3, 11.9, 3.7 Hz, 9H). **^{13}C NMR** (151 MHz, $CDCl_3$) *δ* 154.6, 148.3, 142.2, 138.6, 138.4, 138.2, 128.6 (128.61, 128.57), 128.5 (128.54, 128.52, 128.46), 128.3, 128.2, 128.1, 127.9 (127.91, 127.86), 127.8 (127.84, 127.78), 127.3, 127.2, 123.7, 102.0, 100.5, 79.4, 78.1, 77.8, 77.4, 75.5, 75.4, 75.1, 73.6 (73.60, 73.57), 72.1, 72.0, 71.8, 68.9, 68.8, 35.0, 34.1, 13.4, 12.8. **HRMS** (ESI) m/z: $[M+H]^+$ calcd for $C_{35}H_{37}N_2O_7$ 597.2595; found 597.2607.

diphenylmethanone O-((2R,4R,5S,6R)-4,5-bis(benzyloxy)-6-((benzyloxy)methyl)tetrahydro-2H-pyran-2-yl) oxime (26)

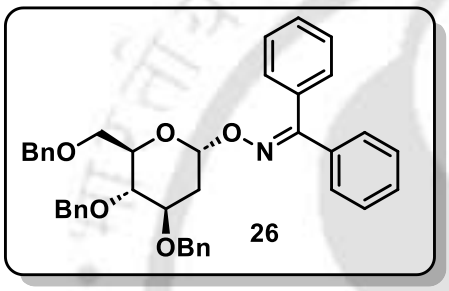

26 was obtained in 82% yield (86 mg), as a colorless oil, R_f = 0.5 (Hexane/EtOAc, 9:1, v/v), **$[\alpha]^{25}_D$** = +36.1 (*c* 0.10, $CHCl_3$). **^{1}H NMR** (600 MHz, $CDCl_3$) *δ* 7.52 – 7.48 (m, 2H), 7.40 – 7.23 (m, 21H), 7.18 – 7.14 (m, 2H), 5.74 (d, *J* = 3.7 Hz, 1H), 4.83 (d, *J* = 10.8 Hz, 1H), 4.64 (d, *J* = 12.1 Hz, 1H), 4.56 – 4.48 (m, 4H), 3.78 (dd, *J* = 10.7, 2.9 Hz, 1H), 3.71 – 3.59 (m, 4H), 2.25 (dd, *J* = 13.1, 4.6 Hz, 1H), 1.79 (ddd, *J* = 13.5, 10.9, 3.9 Hz, 1H). **^{13}C NMR** (151 MHz, $CDCl_3$) *δ* 158.7, 138.6 (138.62, 138.57), 138.3, 136.2, 133.1, 129.7, 129.2, 129.0, 128.5 (128.50, 128.48), 128.4 (128.43, 128.42, 128.37), 128.3, 128.2, 128.1 (128.12, 128.10, 128.08), 127.9, 127.7 (127.73, 127.70, 127.66), 100.3, 78.2, 74.9, 73.5, 72.1, 71.9, 68.8, 34.2. **HRMS** (ESI) m/z: $[M+H]^+$ calcd for $C_{40}H_{40}NO_5$ 614.2901; found 614.2900.

(E)-4-methylbenzaldehyde O-((2R,4R,5R,6R)-4,5-bis(benzyloxy)-6-((benzyloxy)methyl)tetrahydro-2H-pyran-2-yl) oxime (27)

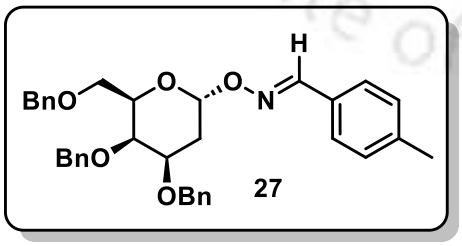

27 was obtained in 85% yield (80 mg), as a white foam, R_f = 0.4 (Hexane/EtOAc, 9:1, v/v), **$[\alpha]^{25}_D$** = +86.0 (*c* 0.10, $CHCl_3$). **^{1}H NMR** (600 MHz, $CDCl_3$) *δ* 8.07 (s, 1H), 7.50 (d, *J* = 7.9 Hz, 2H), 7.37 – 7.23 (m, 15H), 7.17 (d, *J* = 7.8 Hz, 2H), 5.72 (d, *J* = 3.8 Hz, 1H), 4.95 (d, *J* = 11.5 Hz, 1H), 4.64 (d, *J* = 17.2 Hz, 3H), 4.47 (d, *J* = 11.6 Hz, 1H), 4.38 (d, *J* = 11.6 Hz, 1H), 4.02 – 3.93 (m, 3H), 3.67 (dd, *J* = 9.3, 7.6 Hz, 1H), 3.58 (dd, *J* = 9.3, 5.4 Hz, 1H), 2.37 (s, 4H), 2.15 (dd, *J* = 13.0, 4.6 Hz, 1H). **^{13}C NMR** (151 MHz, $CDCl_3$) *δ* 150.6, 140.6, 139.0, 138.6, 138.1, 129.6, 129.2, 128.6, 128.5, 128.4 (128.38, 128.36), 128.1, 127.8, 127.7 (127.72, 127.67),

127.5 (127.49, 127.45), 100.4, 74.6 (74.64, 74.56), 73.6, 72.9, 70.7, 70.5, 69.2, 29.8, 21.6. **HRMS** (ESI) m/z: $[M+H]^+$ calcd for $C_{35}H_{38}NO_5$ 552.2744; found 552.2747.

(E)-4-chlorobenzaldehyde O-((2R,4R,5R,6R)-4,5-bis(benzyloxy)-6-((benzyloxy)methyl)tetrahydro-2H-pyran-2-yl) oxime (28)

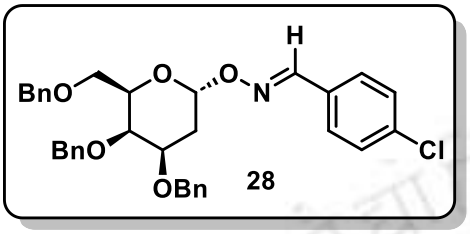

28 was obtained in 82% yield (79 mg), as a white solid, R_f = 0.4 (Hexane/EtOAc, 9:1, v/v), **$[\alpha]^{25}_D$** = +95.4 (*c* 0.04, $CHCl_3$). **^{1}H NMR** (600 MHz, $CDCl_3$) δ 8.06 (s, 1H), 7.57 – 7.51 (m, 2H), 7.39 – 7.19 (m, 17H), 5.72 (d, *J* = 3.8 Hz, 1H), 4.95 (d, *J* = 11.5 Hz, 1H), 4.65 (d, *J* = 17.2 Hz, 3H), 4.47 (d, *J* = 11.6 Hz, 1H), 4.38 (d, *J* = 11.6 Hz, 1H), 4.03 – 3.90 (m, 3H), 3.66 (dd, *J* = 9.4, 7.5 Hz, 1H), 3.58 (dd, *J* = 9.3, 5.5 Hz, 1H), 2.38 (td, *J* = 12.6, 4.0 Hz, 1H), 2.15 (dd, *J* = 13.0, 4.6 Hz, 1H). **^{13}C NMR** (151 MHz, $CDCl_3$) δ 149.4, 138.9, 138.5, 138.1, 136.2, 130.5, 129.1, 128.7, 128.6, 128.5, 128.4 (128.39, 128.36), 128.0, 127.8, 127.7 (127.74, 127.70), 127.4, 100.6, 74.6, 74.5, 73.6, 72.9, 70.9, 70.5, 69.2, 29.7. **HRMS** (ESI) m/z: $[M+Na]^+$ calcd for $C_{34}H_{34}ClNNaO_5$ 594.2018; found 594.2035.

(E)-4-nitrobenzaldehyde O-((2R,4R,5R,6R)-4,5-bis(benzyloxy)-6-((benzyloxy)methyl)tetrahydro-2H-pyran-2-yl) oxime (29)

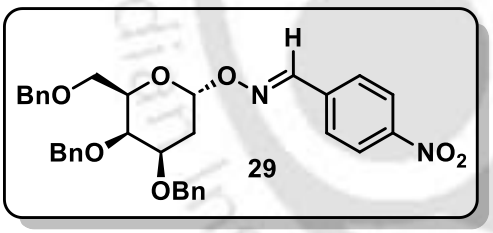

29 was obtained in 84% yield (83 mg), as a white foam, R_f = 0.4 (Hexane/EtOAc, 8:2, v/v), **$[\alpha]^{25}_D$** = +57.3 (*c* 0.06, $CHCl_3$). **^{1}H NMR** (600 MHz, $CDCl_3$) δ 8.22 – 8.19 (m, 2H), 8.15 (s, 1H), 7.76 (d, *J* = 8.5 Hz, 2H), 7.41 – 7.19 (m, 15H), 5.77 (d, *J* = 3.9 Hz, 1H), 4.96 (d, *J* = 11.5 Hz, 1H), 4.69 – 4.61 (m, 3H), 4.47 (d, *J* = 11.6 Hz, 1H), 4.38 (d, *J* = 11.6 Hz, 1H), 4.03 – 3.91 (m, 3H), 3.65 (dd, *J* = 9.3, 7.3 Hz, 1H), 3.59 (dd, *J* = 9.3, 5.6 Hz, 1H), 2.41 (td, *J* = 12.7, 4.0 Hz, 1H), 2.17 (dd, *J* = 13.0, 4.7 Hz, 1H). **^{13}C NMR** (151 MHz, $CDCl_3$) δ 148.6, 148.3, 138.8, 138.4, 138.0, 137.9, 128.6, 128.5, 128.4 (128.40, 128.36), 128.1, 128.0, 127.9, 127.8 (127.79, 127.76), 127.7, 127.4, 124.1 (124.13, 124.06), 101.1, 74.6, 74.3, 73.6, 72.7, 71.1, 70.5, 69.2, 29.6. **HRMS** (ESI) m/z: $[M+NH_4]^+$ calcd for $C_{34}H_{38}N_3O_7$ 600.2704; found 600.2724.

(E)-[1,1'-biphenyl]-4-carbaldehyde O-((2R,4R,5R,6R)-4,5-bis(benzyloxy)-6-((benzyloxy)methyl)tetrahydro-2H-pyran-2-yl) oxime (30)

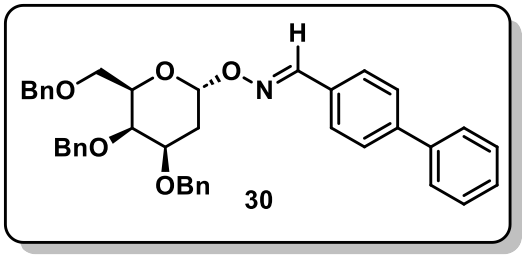

30

30 was obtained in 85% yield (88 mg), as a white foam, R_f = 0.4 (Hexane/EtOAc, 9:1, v/v), **[α]^{25}D** = +85.0 (*c* 0.04, $CHCl_3$). **^{1}H NMR** (600 MHz, $CDCl_3$) δ 8.14 (s, 1H), 7.68 (d, *J* = 8.1 Hz, 2H), 7.64 – 7.58 (m, 4H), 7.45 (t, *J* = 7.6 Hz, 2H), 7.40 – 7.20 (m, 16H), 5.76 (d, *J* = 3.8 Hz, 1H), 4.96 (d, *J* = 11.5 Hz, 1H), 4.65 (d, *J* = 16.1 Hz, 3H), 4.48 (d, *J* = 11.6 Hz, 1H), 4.39 (d, *J* = 11.6 Hz, 1H), 4.06 – 3.93 (m, 3H), 3.68 (dd, *J* = 9.4, 7.5 Hz, 1H), 3.60 (dd, *J* = 9.4, 5.4 Hz, 1H), 2.39 (td, *J* = 12.6, 4.0 Hz, 1H), 2.18 (dd, *J* = 13.0, 4.6 Hz, 1H). **^{13}C NMR** (151 MHz, $CDCl_3$) δ 150.3, 143.0, 140.4, 138.9, 138.6, 138.1, 130.9, 129.0, 128.6, 128.5, 128.4 (128.39, 128.36), 128.1, 127.9 (127.98, 127.89, 127.87), 127.8, 127.7 (127.73, 127.69), 127.6 (127.58, 127.56), 127.5 (127.48, 127.45), 127.2, 100.5, 74.6 (74.61, 74.56), 73.6, 72.9, 70.8, 70.5, 69.3, 29.8. **HRMS** (ESI) m/z: $[M+H]^+$ calcd for $C_{40}H_{40}NO_5$ 614.2901; found 614.2914.

(3S,8S,9S,10R,13S,14S,17R)-17-((E)-1-((((2R,4R,5R,6R)-4,5-bis(benzyloxy)-6-((benzyloxy)methyl)tetrahydro-2H-pyran-2-yl)oxy)imino)ethyl)-10,13-dimethyl-2,3,4,7,8,9,10,11,12,13,14,15,16,17-tetradecahydro-1H-cyclopenta[a]phenanthren-3-yl acetate (31)

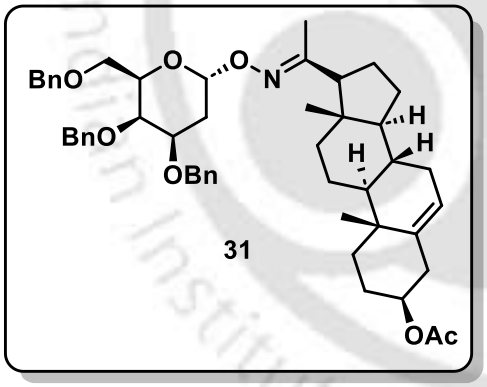

31

31 was obtained in 82% yield (110 mg), as a white foam, R_f = 0.4 (Hexane/EtOAc, 9:1, v/v), **[α]^{25}D** = +6.25 (*c* 0.12, $CHCl_3$). **^{1}H NMR** (600 MHz, $CDCl_3$) δ 7.36 – 7.23 (m, 15H), 5.61 (d, *J* = 2.9 Hz, 1H), 5.37 (d, *J* = 5.4 Hz, 1H), 4.94 (d, *J* = 11.6 Hz, 1H), 4.65 – 4.58 (m, 4H), 4.48 (d, *J* = 11.6 Hz, 1H), 4.41 (d, *J* = 11.7 Hz, 1H), 3.96 (d, *J* = 2.6 Hz, 1H), 3.93 – 3.85 (m, 2H), 3.65 (dd, *J* = 9.3, 7.5 Hz, 1H), 3.56 (dd, *J* = 9.3, 5.5 Hz, 1H), 2.30 (td, *J* = 12.5, 3.9 Hz, 3H), 2.22 – 2.08 (m, 3H), 2.06 – 1.96 (m, 4H), 1.86 (ddt, *J* = 10.0, 7.4, 3.3 Hz, 3H), 1.78 (s, 3H), 1.66 – 1.57 (m, 5H), 1.44 (tdd, *J* = 19.3, 10.3, 5.7 Hz, 3H), 1.14 (td, *J* = 14.5, 4.7 Hz, 3H), 1.03 – 0.97 (m, 4H), 0.61 (s, 3H). **^{13}C NMR** (151 MHz, $CDCl_3$) δ 170.7, 159.3, 139.8, 139.1, 138.6, 138.3, 128.5 (128.53, 128.48), 128.3 (128.34, 128.26), 127.9, 127.8, 127.7, 127.6 (127.59, 127.56, 122.60), 99.6, 74.7, 74.4, 74.0, 73.5, 73.1, 70.8, 70.4, 69.44 56.8, 56.2, 50.2, 43.9, 38.7, 38.2, 37.1, 36.8, 32.1, 31.9, 30.0, 29.8, 27.9, 24.4, 23.2, 21.6, 21.1, 19.5, 15.9, 13.3. **HRMS** (ESI) m/z: $[M+H]^+$ calcd for $C_{50}H_{64}NO_7$ 790.4677; found 790.4657.

(S)-N-(4-((E)-1-((((2R,4R,5R,6R)-4,5-bis(benzyloxy)-6-((benzyloxy)methyl)tetrahydro-2H-pyran-2-yl)oxy)imino)ethyl)phenyl)-2-(4-isobutylphenyl)propanamide (32)

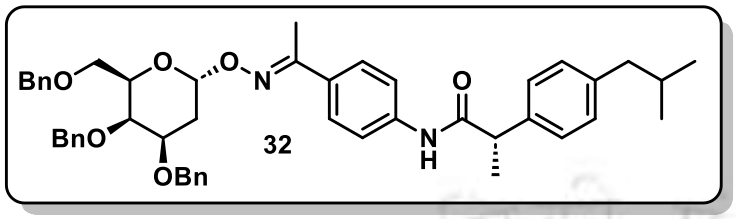

32 was obtained in 81% yield (103 mg), as a white foam, R_f = 0.6 (Hexane/EtOAc, 7:3, v/v), **[α]^{25}D** = +68.1 (*c* 0.16, $CHCl_3$). **^{1}H NMR** (600 MHz, $CDCl_3$) δ 7.49 (d, *J* = 8.5 Hz, 2H), 7.33 (dd, *J* = 8.6, 3.9 Hz, 2H), 7.27 (d, *J* = 7.0 Hz, 6H), 7.22 (t, *J* = 7.3 Hz, 3H), 7.19 – 7.14 (m, 7H), 7.10 – 7.04 (m, 3H), 5.65 (d, *J* = 3.7 Hz, 1H), 4.88 (d, *J* = 11.6 Hz, 1H), 4.59 – 4.51 (m, 3H), 4.38 (d, *J* = 11.5 Hz, 1H), 4.30 (d, *J* = 11.6 Hz, 1H), 3.91 (s, 1H), 3.87 (ddd, *J* = 9.4, 4.5, 2.0 Hz, 2H), 3.60 (dt, *J* = 15.9, 7.7 Hz, 2H), 3.50 (dd, *J* = 9.2, 5.4 Hz, 1H), 2.40 (d, *J* = 7.2 Hz, 2H), 2.29 (td, *J* = 12.6, 3.9 Hz, 1H), 2.06 (s, 4H), 1.79 (dq, *J* = 13.5, 6.7 Hz, 1H), 1.50 (dd, *J* = 7.1, 5.3 Hz, 3H), 0.83 (d, *J* = 6.6 Hz, 6H). **^{13}C NMR** (151 MHz, $CDCl_3$) δ 172.7, 155.6, 141.3, 139.0, 138.4, 138.1 (138.08, 138.05), 138.0, 131.9, 130.0, 128.5 (128.54, 128.46), 128.4, 128.3, 128.1, 127.8, 127.7, 127.6 (127.63, 127.59, 127.55), 127.5, 127.1, 119.2, 100.3, 74.5 (74.52, 74.49), 73.6, 73.0, 47.9, 45.1, 30.3, 29.9, 22.5, 18.7, 12.7. **HRMS** (ESI) m/z: $[M+H]^+$ calcd for $C_{48}H_{55}N_2O_6$ 755.4055; found 755.4033.

(3aR,5S,6aR,Z)-5-((R)-2,2-dimethyl-1,3-dioxolan-4-yl)-2,2-dimethyldihydrofuro[2,3-d][1,3]dioxol-6(5H)-one O-((2R,4R,5R,6R)-4,5-bis(benzyloxy)-6-((benzyloxy)methyl)tetrahydro-2H-pyran-2-yl) oxime (33Z)

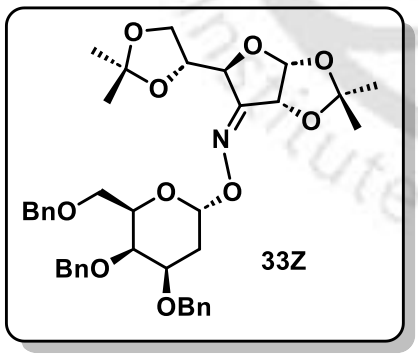

33 (33Z and 33E) was obtained in 85% yield (99 mg), as a white foam, R_f = 0.3 (Hexane/EtOAc, 8:2, v/v), 33Z: **[α]^{25}D** = +64.4 (*c* 0.10, $CHCl_3$). **^{1}H NMR** (600 MHz, $CDCl_3$) δ 7.36 – 7.24 (m, 15H), 5.97 (d, *J* = 4.5 Hz, 1H), 5.66 (d, *J* = 3.7 Hz, 1H), 5.11 (dd, *J* = 4.5, 1.4 Hz, 1H), 4.94 (d, *J* = 11.6 Hz, 1H), 4.82 (t, *J* = 1.9 Hz, 1H), 4.67 – 4.60 (m, 3H), 4.42 (d, *J* = 11.7 Hz, 1H), 4.40 – 4.35 (m, 2H), 4.17 (dd, *J* = 8.0, 5.4 Hz, 1H), 4.01 – 3.92 (m, 4H), 3.62 (t, *J* = 8.5 Hz, 1H), 3.50 (dd, *J* = 8.9, 5.3 Hz, 1H), 2.36 (td, *J* = 12.6, 3.9 Hz, 1H), 2.09 (dd, *J* = 12.9, 4.5 Hz, 1H), 1.36 (d, *J* = 3.5 Hz, 9H), 1.33 (s, 3H). **^{13}C NMR** (151 MHz, $CDCl_3$) δ 159.8, 138.9, 138.5, 138.1, 128.5, 128.4 (128.44, 128.42, 128.37), 128.1, 127.8, 127.7 (127.72, 127.69), 127.6, 113.6, 110.0, 104.9, 100.8, 77.7 (77.74, 77.67), 75.9, 74.5 (74.53, 74.51), 73.5, 72.8, 70.6, 68.9, 64.4, 29.7, 27.7, 27.4, 26.3, 25.4. **HRMS** (ESI) m/z: $[M+NH_4]^+$ calcd for $C_{39}H_{51}N_2O_{10}$ 707.3539; found 707.3515.

4-chlorobenzaldehyde O-((2R,4R,5S,6R)-4,5-bis((4-methylbenzyl)oxy)-6-(((4-methylbenzyl)oxy)methyl)tetrahydro-2H-pyran-2-yl) oxime (*α*/*β* = 88.9:11.1, *α*(E/Z) = 3:1) (34)

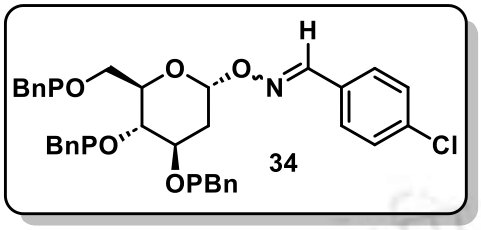

34 was obtained in 85% yield (89 mg), as a white foam, R_f = 0.4 (Hexane/EtOAc, 9:1, v/v), **[α]$^{25}_D$** = +87.5 (*c* 0.04, $CHCl_3$), (*α*/*β* = 88.9:11.1, *α*(E/Z) = 3:1). **^{1}H NMR** (600 MHz, $CDCl_3$) *δ* 8.11 (s, 1H), 8.04 (s, 8H), 7.53 (d, *J* = 8.5 Hz, 18H), 7.36 – 7.31 (m, 18H), 7.26 – 7.03 (m, 156H), 5.70 (dd, *J* = 3.8, 1.4 Hz, 8H), 5.21 (dd, *J* = 10.3, 2.0 Hz, 1H), 5.03 (d, *J* = 3.4 Hz, 3H), 4.83 (t, *J* = 10.2 Hz, 12H), 4.65 – 4.58 (m, 36H), 4.48 – 4.39 (m, 24H), 4.02 – 3.93 (m, 12H), 3.81 – 3.73 (m, 24H), 3.70 – 3.58 (m, 24H), 2.40 (dd, *J* = 13.3, 6.6 Hz, 9H), 2.34 – 2.30 (m, 101H), 1.85 (ddd, *J* = 13.3, 11.6, 3.9 Hz, 9H), 1.73 – 1.70 (m, 3H). **^{13}C NMR** (151 MHz, $CDCl_3$) *δ* 149.9, 149.6, 137.5, 137.4 (137.43, 137.42, 137.40, 137.36), 137.3, 136.3, 135.9, 135.7 (135.71, 135.67), 135.6, 135.2 (135.24, 135.17), 134.8, 130.4, 129.3, 129.2 (129.23, 129.17, 129.16), 129.1 (129.14, 129.11), 128.8, 128.7, 128.3 (128.32, 128.27), 128.2, 128.0, 127.9 (127.90, 127.88), 101.8, 100.1, 96.8, 78.2, 77.9, 77.8, 77.7, 77.3, 75.0, 74.9, 73.5, 73.4 (73.43, 73.39), 71.9 (71.91, 71.87), 71.8, 71.1, 68.8, 68.7, 68.5, 35.6, 33.9, 21.3 (21.32, 21.30), 21.3. **HRMS** (ESI) m/z: $[M+Na]^+$ calcd for $C_{37}H_{40}ClNNaO_5$ 636.2487; found 636.2498.

(E)-4-chlorobenzaldehyde O-((2R,4R,5S,6R)-4,5-dimethoxy-6-(methoxymethyl)tetrahydro-2H-pyran-2-yl) oxime (35)

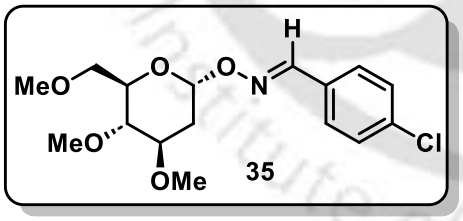

35 was obtained in 82% yield (48 mg), as a white foam, R_f = 0.5 (Hexane/EtOAc, 7:3, v/v), **[α]$^{25}_D$** = +51.1 (*c* 0.17, $CHCl_3$). **^{1}H NMR** (600 MHz, $CDCl_3$) *δ* 8.08 (s, 1H), 7.56 (d, *J* = 8.6 Hz, 2H), 7.35 (d, *J* = 8.5 Hz, 2H), 5.71 – 5.66 (m, 1H), 3.68 – 3.61 (m, 3H), 3.57 (d, *J* = 6.5 Hz, 4H), 3.48 (s, 3H), 3.38 (s, 3H), 3.28 (t, *J* = 9.4 Hz, 1H), 2.37 (dd, *J* = 13.3, 4.7 Hz, 1H), 1.75 – 1.69 (m, 1H). **^{13}C NMR** (151 MHz, $CDCl_3$) *δ* 149.6, 136.3, 130.4, 129.1, 128.7, 100.1, 79.8, 78.7, 71.5, 71.2, 60.7, 59.2, 57.5, 33.4. **HRMS** (ESI) m/z: $[M+Na]^+$ calcd for $C_{16}H_{22}ClNNaO_5$ 366.1079; found 366.1079.

4-chlorobenzaldehyde O-((2R,4R,5S,6R)-4,5-diethoxy-6-(ethoxymethyl)tetrahydro-2H-pyran-2-yl) oxime (*α*(E)/*α*(Z) = 7:1) (36)

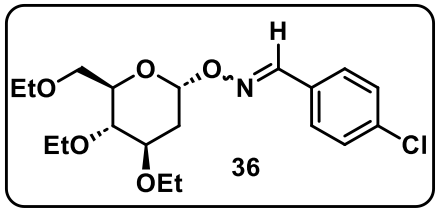

36 was obtained in 81% yield (53 mg), as a white foam, R_f = 0.5 (Hexane/EtOAc, 8:2, v/v), **[α]^{25}D** = +81.6 (*c* 0.06, $CHCl_3$). **^{1}H NMR** (600 MHz, $CDCl_3$) δ 8.06 (s, 1H), 7.54 (d, *J* = 8.4 Hz, 2H), 7.34 (d, *J* = 8.5 Hz, 2H), 5.67 (d, *J* = 3.0 Hz, 1H), 3.89 (dt, *J* = 9.2, 7.1 Hz, 1H), 3.73 – 3.54 (m, 10H), 3.50 – 3.44 (m, 1H), 3.40 (t, *J* = 9.3 Hz, 1H), 2.31 (dd, *J* = 13.0, 4.7 Hz, 1H), 1.75 (dd, *J* = 11.8, 3.8 Hz, 1H), 1.23 – 1.15 (m, 11H). **^{13}C NMR** (151 MHz, $CDCl_3$) δ 149.5, 136.2, 130.5, 129.1, 128.7, 100.2, 97.2, 78.6, 78.1, 77.3, 77.1, 71.8, 70.8, 69.4, 69.1, 68.3, 68.2, 66.9, 66.8, 65.6, 65.5, 62.6, 35.9, 34.2, 15.9, 15.9, 15.9, 15.2. **HRMS** (ESI) m/z: $[M+Na]^+$ calcd for $C_{19}H_{28}ClNNaO_5$ 408.1548; found 408.1561.

(E)-4-chlorobenzaldehyde O-((2R,4R,5S,6R)-4,5-bis((tert-butyldimethylsilyl)oxy)-6-(((tert-butyldimethylsilyl)oxy)methyl)tetrahydro-2H-pyran-2-yl) oxime (37)

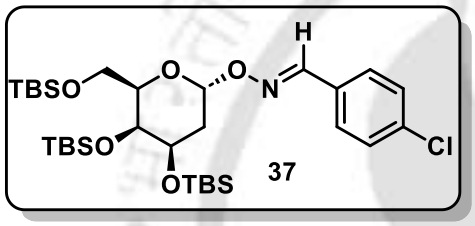

37 was obtained in 83% yield (90 mg), as a white foam, R_f = 0.5 (Hexane/EtOAc, 95:5, v/v), **[α]^{25}D** = +96.4 (*c* 0.05, $CHCl_3$). **^{1}H NMR** (600 MHz, $CDCl_3$) δ 8.08 (s, 1H), 7.55 (d, *J* = 8.6 Hz, 2H), 7.34 (d, *J* = 8.5 Hz, 2H), 5.61 (d, *J* = 3.4 Hz, 1H), 4.04 (ddd, *J* = 11.9, 4.5, 2.4 Hz, 1H), 3.90 (s, 1H), 3.72 – 3.62 (m, 3H), 2.25 (td, *J* = 12.4, 4.1 Hz, 1H), 1.80 (dd, *J* = 12.8, 4.5 Hz, 1H), 0.92 (d, *J* = 9.9 Hz, 18H), 0.83 (s, 9H), 0.11 (dd, *J* = 13.4, 7.2 Hz, 12H), -0.00 (d, *J* = 9.5 Hz, 6H). **^{13}C NMR** (151 MHz, $CDCl_3$) δ 148.9, 136.0, 130.8, 129.1, 128.6, 100.9, 73.7, 69.9, 68.5, 62.2, 32.1, 26.4, 26.3, 25.9, 18.8, 18.7, 18.3, -3.7, -4.2, -4.5, -4.8, -5.1, -5.2. **HRMS** (ESI) m/z: $[M+Na]^+$ calcd for $C_{31}H_{58}ClNNaO_5Si_3$ 666.3204; found 666.3179.

(E)-4-chlorobenzaldehyde O-((2R,4R,5R,6R)-4,5-dimethoxy-6-(methoxymethyl)tetrahydro-2H-pyran-2-yl) oxime (38)

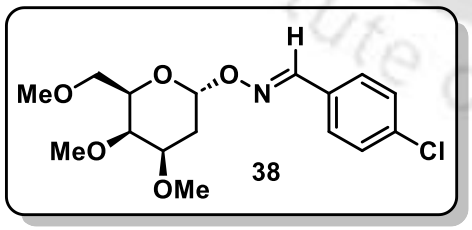

38 was obtained in 82% yield (48 mg), as a white foam, R_f = 0.4 (Hexane/EtOAc, 8:2, v/v), **[α]^{25}D** = +33.3 (*c* 0.18, $CHCl_3$). **^{1}H NMR** (600 MHz, $CDCl_3$) δ 8.08 (s, 1H), 7.56 (d, *J* = 8.5 Hz, 2H), 7.35 (d, *J* = 8.5 Hz, 2H), 5.70 (d, *J* = 3.5 Hz, 1H), 3.92 (t, *J* = 6.6 Hz, 1H), 3.71 – 3.64 (m, 2H), 3.59 (s, 4H), 3.51 (dd, *J* = 9.3, 5.7 Hz, 1H), 3.45 (s, 3H), 3.36 (s, 3H), 2.16 (td, *J* = 12.6, 4.0 Hz, 1H), 2.08 (dd, *J* = 13.0, 4.8 Hz, 1H). **^{13}C NMR** (151 MHz, $CDCl_3$) δ 149.3, 136.2, 130.5, 129.1, 128.7, 100.6, 76.0, 74.4, 71.3, 70.4, 61.1, 59.2, 56.3, 29.3. **HRMS** (ESI) m/z: $[M+Na]^+$ calcd for $C_{16}H_{22}ClNNaO_5$ 366.1079; found 366.1068.

N-(((2R,4R,5R,6R)-4,5-bis(benzyloxy)-6-((benzyloxy)methyl)tetrahydro-2H-pyran-2-yl)oxy)-N-methylbenzamide (39)

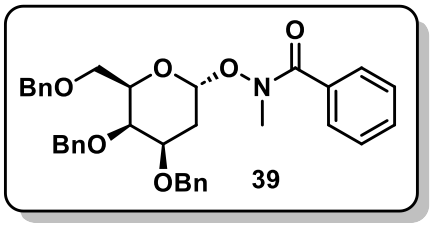

39 was obtained in 83% yield (80 mg), as a colorless oil, R_f = 0.5 (Hexane/EtOAc, 7:3, v/v), **[α]^{25}D** = +54.1 (*c* 0.38, $CHCl_3$). **^{1}H NMR** (600 MHz, $CDCl_3$) δ 7.57 – 7.52 (m, 2H), 7.42 (t, *J* = 7.4 Hz, 1H), 7.37 – 7.25 (m, 17H), 5.21 (s, 1H), 4.88 (d, *J* = 11.6 Hz, 1H), 4.58 – 4.54 (m, 3H), 4.48 (d, *J* = 11.8 Hz, 1H), 4.40 (d, *J* = 11.8 Hz, 1H), 3.86 (d, *J* = 18.3 Hz, 2H), 3.76 (d, *J* = 10.1 Hz, 1H), 3.55 – 3.48 (m, 2H), 3.40 (s, 3H), 2.14 (td, *J* = 12.8, 4.1 Hz, 1H), 1.83 (d, *J* = 10.5 Hz, 1H). **^{13}C NMR** (151 MHz, $CDCl_3$) δ 170.3, 138.7, 138.3, 138.1, 134.6, 130.6, 128.8, 128.6 (128.59, 128.56), 128.5, 128.4, 128.2, 128.1, 127.9 (127.88, 127.85), 127.8, 127.7, 127.5, 103.2, 74.4, 73.9, 73.6, 72.7, 71.9, 70.5, 69.5, 29.3. **HRMS** (ESI) m/z: $[M+H]^+$ calcd for $C_{35}H_{38}NO_6$ 568.2694; found 568.2698.

N-(((2R,4R,5R,6R)-4,5-bis(benzyloxy)-6-((benzyloxy)methyl)tetrahydro-2H-pyran-2-yl)oxy)-N,4-dimethylbenzamide (40)

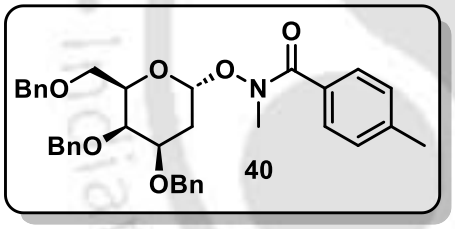

40 was obtained in 85% yield (84 mg), as a colorless oil, R_f = 0.5 (Hexane/EtOAc, 7:3, v/v), **[α]^{25}D** = +67.5 (*c* 0.32, $CHCl_3$). **^{1}H NMR** (600 MHz, $CDCl_3$) δ 7.47 (d, *J* = 8.0 Hz, 2H), 7.39 – 7.35 (m, 2H), 7.34 – 7.24 (m, 13H), 7.15 (d, *J* = 7.8 Hz, 2H), 5.20 (d, *J* = 3.1 Hz, 1H), 4.89 (d, *J* = 11.6 Hz, 1H), 4.59 – 4.55 (m, 3H), 4.48 (d, *J* = 11.7 Hz, 1H), 4.40 (d, *J* = 11.7 Hz, 1H), 3.87 (d, *J* = 11.5 Hz, 2H), 3.79 (d, *J* = 10.4 Hz, 1H), 3.52 (ddd, *J* = 27.1, 9.3, 6.5 Hz, 2H), 3.40 (s, 3H), 2.36 (s, 3H), 2.15 (td, *J* = 12.8, 4.2 Hz, 1H), 1.88 (d, *J* = 12.3 Hz, 1H). **^{13}C NMR** (151 MHz, $CDCl_3$) δ 170.3, 140.9, 138.8, 138.3, 138.1, 131.6, 128.8, 128.6, 128.5, 128.4, 128.3, 128.2, 127.8, 127.7, 127.5, 103.1, 74.4, 73.9, 73.7, 72.8, 71.9, 70.5, 69.5, 37.9, 29.4, 21.6. **HRMS** (ESI) m/z: $[M+H]^+$ calcd for $C_{36}H_{40}NO_6$ 582.2850; found 582.2877.

N-(((2R,4R,5R,6R)-4,5-bis(benzyloxy)-6-((benzyloxy)methyl)tetrahydro-2H-pyran-2-yl)oxy)-4-(tert-butyl)-N-methylbenzamide (41)

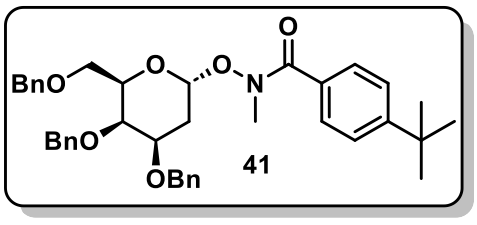

41 was obtained in 82% yield (87 mg), as a colorless oil, R_f = 0.6 (Hexane/EtOAc, 7:3, v/v), **[α]^{25}D** = +60.0 (*c* 0.34, $CHCl_3$). **^{1}H NMR** (600 MHz, $CDCl_3$) δ 7.49 (d, *J* = 8.5 Hz, 2H), 7.36 (dd, *J* = 7.8, 3.5 Hz, 4H), 7.33 – 7.26 (m, 13H), 5.25 – 5.20 (m, 1H), 4.89 (d, *J* = 11.5 Hz, 1H), 4.57 (d, *J* = 11.3 Hz, 3H), 4.49 (d, *J* = 11.8 Hz,

1H), 4.41 (d, *J* = 11.8 Hz, 1H), 3.88 (s, 2H), 3.80 (d, *J* = 12.5 Hz, 1H), 3.54 (q, *J* = 7.5, 5.6 Hz, 2H), 3.40 (s, 3H), 2.16 (dt, *J* = 12.6, 7.3 Hz, 1H), 1.89 (d, *J* = 11.6 Hz, 1H), 1.31 (s, 9H). **^{13}C NMR** (151 MHz, $CDCl_3$) *δ* 170.4, 154.1, 138.8, 138.3, 138.1, 131.6, 128.6, 128.5, 128.4, 128.2, 128.1, 127.9, 127.8, 127.7, 127.5, 125.1, 103.1, 74.4, 73.9, 73.7, 72.8, 71.9, 70.5, 69.6, 35.0, 31.3, 29.9, 29.3. **HRMS** (ESI) m/z: $[M+H]^+$ calcd for $C_{39}H_{46}NO_6$ 624.3320; found 624.3335.

N-(((2R,4R,5R,6R)-4,5-bis(benzyloxy)-6-((benzyloxy)methyl)tetrahydro-2H-pyran-2-yl)oxy)-4-methoxy-N-methylbenzamide (42)

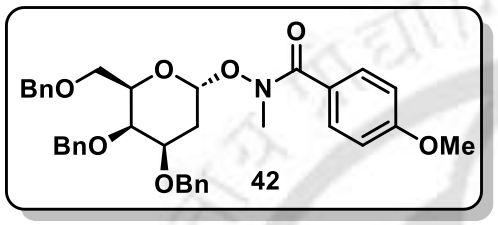

42 was obtained in 88% yield (89 mg), as a colorless oil, R_f = 0.4 (Hexane/EtOAc, 7:3, v/v), **$[\alpha]^{25}_D$** = +56.6 (*c* 0.27, $CHCl_3$). **^{1}H NMR** (600 MHz, $CDCl_3$) *δ* 7.57 (d, *J* = 8.8 Hz, 2H), 7.38 – 7.26 (m, 15H), 6.85 (d, *J* = 8.8 Hz, 2H), 5.20 (d, *J* = 3.7 Hz, 1H), 4.89 (d, *J* = 11.6 Hz, 1H), 4.60 – 4.55 (m, 3H), 4.47 (d, *J* = 11.8 Hz, 1H), 4.40 (d, *J* = 11.7 Hz, 1H), 3.87 (dd, *J* = 13.0, 6.4 Hz, 2H), 3.81 (s, 4H), 3.54 (dd, *J* = 9.3, 6.7 Hz, 1H), 3.49 (dd, *J* = 9.4, 6.2 Hz, 1H), 3.40 (s, 3H), 2.20 – 2.14 (m, 1H), 1.90 (dd, *J* = 13.0, 3.8 Hz, 1H). **^{13}C NMR** (151 MHz, $CDCl_3$) *δ* 169.9, 161.5, 138.8, 138.3, 138.1, 130.4, 128.6, 128.5, 128.4, 128.2, 127.8, 127.7, 127.5, 126.5, 113.5, 103.1, 74.4, 73.9, 73.7, 72.7, 71.9, 70.5, 69.5, 55.5, 37.9, 29.4. **HRMS** (ESI) m/z: $[M+Na]^+$ calcd for $C_{36}H_{39}NNaO_7$ 620.2619; found 620.2619.

N-(((2R,4R,5R,6R)-4,5-bis(benzyloxy)-6-((benzyloxy)methyl)tetrahydro-2H-pyran-2-yl)oxy)-4-iodo-N-methylbenzamide (43)

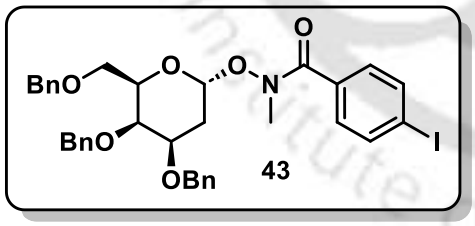

43 was obtained in 84% yield (99 mg), as a colorless oil, R_f = 0.5 (Hexane/EtOAc, 7:3, v/v), **$[\alpha]^{25}_D$** = +46.5 (*c* 0.20, $CHCl_3$). **^{1}H NMR** (600 MHz, $CDCl_3$) *δ* 7.69 (d, *J* = 8.4 Hz, 2H), 7.40 – 7.36 (m, 2H), 7.34 – 7.25 (m, 15H), 5.19 – 5.14 (m, 1H), 4.88 (d, *J* = 11.5 Hz, 1H), 4.56 (d, *J* = 11.5 Hz, 3H), 4.48 (d, *J* = 11.7 Hz, 1H), 4.39 (d, *J* = 11.7 Hz, 1H), 3.87 (s, 1H), 3.80 (s, 1H), 3.74 (d, *J* = 10.8 Hz, 1H), 3.53 – 3.47 (m, 2H), 3.39 (s, 3H), 2.16 (td, *J* = 12.9, 4.2 Hz, 1H), 1.80 (d, *J* = 11.1 Hz, 1H). **^{13}C NMR** (151 MHz, $CDCl_3$) *δ* 169.2, 138.7, 138.2, 138.0, 137.4, 133.9, 129.9, 128.7, 128.5, 128.4, 128.2, 127.9 (127.90, 127.88), 127.8, 127.5, 103.3, 97.3, 74.4, 73.7 (73.74, 73.68), 72.6, 72.1, 70.5, 69.5, 37.5, 29.4. **HRMS** (ESI) m/z: $[M+H]^+$ calcd for $C_{35}H_{37}INO_6$ 694.1660; found 694.1664.

N-(((2R,4R,5R,6R)-4,5-bis(benzyloxy)-6-((benzyloxy)methyl)tetrahydro-2H-pyran-2-yl)oxy)-4-bromo-N-methylbenzamide (44)

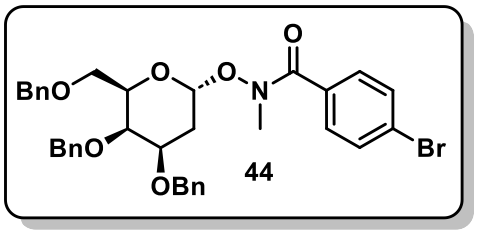

44 was obtained in 82% yield (90 mg), as a colorless oil, R_f = 0.5 (Hexane/EtOAc, 7:3, v/v), **[α]^{25}D** = +65.2 (*c* 0.23, $CHCl_3$). **^{1}H NMR** (600 MHz, $CDCl_3$) δ 7.48 (d, *J* = 8.6 Hz, 2H), 7.43 (d, *J* = 8.5 Hz, 2H), 7.39 – 7.36 (m, 2H), 7.34 – 7.25 (m, 13H), 5.19 – 5.14 (m, 1H), 4.88 (d, *J* = 11.5 Hz, 1H), 4.57 (t, *J* = 11.6 Hz, 3H), 4.47 (d, *J* = 11.7 Hz, 1H), 4.39 (d, *J* = 11.7 Hz, 1H), 3.87 (s, 1H), 3.82 – 3.72 (m, 2H), 3.54 – 3.46 (m, 2H), 3.39 (s, 3H), 2.16 (td, *J* = 12.9, 4.2 Hz, 1H), 1.80 (d, *J* = 10.8 Hz, 1H). **^{13}C NMR** (151 MHz, $CDCl_3$) δ 169.1, 138.7, 138.2, 138.0, 133.3, 131.4, 129.9, 128.6, 128.5, 128.4, 128.2, 127.9 (127.88, 127.86), 127.8, 127.5, 125.1, 103.3, 74.4, 73.7 (73.72, 73.66), 72.6, 72.1, 70.5, 69.5, 37.4, 29.4. **HRMS** (ESI) m/z: $[M+H]^+$ calcd for $C_{35}H_{37}BrNO_6$ 646.1799; found 646.1812.

N-(((2R,4R,5R,6R)-4,5-bis(benzyloxy)-6-((benzyloxy)methyl)tetrahydro-2H-pyran-2-yl)oxy)-N-methyl-2-phenylacetamide (45)

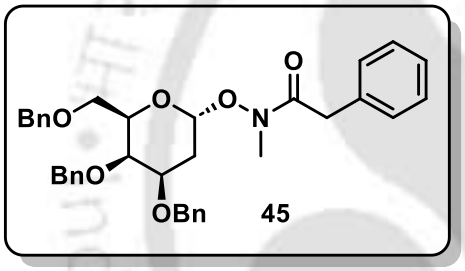

45 was obtained in 85% yield (84 mg), as a colorless oil, R_f = 0.6 (Hexane/EtOAc, 7:3, v/v), **[α]^{25}D** = +55.7 (*c* 0.19, $CHCl_3$). **^{1}H NMR** (600 MHz, $CDCl_3$) δ 7.39 – 7.20 (m, 20H), 5.11 (s, 1H), 4.91 (d, *J* = 11.5 Hz, 1H), 4.64 – 4.57 (m, 3H), 4.49 (d, *J* = 11.8 Hz, 1H), 4.40 (d, *J* = 11.8 Hz, 1H), 4.07 (s, 1H), 3.93 (s, 1H), 3.83 (d, *J* = 10.9 Hz, 1H), 3.79 – 3.68 (m, 2H), 3.55 (t, *J* = 6.2 Hz, 2H), 3.29 (s, 3H), 2.23 (td, *J* = 12.9, 4.2 Hz, 1H), 2.04 (s, 1H). **^{13}C NMR** (151 MHz, $CDCl_3$) δ 173.4, 138.6, 138.2, 137.9, 129.1, 128.7, 128.6, 128.5, 128.4, 128.3, 127.9, 127.8 (127.83, 127.82), 127.5, 127.0, 104.6, 74.5, 73.9, 73.7, 72.7, 71.8, 70.7, 69.7, 40.0, 36.8, 29.8. **HRMS** (ESI) m/z: $[M+H]^+$ calcd for $C_{36}H_{40}NO_6$ 582.2851; found 582.2872.

N-(((2R,4R,5R,6R)-4,5-bis(benzyloxy)-6-((benzyloxy)methyl)tetrahydro-2H-pyran-2-yl)oxy)benzamide (46)

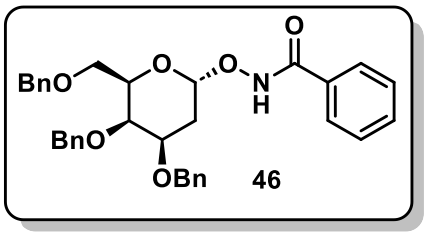

46 was obtained in 88% yield (83 mg), as a colorless oil, R_f = 0.5 (Hexane/EtOAc, 1:1, v/v), **[α]^{25}D** = +86.7 (*c* 0.06, $CHCl_3$). **^{1}H NMR** (600 MHz, $CDCl_3$) δ 9.44 (s, 1H), 7.69 (d, *J* = 7.4 Hz, 2H), 7.47 (t, *J* = 7.4 Hz, 1H), 7.37 – 7.26 (m, 17H), 5.38 (d, *J* = 3.4 Hz, 1H), 4.94 (d, *J* = 11.7 Hz, 1H), 4.65 – 4.60 (m, 2H), 4.58 (d, *J* = 11.9 Hz, 1H), 4.51 (d, *J* = 11.7 Hz, 1H), 4.41 (d, *J* = 11.7 Hz, 1H), 4.14 – 4.08 (m, 1H), 3.95 (dd, *J* = 14.1, 2.1 Hz, 1H), 3.86 (s, 1H), 3.67 (dd, *J* = 9.6, 7.4 Hz, 1H), 3.46 (dd, *J* = 9.7, 4.7 Hz, 1H), 2.39 (dd, *J* = 13.2, 4.3 Hz, 1H), 2.30 (td, *J* = 12.9, 4.0 Hz, 1H). **^{13}C**

NMR (151 MHz, $CDCl_3$) δ 166.0, 138.6, 138.3, 137.7, 132.1, 131.9, 128.7, 128.6 (128.60, 128.57), 128.5, 128.4, 128.0, 127.9, 127.8 (127.84, 127.79), 127.5, 127.3, 102.8, 74.3, 74.2, 73.8, 72.9, 71.9, 28.9. **HRMS** (ESI) m/z: $[M+Na]^+$ calcd for $C_{34}H_{36}NNaO_6$ 576.2357; found 576.2354.

4-((2S,5R,6R)-4,5-bis(benzyloxy)-6-((benzyloxy)methyl)-5,6-dihydro-2H-pyran-2-yl)-N-(((2R,4R,5R,6R)-4,5-bis(benzyloxy)-6-((benzyloxy)methyl)tetrahydro-2H-pyran-2-yl)oxy)-N-methylbenzamide (47)

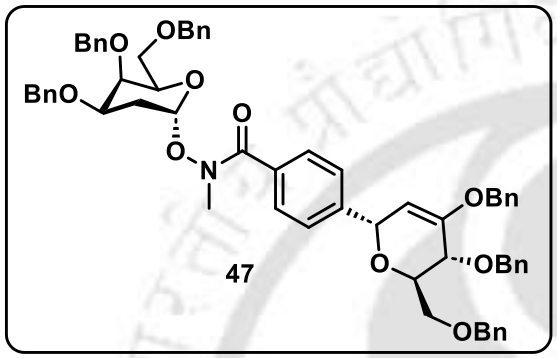

47 was obtained in 90% yield (106 mg), as a colorless oil, R_f = 0.4 (Hexane/EtOAc, 7:3, v/v), $[\alpha]^{25}_D$ = +70.1 (*c* 0.37, $CHCl_3$). **^{1}H NMR** (600 MHz, $CDCl_3$) δ 7.50 (d, *J* = 8.1 Hz, 2H), 7.41 (d, *J* = 8.0 Hz, 2H), 7.40 – 7.21 (m, 30H), 5.35 (d, *J* = 2.8 Hz, 1H), 5.21 (s, 1H), 4.97 (d, *J* = 3.5 Hz, 1H), 4.92 – 4.81 (m, 4H), 4.59 – 4.51 (m, 5H), 4.49 – 4.38 (m, 3H), 4.20 (d, *J* = 6.3 Hz, 1H), 3.91 – 3.74 (m, 4H), 3.64 (dd, *J* = 10.4, 4.8 Hz, 1H), 3.56 – 3.48 (m, 3H), 3.38 (s, 3H), 2.17 – 2.11 (m, 1H), 1.91 – 1.85 (m, 1H). **^{13}C NMR** (151 MHz, $CDCl_3$) δ 170.0, 153.6, 143.6, 138.8, 138.4, 138.3, 138.1, 138.0, 136.8, 134.0, 128.7, 128.6, 128.5 (128.52, 128.49), 128.4 (128.38, 128.37), 128.3, 128.2 (128.20, 128.17), 128.0, 127.9 (127.99, 127.89, 127.87), 127.8 (127.81, 127.75), 127.7, 127.5 (127.51, 127.48), 103.2, 98.5, 74.4, 73.9, 73.7 (73.72, 73.65), 73.4, 73.3, 72.8, 71.9, 71.3, 36.8, 29.3. **HRMS** (ESI) m/z: $[M+H]^+$ calcd for $C_{62}H_{64}NO_{10}$ 982.4525; found 982.4514.

N-(((2R,4R,5R,6R)-4,5-bis(benzyloxy)-6-((benzyloxy)methyl)tetrahydro-2H-pyran-2-yl)oxy)-4-(3-hydroxyprop-1-yn-1-yl)-N-methylbenzamide (48)

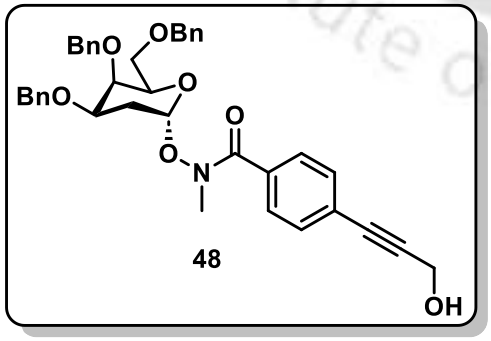

48 was obtained in 95% yield (106 mg), as a colorless oil, R_f = 0.4 (Hexane/EtOAc, 1:1, v/v), **^{1}H NMR** (600 MHz, $CDCl_3$) δ 7.51 (d, *J* = 8.3 Hz, 2H), 7.41 (d, *J* = 8.3 Hz, 2H), 7.39 – 7.23 (m, 15H), 5.18 (s, 1H), 4.88 (d, *J* = 11.5 Hz, 1H), 4.59 – 4.53 (m, 3H), 4.47 (d, *J* = 9.8 Hz, 3H), 4.39 (d, *J* = 11.7 Hz, 1H), 4.28 (s, 1H), 3.87 (s, 1H), 3.82 – 3.71 (m, 2H), 3.52 (dd, *J* = 9.3, 6.6 Hz, 1H), 3.46 (dd, *J* = 9.1, 6.4 Hz, 1H), 3.40 (s, 3H), 2.15 (td, *J* = 12.9, 4.1 Hz, 1H), 1.81 (d, *J* = 9.4 Hz, 1H). **^{13}C NMR** (151 MHz, $CDCl_3$) δ 169.5, 138.7, 138.2, 138.0, 134.2, 131.5, 128.6, 128.5, 128.4, 128.3 (128.27, 128.25), 127.9, 127.8 (127.84, 127.76), 127.5,

125.0, 103.4, 89.4, 84.9, 74.4, 73.7, 73.6, 72.6, 72.0, 70.5, 69.5, 51.6, 51.4, 37.5, 29.3. **HRMS** (ESI) m/z: $[M+H]^+$ calcd for $C_{38}H_{39}NNaO_7$ 644.2619; found 644.2597.

2.6. References

1. Pifferi, C.; Daskhan, G. C.; Fiore, M.; Shiao, T. C.; Roy, R.; Renaudet, O., Aminooxylated Carbohydrates: Synthesis and Applications. *Chem. Rev.* **2017,** *117* (15), 9839-9873.
2. Chen, N.; Xie, J., N-O linkage in carbohydrates and glycoconjugates. *Org. Biomol. Chem* **2016,** *14* (47), 11028-11047.
3. Lee, M. D.; Ellestad, G. A.; Borders, D. B., Calicheamicins: discovery, structure, chemistry, and interaction with DNA. *Acc. Chem. Res.* **1991,** *24* (8), 235-243.
4. Nicolaou, K. C.; Smith, A. L., Molecular design, chemical synthesis, and biological action of enediynes. *Acc. Chem. Res.* **1992,** *25* (11), 497-503.
5. Zein, N.; Poncin, M.; Nilakantan, R.; Ellestad, G. A., Calicheamicin gamma 1I and DNA: molecular recognition process responsible for site-specificity. *Science* **1989,** *244* (4905), 697-9.
6. Kölmel, D. K.; Kool, E. T., Oximes and Hydrazones in Bioconjugation: Mechanism and Catalysis. *Chem. Rev.* **2017,** *117* (15), 10358-10376.
7. De Silva, R. A.; Wang, Q.; Chidley, T.; Appulage, D. K.; Andreana, P. R., Immunological Response from an Entirely Carbohydrate Antigen: Design of Synthetic Vaccines Based on Tn−PS A1 Conjugates. *J. Am. Chem. Soc.* **2009,** *131* (28), 9622-9623.
8. Hudak, J. E.; Yu, H. H.; Bertozzi, C. R., Protein Glycoengineering Enabled by the Versatile Synthesis of Aminooxy Glycans and the Genetically Encoded Aldehyde Tag. *J. Am. Chem. Soc.* **2011,** *133* (40), 16127-16135.
9. Marcaurelle, L. A.; Rodriguez, E. C.; Bertozzi, C. R., Synthesis of an oxime-linked neoglycopeptide with glycosylation-dependent activity similar to its native counterpart. *Tetrahedron Lett.* **1998,** *39* (46), 8417-8420.
10. Rodriguez, E. C.; Winans, K. A.; King, D. S.; Bertozzi, C. R., A Strategy for the Chemoselective Synthesis of O-Linked Glycopeptides with Native Sugar−Peptide Linkages. *J. Am. Chem. Soc.* **1997,** *119* (41), 9905-9906.
11. Bednarczyk-Cwynar, B.; Zaprutko, L., Recent advances in synthesis and biological activity of triterpenic acylated oximes. *Phytochem. Rev.* **2015,** *14* (2), 203-231.
12. Nicolaou, K. C.; Hummel, C. W.; Nakada, M.; Shibayama, K.; Pitsinos, E. N.; Saimoto, H.; Mizuno, Y.; Baldenius, K. U.; Smith, A. L., Total synthesis of calicheamicin .gamma.1I. 3. The final stages. *J. Am. Chem. Soc.* **1993,** *115* (17), 7625-7635.
13. Yang, D.; Kim, S. H.; Kahne, D., Construction of glycosidic N-O linkages in oligosaccharides. *J. Am. Chem. Soc.* **1991,** *113* (12), 4715-4716.
14. Moutel, S.; Prandi, J., Synthesis of novel analogues of the calicheamicin γ1I and esperamicin A1B oligosaccharides. *J. Chem. Soc., Perkin Trans. 1* **2001,** (3), 305-315.
15. Kaur, K.; Srivastava, S., Beckmann rearrangement catalysis: a review of recent advances. *New J. Chem.* **2020,** *44* (43), 18530-18572.
16. Bolotin, D. S.; Bokach, N. A.; Demakova, M. Y.; Kukushkin, V. Y., Metal-Involving Synthesis and Reactions of Oximes. *Chem. Rev.* **2017,** *117* (21), 13039-13122.
17. Yu, J.; Sun, J.; Yu, B., Construction of Interglycosidic N–O Linkage via Direct Glycosylation of Sugar Oximes. *Org. Lett.* **2012,** *14* (15), 4022-4025.
18. Wang, Y.; Cheng, Y.; Zhong, L.; Lei, S.; He, Y.; Dai, Y., Stereospecific Palladium-Catalyzed Direct Glycosylation of Oximes: Access to N–O-Linked Glycosides. *Org. Lett.* **2023,** *25* (22), 4177-4182.
19. Wang, Y.; Cheng, Y.; Tao, X.; Yang, W.; Zhou, Z.; Dai, Y., Palladium-Catalyzed Stereospecific Glycosylation Enables Divergent Synthesis of N–O-Linked Glycosides. *Org. Lett.* **2025,** *27* (3), 915-921.
20. Zhao, R.; Gong, Y.; Zhou, H.; Yang, W.; Yu, B.; Xu, P., Late-Stage Oxime O-Glycosylation with Unprotected Glycosyl Fluorides. *Org. Lett.* **2025,** *27* (24), 6533-6538.
21. Crich, D.; Dudkin, V., An unusual example of steric buttressing in glycosylation. *Tetrahedron Lett.* **2000,** *41* (30), 5643-5646.
22. Xu, X.-H.; Liu, G.-K.; Azuma, A.; Tokunaga, E.; Shibata, N., Synthesis of Indole and Biindolyl Triflones: Trifluoromethanesulfonylation of Indoles with Tf_2O/TTBP (2,4,6-tri-tert-butylpyridine) System. *Org. Lett.* **2011,** *13* (18), 4854-4857.

23. Mukherji, A.; Kancharla, P. K., C–H···Anion Interactions Assisted Addition of Water to Glycals by Sterically Hindered 2,4,6-Tri-tert-butylpyridinium Hydrochloride. *Org. Lett.* **2020,** *22* (6), 2191-2195.
24. Ghosh, T.; Mukherji, A.; Kancharla, P. K., Sterically Hindered 2,4,6-Tri-tert-butylpyridinium Salts as Single Hydrogen Bond Donors for Highly Stereoselective Glycosylation Reactions of Glycals. *Org. Lett.* **2019,** *21* (10), 3490-3495.
25. Thadke, S. A.; Neralkar, M.; Hotha, S., Facile synthesis of aminooxy glycosides by gold(III)-catalyzed glycosidation. *Carbohydr. Res.* **2016,** *430*, 16-23.
26. Renaudet, O.; Dumy, P., Expedient synthesis of aminooxylated-carbohydrates for chemoselective access of glycoconjugates. *Tetrahedron Lett.* **2001,** *42* (43), 7575-7578.
27. Pradhan, P.; Moktan, S.; Biswas, A.; Das, A.; Lenka, R.; Kancharla, P. K., Triple Role of Proton Sponge (DMAN) in the Palladium-Catalyzed Direct Stereoselective Synthesis of C-Aryl Glycosides from Glycals. *Org. Lett.* **2024,** *26* (17), 3563-3568.
28. Balijepalli, A. S.; McNeely, J. H.; Hamoud, A.; Grinstaff, M. W., Guidelines for β-Lactam Synthesis: Glycal Protecting Groups Dictate Stereoelectronics and [2+2] Cycloaddition Kinetics. *J. Org. Chem.* **2020,** *85* (19), 12044-12057.
29. Xiong, D.-C.; Zhang, L.-H.; Ye, X.-S., Oxidant-Controlled Heck-Type C-Glycosylation of Glycals with Arylboronic Acids: Stereoselective Synthesis of Aryl 2-Deoxy-C-glycosides. *Org. Lett.* **2009,** *11* (8), 1709-1712.
30. Wang, B.; Xiong, D.-C.; Ye, X.-S., Direct C–H Trifluoromethylation of Glycals by Photoredox Catalysis. *Org. Lett.* **2015,** *17* (22), 5698-5701.
31. Fang, W.; Luo, Z.-W.; Wang, Y.-C.; Zhou, W.; Li, L.; Chen, Y.; Zhang, X.; Dai, M.; Dai, J.-J., SN2 Reaction at the Amide Nitrogen Center Enables Hydrazide Synthesis. *Angew. Chem. Int. Ed.* **2024,** *63* (14), e202317570.
32. Hoffman, R. V.; Nayyar, N. K.; Chen, W., Base-promoted reaction of O-sulfonylated hydroxamic acids with nucleophiles. A new method for the synthesis of .alpha.-substituted amides. *J. Org. Chem.* **1992,** *57* (21), 5700-5707.

2.7. Selected spectra

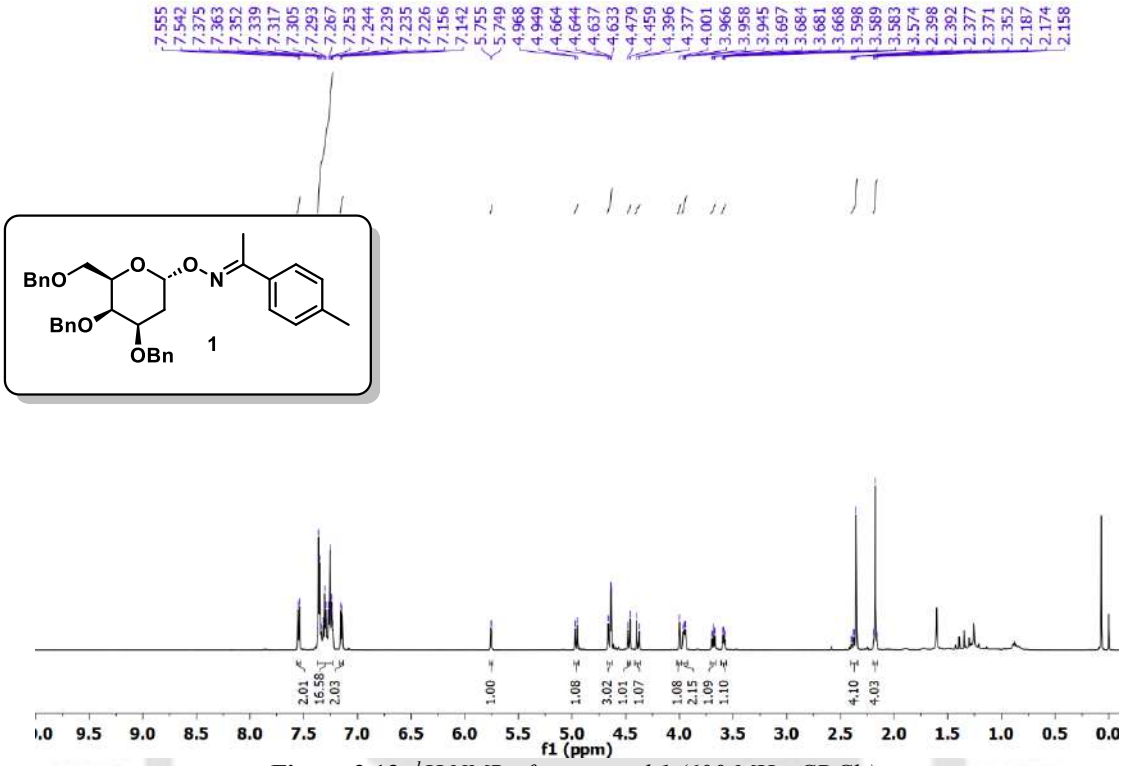

Figure 2.13. *^{1}H NMR of compound **1** (600 MHz, $CDCl_3$).*

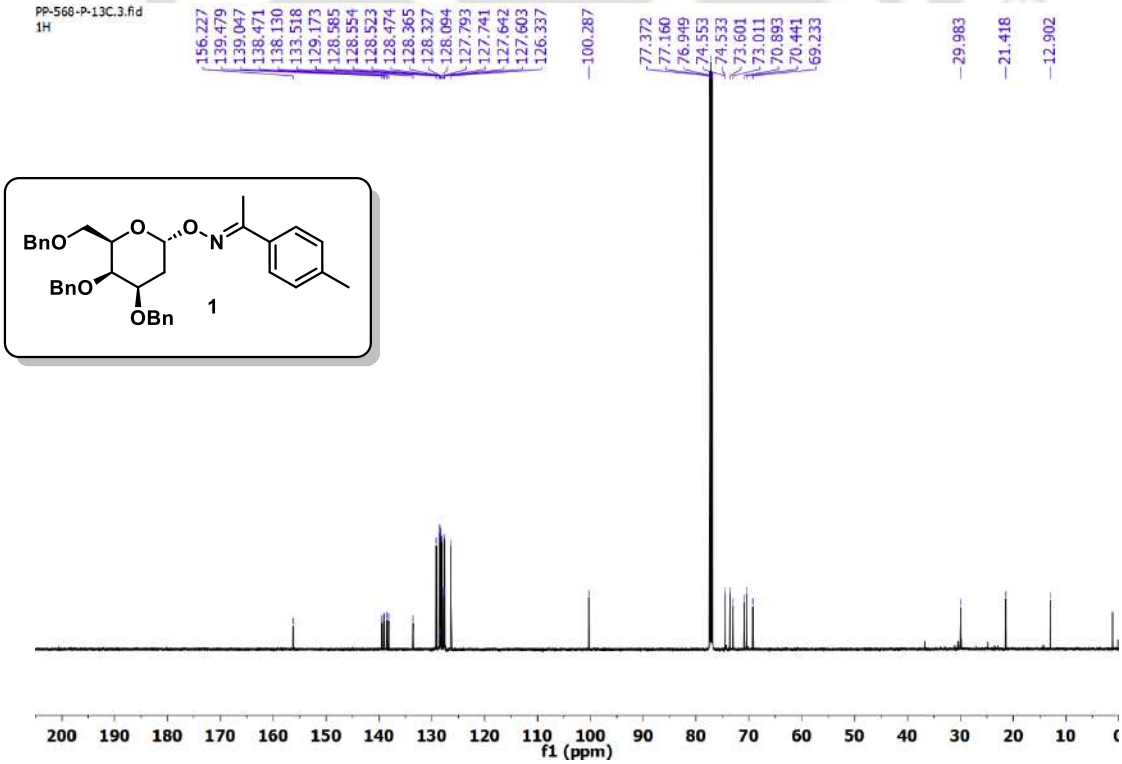

Figure 2.14. *^{13}C NMR of compound **1** (151 MHz, $CDCl_3$).*

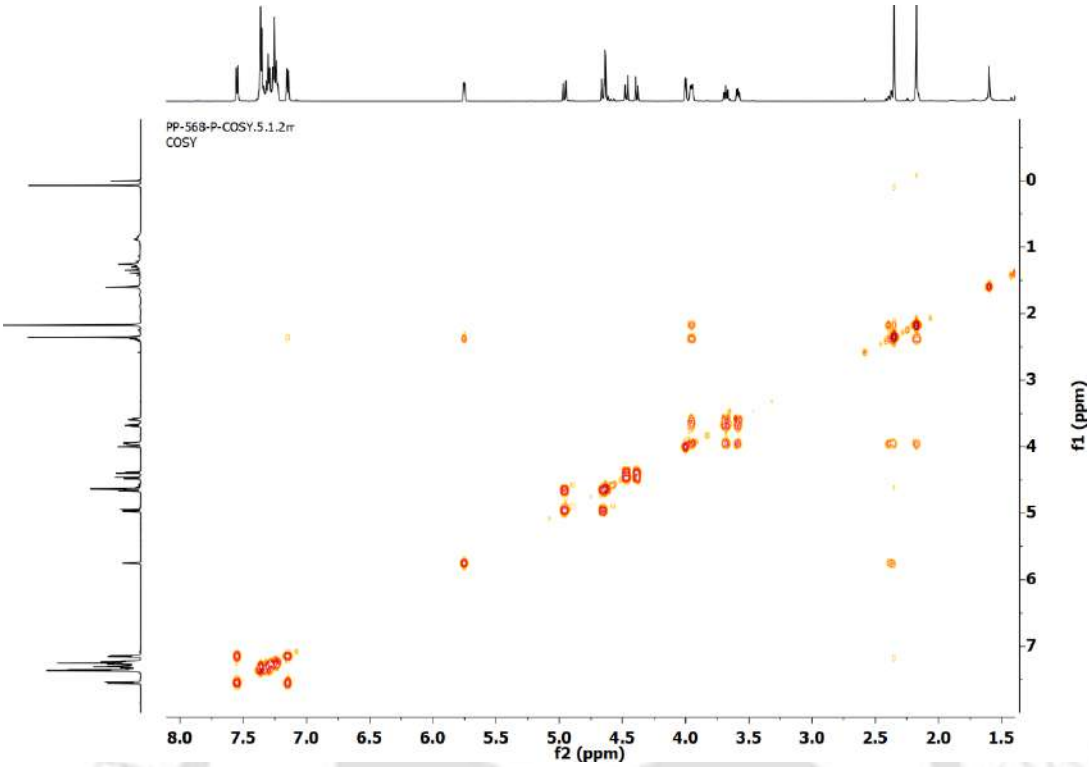

Figure 2.15. *COSY NMR of compound **1** (600 MHz, $CDCl_3$).*

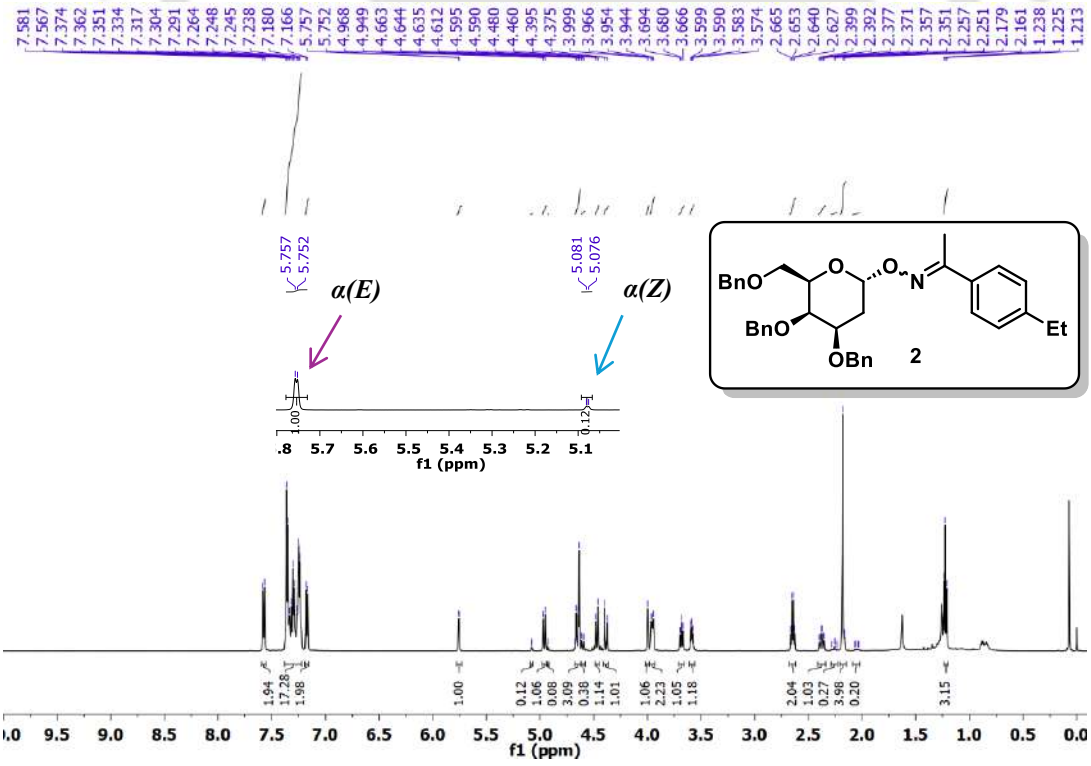

Figure 2.16. *^{1}H NMR of compound **2** (600 MHz, $CDCl_3$).*

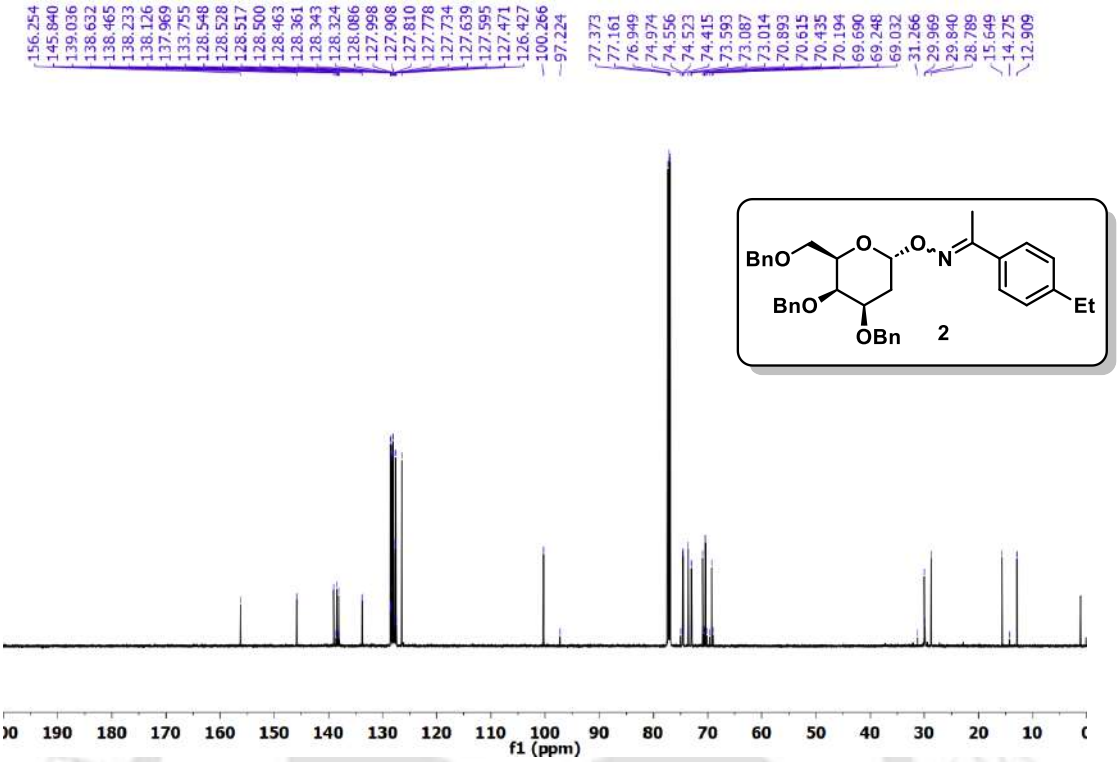

Figure 2.17. *^{13}C NMR of compound **2** (151 MHz, $CDCl_3$).*

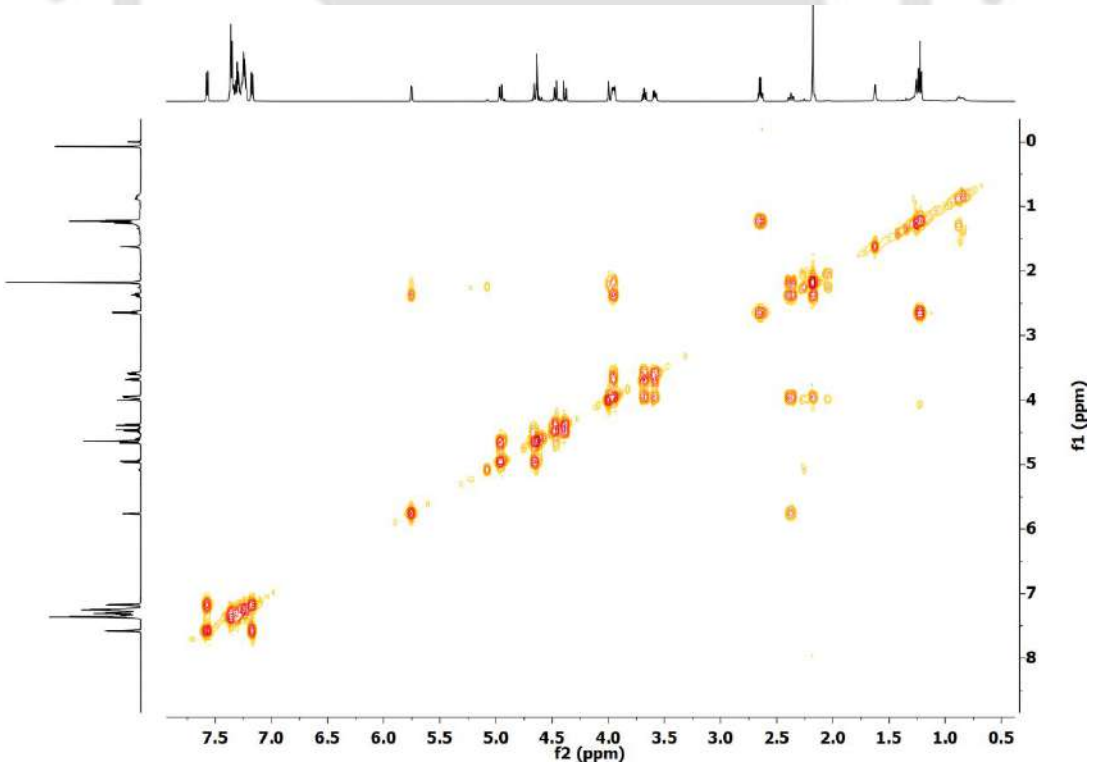

Figure 2.18. *COSY NMR of compound **2** (600 MHz, $CDCl_3$).*

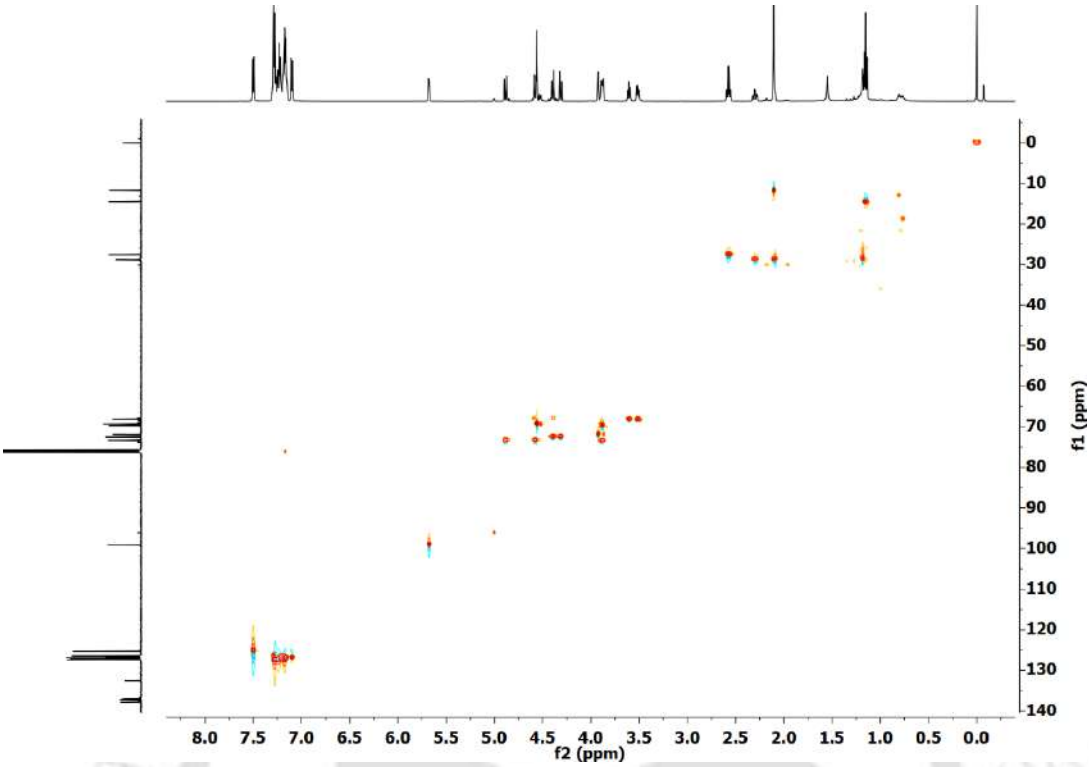

Figure 2.19. *HSQC-GP NMR of compound **2** (600 MHz, $CDCl_3$).*

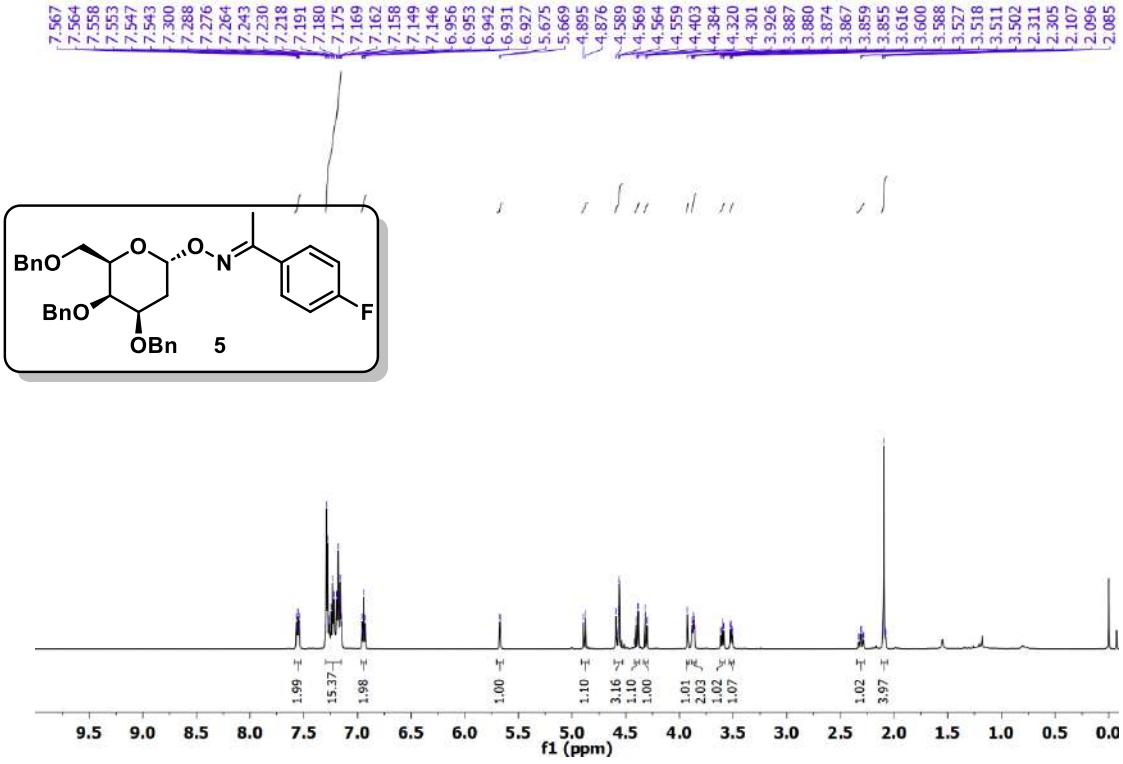

Figure 2.20. *^{1}H NMR of compound **5** (600 MHz, $CDCl_3$).*

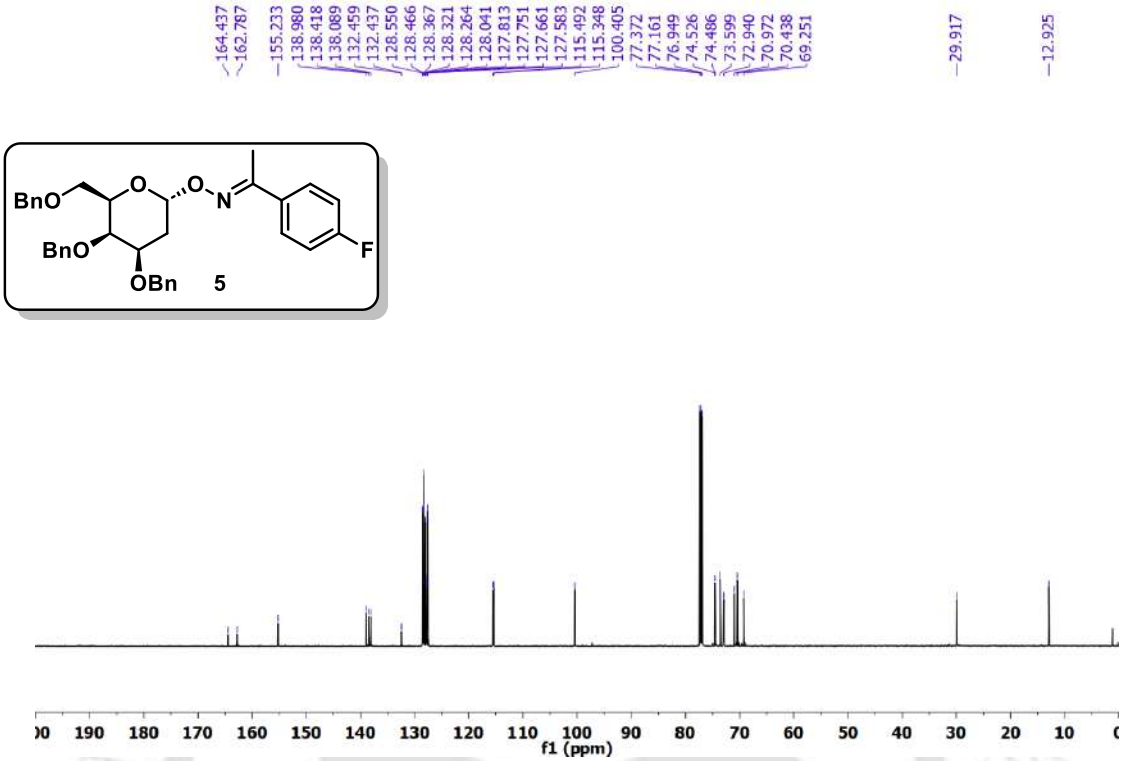

Figure 2.21. *^{13}C NMR of compound **5** (151 MHz, $CDCl_3$).*

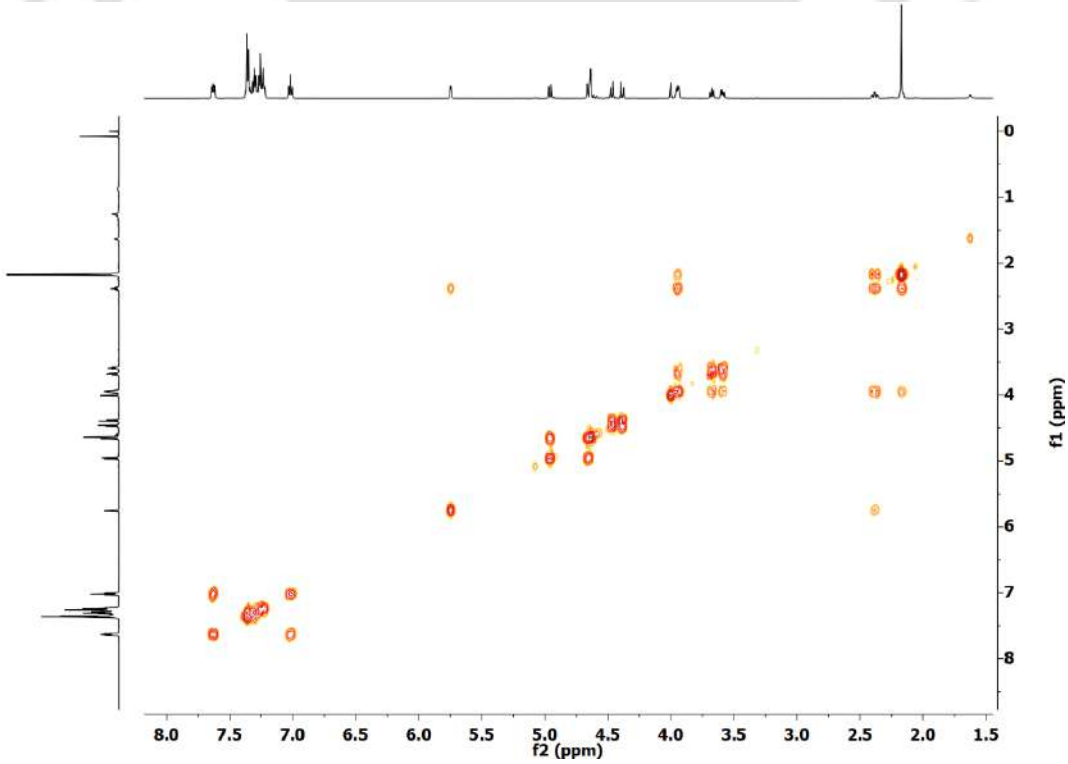

Figure 2.22. *COSY NMR of compound **5** (600 MHz, $CDCl_3$).*

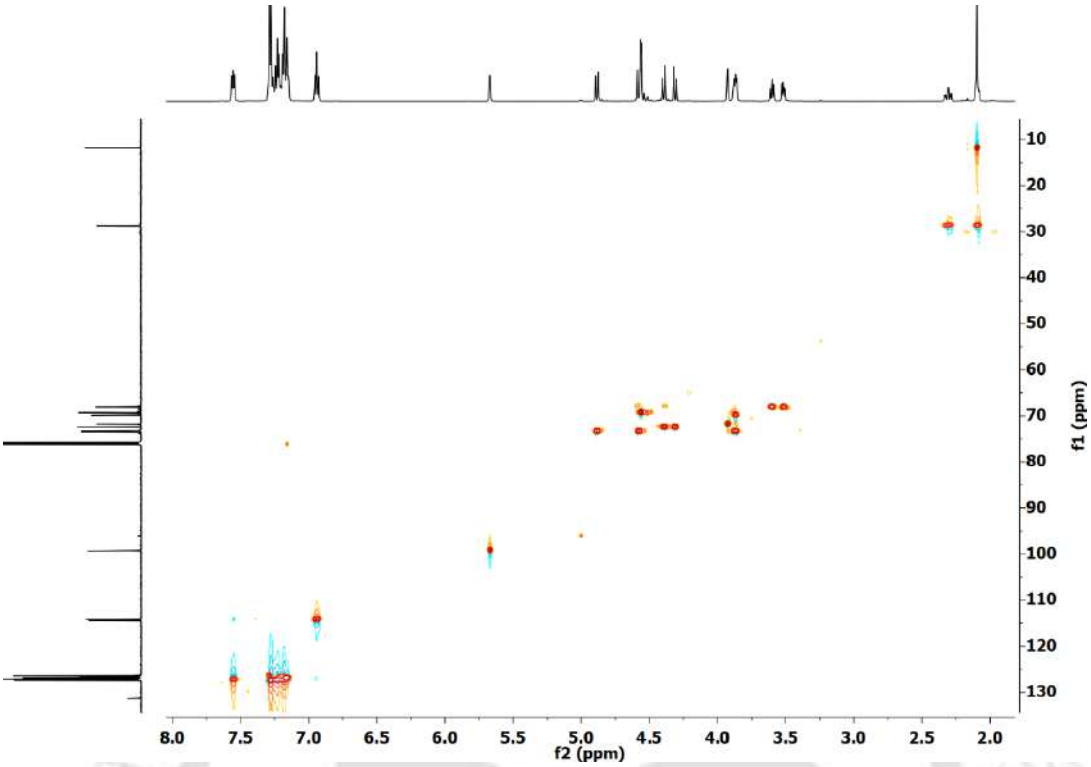

Figure 2.23. *HSQC-GP NMR of compound* ***5*** *(600 MHz, $CDCl_3$).*

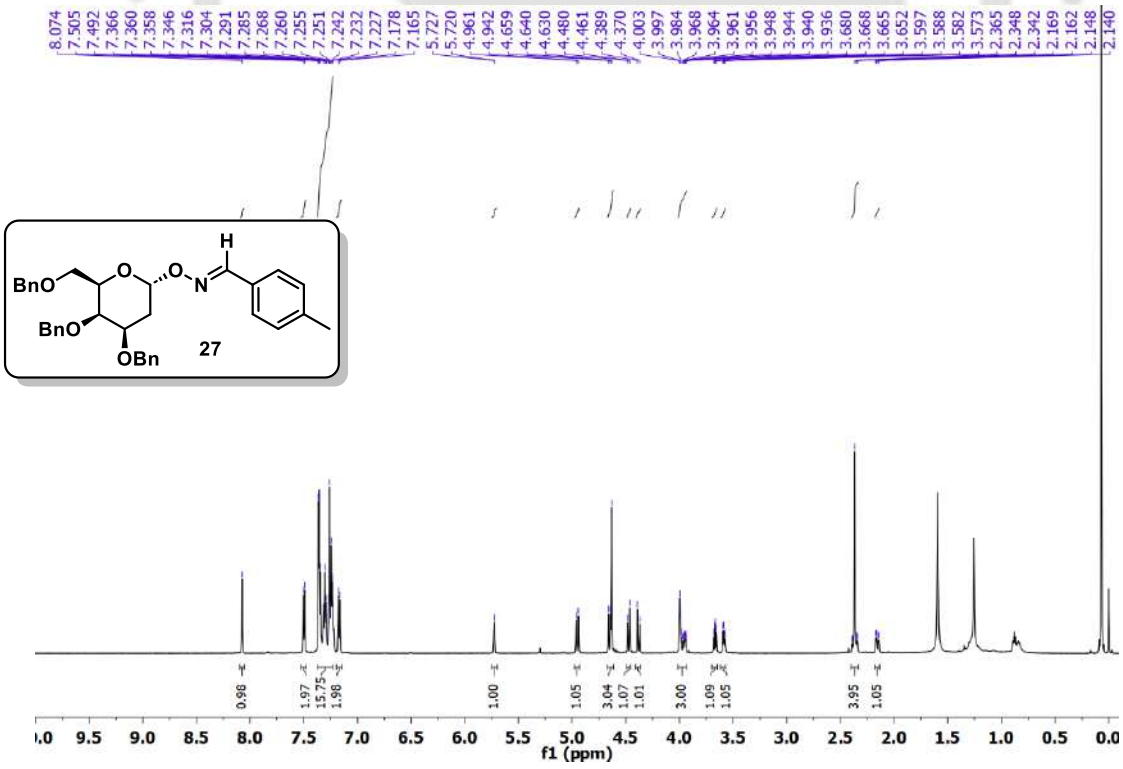

Figure 2.24. *^{1}H NMR of compound* ***27*** *(600 MHz, $CDCl_3$).*

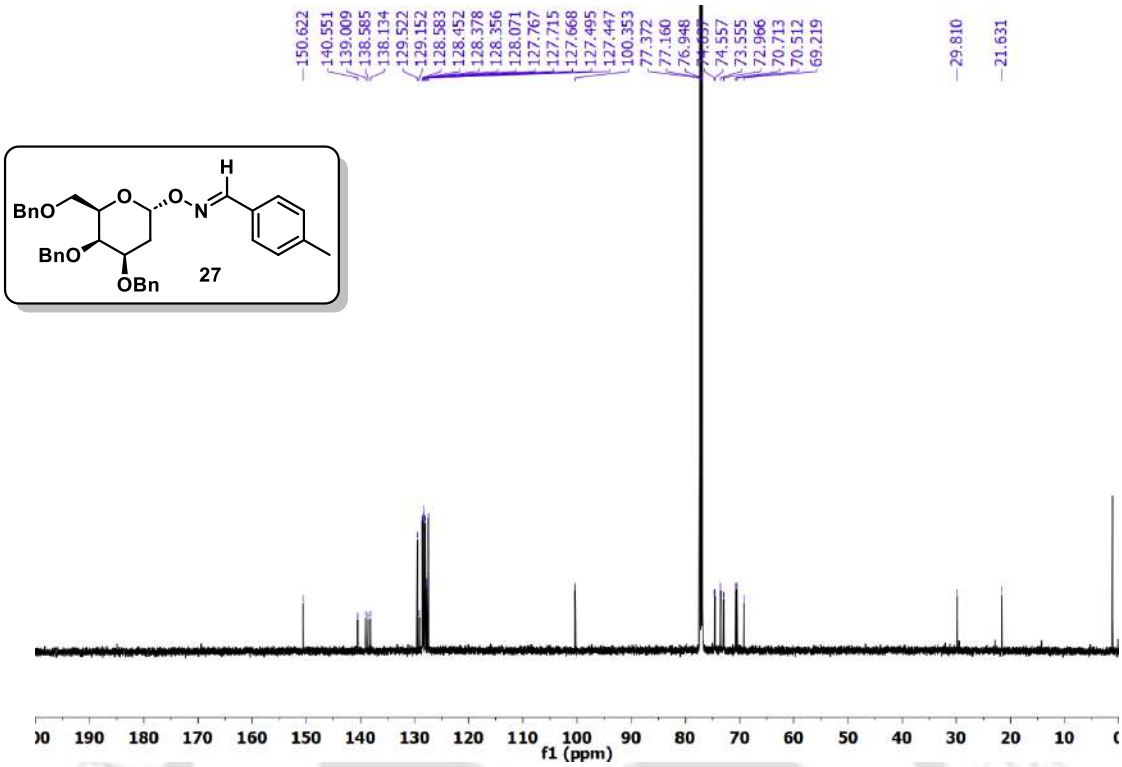

Figure 2.25. *^{13}C NMR of compound **27** (151 MHz, $CDCl_3$).*

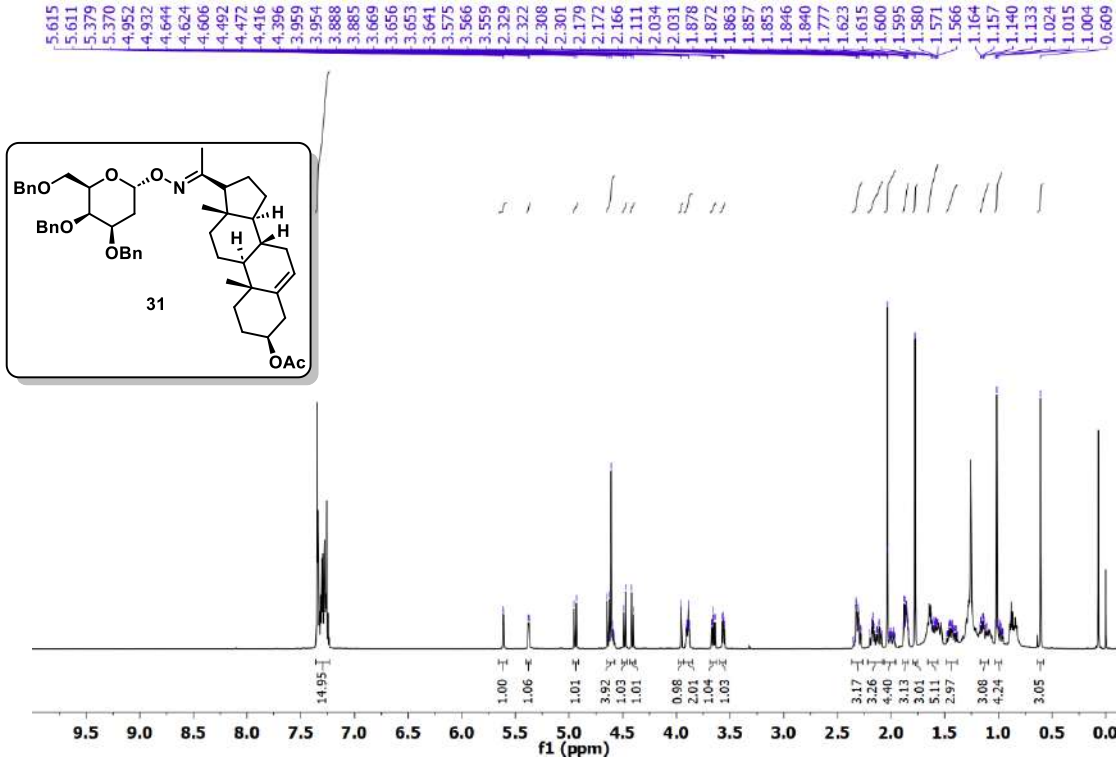

Figure 2.26. *^{1}H NMR of compound **31** (600 MHz, $CDCl_3$).*

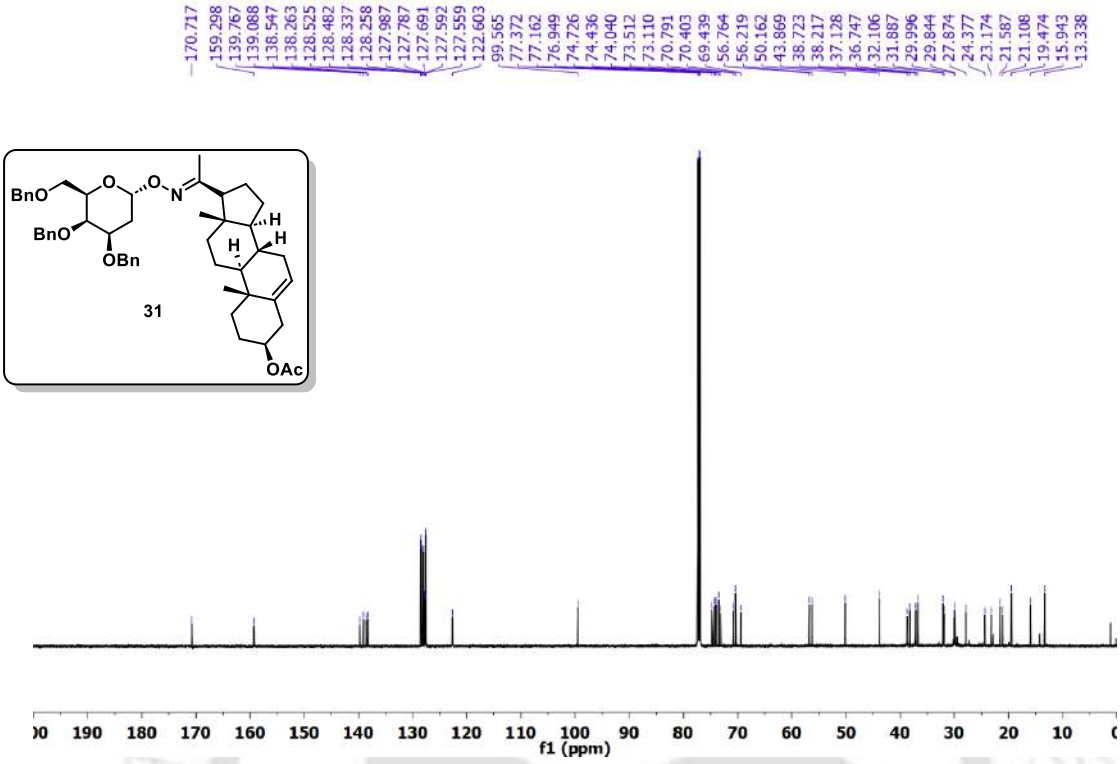

Figure 2.27. *^{13}C NMR of compound **31** (151 MHz, $CDCl_3$).*

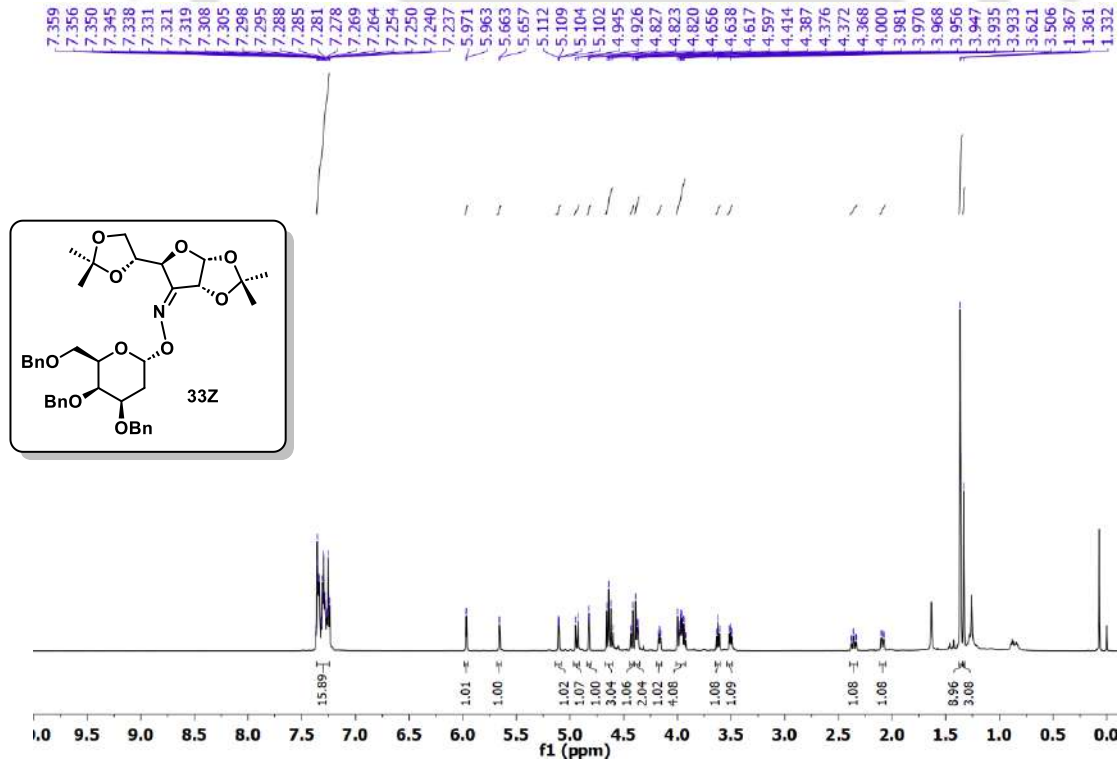

Figure 2.28. *^{1}H NMR of compound **33Z** (600 MHz, $CDCl_3$).*

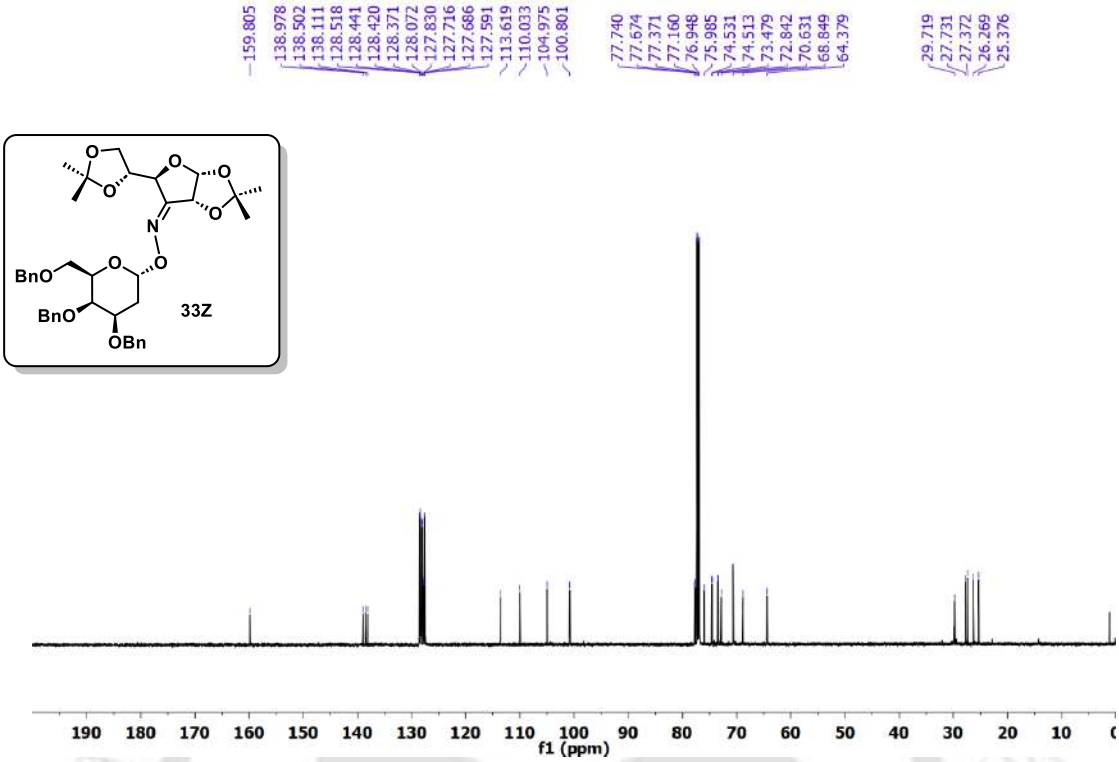

Figure 2.29. *^{13}C NMR of compound **33Z** (151 MHz, $CDCl_3$).*

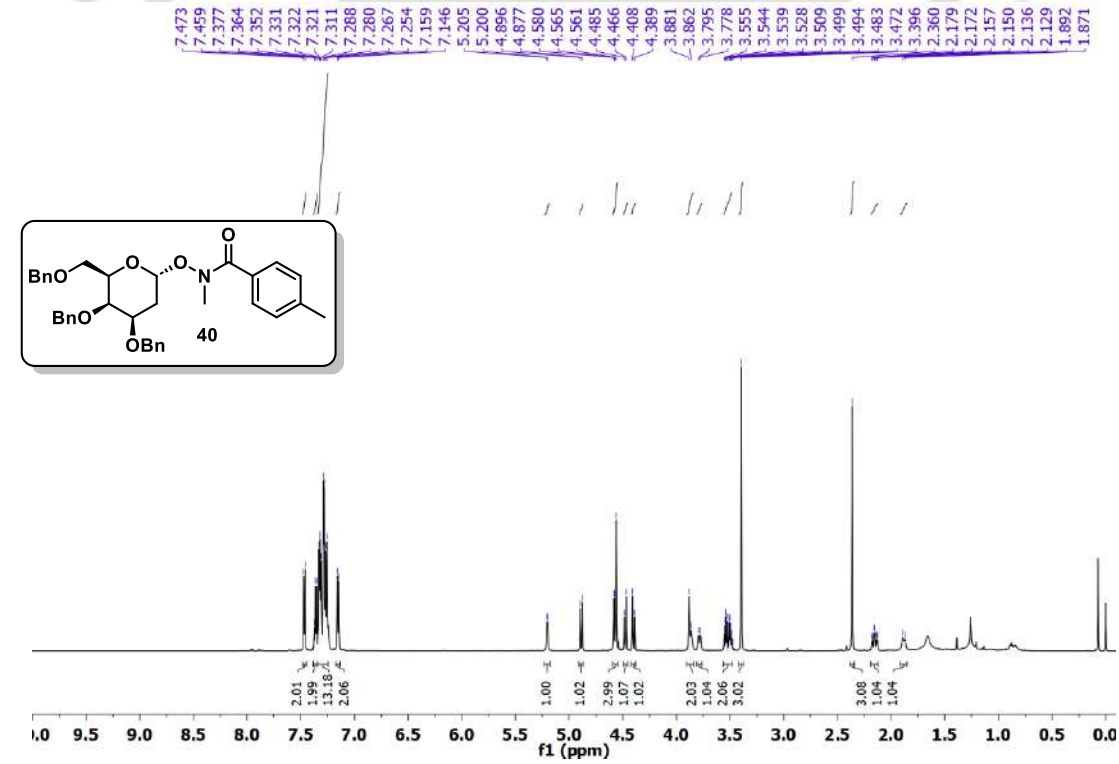

Figure 2.30. *^{1}H NMR of compound **40** (600 MHz, $CDCl_3$).*

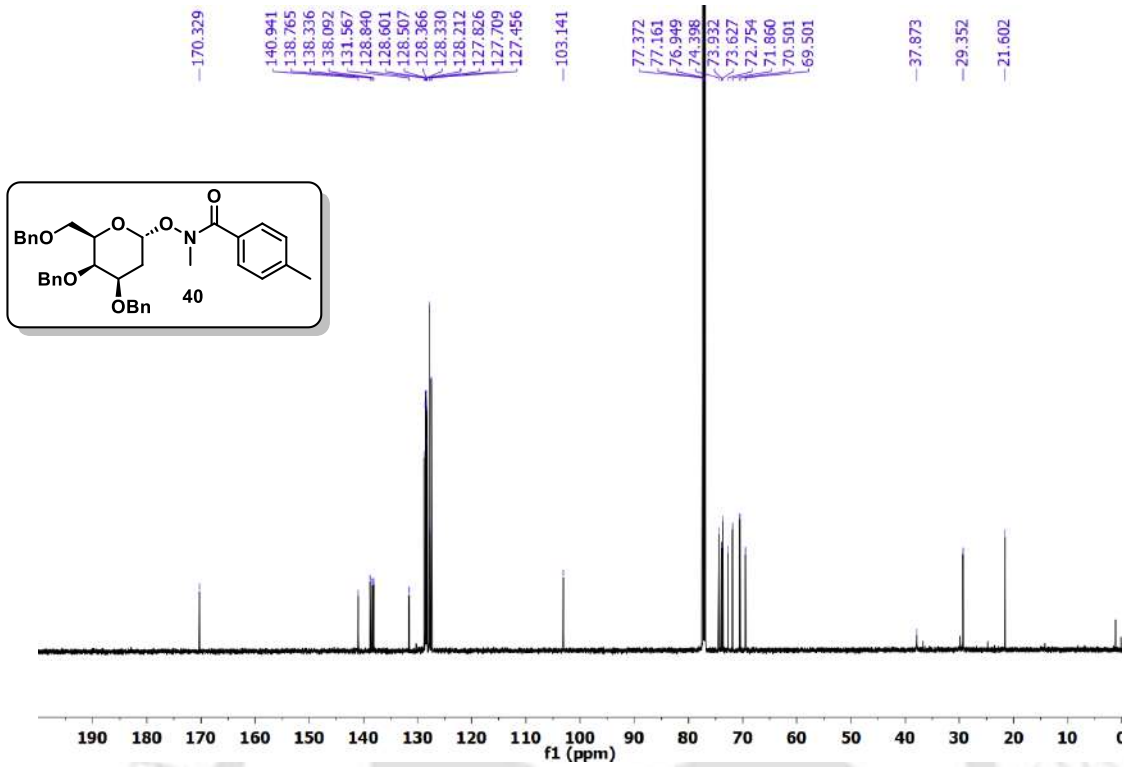

Figure 2.31. *^{13}C NMR of compound **40** (151 MHz, $CDCl_3$).*

2.8. SC-XRD data of 48

The ORTEP diagram with an ellipsoid of 30% probability.

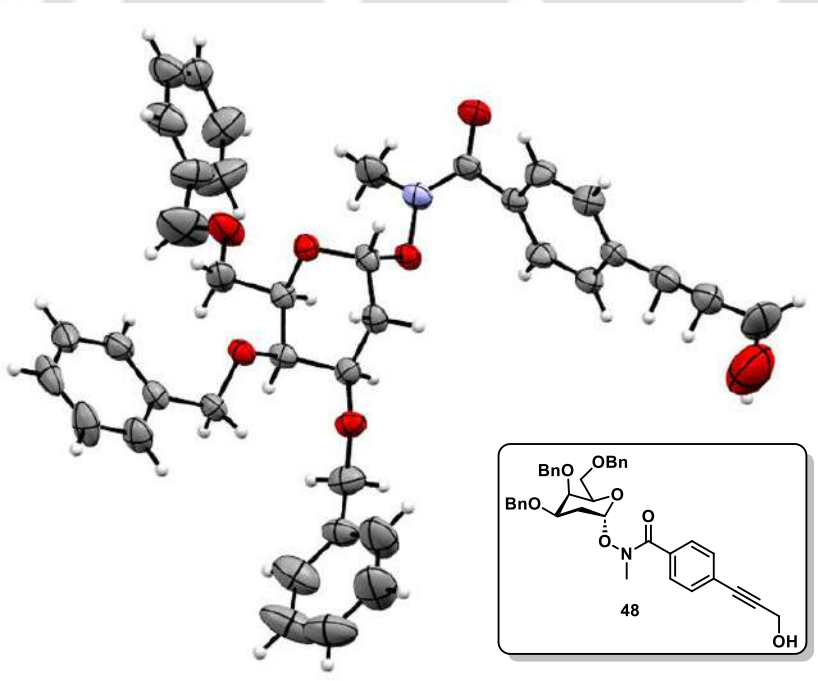

Table 2.5: Crystal parameters and refinement data of **48**

Parameters	Substrate 48
Formula	$C_{38}H_{39}NO_7$
Fw	621.70
Crystal system	monoclinic
Space group	*P 21*
a/Å	11.7715(11)
b/Å	9.3506(9)
c/Å	15.6304(14)
α/°	90.00
β/°	104.025(3)
γ/°	90.00
V/Å^3	1669.2(3)
Z	2
D_c/g cm^{-3}	1.237
μ Mo K_α/mm^{-1}	0.085
F000	660
T/K	295(2)
θ max.	25.68
Total no. of reflections	37645
Independent reflections	5850
Observed reflections	3082
Parameters refined	484
R_1, I > 2σ(I)	0.0833
wR_2, I > 2σ(I)	0.1270
GOF (F^2)	1.036
CCDC No.	2382914

Chapter 3

Sulfonium Stabilized Phenols as Hydrogen Bonding Catalysts toward Diastereoselective Glycosylation of Cyclopropanated Sugars

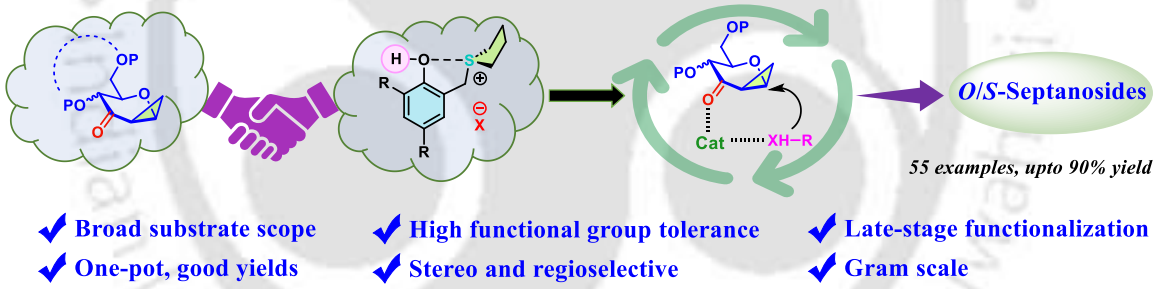

✔ Broad substrate scope
✔ One-pot, good yields
✔ High functional group tolerance
✔ Stereo and regioselective
✔ Late-stage functionalization
✔ Gram scale

(*Org. Lett.* **2025**, *27*, 11650–11655)

3.1. Introduction

3.1.1. Importance of septanosides

Imitating natural glycans[1] is a clever strategy to mislead microorganisms and enzymes responsible for numerous diseases. A key strategy for mimicking natural carbohydrates is to modify ring size, where ring-expanded hexoses, such as septanoses or oxepanes, serve as highly effective carbohydrate mimics (Figure 3.1).[2]

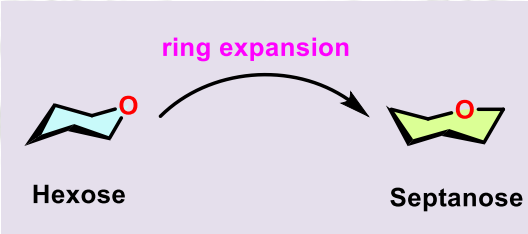

Figure 3.1. Carbohydrate-based oxepane.

The oxepanone scaffold is featured in a diverse array of marine natural products, including hemibrevetoxin B, raspacionin B, sipholenol A, neviotine A, dahabinone A, and aplysistatin (Figure 3.2).[3]

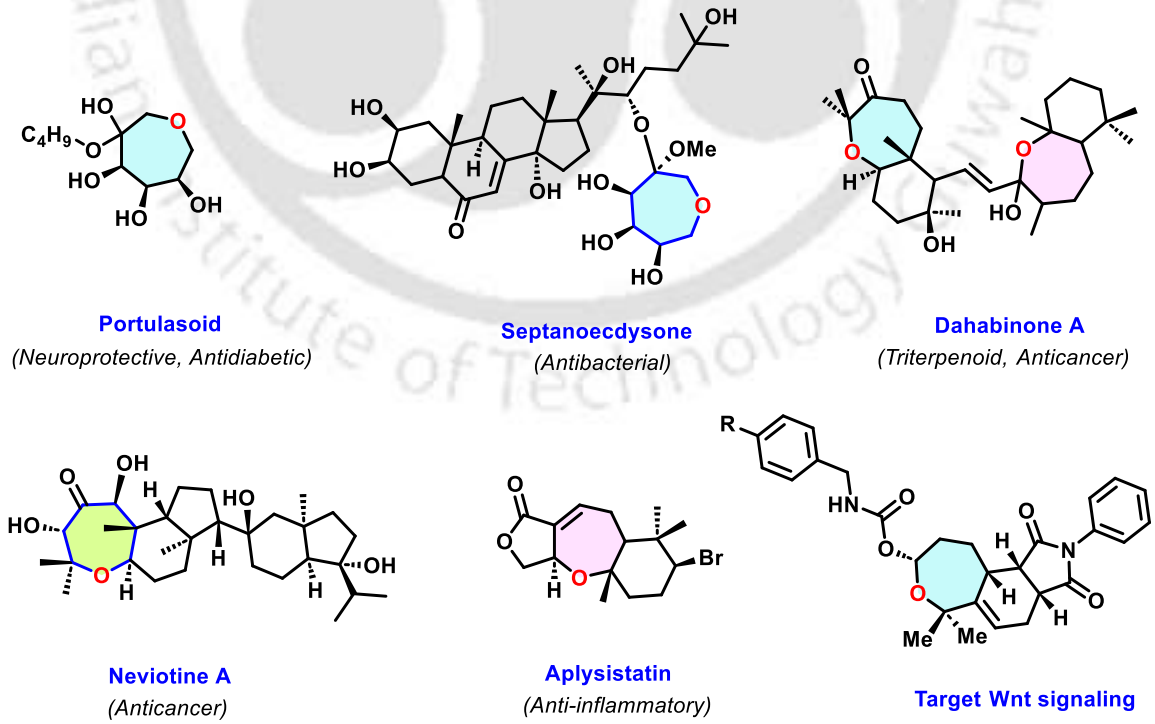

Figure 3.2. Bioactive oxepanes.

Kuszmann et al. reported that septanose analogues of thio-pyranose exhibited a tenfold increase in biological activity relative to beciparcil, a clinically used oral anti-thrombotic agent.[4] Similarly, research by Peczuh and colleagues into carbohydrate-protein interactions, specifically involving methyl septanosides and concanavalin A, has provided initial evidence that septanosides can mimic pyranosides.[5] Damha et al. developed DNA and RNA mimics by substituting the natural pentofuranose ring with a cyclic seven-membered septanose unit. The resulting septanose-based nucleic acids exhibit enhanced resistance to nuclease degradation while retaining key structural features of native DNA (Figure 3.3).[6] In addition, septanoecdysone and portulasoid, isolated from *Atriplex portulacoides*, exhibit anticholinesterase and antibacterial activities (Figure 3.2).[7] More recently, these septanosides have been identified as biological probes capable of penetrating the *Escherichia coli* membrane.[8] The notable bioactivity has prompted extensive efforts to develop synthetic pathways for carbohydrate-derived oxepanes and septanose-based glycoconjugates.[9]

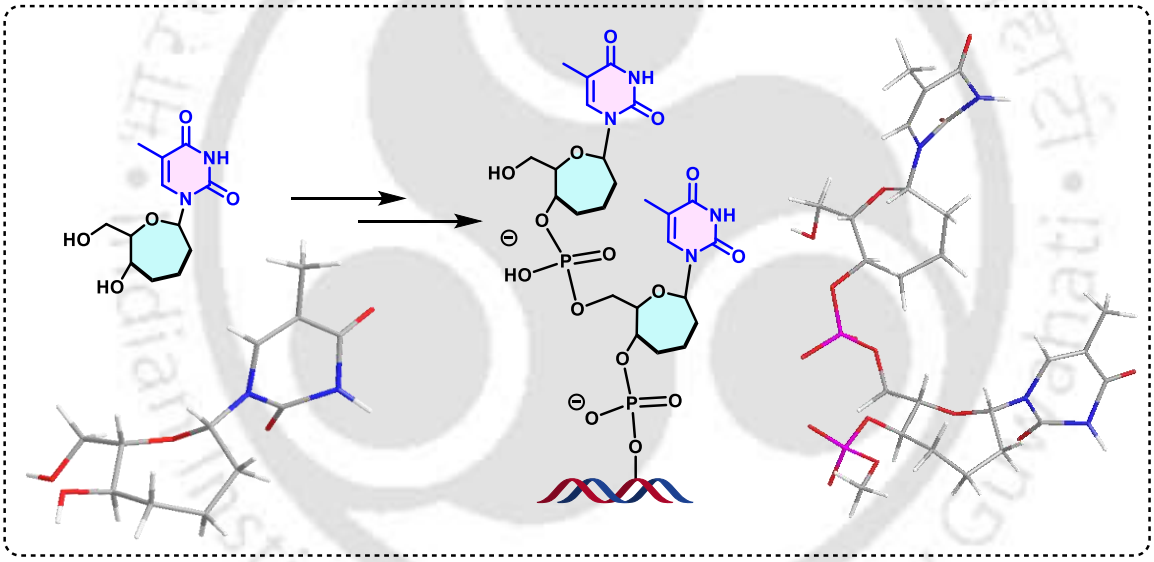

Figure 3.3. Seven-membered carbohydrate ring-modified oligonucleotides.

3.1.2. Existing methods for synthesizing septanosides

Carbohydrate-derived donor-acceptor cyclopropanes (DACs) constitute a class of compounds currently being explored for their potential to create a variety of biologically essential carbohydrate mimics.[10] The introduction of an electron-withdrawing group at the C-3 position of 1,2-cyclopropanated sugar derivatives would create cyclic donor-acceptor cyclopropanes, which could undergo regioselective electrophilic ring-opening reactions, assisted by the endocyclic oxygen, to form oxepane derivatives. In 2012, Ramu Sridhar and Venukumar investigated a stereoselective methodology for the synthesis of 2,3-dideoxyseptanohexoses via ring-expansion septanosylation of 1,2-cyclopropanated

donors, promoted by 20 mol% TMSOTf. Despite its efficiency, this approach exhibited reduced anomeric selectivity in the resulting glycosides (Scheme 3.1).[11]

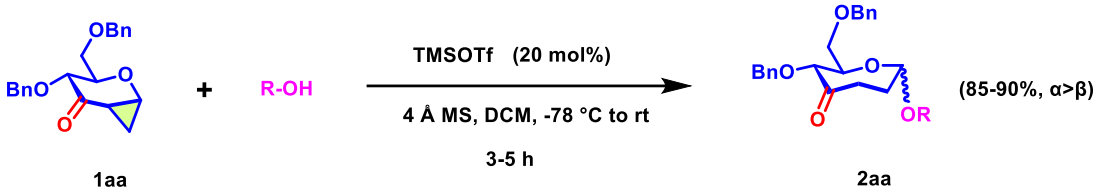

Scheme 3.1. Ring-expansion-septanosylation using 1,2-cyclopropanated donor.

In 2022, the Sridhar group developed a diastereoselective (3+2) cycloaddition using 50 mol% TMSOTf at −10 °C to access bridged oxepanone-indole hybrids as enantiopure products. The reaction scope was assessed using chiral monosaccharide-based cyclopropanes, racemic aryl DACs, and indole substrates bearing electron-donating, electron-withdrawing, and N-alkyl groups (Scheme 3.2).[12]

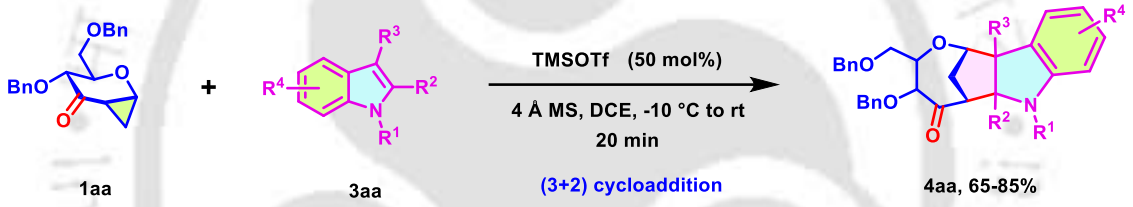

Scheme 3.2. Synthesis of sugar-based bridged oxepanone-indole hybrids.

In 2023, Ma et al. developed a stereoselective glycosylation protocol utilizing 2 mol% phosphonoselenium catalyst at 40-50 °C, where C2-substituted cyclopropanated sugars undergo activation via hydrogen and bifurcated chalcogen bonding to achieve both substrate activation and anomeric control (Scheme 3.3).[13]

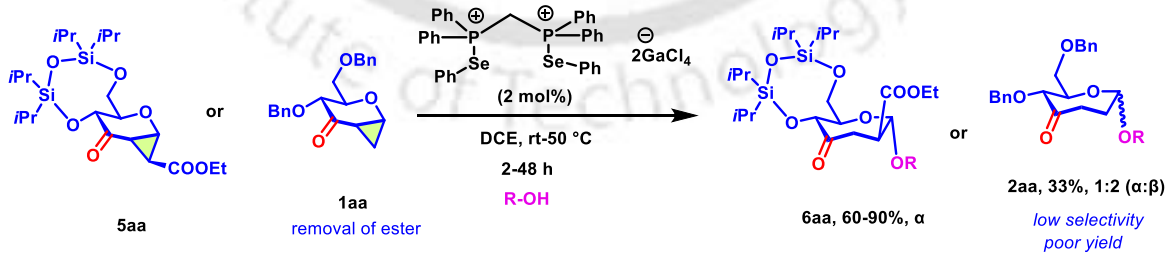

Scheme 3.3. Diphosphonoselenium-catalyzed septanosylation.

3.1.3. Knowledge gap

Despite its potential and recent advancements, stereoselective septanosylation remains largely underexplored, with only a limited number of examples reported to date.[11, 13] A

persistent challenge lies in achieving reliable anomeric control, which has yet to be satisfactorily addressed.[11, 14] In existing literature, both acidic and basic reaction conditions have resulted in poor anomeric selectivity, as Brønsted acids promote hydrolytic cleavage of the glycosidic bond[15]. At the same time, strong bases increase epimerization susceptibility.[14, 16] Notably, harsh reaction conditions, particularly with silylated donors, hamper direct glycosylation due to the susceptibility of silyl protecting groups to strong Lewis acids. Additionally, the substrate scope is limited, and anomeric selectivity remains unsatisfactory with 3-oxo-1,2-cyclopropanated sugar lacking substituents on the cyclopropane ring, even when using the recent developed diphosphonoselenide catalyst.[13] Additionally, creating small-molecule catalysts that can concurrently engage both substrates and drive highly stereoselective coupling reactions continues to be a major synthetic challenge.

3.1.4. Purpose and objectives of the chapter

In Chapter 1, we have discussed the synthetic utility and the electronic properties of phenolic scaffolds, which are cost-effective compounds known for their catalytic efficiency and valued for their dual role as Brønsted acids and hydrogen bond donors.[17-19] Building upon these findings on charge-activated catalytic systems, we designed a phenol-based catalyst incorporating a sulfonium moiety as a charged arm to modulate the catalytic properties of the phenol core.

In this chapter, we present a robust catalytic strategy using a simple, electrostatically tuned phenolic sulfonium salt to enable α-selective strain-release *O*- and *S*-glycosylation toward biologically significant seven-membered oxepane frameworks. The through space interaction of the sulfonium cation with the phenolic oxygen lone pair increases the Bronsted acidity/hydrogen-bonding ability of the phenol, thereby helping the strain-release ring opening of the carbohydrate-derived donor-acceptor cyclopronane, leading to septanosylation. In addition, the simultaneous activation of the alcohol nucleophile by the anion from the same phase as the cation leads to the stereoselective addition of the nucleophile. This unique mode of dual activation by these novel ion-pair catalysts helps us utilize various classes of nucleophiles, such as alcohols, thiols, and even carboxylic acids and amino acids. The unique reactivity of the phenolic cyclic sulfonium salt has been studied by ^{1}H-NMR, IR, UV, and fluorescence spectroscopic studies.

3.2. Results and discussion

3.2.1. Optimization study

We initiated our study by investigating the reaction between cyclopropanated glucosyl donor **1a** and acceptor **2a** as model substrates, systematically evaluating various catalysts and solvents to optimize the reaction conditions (Table 3.1). We hypothesize that using 3-keto cyclopropane-fused pyranoses may offer a thermodynamic advantage by facilitating donor activation through strain release within the pyranosyl ring. Keeping in view the influence of counterion effects in bulky pyridinium salt-catalyzed glycosylation reactions,[20] we examined a series of sulfonium salts bearing Cl, BF_4, triflate, and BArF as counterions for the synthesis of septanosides (Table 3.1). Initially, donor **1a** and acceptor **2a** were subjected to glycosylation using 5 mol% sulfonium chloride salt (**1A**) in DCM at room temperature; however, no product formation was observed (Table 3.1, entry 1). Notably, the use of phenolic tetrafluoroborate salt **1B** under identical conditions furnished septanoside **3a** in 82% yield with a 7:1 α/β selectivity after 5 hours (Table 3.1, entry 2). The stereochemical configuration of **3a** was established through NMR and NOE experiments (see experimental section for details). Treatment with triflate salt **1C** resulted in donor decomposition after 4 hours (Table 3.1, entry 3). BArF salt **1D** also catalyzed the reaction, albeit with slightly reduced yield and selectivity (Table 3.1, entry 4). This observation prompted us to evaluate the influence of anions, revealing that the weakly coordinating BF_4 salt exhibits superior reactivity (**1B**), outperforming its analogues (**1C** and **1D**) in both selectivity and yield. Subsequently, we examined the influence of substituents on the aromatic ring of phenol. Notably, catalyst **1E**, bearing a less sterically demanding methyl group, afforded septanoside **3a** in 86% yield with a 13:1 α/β selectivity after 12 hours (Table 3.1, entry 5). To further explore the hydrogen-bonding interactions between the α-hydrogen atoms of the sulfonium salt and the donor, we conducted the reaction exploiting benzylsulfonium salt **1F**; however, no product formation was observed (Table 3.1, entry 6). Brønsted acid activation with triflic acid resulted in donor decomposition (Table 3.1, entry 7). Catalyst **1E** at 2 mol% gave reduced conversion (73% yield, Table 3.1, entry 8), while increasing the loading to 10 mol% maintained conversion but affected reaction time (Table 3.1, entry 9). Additionally, a series of solvents was screened (Table 3.1, entries 10-14), identifying DCM as the most effective solvent for this transformation. Consequently, the standard reaction conditions were set to 5 mol % of catalyst **1E** in dry DCM at room temperature. The reactions reveal that isolated anionic or charged sulfonium centers exert minimal influence, while the substituted charged arm plays a critical role in regulating phenol's catalytic behavior via through-space electrostatic stabilization of the phenoxide.

Table 3.1. Optimization of the reaction conditions[a]

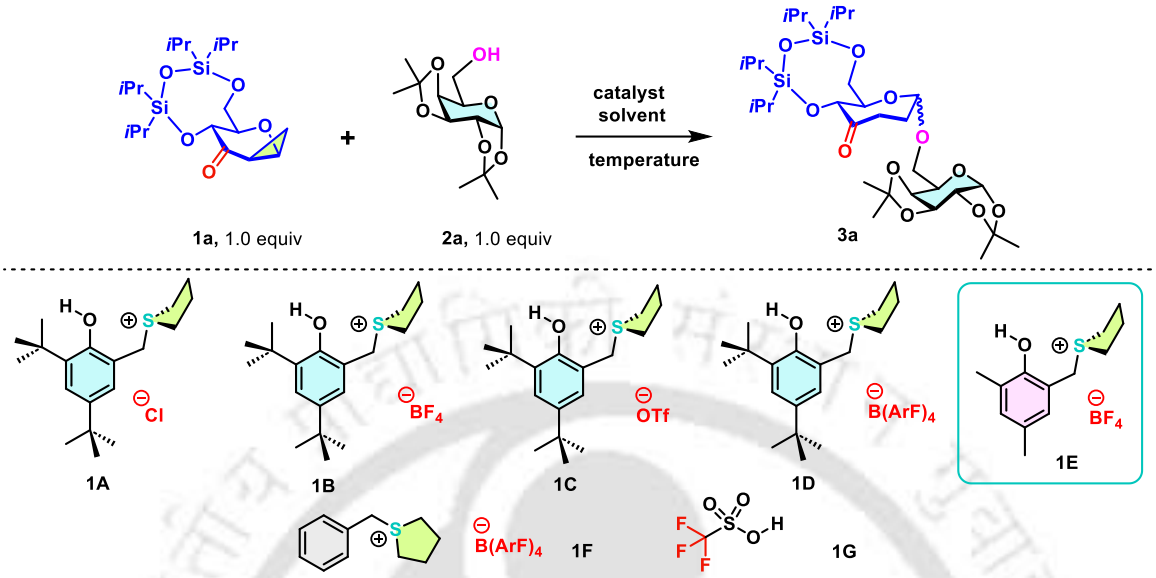

Entry	Catalyst	Solvent	Temp (°C)	Time (h)	(3a) (%)[b] (*α*/*β*)[e]
1	**1A**	DCM	rt-40	24	---
2	**1B**	DCM	rt	5	82 (7:1)
3	**1C**	DCM	rt	4	decomposed
4	**1D**	DCM	rt	14	75 (4:1)
5	**1E**	DCM	rt	12	86 (13:1)
6	**1F**	DCM	rt-40	24	---
7	**1G**	DCM	rt	30 min	decomposed
8[c]	**1E**	DCM	rt	30	73 (10:1)
9[d]	**1E**	DCM	rt	10	80 (13:1)
10	**1E**	Ether	rt-40	48	-----
11	**1E**	Toluene	rt-40	48	-----
12	**1E**	Acetone	rt-40	48	-----
13	**1E**	DMF	rt-40	48	-----
14	**1E**	1,4-dioxane	rt-40	48	-----

[a]Reaction conditions: **1a** (0.25 mmol), **2a** (0.25 mmol), **1A-1G** (5 mol %), solvent (1 mL). [b]Isolated yield. [c]2 mol % **1E** was used. [d]10 mol % **1E** was used. [e]Determined from crude ^{1}H NMR.

3.2.2. Substrate scope

The unique structural attributes of the phenolic sulfonium catalyst promote stereoselective septanosylation and broaden its compatibility with a diverse array of potential reaction partners. With the optimized protocol established, we next evaluated the substrate scope,

which gratifyingly demonstrated broad applicability with consistently robust performance (Table 3.2). Notably, this method delivers septanosides with excellent α-selectivity by employing stereochemically diverse donor-acceptor cyclopropanes (DACs) derived from glucosyl, galactosyl, and rhamnosyl donors, while exhibiting broad tolerance toward a sizable range of *O*-nucleophilic acceptors (Table 3.2). Glycosylation of primary and secondary alcohol acceptors synthesized from pyranose and furanose frameworks selectively furnished disaccharides **3a-3i** and **3zd-3zg** with good to excellent yields and high stereoselectivity (Table 3.2). We extended our study to a variety of readily available alcohols, evaluating less bulky primary (**3j-3o**), more sterically demanding secondary (**3p-3r**), and highly hindered tertiary alcohols (**3s**) as nucleophilic partners. This broad array proved amenable to our strategy, affording *O*-septanosides **3j-3s** with good to excellent anomeric selectivities (Table 3.2). Furthermore, biologically important chiral monoterpenoid alcohols, including Citronellol, L-borneol, and L-menthol, were well tolerated, offering the corresponding glycosides **3t-3v** in good yields with high α-selectivity (Table 3.2). Lipids such as cholesterol, steroids like pregnenolone and diosgenin, and the lipid-lowering drug simvastatin, each bearing hydroxyl groups at distinct positions along with various functional groups, underwent smooth transformation to afford glycolipid-type derivatives **3w-3z** and **3zc** (Table 3.2). These compounds hold promise for applications in glycolipid research and cardiac glycoside studies.[21] Other biologically important acceptors, such as protected L-serine and L-threonine, exhibited excellent reactivity, affording **3za** and **3zb** (Table 3.2). These results may open promising avenues for further exploration in glycopeptide research.

Subsequently, we investigated the reactivity and selectivity of phenolic nucleophiles under optimized conditions (Table 3.3). However, the selective synthesis of *O*-aryl glycosides via nucleophilic substitution between a carbohydrate electrophile and phenol remains challenging,[22] owing to the electron-withdrawing nature of the aromatic ring, steric and electronic effects from phenolic substituents, and the propensity of *O*-aryl glycosides to undergo facile rearrangement to *C*-aryl glycosides.[23] Consequently, the pursuit of advanced glycosylation methodologies to synthesize *O*-aryl septanosides with improved efficiency, selectivity, and functional group tolerance remains an area of sustained research interest. Phenols containing electron-donating groups, along with biologically significant substrates like eugenol, α-tocopherol, and sesamol, were well tolerated, offering products **5a-5g** in good yields with α-selectivity (Table 3.3). The milder sulfonium salt-catalyzed methods, in contrast to the harsher Lewis acid TMSOTf-catalyzed protocols,[24] enabled efficient incorporation of thiol-based acceptors, thereby offering access to *S*-septanosides **5h-5l** with good to high yields (Table 3.3).

Table 3.2. Substrate scope of *O*-septanosides[a]

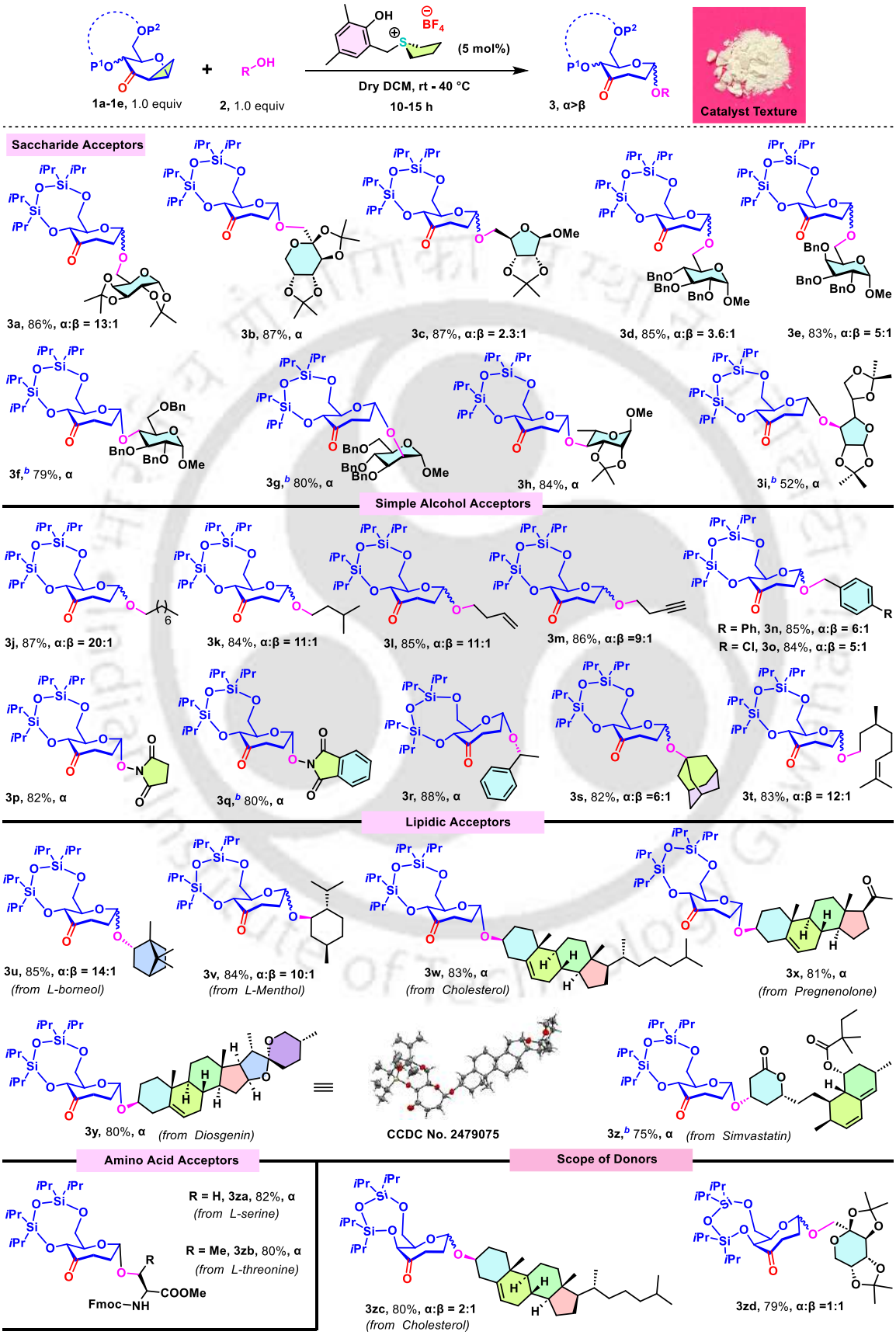

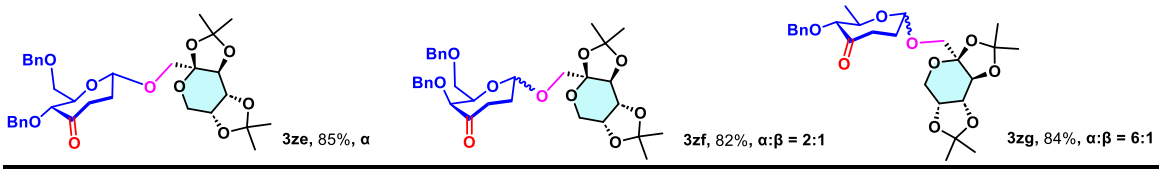

[a]Reaction conditions: **1a**-**1e** (0.25 mmol), **2** (0.25 mmol), **1E** (5 mol %), Dry DCM (1.0 mL), rt (10-15 h). Isolated yield. *α*/*β* ratios were determined using crude ^{1}H NMR analysis. [b]40 °C (4-5 h).

Table 3.3. Substrate scope of *O*/*S*-aryl septanosides[a]

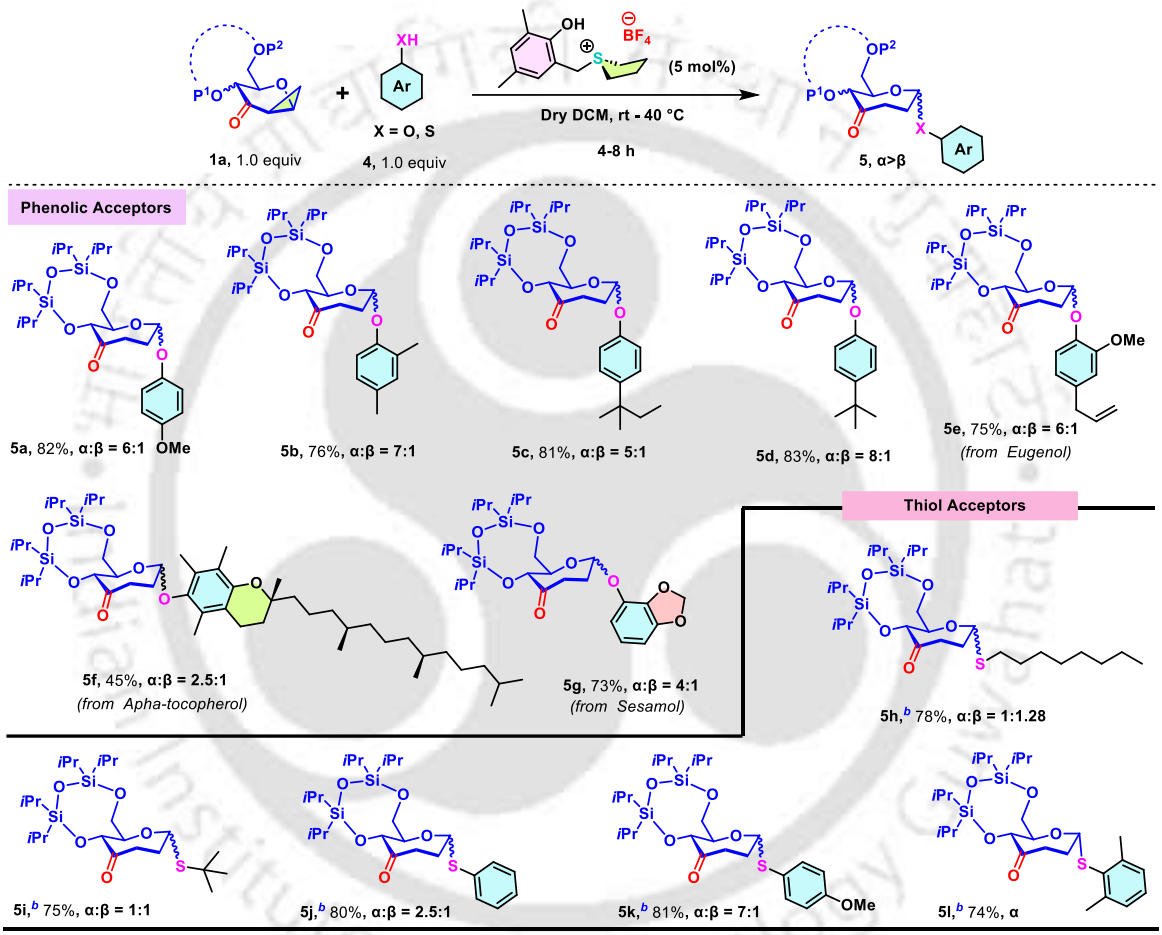

[a]Reaction conditions: **1a** (0.25 mmol), **4** (0.25 mmol), **1E** (5 mol %), Dry DCM (1.0 mL), 40 °C (4-5 h). Isolated yield. *α*/*β* ratios were determined using crude ^{1}H NMR analysis. [b]rt (4-8 h).

To evaluate the generality of the protocol, we investigated its applicability to a range of carboxylic acid acceptors. As summarized in Table 3.4, various structurally sensitive carboxylic acids underwent efficient glycosylation with excellent selectivity. A broad range of carboxylic acids, including dodecanoic acid, 4-methoxyphenylacetic acid, and benzoic acid, were well tolerated, highlighting the method's high functional group compatibility. These substrates furnished septanosyl esters **7a**-**7b** and **7i** in excellent yields with remarkable α-selectivity (Table 3.4). In addition, the robustness of the method was further demonstrated by biologically active drug acids as coupling partners. Application of nonsteroidal anti-inflammatory agents, including ibuprofen, (*S*)-naproxen,

indomethacin, diclofenac, and aceclofenac, as well as the lipid-lowering drug gemfibrozil, enabled rapid access to septanosyl esters **7c-7h** in 80-83% yield with excellent α-stereoselectivity (Table 3.4). For the first time, we have developed a catalytic, highly α-stereoselective septanosylation reaction that employs a diverse array of structurally complex carboxylic acids as acceptors.

Table 3.4. Substrate scope of septanosyl esters[a]

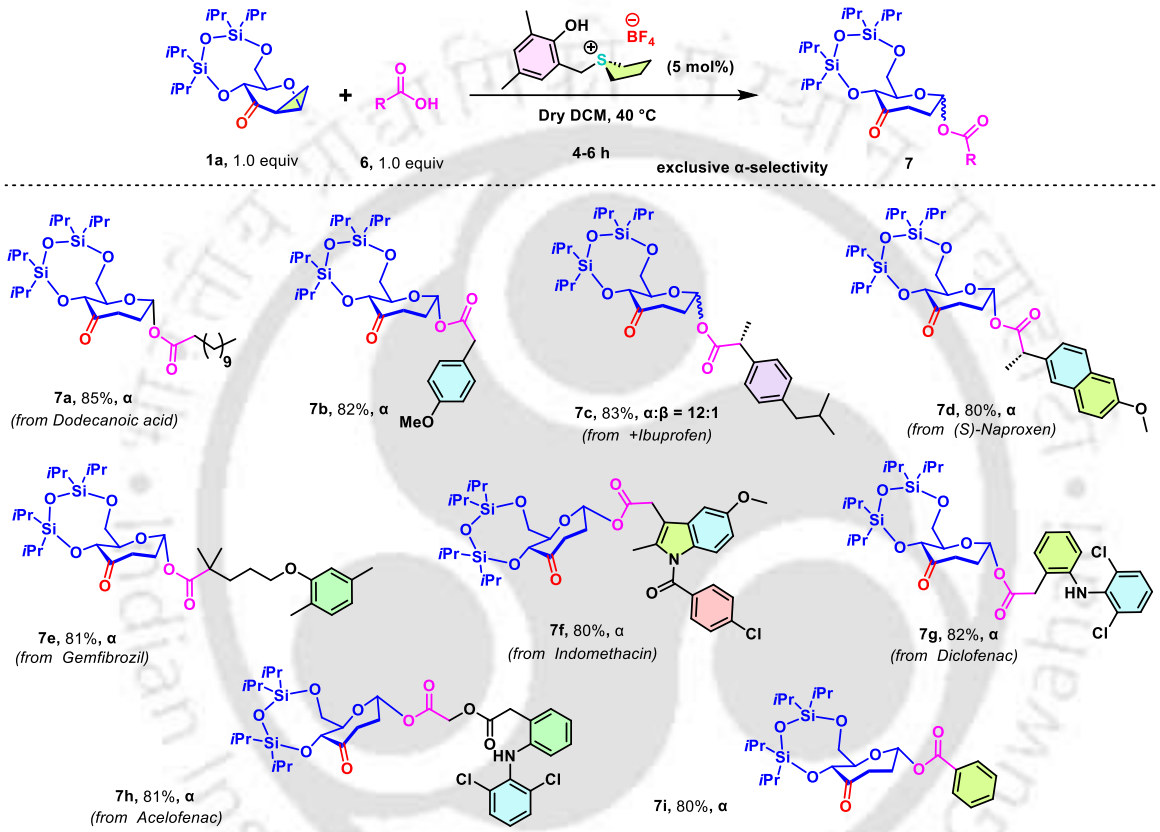

[a]Reaction conditions: **1a** (0.25 mmol), **6** (0.25 mmol), **1E** (5 mol %), Dry DCM (1.0 mL), 40 °C (4-6 h). Isolated yield. *α*/*β* ratios were determined using crude ^{1}H NMR analysis.

3.2.3. Investigation of the mechanism

3.2.3.1. Control experiments

A series of control experiments, as shown in Scheme 3.4, was performed to investigate the mechanism of the current transformation. To elucidate the role of the phenolic O-H in the reaction, the O-H group was masked with a methyl protecting group (**1H**). The absence of the phenolic O-H resulted in the complete shutdown of the catalytic activity, resulting in no product formation (Scheme 3.4). This outcome underscores its essential role, as the acidic hydroxyl group appears to provide a critical driving force in activating the keto functionality of the donor. Also, when the reaction was performed with Brønsted

acid, hydrofluoroboric acid, it completely led to the decomposition of the starting material, signaling that the current method is not proceeding via a typical Brønsted acidic mechanism (Scheme 3.4). To further examine the catalytic activity and assess the influence of the charged arm, the reaction was carried out in the presence of neutral 4-nitrophenol, which failed to catalyze the reaction (Scheme 3.4). To demonstrate the importance of the intramolecular interaction between the sulfonium ion and phenol hydroxyl group, the reaction was carried out in the presence of catalyst **1F** and 4-nitrophenol, which failed to catalyze the reaction (Scheme 3.4). This observation clearly suggests that the catalytic nature of the phenolic sulfonium salt is governed not only by its acidity, but also by the presence of the charged arm within the phenolic framework, which renders the electrostatic interactions.

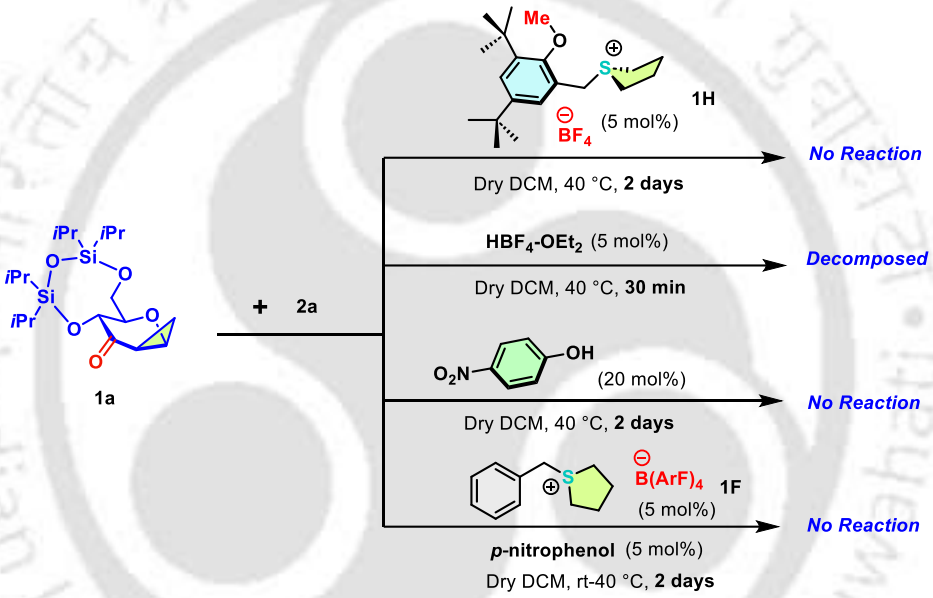

Scheme 3.4. Control experiments.

3.2.3.2. ^{1}H NMR titration experiments

To investigate the mechanism of the current transformation, ^{1}H NMR experiments were conducted in ACN-d_3 (Figure 3.4). Upon mixing catalyst **1E** and alcohol **2k** in ratios ranging from 1:1 to 1:10, a notable downfield shift was observed for the OH proton of **1E** (**H**$_A$, from δ 6.656 to 6.882 ppm), along with a significant downfield shift for the OH proton of **2k** (**H**$_E$, from δ 2.171 to 2.507 ppm). These observations strongly indicate the presence of a hydrogen bond between the catalyst and alcohol.

Similarly, titration of **1E** with donor **1a** in ratios ranging from 1:1 to 1:6, a significant downfield shift was observed for the OH proton of **1E** (**H**$_A$, from δ 6.656 to 6.741 ppm), along with a modest downfield shift for the methylene proton adjacent to the sulfonium center (**H**$_D$, from δ 4.307 to 4.338 ppm). Furthermore, slight downfield shifts

were also detected for the remaining protons of both catalyst **1E** and donor **1a** throughout the titration (Figure 3.5).

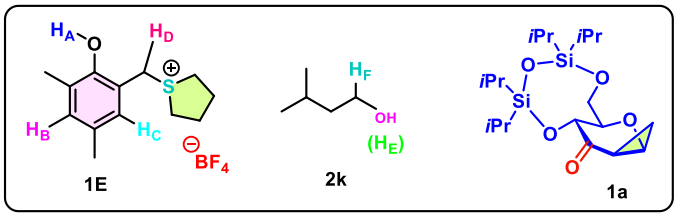

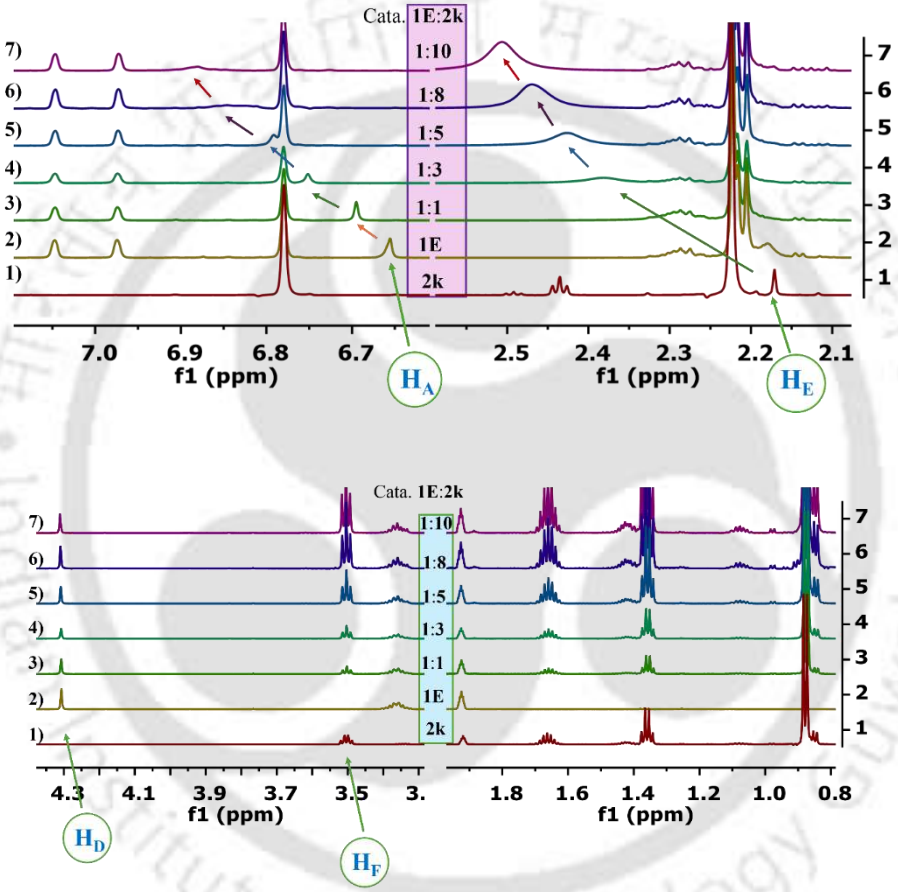

Figure 3.4. ^{1}H NMR titration of catalyst **1E** with alcohol **2k**.

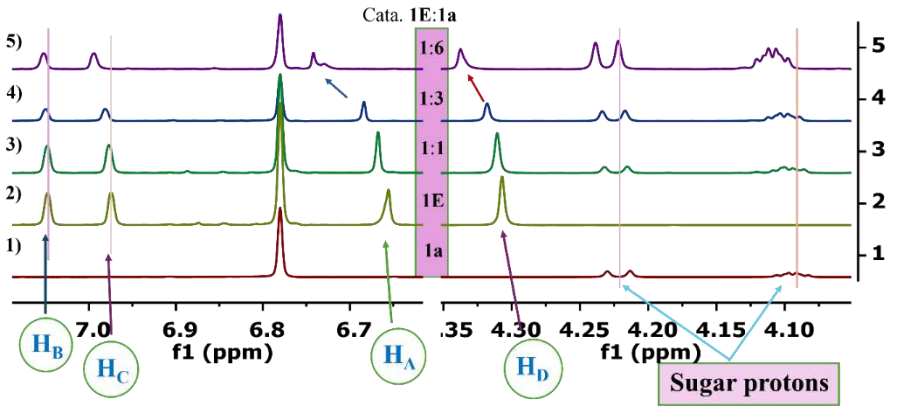

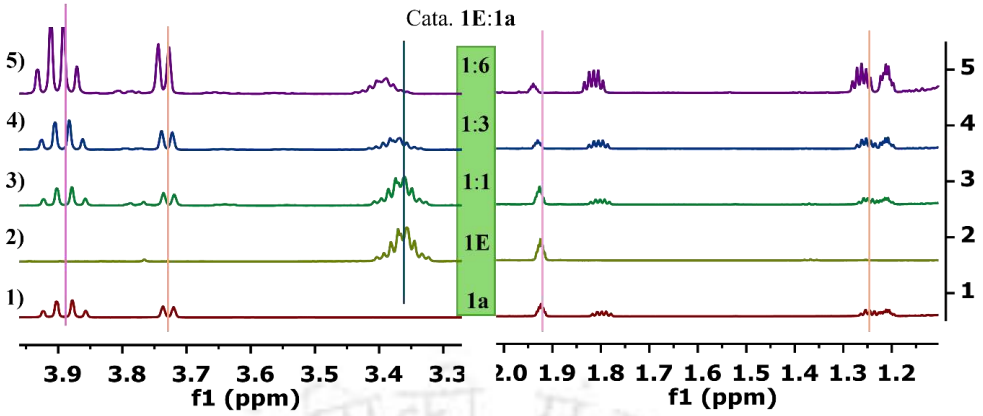

Figure 3.5. ^{1}H NMR titration of catalyst **1E** with donor **1a**.

Also, the ^{13}C NMR revealed an upfield shift of the 3-keto group of the donor from δ 203.924 to 203.820 ppm, along with the emergence of new carbon peaks throughout the titration. This demonstrates a strong interaction of the catalyst with the donor. Furthermore, ^{19}F NMR clearly suggested a downfield shift of the fluorine resonance (δ –151.584 to –151.493 ppm), underscoring a significant change in the electronic environment of the fluorinated moiety upon donor association (Figure 3.6).

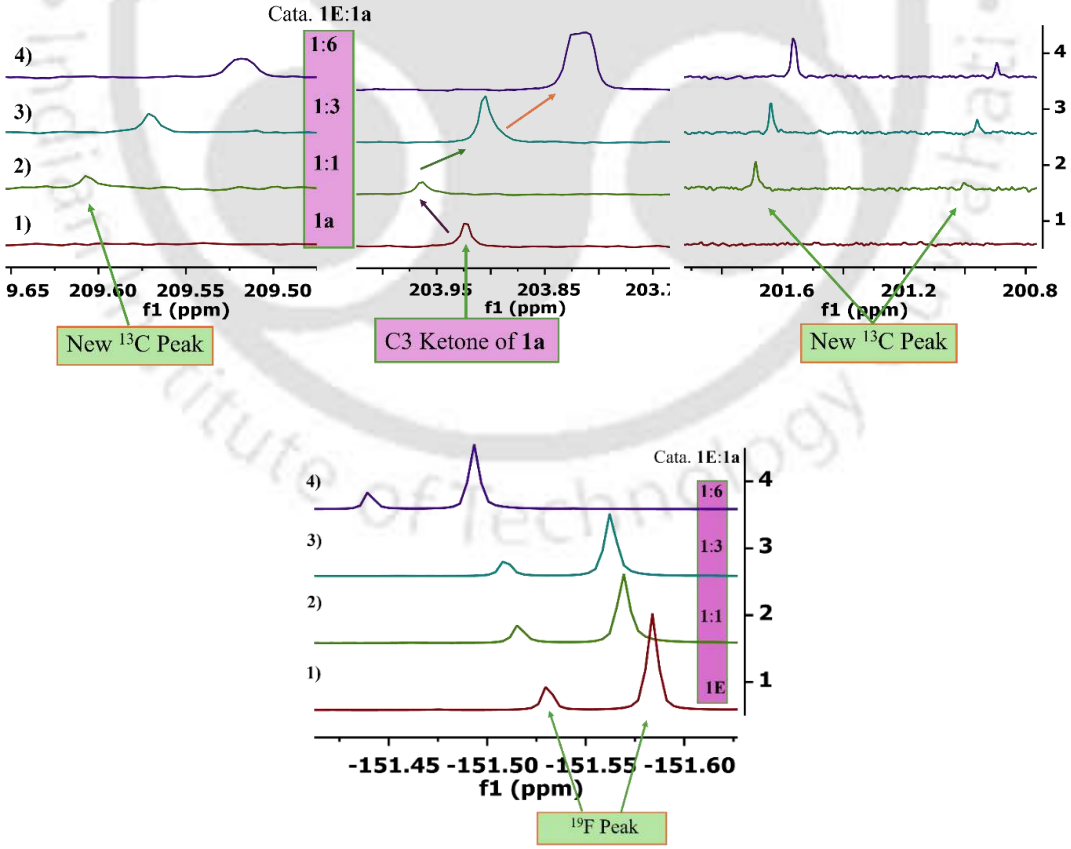

Figure 3.6. ^{13}C and ^{19}F NMR titration of catalyst **1E** with donor **1a**.

3.2.3.3. The UV-Vis titration experiments in ACN

Three experimental groups were established. The first group consisted of UV-Vis measurement for a catalyst **1E** with a concentration of 0.12 mM in ACN (acetonitrile). In the second group, four UV-Vis measurements were taken for a mixture of catalyst **1E** (with a constant concentration of 0.12 mM) and alcohol **2k** at varying concentrations (0.06 mM, 0.12 mM, 0.36 mM, and 0.60 mM) in ACN (Figure 3.7, a). The third group consisted of four UV-Vis measurements were taken for a mixture of catalyst **1E** (with a constant concentration of 0.12 mM) and donor **1a** at varying concentrations (0.06 mM, 0.12 mM, 0.36 mM, and 0.60 mM) in ACN (Figure 3.7, b).

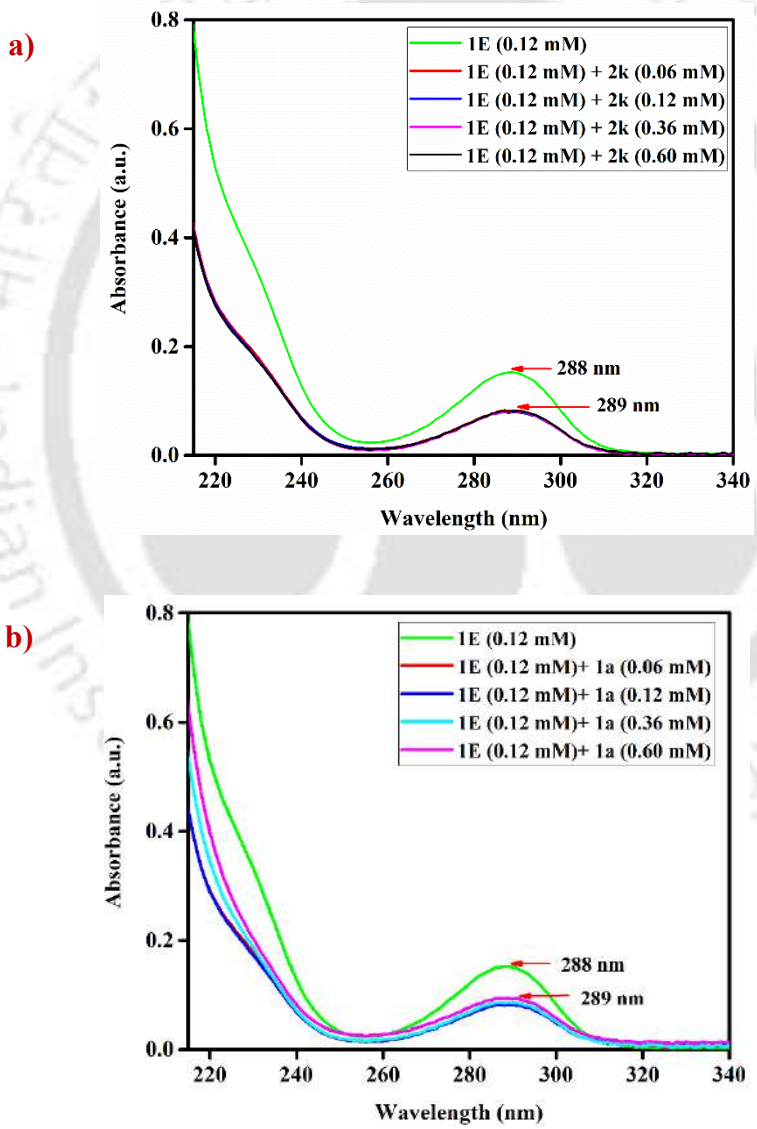

Figure 3.7. a) UV-Vis spectra of **1E** and mixture of **1E** and **2k** b) UV-Vis spectra of **1E** and mixture of **1E** and **1a**.

3.2.3.4. Fluorescence titration experiments in ACN

Three experimental groups were established. The first group consisted of Fluorescence titration for a catalyst **1E** with a concentration of 0.12 mM in ACN (acetonitrile). In the second group, four Fluorescence titrations were taken for a mixture of catalyst **1E** (with a constant concentration of 0.12 mM) and alcohol **2k** at varying concentrations (0.06 mM, 0.12 mM, 0.36 mM, and 0.60 mM) in ACN (Figure 3.8, a). The third group consisted of four Fluorescence titrations were taken for a mixture of catalyst **1E** (with a constant concentration of 0.12 mM) and donor **1a** at varying concentrations (0.06 mM, 0.12 mM, 0.36 mM, and 0.60 mM) in ACN (Figure 3.8, b).

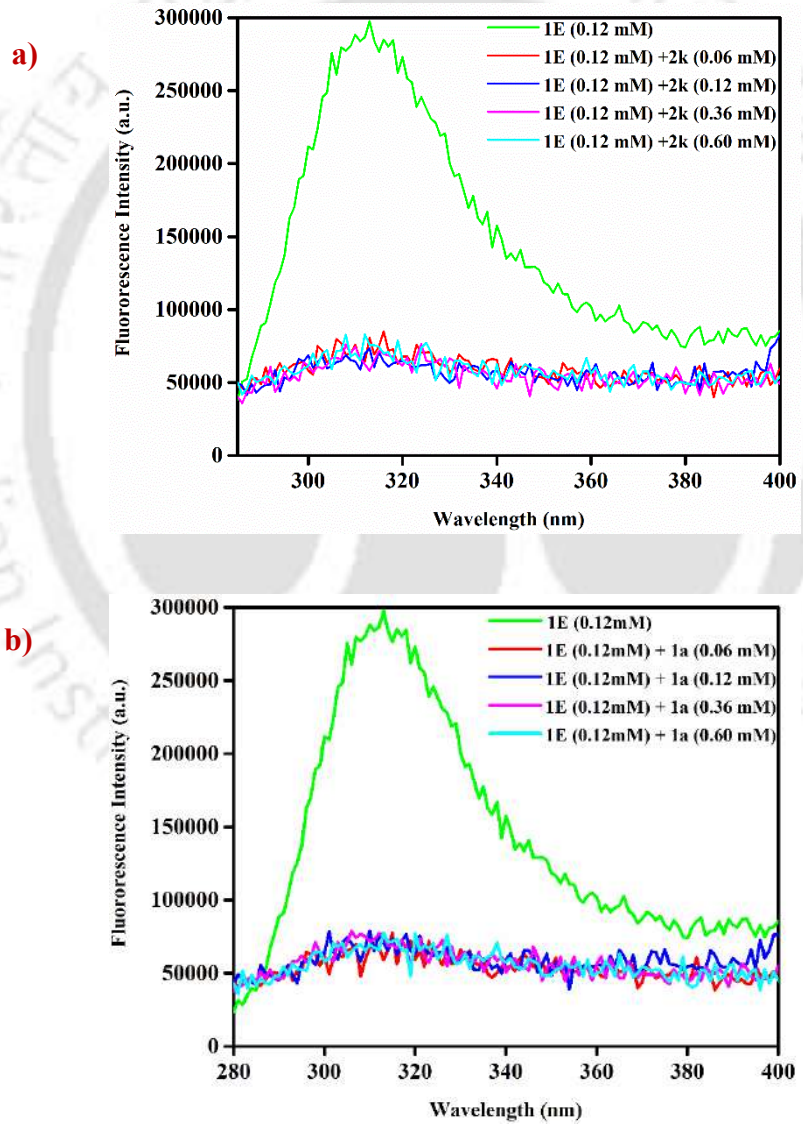

Figure 3.8. a) Fluorescence spectra of **1E** and mixture of **1E** and **2k** b) Fluorescence spectra of **1E** and mixture of **1E** and **1a**.

UV-absorbance and fluorescence of the catalyst are quenched in the presence of the donor, reiterating the strong interactions between the catalyst and the donor (Figure 3.7, 3.8).

3.2.3.5. Analysis of O-H stretching frequency of catalyst 1E via IR spectroscopy

We recorded the IR spectra of catalyst **1E**, donor **1a**, and their mixture (Figure 3.9). The merged spectrum is shown below.

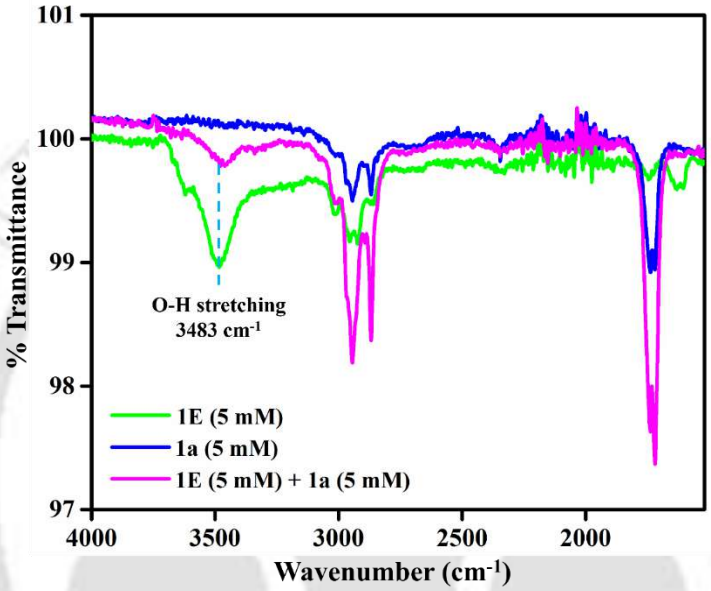

Figure 3.9. IR spectroscopy.

Also, the IR studies showed a decrease in the intensity of the O-H stretching frequency in the presence of the donor, presumably, again due to the interactions with the carbonyl moiety (Figure 3.9).

Collectively, these data strongly support the formation of a non-covalent complex between catalyst **1E,** donor **1a,** and the alcohol nucleophile, likely mediated by a combination of hydrogen bonding, electrostatic interactions, and possible electronic delocalization leading to the stereoselective product formation.

3.2.4. Synthetic applications

3.2.4.1. Gram-scale synthesis

To demonstrate the scalability of our glycosylation protocol, we conducted a gram-scale reaction using 5 mol% catalyst loading (Scheme 3.5). Pleasingly, the gram-scale reaction

proceeded proficiently, offering **3b** and **7f** in 87% and 80% yield, respectively, with excellent α-stereoselectivity (Scheme 3.5).

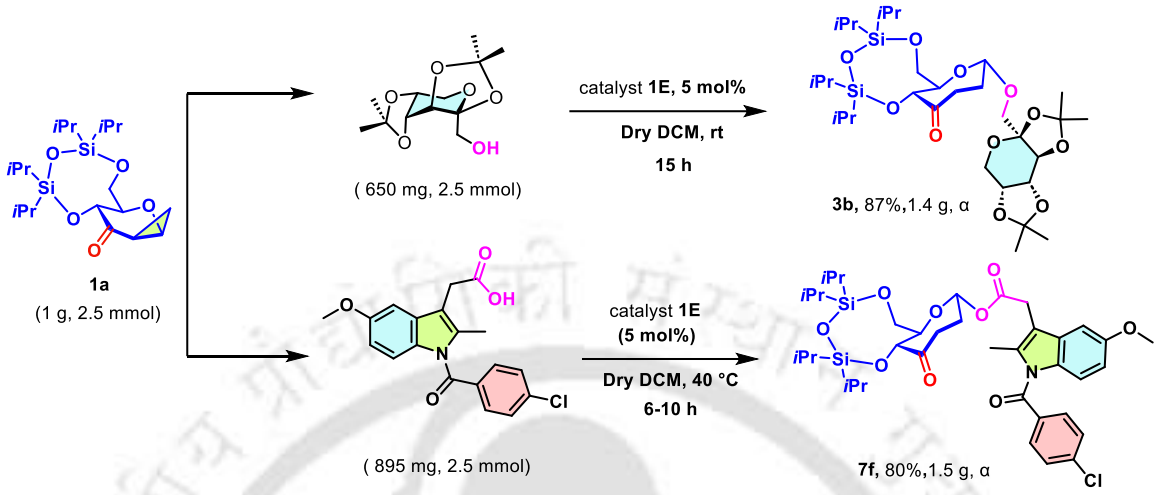

Scheme 3.5. Gram-scale synthesis of compound **3b** and **7f**.

Procedure for 3b: In a screw-capped vial equipped with a magnetic stir bar, donor **1a** (1 g, 2.5 mmol), acceptor **2b** (650 mg, 2.5 mmol), and the catalyst **1E** (39 mg, 0.125 mmol, 5 mol%) were placed under an inert atmosphere. Then, dry DCM (8 mL) was added, and the resulting solution was stirred at room temperature for 15 hours. After completion of the reaction, the solvent was removed in vacuo, and the reaction mixture was purified by using column chromatography (hexane/ethyl acetate = 93/7) to afford the corresponding product **3b** (1.4 g, 87% yield) as a colorless oil.

Procedure for 7f: In a screw-capped vial equipped with a magnetic stir bar, donor **1a** (1 g, 2.5 mmol), acid acceptor (895 mg, 2.5 mmol), and the catalyst **1E** (39 mg, 0.125 mmol, 5 mol%) were placed under an inert atmosphere. Then, dry DCM (5 mL) was added, and the resulting solution was stirred at 40 °C for 8-10 h. After completion of the reaction, the solvent was removed in vacuo, and the reaction mixture was purified by using column chromatography (hexane/ethyl acetate = 88/12) to afford the corresponding product **5g** (1.5 g, 80% yield) as a white sticky foam.

3.2.4.2. Trisaccharide synthesis

Furthermore, our strategy highlighted robust performance in iterative oligosaccharide synthesis (Scheme 3.6). Initially, tetrabutylammonium fluoride (TBAF) was used to cleave the disiloxane protecting group in compound **3b**, thereby unmasking the O5 and O7 hydroxyl groups to furnish diol **8**. Subsequent reapplication of donor **1a** under

sulfonium catalysis with diol **8** enabled regio- and stereoselective formation of the α-glycosidic linkage, offering trisaccharide **9** in 62% yield.

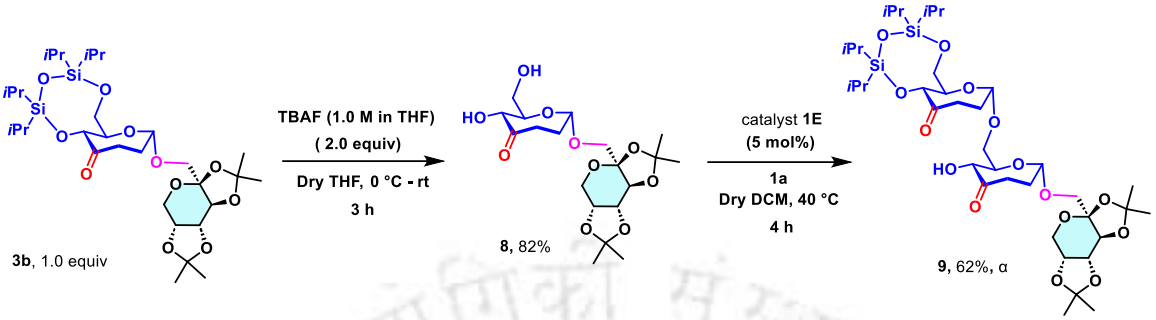

Scheme 3.6. Trisaccharide synthesis.

Procedure: To a stirred solution of compound **3b** (600 mg, 0.91 mmol) in dry THF (5 mL) was added tetrabutylammonium fluoride (TBAF, 1.0 M in THF, 1.82 mmol) dropwise at 0 °C under an inert atmosphere. The reaction mixture was then allowed to warm to room temperature and stirred for 3 hours. After completion of the reaction, the solvent was removed in vacuo, and the reaction mixture was purified by using column chromatography (hexane/ethyl acetate = 30/70) to obtain the desired glycoside **8** (312 mg, 82% yield) as a colorless oil.

In a screw-capped vial equipped with a magnetic stir bar, donor **1a** (100 mg, 0.25 mmol), acceptor **8** (105 mg, 0.25 mmol), and the catalyst **1E** (3.9 mg, 5 mol%) were placed under an inert atmosphere. Then, dry DCM (1 mL) was added, and the resulting solution was stirred at 40 °C for 3-4 hours. After completion of the reaction, the solvent was removed in vacuo, and the reaction mixture was purified by using column chromatography (hexane/ethyl acetate = 60/40) to obtain the desired glycoside **9** (127 mg, 62% yield) as a colorless oil.

3.2.4.3. Pseudodisaccharide synthesis

Additionally, compound **3m** was transformed into benzylic alcohol derivative **10** via Sonogashira coupling[25] (Scheme 3.7). Subsequent reapplication of donor **1a** under sulfonium catalysis with glycoside **10** enabled regio- and stereoselective formation of the α-glycosidic linkage, offering pseudodisaccharide **11** in 75% yield, retaining stereoselectivity (Scheme 3.7).

Procedure: In a 5 mL dry flask with a stirring bar, iodoarene (75 mg, 0.32 mmol), $Pd(PPh_3)_2Cl_2$ (1.5 mg, 0.0021 mmol, 1 mol%), CuI (1 mg, 0.0042 mmol, 2 mol%), and Et_3N (2 mL) were added and stirred for 5 minutes at room temperature. Propargyl donor **3m** (100 mg, 0.21 mmol) was then added, and the reaction was allowed to proceed for 3

hours. After completion of the reaction, the solvent was removed in vacuo, and the reaction mixture was purified by using column chromatography (hexane/ethyl acetate = 80/20) to obtain the desired glycoside **10** (103 mg, 85% yield) as a colorless oil.

In a screw-capped vial equipped with a magnetic stir bar, donor **1a** (50 mg, 0.125 mmol), acceptor **10** (72 mg, 0.125 mmol), and the catalyst (**1E,** 2.0 mg, 5 mol%) were placed under an inert atmosphere. Then, dry DCM (0.5 mL) was added, and the resulting solution was stirred at 40 °C for 3-4 hours. After completion of the reaction, the solvent was removed in vacuo, and the reaction mixture was purified by using column chromatography (hexane/ethyl acetate = 93/7) to afford the desired product **11** (90 mg, 75% yield) as a colorless oil.

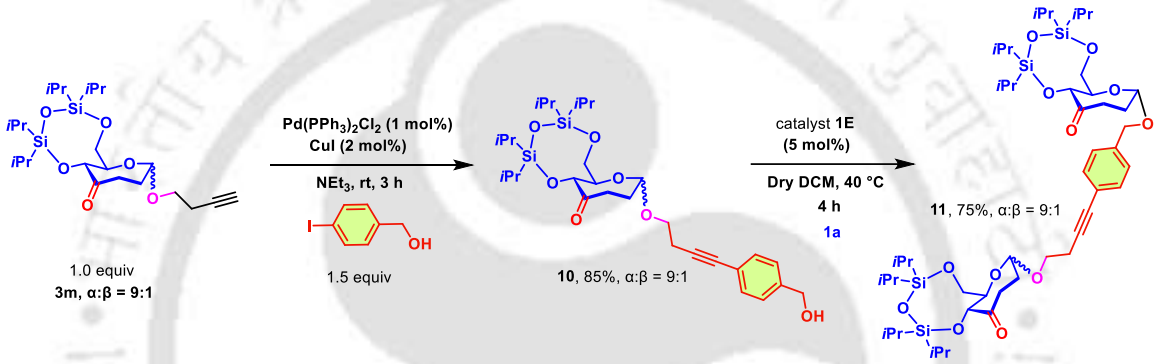

Scheme 3.7. Pseudodisaccharide synthesis.

3.3. Proposed mechanism

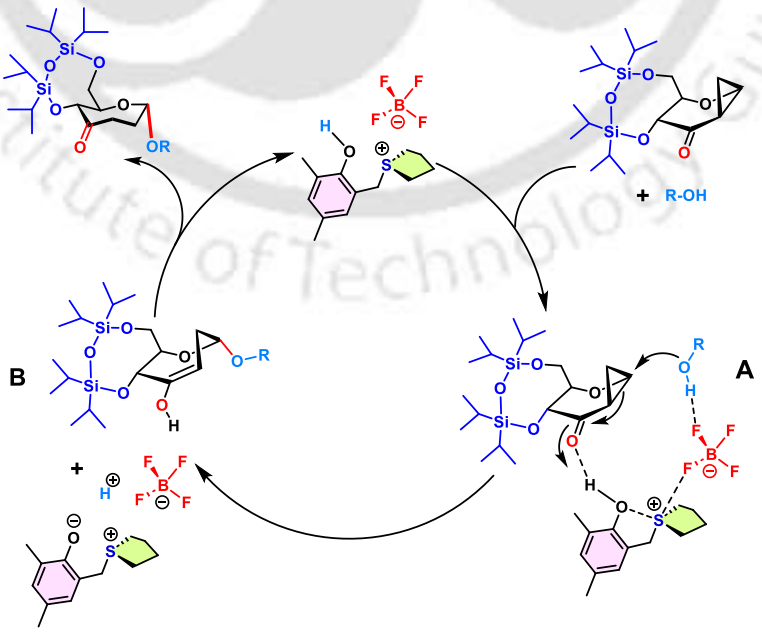

Scheme 3.8. Plausible reaction mechanism.

Based on all the above studies, we propose a tentative mechanism for the observed transformation (Scheme 3.8). The phenolic O-H of the sulfonium catalyst activates the carbonyl group of the cyclopropane donor, whereas the tetrafluoroborate anion simultaneously activates the alcohol from below the plane of cyclopropane via H-bonding, thus making the alcohol more nucleophilic (Scheme 3.8, A). This leads to the cleavage of the internal C-C bond of the cyclopropane, thus providing the septano-glycosides in a stereoselective fashion, also regenerating the catalyst via the transfer of a proton from the alcohol to the phenolic oxygen.

3.4. Conclusion

In conclusion, we report a highly efficient, sulfonium-stabilized phenolic ion-pairs as an organocatalyst for stereoselective strain-release septanosylation, capable of accommodating a diverse array of complex alcohols, thiols, and carboxylic acid acceptors. Also, cooperative hydrogen bonding among the catalyst, donor, and reaction partners facilitates the formation of a ternary complex, thereby enhancing both the reactivity and selectivity of the transformation. Our protocol thus establishes a new paradigm for harnessing nonclassical noncovalent interactions (NCIs) in selective aglycone delivery, unlocking synthetic access to structurally valuable seven-membered glycomimetics. The importance of this method is underscored by its effectiveness in late-stage modification of key bioactive and drug molecules, as well as downstream transformations to trisaccharide and pseudodisaccharide. Moreover, the distinctive reactivity profile of the phenolic sulfonium salt offers broad potential for catalyzing a wide range of organic reactions, and exploration in this direction is in progress in our laboratory.

3.5. Experimental section

3.5.1. Donors and acceptors used in the present study

The following donors (**1a-1e**), along with alcohols, thiols, and acids as acceptors, were used in this method.

Donors:

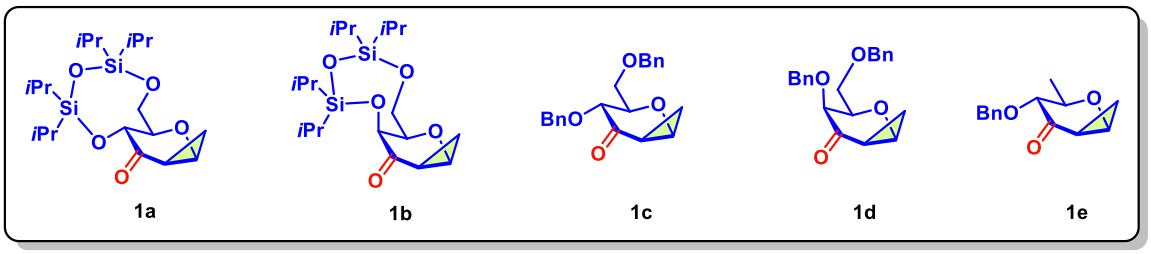

Donors **1a**–**1e** were synthesized according to reported procedures.[13,26,11,27] The acceptors (**2a-2i**) were synthesized using the following literature procedures.[28,29,30,31,32,33,34,35]

Alcohol acceptors:

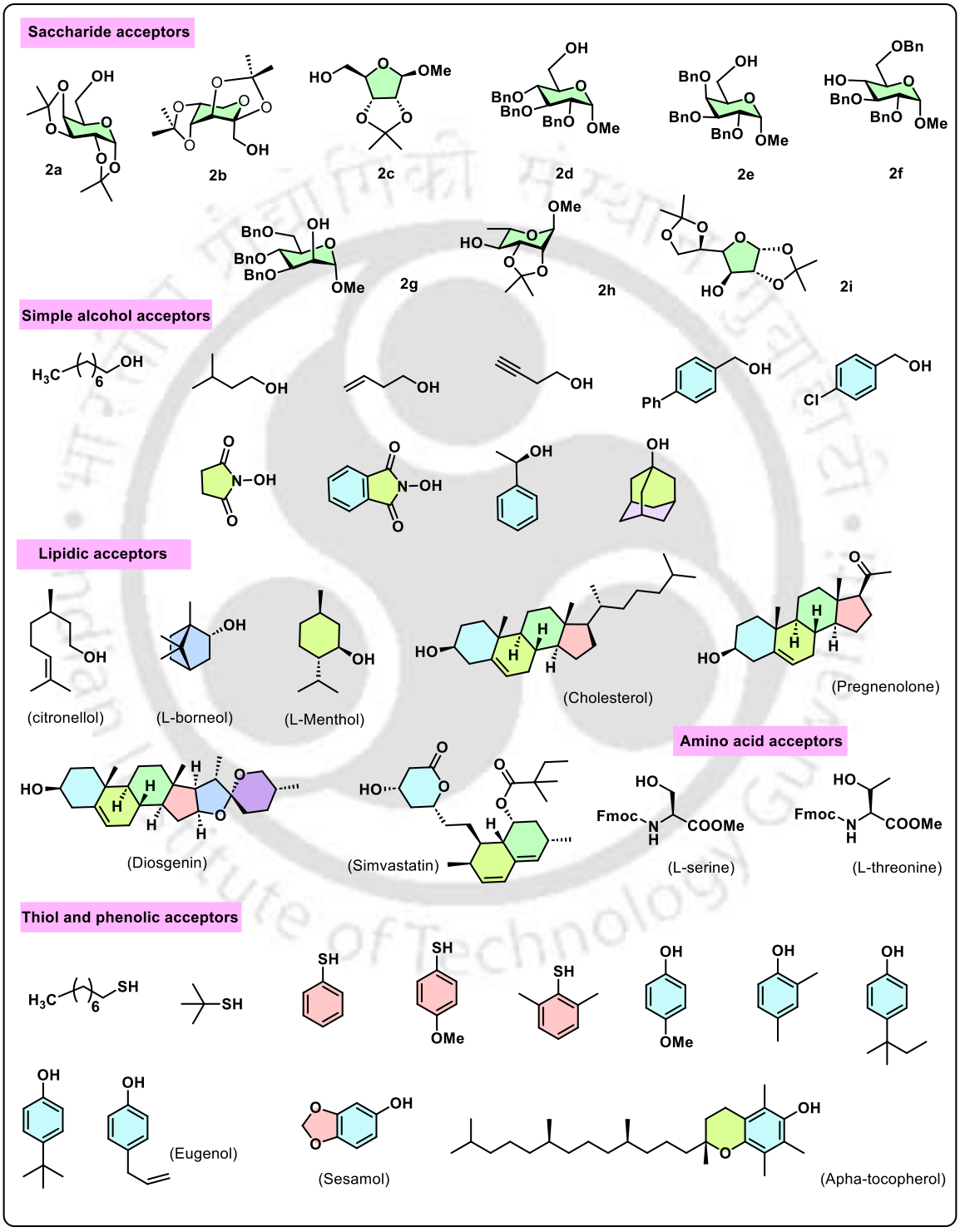

Acid acceptors:

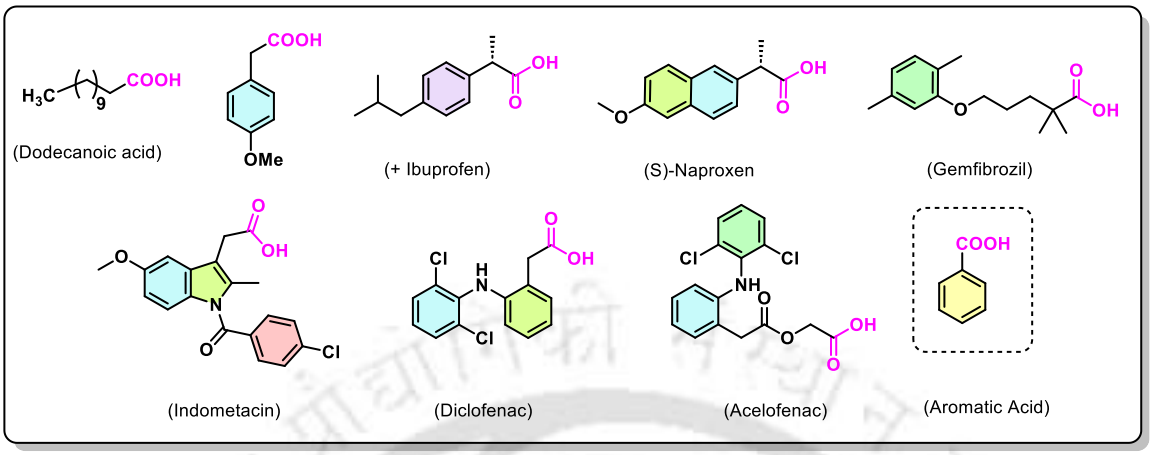

3.5.2. Spectroscopic data of donors (1a-1e)

(6aR,7aS,8aR,9aR)-2,2,4,4-tetraisopropyltetrahydro-6H-cyclopropa[5,6]pyrano[3,2-f][1,3,5,2,4]trioxadisilocin-9(7aH)-one (1a)

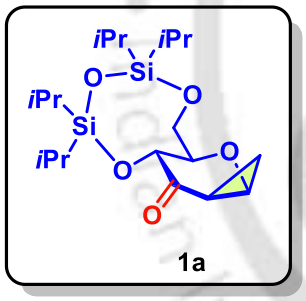

^{1}H NMR (600 MHz, $CDCl_3$) δ 4.28 (d, J = 9.9 Hz, 1H), 4.16 (q, J = 5.2 Hz, 1H), 3.97 (s, 2H), 3.79 (d, J = 9.9 Hz, 1H), 1.92 (dt, J = 11.5, 6.0 Hz, 1H), 1.31 – 1.28 (m, 1H), 1.25 (d, J = 2.8 Hz, 1H), 1.12 – 1.01 (m, 28H). **^{13}C NMR** (151 MHz, $CDCl_3$) δ 204.0, 83.6, 70.6, 61.0, 58.1, 25.8, 20.3, 17.4 (17.38, 17.37, 17.36), 17.3, 17.2 (17.19, 17.17), 17.1, 13.6, 13.4, 12.5, 12.4. **HRMS** (ESI) m/z: $[M+H]^+$ calcd for $C_{19}H_{37}O_5Si_2$ 401.2175; found 401.2155.

(6aR,7aS,8aR,9aS)-2,2,4,4-tetraisopropyltetrahydro-6H-cyclopropa[5,6]pyrano[3,2-f][1,3,5,2,4]trioxadisilocin-9(7aH)-one (1b)

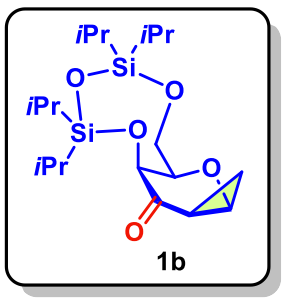

Compound **1b** was synthesized using the general procedure **1.1**. **1b** was obtained in 92% yield (4.4 gm) as a colorless oil, R_f = 0.6 (Hexane/EtOAc, 9:1, v/v). **^{1}H NMR** (600 MHz, $CDCl_3$) δ 4.11 (q, J = 5.0 Hz, 1H), 4.07 (s, 1H), 3.94 (dd, J = 9.9, 5.5 Hz, 1H), 3.81 (dd, J = 10.4, 5.4 Hz, 1H), 3.70 (t, J = 10.2 Hz, 1H), 1.91 (q, J = 5.7 Hz, 1H), 1.76 (dt, J = 11.6, 5.9 Hz, 1H), 1.25 (d, J = 5.2 Hz, 1H), 1.08 – 1.00 (m, 28H). **^{13}C NMR** (151 MHz, $CDCl_3$) δ 201.6, 80.4, 72.6, 58.8, 58.2, 24.1, 18.9, 17.5 (17.48, 17.45), 17.4, 17.3, 17.2 (17.23, 17.18), 17.1, 13.4, 13.3, 12.8, 12.7. **HRMS** (ESI) m/z: $[M+H]^+$ calcd for $C_{19}H_{37}O_5Si_2$ 401.2175; found 401.2155.

(1S,3R,4R,6R)-4-(benzyloxy)-3-((benzyloxy)methyl)-2-oxabicyclo[4.1.0]heptan-5-one (1c)

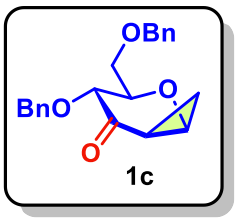

^{1}H NMR (600 MHz, $CDCl_3$) δ 7.23 (dq, J = 14.0, 8.2, 7.0 Hz, 10H), 4.88 (d, J = 11.0 Hz, 1H), 4.51 (d, J = 12.1 Hz, 1H), 4.43 (dd, J = 24.3, 11.5 Hz, 2H), 4.11 (q, J = 5.1 Hz, 1H), 3.92 (dd, J = 10.0, 3.6 Hz, 1H), 3.83 (d, J = 10.1 Hz, 1H), 3.64 (d, J = 10.7 Hz, 1H), 3.54 (dd, J = 10.8, 4.4 Hz, 1H), 1.84 (dt, J = 11.5, 5.9 Hz, 1H), 1.28 (td, J = 6.3, 3.2 Hz, 1H), 1.25 – 1.22 (m, 1H). **^{13}C NMR** (151 MHz, $CDCl_3$) δ 205.2, 138.0, 137.6, 128.5 (128.52, 128.49), 128.3, 128.0, 127.9, 127.8, 81.7, 77.8, 74.4, 73.8, 69.0, 58.1, 25.9, 20.0. **HRMS** (ESI) m/z: $[M+NH_4]^+$ calcd for $C_{21}H_{26}NO_4$ 356.1856; found 356.1854.

(1S,3R,4S,6R)-4-(benzyloxy)-3-((benzyloxy)methyl)-2-oxabicyclo[4.1.0]heptan-5-one (1d)

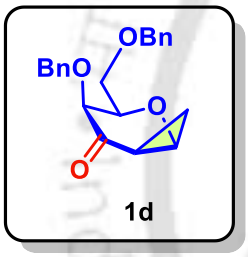

Compound **1d** was synthesized using the general procedure **1.2**. **1d** was obtained in 92% yield (623 mg) as a colorless oil, R_f = 0.4 (Hexane/EtOAc, 7:3, v/v). **^{1}H NMR** (600 MHz, $CDCl_3$) δ 7.27 – 7.18 (m, 10H), 4.55 (d, J = 11.8 Hz, 1H), 4.46 (d, J = 11.9 Hz, 1H), 4.37 – 4.31 (m, 2H), 4.12 (q, J = 5.3 Hz, 1H), 3.97 (t, J = 6.1 Hz, 1H), 3.60 – 3.55 (m, 2H), 3.43 (dd, J = 9.8, 6.0 Hz, 1H), 1.80 (td, J = 6.0, 3.4 Hz, 1H), 1.70 (dt, J = 11.3, 5.8 Hz, 1H), 1.19 (d, J = 5.7 Hz, 1H). **^{13}C NMR** (151 MHz, $CDCl_3$) δ 202.3, 137.9, 137.1, 128.5 (128.54, 128.53), 128.3, 128.1, 127.9, 80.4, 79.8, 73.7, 71.9, 68.6, 58.3, 24.1, 19.3. **HRMS** (ESI) m/z: $[M+NH_4]^+$ calcd for $C_{21}H_{26}NO_4$ 356.1856; found 356.1854.

(1S,3R,4R,6R)-4-(benzyloxy)-3-methyl-2-oxabicyclo[4.1.0]heptan-5-one (1e)

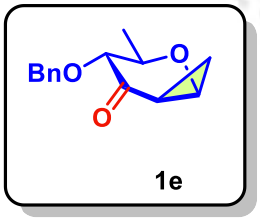

Compound **1e** was synthesized using the general procedure **1.2**. **1e** was obtained in 90% yield (418 mg) as a colorless oil, R_f = 0.4 (Hexane/EtOAc, 8:2, v/v). **^{1}H NMR** (600 MHz, $CDCl_3$) δ 7.32 – 7.18 (m, 5H), 4.92 (d, J = 11.4 Hz, 1H), 4.47 (d, J = 11.4 Hz, 1H), 4.05 (q, J = 4.5 Hz, 1H), 3.90 – 3.84 (m, 1H), 3.39 (d, J = 9.7 Hz, 1H), 1.86 – 1.80 (m, 1H), 1.21 – 1.18 (m, 5H). **^{13}C NMR** (151 MHz, $CDCl_3$) δ 205.2, 137.6, 128.5, 128.4, 128.1, 82.2, 79.0, 74.1, 57.9, 26.1, 20.1, 18.4. **HRMS** (ESI) m/z: $[M+NH_4]^+$ calcd for $C_{14}H_{20}NO_3$ 250.1438; found 250.1422.

3.5.3. Synthesis of catalysts

The following catalysts (**1A-1F** and **1H**) were used in this method.

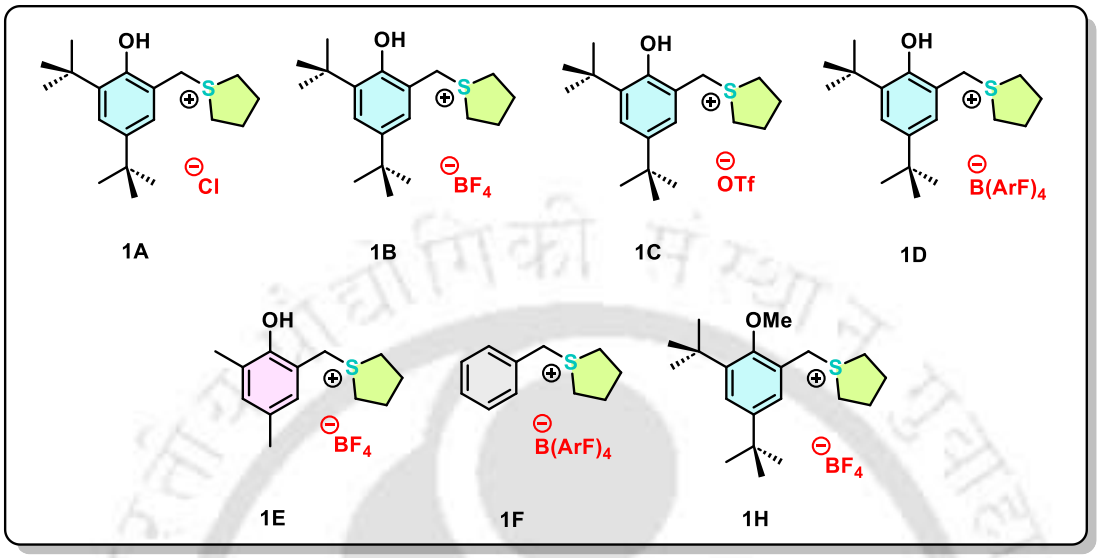

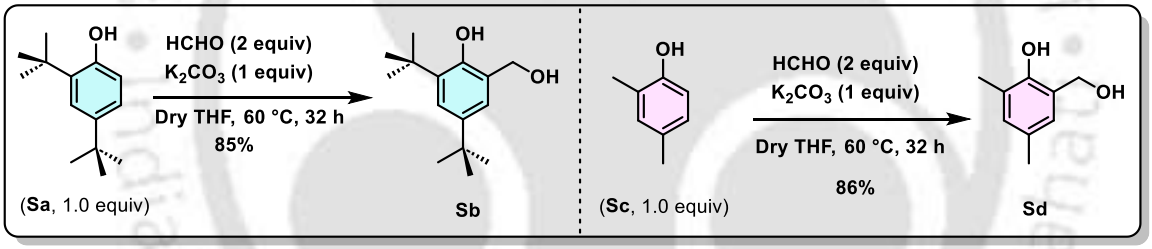

To a stirred solution of 2,4-di-*tert*-butylphenol **Sa** (2.0 g, 9.7 mmol) in dry THF (50 mL), potassium carbonate (K_2CO_3, 1.3 g, 9.7 mmol) and paraformaldehyde (600 mg, 19.4 mmol) were added sequentially. The reaction mixture was heated at 60 °C and stirred for 32 h. Upon completion, it was diluted with dichloromethane (DCM, 50 mL), and the organic layer was washed with brine, dried over anhydrous sodium sulfate (Na_2SO_4), and concentrated under reduced pressure. The crude residue was purified by column chromatography on silica gel (petroleum ether/ethyl acetate = 95:5) to afford compound **Sb** as a white solid (2.3 g, 85% yield). **^{1}H NMR** (500 MHz, $CDCl_3$) δ 7.54 (s, 1H), 7.29 (d, J = 2.5 Hz, 1H), 6.90 (d, J = 2.5 Hz, 1H), 4.86 (d, J = 5.5 Hz, 2H), 1.43 (s, 9H), 1.29 (s, 9H). **^{13}C NMR** (126 MHz, $CDCl_3$) δ 153.2, 141.8, 136.7, 124.2, 124.1, 122.7, 66.0, 35.1, 34.4, 31.7, 29.8, 1.2. **HRMS** (ESI) m/z: $[M+Na]^+$ calcd for $C_{15}H_{24}NaO_2$ 259.1669; found 259.1661.

To a stirred solution of 2,4-dimethylphenol **Sc** (2.0 g, 16.4 mmol) in dry THF (50 mL), potassium carbonate (K_2CO_3, 2.3 g, 16.4 mmol) and paraformaldehyde (1.0 g, 32.8 mmol) were added sequentially. The reaction mixture was heated at 60 °C and stirred for

32 h. Upon completion, it was diluted with dichloromethane (DCM, 50 mL), and the organic layer was washed with brine, dried over anhydrous sodium sulfate (Na_2SO_4), and concentrated under reduced pressure. The crude residue was purified by column chromatography on silica gel (petroleum ether/ethyl acetate = 95:5) to afford compound **Sd** as a colorless oil (2.1 g, 86% yield). **^{1}H NMR** (600 MHz, $CDCl_3$) δ 7.18 (s, 1H), 6.91 (s, 1H), 6.68 (s, 1H), 4.79 (d, J = 5.1 Hz, 2H), 2.23 (d, J = 2.0 Hz, 6H). **^{13}C NMR** (151 MHz, $CDCl_3$) δ 152.1, 131.6, 128.9, 126.0, 125.3, 124.0, 64.9, 20.5, 15.7. **HRMS** (ESI) m/z: $[M+Na]^+$ calcd for $C_9H_{12}NaO_2$ 175.0730; found 175.0735.

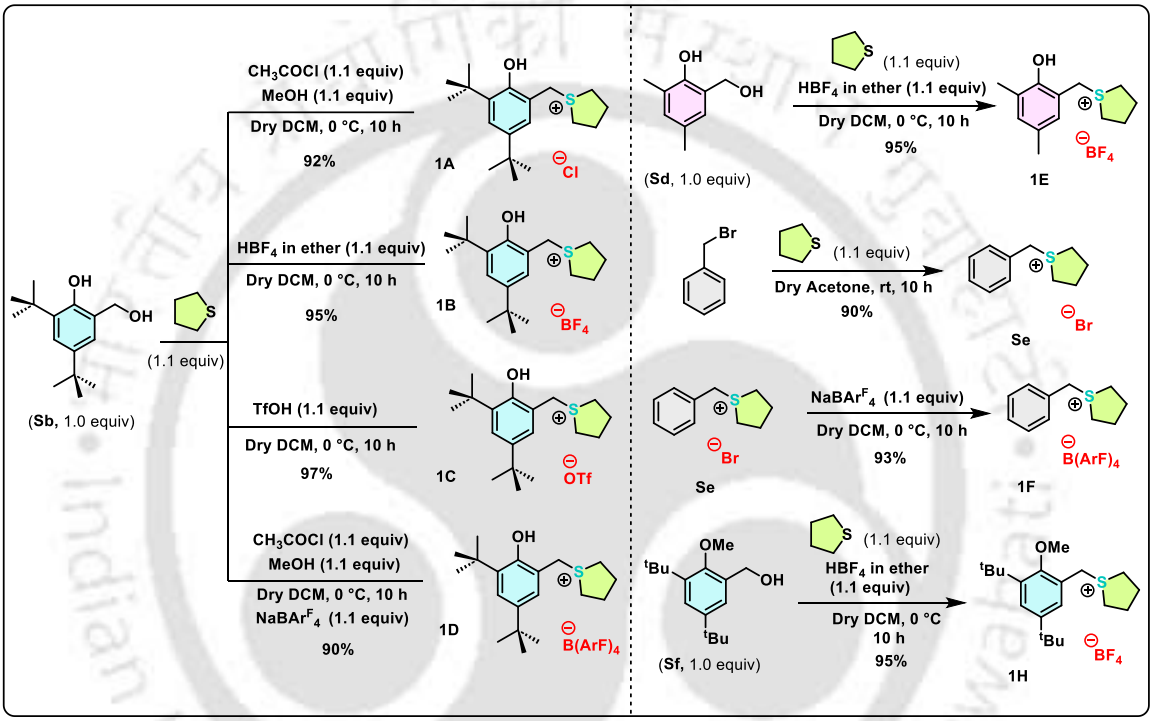

1-(3,5-di-*tert*-butyl-2-hydroxybenzyl)tetrahydro-1H-thiophen-1-ium chloride salt (1A):

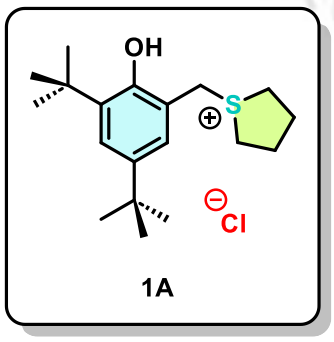

To a stirred solution of compound **Sb** (100 mg, 0.42 mmol) and tetrahydrothiophene (42 µL, 0.47 mmol) in dry dichloromethane (DCM, 2 mL), acetyl chloride (34 µL, 0.47 mmol) and methanol (0.47 mmol) were added sequentially at 0 °C. The reaction mixture was stirred for 10 h, then concentrated under reduced pressure to get a white solid. The residue was washed with diethyl ether (4 ×) to afford **1A** as a white solid (133 mg, 92% yield). **^{1}H NMR** (500 MHz, $CDCl_3$) δ 7.34 (s, 1H), 7.08 (s, 1H), 5.39 (s, 1H), 4.70 (s, 2H), 3.52 – 3.44 (m, 1H), 2.84 (s, 3H), 1.94 (s, 4H), 1.43 (s, 9H), 1.29 (s, 9H). **^{13}C NMR** (126 MHz, $CDCl_3$) δ 151.8, 143.0, 137.2, 125.6, 124.8, 123.2, 45.2, 35.1, 34.5, 31.9, 31.7, 31.2, 30.0.

1-(3,5-di-*tert*-butyl-2-hydroxybenzyl)tetrahydro-1H-thiophen-1-ium tetrafluoroborate salt (1B):

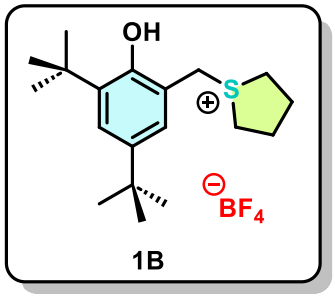

To a stirred solution of compound **Sb** (100 mg, 0.42 mmol) and tetrahydrothiophene (42 µL, 0.47 mmol) in dry dichloromethane (DCM, 2 mL), a solution of fluoroboric acid (HBF_4) in diethyl ether (35 µL, 0.47 mmol) was added dropwise at 0 °C. The reaction mixture was stirred for 10 h, then concentrated under reduced pressure to get a white solid. The residue was washed with diethyl ether (4 ×) to afford **1B** as a white solid (157 mg, 95% yield). **^{1}H NMR** (600 MHz, ACN-d_3) δ 7.49 (d, J = 2.5 Hz, 1H), 7.30 (d, J = 2.5 Hz, 1H), 6.31 (s, 1H), 4.43 (s, 2H), 3.50 – 3.39 (m, 4H), 2.29 (ddd, J = 28.0, 13.5, 6.6 Hz, 4H), 1.45 (s, 9H), 1.34 (s, 9H). **^{13}C NMR** (151 MHz, ACN-d_3) δ 152.1, 145.4, 139.7, 127.8, 127.3, 118.6, 44.1, 43.9, 35.5, 35.1, 31.5, 30.2, 29.3.

1-(3,5-di-*tert*-butyl-2-hydroxybenzyl)tetrahydro-1H-thiophen-1-ium triflate salt (1C):

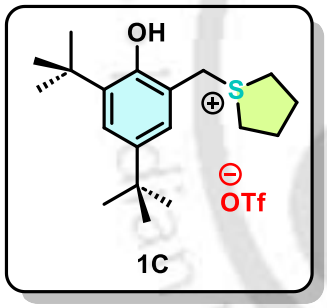

To a stirred solution of compound **Sb** (100 mg, 0.42 mmol) and tetrahydrothiophene (42 µL, 0.47 mmol) in dry dichloromethane (DCM, 2 mL), triflic acid (42 µL, 0.47 mmol) was added dropwise at 0 °C. The reaction mixture was stirred for 10 h, then concentrated under reduced pressure to get a white solid. The residue was washed with diethyl ether (4 ×) to afford **1C** as a white solid (186 mg, 97% yield). **^{1}H NMR** (600 MHz, ACN-d_3) δ 7.49 (d, J = 2.5 Hz, 1H), 7.29 (d, J = 2.4 Hz, 1H), 6.68 (s, 1H), 4.47 (s, 2H), 3.45 (dtd, J = 25.3, 13.1, 6.3 Hz, 4H), 2.36 – 2.30 (m, 2H), 2.29 – 2.23 (m, 2H), 1.44 (s, 9H), 1.34 (s, 9H). **^{13}C NMR** (151 MHz, ACN-d_3) δ 152.4, 145.2, 139.9, 127.7, 127.3, 118.6, 44.2, 43.9, 35.6, 35.1, 31.6, 30.1, 29.3.

1-(3,5-di-*tert*-butyl-2-hydroxybenzyl)tetrahydro-1H-thiophen-1-ium tetrakis[3,5 bis(trifluoromethyl)phenyl]borate salt (1D):

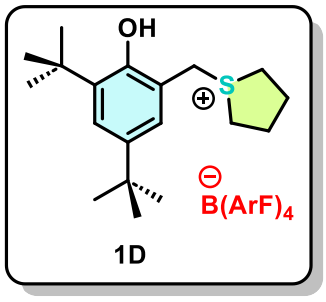

Chloride salt **1A** (100 mg, 0.29 mmol) and sodium tetrakis[3,5-bis(trifluoromethyl)phenyl]borate (285 mg, 0.32 mmol) were dissolved in dry dichloromethane (DCM, 2 mL) and stirred at 0 °C for 1 h. A white precipitate of sodium chloride (NaCl) formed immediately upon mixing. After allowing the mixture to settle for a few minutes, the supernatant was carefully decanted and concentrated under reduced pressure to afford compound **1D** as a white solid (90% yield). **^{1}H NMR** (500

MHz, $CDCl_3$) δ 7.70 (s, 8H), 7.54 (s, 4H), 7.46 (s, 1H), 7.26 (s, 1H), 7.02 (s, 1H), 4.27 (s, 2H), 3.28 (d, J = 6.7 Hz, 4H), 2.17 (dq, J = 25.3, 7.2 Hz, 4H). **^{13}C NMR** (126 MHz, $CDCl_3$) δ 162.4, 162.0, 161.6, 161.2, 150.7, 145.6, 135.9, 134.9, 129.23, 129.19, 128.98, 128.94, 128.1, 127.9, 126.5, 125.8, 123.6, 121.4, 117.71, 117.68, 117.65, 113.3, 44.8, 43.0, 31.4, 30.4, 30.2, 29.9, 28.8.

1-(2-hydroxy-3,5-dimethylbenzyl)tetrahydro-1H-thiophen-1-ium tetrafluoroborate salt (1E):

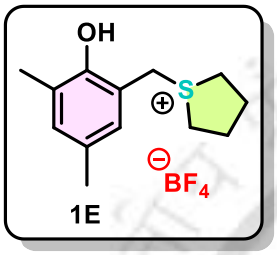

To a stirred solution of compound **Sd** (100 mg, 0.66 mmol) and tetrahydrothiophene (64 µL, 0.72 mmol) in dry dichloromethane (DCM, 2 mL), a solution of fluoroboric acid (HBF_4) in diethyl ether (54 µL, 0.72 mmol) was added dropwise at 0 °C. The reaction mixture was stirred for 10 h, then concentrated under reduced pressure to get a white solid. The residue was washed with diethyl ether (4 ×) to afford **1E** as a white solid (194 mg, 95% yield). **^{1}H NMR** (600 MHz, ACN-d_3) δ 7.10 (s, 1H), 7.04 (s, 1H), 6.74 (s, 1H), 4.37 (s, 2H), 3.47 – 3.39 (m, 4H), 2.35 (dd, J = 10.7, 5.8 Hz, 2H), 2.27 (d, J = 5.8 Hz, 8H). **^{13}C NMR** (151 MHz, ACN-d_3) δ 152.2, 134.6, 131.3, 130.8, 126.1, 116.3, 43.8, 43.1, 29.3, 20.2, 16.59, 16.57. **HRMS** (ESI) m/z: $[M]^+$ calcd for $C_{13}H_{19}OS$ 223.1152; found 223.1151.

1-benzyltetrahydro-1H-thiophen-1-ium tetrakis[3,5 bis(trifluoromethyl)phenyl]borate salt (1F):

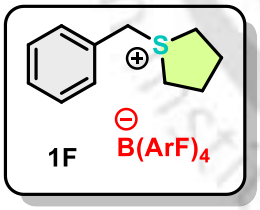

A solution of tetrahydrothiophene (0.12 mL, 1.32 mmol) and benzyl bromide (0.14 mL, 1.20 mmol) in acetone (2 mL) was stirred at room temperature for 10 hours. The resulting precipitate was collected by filtration, washed thoroughly with cold acetone, and dried under vacuum to yield the sulfonium salt (**Se**) as a solid (280 mg, 90%). Bromide salt **Se** (280 mg, 1.1 mmol) and sodium tetrakis[3,5-bis(trifluoromethyl)phenyl]borate (1.1 g, 1.2 mmol) were dissolved in dry dichloromethane (DCM, 5 mL) and stirred at 0 °C for 2 h. A white precipitate of sodium chloride (NaCl) formed immediately upon mixing. After allowing the mixture to settle for a few minutes, the supernatant was carefully decanted and concentrated under reduced pressure to afford salt **1F** as a white solid (93% yield). **^{1}H NMR** (500 MHz, $CDCl_3$) δ 7.70 (s, 8H), 7.54 (s, 5H), 7.45 (t, J = 7.7 Hz, 2H), 7.19 (d, J = 7.5 Hz, 2H), 4.14 (s, 2H), 3.32 – 3.24 (m, 2H), 3.20 – 3.12 (m, 2H), 2.16 (dt, J = 7.1, 3.6 Hz, 4H). **^{13}C NMR** (126 MHz, $CDCl_3$) δ 162.4, 162.0, 161.6, 161.2, 134.9, 132.0, 130.9, 129.9, 129.27, 129.25, 129.23, 129.20, 129.02, 129.00, 128.98, 128.96, 127.89, 125.7, 124.8, 123.6, 121.4, 117.78, 117.75, 117.72, 117.69, 117.66, 47.62, 42.58, 28.7.

3.5.4. NMR titration experiments

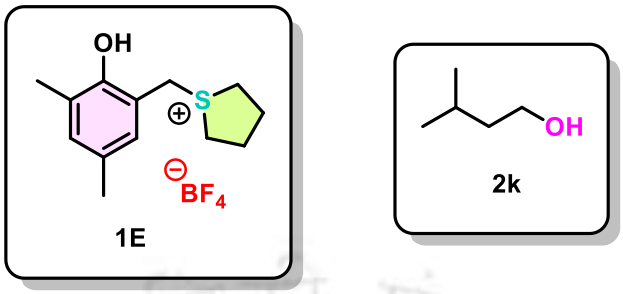

^{1}H NMR titration of the catalyst (**1E**) with alcohol (**2k**) in 0.5 mL solution of ACN-d_3.

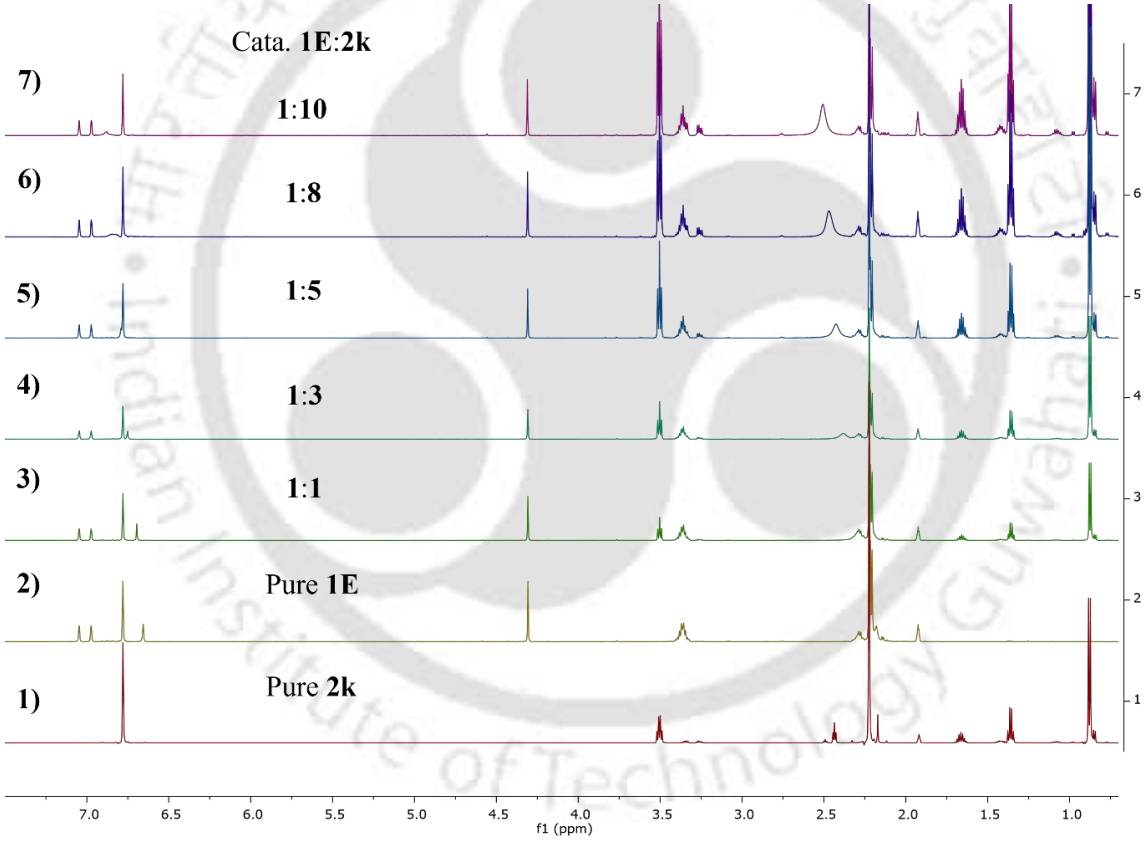

1) 0.032 mmol of **2k** 2) 0.032 mmol of **1E** 3) 0.032 mmol of **1E** and 0.032 mmol of **2k** (1:1 ratio) 4) 0.032 mmol of **1E** and 0.096 mmol of **2k** (1:3 ratio) 5) 0.032 mmol of **1E** and 0.16 mmol of **2k** (1:5 ratio) 6) 0.032 mmol of **1E** and 0.256 mmol of **2k** (1:8 ratio) 7) 0.032 mmol of **1E** and 0.32 mmol of **2k** (1:10 ratio).

In all experiments for calibration, 0.032 mmol of mesitylene is used as an internal standard.

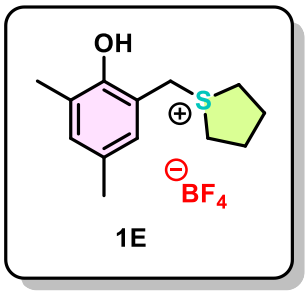

1E

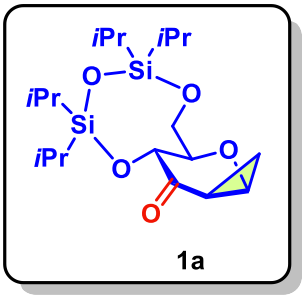

1a

^{1}H NMR titration of the catalyst (**1E)** with donor (**1a)** in 0.5 mL solution of ACN-d_3.

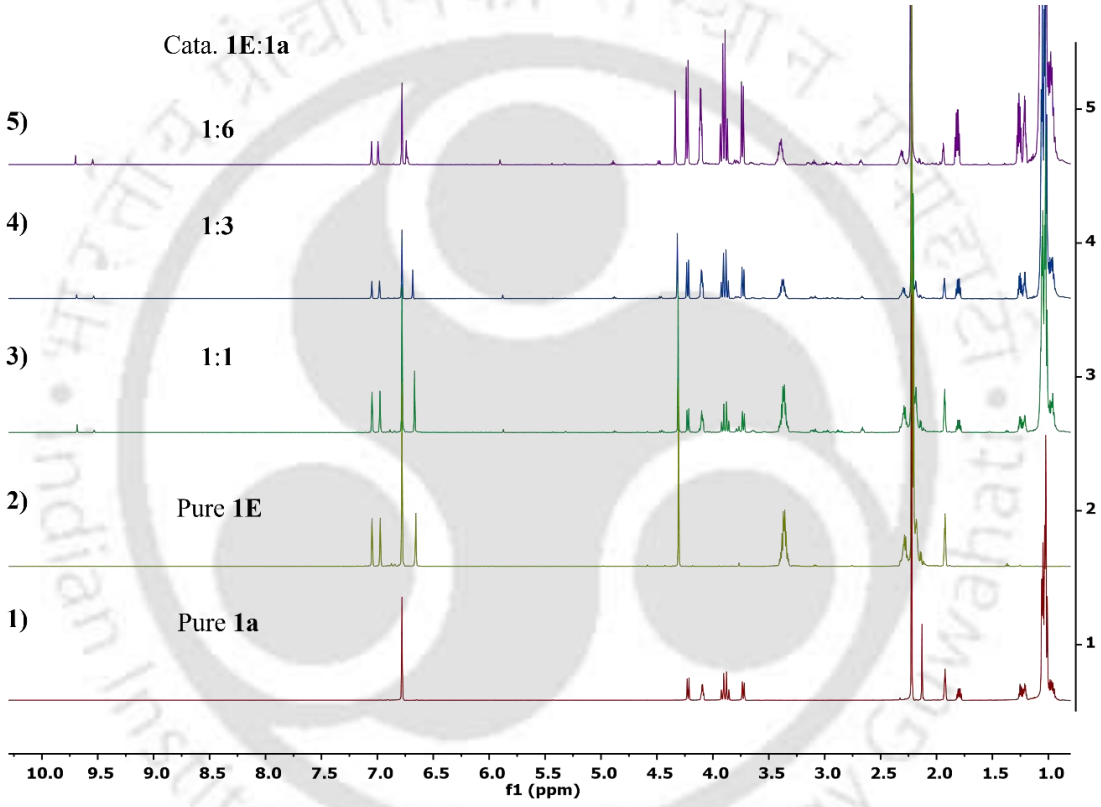

1) 0.032 mmol of **1a** 2) 0.032 mmol of **1E** 3) 0.032 mmol of **1E** and 0.032 mmol of **1a** (1:1 ratio) 4) 0.032 mmol of **1E** and 0.096 mmol of **1a** (1:3 ratio) 5) 0.032 mmol of **1E** and 0.192 mmol of **1a** (1:6 ratio).

In all experiments for calibration, 0.032 mmol of mesitylene is used as an internal standard.

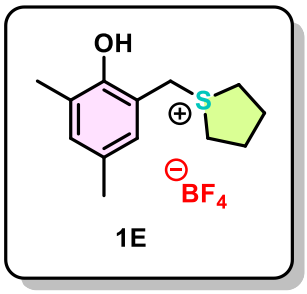

1E

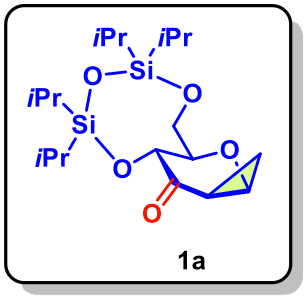

1a

^{13}C NMR titration of the catalyst (**1E)** with donor (**1a)** in 0.5 mL solution of ACN-d_3.

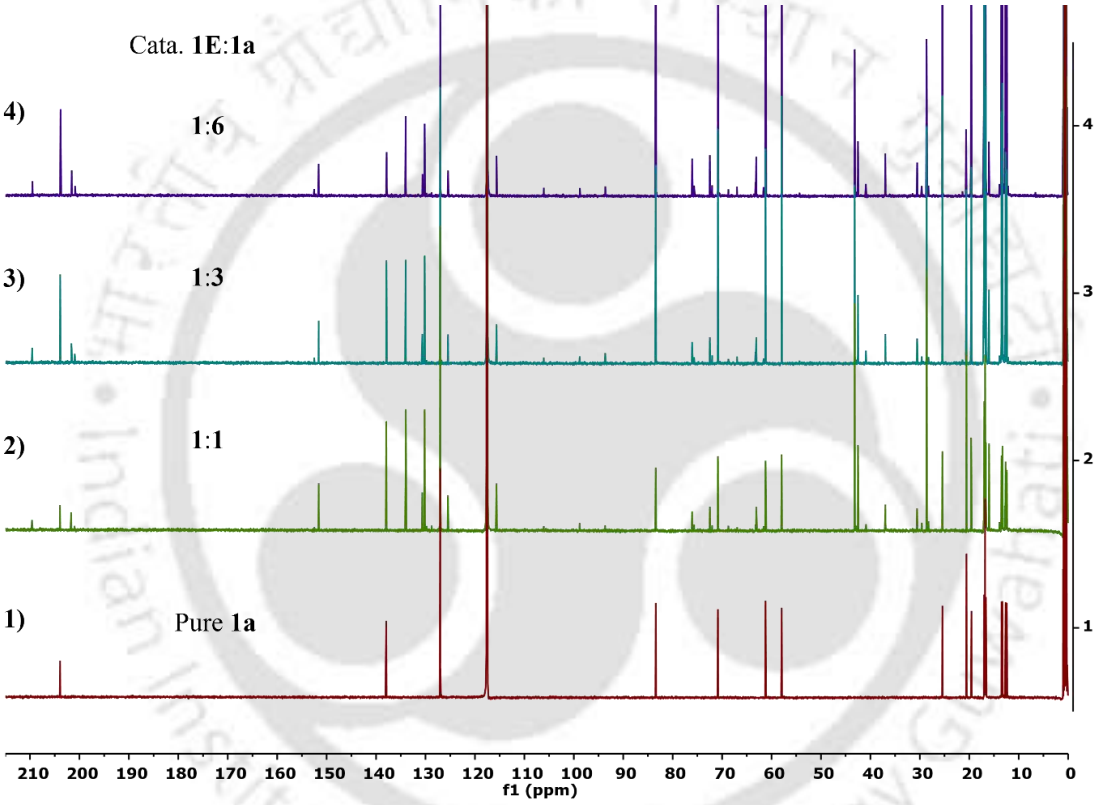

1) 0.032 mmol of **1a** 2) 0.032 mmol of **1E** and 0.032 mmol of **1a** (1:1 ratio) 3) 0.032 mmol of **1E** and 0.096 mmol of **1a** (1:3 ratio) 4) 0.032 mmol of **1E** and 0.192 mmol of **1a** (1:6 ratio). In all experiments for calibration, 0.032 mmol of mesitylene is used as an internal standard.

3.5.5. nOe experiment of 3a

Irradiation of H_1: Upon irradiation of H_1, the enhancement on the H_6 protons (appearing at 3.919 and 3.764 ppm) are found 1.99% and 2.20%, and the enhancement on the H_2 proton (appearing at 2.120 ppm) is found 2.32%. In addition, there is no enhancement on

the **H5** proton (appearing at 4.415 ppm). Hence, **H1** is trans to **H5**. Thus, the compound is in **alpha** configuration (Figure 3.10).

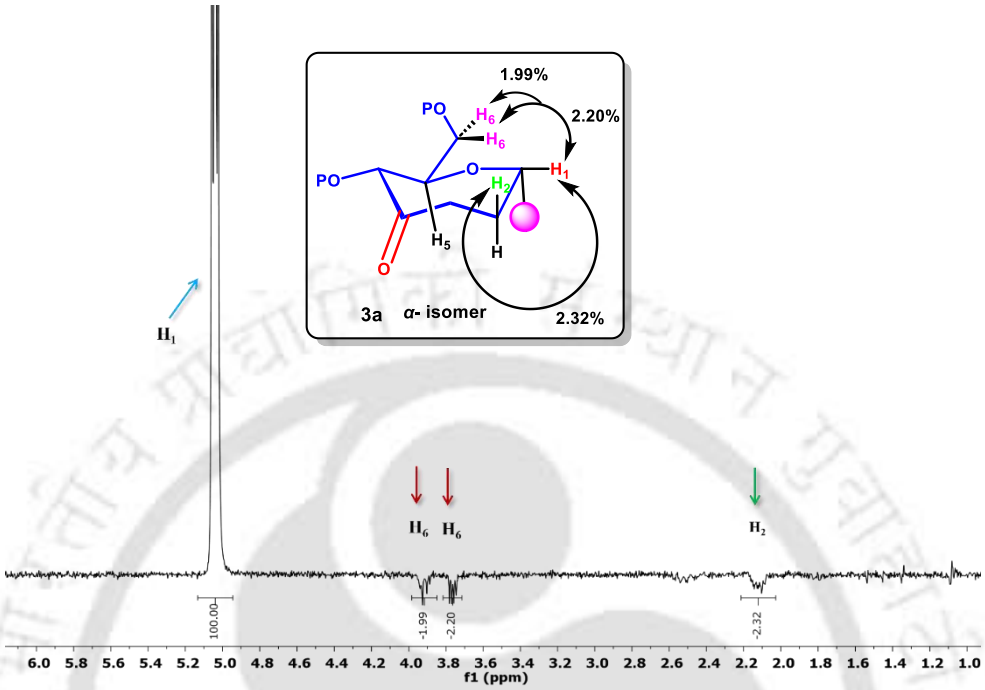

Figure 3.10. *nOe experiment of 3a.*

Irradiation of H2: Upon irradiation of **H2**, the enhancement on the **H1** proton (appearing at 5.041 ppm) is found 3.27%. In addition, there is no enhancement on the **H5** proton (appearing at 4.415 ppm). Hence, **H1** and **H2** are trans to **H5**. Thus, the compound is in **alpha** configuration (Figure 3.11).

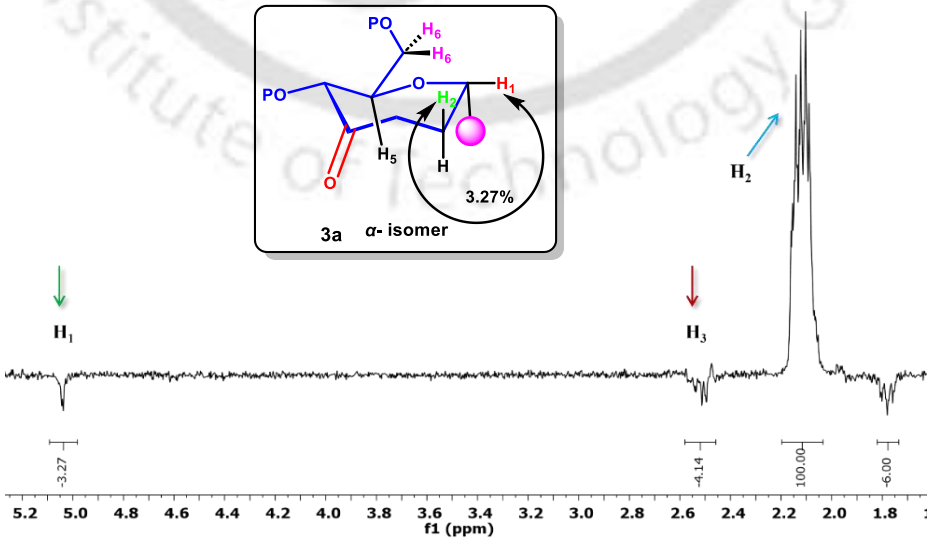

Figure 3.11. nOe experiment of 3a.

3.5.6. General procedure 1.1: synthesis of (*O*/*S*)-septanosides

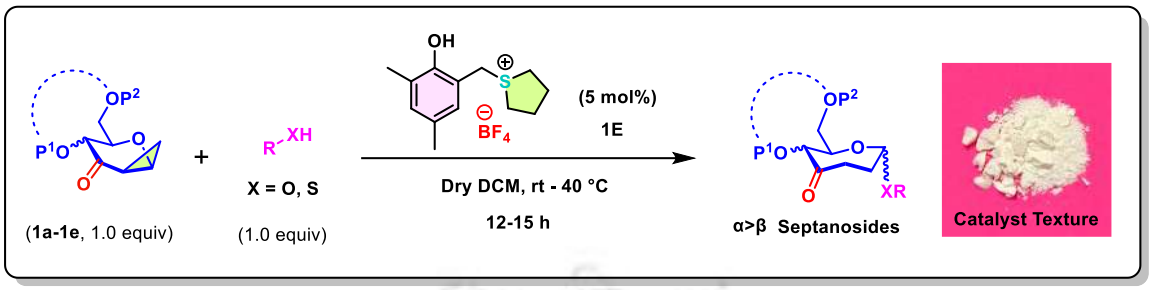

Procedure: In a screw-capped vial equipped with a magnetic stir bar, donor (0.25 mmol, 1.0 equiv), acceptor (0.25 mmol, 1.0 equiv), and the catalyst **1E** (3.9 mg, 0.0125 mmol, 5 mol%) were placed under an argon atmosphere. Then, dry DCM (1 mL) was added, and the resulting solution was stirred at **room temperature** for 12-15 h or **40 °C** for 3-6 h. After completion of the reaction, the solvent was removed in vacuo, and the reaction mixture was purified using column chromatography (SiO_2, EtOAc/Hexane) to obtain the desired septanosides. The anomerization of septanosides was confirmed on their **^{1}H NMR** and **^{13}C NMR** data. Also, the ***α***-configuration of the septanosides was confirmed based on **NOE** experiments and SC-XRD data.

3.5.7. General procedure 1.2: synthesis of septanosyl esters

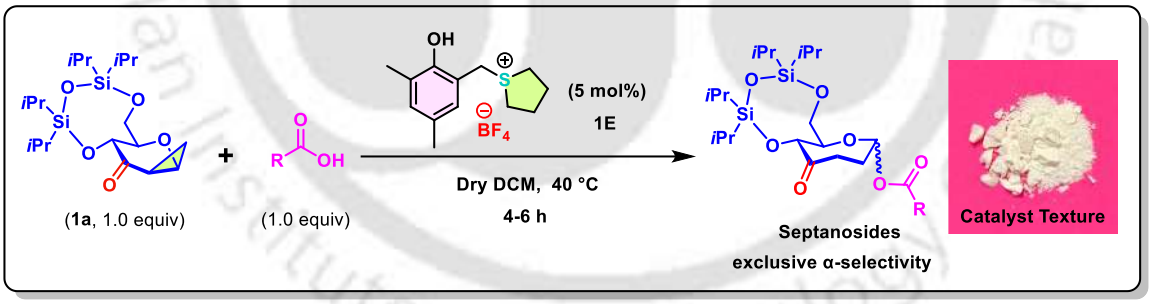

Procedure: In a screw-capped vial equipped with a magnetic stir bar, donor **1a** (0.25 mmol, 1.0 equiv), acid acceptor (0.25 mmol, 1.0 equiv), and the catalyst **1E** (3.9 mg, 0.0125 mmol, 5 mol%) were placed under an argon atmosphere. Then, dry DCM (1 mL) was added, and the resulting solution was stirred at **40 °C** for 3-6 h. After completion of the reaction, the solvent was removed in vacuo, and the reaction mixture was purified using column chromatography (SiO_2, EtOAc/Hexane) to obtain the desired septanosyl esters. The anomerization of septanosides was confirmed on their **^{1}H NMR** and **^{13}C NMR** data.

3.5.8. Spectroscopic data of Septanosides (3a-7i)

(6aR,11aR)-2,2,4,4-tetraisopropyl-8-(((3aR,5R,5aS,8aS,8bR)-2,2,7,7-tetramethyltetrahydro-5H-bis([1,3]dioxolo)[4,5-b:4',5'-d]pyran-5-yl)methoxy)tetrahydro-6H-oxepino[3,2-f][1,3,5,2,4]trioxadisilocin-11(8H)-one (3a)

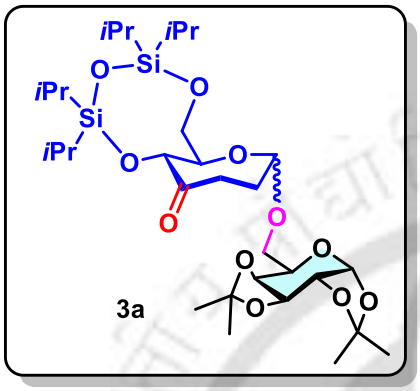

Compound **3a** was synthesized using the general procedure **1.3** (**A**). **3a** was obtained in 86% yield (142 mg), as a colorless oil, R_f = 0.6 (Hexane/EtOAc, 8:2, v/v), **[α]^{25}D** = +28.8 (*c* 0.16, EtOAc), **α/β = 13:1**. α-isomer: **^{1}H NMR** (600 MHz, $CDCl_3$) δ 5.50 (d, *J* = 5.0 Hz, 1H), 5.02 (dd, *J* = 8.0, 5.4 Hz, 1H), 4.60 (dd, *J* = 7.9, 2.4 Hz, 1H), 4.40 (d, *J* = 9.6 Hz, 1H), 4.31 (dd, *J* = 5.0, 2.4 Hz, 1H), 4.20 (dd, *J* = 7.9, 1.7 Hz, 1H), 4.12 (dd, *J* = 11.6, 1.8 Hz, 1H), 3.96 – 3.87 (m, 4H), 3.74 (dd, *J* = 10.0, 5.8 Hz, 1H), 2.50 (d, *J* = 11.8 Hz, 1H), 2.48 – 2.43 (m, 1H), 2.14 – 2.07 (m, 1H), 1.81 – 1.74 (m, 1H), 1.51 (s, 3H), 1.43 (s, 3H), 1.32 (d, *J* = 4.5 Hz, 6H), 1.08 – 1.01 (m, 28H). **^{13}C NMR** (151 MHz, $CDCl_3$) δ 207.9, 109.5, 108.7, 99.8, 96.5, 74.8, 71.2, 70.8, 70.7, 68.8, 66.4, 66.3, 63.4, 35.7, 27.7, 26.2, 26.1, 25.0, 24.7, 17.5, 17.4, 17.3, 17.2, 17.1, 13.5, 13.4, 12.6, 12.4. **HRMS** (ESI) m/z: $[M+Na]^+$ calcd for $C_{31}H_{56}NaO_{11}Si_2$ 683.3254; found 683.3262.

(6aR,8S,11aR)-2,2,4,4-tetraisopropyl-8-(((3aS,5aR,8aR,8bS)-2,2,7,7-tetramethyltetrahydro-3aH-bis([1,3]dioxolo)[4,5-b:4',5'-d]pyran-3a-yl)methoxy)tetrahydro-6H-oxepino[3,2-f][1,3,5,2,4]trioxadisilocin-11(8H)-one (3b)

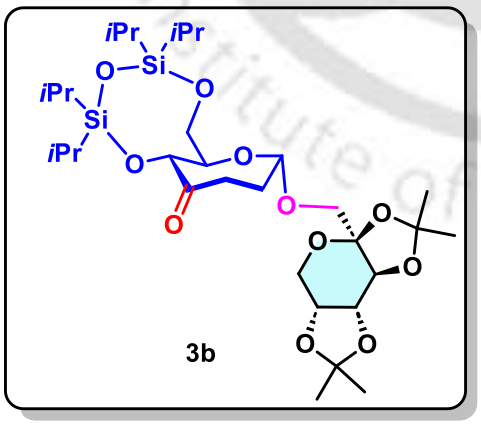

Compound **3b** was synthesized using the general procedure **1.3** (**A**). **3b** was obtained in 87% yield (144 mg), as a colorless oil, R_f = 0.6 (Hexane/EtOAc, 8:2, v/v), **[α]^{25}D** = +13.4 (*c* 0.16, EtOAc). **^{1}H NMR** (600 MHz, $CDCl_3$) δ 5.02 (dd, *J* = 8.0, 5.4 Hz, 1H), 4.59 (dd, *J* = 7.8, 2.6 Hz, 1H), 4.41 (d, *J* = 9.7 Hz, 1H), 4.33 (d, *J* = 2.7 Hz, 1H), 4.24 – 4.20 (m, 1H), 4.12 (dd, *J* = 11.7, 1.9 Hz, 1H), 3.99 – 3.93 (m, 2H), 3.92 – 3.88 (m, 2H), 3.72 (d, *J* = 13.0 Hz, 1H), 3.53 (d, *J* = 10.4 Hz, 1H), 2.56 – 2.50 (m, 1H), 2.48 – 2.43 (m, 1H), 2.19 – 2.12 (m, 1H), 1.83 – 1.76 (m, 1H), 1.51 (s, 3H), 1.46 (s, 3H), 1.34 (d, J = 13.8 Hz, 6H), 1.11 – 1.01 (m, 28H). **^{13}C NMR** (151 MHz, $CDCl_3$) δ 207.7, 109.2, 108.8, 102.4, 100.2, 75.0, 71.2, 70.4, 70.1, 69.5, 69.1, 63.5, 61.3, 35.6, 27.7, 26.7, 26.1, 25.5, 24.3, 17.5 (17.50, 17.46, 17.45), 17.4, 17.3 (17.32,

17.31), 17.2, 17.1, 13.5, 13.4, 12.7, 12.5. **HRMS** (ESI) m/z: $[M+Na]^+$ calcd for $C_{31}H_{56}NaO_{11}Si_2$ 683.3254; found 683.3248.

(6aR,11aR)-2,2,4,4-tetraisopropyl-8-(((3aR,4R,6R,6aR)-6-methoxy-2,2-dimethyltetrahydrofuro[3,4-d][1,3]dioxol-4-yl)methoxy)tetrahydro-6H-oxepino[3,2-f][1,3,5,2,4]trioxadisilocin-11(8H)-one (3c)

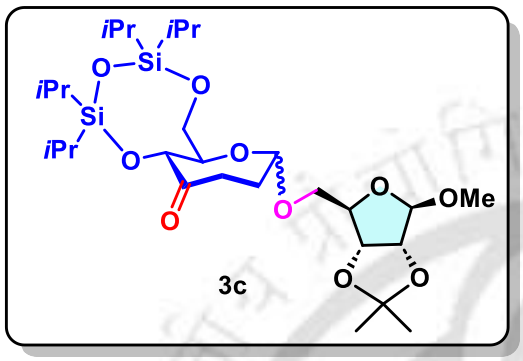

Compound **3c** was synthesized using the general procedure **1.3** (**A**). **3c** was obtained in 87% yield (132 mg), as a colorless oil, R_f = 0.6 (Hexane/EtOAc, 8:2, v/v), **$[\alpha]^{25}_D$** = -2.7 (*c* 0.18, EtOAc). **α/β = 2.3:1**. α-isomer: **^{1}H NMR** (600 MHz, $CDCl_3$) *δ* 4.98 (dd, *J* = 7.9, 5.3 Hz, 1H), 4.94 (s, 1H), 4.64 (d, *J* = 6.0 Hz, 1H), 4.58 – 4.53 (m, 1H), 4.39 (d, *J* = 9.6 Hz, 1H), 4.32 – 4.25 (m, 1H), 4.16 (d, *J* = 11.2 Hz, 1H), 3.91 – 3.81 (m, 3H), 3.48 (t, *J* = 9.3 Hz, 1H), 3.29 (s, 3H), 2.53 – 2.44 (m, 2H), 2.10 (dd, *J* = 14.3, 6.7 Hz, 1H), 1.83 – 1.77 (m, 1H), 1.47 (s, 3H), 1.31 (s, 3H), 1.09 – 1.02 (m, 28H). **^{13}C NMR** (151 MHz, $CDCl_3$) *δ* 207.5, 112.6, 109.6, 100.5, 85.3, 85.1, 82.2, 74.8, 69.2, 69.0, 63.6, 55.2, 35.6, 27.6, 26.6, 25.2, 17.5, 17.4, 17.3 (17.30, 17.26), 17.2, 17.1, 13.5, 13.4, 12.6, 12.4. **HRMS** (ESI) m/z: $[M+Na]^+$ calcd for $C_{28}H_{52}NaO_{10}Si_2$ 627.2992; found 627.2967.

(6aR,11aR)-2,2,4,4-tetraisopropyl-8-(((2R,3R,5R,6S)-3,4,5-tris(benzyloxy)-6-methoxytetrahydro-2H-pyran-2-yl)methoxy)tetrahydro-6H-oxepino[3,2-f][1,3,5,2,4]trioxadisilocin-11(8H)-one (3d)

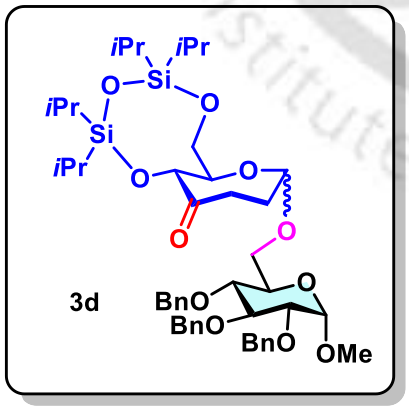

Compound **3d** was synthesized using the general procedure **1.3** (**A**). **3d** was obtained in 85% yield (184 mg), as a colorless oil, R_f = 0.5 (Hexane/EtOAc, 8:2, v/v), **$[\alpha]^{25}_D$** = +56.3 (*c* 0.22, EtOAc). **α/β = 3.6:1**. α-isomer: **^{1}H NMR** (600 MHz, $CDCl_3$) *δ* 7.28 – 7.17 (m, 15H), 4.95 (dd, *J* = 7.6, 5.4 Hz, 1H), 4.91 – 4.88 (m, 1H), 4.85 (d, *J* = 11.4 Hz, 1H), 4.75 – 4.68 (m, 2H), 4.58 (dd, *J* = 12.0, 7.7 Hz, 1H), 4.53 – 4.47 (m, 2H), 4.30 (d, *J* = 9.6 Hz, 1H), 3.89 (dt, *J* = 19.3, 10.4 Hz, 2H), 3.81 (dd, *J* = 11.5, 4.6 Hz, 1H), 3.72 – 3.64 (m, 4H), 3.45 – 3.35 (m, 2H), 3.28 (s, 3H), 2.45 – 2.34 (m, 2H), 2.07 – 1.99 (m, 1H), 1.67 (d, *J* = 24.5 Hz, 1H), 1.02 – 0.94 (m, 28H). **^{13}C NMR** (151 MHz, $CDCl_3$) *δ* 207.8, 138.8, 138.5, 138.3, 128.6, 128.5 (128.51, 128.49), 128.2, 128.1, 128.0, 127.7 (127.74, 127.69), 127.3, 100.4, 98.1, 82.3, 80.2, 77.8, 75.9, 74.8 (74.80, 74.76), 73.5, 70.1, 68.9, 66.8, 63.4,

55.2, 35.6, 27.6, 17.5 (17.48, 17.45), 17.4 (17.41, 17.39), 17.3 (17.32, 17.27), 17.2, 17.1, 13.4, 13.3, 12.5, 12.4. **HRMS** (ESI) m/z: $[M+Na]^+$ calcd for $C_{47}H_{68}NaO_{11}Si_2$ 887.4193; found 887.4202.

(6aR,11aR)-2,2,4,4-tetraisopropyl-8-(((2R,3S,5R,6S)-3,4,5-tris(benzyloxy)-6-methoxytetrahydro-2H-pyran-2-yl)methoxy)tetrahydro-6H-oxepino[3,2-f][1,3,5,2,4]trioxadisilocin-11(8H)-one (3e)

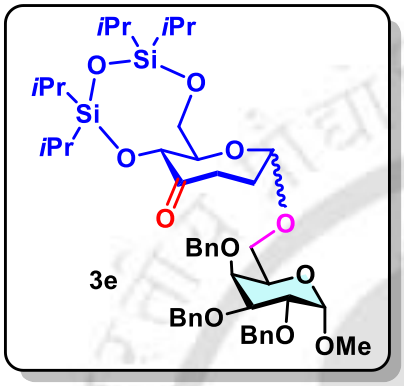

Compound **3e** was synthesized using the general procedure **1.3** (**A**). **3e** was obtained in 83% yield (179 mg), as a colorless oil, R_f = 0.5 (Hexane/EtOAc, 8:2, v/v), **$[\alpha]^{25}_D$** = +47.3 (*c* 0.18, EtOAc). **α/β = 5:1**. α-isomer: **^{1}H NMR** (600 MHz, $CDCl_3$) δ 7.29 – 7.17 (m, 15H), 4.95 (dd, *J* = 7.7, 5.4 Hz, 1H), 4.89 (d, *J* = 10.8 Hz, 1H), 4.85 (d, *J* = 11.4 Hz, 1H), 4.71 (d, *J* = 11.8 Hz, 2H), 4.58 (dd, *J* = 12.0, 7.7 Hz, 1H), 4.52 – 4.47 (m, 2H), 4.30 (d, *J* = 9.6 Hz, 1H), 3.94 – 3.86 (m, 2H), 3.81 (dd, *J* = 11.5, 4.6 Hz, 1H), 3.70 – 3.63 (m, 4H), 3.43 (dd, *J* = 10.4, 4.7 Hz, 2H), 3.28 (s, 3H), 2.44 – 2.34 (m, 2H), 2.07 – 1.99 (m, 1H), 1.71 – 1.64 (m, 1H), 1.02 – 0.94 (m, 28H). **^{13}C NMR** (151 MHz, $CDCl_3$) δ 207.8, 138.8, 138.5, 138.3, 128.6, 128.51, 128.48, 128.2, 128.1, 128.0, 127.74, 127.69, 127.3, 100.4, 98.1, 82.3, 80.2, 77.8, 75.9, 74.8, 74.8, 73.5, 70.1, 68.9, 66.8, 63.4, 55.2, 35.6, 27.6, 17.48, 17.45, 17.41, 17.38, 17.32, 17.27, 17.2, 17.1, 13.4, 13.3, 12.5, 12.4. **HRMS** (ESI) m/z: $[M+Na]^+$ calcd for $C_{47}H_{68}NaO_{11}Si_2$ 887.4193; found 887.4201.

(6aR,8R,11aR)-8-(((2R,3R,5R,6S)-4,5-bis(benzyloxy)-2-((benzyloxy)methyl)-6-methoxytetrahydro-2H-pyran-3-yl)oxy)-2,2,4,4-tetraisopropyltetrahydro-6H-oxepino[3,2-f][1,3,5,2,4]trioxadisilocin-11(8H)-one (3f)

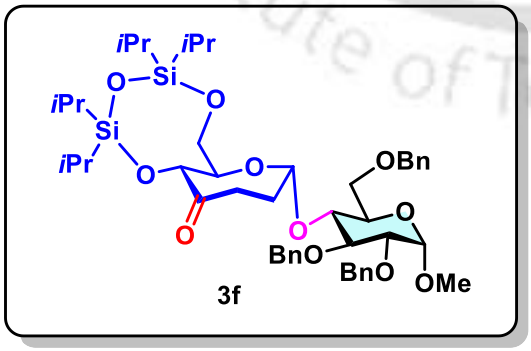

Compound **3f** was synthesized using the general procedure **1.3** (**B**). **3f** was obtained in 79% yield (170 mg), as a colorless oil, R_f = 0.5 (Hexane/EtOAc, 8:2, v/v), **$[\alpha]^{25}_D$** = +52.5 (*c* 0.16, EtOAc). **^{1}H NMR** (600 MHz, $CDCl_3$) δ 7.27 – 7.17 (m, 15H), 5.36 (dd, *J* = 8.9, 5.0 Hz, 1H), 4.98 (d, *J* = 11.5 Hz, 1H), 4.66 (d, *J* = 12.0 Hz, 1H), 4.57 – 4.51 (m, 4H), 4.46 (d, *J* = 12.3 Hz, 1H), 4.23 (d, *J* = 9.2 Hz, 1H), 3.86 – 3.80 (m, 2H), 3.68 (d, *J* = 7.3 Hz, 3H), 3.60 – 3.54 (m, 3H), 3.46 (dd, *J* = 9.6, 3.5 Hz, 1H), 3.33 (s, 3H), 2.18 – 2.10 (m, 2H), 1.65 – 1.60 (m, 1H), 1.49 (m, 1H), 1.00 – 0.93 (m, 28H). **^{13}C NMR** (151 MHz, $CDCl_3$) δ 207.5, 138.8, 138.3, 138.0, 128.63, 128.56, 128.5, 128.3, 128.1, 127.73, 127.71, 127.68,

127.5, 101.1, 97.8, 82.5, 80.3, 75.6, 75.4, 74.4, 73.4, 70.2, 69.9, 69.3, 63.6, 55.3, 35.6, 27.2, 17.5, 17.41, 17.39, 17.36, 17.3, 17.2, 17.1, 13.4, 13.3, 12.7, 12.4. **HRMS** (ESI) m/z: $[M+Na]^+$ calcd for $C_{47}H_{68}NaO_{11}Si_2$ 887.4193; found 887.4202.

(6aR,8R,11aR)-8-(((2S,3S,5R,6R)-4,5-bis(benzyloxy)-6-((benzyloxy)methyl)-2-methoxytetrahydro-2H-pyran-3-yl)oxy)-2,2,4,4-tetraisopropyltetrahydro-6H-oxepino[3,2-f][1,3,5,2,4]trioxadisilocin-11(8H)-one (3g)

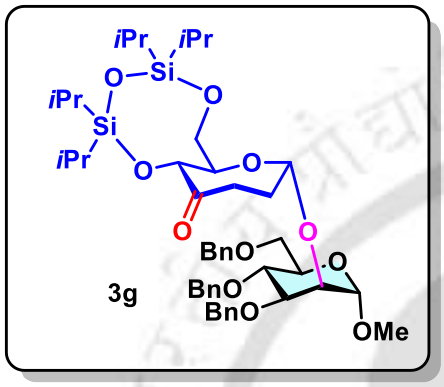

Compound **3g** was synthesized using the general procedure **1.3** (**B**). **3g** was obtained in 80% yield (173 mg), as a colorless oil, R_f = 0.6 (Hexane/EtOAc, 8:2, v/v), **[α]^{25}D** = +32.7 (*c* 0.19, EtOAc). **^{1}H NMR** (600 MHz, $CDCl_3$) δ 7.28 – 7.17 (m, 13H), 7.09 – 7.04 (m, 2H), 5.16 (dd, *J* = 8.3, 5.2 Hz, 1H), 4.71 (d, *J* = 10.8 Hz, 1H), 4.58 (d, *J* = 29.1 Hz, 4H), 4.45 (d, *J* = 12.1 Hz, 1H), 4.40 (d, *J* = 10.8 Hz, 1H), 4.30 (d, *J* = 9.6 Hz, 1H), 4.18 (s, 1H), 4.08 (d, *J* = 10.3 Hz, 1H), 3.89 (d, *J* = 9.6 Hz, 1H), 3.80 (dd, *J* = 9.3, 2.7 Hz, 1H), 3.76 – 3.72 (m, 2H), 3.68 – 3.62 (m, 3H), 3.28 (s, 3H), 2.40 – 2.34 (m, 2H), 2.09 (dd, *J* = 11.5, 6.3 Hz, 1H), 1.77 (dd, *J* = 17.4, 8.6 Hz, 1H), 1.03 – 0.98 (m, 28H).**^{13}C NMR** (151 MHz, $CDCl_3$) δ 207.6, 138.5, 128.6, 128.5, 128.0, 127.81, 127.78, 127.75, 127.7, 127.5, 101.5, 100.5, 80.4, 75.1, 74.9, 73.6, 73.5, 72.6, 71.9, 69.3, 69.1, 63.8, 54.9, 35.7, 27.3, 17.53, 17.50, 17.4, 17.32, 17.31, 17.2, 17.1, 13.5, 13.4, 12.6, 12.4. **HRMS** (ESI) m/z: $[M+Na]^+$ calcd for $C_{47}H_{68}NaO_{11}Si_2$ 887.4193; found 887.4199.

(6aR,8R,11aR)-2,2,4,4-tetraisopropyl-8-(((3aR,4R,6S,7S,7aR)-4-methoxy-2,2,6-trimethyltetrahydro-4H-[1,3]dioxolo[4,5-c]pyran-7-yl)oxy)tetrahydro-6H-oxepino[3,2-f][1,3,5,2,4]trioxadisilocin-11(8H)-one (3h)

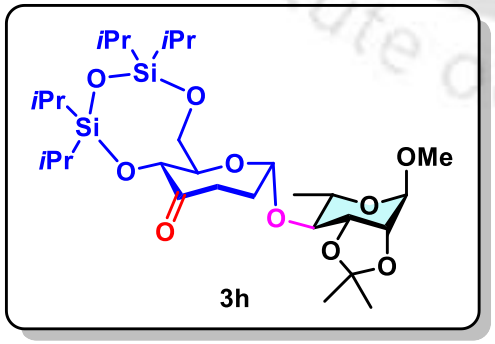

Compound **3h** was synthesized using the general procedure **1.3** (**A**). **3h** was obtained in 84% yield (130 mg), as a colorless oil, R_f = 0.6 (Hexane/EtOAc, 8:2, v/v), **[α]^{25}D** = +57.1 (*c* 0.18, EtOAc). **^{1}H NMR** (600 MHz, $CDCl_3$) δ 5.09 (dd, *J* = 8.4, 4.9 Hz, 1H), 4.83 (s, 1H), 4.44 (d, *J* = 9.4 Hz, 1H), 4.37 – 4.32 (m, 1H), 4.13 – 4.07 (m, 2H), 4.04 (t, *J* = 6.4 Hz, 1H), 3.95 (d, *J* = 9.3 Hz, 1H), 3.59 (dq, *J* = 12.5, 6.2 Hz, 1H), 3.49 (dd, *J* = 9.9, 7.4 Hz, 1H), 3.35 (s, 3H), 2.51 – 2.43 (m, 2H), 2.10 – 2.03 (m, 1H), 1.87 (dt, *J* = 16.0, 8.0 Hz, 1H), 1.59 (s, 3H), 1.33 (s, 3H), 1.23 (d, *J* = 6.2 Hz, 3H), 1.10 – 1.03 (m, 28H). **^{13}C NMR** (151 MHz, $CDCl_3$) δ 207.7, 109.3, 101.3, 98.2, 80.9, 77.1, 76.2, 75.5, 69.9, 65.1, 62.7, 54.9, 35.8, 28.1, 27.4,

26.6, 17.7, 17.6, 17.50, 17.48, 17.46, 17.43, 17.35, 17.3, 17.2, 13.4, 13.4, 12.9, 12.5. **HRMS** (ESI) m/z: $[M+H]^+$ calcd for $C_{29}H_{55}O_{10}Si_2$ 619.3329; found 619.3299.

(6aR,8R,11aR)-8-(((6S)-5-(2,2-dimethyl-1,3-dioxolan-4-yl)-2,2-dimethyltetrahydrofuro[2,3-d][1,3]dioxol-6-yl)oxy)-2,2,4,4-tetraisopropyltetrahydro-6H-oxepino[3,2-f][1,3,5,2,4]trioxadisilocin-11(8H)-one (3i)

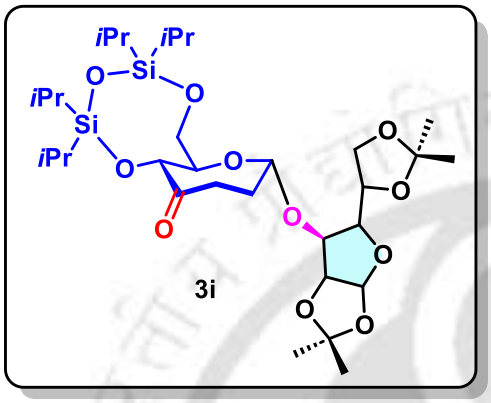

Compound **3i** was synthesized using the general procedure **1.3** (**B**). **3i** was obtained in 52% yield (86 mg), as a colorless oil, R_f = 0.5 (Hexane/EtOAc, 8:2, v/v), **$[\alpha]^{25}_D$** = +26.3 (*c* 0.08, EtOAc). **^{1}H NMR** (600 MHz, $CDCl_3$) δ 5.98 (d, *J* = 3.7 Hz, 1H), 5.02 (dd, *J* = 7.9, 5.5 Hz, 1H), 4.57 (d, *J* = 3.7 Hz, 1H), 4.40 (d, *J* = 9.9 Hz, 1H), 4.30 (dd, *J* = 7.3, 3.9 Hz, 1H), 4.19 (d, *J* = 3.8 Hz, 1H), 4.11 (d, *J* = 11.4 Hz, 1H), 3.96 (d, *J* = 11.8 Hz, 1H), 3.93 – 3.86 (m, 2H), 3.77 (d, *J* = 11.1 Hz, 1H), 3.67 (t, *J* = 5.9 Hz, 1H), 2.53 (t, *J* = 12.5 Hz, 1H), 2.47 – 2.42 (m, 1H), 2.15 – 2.09 (m, 1H), 1.78 (d, *J* = 12.7 Hz, 1H), 1.46 (s, 3H), 1.33 (d, *J* = 6.5 Hz, 9H), 1.10 – 1.04 (m, 28H). **^{13}C NMR** (151 MHz, $CDCl_3$) δ 207.9, 112.3, 106.5, 101.1, 99.6, 84.2, 79.3, 75.2, 74.8, 71.4, 68.8, 67.6, 63.4, 35.7, 27.6, 27.3, 26.7, 24.1, 17.52, 17.48, 17.46, 17.4, 17.3, 17.2, 17.1, 13.5, 13.4, 12.6, 12.3. **HRMS** (ESI) m/z: $[M+Na]^+$ calcd for $C_{31}H_{56}NaO_{11}Si_2$ 683.3254; found 683.3257.

(6aR,8S,11aR)-2,2,4,4-tetraisopropyl-8-(octyloxy)tetrahydro-6H-oxepino[3,2-f][1,3,5,2,4]trioxadisilocin-11(8H)-one (3j)

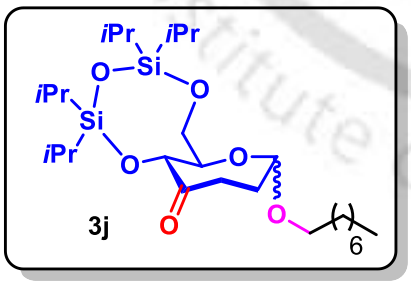

Compound **3j** was synthesized using the general procedure **1.3** (**A**). **3j** was obtained in 87% yield (115 mg), as a colorless oil, R_f = 0.7 (Hexane/EtOAc, 9:1, v/v), **$[\alpha]^{25}_D$** = +65.9 (*c* 0.13, EtOAc). **α/β = 20:1**. α-isomer: **^{1}H NMR** (600 MHz, $CDCl_3$) δ 4.98 – 4.90 (m, 1H), 4.41 (d, *J* = 9.4 Hz, 1H), 4.15 (d, *J* = 11.5 Hz, 1H), 3.85 (dd, *J* = 16.5, 10.6 Hz, 2H), 3.70 – 3.63 (m, 1H), 3.34 (dt, *J* = 9.6, 6.1 Hz, 1H), 2.56 – 2.44 (m, 2H), 2.11 – 2.05 (m, 1H), 1.82 – 1.73 (m, 1H), 1.63 – 1.58 (m, 1H), 1.50 – 1.44 (m, 1H), 1.39 – 1.26 (m, 6H), 1.10 – 1.02 (m, 28H), 0.87 (dt, *J* = 12.5, 7.1 Hz, 7H). **^{13}C NMR** (151 MHz, $CDCl_3$) δ 208.0, 100.21, 100.16, 75.0, 71.31, 71.26, 68.9, 63.6, 39.80, 39.78, 35.66, 30.65, 30.6, 29.3, 29.2, 27.9, 24.0, 23.2, 17.51, 17.46, 17.44, 17.42, 17.31, 17.29, 17.2, 17.1, 14.2, 13.5, 13.4, 12.6, 12.4, 11.32, 11.25. **HRMS** (ESI) m/z: $[M+H]^+$ calcd for $C_{27}H_{55}O_6Si_2$ 531.3532; found 531.3532.

(6aR,11aR)-8-(isopentyloxy)-2,2,4,4-tetraisopropyltetrahydro-6H-oxepino[3,2-f][1,3,5,2,4]trioxadisilocin-11(8H)-one (3k)

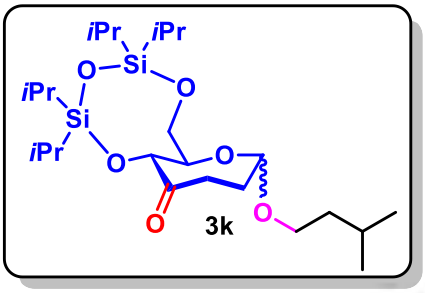

Compound **3k** was synthesized using the general procedure **1.3** (**A**). **3k** was obtained in 84% yield (103 mg), as a colorless oil, R_f = 0.7 (Hexane/EtOAc, 9:1, v/v), **[α]$^{25}_D$** = +45.0 (*c* 0.22, EtOAc). **α/β = 11:1**. α-isomer: **^{1}H NMR** (500 MHz, $CDCl_3$) δ 4.99 – 4.92 (m, 1H), 4.40 (d, *J* = 9.6 Hz, 1H), 4.15 (d, *J* = 11.0 Hz, 1H), 3.82 (dt, *J* = 34.3, 8.4 Hz, 3H), 3.56 – 3.45 (m, 1H), 2.55 – 2.43 (m, 2H), 2.13 – 2.04 (m, 1H), 1.82 – 1.73 (m, 1H), 1.67 (dd, *J* = 13.4, 6.6 Hz, 1H), 1.44 (q, *J* = 6.8 Hz, 2H), 1.10 – 1.02 (m, 28H), 0.89 (d, *J* = 6.4 Hz, 6H). **^{13}C NMR** (126 MHz, $CDCl_3$) δ 207.9, 99.9, 74.9, 68.8, 66.8, 63.6, 38.5, 35.7, 27.9, 25.2, 22.8, 22.7, 17.51, 17.46, 17.43, 17.42, 17.32, 17.28, 17.2, 17.1, 13.5, 13.4, 12.6, 12.4. **HRMS** (ESI) m/z: $[M+H]^+$ calcd for $C_{24}H_{49}O_6Si_2$ 489.3063; found 489.3059.

(6aR,8S,11aR)-8-(but-3-en-1-yloxy)-2,2,4,4-tetraisopropyltetrahydro-6H-oxepino[3,2-f][1,3,5,2,4]trioxadisilocin-11(8H)-one (3l)

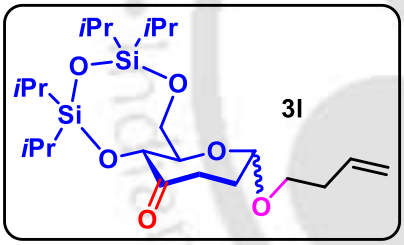

Compound **3l** was synthesized using the general procedure **1.3** (**A**). **3l** was obtained in 85% yield (100 mg), as a colorless oil, R_f = 0.6 (Hexane/EtOAc, 9:1, v/v), **[α]$^{25}_D$** = +45.1 (*c* 0.26, EtOAc). **α/β = 11:1**. α-isomer: **^{1}H NMR** (600 MHz, $CDCl_3$) δ 5.79 (ddt, *J* = 17.0, 10.2, 6.7 Hz, 1H), 5.10 – 5.06 (m, 1H), 5.03 (d, *J* = 10.2 Hz, 1H), 4.97 (dd, *J* = 8.0, 5.3 Hz, 1H), 4.40 (d, *J* = 9.7 Hz, 1H), 4.17 – 4.13 (m, 1H), 3.88 – 3.78 (m, 3H), 3.54 (dt, *J* = 9.6, 6.6 Hz, 1H), 2.55 – 2.43 (m, 2H), 2.31 (q, *J* = 6.8 Hz, 2H), 2.12 – 2.05 (m, 1H), 1.81 – 1.72 (m, 1H), 1.14 – 0.99 (m, 28H). **^{13}C NMR** (151 MHz, $CDCl_3$) δ 207.9, 135.0, 116.8, 99.8, 74.9, 68.8, 67.4, 63.6, 35.7, 34.1, 27.7, 17.52, 17.46, 17.43, 17.42, 17.31, 17.28, 17.2, 17.1, 13.5, 13.4, 12.6, 12.4. **HRMS** (ESI) m/z: $[M+H]^+$ calcd for $C_{23}H_{45}O_6Si_2$ 473.2750; found 473.2749.

(6aR,11aR)-8-(but-3-yn-1-yloxy)-2,2,4,4-tetraisopropyltetrahydro-6H-oxepino[3,2-f][1,3,5,2,4]trioxadisilocin-11(8H)-one (3m)

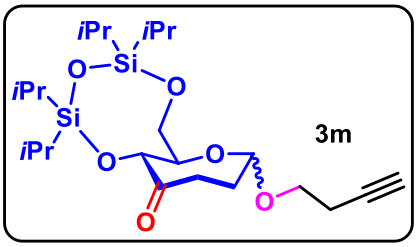

Compound **3m** was synthesized using the general procedure **1.3** (**A**). **3m** was obtained in 86% yield (101 mg), as a colorless oil, R_f = 0.5 (Hexane/EtOAc, 9:1, v/v), **[α]$^{25}_D$** = +35.2 (*c* 0.11, EtOAc). **α/β = 9:1**. α-isomer: **^{1}H NMR** (600 MHz, $CDCl_3$) δ 5.02 (dd, *J* = 8.0, 5.4 Hz, 1H), 4.40 (d, *J* = 9.5 Hz, 1H), 4.15 (d, *J* =

10.3 Hz, 1H), 3.93 – 3.86 (m, 3H), 3.63 (dt, J = 9.5, 6.5 Hz, 1H), 2.56 – 2.43 (m, 4H), 2.11 (dt, J = 13.4, 5.6 Hz, 1H), 1.95 (t, J = 2.5 Hz, 1H), 1.82 – 1.74 (m, 1H), 1.13 – 1.01 (m, 28H), 0.96 – 0.91 (m, 1H). **^{13}C NMR** (151 MHz, $CDCl_3$) δ 207.7, 99.8, 81.2, 74.9, 69.5, 68.9, 65.9, 63.6, 35.7, 27.6, 19.9, 17.51, 17.46, 17.43, 17.42, 17.30, 17.28, 17.2, 17.1, 13.5, 13.4, 12.6, 12.4. **HRMS** (ESI) m/z: $[M+H]^+$ calcd for $C_{23}H_{43}O_6Si_2$ 471.2593; found 471.2593.

(6aR,11aR)-8-([1,1'-biphenyl]-4-ylmethoxy)-2,2,4,4-tetraisopropyltetrahydro-6H-oxepino[3,2-f][1,3,5,2,4]trioxadisilocin-11(8H)-one (3n)

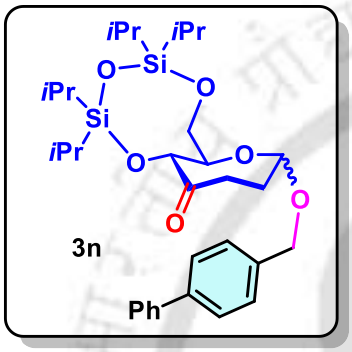

Compound **3n** was synthesized using the general procedure **1.3** (**A**). **3n** was obtained in 85% yield (124 mg), as a colorless oil, R_f = 0.5 (Hexane/EtOAc, 9:1, v/v), **$[\alpha]^{25}_D$** = +27.1 (c 0.24, EtOAc). **α/β = 6:1**. α-isomer: **^{1}H NMR** (600 MHz, $CDCl_3$) δ 7.50 (d, J = 7.5 Hz, 4H), 7.36 (t, J = 7.6 Hz, 2H), 7.32 (d, J = 8.0 Hz, 2H), 7.27 (t, J = 7.3 Hz, 1H), 5.04 (dd, J = 8.1, 5.3 Hz, 1H), 4.80 (d, J = 12.1 Hz, 1H), 4.58 (d, J = 12.1 Hz, 1H), 4.37 (d, J = 9.5 Hz, 1H), 4.10 (d, J = 10.2 Hz, 1H), 3.89 (d, J = 9.5 Hz, 1H), 3.81 (dd, J = 11.6, 1.8 Hz, 1H), 2.51 – 2.41 (m, 2H), 2.08 (dt, J = 13.2, 5.4 Hz, 1H), 1.82 (dt, J = 12.9, 9.0 Hz, 1H), 1.08 – 0.93 (m, 28H). **^{13}C NMR** (151 MHz, $CDCl_3$) δ 207.7, 140.9, 136.9, 128.9, 128.1, 127.5, 127.4, 127.2, 99.6, 75.0, 69.5, 69.2, 63.6, 35.8, 27.7, 17.52, 17.49, 17.45, 17.4, 17.32, 17.24, 17.1, 13.5, 13.4, 12.7, 12.4. **HRMS** (ESI) m/z: $[M+Na]^+$ calcd for $C_{32}H_{48}NaO_6Si_2$ 607.2882; found 607.2878.

(6aR,11aR)-8-((4-chlorobenzyl)oxy)-2,4,4-triisopropyltetrahydro-6H-2l3-oxepino[2,3-g][1,3,5,2,4]trioxadisilocin-11(8H)-one (3o)

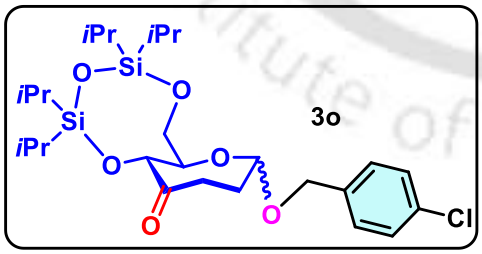

Compound **3o** was synthesized using the general procedure **1.3** (**A**). **3o** was obtained in 84% yield (105 mg), as a colorless oil, R_f = 0.5 (Hexane/EtOAc, 9:1, v/v), **$[\alpha]^{25}_D$** = +27.1 (c 0.24, EtOAc). **α/β = 5:1**. α-isomer: **^{1}H NMR** (600 MHz, $CDCl_3$) δ 7.24 (d, J = 8.3 Hz, 2H), 7.18 (t, J = 6.6 Hz, 2H), 4.99 (dd, J = 8.1, 5.3 Hz, 1H), 4.71 (d, J = 12.4 Hz, 1H), 4.51 (d, J = 12.4 Hz, 1H), 4.37 (dd, J = 16.6, 10.9 Hz, 1H), 4.08 (d, J = 10.3 Hz, 1H), 3.84 (d, J = 9.5 Hz, 1H), 3.77 – 3.74 (m, 1H), 2.49 – 2.40 (m, 2H), 2.05 (dt, J = 13.1, 5.3 Hz, 1H), 1.79 (dt, J = 12.8, 9.0 Hz, 1H), 1.06 – 0.94 (m, 28H). **^{13}C NMR** (151 MHz, $CDCl_3$) δ 207.5, 136.4, 133.6, 128.9, 128.8, 99.6, 74.9, 69.3, 68.9, 63.6, 35.7, 27.6, 17.50, 17.47, 17.43, 17.41, 17.3, 17.2, 17.1, 13.5, 13.4, 12.6, 12.4. **HRMS** (ESI) m/z: $[M+H]^+$ calcd for $C_{26}H_{44}ClO_6Si_2$ 543.2360; found 543.2330.

1-(((6aR,8R,11aR)-2,2,4,4-tetraisopropyl-11-oxohexahydro-6H-oxepino[3,2-f][1,3,5,2,4]trioxadisilocin-8-yl)oxy)pyrrolidine-2,5-dione (3p)

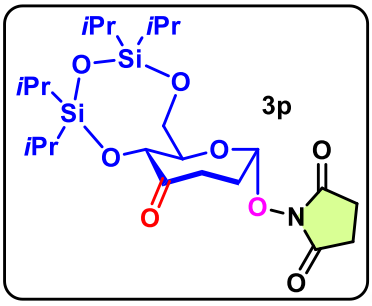

Compound **3p** was synthesized using the general procedure **1.3** (**A**). **3p** was obtained in 82% yield (106 mg), as a white foam, R_f = 0.4 (Hexane/EtOAc, 7:3, v/v), **[α]$^{25}_D$** = +71.9 (*c* 0.16, EtOAc). **^{1}H NMR** (600 MHz, $CDCl_3$) *δ* 5.60 (dd, *J* = 8.8, 5.5 Hz, 1H), 4.42 (d, *J* = 9.5 Hz, 1H), 4.23 (d, *J* = 9.5 Hz, 1H), 4.16 (d, *J* = 12.0 Hz, 1H), 3.93 (d, *J* = 10.8 Hz, 1H), 2.72 (s, 4H), 2.57 – 2.48 (m, 2H), 2.40 (dt, *J* = 13.1, 5.6 Hz, 1H), 1.94 (dt, *J* = 13.1, 9.7 Hz, 1H), 1.09 – 1.04 (m, 28H). **^{13}C NMR** (151 MHz, $CDCl_3$) *δ* 206.3, 171.3, 104.1, 74.6, 71.4, 63.2, 34.9, 25.7, 24.8, 17.5, 17.43, 17.40, 17.36, 17.3, 17.22, 17.19, 17.1, 13.5, 13.3, 12.41, 12.36. **HRMS** (ESI) m/z: $[M+H]^+$ calcd for $C_{23}H_{42}NO_8Si_2$ 516.2444; found 516.2416.

2-(((6aR,8R,11aR)-2,2,4,4-tetraisopropyl-11-oxohexahydro-6H-oxepino[3,2-f][1,3,5,2,4]trioxadisilocin-8-yl)oxy)isoindoline-1,3-dione (3q)

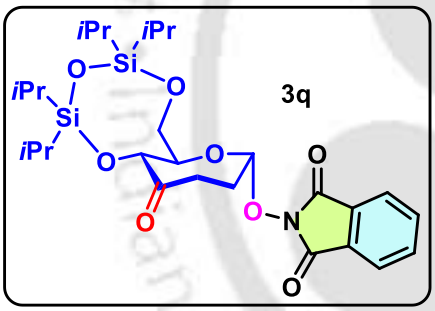

Compound **3q** was synthesized using the general procedure **1.3** (**B**). **3q** was obtained in 80% yield (113 mg), as a white foam, R_f = 0.7 (Hexane/EtOAc, 7:3, v/v), **[α]$^{25}_D$** = +79.2 (*c* 0.14, EtOAc). **^{1}H NMR** (600 MHz, $CDCl_3$) *δ* 7.83 (dd, *J* = 5.2, 3.2 Hz, 2H), 7.76 (dd, *J* = 5.4, 3.1 Hz, 2H), 5.69 (dd, *J* = 8.8, 5.5 Hz, 1H), 4.46 (d, *J* = 9.6 Hz, 1H), 4.33 (d, *J* = 9.5 Hz, 1H), 4.23 (d, *J* = 11.9 Hz, 1H), 4.02 (d, *J* = 10.6 Hz, 1H), 2.62 – 2.46 (m, 3H), 2.05 – 1.98 (m, 1H), 1.11 – 1.02 (m, 28H). **^{13}C NMR** (151 MHz, $CDCl_3$) *δ* 206.5, 163.8, 134.7, 129.2, 123.7, 105.3, 74.7, 71.4, 63.3, 35.1, 24.9, 17.5, 17.42, 17.41, 17.40, 17.3, 17.23, 17.22, 17.1, 13.5, 13.3, 12.43, 12.38. **HRMS** (ESI) m/z: $[M+H]^+$ calcd for $C_{27}H_{42}NO_8Si_2$ 564.2444; found 564.2416.

(6aR,8S,11aR)-2,2,4,4-tetraisopropyl-8-((R)-1-phenylethoxy)tetrahydro-6H-oxepino[3,2-f][1,3,5,2,4]trioxadisilocin-11(8H)-one (3r)

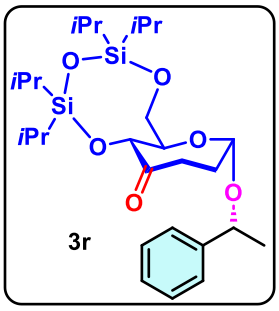

Compound **3r** was synthesized using the general procedure **1.3** (**A**). **3r** was obtained in 88% yield (115 mg), as a colorless oli, R_f = 0.7 (Hexane/EtOAc, 9:1, v/v), **[α]$^{25}_D$** = +105.5 (*c* 0.13, EtOAc). **^{1}H NMR** (600 MHz, $CDCl_3$) *δ* 7.23 (ddd, *J* = 24.6, 16.2, 7.6 Hz, 5H), 4.89 (q, *J* = 6.6 Hz, 1H), 4.72 (dd, *J* = 8.2, 5.3 Hz, 1H), 4.33 (d, *J* = 9.6 Hz, 1H), 4.16 (dd, *J* = 11.6, 1.5 Hz, 1H), 3.92 (d, *J* = 9.6 Hz, 1H), 3.86 (dd, *J* = 11.6, 2.0 Hz, 1H), 2.36 (q, *J* = 9.3, 7.7

Hz, 2H), 1.91 (dq, *J* = 15.3, 8.5, 6.8 Hz, 1H), 1.79 – 1.72 (m, 1H), 1.33 (d, *J* = 6.6 Hz, 3H), 1.12 – 0.93 (m, 28H). **^{13}C NMR** (151 MHz, $CDCl_3$) *δ* 207.9, 143.5, 128.6, 127.7, 126.3, 97.4, 75.1, 73.9, 69.2, 63.9, 35.8, 27.7, 24.6, 17.6, 17.5, 17.43, 17.42, 17.34, 17.33, 17.25, 17.1, 13.5, 13.4, 12.7, 12.4. **HRMS** (ESI) m/z: $[M+Na]^+$ calcd for $C_{27}H_{46}NaO_6Si_2$ 545.2726; found 545.2713.

(6aR,11aR)-8-(((3S,5S,7S)-adamantan-1-yl)oxy)-2,2,4,4-tetraisopropyltetrahydro-6H-oxepino[3,2-f][1,3,5,2,4]trioxadisilocin-11(8H)-one (3s)

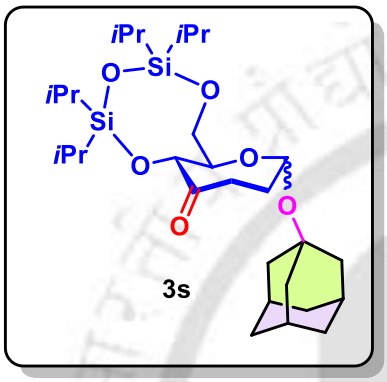

Compound **3s** was synthesized using the general procedure **1.3** (**A**). **3s** was obtained in 82% yield (113 mg), as a colorless oil, R_f = 0.7 (Hexane/EtOAc, 9:1, v/v), **$[\alpha]^{25}_D$** = +24.4 (*c* 0.36, EtOAc). **α/β = 6:1**. α-isomer: **^{1}H NMR** (600 MHz, $CDCl_3$) *δ* 5.35 (dd, *J* = 7.4, 4.7 Hz, 1H), 4.39 (d, *J* = 8.8 Hz, 1H), 4.13 (dd, *J* = 11.4, 2.1 Hz, 1H), 3.97 (d, *J* = 9.0 Hz, 1H), 3.83 (dd, *J* = 11.5, 3.0 Hz, 1H), 2.61 – 2.50 (m, 1H), 2.44 (ddd, *J* = 14.2, 10.2, 3.2 Hz, 1H), 2.13 (s, 3H), 1.97 – 1.85 (m, 2H), 1.79 (d, *J* = 15.5 Hz, 6H), 1.64 – 1.58 (m, 6H), 1.11 – 1.02 (m, 28H). **^{13}C NMR** (151 MHz, $CDCl_3$) *δ* 208.4, 92.2, 75.9, 74.1, 69.8, 63.9, 42.8, 36.4, 35.7, 30.7, 29.5, 17.60, 17.60, 17.5, 17.41, 17.38, 17.34, 17.26, 17.2, 13.48, 13.46, 12.8, 12.5. **HRMS** (ESI) m/z: $[M+H]^+$ calcd for $C_{29}H_{53}O_6Si_2$ 553.3376; found 553.3374.

(6aR,11aR)-8-(((S)-3,7-dimethyloct-6-en-1-yl)oxy)-2,2,4,4-tetraisopropyltetrahydro-6H-oxepino[3,2-f][1,3,5,2,4]trioxadisilocin-11(8H)-one (3t)

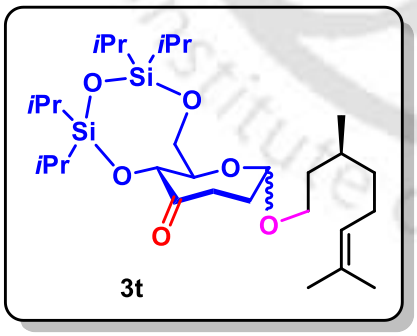

Compound **3t** was synthesized using the general procedure **1.3** (**A**). **3t** was obtained in 83% yield (116 mg), as a colorless oil, R_f = 0.6 (Hexane/EtOAc, 9:1, v/v), **$[\alpha]^{25}_D$** = +27.3 (*c* 0.13, EtOAc). **α/β = 12:1**. α-isomer: **^{1}H NMR** (600 MHz, $CDCl_3$) *δ* 5.07 (t, *J* = 6.4 Hz, 1H), 4.96 (dd, *J* = 7.7, 5.3 Hz, 1H), 4.41 (d, *J* = 9.5 Hz, 1H), 4.16 (d, *J* = 10.4 Hz, 1H), 3.82 (dt, *J* = 38.2, 9.9 Hz, 3H), 3.53 – 3.44 (m, 1H), 2.55 – 2.44 (m, 2H), 2.08 (dd, *J* = 11.5, 3.9 Hz, 1H), 1.95 (dq, *J* = 22.7, 7.5 Hz, 2H), 1.76 (q, *J* = 11.7 Hz, 1H), 1.67 (s, 3H), 1.59 (s, 3H), 1.55 – 1.50 (m, 1H), 1.40 – 1.31 (m, 2H), 1.17 (dd, *J* = 13.5, 6.3 Hz, 1H), 1.10 – 1.04 (m, 28H), 0.90 – 0.86 (m, 4H). **^{13}C NMR** (151 MHz, $CDCl_3$) *δ* 207.9, 131.4, 124.8, 99.94, 99.87, 75.0, 74.9, 68.9, 68.8, 66.69, 66.68, 63.7, 37.3, 37.2, 36.7, 36.6, 35.7, 29.74, 29.68, 27.9, 25.8, 25.59, 25.56, 19.8, 19.7, 17.8, 17.52, 17.47, 17.44, 17.43, 17.33, 17.29, 17.24, 17.1, 13.5, 13.4, 12.6, 12.4. **HRMS** (ESI) m/z: $[M+H]^+$ calcd for $C_{29}H_{57}O_6Si_2$ 557.3689; found 557.3689.

(6aR,11aR)-2,2,4,4-tetraisopropyl-8-(((1R,2S,4R)-1,7,7-trimethylbicyclo[2.2.1]heptan-2-yl)oxy)tetrahydro-6H-oxepino[3,2-f][1,3,5,2,4]trioxadisilocin-11(8H)-one (3u)

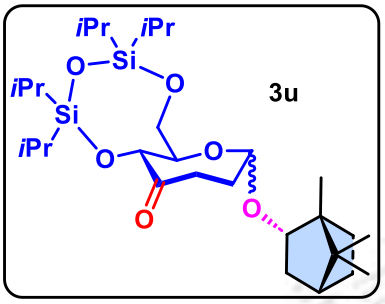

Compound **3u** was synthesized using the general procedure **1.3** (**A**). **3u** was obtained in 85% yield (118 mg), as a colorless oil, R_f = 0.7 (Hexane/EtOAc, 9:1, v/v), **[α]$^{25}_D$** = +25.0 (*c* 0.16, EtOAc). **α/β = 14:1**. α-isomer: **^{1}H NMR** (500 MHz, $CDCl_3$) δ 4.99 – 4.92 (m, 1H), 4.41 (d, *J* = 9.3 Hz, 1H), 4.15 (d, *J* = 11.4 Hz, 1H), 3.97 (d, *J* = 10.1 Hz, 1H), 3.89 (d, *J* = 9.3 Hz, 1H), 3.82 (d, *J* = 11.4 Hz, 1H), 2.52 – 2.43 (m, 2H), 2.28 – 2.18 (m, 1H), 2.10 (dd, *J* = 10.5, 5.1 Hz, 1H), 1.95 – 1.79 (m, 2H), 1.68 (s, 1H), 1.60 (s, 1H), 1.19 (d, *J* = 12.2 Hz, 2H), 1.10 – 1.02 (m, 28H), 0.86 – 0.78 (m, 10H). **^{13}C NMR** (126 MHz, $CDCl_3$) δ 208.2, 101.4, 83.9, 75.1, 68.9, 63.9, 49.8, 47.8, 45.2, 37.6, 35.6, 28.3, 28.1, 26.8, 19.9, 18.9, 17.53, 17.46, 17.44, 17.43, 17.33, 17.26, 17.25, 17.1, 13.9, 13.5, 13.4, 12.5, 12.4. **HRMS** (ESI) m/z: $[M+H]^+$ calcd for $C_{29}H_{55}O_6Si_2$ 555.3532; found 555.3532.

(6aR,11aR)-2,2,4,4-tetraisopropyl-8-(((1R,2S,5R)-2-isopropyl-5-methylcyclohexyl)oxy)tetrahydro-6H-oxepino[3,2-f][1,3,5,2,4]trioxadisilocin-11(8H)-one (3v)

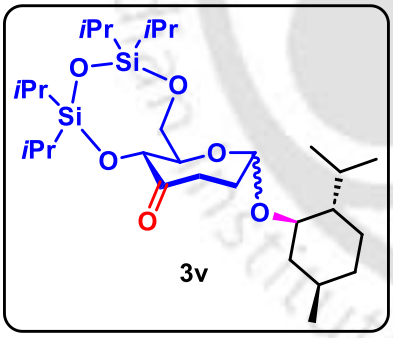

Compound **3v** was synthesized using the general procedure **1.3** (**A**). **3v** was obtained in 84% yield (120 mg), as a colorless oil, R_f = 0.8 (Hexane/EtOAc, 9:1, v/v), **[α]$^{25}_D$** = -3.9 (*c* 0.18, EtOAc). **α/β = 10:1**. α-isomer: **^{1}H NMR** (500 MHz, $CDCl_3$) δ 5.00 (dd, *J* = 7.7, 5.1 Hz, 1H), 4.41 (d, *J* = 8.9 Hz, 1H), 4.15 (d, *J* = 11.1 Hz, 1H), 3.91 (dd, *J* = 19.1, 10.3 Hz, 2H), 3.41 (dt, *J* = 10.5, 5.3 Hz, 1H), 2.53 – 2.42 (m, 2H), 2.09 (d, *J* = 12.2 Hz, 2H), 2.03 – 1.95 (m, 1H), 1.93 – 1.83 (m, 1H), 1.64 (s, 1H), 1.39 (s, 1H), 1.22 – 1.13 (m, 2H), 1.12 – 1.00 (m, 28H), 0.89 (t, *J* = 6.1 Hz, 7H), 0.86 – 0.78 (m, 2H), 0.74 (d, *J* = 6.9 Hz, 3H). **^{13}C NMR** (126 MHz, $CDCl_3$) δ 208.0, 101.9, 80.3, 75.6, 69.7, 63.7, 49.2, 43.7, 35.6, 34.4, 31.8, 27.9, 25.8, 23.2, 22.4, 21.3, 17.54, 17.48, 17.44, 17.42, 17.32, 17.2, 17.1, 16.3, 13.5, 13.4, 12.6, 12.4. **HRMS** (ESI) m/z: $[M+H]^+$ calcd for $C_{29}H_{57}O_6Si_2$ 557.3689; found 557.3677.

(6aR,8S,11aR)-8-(((3S,8S,9S,10R,13R,14S,17R)-10,13-dimethyl-17-((R)-6-methylheptan-2-yl)-2,3,4,7,8,9,10,11,12,13,14,15,16,17-tetradecahydro-1H-cyclopenta[a]phenanthren-3-yl)oxy)-2,2,4,4-tetraisopropyltetrahydro-6H-oxepino[3,2-f][1,3,5,2,4]trioxadisilocin-11(8H)-one (3w)

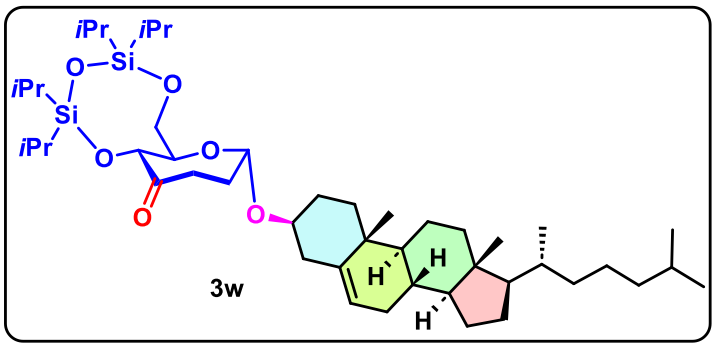

Compound **3w** was synthesized using the general procedure **1.3** (**A**). **3w** was obtained in 83% yield (163 mg), as a colorless oil, R_f = 0.8 (Hexane/EtOAc, 9:1, v/v), **[α]$^{25}_D$** = +43.9 (*c* 0.21, EtOAc). **^{1}H NMR** (600 MHz, $CDCl_3$) δ 5.33 (d, *J* = 4.8 Hz, 1H), 5.12 (dd, J = 7.9, 5.1 Hz, 1H), 4.40 (d, *J* = 9.4 Hz, 1H), 4.17 (d, *J* = 10.1 Hz, 1H), 3.90 (d, *J* = 9.4 Hz, 1H), 3.86 – 3.80 (m, 1H), 3.66 (dt, *J* = 11.4, 6.7 Hz, 1H), 2.55 – 2.44 (m, 2H), 2.29 (t, *J* = 11.5 Hz, 1H), 2.19 – 2.15 (m, 1H), 2.07 – 1.95 (m, 3H), 1.89 – 1.77 (m, 4H), 1.58 – 1.32 (m, 11H), 1.27 (d, *J* = 17.7 Hz, 4H), 1.16 (dd, *J* = 13.1, 8.8 Hz, 3H), 1.11 – 1.05 (m, 28H), 0.99 (s, 4H), 0.91 (d, *J* = 6.5 Hz, 4H), 0.86 (dd, *J* = 6.6, 2.6 Hz, 7H), 0.67 (s, 3H). **^{13}C NMR** (151 MHz, $CDCl_3$) δ 207.9, 140.9, 121.9, 96.8, 75.4, 75.2, 69.0, 63.8, 56.9, 56.3, 50.2, 42.5, 40.2, 39.9, 39.7, 37.0, 36.9, 36.4, 35.9, 35.8, 32.08, 32.05, 28.4, 28.24, 28.16, 27.8, 24.4, 23.9, 22.9, 22.7, 21.2, 19.5, 18.9, 17.6, 17.53, 17.45, 17.43, 17.35, 17.32, 17.26, 17.1, 13.5, 13.4, 12.6, 12.5, 12.0. **HRMS** (ESI) m/z: $[M+H]^+$ calcd for $C_{46}H_{83}O_6Si_2$ 787.5723; found 787.5717.

(6aR,8S,11aR)-8-(((3S,8S,9S,10R,13S,14S,17S)-17-acetyl-10,13-dimethyl-2,3,4,7,8,9,10,11,12,13,14,15,16,17-tetradecahydro-1H-cyclopenta[a]phenanthren-3-yl)oxy)-2,2,4,4-tetraisopropyltetrahydro-6H-oxepino[3,2-f][1,3,5,2,4]trioxadisilocin-11(8H)-one (3x)

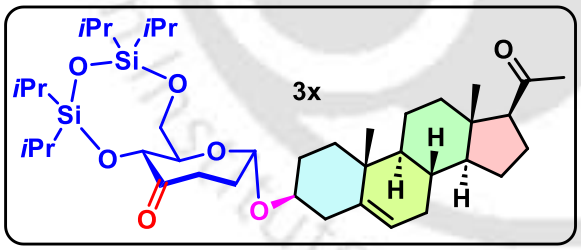

Compound **3x** was synthesized using the general procedure **1.3** (**A**). **3x** was obtained in 81% yield (145 mg), as a colorless oil, R_f = 0.5 (Hexane/EtOAc, 9:1, v/v), **[α]$^{25}_D$** = +63.0 (*c* 0.19, EtOAc). **^{1}H NMR** (600 MHz, $CDCl_3$) δ 5.33 (d, *J* = 4.9 Hz, 1H), 5.11 (dd, *J* = 8.0, 5.1 Hz, 1H), 4.39 (d, *J* = 9.4 Hz, 1H), 4.17 (d, *J* = 10.1 Hz, 1H), 3.90 (d, *J* = 9.4 Hz, 1H), 3.82 (dd, *J* = 11.6, 2.0 Hz, 1H), 3.66 (tt, *J* = 11.3, 4.4 Hz, 1H), 2.56 – 2.44 (m, 3H), 2.28 (t, *J* = 11.6 Hz, 1H), 2.19 (dd, *J* = 19.3, 8.5 Hz, 2H), 2.12 (s, 3H), 2.08 – 1.97 (m, 3H), 1.90 – 1.82 (m, 2H), 1.80 – 1.74 (m, 1H), 1.64 – 1.53 (m, 3H), 1.52 – 1.36 (m, 5H), 1.22 – 1.20 (m, 1H), 1.15 (dt, *J* = 11.5, 5.9 Hz, 1H), 1.11 – 1.03 (m, 28H), 0.99 (s, 3H), 0.85 (dt, *J* = 20.7, 5.5 Hz, 2H), 0.62 (s, 3H). **^{13}C NMR** (151 MHz, $CDCl_3$) δ 209.7, 207.9, 140.8, 121.5, 96.8, 75.13, 75.06, 68.9, 63.8, 63.7, 57.0, 50.0, 44.1, 40.1, 38.9, 36.99, 36.92, 35.8, 31.96, 31.90, 31.7, 28.2, 27.7, 24.6, 22.9, 21.2, 19.5, 17.54, 17.50, 17.43, 17.41, 17.33, 17.29, 17.23, 17.1, 13.5, 13.4, 13.3, 12.6, 12.4. **HRMS** (ESI) m/z: $[M+H]^+$ calcd for $C_{40}H_{69}O_7Si_2$ 717.4577; found 717.4566.

(6aR,8S,11aR)-2,2,4,4-tetraisopropyl-8-(((4S,5'R,6aR,6bS,8aS,8bR,9S,10R,11aS,12aS,12bS)-5',6a,8a,9-tetramethyl-1,3,3',4,4',5,5',6,6a,6b,6',7,8,8a,8b,9,11a,12,12a,12b-icosahydrospiro[naphtho[2',1':4,5]indeno[2,1-b]furan-10,2'-pyran]-4-yl)oxy)tetrahydro-6H-oxepino[3,2-f][1,3,5,2,4]trioxadisilocin-11(8H)-one (3y)

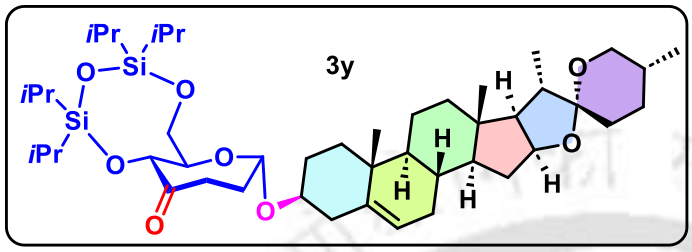

Compound **3y** was synthesized using the general procedure **1.3** (**A**). **3y** was obtained in 80% yield (163 mg), as a white foam, R_f = 0.5 (Hexane/EtOAc, 9:1, v/v), $[\alpha]^{25}_{D}$ = +3.5 (*c* 0.20, EtOAc). **^{1}H NMR** (600 MHz, $CDCl_3$) δ 5.32 (s, 1H), 5.11 (dd, *J* = 7.7, 5.2 Hz, 1H), 4.39 (d, *J* = 9.4 Hz, 2H), 4.16 (d, *J* = 10.9 Hz, 1H), 3.89 (d, *J* = 9.4 Hz, 1H), 3.82 (d, *J* = 11.6 Hz, 1H), 3.66 (dt, *J* = 11.3, 6.7 Hz, 1H), 3.46 (d, *J* = 9.3 Hz, 1H), 3.37 (t, *J* = 11.0 Hz, 1H), 2.49 (p, *J* = 12.0 Hz, 2H), 2.28 (t, *J* = 11.8 Hz, 1H), 2.17 (d, *J* = 10.1 Hz, 1H), 2.07 – 1.96 (m, 3H), 1.80 (ddt, *J* = 56.6, 24.6, 9.9 Hz, 7H), 1.65 – 1.36 (m, 11H), 1.29 (dd, *J* = 13.2, 6.4 Hz, 1H), 1.21 – 1.16 (m, 1H), 1.10 – 1.01 (m, 28H), 1.01 (s, 3H), 0.96 (d, *J* = 6.9 Hz, 4H), 0.78 (d, *J* = 5.5 Hz, 6H). **^{13}C NMR** (151 MHz, $CDCl_3$) δ 207.9, 140.9, 121.6, 109.4, 96.8, 80.9, 75.2, 75.1, 68.9, 66.9, 63.7, 62.2, 56.6, 50.1, 41.7, 40.4, 40.1, 39.9, 37.1, 36.9, 35.8, 32.2, 31.9, 31.6, 31.5, 30.4, 28.9, 28.2, 27.8, 20.9, 19.5, 17.54, 17.51, 17.44, 17.42, 17.34, 17.30, 17.27, 17.24, 17.1, 16.4, 14.7, 13.5, 13.4, 12.6, 12.4. **HRMS** (ESI) m/z: $[M+H]^+$ calcd for $C_{46}H_{79}O_8Si_2$ 815.5308; found 815.5308.

(1R,3S,7R,8R,8aS)-3,7-dimethyl-8-(2-((2R,4S)-6-oxo-4-(((6aR,8S,11aR)-2,2,4,4-tetraisopropyl-11-oxohexahydro-6H-oxepino[3,2-f][1,3,5,2,4]trioxadisilocin-8-yl)oxy)tetrahydro-2H-pyran-2-yl)ethyl)-1,2,3,7,8,8a-hexahydronaphthalen-1-yl 2,2-dimethylbutanoate (3z)

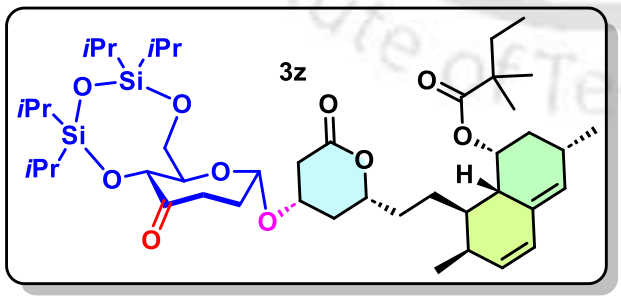

Compound **3z** was synthesized using the general procedure **1.3** (**B**). **3z** was obtained in 75% yield (154 mg), as a colorless oil, R_f = 0.3 (Hexane/EtOAc, 8:2, v/v), $[\alpha]^{25}_{D}$ = +123.5 (*c* 0.20, EtOAc). **^{1}H NMR** (600 MHz, $CDCl_3$) δ 5.98 (d, *J* = 9.6 Hz, 1H), 5.76 (dd, *J* = 9.4, 6.2 Hz, 1H), 5.50 (s, 1H), 5.35 (d, *J* = 2.9 Hz, 1H), 5.08 (dd, *J* = 8.1, 5.4 Hz, 1H), 4.54 – 4.44 (m, 2H), 4.41 (d, *J* = 9.7 Hz, 1H), 4.21 (d, *J* = 10.4 Hz, 1H), 3.86 – 3.77 (m, 2H), 2.67 (d, *J* = 17.3 Hz, 1H), 2.60 (dd, *J* = 17.7, 4.6 Hz, 1H), 2.53 (t, *J* = 12.1 Hz, 1H), 2.45 (dd, *J* = 12.5, 8.3 Hz, 2H), 2.38 – 2.32 (m, 1H), 2.24 (d, *J* = 9.8 Hz, 1H), 2.08 (dt, *J* = 13.5, 5.7 Hz, 1H), 1.95 – 1.88 (m, 3H), 1.85 (dd, *J* = 13.8, 6.5 Hz, 1H), 1.77 – 1.68 (m,

2H), 1.66 – 1.62 (m, 1H), 1.53 (ddt, *J* = 28.3, 13.7, 7.2 Hz, 3H), 1.46 – 1.38 (m, 1H), 1.34 (dd, *J* = 13.8, 10.0 Hz, 1H), 1.12 – 1.03 (m, 37H), 0.88 – 0.86 (m, 3H), 0.80 (t, *J* = 7.5 Hz, 3H). **^{13}C NMR** (151 MHz, $CDCl_3$) *δ* 207.2, 177.7, 169.6, 132.9, 131.6, 129.9, 128.5, 97.0, 76.9, 74.7, 69.2, 67.9, 65.6, 63.6, 43.1, 37.6, 36.8, 35.6, 34.9, 34.7, 33.2, 33.1, 32.9, 30.8, 27.7, 27.4, 24.98, 24.87, 24.2, 23.6, 17.49, 17.45, 17.40, 17.38, 17.29, 17.25, 17.20, 17.1, 14.0, 13.42, 13.36, 12.5, 12.4, 9.5. **HRMS** (ESI) m/z: $[M+H]^+$ calcd for $C_{44}H_{75}O_{10}Si_2$ 819.4894; found 819.4886.

methyl N-(((9H-fluoren-9-yl)methoxy)carbonyl)-O-((6aR,8S,11aR)-2,2,4,4-tetraisopropyl-11-oxohexahydro-6H-oxepino[3,2-f][1,3,5,2,4]trioxadisilocin-8-yl)-L-serinate (3za)

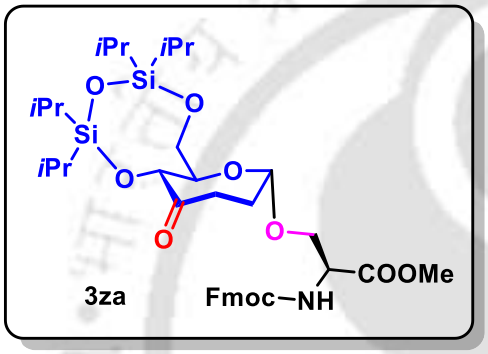

Compound **3za** was synthesized using the general procedure **1.3** (**A**). **3za** was obtained in 82% yield (152 mg), as a colorless oil, R_f = 0.2 (Hexane/EtOAc, 8:2, v/v), **$[\alpha]^{25}_D$** = +17.9 (*c* 0.17, EtOAc). **^{1}H NMR** (500 MHz, $CDCl_3$) *δ* 7.69 (d, *J* = 7.5 Hz, 2H), 7.52 (d, *J* = 7.6 Hz, 2H), 7.33 (t, *J* = 7.6 Hz, 2H), 7.24 (t, *J* = 7.7 Hz, 2H), 5.51 (d, *J* = 8.5 Hz, 1H), 4.89 (t, *J* = 6.8 Hz, 1H), 4.49 (d, *J* = 8.5 Hz, 1H), 4.34 (t, *J* = 9.9 Hz, 2H), 4.27 (t, *J* = 9.0 Hz, 1H), 4.16 (d, *J* = 7.3 Hz, 1H), 4.07 – 4.00 (m, 2H), 3.91 – 3.85 (m, 1H), 3.77 (dd, *J* = 19.2, 10.8 Hz, 2H), 3.70 (s, 3H), 2.47 – 2.35 (m, 2H), 1.99 (dd, *J* = 14.0, 6.9 Hz, 1H), 1.68 (dd, *J* = 12.8, 5.2 Hz, 1H), 0.99 – 0.93 (m, 28H). **^{13}C NMR** (126 MHz, $CDCl_3$) *δ* 207.3, 170.7, 156.0, 143.9, 143.8, 141.44, 141.42, 127.9, 127.3, 127.2, 125.2, 120.1, 100.5, 74.7, 69.3, 68.3, 67.5, 63.3, 54.3, 52.8, 47.2, 35.6, 27.3, 17.44, 17.40, 17.30, 17.26, 17.2, 17.1, 13.4, 13.3, 12.6, 12.5. **HRMS** (ESI) m/z: $[M+H]^+$ calcd for $C_{38}H_{56}NO_{10}Si_2$ 742.3438; found 742.3429.

methyl N-(((9H-fluoren-9-yl)methoxy)carbonyl)-O-((6aR,8S,11aR)-2,2,4,4-tetraisopropyl-11-oxohexahydro-6H-oxepino[3,2-f][1,3,5,2,4]trioxadisilocin-8-yl)-L-threoninate (3zb)

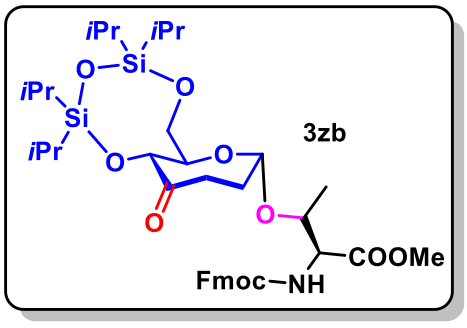

Compound **3zb** was synthesized using the general procedure **1.3** (**A**). **3zb** was obtained in 80% yield (151 mg), as a colorless oil, R_f = 0.2 (Hexane/EtOAc, 8:2, v/v), **$[\alpha]^{25}_D$** = +20.0 (*c* 0.20, EtOAc). **^{1}H NMR** (500 MHz, $CDCl_3$) *δ* 7.70 (d, *J* = 7.5 Hz, 2H), 7.54 (t, *J* = 7.6 Hz, 2H), 7.34 (dt, *J* = 10.6, 5.1 Hz, 2H), 7.25 (t, *J* = 7.8 Hz, 2H), 5.33 (d, *J* = 9.7 Hz, 1H), 4.84 (dd, *J* = 8.3, 5.3 Hz, 1H), 4.35 (dd, *J* = 13.2, 8.3 Hz, 3H), 4.18 (t, *J* = 7.2 Hz, 1H), 4.10 (d, *J* = 11.3 Hz, 1H), 3.81 –

3.77 (m, 2H), 3.68 (s, 3H), 2.37 (t, J = 5.9 Hz, 2H), 1.93 (dt, J = 16.3, 5.2 Hz, 1H), 1.70 (dt, J = 15.9, 8.1 Hz, 1H), 1.20 (d, J = 6.7 Hz, 3H), 1.04 – 0.98 (m, 28H). **^{13}C NMR** (126 MHz, $CDCl_3$) δ 207.4, 171.4, 156.7, 144.0, 143.8, 141.5, 127.9, 127.2, 125.2, 120.2, 120.1, 101.1, 75.1, 74.8, 69.7, 67.4, 63.6, 58.4, 52.6, 47.3, 35.5, 27.6, 19.2, 17.51, 17.48, 17.41, 17.39, 17.30, 17.29, 17.2, 17.1, 13.44, 13.40, 12.6, 12.4. **HRMS** (ESI) m/z: $[M+H]^+$ calcd for $C_{39}H_{58}NO_{10}Si_2$ 756.3594; found 756.3586.

(6aR,11aS)-8-(((3S,8S,9S,10R,13R,14S,17R)-10,13-dimethyl-17-((R)-6-methylheptan-2-yl)-2,3,4,7,8,9,10,11,12,13,14,15,16,17-tetradecahydro-1H-cyclopenta[a]phenanthren-3-yl)oxy)-2,2,4,4-tetraisopropyltetrahydro-6H-oxepino[3,2-f][1,3,5,2,4]trioxadisilocin-11(8H)-one (3zc)

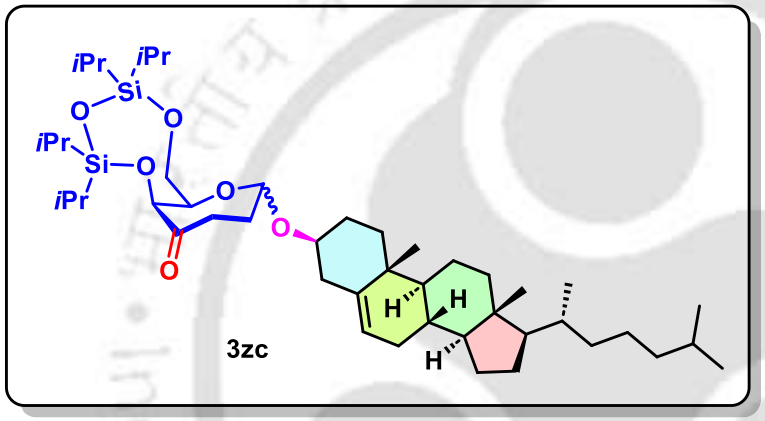

Compound **3zc** was synthesized using the general procedure **1.3** (**A**). **3zc** was obtained in 80% yield (157 mg), as a colorless oil, R_f = 0.8 (Hexane/EtOAc, 9:1, v/v), **$[\alpha]^{25}_D$** = +44.7 (*c* 0.15, EtOAc). **α/β = 2:1**. α-isomer: **^{1}H NMR** (600 MHz, $CDCl_3$) δ 5.36 (s, 1H), 5.15 – 5.10 (m, 1H), 4.37 (s, 1H), 4.11 (dd, J = 9.4, 6.2 Hz, 1H), 3.82 – 3.73 (m, 2H), 3.43 (dt, J = 11.1, 6.2 Hz, 1H), 2.73 – 2.67 (m, 1H), 2.56 (td, J = 13.8, 12.1, 4.0 Hz, 1H), 2.32 – 2.20 (m, 3H), 2.00 (d, J = 12.7 Hz, 2H), 1.88 – 1.81 (m, 3H), 1.78 (dd, J = 13.1, 6.7 Hz, 1H), 1.53 – 1.32 (m, 11H), 1.28 (s, 4H), 1.15 (dt, J = 12.2, 6.4 Hz, 3H), 1.12 – 1.03 (m, 28H), 0.99 (s, 4H), 0.91 (d, J = 6.4 Hz, 4H), 0.86 (dd, J = 6.6, 2.6 Hz, 7H), 0.67 (s, 3H). **^{13}C NMR** (151 MHz, $CDCl_3$) δ 208.9, 140.8, 121.9, 96.4, 77.0, 76.2, 68.0, 60.3, 56.9, 56.3, 50.3, 42.5, 39.9, 39.8, 39.7, 37.2, 36.9, 36.3, 35.9, 34.7, 32.1, 32.0, 29.6, 28.4, 28.2, 27.7, 24.4, 23.9, 22.9, 22.7, 21.2, 19.5, 18.9, 17.6, 17.5, 17.4, 17.34, 17.29, 17.26, 13.4, 12.8, 12.8, 12.0. **HRMS** (ESI) m/z: $[M+Na]^+$ calcd for $C_{46}H_{82}NaO_6Si_2$ 809.5543; found 809.5530.

(6aR,11aS)-2,2,4,4-tetraisopropyl-8-(((3aS,5aR,8aR,8bS)-2,2,7,7-tetramethyltetrahydro-3aH-bis([1,3]dioxolo)[4,5-b:4',5'-d]pyran-3a-yl)methoxy)tetrahydro-6H-oxepino[3,2-f][1,3,5,2,4]trioxadisilocin-11(8H)-one (3zd)

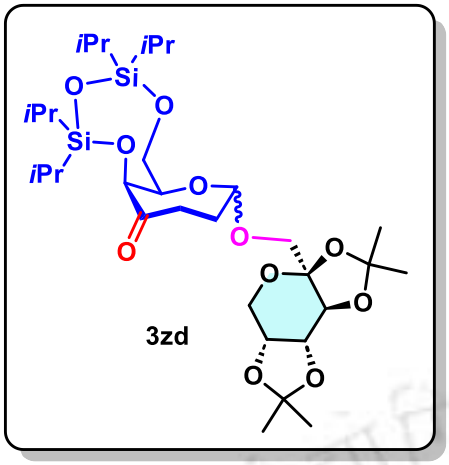

Compound **3zd** was synthesized using the general procedure **1.3** (**A**). **3zd** was obtained in 79% yield (130 mg), as a colorless oil, R_f = 0.6 (Hexane/EtOAc, 8:2, v/v), **[α]^{25}D** = +18.2 (*c* 0.15, EtOAc). **α/β = 1:1**. α-isomer: **^{1}H NMR** (600 MHz, $CDCl_3$) *δ* 4.98 (t, *J* = 4.4 Hz, 1H), 4.60 (dd, *J* = 7.9, 2.5 Hz, 1H), 4.38 – 4.32 (m, 2H), 4.27 (t, *J* = 7.8 Hz, 1H), 4.23 (d, *J* = 8.0 Hz, 1H), 3.92 (d, *J* = 11.6 Hz, 1H), 3.87 (d, *J* = 10.5 Hz, 1H), 3.84 – 3.79 (m, 2H), 3.74 (d, *J* = 13.0 Hz, 1H), 3.48 (d, *J* = 10.5 Hz, 1H), 2.68 (ddd, *J* = 12.3, 8.5, 3.5 Hz, 1H), 2.63 – 2.56 (m, 1H), 2.18 (td, *J* = 10.6, 5.1 Hz, 1H), 1.83 (dt, *J* = 13.8, 4.9 Hz, 1H), 1.54 (s, 3H), 1.46 (s, 3H), 1.41 (s, 3H), 1.34 (s, 3H), 1.11 – 0.99 (m, 28H). **^{13}C NMR** (151 MHz, $CDCl_3$) *δ* 208.4, 109.1, 108.9, 102.2, 99.9, 76.4, 71.1, 70.3, 70.0, 69.6, 67.8, 61.2, 60.1, 34.6, 29.9, 26.7, 26.1, 25.5, 24.2, 17.50, 17.45, 17.43, 17.41, 17.38, 17.33, 17.28, 17.2, 13.4, 13.3, 12.8, 12.7. **HRMS** (ESI) m/z: $[M+Na]^+$ calcd for $C_{31}H_{56}NaO_{11}Si_2$ 683.3254; found 683.3248.

(2R,3R,7S)-3-(benzyloxy)-2-((benzyloxy)methyl)-7-(((3aS,5aR,8aR,8bS)-2,2,7,7-tetramethyltetrahydro-3aH-bis([1,3]dioxolo)[4,5-b:4',5'-d]pyran-3a-yl)methoxy)oxepan-4-one (3ze)

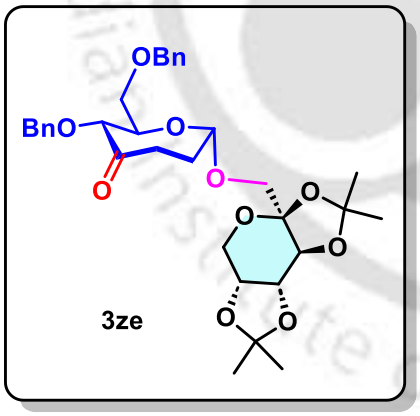

Compound **3ze** was synthesized using the general procedure **1.3** (**A**). **3ze** was obtained in 85% yield (127 mg), as a colorless oil, R_f = 0.6 (Hexane/EtOAc, 7:3, v/v), **[α]^{25}D** = +21.7 (*c* 0.18, CH_2Cl_2). **^{1}H NMR** (600 MHz, $CDCl_3$) *δ* 7.25 – 7.17 (m, 10H), 4.89 (dd, *J* = 8.0, 4.5 Hz, 1H), 4.58 – 4.51 (m, 3H), 4.44 (t, *J* = 12.4 Hz, 1H), 4.34 (d, *J* = 11.3 Hz, 1H), 4.27 (d, *J* = 2.3 Hz, 1H), 4.20 – 4.15 (m, 2H), 3.94 (d, *J* = 7.2 Hz, 1H), 3.89 (d, *J* = 10.5 Hz, 1H), 3.83 (d, *J* = 12.0 Hz, 1H), 3.67 (d, *J* = 12.9 Hz, 1H), 3.60 (dd, *J* = 10.1, 4.3 Hz, 1H), 3.50 (dd, *J* = 10.1, 3.7 Hz, 1H), 3.45 (d, *J* = 10.5 Hz, 1H), 2.55 – 2.48 (m, 1H), 2.41 – 2.33 (m, 1H), 2.26 – 2.20 (m, 1H), 2.04 – 1.98 (m, 1H), 1.45 (s, 3H), 1.40 (s, 3H), 1.31 (s, 3H), 1.27 (s, 3H). **^{13}C NMR** (151 MHz, $CDCl_3$) *δ* 208.6, 138.1, 137.5, 128.5, 128.1, 128.0, 127.9, 127.7, 109.1, 108.7, 102.4, 100.7, 84.4, 73.6, 73.2, 71.1, 70.6, 70.3, 70.2, 69.3, 68.7, 61.2, 35.8, 28.2, 26.7, 26.1, 25.5, 24.2. **HRMS** (ESI) m/z: $[M+NH_4]^+$ calcd for $C_{33}H_{46}NO_{10}$ 616.3117; found 616.3107.

(2R,3S)-3-(benzyloxy)-2-((benzyloxy)methyl)-7-(((3aS,5aR,8aR,8bS)-2,2,7,7-tetramethyltetrahydro-3aH-bis([1,3]dioxolo)[4,5-b:4',5'-d]pyran-3a-yl)methoxy)oxepan-4-one (3zf)

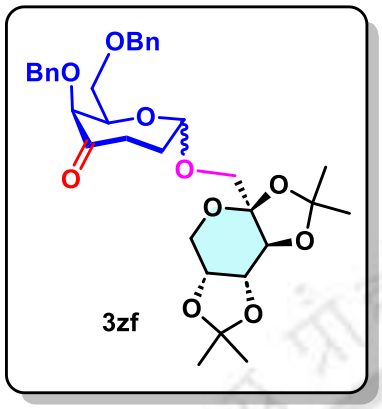

Compound **3zf** was synthesized using the general procedure **1.3** (**A**). **3zf** was obtained in 82% yield (123 mg), as a colorless oil, R_f = 0.6 (Hexane/EtOAc, 7:3, v/v), **$[\alpha]^{25}_D$** = -15.3 (*c* 0.31, CH_2Cl_2). **α/β = 2:1**. α-isomer: **^{1}H NMR** (600 MHz, $CDCl_3$) δ 7.25 – 7.14 (m, 11H), 4.97 – 4.93 (m, 1H), 4.59 (d, *J* = 11.7 Hz, 1H), 4.52 (dd, *J* = 7.8, 2.4 Hz, 1H), 4.36 (dd, *J* = 24.6, 11.8 Hz, 2H), 4.29 – 4.24 (m, 2H), 4.17 – 4.13 (m, 2H), 3.88 (d, *J* = 8.8 Hz, 2H), 3.84 (d, *J* = 12.1 Hz, 1H), 3.66 (d, *J* = 13.0 Hz, 1H), 3.58 – 3.52 (m, 2H), 3.44 (d, *J* = 10.6 Hz, 1H), 2.64 (t, *J* = 10.9 Hz, 1H), 2.39 – 2.33 (m, 1H), 2.24 – 2.18 (m, 1H), 1.71 (dt, *J* = 15.1, 7.5 Hz, 1H), 1.44 (s, 3H), 1.39 (s, 3H), 1.29 (s, 3H), 1.27 (s, 3H). **^{13}C NMR** (151 MHz, $CDCl_3$) δ 209.2, 138.1, 137.2, 128.7, 128.53, 128.45, 128.2, 127.8, 127.7, 109.1, 108.7, 102.3, 100.2, 82.6, 73.3, 73.2, 71.1, 70.3, 70.1, 69.3, 68.6, 66.2, 61.2, 34.9, 28.7, 26.7, 26.1, 25.5, 24.1. **HRMS** (ESI) m/z: $[M+NH_4]^+$ calcd for $C_{33}H_{46}NO_{10}$ 616.3117; found 616.3106.

(2R,3R)-3-(benzyloxy)-2-methyl-7-(((3aS,5aR,8aR,8bS)-2,2,7,7-tetramethyltetrahydro-3aH-bis([1,3]dioxolo)[4,5-b:4',5'-d]pyran-3a-yl)methoxy)oxepan-4-one (3zg)

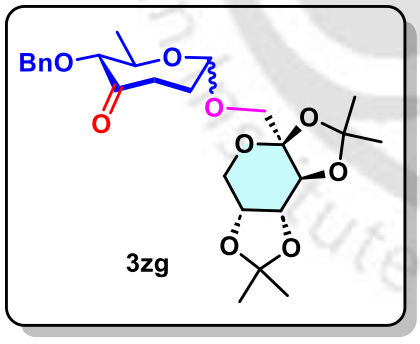

Compound **3zg** was synthesized using the general procedure **1.3** (**A**). **3zg** was obtained in 84% yield (103 mg), as a colorless oil, R_f = 0.6 (Hexane/EtOAc, 7:3, v/v), **$[\alpha]^{25}_D$** = -44.2 (*c* 0.10, CH_2Cl_2). **α/β = 6:1**. α-isomer: **^{1}H NMR** (600 MHz, $CDCl_3$) δ 7.37 – 7.30 (m, 5H), 4.90 (dd, *J* = 8.0, 4.5 Hz, 1H), 4.69 (d, *J* = 11.5 Hz, 1H), 4.59 (dd, *J* = 7.8, 2.4 Hz, 1H), 4.42 (d, *J* = 11.5 Hz, 1H), 4.36 (d, *J* = 2.4 Hz, 1H), 4.23 (d, *J* = 8.0 Hz, 1H), 4.13 (p, *J* = 6.5 Hz, 1H), 3.90 (d, *J* = 13.0 Hz, 1H), 3.74 (dd, *J* = 23.1, 11.8 Hz, 2H), 3.65 – 3.59 (m, 2H), 2.55 (ddd, *J* = 14.9, 6.8, 3.0 Hz, 1H), 2.46 – 2.39 (m, 1H), 2.28 – 2.20 (m, 1H), 2.09 – 2.01 (m, 1H), 1.53 (s, 3H), 1.45 (s, 3H), 1.38 (s, 3H), 1.33 (s, 3H), 1.29 (d, *J* = 6.4 Hz, 3H). **^{13}C NMR** (151 MHz, $CDCl_3$) δ 208.7, 137.5, 128.6, 128.3, 128.2, 109.1, 108.7, 102.6, 100.6, 88.9, 73.2, 71.1, 70.2, 70.1, 68.7, 65.9, 61.2, 35.9, 28.1, 26.7, 26.0, 25.6, 24.1, 20.4. **HRMS** (ESI) m/z: $[M+NH_4]^+$ calcd for $C_{26}H_{40}NO_9$ 510.2698; found 510.2690.

(6aR,11aR)-2,2,4,4-tetraisopropyl-8-(4-methoxyphenoxy)tetrahydro-6H-oxepino[3,2-f][1,3,5,2,4]trioxadisilocin-11(8H)-one (5a)

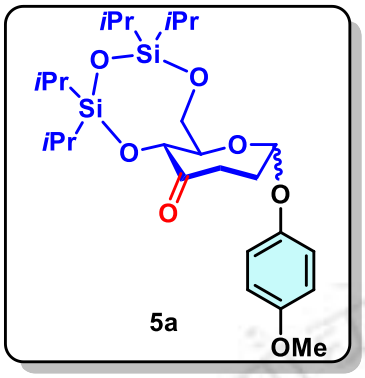

Compound **5a** was synthesized using the general procedure **1.3** (**B**). **5a** was obtained in 82% yield (108 mg), as a colorless oil, R_f = 0.6 (Hexane/EtOAc, 8:2, v/v), **[α]$^{25}_D$** = +36.3 (*c* 0.16, EtOAc). **α/β = 6:1**. α-isomer: **^{1}H NMR** (400 MHz, $CDCl_3$) δ 7.06 – 6.98 (m, 2H), 6.91 – 6.77 (m, 2H), 5.59 (dd, *J* = 7.6, 5.1 Hz, 1H), 4.45 (d, *J* = 9.5 Hz, 1H), 4.04 (dd, *J* = 11.6, 2.1 Hz, 1H), 4.01 – 3.95 (m, 1H), 3.77 (d, *J* = 1.9 Hz, 3H), 3.70 (dd, *J* = 11.6, 2.3 Hz, 1H), 2.67 – 2.54 (m, 2H), 2.32 – 2.24 (m, 1H), 2.15 – 2.03 (m, 1H), 1.10 – 1.00 (m, 28H). **^{13}C NMR** (101 MHz, $CDCl_3$) δ 207.7, 154.9, 150.8, 117.8, 114.7, 98.6, 74.9, 69.8, 63.3, 55.8, 35.6, 27.9, 17.48, 17.46, 17.44, 17.40, 17.34, 17.28, 17.2, 17.1, 13.5, 13.3, 12.7, 12.4. **HRMS** (ESI) m/z: $[M+H]^+$ calcd for $C_{26}H_{45}O_7Si_2$ 525.2699; found 525.2700.

(6aR,11aR)-8-(2,4-dimethylphenoxy)-2,2,4,4-tetraisopropyltetrahydro-6H-oxepino[3,2-f][1,3,5,2,4]trioxadisilocin-11(8H)-one (5b)

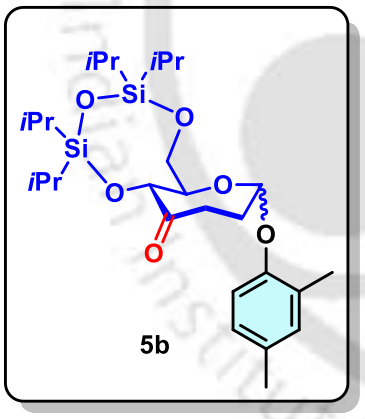

Compound **5b** was synthesized using the general procedure **1.3** (**B**). **5b** was obtained in 76% yield (99 mg), as a colorless oil, R_f = 0.8 (Hexane/EtOAc, 9:1, v/v), **[α]$^{25}_D$** = +55.8 (*c* 0.21, EtOAc). **α/β = 7:1**. α-isomer: **^{1}H NMR** (400 MHz, $CDCl_3$) δ 7.13 (d, *J* = 8.4 Hz, 1H), 6.95 (d, *J* = 7.4 Hz, 2H), 5.66 (dd, *J* = 7.3, 4.8 Hz, 1H), 4.50 (d, *J* = 9.5 Hz, 1H), 4.04 (dd, *J* = 11.6, 2.1 Hz, 1H), 3.94 (t, *J* = 9.9 Hz, 1H), 3.72 (dd, *J* = 11.6, 2.3 Hz, 1H), 2.72 – 2.55 (m, 2H), 2.26 (s, 4H), 2.18 (d, *J* = 2.6 Hz, 1H), 2.15 (s, 3H), 1.12 – 1.00 (m, 28H). **^{13}C NMR** (101 MHz, $CDCl_3$) δ 207.8, 152.8, 131.6, 131.2, 127.4, 126.9, 114.2, 97.7, 75.0, 69.9, 63.4, 35.6, 28.2, 20.6, 17.48, 17.45, 17.41, 17.35, 17.3, 17.2, 17.1, 16.3, 13.5, 13.3, 12.7, 12.4. **HRMS** (ESI) m/z: $[M+H]^+$ calcd for $C_{27}H_{47}O_6Si_2$ 523.2906; found 523.2888.

(6aR,11aR)-2,2,4,4-tetraisopropyl-8-(4-(tert-pentyl)phenoxy)tetrahydro-6H-oxepino[3,2-f][1,3,5,2,4]trioxadisilocin-11(8H)-one (5c)

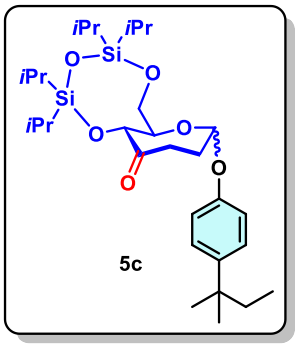

Compound **5c** was synthesized using the general procedure **1.3** (**B**). **5c** was obtained in 81% yield (114 mg), as a colorless oil, R_f = 0.8 (Hexane/EtOAc, 9:1, v/v), **[α]^{25}D** = +82.0 (*c* 0.23, EtOAc). **α/β = 5:1**. α-isomer: **^{1}H NMR** (400 MHz, $CDCl_3$) *δ* 7.24 (dq, *J* = 8.1, 3.1 Hz, 2H), 7.02 (d, *J* = 8.9 Hz, 2H), 5.66 (dd, *J* = 7.6, 5.1 Hz, 1H), 4.46 (d, *J* = 9.4 Hz, 1H), 4.07 – 3.95 (m, 2H), 3.70 (dd, *J* = 11.6, 2.2 Hz, 1H), 2.68 – 2.55 (m, 2H), 2.32 – 2.20 (m, 1H), 2.16 – 2.06 (m, 1H), 1.67 – 1.56 (m, 3H), 1.26 (d, *J* = 3.1 Hz, 5H), 1.14 – 0.94 (m, 28H), 0.66 (td, *J* = 7.4, 3.9 Hz, 3H). **^{13}C NMR** (101 MHz, $CDCl_3$) *δ* 207.8, 154.5, 143.4, 127.1, 116.2, 98.2, 74.9, 69.8, 63.4, 37.5, 37.1, 35.6, 28.7, 28.1, 17.47, 17.45, 17.40, 17.36, 17.28, 17.2, 17.1, 13.5, 13.3, 12.7, 12.4. **HRMS** (ESI) m/z: $[M+H]^+$ calcd for $C_{30}H_{53}O_6Si_2$ 565.3376; found 565.3360.

(6aR,11aR)-8-(4-(tert-butyl)phenoxy)-2,2,4,4-tetraisopropyltetrahydro-6H-oxepino[3,2-f][1,3,5,2,4]trioxadisilocin-11(8H)-one (5d)

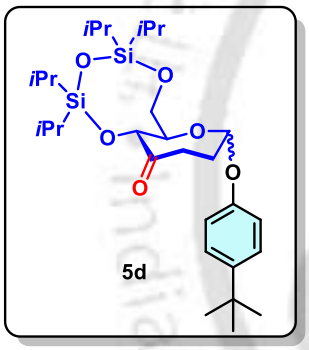

Compound **5d** was synthesized using the general procedure **1.3** (**B**). **5d** was obtained in 83% yield (114 mg), as a colorless oil, R_f = 0.8 (Hexane/EtOAc, 9:1, v/v), **[α]^{25}D** = +47.9 (*c* 0.28, EtOAc). **α/β = 8:1**. α-isomer: **^{1}H NMR** (400 MHz, $CDCl_3$) *δ* 7.30 (td, *J* = 6.0, 5.6, 2.4 Hz, 2H), 7.09 – 6.98 (m, 2H), 5.65 (dd, *J* = 7.5, 4.9 Hz, 1H), 4.47 (d, *J* = 9.5 Hz, 1H), 4.02 (ddd, *J* = 17.6, 10.5, 2.2 Hz, 2H), 3.73 (dd, *J* = 11.6, 2.2 Hz, 1H), 2.67 – 2.55 (m, 2H), 2.30 – 2.20 (m, 1H), 2.18 – 2.07 (m, 1H), 1.30 (d, *J* = 3.4 Hz, 9H), 1.12 – 1.00 (m, 28H). **^{13}C NMR** (126 MHz, $CDCl_3$) *δ* 207.7, 154.7, 145.2, 126.5, 116.3, 98.3, 75.1, 69.9, 63.5, 35.6, 34.3, 31.6, 28.1, 17.49, 17.46, 17.40, 17.37, 17.3, 17.2, 17.1, 13.5, 13.4, 12.8, 12.4. **HRMS** (ESI) m/z: $[M+H]^+$ calcd for $C_{29}H_{51}O_6Si_2$ 551.3219; found 551.3209.

(6aR,11aR)-8-(4-allyl-2-methoxyphenoxy)-2,2,4,4-tetraisopropyltetrahydro-6H-oxepino[3,2-f][1,3,5,2,4]trioxadisilocin-11(8H)-one (5e)

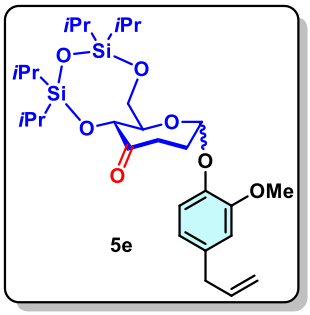

Compound **5e** was synthesized using the general procedure **1.3** (**B**). **5e** was obtained in 75% yield (106 mg), as a colorless oil, R_f = 0.4 (Hexane/EtOAc, 8:2, v/v), **[α]^{25}D** = +52.7 (*c* 0.18, EtOAc). **α/β = 6:1**. α-isomer: **^{1}H NMR** (400 MHz, $CDCl_3$) *δ* 7.06 (d, *J* = 7.9 Hz, 1H), 6.72 (d, *J* = 8.1 Hz, 2H), 5.95 (ddt, *J* = 16.9, 10.1, 6.7 Hz, 1H), 5.63 (dd, *J* = 8.1, 5.3 Hz, 1H), 5.12 – 5.05 (m, 2H), 4.43 (d, *J* = 9.5 Hz, 1H), 4.16 – 4.06 (m, 2H), 3.83 – 3.74 (m, 4H), 3.34 (d, *J* = 6.6 Hz, 2H), 2.65 – 2.55 (m, 2H), 2.41 – 2.31 (m, 1H), 2.18 – 2.08 (m, 1H), 1.09 – 1.02 (m, 28H). **^{13}C NMR** (101

MHz, $CDCl_3$) δ 207.7, 150.6, 144.1, 137.6, 135.6, 120.9, 119.2, 115.9, 112.7, 99.9, 74.9, 69.8, 63.4, 55.9, 40.1, 35.7, 29.8, 27.8, 17.49, 17.46, 17.42, 17.3, 17.2, 17.1, 13.5, 13.3, 12.6, 12.4. **HRMS** (ESI) m/z: $[M+NH_4]^+$ calcd for $C_{29}H_{52}NO_7Si_2$ 582.3277; found 582.3276.

(6aR,11aR)-2,2,4,4-tetraisopropyl-8-(((R)-2,5,7,8-tetramethyl-2-((4R,8R)-4,8,12-trimethyltridecyl)chroman-6-yl)oxy)tetrahydro-6H-oxepino[3,2-f][1,3,5,2,4]trioxadisilocin-11(8H)-one (5f)

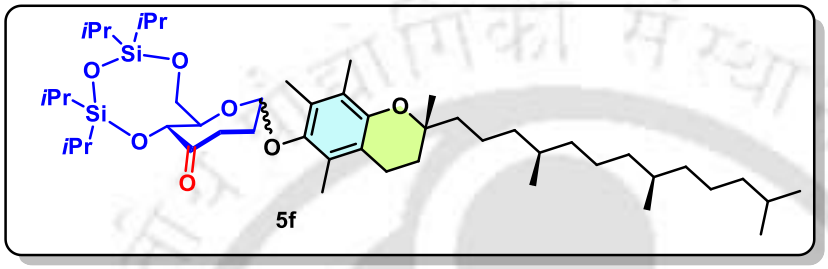

Compound **5f** was synthesized using the general procedure **1.3** (**B**). **5f** was obtained in 45% yield (93 mg), as a colorless oil, R_f = 0.8 (Hexane/EtOAc, 9:1, v/v), **[α]$^{25}_D$** = +9.4 (*c* 0.13, CH_2Cl_2). **α/β = 2.5:1**. **^{1}H NMR** (600 MHz, $CDCl_3$) δ 5.28 – 5.21 (m, 1H), 4.46 (d, *J* = 8.5 Hz, 1H), 4.18 (dd, *J* = 22.1, 9.9 Hz, 2H), 3.91 (s, 1H), 2.65 – 2.47 (m, 5H), 2.37 (d, *J* = 15.6 Hz, 1H), 2.26 – 2.20 (m, 1H), 2.14 (s, 4H), 2.10 (s, 4H), 2.07 (d, *J* = 7.9 Hz, 4H), 1.85 – 1.73 (m, 3H), 1.56 – 1.49 (m, 3H), 1.37 (s, 3H), 1.11 – 1.04 (m, 33H), 0.87 – 0.84 (m, 12H). **^{13}C NMR** (151 MHz, $CDCl_3$) δ 207.6, 148.1, 146.6, 146.4, 127.4, 125.4, 123.2, 117.8, 103.4, 80.6, 75.8, 74.9, 71.9, 63.9, 39.5, 37.61, 37.56, 37.5, 37.4, 35.8, 32.94, 32.93, 32.87, 32.85, 28.1, 24.97, 24.95, 24.6, 22.9, 22.8, 19.9, 19.8, 17.5, 17.43, 17.40, 17.3, 17.2, 17.1, 14.2, 13.5, 13.4, 13.3, 12.7, 12.5, 12.0. **HRMS** (ESI) m/z: $[M+H]^+$ calcd for $C_{48}H_{87}O_7Si_2$ 831.5985; found 831.5962.

(6aR,11aR)-8-(benzo[d][1,3]dioxol-4-yloxy)-2,2,4,4-tetraisopropyltetrahydro-6H-oxepino[3,2-f][1,3,5,2,4]trioxadisilocin-11(8H)-one (5g)

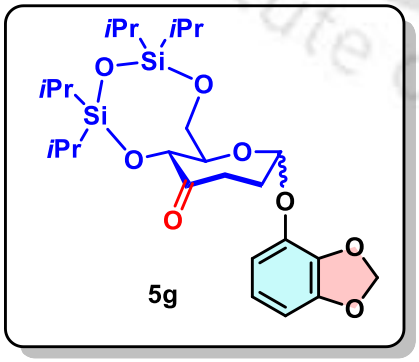

Compound **5g** was synthesized using the general procedure **1.3** (**B**). **5g** was obtained in 73% yield (98 mg), as a colorless oil, R_f = 0.5 (Hexane/EtOAc, 9:1, v/v), **[α]$^{25}_D$** = +27.9 (*c* 0.17, CH_2Cl_2). **α/β = 4:1**. α-isomer: **^{1}H NMR** (400 MHz, $CDCl_3$) δ 6.70 (dd, *J* = 8.4, 6.2 Hz, 1H), 6.65 (d, *J* = 2.6 Hz, 1H), 6.58 – 6.52 (m, 1H), 5.96 – 5.90 (m, 2H), 5.56 (dd, *J* = 7.7, 5.2 Hz, 1H), 4.45 (d, *J* = 9.5 Hz, 1H), 4.05 (dd, *J* = 11.6, 2.2 Hz, 1H), 3.99 – 3.93 (m, 1H), 3.73 (dd, *J* = 11.6, 2.6 Hz, 1H), 2.65 – 2.54 (m, 2H), 2.30 – 2.22 (m, 1H), 2.13 – 2.03 (m, 1H), 1.11 – 1.01 (m, 28H). **^{13}C NMR** (126 MHz, $CDCl_3$) δ 207.5, 152.1, 148.3, 142.9, 108.9, 108.2, 101.4, 99.9, 98.9, 75.1, 69.9, 63.4, 35.6, 27.9, 17.5, 17.44, 17.40, 17.35, 17.3, 17.2, 17.1, 13.5,

13.4, 12.7, 12.4. **HRMS** (ESI) m/z: $[M+H]^+$ calcd for $C_{26}H_{43}NO_8Si_2$ 539.2491; found 539.2483.

(6aR,11aR)-2,2,4,4-tetraisopropyl-8-(octylthio)tetrahydro-6H-oxepino[3,2-f][1,3,5,2,4]trioxadisilocin-11(8H)-one (5h)

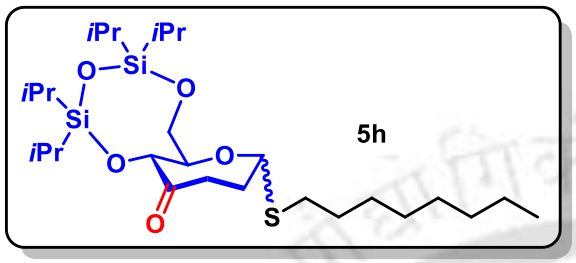

Compound **5h** was synthesized using the general procedure **1.3** (**A**). **5h** was obtained in 78% yield (107 mg), as a colorless oil, R_f = 0.8 (Hexane/EtOAc, 9:1, v/v), **$[\alpha]^{25}_D$** = +30.0 (*c* 0.10, EtOAc). **α/β = 1:1.28**. **^{1}H NMR** (600 MHz, $CDCl_3$) δ 5.28 (dd, *J* = 10.5, 5.6 Hz, 1H), 4.58 (dd, *J* = 9.4, 5.9 Hz, 2.H), 4.48 (d, *J* = 9.4 Hz, 1H), 4.16 – 4.09 (m, 2.H), 4.02 (d, *J* = 11.2 Hz, 2.H), 3.79 (dd, *J* = 11.6, 2.5 Hz, 1H), 3.28 (d, *J* = 8.8 Hz, 1.H), 2.76 – 2.63 (m, 4H), 2.58 (tt, *J* = 15.6, 7.2 Hz, 4H), 2.49 (dd, *J* = 13.2, 7.3 Hz, 1H), 2.21 (dt, *J* = 13.4, 5.7 Hz, 1H), 2.11 (ddt, *J* = 14.1, 9.7, 5.2 Hz, 1H), 1.94 – 1.88 (m, 1H), 1.82 – 1.76 (m, 1H), 1.59 (dq, *J* = 14.7, 7.2 Hz, 4H), 1.41 – 1.32 (m, 5H), 1.29 – 1.24 (m, 18H), 1.11 – 0.98 (m, 63H), 0.87 (t, *J* = 6.9 Hz, 8H). **^{13}C NMR** (151 MHz, $CDCl_3$) δ 208.9, 207.8, 86.7, 83.8, 83.5, 75.9, 75.1, 70.3, 64.0, 63.2, 37.5, 37.0, 31.9, 31.1, 30.8, 30.5, 30.0, 29.6, 29.34, 29.30, 29.1, 29.0, 28.6, 22.8, 17.52, 17.51, 17.45, 17.41, 17.39, 17.34, 17.32, 17.31, 17.25, 17.22, 17.21, 17.14, 17.13, 17.07, 14.2, 13.53, 13.47, 13.39, 13.37, 12.73, 12.70, 12.40, 12.38. **HRMS** (ESI) m/z: $[M+H]^+$ calcd for $C_{27}H_{55}O_5SSi_2$ 547.3304; found 547.3291.

(6aR,11aR)-8-(tert-butylthio)-2,2,4,4-tetraisopropyltetrahydro-6H-oxepino[3,2-f][1,3,5,2,4]trioxadisilocin-11(8H)-one (5i)

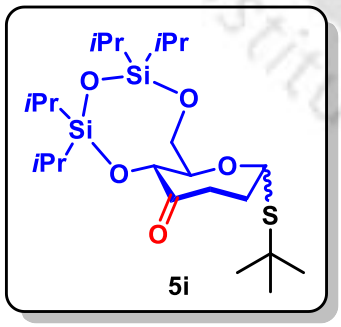

Compound **5i** was synthesized using the general procedure **1.3** (**A**). **5i** was obtained in 75% yield (92 mg), as a colorless oil, R_f = 0.8 (Hexane/EtOAc, 9:1, v/v), **$[\alpha]^{25}_D$** = +54.4 (*c* 0.07, EtOAc). **α/β = 1:1**. **^{1}H NMR** (600 MHz, $CDCl_3$) δ 5.45 (dd, *J* = 10.7, 5.2 Hz, 1H), 4.72 (dd, *J* = 10.3, 4.8 Hz, 1H), 4.61 (d, *J* = 8.8 Hz, 1H), 4.46 (d, *J* = 8.4 Hz, 1H), 4.10 (td, *J* = 11.4, 2.4 Hz, 2H), 4.03 – 3.97 (m, 2H), 3.81 (dd, *J* = 11.5, 3.7 Hz, 1H), 3.36 (d, *J* = 8.8 Hz, 1H), 2.75 – 2.67 (m, 1H), 2.62 – 2.50 (m, 3H), 2.20 – 2.14 (m, 1H), 2.08 (ddt, *J* = 14.5, 10.1, 5.4 Hz, 1H), 2.03 – 1.97 (m, 1H), 1.92 (dt, *J* = 14.3, 8.1 Hz, 1H), 1.37 (d, *J* = 16.7 Hz, 18H), 1.11 – 0.97 (m, 56H). **^{13}C NMR** (151 MHz, $CDCl_3$) δ 208.9, 207.9, 84.7, 82.9, 81.6, 75.99, 75.95, 71.4, 63.7, 63.3, 44.1, 44.0, 37.8, 36.9, 31.9, 31.7, 30.6, 29.2, 17.60, 17.56, 17.50, 17.45, 17.44, 17.42, 17.40, 17.34, 17.32, 17.29, 17.26, 17.22, 17.20, 17.18, 17.14, 17.06, 13.53, 13.45,

13.4, 12.9, 12.7, 12.42, 12.36. **HRMS** (ESI) m/z: $[M+H]^+$ calcd for $C_{23}H_{47}O_5SSi_2$ 491.2678; found 491.2675.

(6aR,11aR)-2,2,4,4-tetraisopropyl-8-(phenylthio)tetrahydro-6H-oxepino[3,2-f][1,3,5,2,4]trioxadisilocin-11(8H)-one (5j)

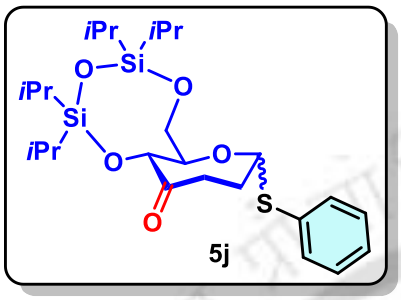

Compound **5j** was synthesized using the general procedure **1.3** (**A**). **5j** was obtained in 80% yield (102 mg), as a colorless oil, R_f = 0.7 (Hexane/EtOAc, 9:1, v/v), **$[\alpha]^{25}_D$** = +55.6 (*c* 0.14, CH_2Cl_2). **α/β = 2.5:1**. α-isomer: **^{1}H NMR** (600 MHz, $CDCl_3$) δ 7.43 (t, *J* = 7.7 Hz, 2H), 7.26 – 7.21 (m, 2H), 7.20 – 7.16 (m, 1H), 5.55 (dd, *J* = 10.6, 5.5 Hz, 1H), 4.44 (d, *J* = 8.8 Hz, 1H), 4.08 – 3.98 (m, 2H), 3.69 (dd, *J* = 11.6, 2.9 Hz, 1H), 2.66 – 2.55 (m, 1H), 2.50 (dd, *J* = 12.3, 7.4 Hz, 1H), 2.29 (dt, *J* = 12.7, 5.2 Hz, 1H), 2.01 – 1.93 (m, 1H), 1.06 – 0.90 (m, 28H). **^{13}C NMR** (151 MHz, $CDCl_3$) δ 207.5, 133.4, 131.0, 129.2, 127.3, 86.7, 75.4, 71.4, 63.7, 37.5, 28.7, 17.53, 17.51, 17.43, 17.36, 17.32, 17.2, 17.14, 13.5, 13.4, 12.8, 12.4. **HRMS** (ESI) m/z: $[M+H]^+$ calcd for $C_{25}H_{43}O_5SSi_2$ 511.2365; found 511.2352.

(6aR,11aR)-2,2,4,4-tetraisopropyl-8-((4-methoxyphenyl)thio)tetrahydro-6H-oxepino[3,2-f][1,3,5,2,4]trioxadisilocin-11(8H)-one (5k)

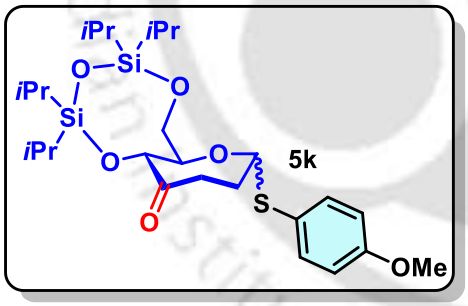

Compound **5k** was synthesized using the general procedure **1.3** (**A**). **5k** was obtained in 81% yield (109 mg), as a colorless oil, R_f = 0.5 (Hexane/EtOAc, 9:1, v/v), **$[\alpha]^{25}_D$** = +74.1 (*c* 0.12, EtOAc). **α/β = 7:1**. α-isomer: **^{1}H NMR** (500 MHz, $CDCl_3$) δ 7.42 (d, *J* = 7.8 Hz, 2H), 6.85 (d, *J* = 7.8 Hz, 2H), 5.49 – 5.42 (m, 1H), 4.49 (d, *J* = 8.4 Hz, 1H), 4.12 (d, *J* = 10.0 Hz, 2H), 3.80 (s, 4H), 2.70 – 2.53 (m, 2H), 2.33 (d, J = 16.3 Hz, 1H), 2.07 – 1.99 (m, 1H), 1.10 – 1.01 (m, 28H). **^{13}C NMR** (126 MHz, $CDCl_3$) δ 207.5, 159.8, 134.3, 124.6, 114.8, 87.9, 75.5, 71.4, 63.9, 55.5, 37.5, 28.7, 17.6, 17.5, 17.44, 17.36, 17.34, 17.23, 17.15, 13.5, 13.4, 12.8, 12.4. **HRMS** (ESI) m/z: $[M+H]^+$ calcd for $C_{26}H_{45}O_6SSi_2$ 541.2470; found 541.2459.

(6aR,11aR)-8-((2,6-dimethylphenyl)thio)-2,2,4,4-tetraisopropyltetrahydro-6H-oxepino[3,2-f][1,3,5,2,4]trioxadisilocin-11(8H)-one (5l)

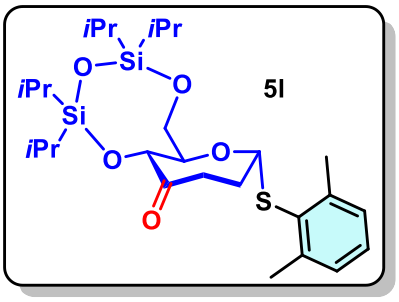

Compound **5l** was synthesized using the general procedure **1.3** (**A**). **5l** was obtained in 74% yield (99 mg), as a colorless oil, R_f = 0.7 (Hexane/EtOAc, 9:1, v/v), **[α]^{25}D** = +71.4 (*c* 0.08, CH_2Cl_2). **^{1}H NMR** (600 MHz, $CDCl_3$) *δ* 7.15 – 7.07 (m, 3H), 5.34 (dd, *J* = 10.6, 5.4 Hz, 1H), 4.48 (d, *J* = 8.6 Hz, 1H), 4.16 – 4.06 (m, 2H), 3.79 (dd, *J* = 11.3, 2.8 Hz, 1H), 2.58 (t, *J* = 5.1 Hz, 2H), 2.51 (s, 6H), 2.37 – 2.30 (m, 1H), 2.14 (ddd, *J* = 17.1, 10.7, 6.0 Hz, 1H), 1.13 – 0.97 (m, 28H). **^{13}C NMR** (151 MHz, $CDCl_3$) *δ* 207.6, 142.9, 131.9, 128.7, 128.4, 87.3, 75.5, 72.6, 63.8, 37.5, 22.4, 17.50, 17.48, 17.40, 17.37, 17.34, 17.30, 17.2, 17.1, 13.5, 13.4, 12.6, 12.4. **HRMS** (ESI) m/z: $[M+H]^+$ calcd for $C_{27}H_{47}O_5SSi_2$ 539.2678; found 539.2684.

(6aR,8R,11aR)-2,2,4,4-tetraisopropyl-11-oxohexahydro-6H-oxepino[3,2-f][1,3,5,2,4]trioxadisilocin-8-yl dodecanoate (7a)

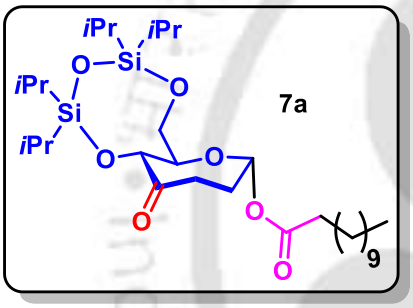

Compound **7a** was synthesized using the general procedure **1.4**. **7a** was obtained in 85% yield (128 mg), as a colorless oil, R_f = 0.7 (Hexane/EtOAc, 9:1, v/v), **[α]^{25}D** = +35.6 (*c* 0.16, EtOAc). **^{1}H NMR** (400 MHz, $CDCl_3$) *δ* 6.24 (dd, *J* = 8.9, 5.6 Hz, 1H), 4.41 (d, *J* = 9.5 Hz, 1H), 4.14 (dd, *J* = 11.6, 1.6 Hz, 1H), 3.94 – 3.84 (m, 2H), 2.63 – 2.47 (m, 2H), 2.32 – 2.20 (m, 3H), 1.93 – 1.82 (m, 1H), 1.64 – 1.56 (m, 2H), 1.26 (d, *J* = 9.9 Hz, 16H), 1.10 – 1.03 (m, 28H), 0.87 (t, *J* = 6.9 Hz, 3H). **^{13}C NMR** (101 MHz, $CDCl_3$) *δ* 206.8, 172.2, 94.3, 74.9, 71.5, 63.3, 35.8, 34.5, 32.0, 29.7, 29.6, 29.5, 29.4, 29.2, 26.3, 24.9, 22.8, 17.5, 17.37, 17.36, 17.28, 17.26, 17.2, 17.1, 14.3, 13.40, 13.36, 12.6, 12.4. **HRMS** (ESI) m/z: $[M+NH_4]^+$ calcd for $C_{31}H_{64}NO_7Si_2$ 618.4216; found 618.4216.

(6aR,8R,11aR)-2,2,4,4-tetraisopropyl-11-oxohexahydro-6H-oxepino[3,2-f][1,3,5,2,4]trioxadisilocin-8-yl 2-(4-methoxyphenyl)acetate (7b)

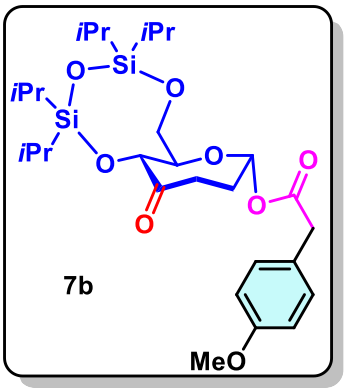

Compound **7b** was synthesized using the general procedure **1.4**. **7b** was obtained in 82% yield (116 mg), as a colorless oil, R_f = 0.5 (Hexane/EtOAc, 8:2, v/v), **[α]^{25}D** = +58.3 (*c* 0.05, EtOAc). **^{1}H NMR** (400 MHz, $CDCl_3$) *δ* 7.18 (d, *J* = 8.7 Hz, 2H), 6.84 (d, *J* = 8.7 Hz, 2H), 6.23 (dd, *J* = 8.8, 5.7 Hz, 1H), 4.36 (d, *J* = 9.8 Hz, 1H), 3.93 (d, J = 9.9 Hz, 1H), 3.78 (s, 4H), 3.53 (s, 2H), 3.47 (dd, *J* = 11.8, 2.1 Hz, 1H), 2.60 – 2.45 (m, 2H), 2.27 – 2.18 (m, 1H), 1.91 – 1.80 (m, 1H), 1.10 – 1.00 (m, 28H). **^{13}C NMR** (126 MHz, $CDCl_3$) *δ* 206.8, 170.1, 159.1, 130.5, 125.6, 114.2, 94.4, 74.7, 71.3, 62.9, 55.3, 40.9, 35.7, 26.3,

17.5, 17.37, 17.35, 17.29, 17.26, 17.2, 17.1, 13.4, 13.3, 12.7, 12.4. **HRMS** (ESI) m/z: $[M+NH_4]^+$ calcd for $C_{28}H_{50}NO_8Si_2$ 584.3070; found 584.3061.

(6aR,11aR)-2,2,4,4-tetraisopropyl-11-oxohexahydro-6H-oxepino[3,2-f][1,3,5,2,4]trioxadisilocin-8-yl (R)-2-(4-isobutylphenyl)propanoate (7c)

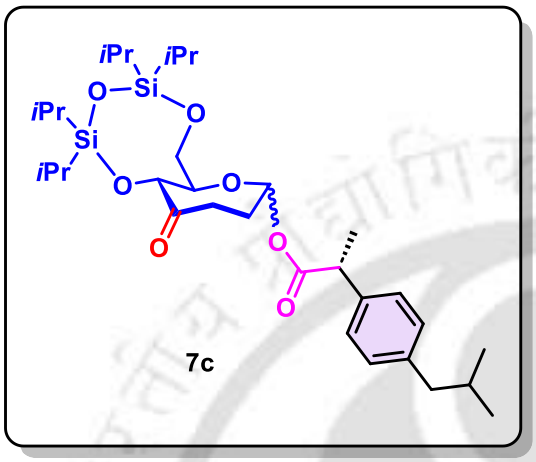

Compound **7c** was synthesized using the general procedure **1.4**. **7c** was obtained in 83% yield (121 mg), as a white foam, R_f = 0.7 (Hexane/EtOAc, 8:2, v/v), **[α]^{25}D** = +13.9 (*c* 0.18, EtOAc). **α/β = 12:1**. α-isomer: **^{1}H NMR** (500 MHz, $CDCl_3$) *δ* 7.16 (d, *J* = 7.6 Hz, 2H), 7.07 (d, *J* = 7.6 Hz, 2H), 6.21 (t, *J* = 6.9 Hz, 1H), 4.37 (d, *J* = 9.6 Hz, 1H), 4.00 (d, *J* = 11.7 Hz, 1H), 3.76 (d, *J* = 9.8 Hz, 1H), 3.71 – 3.57 (m, 2H), 2.52 (t, *J* = 13.0 Hz, 1H), 2.43 (d, *J* = 7.0 Hz, 3H), 2.21 – 2.12 (m, 1H), 1.88 – 1.71 (m, 2H), 1.49 (d, *J* = 7.0 Hz, 3H), 1.06 (d, *J* = 7.6 Hz, 28H), 0.88 (d, *J* = 6.6 Hz, 6H). **^{13}C NMR** (126 MHz, $CDCl_3$) *δ* 206.7, 172.8, 140.9, 137.1, 129.5, 127.3, 94.5, 74.8, 71.5, 63.1, 45.5, 45.1, 35.6, 30.3, 26.2, 22.5, 18.0, 17.5, 17.4, 17.27, 17.26, 17.2, 17.1, 13.39, 13.36, 12.6, 12.4. **HRMS** (ESI) m/z: $[M+NH_4]^+$ calcd for $C_{32}H_{58}NO_7Si_2$ 624.3747; found 624.3746.

(6aR,8R,11aR)-2,2,4,4-tetraisopropyl-11-oxohexahydro-6H-oxepino[3,2-f][1,3,5,2,4]trioxadisilocin-8-yl (S)-2-(6-methoxynaphthalen-2-yl)propanoate (7d)

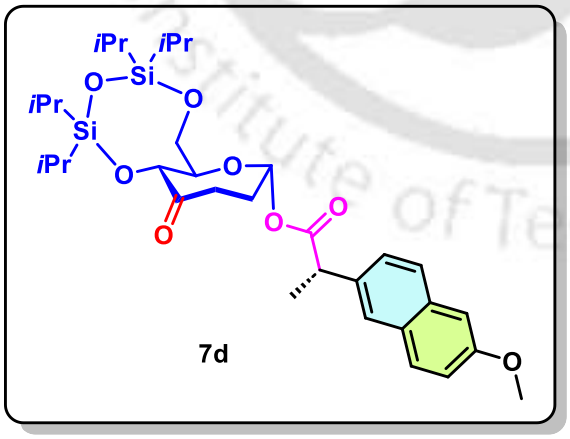

Compound **7d** was synthesized using the general procedure **1.4**. **7d** was obtained in 80% yield (126 mg), as a white foam, R_f = 0.6 (Hexane/EtOAc, 8:2, v/v), **[α]^{25}D** = +16.7 (*c* 0.12, EtOAc). **^{1}H NMR** (600 MHz, $CDCl_3$) *δ* 7.71 – 7.63 (m, 3H), 7.38 (d, *J* = 8.4 Hz, 1H), 7.13 (dd, *J* = 8.9, 2.4 Hz, 1H), 7.09 (d, *J* = 2.1 Hz, 1H), 6.22 (dd, *J* = 8.6, 5.8 Hz, 1H), 4.30 (d, *J* = 9.8 Hz, 1H), 3.90 (s, 3H), 3.85 (q, *J* = 7.1 Hz, 1H), 3.69 (d, *J* = 11.8 Hz, 1H), 3.65 (d, *J* = 9.7 Hz, 1H), 3.24 (dd, *J* = 11.8, 1.6 Hz, 1H), 2.52 (t, *J* = 12.4 Hz, 1H), 2.43 (dd, *J* = 12.9, 7.8 Hz, 1H), 2.16 (dt, *J* = 13.7, 6.0 Hz, 1H), 1.79 – 1.73 (m, 1H), 1.60 (d, *J* = 7.2 Hz, 3H), 1.11 – 0.91 (m, 28H). **^{13}C NMR** (126 MHz, $CDCl_3$) *δ* 206.8, 172.7, 157.9, 134.8, 133.9, 129.3, 128.9, 127.34, 126.27, 126.2, 119.4, 105.6, 94.3, 74.6, 71.3, 62.8, 55.4, 46.0, 35.6, 26.1, 17.7, 17.41, 17.39, 17.32, 17.27,

17.23, 17.16, 17.1, 13.4, 13.2, 12.6, 12.3. **HRMS** (ESI) m/z: $[M+NH_4]^+$ calcd for $C_{33}H_{54}NO_8Si_2$ 648.3383; found 648.3382.

(6aR,8R,11aR)-2,2,4,4-tetraisopropyl-11-oxohexahydro-6H-oxepino[3,2-f][1,3,5,2,4]trioxadisilocin-8-yl 5-(2,5-dimethylphenoxy)-2,2-dimethylpentanoate (7e)

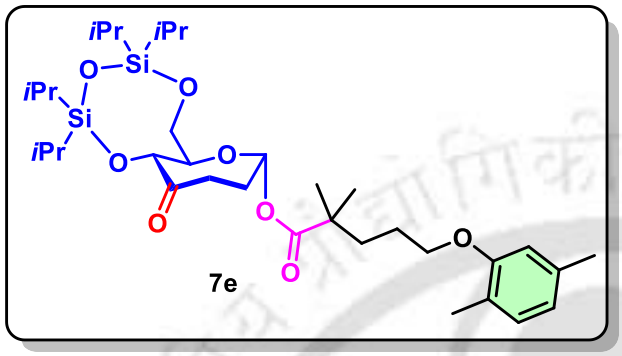

Compound **7e** was synthesized using the general procedure **1.4**. **7e** was obtained in 81% yield (132 mg), as a colorless oil, R_f = 0.5 (Hexane/EtOAc, 9:1, v/v), **[α]$^{25}_D$** = +22.6 (*c* 0.20, EtOAc). **^{1}H NMR** (500 MHz, $CDCl_3$) δ 6.99 (d, *J* = 7.4 Hz, 1H), 6.65 (d, *J* = 7.1 Hz, 1H), 6.59 (s, 1H), 6.25 (t, *J* = 6.7 Hz, 1H), 4.43 (d, *J* = 9.5 Hz, 1H), 4.14 (d, *J* = 11.6 Hz, 1H), 3.94 – 3.83 (m, 4H), 2.64 – 2.47 (m, 2H), 2.30 (s, 3H), 2.27 – 2.19 (m, 1H), 2.15 (s, 3H), 1.85 (q, *J* = 12.9, 12.0 Hz, 1H), 1.78 – 1.67 (m, 4H), 1.22 (s, 6H), 1.07 – 1.04 (m, 28H). **^{13}C NMR** (126 MHz, $CDCl_3$) δ 206.6, 175.9, 156.9, 136.6, 130.5, 123.6, 120.9, 112.1, 94.5, 74.9, 71.8, 67.9, 63.3, 42.3, 37.1, 35.7, 26.4, 25.4, 25.2, 24.9, 21.5, 17.5, 17.43, 17.38, 17.37, 17.29, 17.26, 17.2, 17.1, 15.9, 13.42, 13.36, 12.7, 12.5. **HRMS** (ESI) m/z: $[M+NH_4]^+$ calcd for $C_{34}H_{62}NO_8Si_2$ 668.4009; found 668.4008.

(6aR,8R,11aR)-2,2,4,4-tetraisopropyl-11-oxohexahydro-6H-oxepino[3,2-f][1,3,5,2,4]trioxadisilocin-8-yl 2-(1-(4-chlorobenzoyl)-5-methoxy-2-methyl-1H-indol-3-yl)acetate (7f)

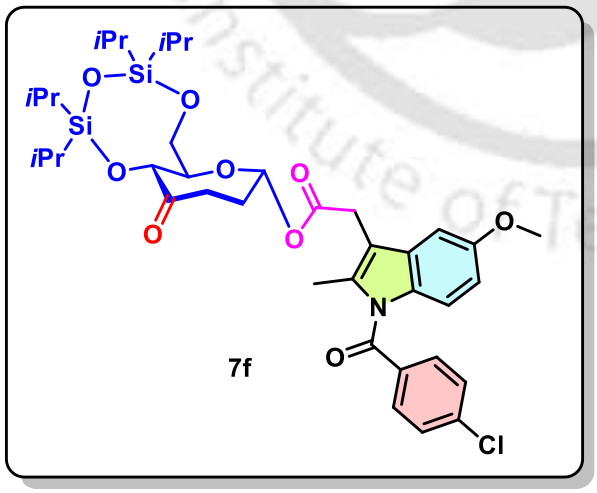

Compound **7f** was synthesized using the general procedure **1.4**. **7f** was obtained in 80% yield (152 mg), as a white foam, R_f = 0.4 (Hexane/EtOAc, 8:2, v/v), **[α]$^{25}_D$** = +9.8 (*c* 0.26, EtOAc). **^{1}H NMR** (500 MHz, $CDCl_3$) δ 7.65 (d, *J* = 8.2 Hz, 2H), 7.47 (d, *J* = 8.2 Hz, 2H), 6.94 (s, 1H), 6.88 (d, *J* = 8.9 Hz, 1H), 6.66 (d, *J* = 8.9 Hz, 1H), 6.24 (t, *J* = 6.7 Hz, 1H), 4.33 (d, *J* = 9.7 Hz, 1H), 3.82 (d, *J* = 16.3 Hz, 4H), 3.71 – 3.61 (m, 3H), 3.33 (d, *J* = 11.8 Hz, 1H), 2.60 – 2.44 (m, 2H), 2.37 (s, 3H), 2.28 – 2.22 (m, 1H), 1.87 – 1.80 (m, 1H), 1.05 – 0.97 (m, 28H). **^{13}C NMR** (126 MHz, $CDCl_3$) δ 206.6, 168.9, 168.3, 156.2, 139.5, 136.2, 133.9, 131.3, 130.9, 130.5, 129.3, 115.2, 112.1, 111.7, 101.6, 94.8, 74.5, 71.5, 62.8, 55.8, 35.7, 30.8, 26.5, 17.44,

17.36, 17.32, 17.28, 17.22, 17.19, 17.1, 13.5, 13.4, 13.3, 12.6, 12.3. **HRMS** (ESI) m/z: $[M+H]^+$ calcd for $C_{38}H_{53}ClNO_9Si_2$ 758.2942; found 758.2941.

(6aR,8R,11aR)-2,2,4,4-tetraisopropyl-11-oxohexahydro-6H-oxepino[3,2-f][1,3,5,2,4]trioxadisilocin-8-yl 2-(2-((2,6-dichlorophenyl)amino)phenyl)acetate (7g)

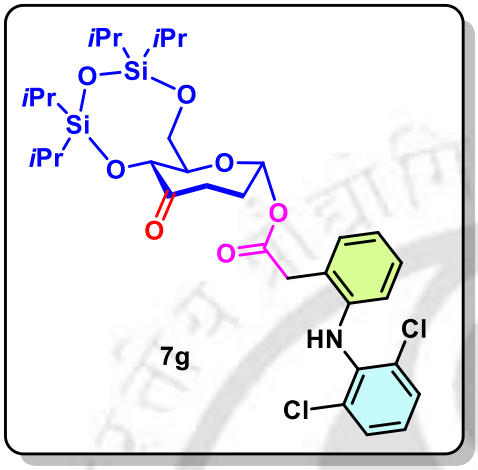

Compound **7g** was synthesized using the general procedure **1.4**. **7g** was obtained in 82% yield (143 mg), as a colorless oil, R_f = 0.6 (Hexane/EtOAc, 8:2, v/v), **[α]^{25}D** = +12.9 (*c* 0.25, EtOAc). **^{1}H NMR** (500 MHz, $CDCl_3$) δ 7.34 (d, *J* = 7.9 Hz, 2H), 7.21 (d, *J* = 7.6 Hz, 1H), 7.12 (t, *J* = 7.6 Hz, 1H), 6.97 (dt, *J* = 22.4, 7.6 Hz, 2H), 6.65 (s, 1H), 6.53 (d, *J* = 7.9 Hz, 1H), 6.32 – 6.26 (m, 1H), 4.38 (d, *J* = 9.7 Hz, 1H), 3.93 (d, *J* = 11.6 Hz, 1H), 3.84 (d, *J* = 10.0 Hz, 1H), 3.80 (s, 2H), 3.52 (d, *J* = 11.8 Hz, 1H), 2.54 (dt, *J* = 23.7, 13.3 Hz, 2H), 2.30 – 2.22 (m, 1H), 1.99 – 1.90 (m, 1H), 1.06 – 1.01 (m, 28H). **^{13}C NMR** (126 MHz, $CDCl_3$) δ 206.6, 170.7, 142.9, 137.8, 130.9, 129.9, 128.9, 128.4, 124.4, 123.9, 122.3, 118.5, 94.9, 74.8, 71.5, 62.9, 38.8, 35.7, 26.2, 17.42, 17.36, 17.28, 17.2, 17.1, 13.4, 13.3, 12.7, 12.4. **HRMS** (ESI) m/z: $[M+NH_4]^+$ calcd for $C_{33}H_{51}Cl_2N_2O_7Si_2$ 713.2607; found 713.2589.

2-oxo-2-(((6aR,8R,11aR)-2,2,4,4-tetraisopropyl-11-oxohexahydro-6H-oxepino[3,2-f][1,3,5,2,4]trioxadisilocin-8-yl)oxy)ethyl 2-(2-((2,6-dichlorophenyl)amino)phenyl)acetate (7h)

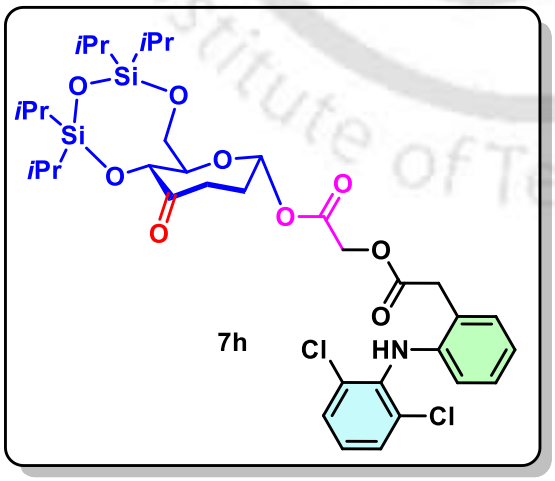

Compound **7h** was synthesized using the general procedure **1.4**. **7h** was obtained in 81% yield (153 mg), as a colorless oil, R_f = 0.6 (Hexane/EtOAc, 8:2, v/v), **[α]^{25}D** = +41.7 (*c* 0.16, EtOAc). **^{1}H NMR** (400 MHz, $CDCl_3$) δ 7.33 (d, *J* = 8.1 Hz, 2H), 7.24 (dd, *J* = 7.5, 1.3 Hz, 1H), 7.17 – 7.09 (m, 1H), 6.97 (dt, *J* = 15.1, 7.4 Hz, 2H), 6.78 (s, 1H), 6.53 (d, *J* = 8.0 Hz, 1H), 6.26 (dd, *J* = 9.1, 5.8 Hz, 1H), 4.74 – 4.59 (m, 2H), 4.33 (d, *J* = 9.8 Hz, 1H), 4.04 (dd, *J* = 11.8, 1.6 Hz, 1H), 3.90 (s, 2H), 3.82 (dd, *J* = 11.9, 2.0 Hz, 1H), 3.59 (d, *J* = 9.8 Hz, 1H), 2.54 – 2.39 (m, 2H), 2.17 – 2.06 (m, 1H), 1.61 (dd, *J* = 7.7, 4.8 Hz, 1H), 1.11 – 1.01 (m, 28H). **^{13}C NMR** (101 MHz, $CDCl_3$) δ 205.9, 171.4, 166.1, 142.7, 137.7, 130.9, 129.5, 129.0, 128.6,

124.3, 123.6, 122.4, 118.5, 95.5, 74.6, 71.4, 62.9, 61.3, 38.1, 35.6, 25.6, 17.5, 17.38, 17.35, 17.28, 17.27, 17.2, 17.1, 13.4, 13.3, 12.6, 12.5. **HRMS** (ESI) m/z: $[M+H]^+$ calcd for $C_{35}H_{50}Cl_2NO_9Si_2$ 754.2396; found 754.2393.

(6aR,8R,11aR)-2,2,4,4-tetraisopropyl-11-oxohexahydro-6H-oxepino[3,2-f][1,3,5,2,4]trioxadisilocin-8-yl benzoate (7i)

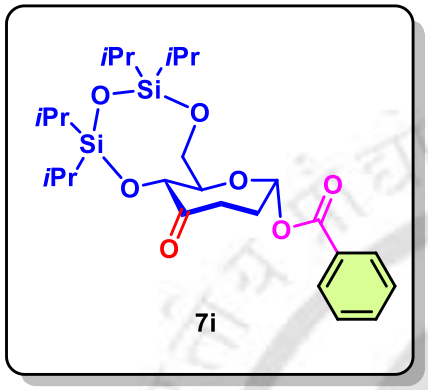

Compound **7i** was synthesized using the general procedure **1.4**. **7i** was obtained in 80% yield (108 mg), as a colorless oil, R_f = 0.6 (Hexane/EtOAc, 9:1, v/v), **[α]$^{25}_D$** = +5.8 (*c* 0.22, EtOAc). **^{1}H NMR** (400 MHz, $CDCl_3$) δ 8.05 – 7.96 (m, 2H), 7.63 – 7.53 (m, 1H), 7.45 (t, *J* = 7.8 Hz, 2H), 6.50 (dd, *J* = 8.8, 5.6 Hz, 1H), 4.48 (d, *J* = 9.6 Hz, 1H), 4.17 (dd, *J* = 11.6, 1.9 Hz, 1H), 4.06 (d, *J* = 9.6 Hz, 1H), 3.91 (dd, *J* = 11.7, 2.3 Hz, 1H), 2.73 – 2.55 (m, 2H), 2.44 – 2.37 (m, 1H), 2.12 – 2.01 (m, 1H), 1.12 – 1.01 (m, 28H). **^{13}C NMR** (101 MHz, $CDCl_3$) δ 206.7, 164.8, 133.6, 129.8, 128.7, 95.1, 74.9, 71.8, 63.3, 35.8, 26.5, 17.5, 17.44, 17.38, 17.37, 17.30, 17.28, 17.2, 17.1, 13.41, 13.36, 12.7, 12.4. **HRMS** (ESI) m/z: $[M+H]^+$ calcd for $C_{26}H_{46}NO_7Si_2$ 540.2808; found 540.2808.

3.5.9. Spectroscopic data of Septanosides (8-11)

(2R,3R,7S)-3-hydroxy-2-(hydroxymethyl)-7-(((3aS,5aR,8aR,8bS)-2,2,7,7-tetramethyltetrahydro-3aH-bis([1,3]dioxolo)[4,5-b:4',5'-d]pyran-3a-yl)methoxy)oxepan-4-one (8)

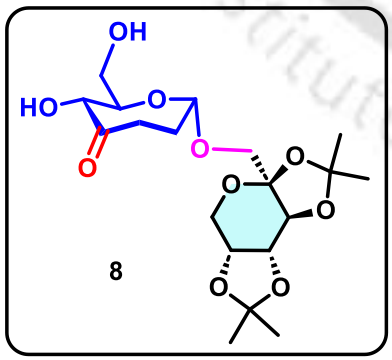

[α]$^{25}_D$ = +27.0 (*c* 0.10, EtOAc). **^{1}H NMR** (400 MHz, $CDCl_3$) δ 5.03 (dd, *J* = 7.7, 4.6 Hz, 1H), 4.59 (dd, *J* = 8.0, 2.6 Hz, 1H), 4.32 (d, *J* = 2.7 Hz, 1H), 4.21 (dd, *J* = 14.7, 9.7 Hz, 2H), 4.00 (d, *J* = 10.4 Hz, 1H), 3.94 – 3.88 (m, 2H), 3.83 – 3.70 (m, 3H), 3.56 (d, *J* = 10.3 Hz, 1H), 2.70 – 2.59 (m, 2H), 2.26 (s, 1H), 2.22 (dd, *J* = 11.6, 6.4 Hz, 1H), 1.85 – 1.76 (m, 1H), 1.68 (s, 1H), 1.52 (s, 3H), 1.47 (s, 3H), 1.35 (d, *J* = 9.1 Hz, 6H). **^{13}C NMR** (151 MHz, $CDCl_3$) δ 210.2, 109.2, 108.8, 102.2, 99.7, 76.6, 71.1, 70.3, 70.1, 69.3, 68.7, 63.9, 61.2, 34.2, 27.3, 26.6, 26.1, 25.5, 24.1. **HRMS** (ESI) m/z: $[M+H]^+$ calcd for $C_{19}H_{31}O_{10}$ 419.1912; found 419.1908.

(6aR,8S,11aR)-8-(((2R,3R,7S)-3-hydroxy-4-oxo-7-(((3aS,5aR,8aR,8bS)-2,2,7,7-tetramethyltetrahydro-3aH-bis([1,3]dioxolo)[4,5-b:4',5'-d]pyran-3a-yl)methoxy)oxepan-2-yl)methoxy)-2,2,4,4-tetraisopropyltetrahydro-6H-oxepino[3,2-f][1,3,5,2,4]trioxadisilocin-11(8H)-one (9)

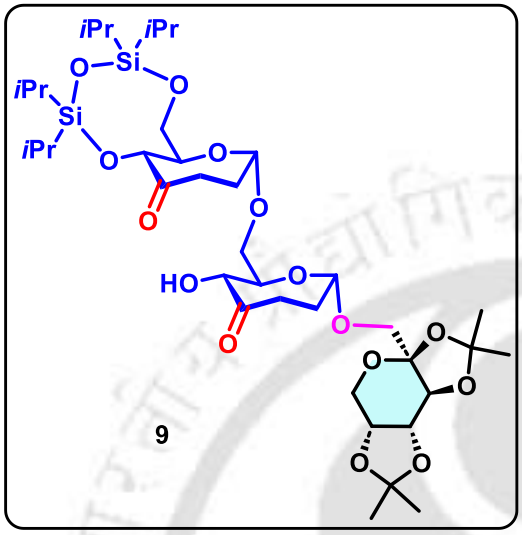

[α]$^{25}_{D}$ = +17.5 (*c* 0.20, CH_2Cl_2). **^{1}H NMR** (600 MHz, $CDCl_3$) *δ* 4.92 (dd, *J* = 7.8, 5.0 Hz, 1H), 4.59 (d, *J* = 5.4 Hz, 2H), 4.31 (d, *J* = 2.3 Hz, 1H), 4.23 – 4.18 (m, 2H), 4.10 (d, *J* = 12.6 Hz, 2H), 3.99 (d, *J* = 10.1 Hz, 1H), 3.89 (dd, *J* = 21.2, 11.6 Hz, 4H), 3.74 (s, 1H), 3.61 – 3.58 (m, 1H), 3.50 (d, *J* = 10.3 Hz, 1H), 3.44 (t, *J* = 10.4 Hz, 1H), 2.85 (t, *J* = 6.6 Hz, 3H), 2.52 (d, *J* = 9.8 Hz, 2H), 2.17 (dd, *J* = 11.2, 7.0 Hz, 1H), 2.09 – 2.05 (m, 1H), 2.01 – 1.98 (m, 1H), 1.74 (s, 1H), 1.52 (s, 3H), 1.46 (s, 3H), 1.37 (s, 3H), 1.33 (s, 3H), 1.07 – 1.01 (m, 28H). **^{13}C NMR** (151 MHz, $CDCl_3$) *δ* 212.6, 203.6, 109.1, 108.8, 102.1, 100.4, 99.9, 84.0, 75.9, 72.5, 71.1, 70.2, 70.0, 69.5, 68.9, 62.3, 61.2, 59.4, 35.6, 32.6, 27.4, 27.2, 26.7, 26.0, 25.5, 24.1, 17.47, 17.45, 17.40, 17.39, 17.38, 17.32, 17.31, 17.25, 13.4, 13.3, 12.8. **HRMS** (ESI) m/z: $[M+NH_4]^+$ calcd for $C_{38}H_{70}NO_{15}Si_2$ 836.4279; found 836.4286.

(6aR,11aR)-8-((4-(4-(hydroxymethyl)phenyl)but-3-yn-1-yl)oxy)-2,2,4,4-tetraisopropyltetrahydro-6H-oxepino[3,2-f][1,3,5,2,4]trioxadisilocin-11(8H)-one (10)

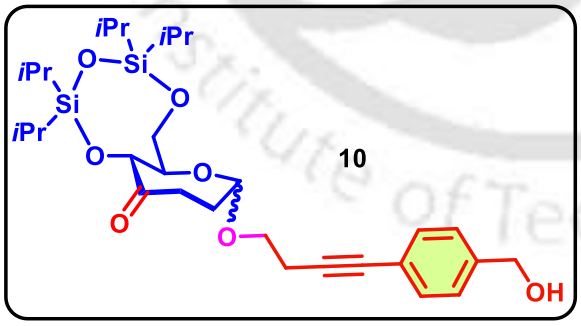

[α]$^{25}_{D}$ = +25.9 (*c* 0.56, CH_2Cl_2). **α/β = 9:1**. α-isomer: **^{1}H NMR** (600 MHz, $CDCl_3$) *δ* 7.36 (d, *J* = 8.1 Hz, 2H), 7.28 – 7.26 (m, 2H), 5.05 (dd, *J* = 8.0, 5.5 Hz, 1H), 4.67 (d, *J* = 3.4 Hz, 2H), 4.40 (d, *J* = 9.7 Hz, 1H), 4.06 (d, *J* = 11.1 Hz, 1H), 4.01 – 3.91 (m, 3H), 3.71 (dt, *J* = 9.4, 6.1 Hz, 1H), 2.72 – 2.66 (m, 2H), 2.54 (t, *J* = 12.2 Hz, 1H), 2.46 (dd, *J* = 12.8, 8.1 Hz, 1H), 2.13 (dt, *J* = 13.6, 5.9 Hz, 1H), 1.79 (dd, *J* = 24.5, 10.5 Hz, 2H), 1.13 – 0.98 (m, 28H). **^{13}C NMR** (151 MHz, $CDCl_3$) *δ* 207.8, 140.7, 131.8, 126.9, 122.8, 99.7, 86.9, 81.4, 74.7, 68.8, 66.0, 65.1, 63.5, 35.7, 27.6, 20.9, 17.5, 17.44, 17.42, 17.40, 17.29, 17.27, 17.2, 17.1, 13.4, 13.3, 12.6, 12.3. **HRMS** (ESI) m/z: $[M+NH_4]^+$ calcd for $C_{30}H_{52}NO_7Si_2$ 594.3277; found 594.3263.

(6aR,8S,11aR)-2,2,4,4-tetraisopropyl-8-((4-(4-(((6aR,11aR)-2,2,4,4-tetraisopropyl-11-oxohexahydro-6H-oxepino[3,2-f][1,3,5,2,4]trioxadisilocin-8-yl)oxy)but-1-yn-1-yl)benzyl)oxy)tetrahydro-6H-oxepino[3,2-f][1,3,5,2,4]trioxadisilocin-11(8H)-one (11)

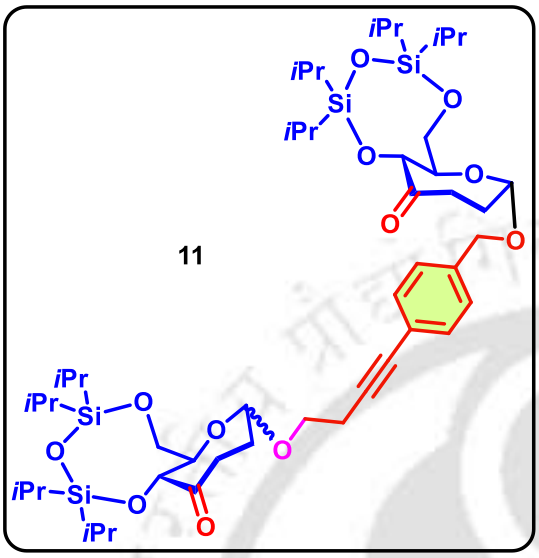

$[\alpha]^{25}_{D}$ = +29.3 (*c* 0.46, CH_2Cl_2). **α/β = 9:1**. α-isomer: **^{1}H NMR** (600 MHz, $CDCl_3$) *δ* 7.34 (d, *J* = 8.0 Hz, 2H), 7.21 (d, *J* = 8.0 Hz, 2H), 5.05 (q, *J* = 8.4 Hz, 2H), 4.79 (d, *J* = 12.6 Hz, 1H), 4.57 (d, *J* = 12.5 Hz, 1H), 4.41 (dd, *J* = 19.0, 9.6 Hz, 2H), 4.15 (d, *J* = 11.4 Hz, 1H), 4.06 (d, *J* = 10.6 Hz, 1H), 4.00 – 3.90 (m, 4H), 3.87 – 3.82 (m, 1H), 3.72 – 3.69 (m, 1H), 2.67 (t, *J* = 6.5 Hz, 2H), 2.57 – 2.43 (m, 4H), 2.16 – 2.10 (m, 2H), 1.88 – 1.75 (m, 3H), 1.09 – 1.02 (m, 56H). **^{13}C NMR** (151 MHz, $CDCl_3$) *δ* 207.8, 207.6, 137.6, 131.8, 127.8, 127.3, 122.9, 99.7, 99.6, 87.0, 81.4, 74.9, 74.7, 69.3, 69.2, 68.9, 66.0, 63.6, 63.5, 35.72, 35.70, 27.6, 20.9, 17.50, 17.49, 17.45, 17.42, 17.30, 17.27, 17.2, 17.10, 17.07, 13.5, 13.44, 13.38, 13.3, 12.61, 12.55, 12.4, 12.3. **HRMS** (ESI) m/z: $[M+H]^+$ calcd for $C_{49}H_{85}O_{12}Si_4$ 977.5113; found 977.5099.

3.6. References

1. Koester, D. C.; Holkenbrink, A.; Werz, D. B., Recent Advances in the Synthesis of Carbohydrate Mimetics. *Synthesis* **2010,** *2010* (19), 3217-3242.
2. Hoberg, J. O., Formation of Seven-Membered Oxacycles through Ring Expansion of Cyclopropanated Carbohydrates. *J. Org. Chem.* **1997,** *62* (19), 6615-6618.
3. Barbero, H.; Díez-Poza, C.; Barbero, A. The Oxepane Motif in Marine Drugs. *Mar. Drugs* **2017**, *15* (11), 361
4. Bozó, É.; Medgyes, A.; Boros, S.; Kuszmann, J., Synthesis of 4-substituted phenyl 2,5-anhydro-1,6-dithio-α-d-gluco- and -α-l-guloseptanosides possessing antithrombotic activity. *Carbohydr. Res.* **2000,** *329* (1), 25-40.
5. Duff Jr, M. R.; Fyvie, W. S.; Markad, S. D.; Frankel, A. E.; Kumar, C. V.; Gascón, J. A.; Peczuh, M. W., Computational and experimental investigations of mono-septanoside binding by Concanavalin A: correlation of ligand stereochemistry to enthalpies of binding. *Org. Biomol. Chem.* **2011,** *9* (1), 154-164.
6. Sabatino, D.; Damha, M. J., Oxepane Nucleic Acids: Synthesis, Characterization, and Properties of Oligonucleotides Bearing a Seven-Membered Carbohydrate Ring. *J. Am. Chem. Soc.* **2007,** *129* (26), 8259-8270.
7. Ben Nejma, A.; Nguir, A.; Ben Jannet, H.; Hamza, M. h. A.; Daïch, A.; Othman, M.; Lawson, A. M., New septanoside and 20-hydroxyecdysone septanoside derivative from Atriplex portulacoides roots with preliminary biological activities. *Bioorg. Med. Chem. Lett.* **2015,** *25* (8), 1665-1670.
8. Pote, A. R.; Pascual, S.; Planas, A.; Peczuh, M. W. Indolyl Septanoside Synthesis for In Vivo Screening of Bacterial Septanoside Hydrolases. *Int. J. Mol. Sci.* **2021**, *22* (9), 4497.

9. Saha, J.; Peczuh, M. W., Expanding the Scope of Aminosugars: Synthesis of 2-Amino Septanosyl Glycoconjugates Using Septanosyl Fluoride Donors. *Chem. Eur. J.* **2011,** *17* (26), 7357-7365.
10. Schneider, T. F.; Kaschel, J.; Werz, D. B., A New Golden Age for Donor–Acceptor Cyclopropanes. *Angew. Chem. Int. Ed.* **2014,** *53* (22), 5504-5523.
11. Sridhar, P. R.; Venukumar, P., A Ring Expansion–Glycosylation Strategy toward the Synthesis of Septano-oligosaccharides. *Org. Lett.* **2012,** *14* (21), 5558-5561.
12. Kamala Lakshmi, M. V.; Ali, I.; Perali, R. S., A Ring Expansion─Stereoselective Cycloaddition of Carbohydrate-Derived Donor–Acceptor Cyclopropanes: Synthesis of Bridged Oxepanone–Indole Hybrids. *J. Org. Chem.* **2022,** *87* (18), 12370-12385.
13. Ma, W.; Kirchhoff, J.-L.; Strohmann, C.; Grabe, B.; Loh, C. C. J., Cooperative Bifurcated Chalcogen Bonding and Hydrogen Bonding as Stereocontrolling Elements for Selective Strain-Release Septanosylation. *J. Am. Chem. Soc.* **2023,** *145* (49), 26611-26622.
14. Ganesh, N. V.; Jayaraman, N., Synthesis of Aryl, Glycosyl, and Azido Septanosides through Ring Expansion of 1,2-Cyclopropanated Sugars. *J. Org. Chem.* **2009,** *74* (2), 739-746.
15. Dey, S.; Jayaraman, N., Glycosidic bond hydrolysis in septanosides: a comparison of mono-, di-, and 2-chloro-2-deoxy-septanosides. *Carbohydr. Res.* **2014,** *399*, 49-56.
16. Ganesh, N. V.; Raghothama, S.; Sonti, R.; Jayaraman, N., Ring Expansion of Oxyglycals. Synthesis and Conformational Analysis of Septanoside-Containing Trisaccharides. *J. Org. Chem.* **2010,** *75* (1), 215-218.
17. Türkmen, Y. E.; Rawal, V. H., Exploring the Potential of Diarylacetylenediols as Hydrogen Bonding Catalysts. *J. Org. Chem.* **2013,** *78* (17), 8340-8353.
18. Beddoe, R. H.; Andrews, K. G.; Magné, V.; Cuthbertson, J. D.; Saska, J.; Shannon-Little, A. L.; Shanahan, S. E.; Sneddon, H. F.; Denton, R. M., Redox-neutral organocatalytic Mitsunobu reactions. *Science* **2019,** *365* (6456), 910-914.
19. Biswas, A.; Pradhan, P.; Wakpanjar, S. A.; Kancharla, P. K., Direct organocatalytic esterification of carboxylic acids and alcohols by redox neutral sulfur(iv) catalysis via intramolecularly interrupted Pummerrer intermediates. *Chem. Commun.* **2025,** *61* (31), 5746-5749.
20. Ghosh, T.; Mukherji, A.; Kancharla, P. K., Sterically Hindered 2,4,6-Tri-tert-butylpyridinium Salts as Single Hydrogen Bond Donors for Highly Stereoselective Glycosylation Reactions of Glycals. *Org. Lett.* **2019,** *21* (10), 3490-3495.
21. Prassas, I.; Diamandis, E. P., Novel therapeutic applications of cardiac glycosides. *Nat. Rev. Drug Discov.* **2008,** *7* (11), 926-935.
22. Dimakos, V.; Taylor, M. S., Recent advances in the direct O-arylation of carbohydrates. *Org. Biomol. Chem.* **2021,** *19* (3), 514-524.
23. Mahling, J.-A.; Schmidt, R. R., Aryl C-Glycosides from O-Glycosyltrichloroacetimidates and Phenol Derivatives with Trimethylsilyl Trifluoromethanesulfonate (TMSOTf) as the Catalyst. *Synthesis* **1993,** *1993* (03), 325-328.
24. Venukumar, P.; Sudharani, C.; Sridhar, P. R., A one-pot septanoside formation and glycosylation of acyclic dithioacetals derived from 1,2-cyclopropanated sugars. *Chem. Commun.* **2014,** *50* (17), 2218-2221.
25. Pradhan, P.; Moktan, S.; Biswas, A.; Das, A.; Lenka, R.; Kancharla, P. K., Triple Role of Proton Sponge (DMAN) in the Palladium-Catalyzed Direct Stereoselective Synthesis of C-Aryl Glycosides from Glycals. *Org. Lett.* **2024,** *26* (17), 3563-3568.
26. Ma, W.; Schmidt, A.; Strohmann, C.; Loh, C. C. J., Stereoselective Entry into α,α'-C-Oxepane Scaffolds through a Chalcogen Bonding Catalyzed Strain-Release C-Septanosylation Strategy. *Angew. Chem. Int. Ed.* **2024,** *63* (29), e202405706.
27. Chennaiah, A.; Verma, A. K.; Vankar, Y. D., TEMPO-Catalyzed Oxidation of 3-O-Benzylated/Silylated Glycals to the Corresponding Enones Using a PIFA–Water Reagent System. *J. Org. Chem.* **2018,** *83* (17), 10535-10540.

28. Kalikanda, J.; Li, Z., Study of the stereoselectivity of 2-azido-2-deoxygalactosyl donors: relationship to the steric factors of glycosyl acceptors. *Carbohydr. Res.* **2011,** *346* (15), 2380-2383.
29. Sahu, D.; Dey, S.; Pathak, T.; Ganguly, B., Regioselectivity of Vinyl Sulfone Based 1,3-Dipolar Cycloaddition Reactions with Sugar Azides by Computational and Experimental Studies. *Org. Lett.* **2014,** *16* (8), 2100-2103.
30. Lambrecht, M. J.; Brichacek, M.; Barkauskaite, E.; Ariza, A.; Ahel, I.; Hergenrother, P. J., Synthesis of Dimeric ADP-Ribose and Its Structure with Human Poly(ADP-ribose) Glycohydrolase. *J. Am. Chem. Soc.* **2015,** *137* (10), 3558-3564.
31. Viuff, A. H.; Besenbacher, L. M.; Kamori, A.; Jensen, M. T.; Kilian, M.; Kato, A.; Jensen, H. H., Stable analogues of nojirimycin – synthesis and biological evaluation of nojiristegine and manno-nojiristegine. *Org. Biomol. Chem.* **2015,** *13* (37), 9637-9658.
32. Callari, M.; De Souza, P. L.; Rawal, A.; Stenzel, M. H., The Effect of Drug Loading on Micelle Properties: Solid-State NMR as a Tool to Gain Structural Insight. *Angew. Chem. Int. Ed.* **2017,** *56* (29), 8441-8445.
33. Zhang, Y. K.; Sanchez-Ayala, M. A.; Sternberg, P. W.; Srinivasan, J.; Schroeder, F. C., Improved Synthesis for Modular Ascarosides Uncovers Biological Activity. *Org. Lett.* **2017,** *19* (11), 2837-2840.
34. Meng, S.; Zhong, W.; Yao, W.; Li, Z., Stereoselective Phenylselenoglycosylation of Glycals Bearing a Fused Carbonate Moiety toward the Synthesis of 2-Deoxy-β-galactosides and β-Mannosides. *Org. Lett.* **2020,** *22* (8), 2981-2986.
35. Desireddi, J. R.; Rao, M. M.; Murahari, K. K.; Nimmareddy, R. R.; Mothe, T.; Lingala, A. K.; Maiti, B.; Manchal, R., Study of the β-oxygen effect in the Barton–McCombie reaction for the total synthesis of (4R,5R)-4-hydroxy-γ-decalactone (Japanese orange fly lactone): a carbohydrate based approach. *RSC Adv.* **2022,** *12* (39), 25520-25527.

3.7. Selected spectra

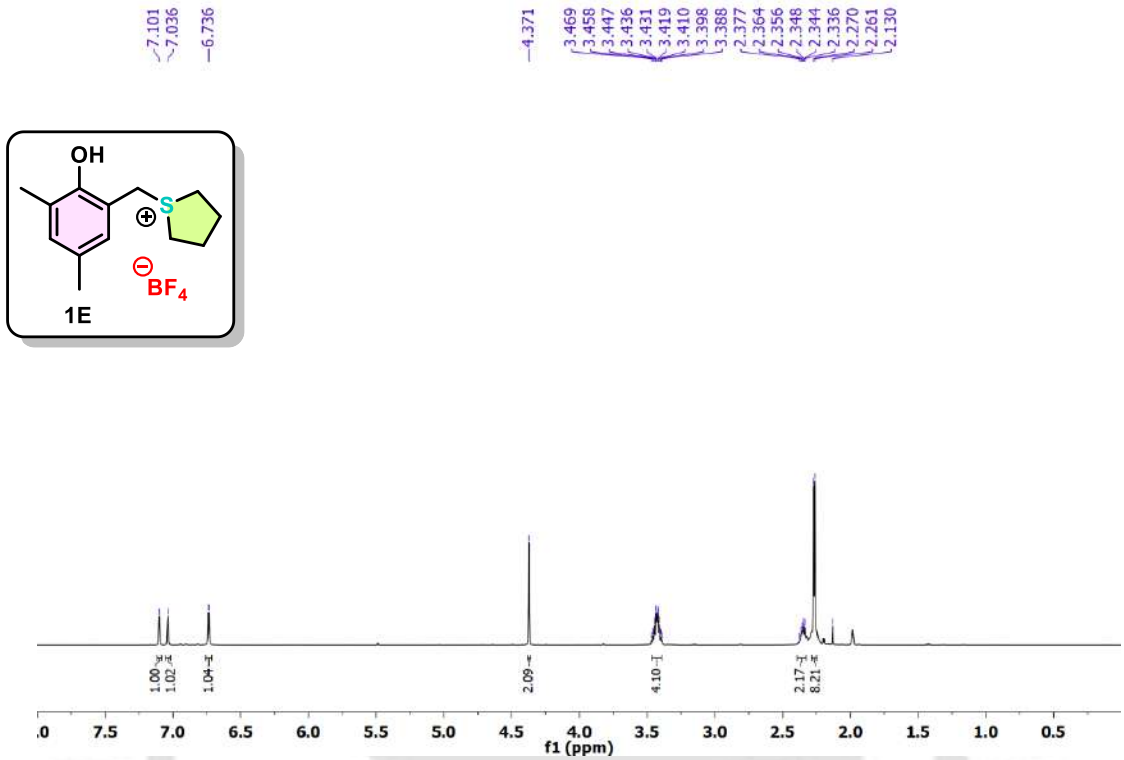

Figure 3.12. *[1]H NMR of compound **1E** (600 MHz, ACN-d_3).*

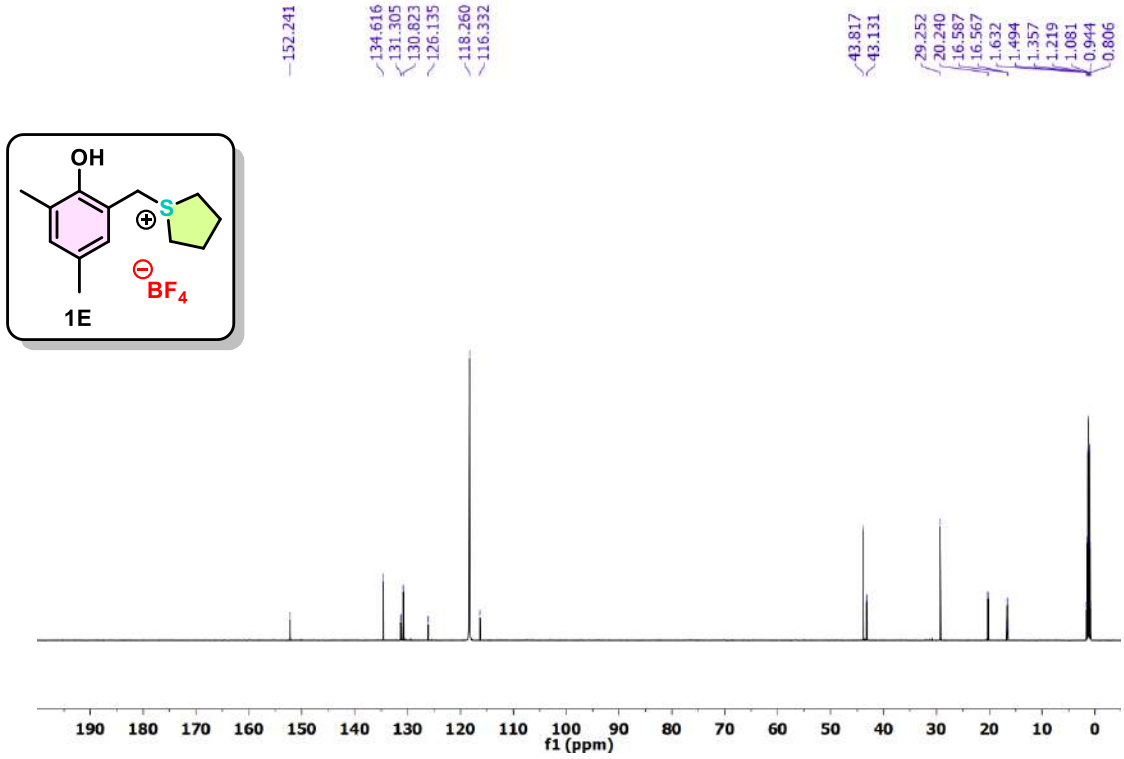

Figure 3.13. *[13]C NMR of compound **1E** (151 MHz, ACN-d_3).*

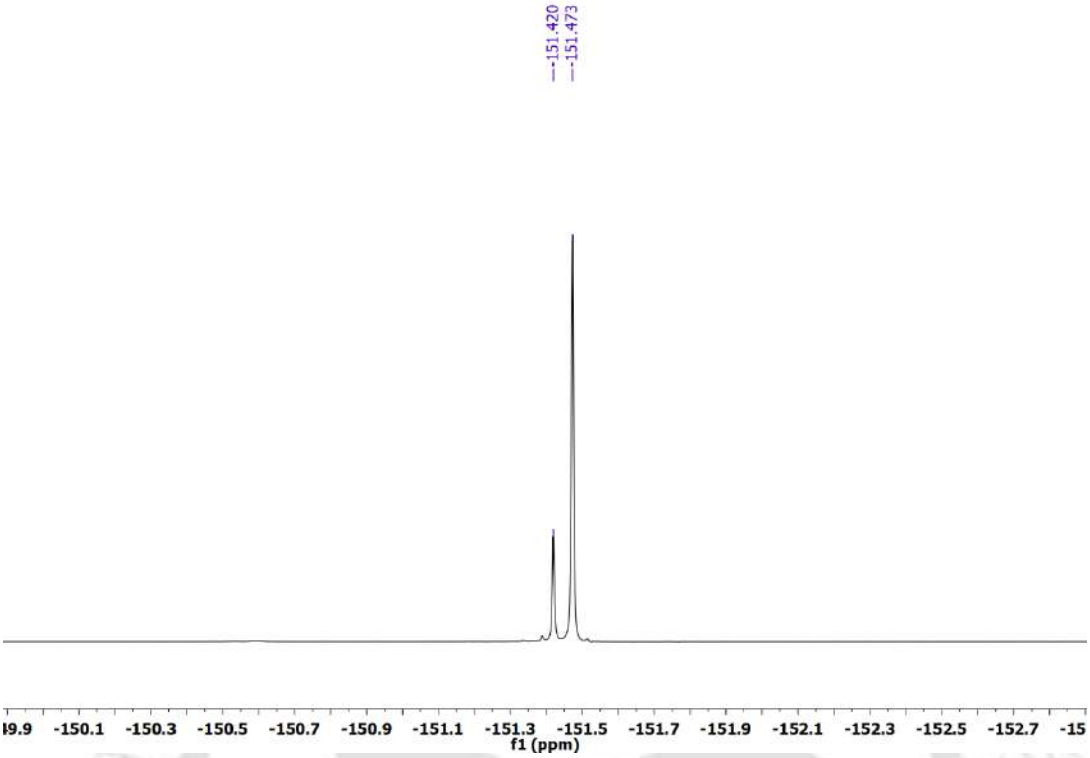

Figure 3.14. *^{19}F NMR of compound **1E** (500 MHz, ACN-d_3).*

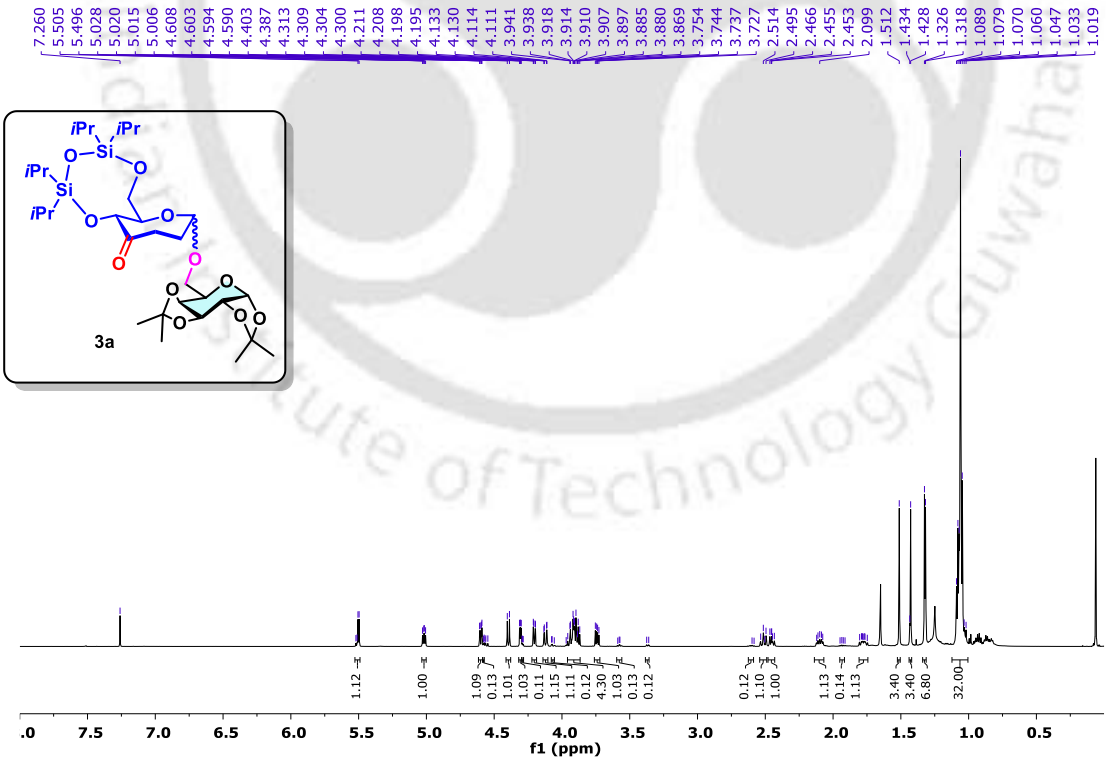

Figure 3.15. *^{1}H NMR of compound **3a** (600 MHz, $CDCl_3$).*

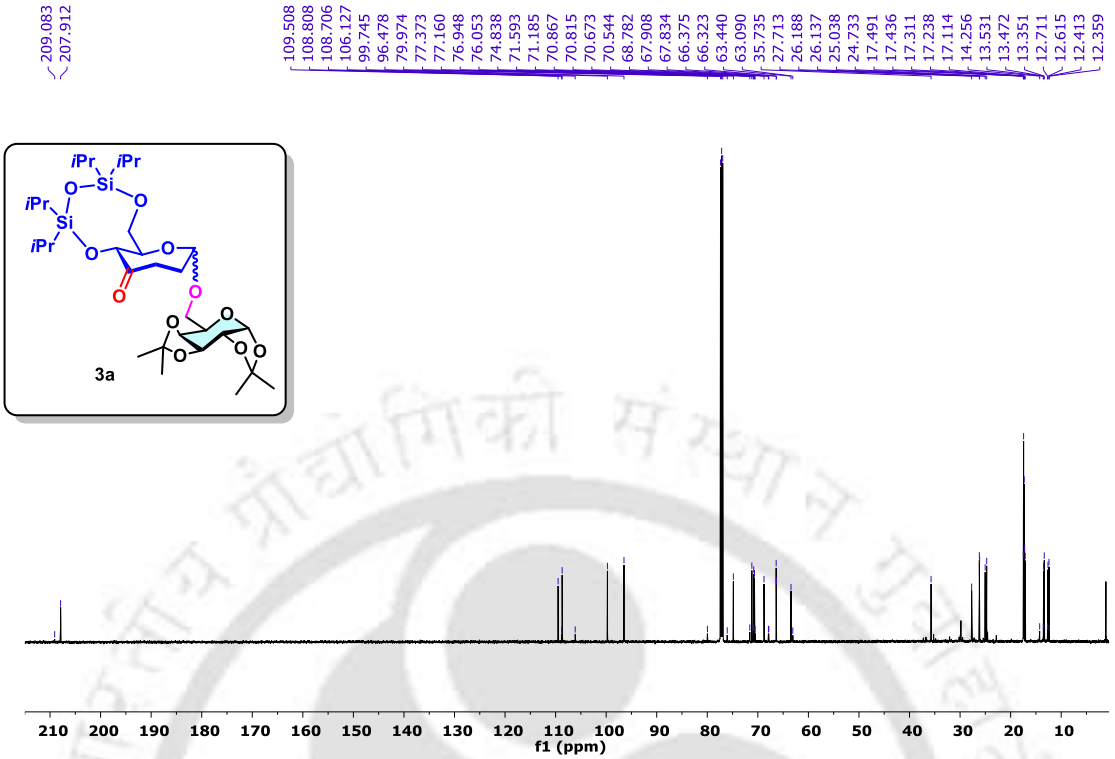

Figure 3.16. *^{13}C NMR of compound **3a** (151 MHz, $CDCl_3$).*

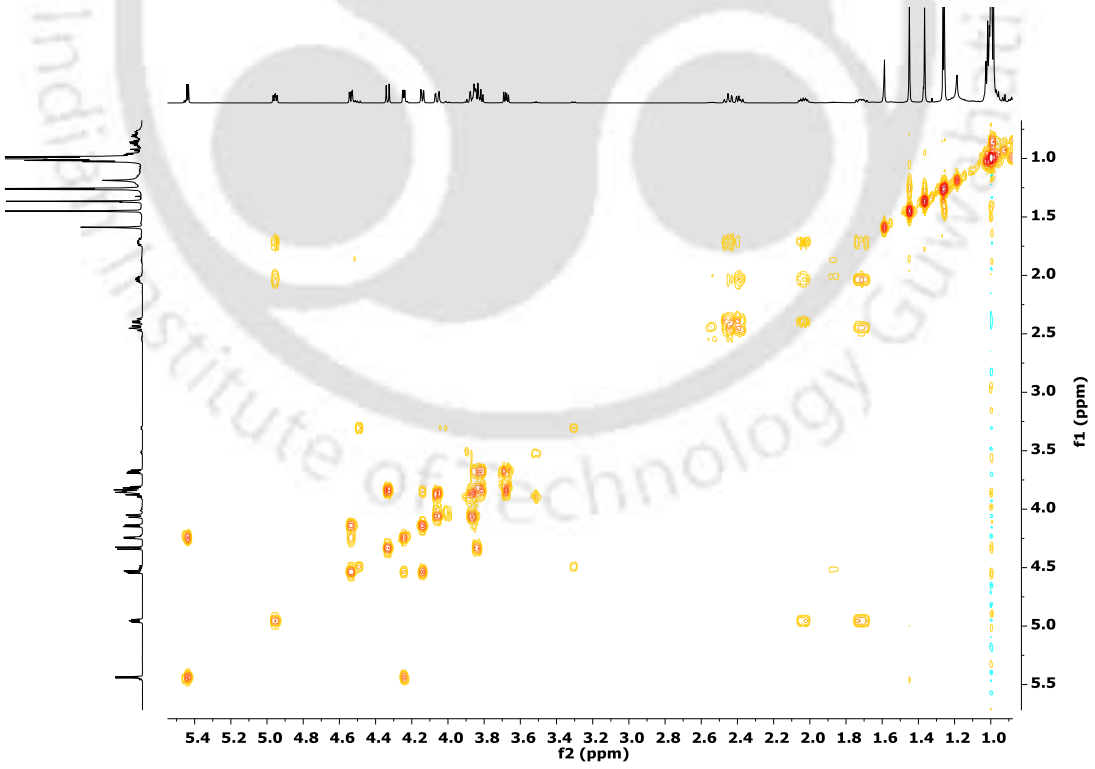

Figure 3.17. *COSY NMR of compound **3a** (600 MHz, $CDCl_3$).*

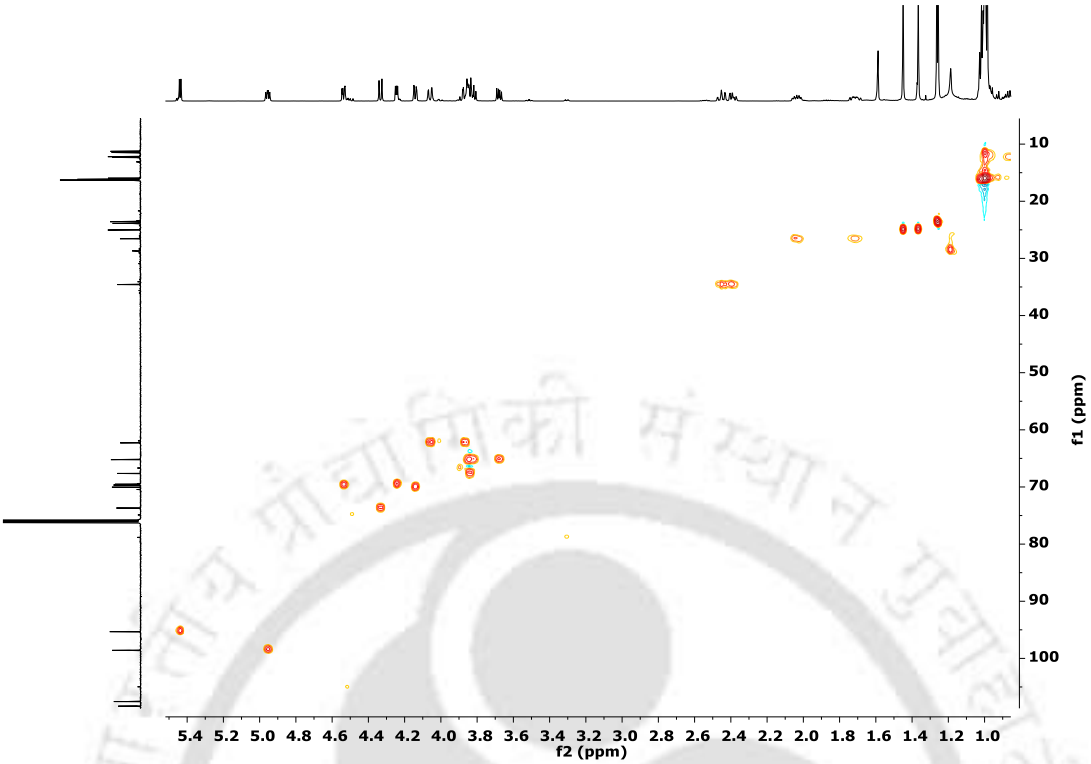

Figure 3.18. *HSQC-GP NMR of compound **3a** (600 MHz, $CDCl_3$).*

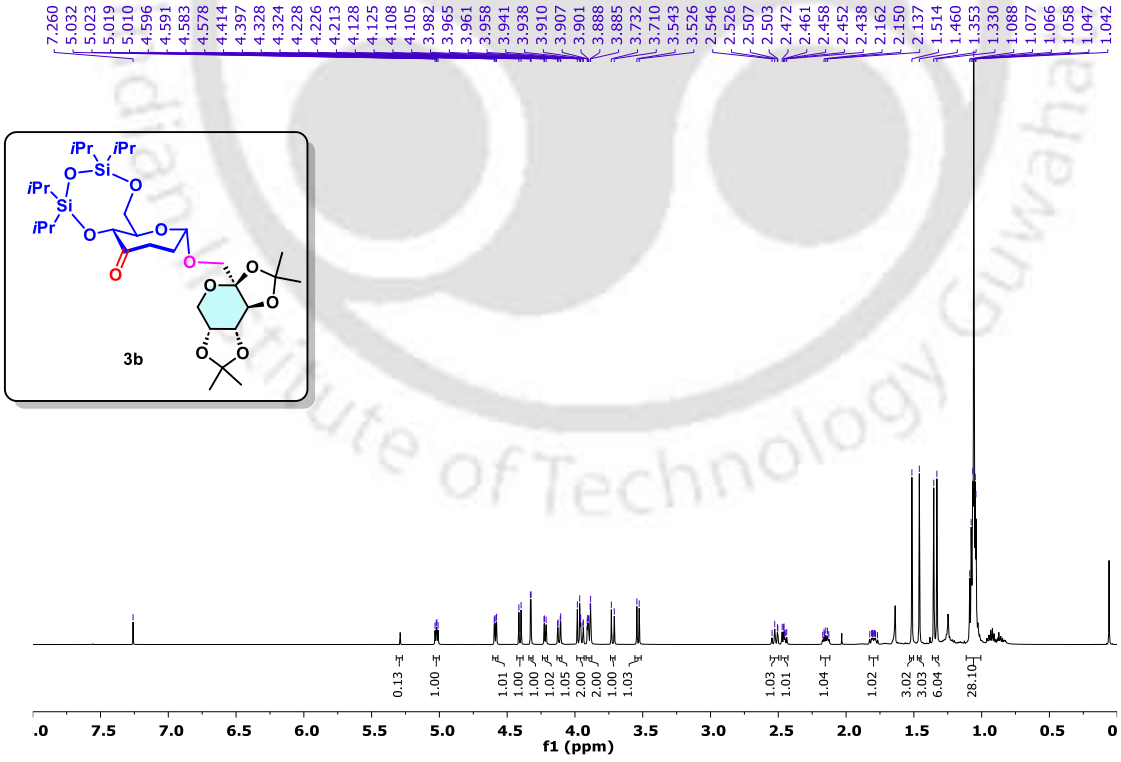

Figure 3.19. *^1H NMR of compound **3b** (600 MHz, $CDCl_3$).*

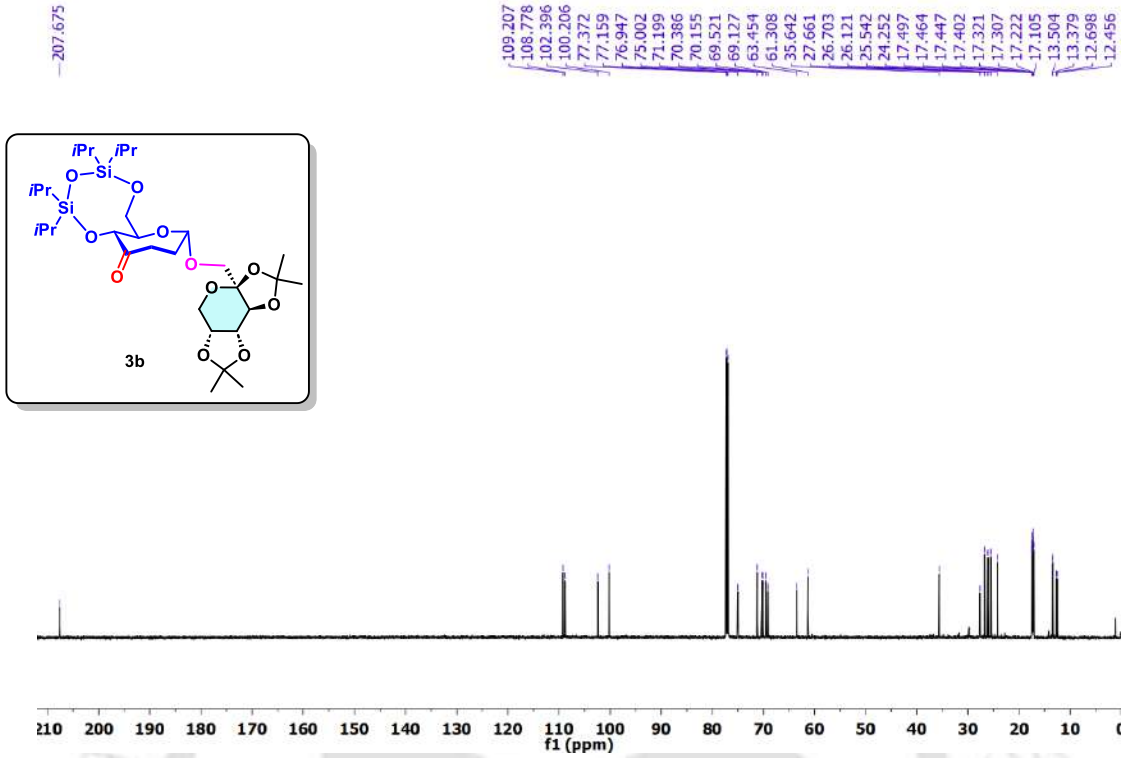

Figure 3.20. *^{13}C NMR of compound **3b** (151 MHz, $CDCl_3$).*

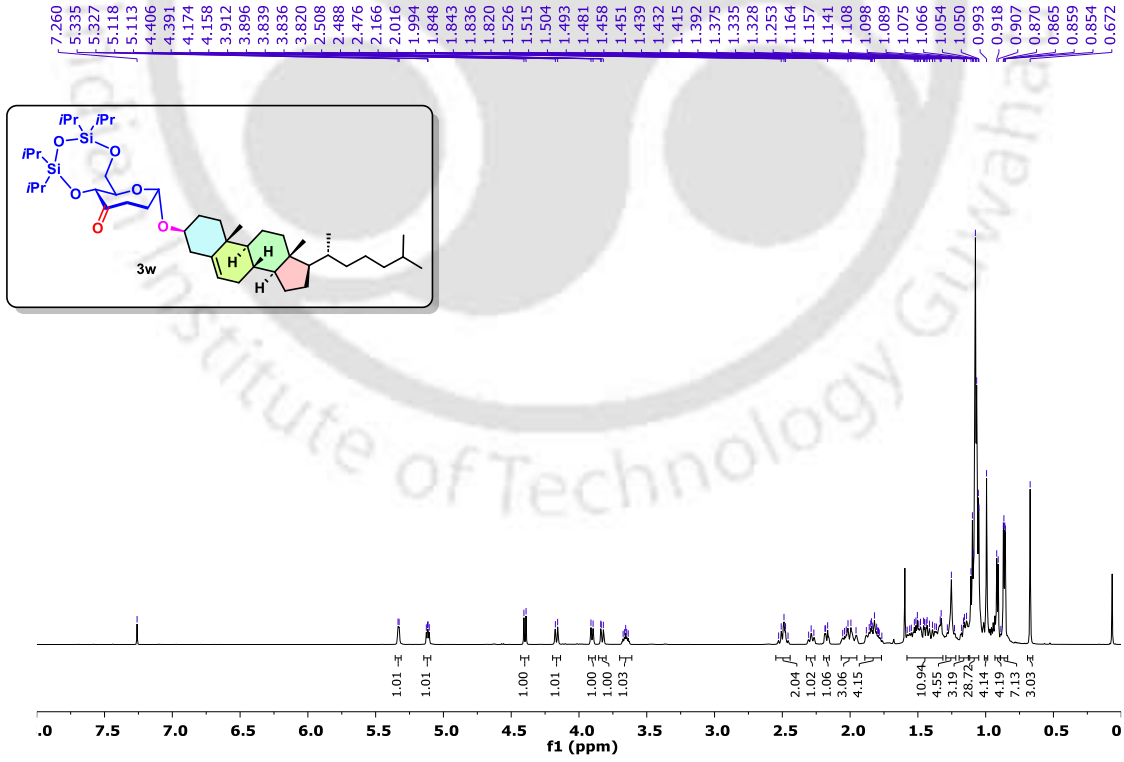

Figure 3.21. *^{1}H NMR of compound **3w** (600 MHz, $CDCl_3$).*

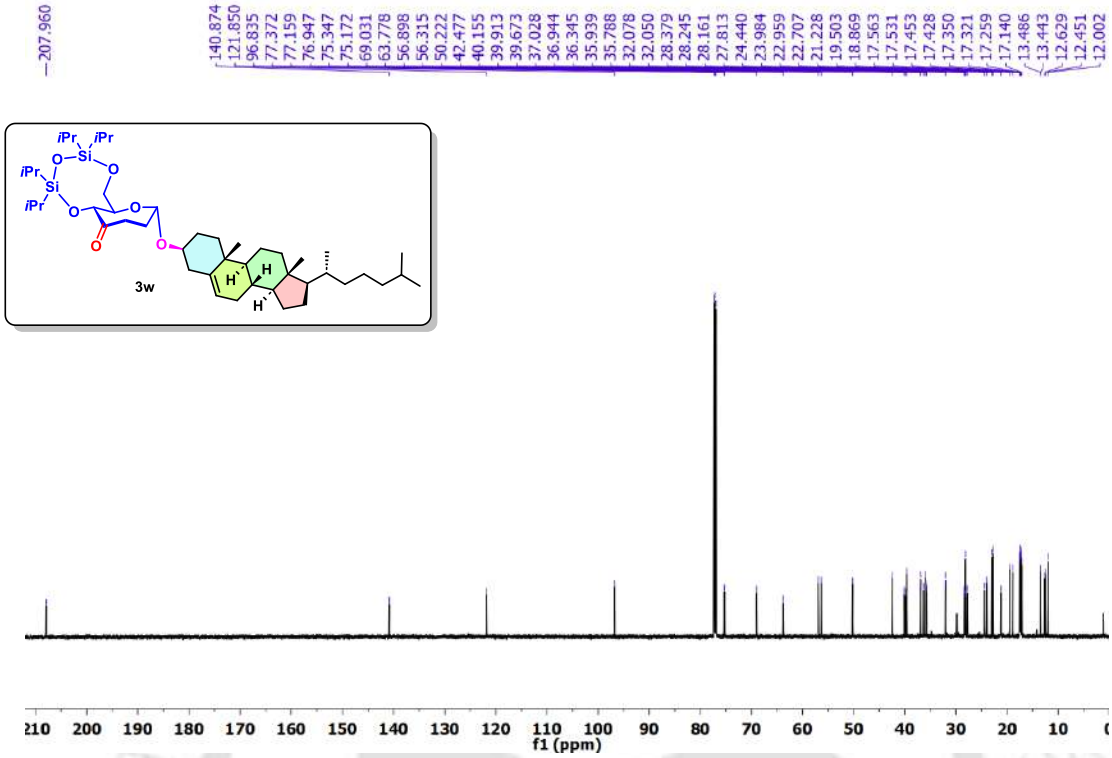

Figure 3.22. *^{13}C NMR of compound **3w** (151 MHz, $CDCl_3$).*

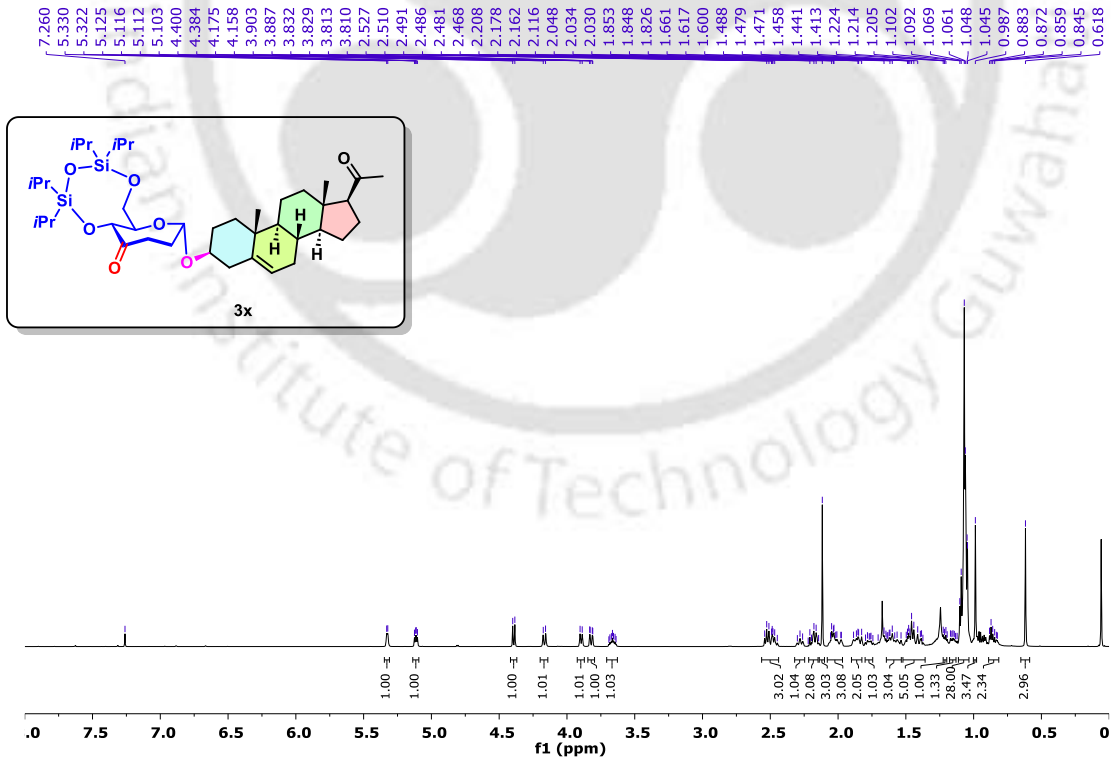

Figure 3.23. *^{1}H NMR of compound **3x** (600 MHz, $CDCl_3$).*

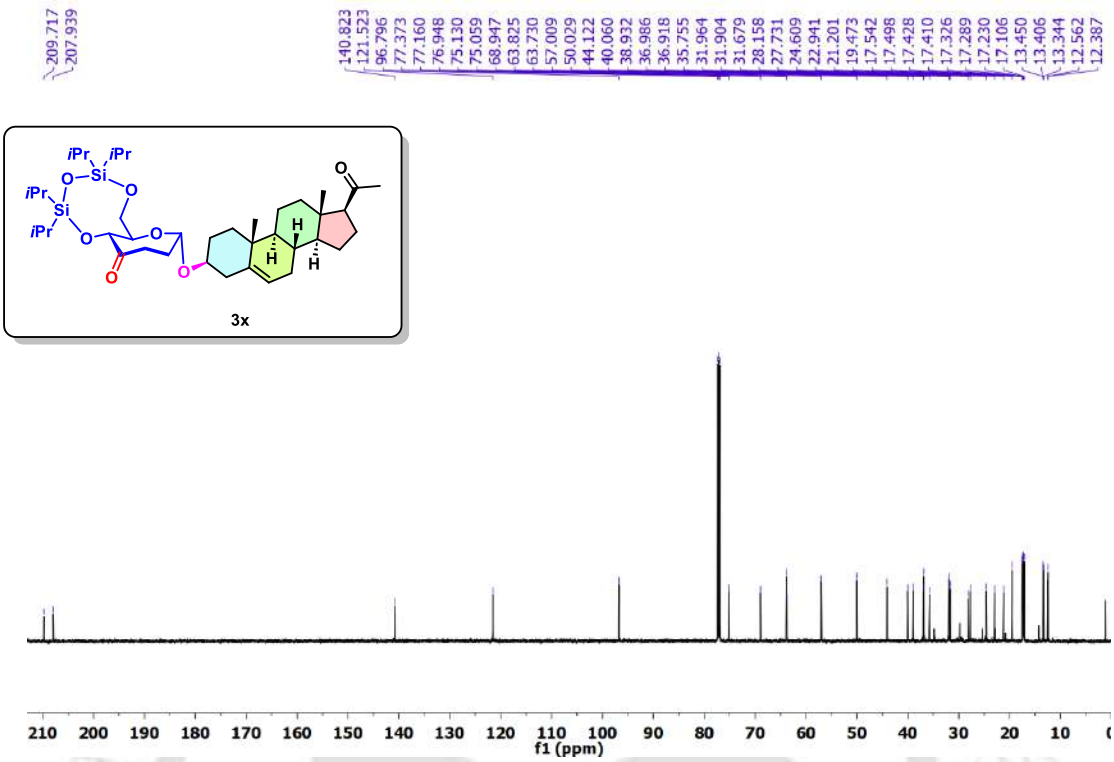

Figure 3.24. *^{13}C NMR of compound **3x** (151 MHz, $CDCl_3$).*

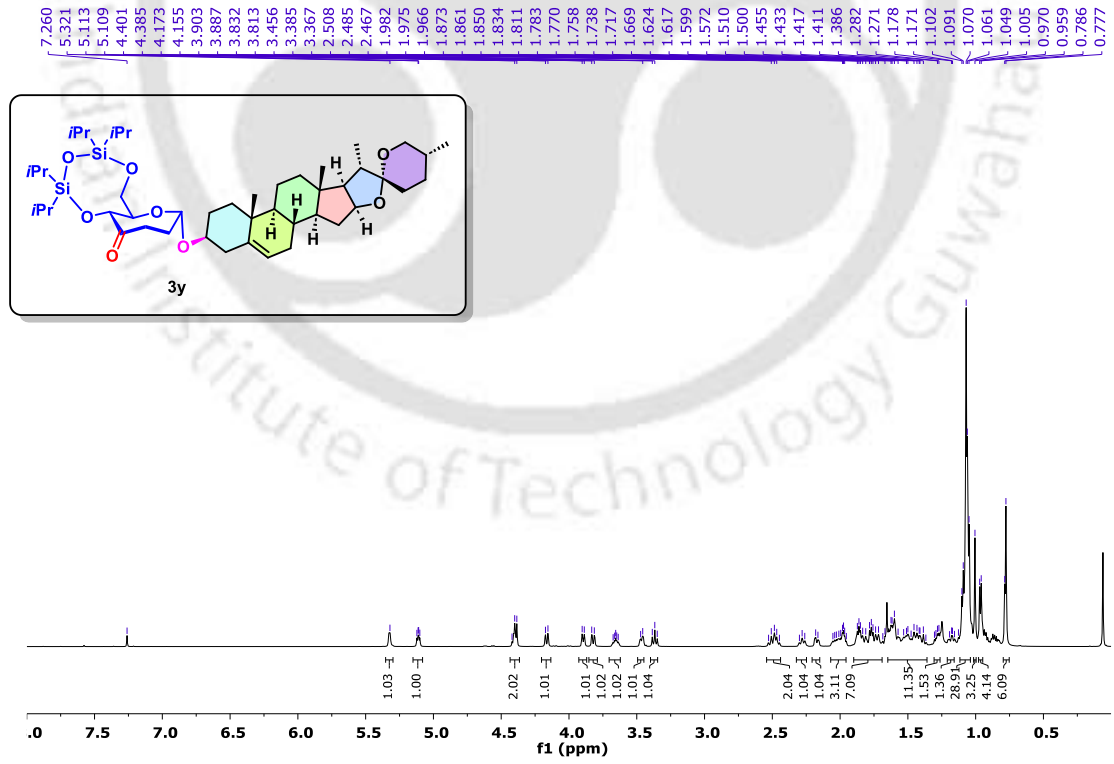

Figure 3.25. *^{1}H NMR of compound **3y** (600 MHz, $CDCl_3$).*

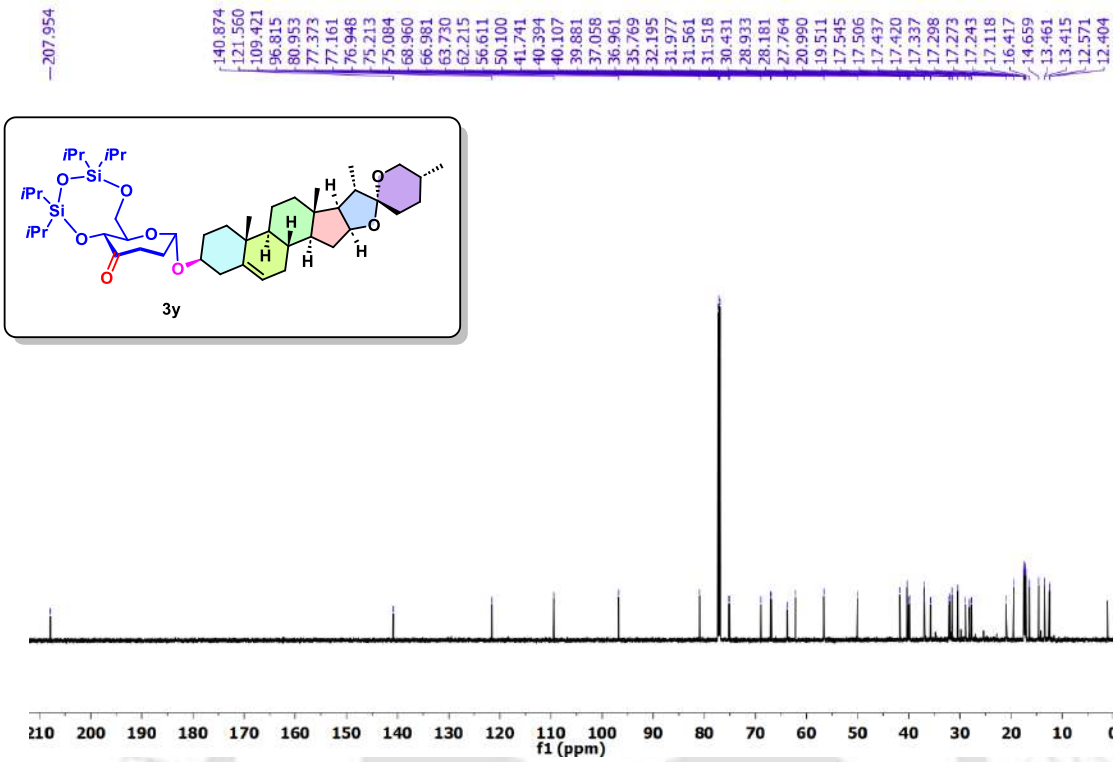

Figure 3.26. *^{13}C NMR of compound **3y** (151 MHz, $CDCl_3$).*

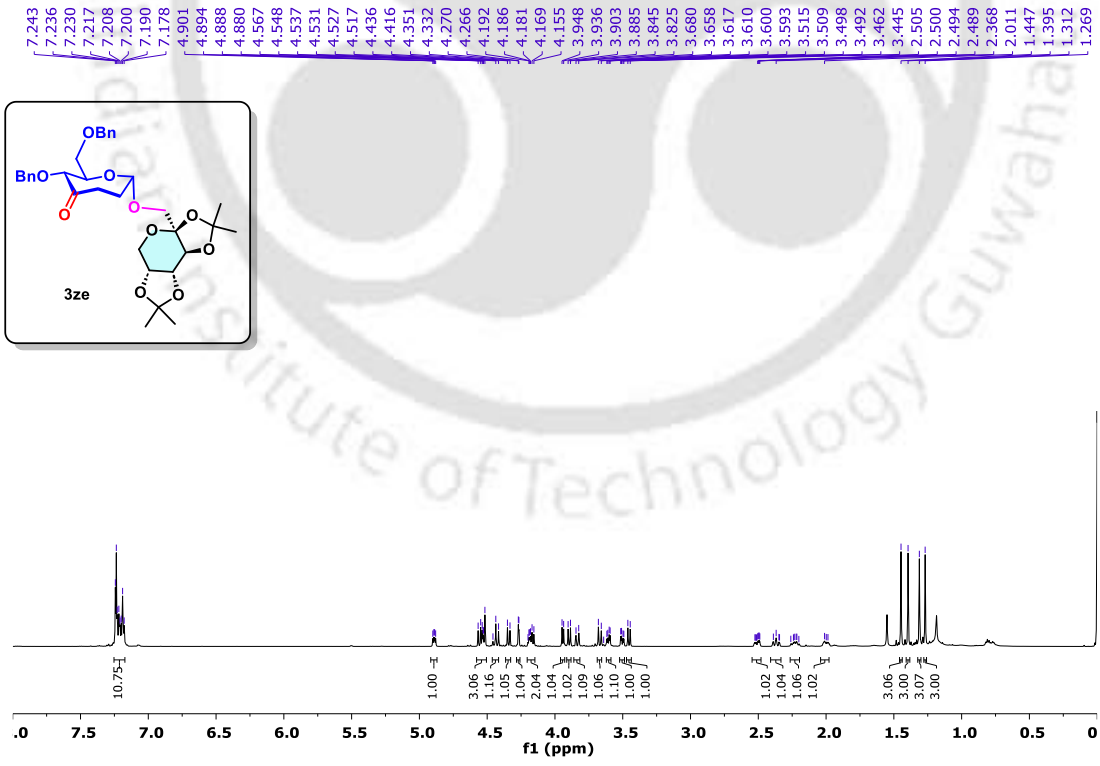

Figure 3.27. *^{1}H NMR of compound **3ze** (600 MHz, $CDCl_3$).*

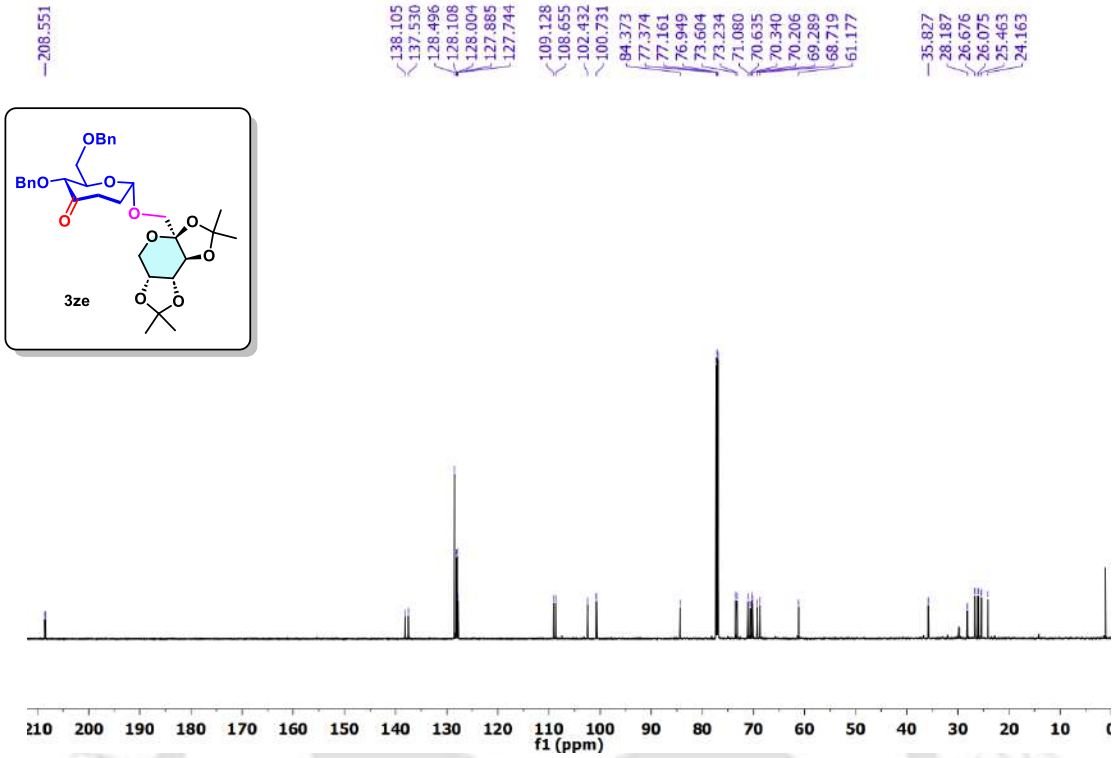

Figure 3.28. *^{13}C NMR of compound **3ze** (151 MHz, $CDCl_3$).*

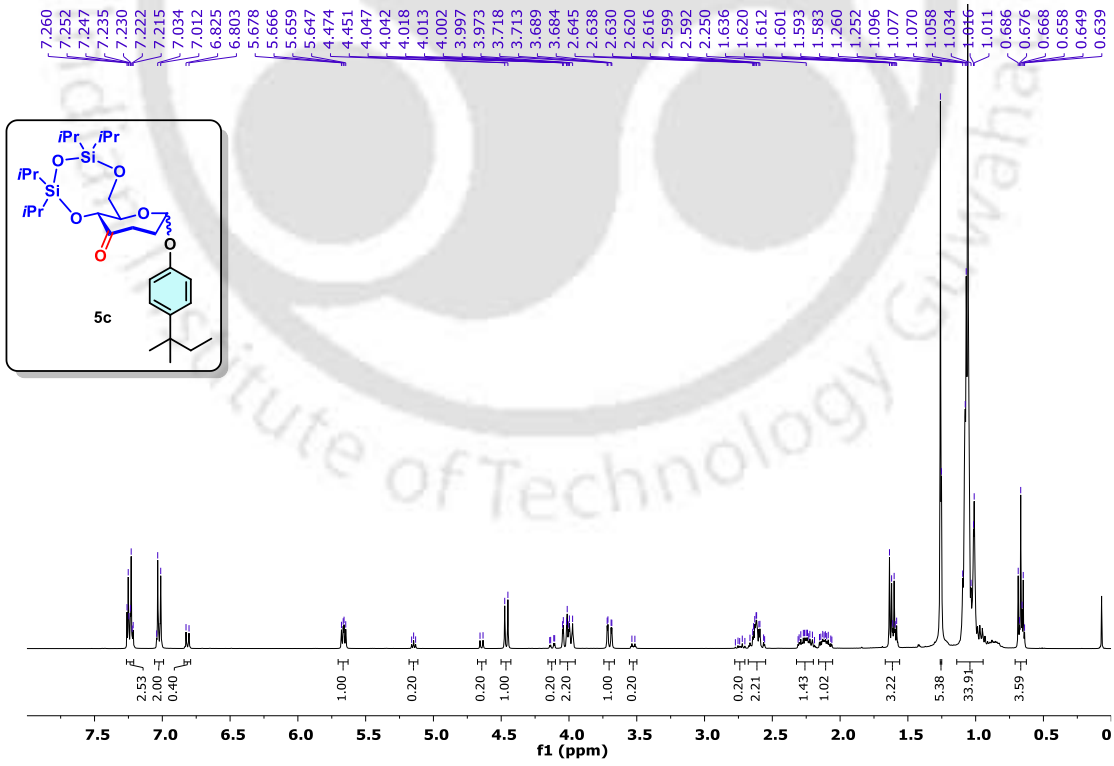

Figure 3.29. *^{1}H NMR of compound **5c** (400 MHz, $CDCl_3$).*

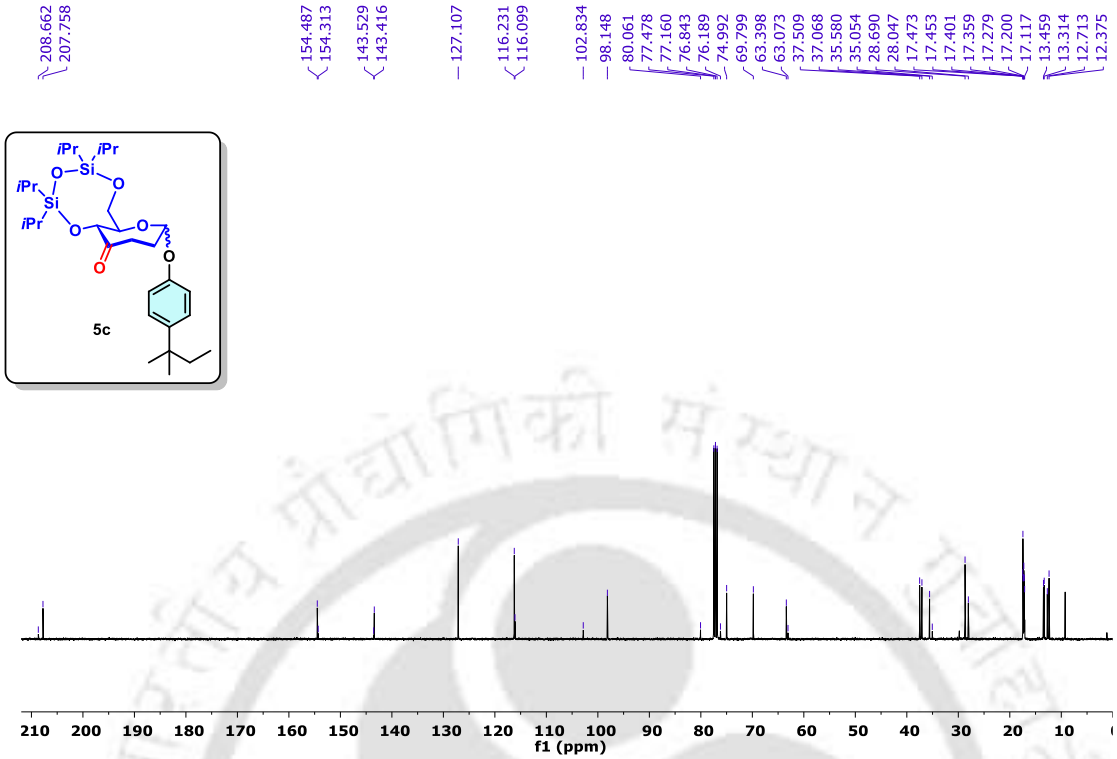

Figure 3.30. *^{13}C NMR of compound **5c** (101 MHz, $CDCl_3$).*

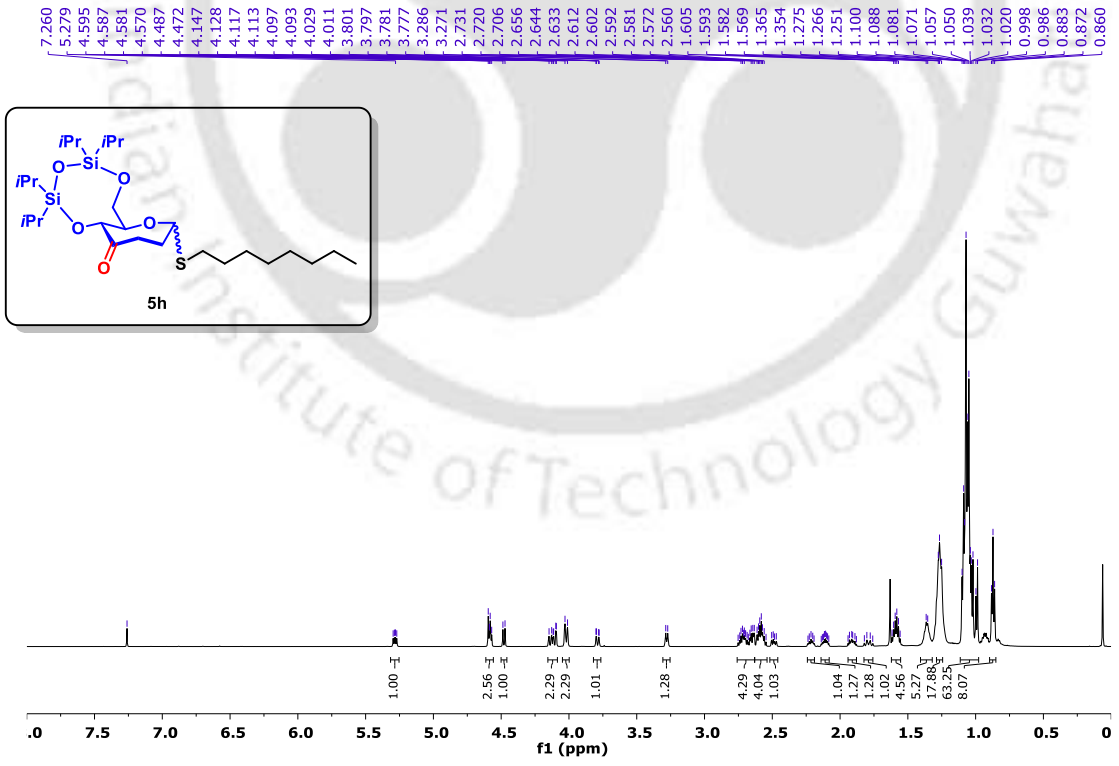

Figure 3.31. *^{1}H NMR of compound **5h** (600 MHz, $CDCl_3$).*

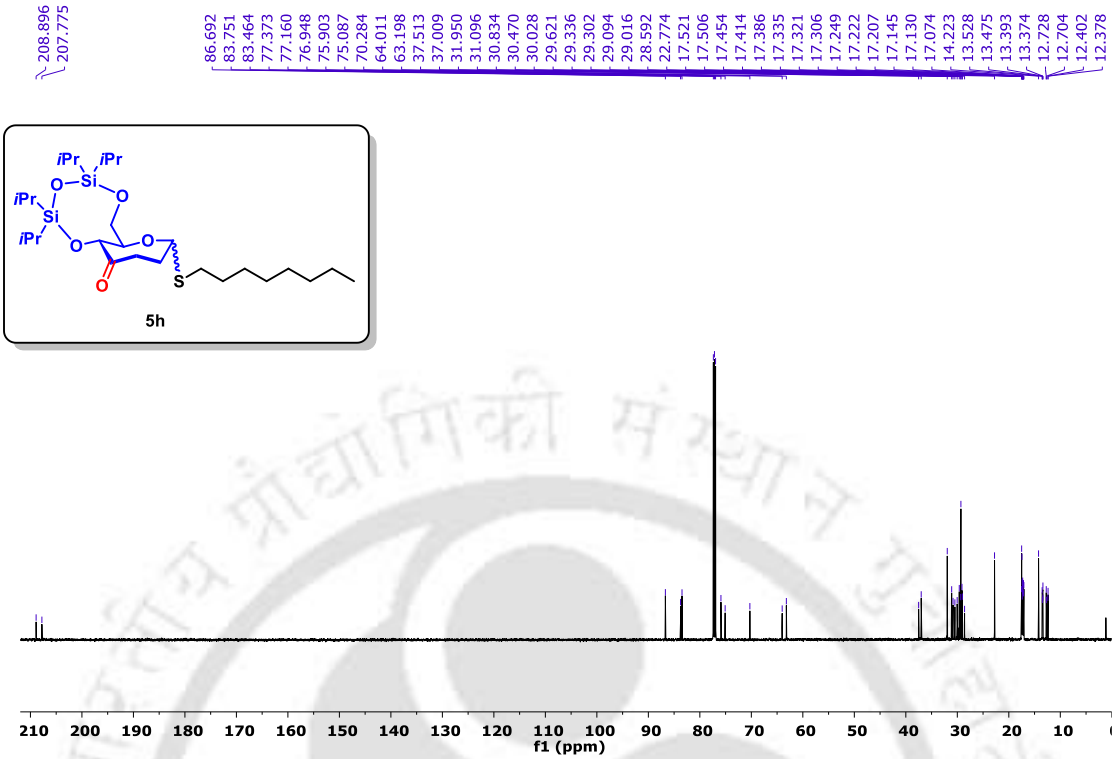

Figure 3.32. *^{13}C NMR of compound **5h** (151 MHz, $CDCl_3$).*

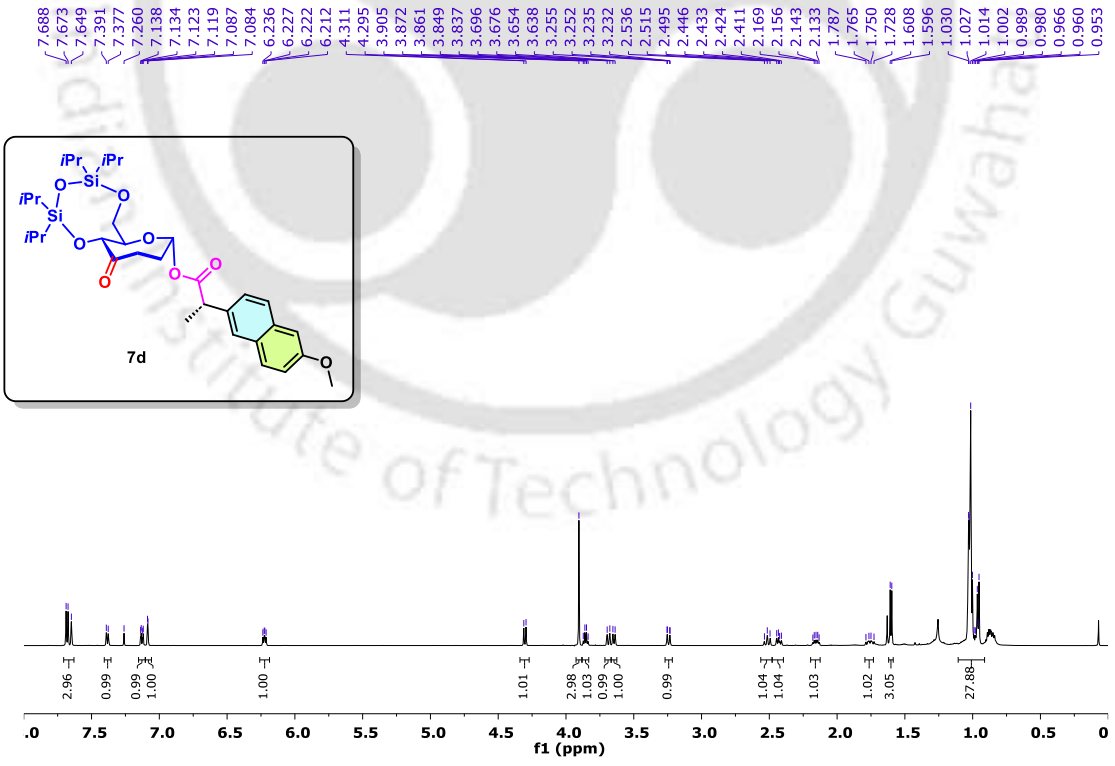

Figure 3.33. *^{1}H NMR of compound **7d** (600 MHz, $CDCl_3$).*

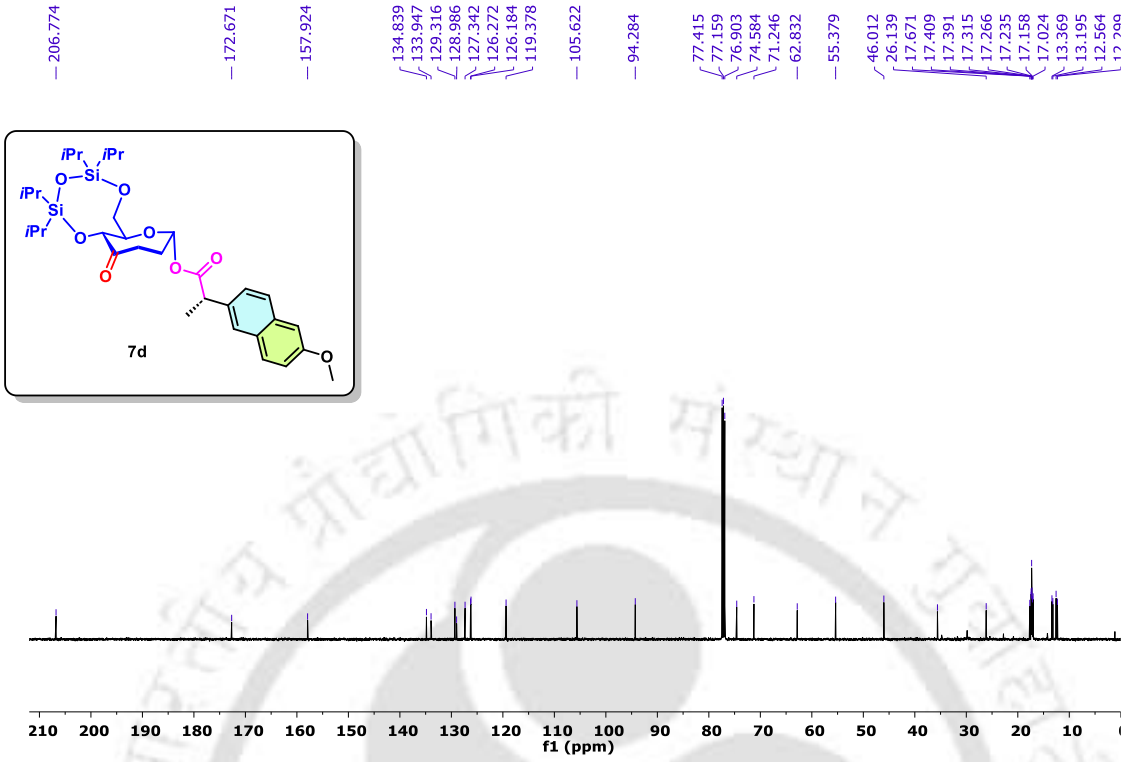

Figure 3.34. *^{13}C NMR of compound **7d** (126 MHz, $CDCl_3$).*

3.8. SC-XRD data of 3y

The ORTEP diagram with an ellipsoid of 30% probability.

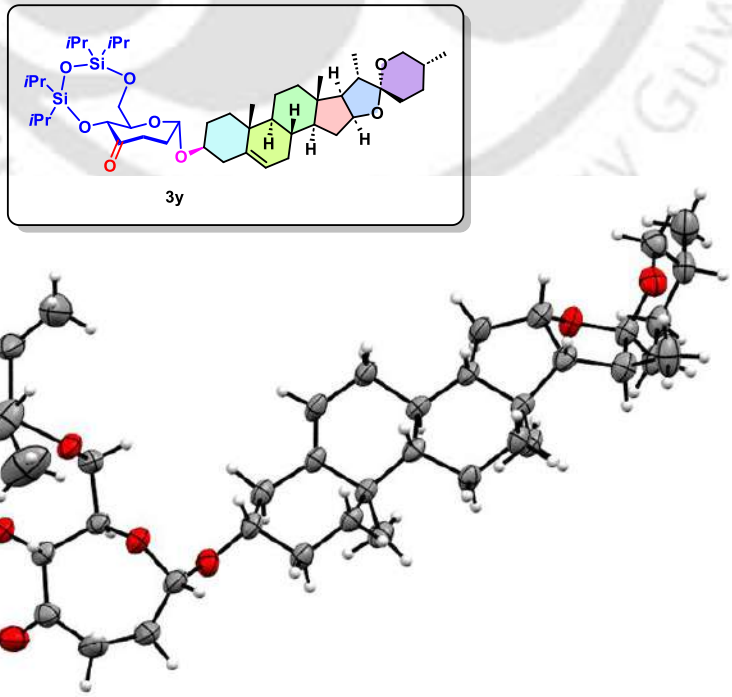

Table 3.5: Crystal parameters and refinement data of **3y**

Parameters	Substrate 3y
Formula	$C_{46}H_{78}O_8Si_2$
Fw	815.2920
Crystal system	monoclinic
Space group	*'P 21'*
a/Å	8.1938(5)
b/Å	9.2358(6)
c/Å	31.5352(19)
α/°	90.00
β/°	97.349(2)
γ/°	90
V/Å^3	2366.9(3)
Z	2
D_c/g cm^{-3}	1.144
μ Mo K_α/mm^{-1}	0.123
F000	892
T/K	295(2)
θ max.	25.65
Total no. of reflections	44827
Independent reflections	8315
Observed reflections	4977
Parameters refined	517
R_1, I > 2σ(I)	0.0657
wR_2, I > 2σ(I)	0.1541
GOF (F^2)	1.086
CCDC No.	2479075

Chapter 4

Triple Role of Proton Sponge (DMAN) in the Palladium-Catalyzed Direct Stereoselective Synthesis of *C*-Aryl Glycosides from Glycals

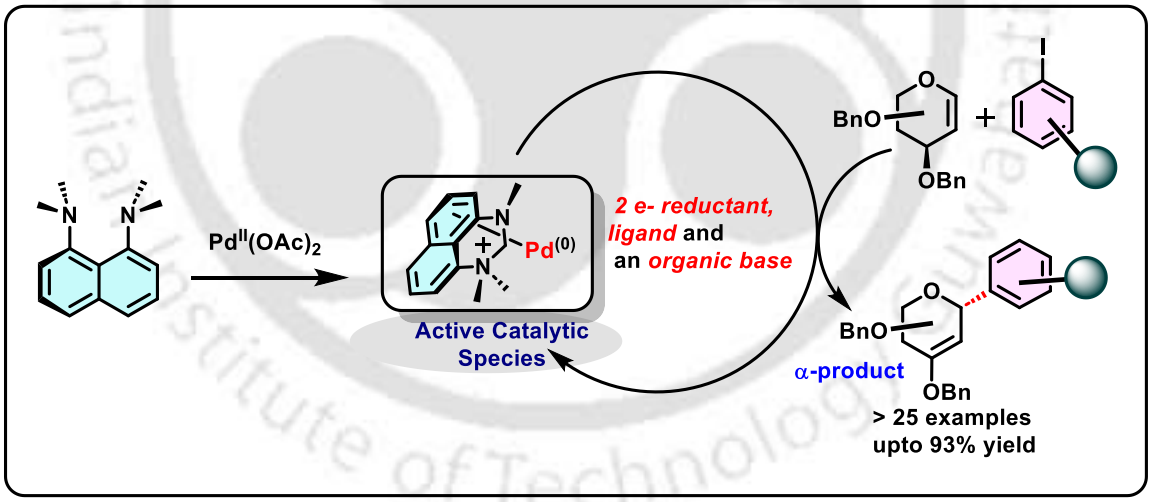

(*Org. Lett.* **2024**, *26*, 3563−3568)

4.1. Introduction

4.1.1. Importance of *C*-aryl glycosides

Carbohydrate motifs featuring a carbon-carbon glycosidic linkage between the aglycone carbon and the anomeric carbon of the sugar unit are known as *C*-glycosides.[1] Among *C*-glycosides, *C*-aryl glycosides are notable for their diverse bioactivities and synthetic utility, such as antibiotic and antitumor properties, along with their usefulness as chiral building blocks.[2] Distinct aryl *C*-glycoside motifs are found across a broad spectrum of drugs and biologically significant natural products, including pluramycin A, urdamycinones A-D, angucyclines, dapagliflozin, marmycin A-B, kidamycin, canagliflozin, and ipragliflozin (Figure 4.1).[3-5] Numerous synthetic *C*-aryl glycosides have recently gained approval as SGLT1/SGLT2 inhibitors for treating type 2 diabetes.[6] Additionally, pluramycin A, an antibacterial and antitumor antibiotic derived from *Streptomyces pluncolorescens*, inhibits both nucleic acid and protein synthesis in intact *E. coli* B cells at concentrations that do not interfere with energy metabolism.[1] Naturally occurring *C*-aryl glycosides predominantly fall into two categories: 2-deoxy and 2-hydroxy-β-aryl *C*-glycosides.[7] Therefore, developing straightforward methods for the stereo- and regioselective synthesis of *C*-aryl glycosides with broad substrate compatibility is highly desirable.

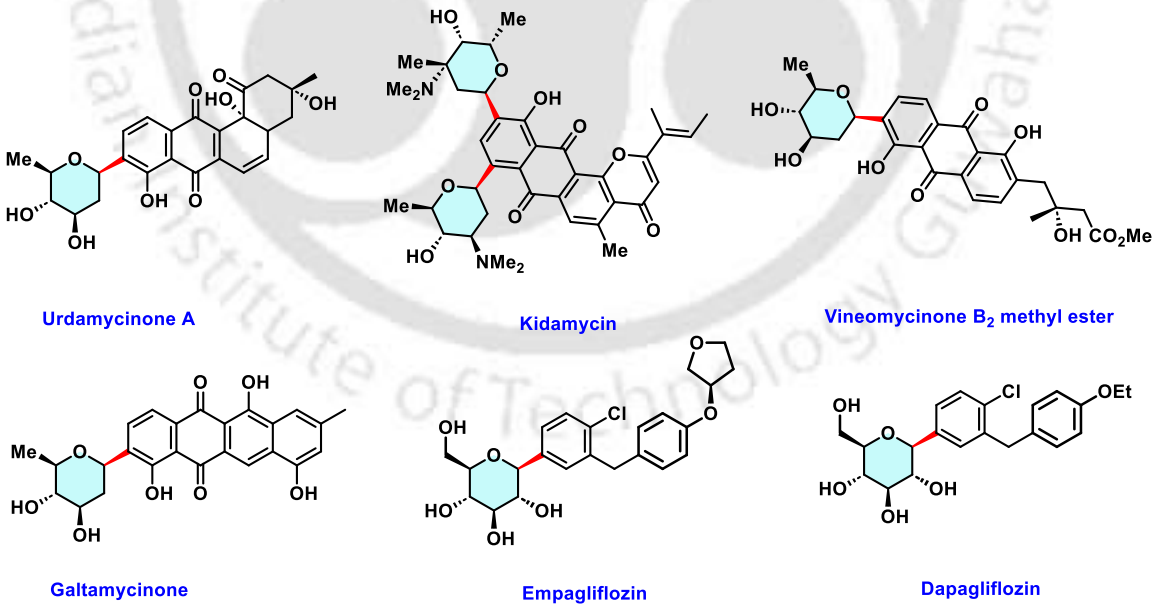

Figure 4.1. Bioactive *C*-aryl glycosides.

4.1.2. Existing methods for synthesizing *C*-aryl glycosides

Few methods enable *C*-aryl glycoside synthesis from glycals with C-3 oxygen retention, but they often require prefunctionalized substrates, directing groups, and exogenous ligands, and show limited substrate scope. Current strategies for constructing *C*-aryl glycosidic linkages include: (1) electrophilic substitution of glycosyl donors with aryl acceptors[8] (2) Lewis acid-mediated *O*-to-*C* migration[9] (3) transition metal-assisted *C*-glycosylation[10, 11], and (4) de novo sugar construction via metathesis[12] and cycloaddition[13]. Among these approaches, transition metal-assisted coupling reactions are highly effective for forming C–C bonds. Primarily, Heck-type arylation reactions of glycals have been developed using a variety of aryl sources, including triarylindium reagents,[14] arylhydrazines,[11] arylboronic acids,[15] aromatic acids, arylzinc reagents[16] and aryl iodides/bromides[17, 18] (Scheme 4.1). Aromatic organoboronic acids stand out among diverse organometallic reagents due to their notable moisture and air resistance, extensive commercial accessibility, and inherent low toxicity.

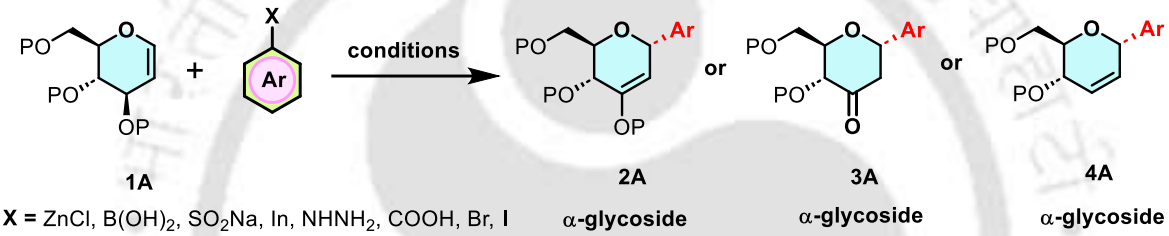

Scheme 4.1. Unlocking *C*-glycosylation with transition metal catalysts.

De la Figuera[19] and Maddaford[20] synthesized 2,3-deoxy-*C*-glycosides via the carbon-Ferrier reaction using glycals and arylboronic acids (Scheme 4.2). However, $Pd(OAc)_2$-catalyzed couplings with arylboronic acids often suffer from substrate ring opening as a major side reaction. To overcome this, recent studies have explored alternative aryl sources for glycal arylation, including aryl carboxylic acids, arylsulfonyl chlorides,[21] and phenylhydrazines[11]. In 2013, Liu *et al.* developed a palladium-mediated *C*-arylation of glycals using phenylhydrazines and later extended the strategy to decarboxylative arylation with aromatic carboxylic acids (Scheme 4.2).[11] In 2015, Kusunuru *et al.* introduced a Pd-catalyzed desulfitative Heck-type coupling method for forming *C*-aryl glycosidic bonds using arylsulfonyl chlorides and glycals bearing good leaving groups (Scheme 4.2).[21]

In 2009, the Xin-Shan Ye group introduced a novel and efficient method for *C*-glycosylation of various glycal donors with several arylboronic acids, marking the first use of $Pd(OAc)_2$ as a catalyst under oxidant-controlled conditions. Using benzoquinone (BQ), DDQ, and $Cu(OAc)_2/O_2$ as oxidants, the reaction selectively yielded ketone, enone, and enol ether type *C*-glycosides, respectively. The coupling reactions exhibited excellent control over both stereoselectivity and regioselectivity (Scheme 4.3).[15]

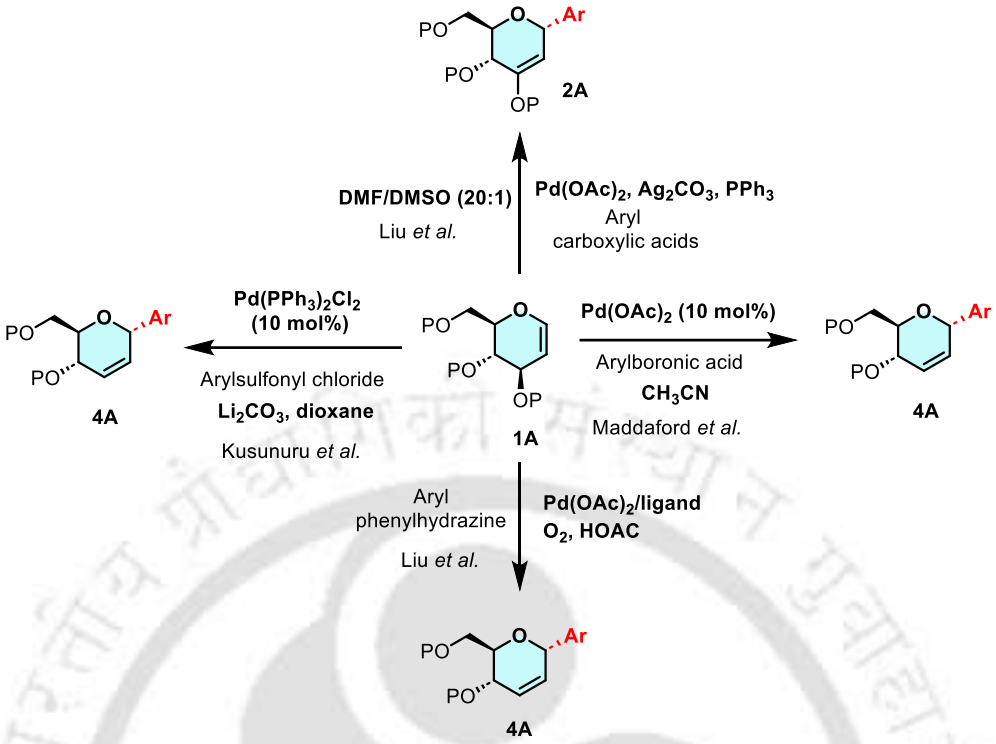

Scheme 4.2. Recent progress in *C*-arylation of glycals via Heck-type reactions.

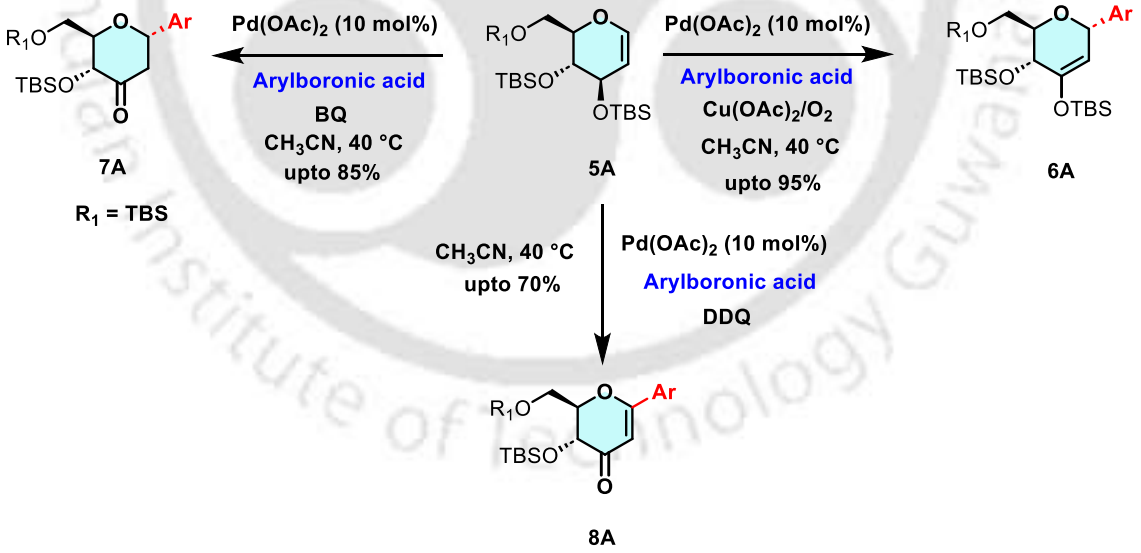

Scheme 4.3. Oxidant-controlled *C*-glycosylation.

In 2014, the same research group developed an innovative "ring-opening-ring-closing" approach for synthesizing aryl *C*-glycosides. This method utilized nickel-mediated regioselective β-O elimination of glycals through reactions with different arylboronic acids, generating ring-opened intermediates that were subsequently cyclized using Lewis

acids, PhSeCl, protonic acids or NBS to produce a diverse array of *C*-glycosides (Scheme 4.4).[1]

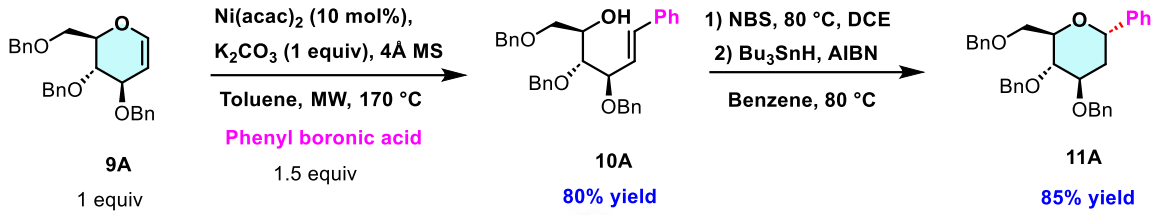

Scheme 4.4. Nickel-catalyzed *C*-glycosylation.

In 2020, Kandasamy and co-workers introduced a robust and selective methodology for synthesizing aryl 2-deoxy-*C*-glycosides, utilizing enone-based donors synthesized from various glycals. Enones prepared from L-rhamnal, D-rhamnal, D-galactal, L-arabinal, and D-glucal participated in regio and stereoselective coupling reactions with arylboronic acids featuring electron-rich and electron-deficient groups, affording enone with *C*-1 aryl in consistently high yields. Additionally, diverse protecting groups in the enone substrates remained intact and showed good compatibility under the coupling conditions (Scheme 4.5).[7]

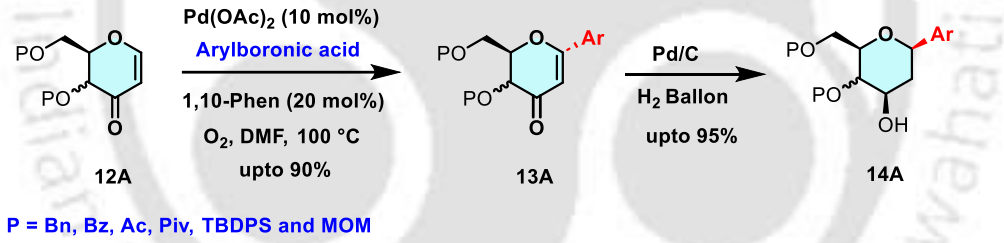

Scheme 4.5. Stereoselective construction of β-Aryl-*C*-glycosides.

4.1.3. Knowledge gap

Palladium-catalyzed functionalization of glycals offers a valuable strategy for synthesizing *C*-aryl glycosides. Despite its potential, Ferrier-type glycosylation remains the predominant pathway in glycal chemistry, often limiting access to alternative C-C bond-forming transformations. Notably, the stereoselective synthesis of *C*-aryl glycosides from glycals while retaining the C-3 oxygen functionality has been explored in limited studies. However, these existing methodologies are constrained by several drawbacks, including the need for substrate prefunctionalization, narrow substrate scope, reliance on directing groups, and the use of exogenous ligands. Moreover, many of these protocols involve toxic and costly reagents, diminishing their practical appeal. In addition, the ligand significantly influences the outcome of Pd-catalyzed reactions. Therefore, developing operationally simple and broadly applicable approaches for the ligand-

controlled stereo- and regioselective construction of *C*-aryl glycosides remains a highly desirable goal.

4.1.4. Purpose and objectives of the chapter

In chapter 1, we have discussed the synthetic applications of proton sponge, a well-known organic superbase. Although not a dominant reagent, it enables mild and selective transformations within organic synthesis. Beyond its practical utility, proton sponge has contributed substantially to developing acid-base theory, hydrogen bonding interactions, general structural principles, and preparative methodologies. Despite its distinctive properties, commercial availability, and affordability, the utilization of this proton sponge in metal catalysis has seen limited progress.

In this chapter, we unveil the triple role of the proton sponge: it acts as a reductant, serves as a ligand precursor to stabilize in situ formed zero-valent palladium, and functions as an organic base. We demonstrate its application in the Heck-type coupling of glycals with aryl iodides, leading to the synthesis of biologically significant aryl *C*-glycosides. Remarkably, this study introduces the first use of a palladium proton sponge complex in coupling reactions. A few β-aryl glycosides were also synthesized using our tri-*tert*-butyl pyridinium salt catalysis.

4.2. Results and discussion

Herein, we report a Pd-catalyzed, stereo- and regioselective strategy for the construction of synthetically challenging *C*-aryl glycosides from aryl iodides and glycals, employing palladium acetate as the catalyst and proton sponge (DMAN) as a multifunctional ligand, base, and reductant. This methodology was further applied to the synthesis of 3-oxo-β-aryl-*C*-glycosides.This method is characterized by the following key features: (i) simple operation, (ii) no use of any air-sensitive ligands, (iii) stereo- and regio-selective because only a single isomer is produced, (iv) Heck coupling reaction goes by the syn β-hydride elimination, and (v) there are no carbon Ferrier products or ring-opening products. Also, the aryl iodides are more easily accessible than the aryl boronic acids. The method allows the direct insertion of the aryl group into the carbohydrate substrate's anomeric center to make the C-C glycosidic bond. It uses readily available aryl halides and glycals as starting materials.

4.2.1. Optimization study

We initiated our investigation into the synthesis of aryl *C*-glycosides by examining the Pd-catalyzed reaction between perbenzylated glucal donor (**1a**) and phenyl iodide (**2a**) in

dry DMF at 80 °C, employing $Pd(OAc)_2$ as the catalyst and DMAN (1,8-bis(dimethylamino)naphthalene) as the base and ligand (Table 4.1).

Table 4.1. Optimization of the reaction conditions[a]

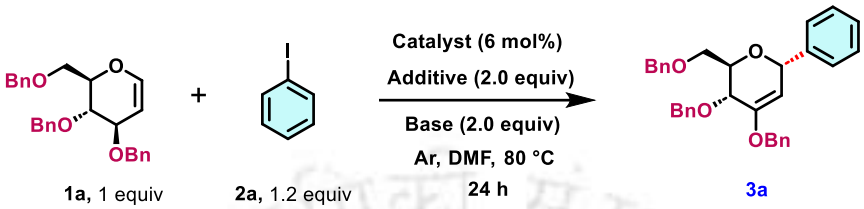

Entry	Catalyst (6 mol%)	Base (2 equ.)	Additive (2 equ.)	Solvent (2 mL)	Temp (°C)	Time (hrs)	Yield of 3a[b] (%)
1	$Pd(OAc)_2$	PS	--------	DMF	80	24	52
2[c]	$Pd(OAc)_2$	PS	Bu_4NCl	DMF	80	24	63
3[d]	$Pd(OAc)_2$	PS	Bu_4NCl	DMF	80	24	77
4	$Pd(OAc)_2$	PS	Bu_4NCl	DMF	80	24	90
5	$Pd(OAc)_2$	DIPEA	Bu_4NCl	DMF	80	24	75
6	$Pd(OAc)_2$	DIPEA	---------	DMF	80	24	25
7	$Pd(OAc)_2$	DBU	Bu_4NCl	DMF	80	48	0
8	$Pd(OAc)_2$	TTBPy	Bu_4NCl	DMF	80	48	0
9	$PdCl_2$	PS	Bu_4NCl	DMF	80	24	80
10	$PdCl_2(PPh_3)_2$	PS	Bu_4NCl	DMF	80	48	0
11[e]	$Pd_2(dba)_3$	Cs_2CO_3	PPh_3	ACN	60	48	30
12[f]	$Pd(OAc)_2$	PS	Bu_4NCl	Toluene	80	24	13
13[g]	$Pd(OAc)_2$	PS	Bu_4NCl	ACN	80	24	20
14[h]	$Pd(OAc)_2$	PS	Bu_4NCl	DCE	80	24	0
15[i]	$Pd(OAc)_2$	PS	Bu_4NCl	THF	80	24	25
16[j]	$Pd(OAc)_2$	PS	Bu_4NCl	DMF	80	24	55

[a]Reaction conditions: Donor **1a** (1.0 equ.), catalyst (0.06 equ.), **2a** (1.2 equ.), base (2.0 equ.), additive (2.0 equ.) at 80 °C in dry solvent (2 ml). [b]Isolated yield. [c]1.0 equ. Bu_4NCl and 1.0 equ. PS, [d]1.0 equ. Bu_4NCl and 2.0 equ. PS were used. [e]In the presence of 1.0 equ. PPh_3. In the presence of dry [f]Toluene, [g]ACN, [h]DCE. [i]THF. [j]10 mol% $Pd(OAc)_2$ was used. PS : Proton Sponge (1,8-Bis(dimethylamino)naphthalene).

Perbenzylated glucal donor (**1a**) was selected due to the electron-donating nature of the benzyl protecting groups, which facilitate the insertion of the aryl-transition metal species. Compared to benzoyl or acetyl moieties, benzyl groups enhance the electron density at the olefinic site, thereby promoting the Pd-catalyzed arylation. Under the initial conditions, the desired glycoside (**3a**) was obtained in 52% yield (Table 4.1, entry 1). The stereochemistry of glycoside **3a** was elucidated through comprehensive 2D NMR

analysis, including ^{1}H NMR and NOE experiments, as well as single-crystal X-ray diffraction (SC-XRD) (see Experimental Section for details). After some initial screenings (Table 4.1, entries 2 & 3), we revealed that the use of 2.0 equivalents each of ammonium salt, tetrabutylammonium chloride (Bu_4NCl), and DMAN (proton sponge) significantly improved the yield to 90% (Table 4.1, entry 4). In contrast, substituting DMAN with the alkylamine DIPEA led to a notable decrease in yield to 75% (Table 4.1, entries 5 & 6). Furthermore, the use of non-nucleophilic bases such as DBU and TTBPy led to no product formation (Table 4.1, entries 7 & 8), highlighting the unique role of DMAN as more than a base in this transformation. To further evaluate the catalytic system, alternative Pd(II) and Pd(0) catalysts, including $PdCl_2$, $PdCl_2(PPh_3)_2$, and $Pd_2(dba)_3$ were tested under these conditions (Table 4.1, entries 9-11). Among the tested catalysts, $PdCl_2$ exhibited comparable efficiency to $Pd(OAc)_2$ in the presence of Bu_4NCl, albeit affording slightly lower yields (Table 4.1, entry 9). Interestingly, no product formation was observed with $PdCl_2(PPh_3)_2$, even in the presence of both TBACl and DMAN (Table 4.1, entry 10), suggesting that Pd(II) may not be the catalytically active species in this transformation. Furthermore, when the reaction was conducted using a catalytic amount of $Pd_2(dba)_3$ and PPh_3, with Cs_2CO_3 as the base in place of DMAN, product **3a** was obtained in only 30% yield (Table 4.1, entry 11). To evaluate the influence of solvent choice on reaction efficiency, the transformation was conducted in toluene, acetonitrile (ACN), dichloroethane (DCE), and THF (Table 4.1, entries 12-15). Each of these solvents led to a substantial decline in product yield, reaffirming DMF as the optimal solvent for this transformation. Moreover, increasing the catalyst loading to 10 mol% unexpectedly led to diminished yield (Table 4.1, entry 16), suggesting that excess palladium may negatively impact the reaction outcome.

4.2.2. Substrate scope

Under the optimized conditions, the protocol was successfully applied to benzyl-protected glucal, galactal, and rhamnal donors using a diverse array of aryl iodides. The resulting aryl *C*-glycosides (**3a-3y**) were obtained in good to excellent yields (73-93%) with complete stereoselectivity across all substrates (Table 4.2). Aryl iodides containing alkyl groups underwent smooth coupling, affording products **3c**, **3d**, **3h**, and **3i** in 85-87% yields within 24 hours (Table 4.2). Gratifyingly, the presence of electron-donating or electron-withdrawing substituents on the aryl iodides had no adverse effect on reaction efficiency, consistently affording the desired glycosides **3b**, **3f**, **3g, 3p** and **3q** in good yields (Table 4.2). Additionally, biphenyl and naphthyl iodides underwent smooth coupling, delivering products **3e** and **3j** in good to excellent yields (Table 4.2). The functional group tolerance of the protocol was further demonstrated by successful coupling with aryl iodides bearing keto, ester, ether, and amide groups, yielding products **3l, 3n, 3r**, **3v,** and **3w**, respectively (Table 4.2).

Table 4.2. Substrate scope of *C*-aryl glycosides[a]

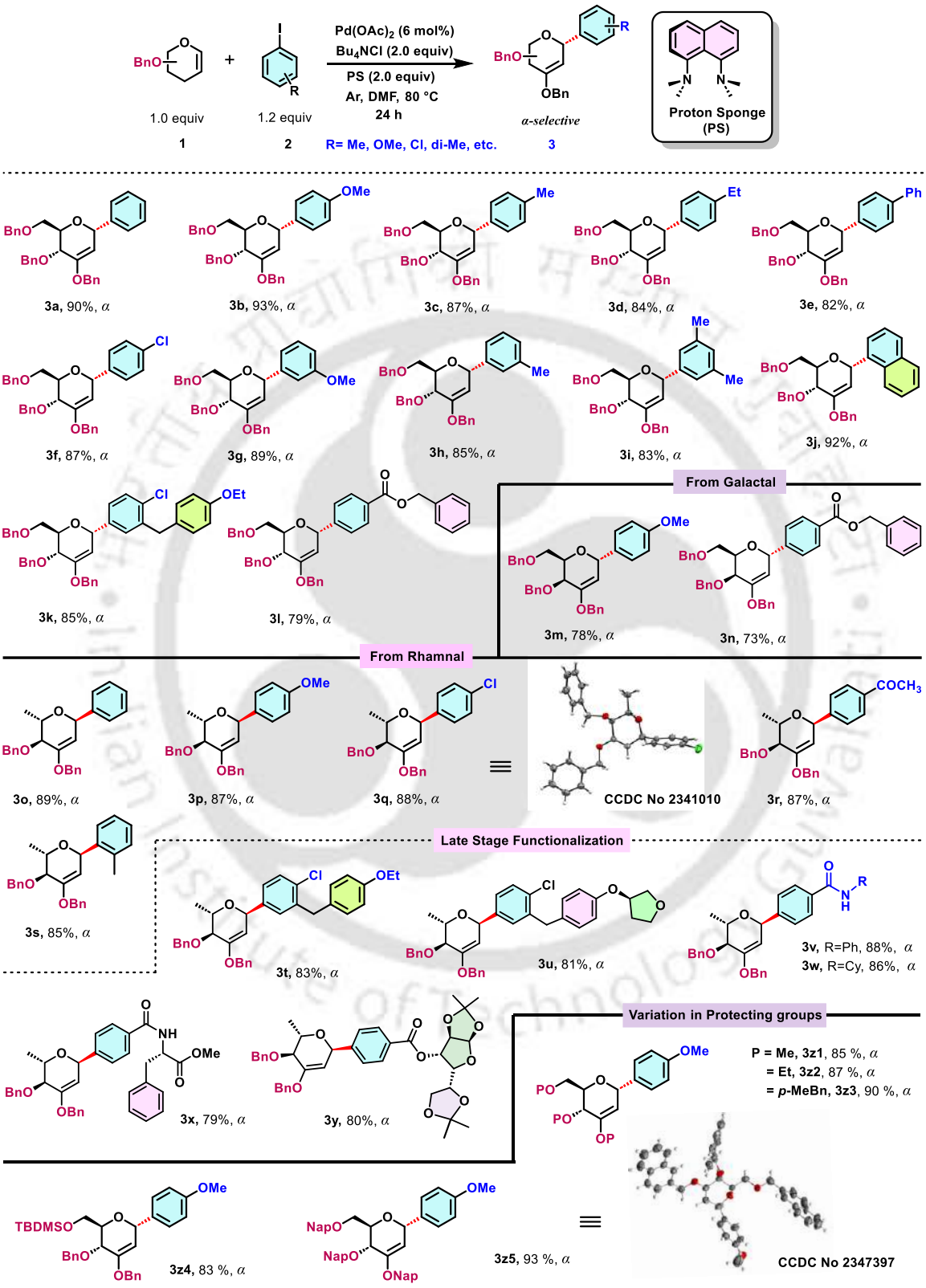

[a]Reaction conditions: glycal (1.0 equiv), aryl iodide (1.2 equiv), $Pd(OAc)_2$ (0.06 equiv), Bu_4NCl (2.0 equiv), and PS (2.0 equiv) in dry DMF (2 ml), 80 °C, 24-48 h under argon atmosphere. [b]Isolated yield.

The applicability of the Pd-catalyzed protocol was further demonstrated through late-stage functionalization of structurally complex, drug-like substrates, yielding aryl glycosides **3k**, **3t**, **3u**, **3x**, and **3y** in 79-85% yields (Table 4.2). Notably, an amino acid-derived aryl iodide furnished **3x** in 79% yield, while the benzoate-linked pseudodisaccharide **3y** was obtained in 80%, highlighting the method's robustness (Table 4.2). All coupling reactions proceeded efficiently, affording the desired glycosides in good to excellent yields with complete stereospecificity, exclusively furnishing the α-anomers.

The protocol's applicability was further demonstrated using glucal substrates bearing armed or disarmed protecting groups, including methyl (Me), ethyl (Et), *p*-methylbenzyl (PMB), silyl, and naphthyl protecting groups. All substrates underwent successful transformation, delivering the corresponding glycosides (Table 4.2, **3z1**-**3z5**) in good to excellent yields and selectivity, with the α-anomer favored. The α-configuration of the aryl glycosides was confirmed by ^{1}H, ^{13}C NMR, NOE, and other spectroscopic techniques, with single-crystal X-ray diffraction (SC-XRD) of **3q** and **3z5** providing unambiguous stereochemical evidence (see Experimental Section for details).

Table 4.3. Synthesis of 3-oxo-β-aryl-*C*-glycosides[a, b]

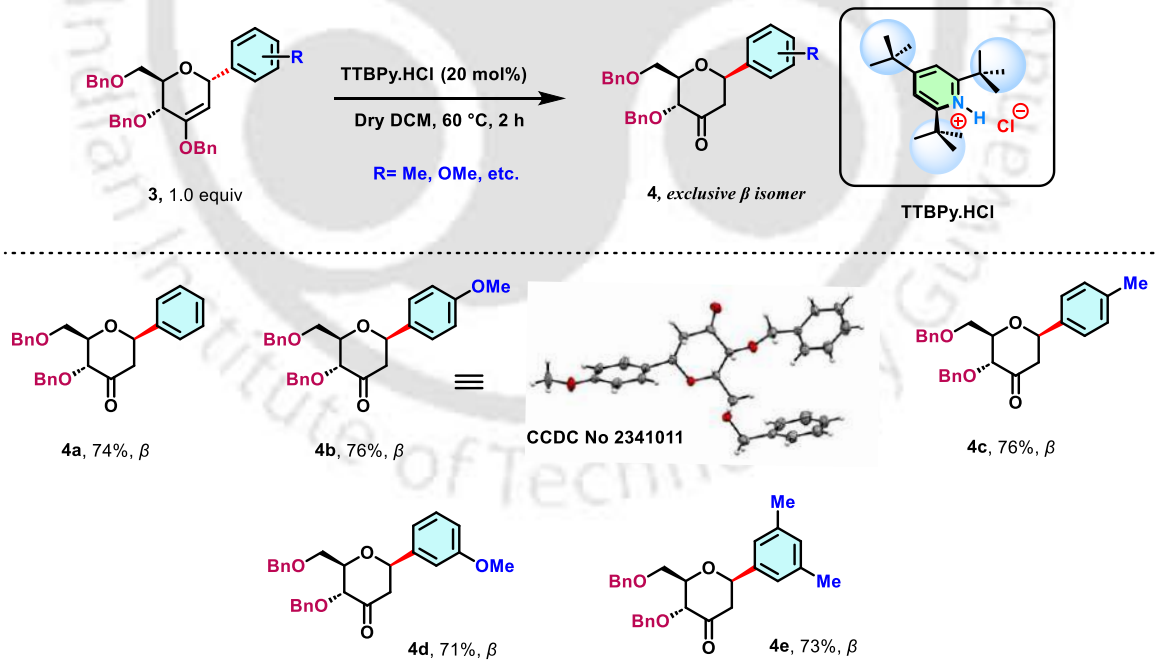

[a]Reaction conditions: *α*-aryl-2-deoxy-*C*-glycosides (1.0 equiv), 2,4,6-tri-*tert*-butyl-pyridium hydrochloride salt (0.2 equiv) in dry DCM (2 ml), 60 °C, 2-4 h under argon atmosphere. [b]Isolated yield.

The *C*-aryl glycosides (**3**) were subjected to mildly Brønsted acidic conditions using sterically bulky 2,4,6-tri-*tert*-butylpyridinium salt in DCM at 60 °C, leading to isomerization and formation of 3-oxo-β-aryl-*C*-glycosides (**4a**-**4e**, Table 4.3) in moderate

to good yields within 2-4 hours. This strategy was subsequently extended to synthesize additional β-*C*-aryl-3-ketoglycosides (Table 4.3). When the same reaction was performed under Lewis-acidic conditions using 20 mol% TMSOTf instead of a Brønsted acid, product **4b** was obtained in 65% yield within just 5 minutes (Scheme 4.6). Interestingly, 5 mol% TMSOTf in dry DCM selectively furnished the ring-opened α,β-unsaturated keto product **5b** in 55% yield (Scheme 4.6). These observations strongly support a ring-opening/ring-closing mechanism for the anomerization process.

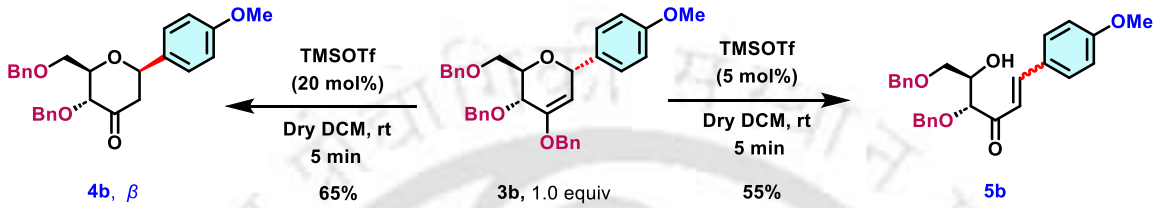

Scheme 4.6. TMSOTf-catalyzed ring-opening isomerization.

4.2.3. Investigation of the mechanism

4.2.3.1. Synthesis of Pd-PS complex

To gain mechanistic insight into the palladium-catalyzed *C*-arylation and specifically evaluate the role of proton sponge (DMAN) in the protocol, a series of control experiments was conducted. Mixing equimolar amounts of $Pd(OAc)_2$ and DMAN in DCM led to the formation of a red-colored charge-transfer complex (Figure 4.2).

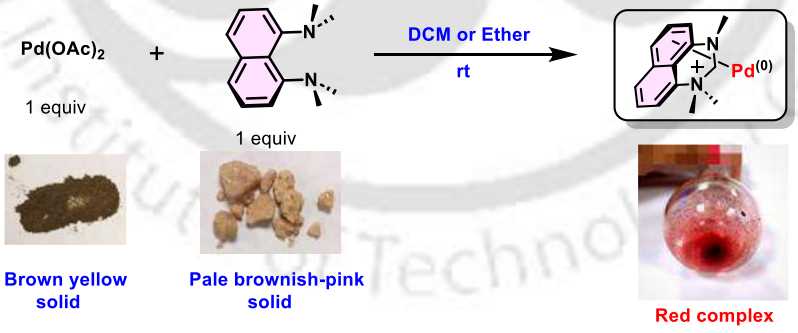

Figure 4.2. Synthesis of the palladium-proton sponge (Pd-PS) complex.

Procedure: In a 5 mL dry flask equipped with a magnetic stir bar, proton sponge (DMAN, 19 mg, 0.089 mmol) was dissolved in dry CH_2Cl_2 (1 mL). To this solution, $Pd(OAc)_2$ (20 mg, 0.089 mmol) in CH_2Cl_2 (2 mL) was added, and the mixture was stirred at room temperature for 10-12 hours. After partial solvent removal under reduced pressure to 0.5 mL, the product was precipitated by slowly adding pentane and collected by filtration, affording a stable red solid in 94% yield (27 mg) (Figure 4.2). HRMS (ESI)

m/z: calcd for $C_{14}H_{17}N_2Pd$ 319.0422; found 319.0425 (Figure 4.3). The mass spectral analysis showcased the formation of the palladium-DMAN adduct with the proper isotopic distribution.

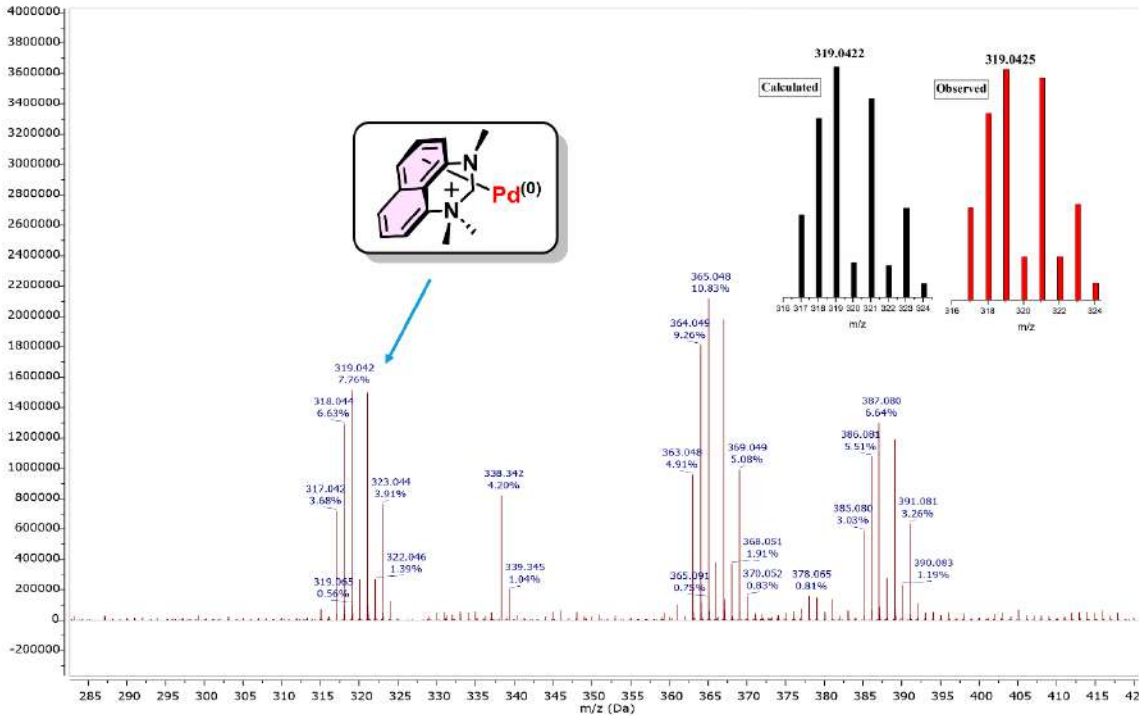

Figure 4.3. HRMS spectrum of Pd-PS complex.

4.2.3.2. The UV-Vis experiments in DCM

UV-Vis absorption spectra of proton sponge (PS), $Pd(OAc)_2$, and the Pd-PS complex (each 1 mM) were recorded in DCM at room temperature using a PerkinElmer Lambda 365+ spectrometer. PS exhibited a sharp absorption band at ~340 nm, while $Pd(OAc)_2$ showed a weak band at ~397 nm. Formation of the Pd-PS complex was accompanied by an intense color change, with characteristic LMCT bands appearing at ~523 nm and ~310 nm (Figure 4.4), consistent with its deep red coloration. The emergence of these new bands indicates a change in the oxidation state of the palladium center, which was further investigated by cyclic voltammetry (CV).

The complex formation was evidenced by the disappearance of the $Pd(OAc)_2$ absorption band at 397 nm and the emergence of a new charge-transfer band with a new λ_{max} at 523 nm (Figure 4.4), confirming successful complex formation.

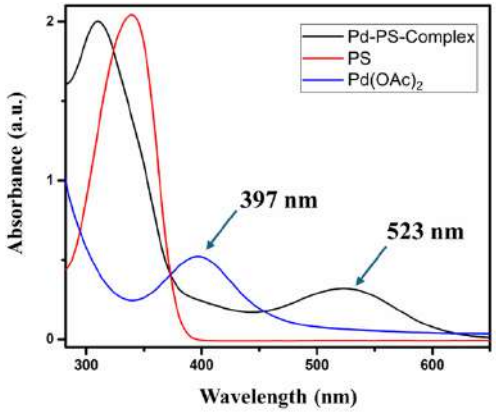

Figure 4.4. UV-Vis spectroscopy of Pd-PS complex.

4.2.3.3. Cyclic voltammetry of Pd-PS complex in DCM

Cyclic voltammograms (CVs) of $Pd(OAc)_2$ and Pd-PS complex were recorded using a VersaSTAT 3 instrument in DCM containing 0.10 M tetrabutylammonium perchlorate ($[(nBu)_4N]ClO_4$) as the supporting electrolyte. The electrochemical cell comprised a glassy carbon working electrode (0.071 cm^2), a platinum wire counter electrode, and an Ag/AgCl reference electrode. Fresh working electrodes were used, and measurements were conducted at 22 °C with a scan rate of 100 mV/s. The concentrations of $Pd(OAc)_2$ and the Pd-PS complex were 1.34 mM and 3.12 mM, respectively. Prior to scanning, solutions were deoxygenated by purging with dry nitrogen for 5-10 minutes. Voltage scans were performed from 0 to negative values, then to positive values, following the IUPAC convention.

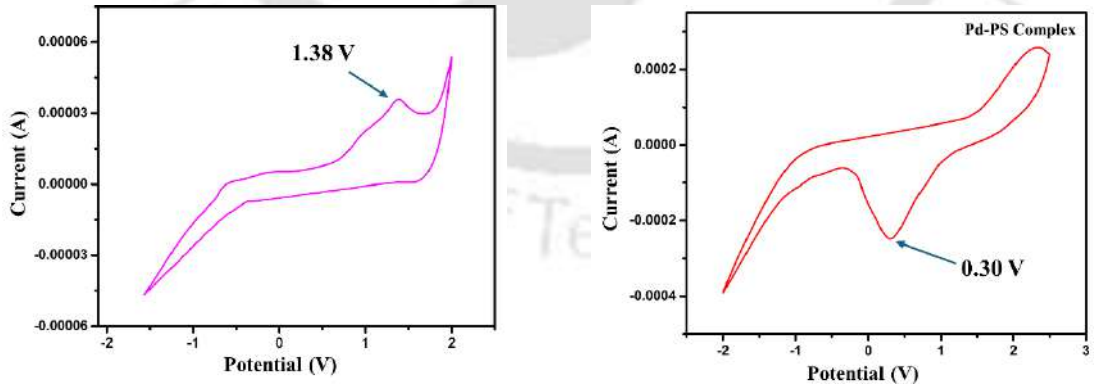

Figure 4.5. Cyclic voltammetry of $Pd(OAc)_2$ and Pd-PS complex.

$Pd(OAc)_2$ exhibited a positive reduction potential at ~1.38 V. Upon addition of proton sponge (PS) in DCM, the resulting Pd-PS complex displayed a significantly lower reduction potential at ~0.30 V. This pronounced shift indicates a change in the oxidation state of the palladium center from +2 to 0 (Figure 4.5).

This analysis revealed the formation of a zero-valent palladium complex, indicated by a peak at E_0 = +0.3 V (Figure 4.5), analogous to the Pd(II) to Pd(0) reduction typically observed with triphenylphosphine.[22]

4.2.3.4. EPR spectroscopy of Pd-PS complex

The EPR spectrum of the Pd-PS complex showed no paramagnetic activity, reaffirming the formation of a zero-valent palladium species (Figure 4.6).

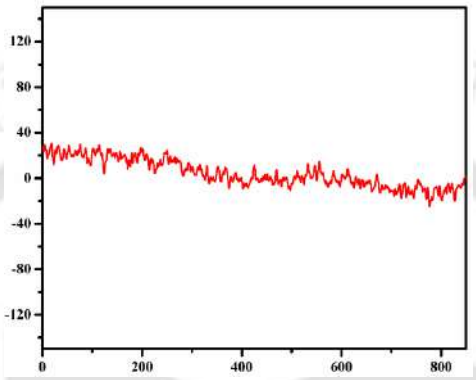

Figure 4.6. EPR spectra of Pd-PS complex.

4.2.3.5. Control experiments

The arylation reaction using the preformed red palladium-DMAN complex yielded a clean product, indicating that this complex functions as the active catalytic species in the transformation (Scheme 4.7). Additionally, high yields obtained with $Pd_2(dba)_3$, a well-known palladium zero-valent catalyst, further support the notion that palladium in the zero-oxidation state is responsible for the catalytic activity under these conditions (Scheme 4.7).

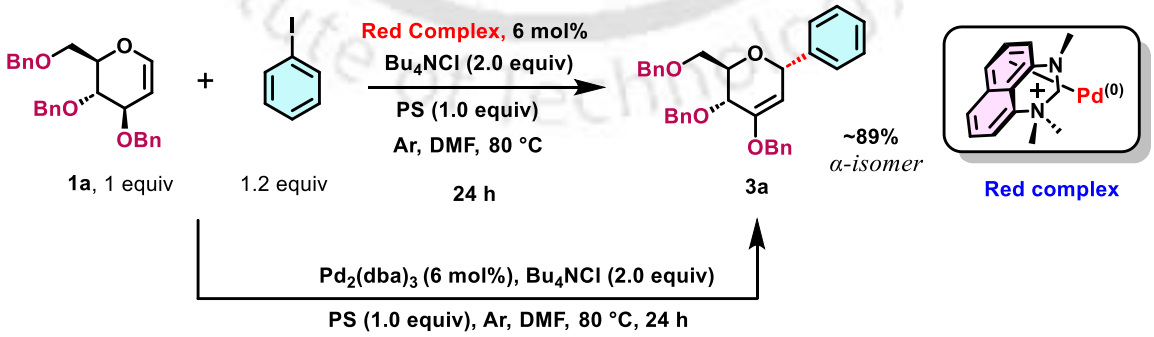

Scheme 4.7. Control experiments.

4.2.4. Gram-scale synthesis

To demonstrate the scalability of the protocol, the coupling reaction between **1a** and **2a** was performed on a 4.80 mmol scale, affording the product **3a** with 89% yield. Notably, glycoside **3a** was exclusively obtained as an α-isomer without any loss in selectivity, even at gram-scale synthesis (Scheme 4.8).

Procedure: $Pd(OAc)_2$ (66 mg, 0.29 mmol, 6.0 mol%) was added to a screw-capped vial equipped with a magnetic stir bar and suspended in dry DMF (15 mL). Under an argon atmosphere, proton sponge (2.1 g, 9.6 mmol, 2.0 equiv), iodobenzene **2a** (0.65 mL, 5.8 mmol, 1.2 equiv), donor **1a** (2.0 g, 4.8 mmol, 1.0 equiv), and Bu_4NCl (2.7 g, 9.6 mmol, 2.0 equiv) were added sequentially. The reaction mixture was stirred at 80 °C in an oil bath (610 rpm) for 2-24 h. Upon completion (monitored by TLC), the mixture was cooled to room temperature, and the crude mixture was purified by column chromatography on silica gel using EtOAc/hexane containing 1% v/v triethylamine to afford glycoside **3a** with 89% yield (2.1 g).

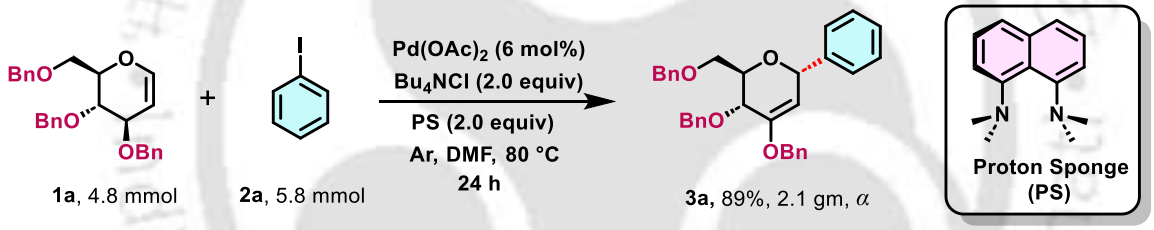

Scheme 4.8. Gram-scale synthesis of compound **3a**.

4.3. Proposed mechanism

Based on the above observations, we propose a mechanism for the current transformation, as illustrated in Scheme 4.9. $Pd(OAc)_2$ reacts with proton sponge (DMAN) to generate an in situ Pd(0) complex **A**, stabilized by the cationic nature of the proton sponge. This Pd(0) species undergoes oxidative addition with aryl iodide to afford the Pd(II) intermediate **B**. Subsequent coordination of intermediate **B** to the glycal enables a regioselective 1,2-migratory insertion, forming the cationic Pd(II) complex **C**, which is stabilized by tetrabutylammonium chloride or the chloride counterion. A β-hydride elimination from complex **C** furnishes the desired *C*-aryl glycoside along with intermediate **D**. Finally, reductive elimination of the Pd(II) species **D**, facilitated by the proton sponge acting as a base, regenerates the catalytically active Pd(0) complex.

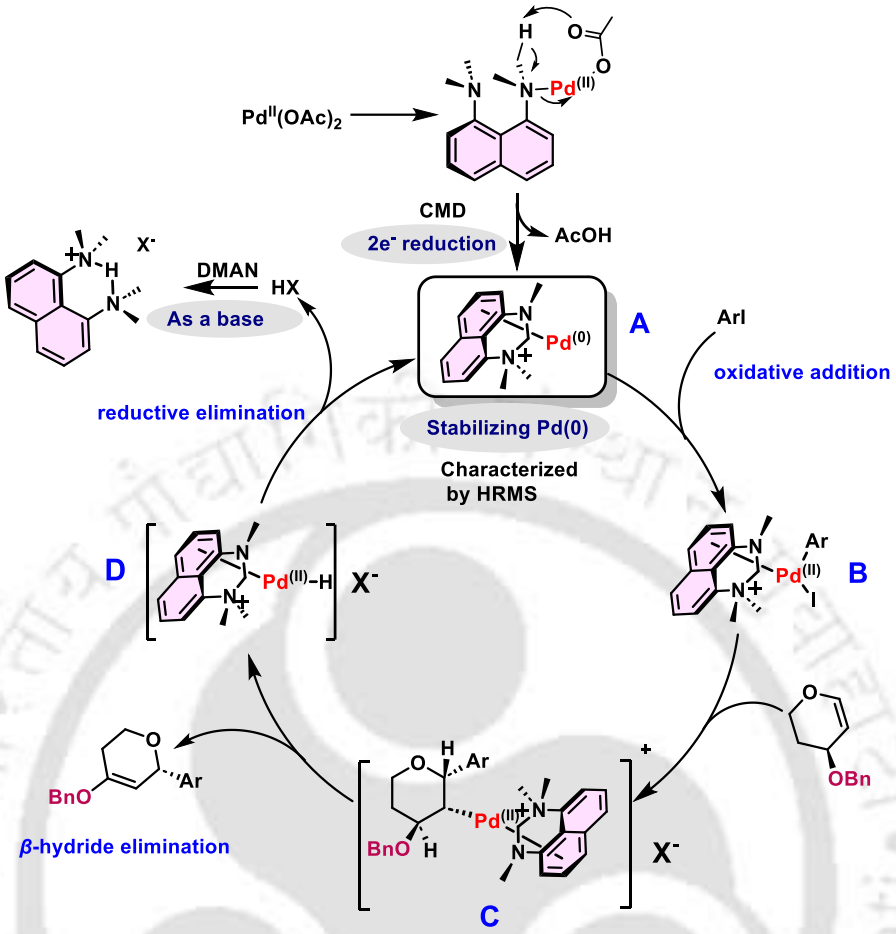

Scheme 4.9. Plausible reaction mechanism.

4.4. Conclusion

In conclusion, we have introduced and demonstrated the triple role of sterically bulky proton sponge (DMAN) for the first time as a reductant of Pd(II) to Pd(0), as an organic base, and reduced DMAN as a stabilizing ligand for Pd(0) in palladium-catalyzed Heck-type coupling of aryl iodides with glycals for the stereoselective synthesis of *C*-aryl glycosides. The Pd-DMAN complex has been thoroughly characterized using various spectroscopic techniques. The robustness of this methodology is exemplified by the efficient synthesis of a range of biologically relevant *C*-aryl glycosides, including successful late-stage modifications of amino acids. Remarkably, this study introduces the first instance of a palladium proton sponge complex being employed in coupling reactions. A few β-aryl glycosides were also synthesized using our tri-*tert*-butyl pyridinium salt catalysis. We anticipate that this palladium–proton sponge system will apply to a broader array of organic transformations, and further exploration is underway in our laboratory.

4.5. Experimental section

4.5.1. Donors and aryl iodides used in the present study

Following donors (**1a-1h**) and aryl iodides (**2a-2s**) were used in this method.

The donors (**1a-1h**) were synthesized by following literature procedures.[23-27] Aryl iodides (**2a-2n**) were commercially available. Compounds (**2o-2s**) were prepared according to literature procedure.[28]

Donors:

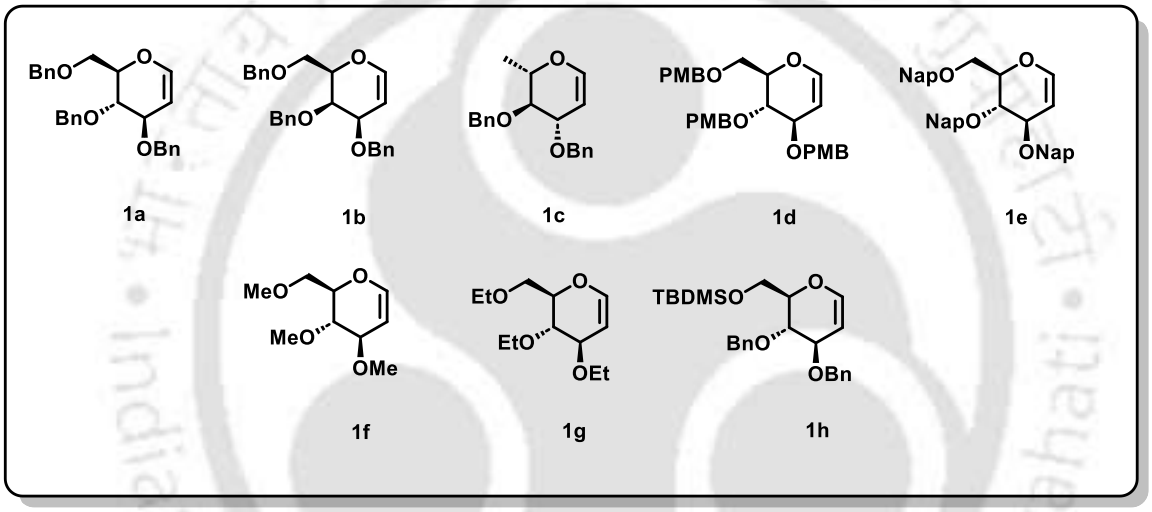

Aryl iodides:

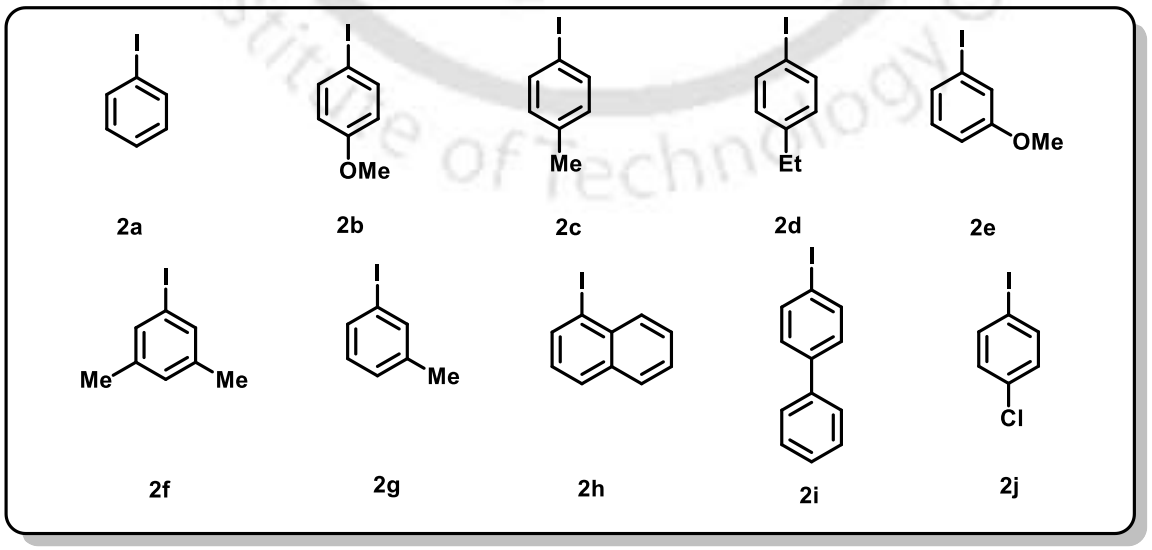

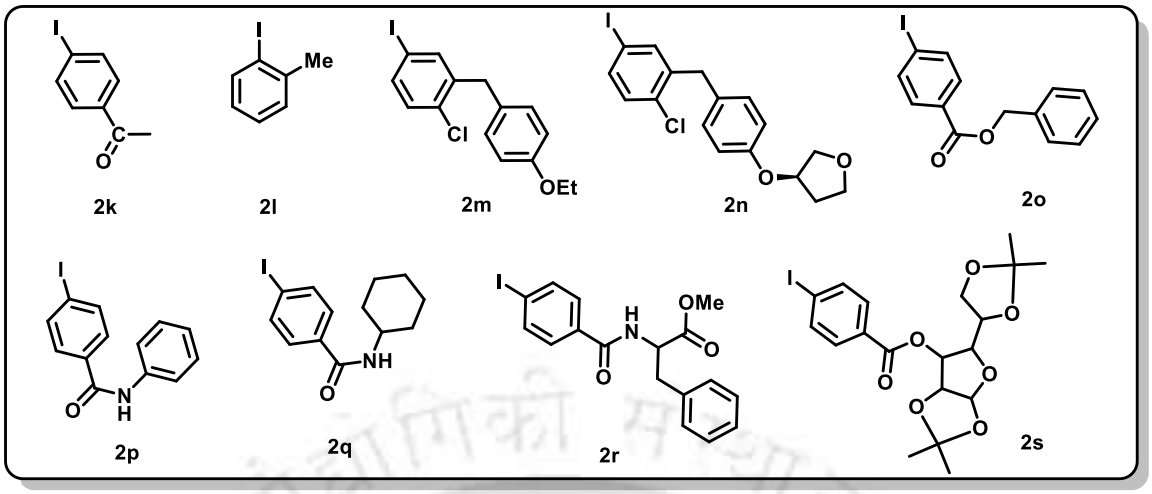

4.5.2. nOe experiments

nOe experiment of 3b

Irradiation of H_1: Upon irradiation of H_1, the enhancement on the H_6 protons (appearing at 3.670 and 3.595 ppm) are found 0.44% and 0.40%, and the enhancement on the H_2 proton (appearing at 5.034 ppm) is found 1.81%. In addition, there is no enhancement on the H_5 proton (appearing at 3.79 ppm). Hence, H_1 is trans to H_5. Thus, the compound is in **alpha** configuration (Figure 4.7).

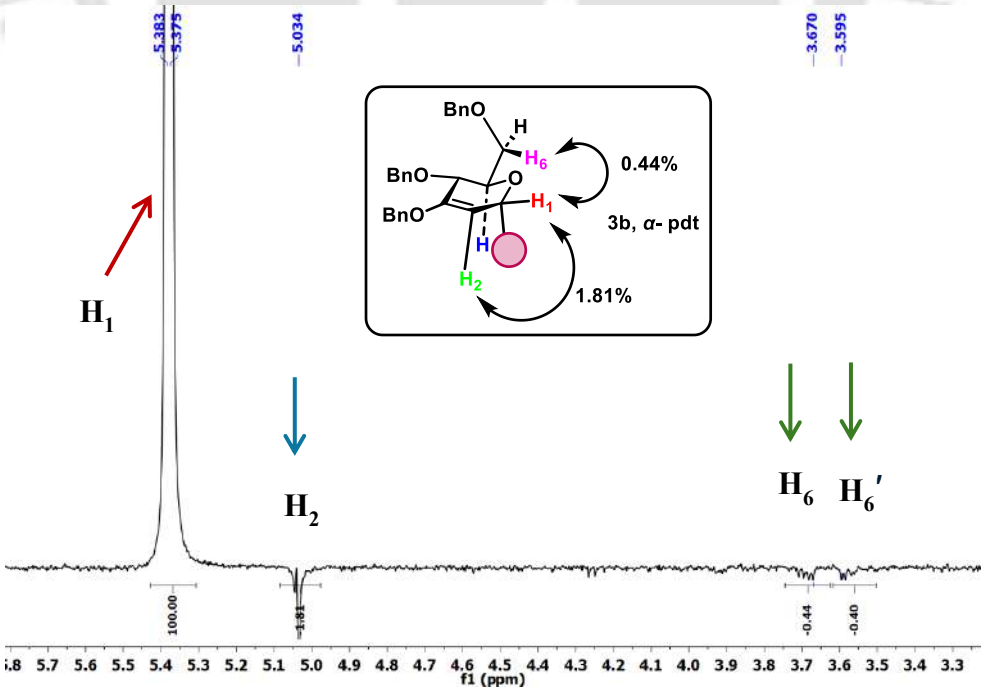

Figure 4.7. *nOe experiment of 3b.*

nOe experiment of 3q

Irradiation of H_1: Upon irradiation of H_1, the enhancement on the CH_3 proton (appearing at 1.265 ppm) is found 1.15% and the enhancement on the H_2 proton (appearing at 4.956 ppm) is found 0.91%. In addition, there is no enhancement on the H_5 proton (appearing at 4.02 ppm). Hence, H_1 is trans to H_5. Thus, the compound is in **alpha** configuration (Figure 4.8).

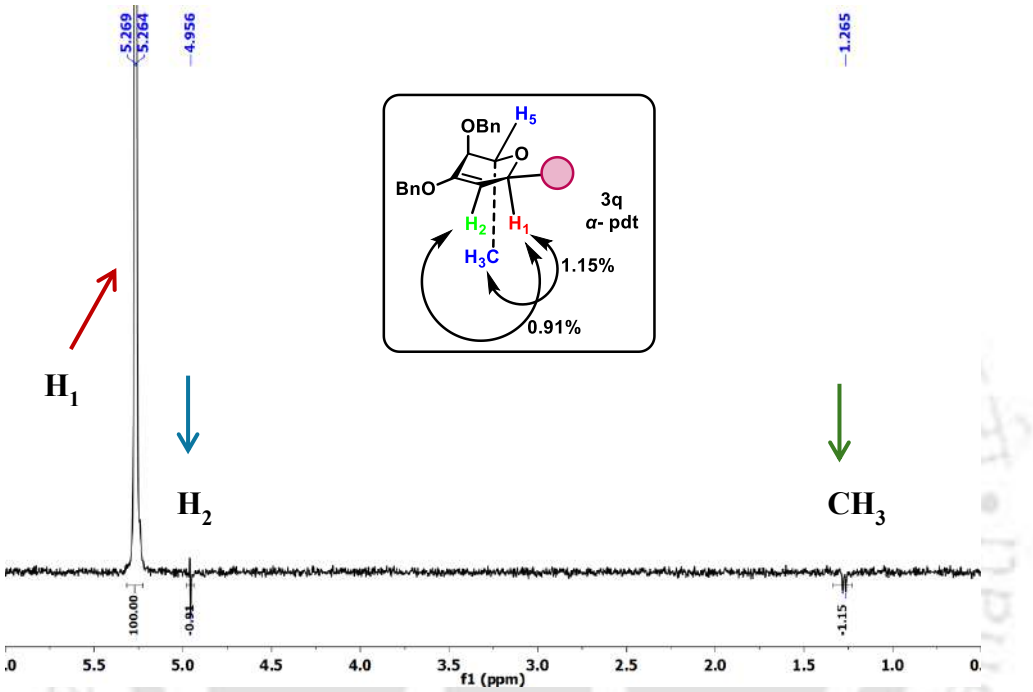

Figure 4.8. *nOe experiment of 3q.*

nOe experiment of 4a

Irradiation of H_1: Upon irradiation of H_1, the enhancement on the H_5 proton (appearing at 3.882 ppm) is found 3.21%, and also the enhancement on the H_2 protons (appearing at 2.796 ppm) is found 2.59%. Hence, H_1 is cis to H_5. Thus, the compound is in **beta** configuration (Figure 4.9).

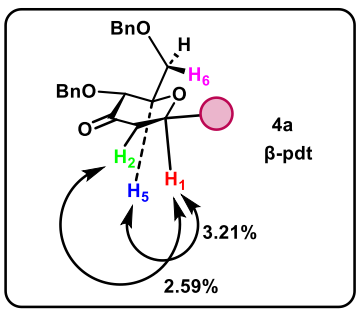

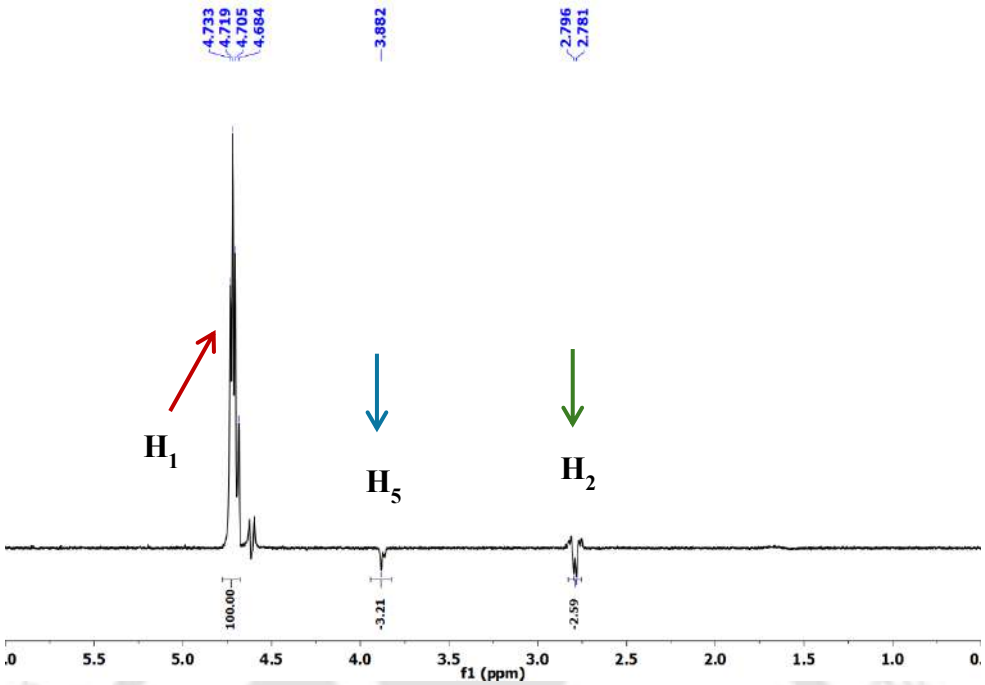

Figure 4.9. *nOe experiment of 4a.*

4.5.3. General procedure 1.1: synthesis of *C*-aryl glycosides

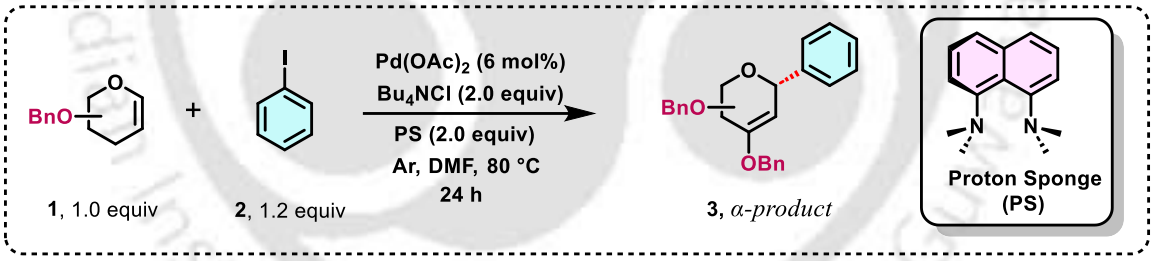

$Pd(OAc)_2$ (0.014 mmol, 6.0 mol%) was added to a screw-capped vial equipped with a magnetic stir bar and suspended in dry DMF (1 mL). Under an argon atmosphere, proton sponge (0.48 mmol, 2.0 equiv), aryl iodide **2** (0.29 mmol, 1.2 equiv), donor **1** (0.24 mmol, 1.0 equiv), and Bu_4NCl (0.48 mmol, 2.0 equiv) were added sequentially. The reaction mixture was stirred at 80 °C in an oil bath (610 rpm) for 2-24 h. Upon completion (monitored by TLC), the mixture was cooled to room temperature, and the crude mixture was purified by column chromatography on silica gel using EtOAc/hexane containing 1% v/v triethylamine to afford the corresponding glycosides **3**. The anomeric configuration of the glycosides was determined by **^{1}H NMR** and **^{13}C NMR** data. **NOE** experiments and **SC-XRD** data further confirmed the **α**-configuration of the glycosides.

Reaction Vial

4.5.4. Spectroscopic data of *C*-aryl glycosides (3a-3z5)

(2R,3R,6S)-3,4-bis(benzyloxy)-2-((benzyloxy)methyl)-6-phenyl-3,6-dihydro-2H-pyran (3a)

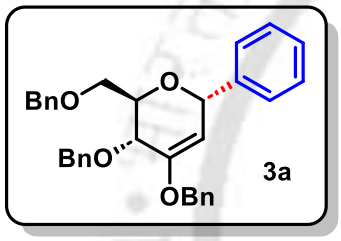

3a was obtained in 90% yield (106.4 mg), as a slightly yellow oil, R_f = 0.5 (Hexane/EtOAc, 9:1, v/v). **^{1}H NMR** (500 MHz, $CDCl_3$) δ 7.46 – 7.35 (m, 6H), 7.34 – 7.23 (m, 14H), 5.36 (s, 1H), 5.03 (d, J = 3.1 Hz, 1H), 4.96 – 4.82 (m, 3H), 4.65 – 4.51 (m, 2H), 4.44 (d, J = 12.1 Hz, 1H), 4.21 (d, J = 6.4 Hz, 1H), 3.92 (dd, J = 9.5, 4.6 Hz, 1H), 3.66 (dd, J = 10.4, 4.7 Hz, 1H), 3.56 (dd, J = 10.4, 3.4 Hz, 1H). **^{13}C NMR** (151 MHz, $CDCl_3$) δ 153.2, 140.7, 138.3, 138.1, 136.8, 128.4, 128.3, 128.2 (128.23, 128.20), 128.1, 127.8 (127.85, 127.83), 127.6, 127.58, 127.3, 98.8, 73.6, 73.5, 73.1, 72.3, 71.3, 69.1, 68.7. **HRMS** (ESI) m/z: $[M+H]^+$ calcd for $C_{33}H_{33}O_4$ 493.2373; found 493.2372.

(2R,3R,6S)-3,4-bis(benzyloxy)-2-((benzyloxy)methyl)-6-(4-methoxyphenyl)-3,6-dihydro-2H-pyran (3b)

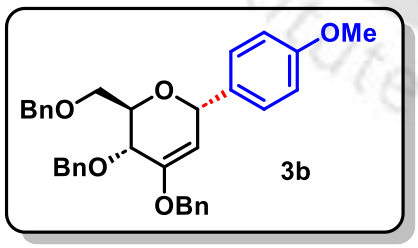

3b was obtained in 93% yield (116.6 mg), as a yellow oil, R_f = 0.3 (Hexane/EtOAc, 9:1, v/v). **^{1}H NMR** (600 MHz, $CDCl_3$) δ 7.43 – 7.35 (m, 4H), 7.35 – 7.28 (m, 7H), 7.25 (dd, J = 12.0, 5.8 Hz, 6H), 6.84 (d, J = 8.4 Hz, 2H), 5.33 (d, J = 2.3 Hz, 1H), 4.99 (d, J = 3.3 Hz, 1H), 4.95 – 4.81 (m, 3H), 4.55 (dd, J = 11.5, 8.6 Hz, 2H), 4.42 (d, J = 12.1 Hz, 1H), 4.21 (d, J = 6.6 Hz, 1H), 3.87 (dd, J = 10.0, 4.4 Hz, 1H), 3.78 (s, 3H), 3.64 (dd, J = 10.4, 4.6 Hz, 1H), 3.53 (dd, J = 10.4, 3.4 Hz, 1H). **^{13}C NMR** (151 MHz, $CDCl_3$) δ 159.3, 153.3, 138.4, 138.1, 136.9, 132.8, 129.6, 128.5, 128.3, 128.2 (128.26, 128.24), 127.9, 127.8, 127.6 (127.62, 127.60), 127.4, 113.5, 99.0, 73.5, 73.3, 73.2, 71.9, 71.4, 69.1, 68.8, 55.3. **HRMS** (ESI) m/z: $[M+H]^+$ calcd for $C_{34}H_{35}O_5$ 523.2479; found 523.2486.

(2R,3R,6S)-3,4-bis(benzyloxy)-2-((benzyloxy)methyl)-6-(p-tolyl)-3,6-dihydro-2H-pyran (3c)

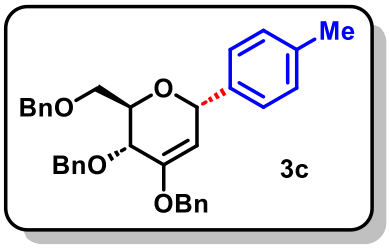

3c was obtained in 87% yield (106 mg), as a colorless oil, R_f = 0.5 (Hexane/EtOAc, 9:1, v/v). **^{1}H NMR** (500 MHz, $CDCl_3$) δ 7.38 (dd, J = 17.4, 7.4 Hz, 4H), 7.34 – 7.28 (m, 7H), 7.28 – 7.21 (m, 6H), 7.12 (d, J = 7.7 Hz, 2H), 5.34 (d, J = 2.4 Hz, 1H), 5.01 (d, J = 3.4 Hz, 1H), 4.98 – 4.81 (m, 3H), 4.55 (dd, J = 11.7, 6.7 Hz, 2H), 4.43 (d, J = 12.1 Hz, 1H), 4.22 (d, J = 6.4 Hz, 1H), 3.90 (dd, J = 10.3, 4.4 Hz, 1H), 3.65 (dd, J = 10.4, 4.7 Hz, 1H), 3.54 (dd, J = 10.4, 3.5 Hz, 1H), 2.33 (s, 3H). **^{13}C NMR** (126 MHz, $CDCl_3$) δ 153.2, 138.4, 138.1, 137.7, 137.6, 136.9, 128.9, 128.4, 128.3, 128.2, 128.1 (128.19, 128.17), 127.8 (127.87, 127.83), 127.5 (127.59, 127.56), 127.4, 99.0, 73.5, 73.4, 73.2, 72.1, 71.4, 69.1, 68.9, 21.1. **HRMS** (ESI) m/z: $[M+H]^+$ calcd for $C_{34}H_{35}O_4$ 507.2530; found 507.2531.

(2R,3R,6S)-3,4-bis(benzyloxy)-2-((benzyloxy)methyl)-6-(4-ethylphenyl)-3,6-dihydro-2H-pyran (3d)

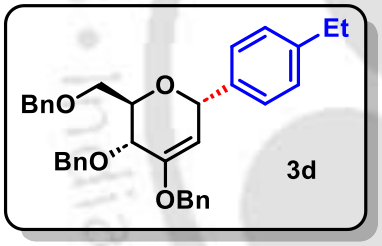

3d was obtained in 84% yield (105 mg), as a yellow oil, R_f = 0.6 (Hexane/EtOAc, 9:1, v/v). **^{1}H NMR** (400 MHz, $CDCl_3$) δ 7.38 (q, J = 7.9 Hz, 4H), 7.35 – 7.28 (m, 7H), 7.27 – 7.19 (m, 6H), 7.14 (d, J = 8.0 Hz, 2H), 5.35 (d, J = 3.0 Hz, 1H), 5.02 (d, J = 3.5 Hz, 1H), 4.95 – 4.81 (m, 3H), 4.55 (dd, J = 11.7, 3.8 Hz, 2H), 4.42 (d, J = 12.1 Hz, 1H), 4.22 (d, J = 6.6 Hz, 1H), 3.97 – 3.86 (m, 1H), 3.65 (dd, J = 10.4, 4.6 Hz, 1H), 3.55 (dd, J = 10.4, 3.6 Hz, 1H), 2.62 (q, J = 7.6 Hz, 2H), 1.21 (t, J = 7.6 Hz, 3H). **^{13}C NMR** (126 MHz, $CDCl_3$) δ 153.1, 143.9, 138.4, 138.1, 137.9, 136.8, 128.4, 128.2 (128.28, 128.20), 128.18, 127.8, 127.7 (127.79, 127.71), 127.5 (127.57, 127.54), 127.3, 99.0, 73.4 (73.49, 73.46), 73.1, 72.1, 71.3, 69.0, 68.8, 28.5, 15.5. **HRMS** (ESI) m/z: $[M+H]^+$ calcd for $C_{35}H_{37}O_4$ 521.2686; found 521.2697.

(2R,3R,6S)-6-([1,1'-biphenyl]-4-yl)-3,4-bis(benzyloxy)-2-((benzyloxy)methyl)-3,6-dihydro-2H-pyran (3e)

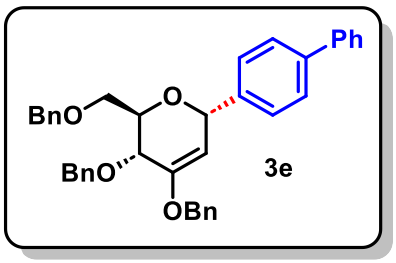

3e was obtained in 82% yield (112 mg), as a white solid, R_f = 0.3 (Hexane/EtOAc, 9:1, v/v), mp 80–82 °C. **^{1}H NMR** (600 MHz, $CDCl_3$) δ 7.56 (d, J = 7.3 Hz, 2H), 7.53 (d, J = 8.2 Hz, 2H), 7.48 (d, J = 8.1 Hz, 2H), 7.39 (dt, J = 14.8, 7.6 Hz, 6H), 7.35 – 7.28 (m, 6H), 7.27 – 7.20 (m, 6H), 5.41 (d, J = 2.9 Hz, 1H), 5.05 (d, J = 3.5 Hz, 1H), 4.96 – 4.84 (m, 3H), 4.57 (dd, J = 11.6, 9.5 Hz, 2H), 4.44 (d, J = 12.1 Hz, 1H),

4.24 (d, J = 6.0 Hz, 1H), 3.94 (dt, J = 6.5, 4.4 Hz, 1H), 3.67 (dd, J = 10.4, 4.8 Hz, 1H), 3.57 (dd, J = 10.4, 3.6 Hz, 1H). **^{13}C NMR** (151 MHz, $CDCl_3$) δ 153.3, 140.8 (140.88, 140.80), 139.8, 138.4, 138.1, 136.8, 128.7, 128.5 (128.57, 128.50), 128.3, 128.2 (128.24, 128.20), 127.8, 127.6, 127.5, 127.3, 127.2, 127.1, 127.0, 98.8, 73.5, 73.3, 73.2, 72.4, 71.4, 69.1, 68.8. **HRMS** (ESI) m/z: $[M+H]^+$ calcd for $C_{39}H_{37}O_4$ 569.2686; found 569.2699.

(2R,3R,6S)-3,4-bis(benzyloxy)-2-((benzyloxy)methyl)-6-(4-chlorophenyl)-3,6-dihydro-2H-pyran (3f)

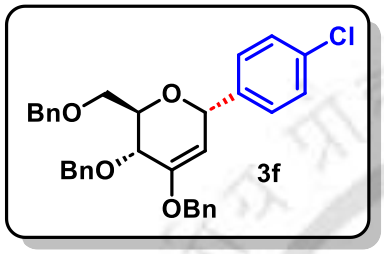

3f was obtained in 87% yield (110 mg), as a colorless oil, R_f = 0.5 (Hexane/EtOAc, 9:1, v/v). **^{1}H NMR** (600 MHz, $CDCl_3$) δ 7.38 (q, J = 7.9 Hz, 4H), 7.33 (dd, J = 7.3, 5.4 Hz, 4H), 7.26 (m, 11H), 5.32 (d, J = 3.1 Hz, 1H), 4.97 (d, J = 3.6 Hz, 1H), 4.93 – 4.81 (m, 3H), 4.55 (dd, J = 11.7, 5.6 Hz, 2H), 4.43 (d, J = 12.1 Hz, 1H), 4.19 (d, J = 6.4 Hz, 1H), 3.85 (dt, J = 6.4, 4.6 Hz, 1H), 3.64 (dd, J = 10.4, 4.9 Hz, 1H), 3.53 (dd, J = 10.4, 3.6 Hz, 1H). **^{13}C NMR** (151 MHz, $CDCl_3$) δ 153.5, 139.3, 138.2, 138.0, 136.6, 133.6, 129.4, 128.5, 128.3 (128.37, 128.33), 128.2, 128.1, 127.8 (127.88, 127.84), 127.6 (127.64, 127.63), 127.3, 98.3, 73.6, 73.2, 72.9, 72.4, 71.2, 69.1, 68.7. **HRMS** (ESI) m/z: $[M+H]^+$ calcd for $C_{33}H_{32}ClO_4$ 527.1984; found 527.1986.

(2R,3R,6S)-3,4-bis(benzyloxy)-2-((benzyloxy)methyl)-6-(3-methoxyphenyl)-3,6-dihydro-2H-pyran (3g)

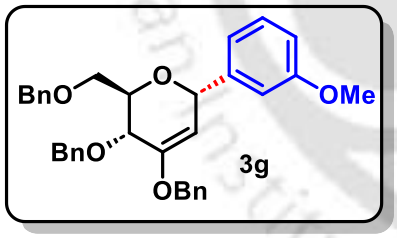

3g was obtained in 89% yield (112 mg), as a yellow oil, R_f = 0.4 (Hexane/EtOAc, 9:1, v/v). **^{1}H NMR** (400 MHz, $CDCl_3$) δ 7.38 (q, J = 7.8 Hz, 4H), 7.34 – 7.28 (m, 5H), 7.29 – 7.18 (m, 7H), 6.99 (dd, J = 8.2, 4.9 Hz, 2H), 6.81 (dd, J = 8.1, 2.2 Hz, 1H), 5.35 (d, J = 3.2 Hz, 1H), 5.04 (d, J = 3.6 Hz, 1H), 4.96 – 4.80 (m, 3H), 4.55 (d, J = 10.9 Hz, 2H), 4.44 (d, J = 12.1 Hz, 1H), 4.27 – 4.16 (m, 1H), 3.93 (dt, J = 6.6, 4.5 Hz, 1H), 3.74 (s, 3H), 3.66 (dd, J = 10.4, 4.9 Hz, 1H), 3.57 (dd, J = 10.4, 3.7 Hz, 1H). **^{13}C NMR** (126 MHz, $CDCl_3$) δ 159.6, 153.3, 142.5, 138.4, 138.1, 136.8, 129.1, 128.5, 128.3, 128.2, 128.1, 127.8 (127.89, 127.85), 127.6, 127.5, 127.3, 120.3, 113.6, 113.3, 98.7, 73.5, 73.4, 73.2, 72.4, 71.4, 69.1, 68.9, 55.2. **HRMS** (ESI) m/z: $[M+H]^+$ calcd for $C_{34}H_{35}O_5$ 523.2479; found 523.2481.

(2R,3R,6S)-3,4-bis(benzyloxy)-2-((benzyloxy)methyl)-6-(m-tolyl)-3,6-dihydro-2H-pyran (3h)

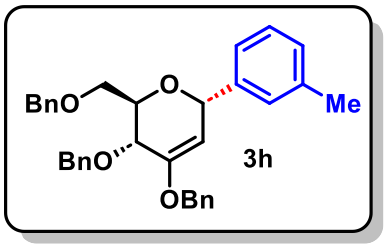

3h was obtained in 85% yield (103.3 mg) as a colorless oil, R_f = 0.6 (Hexane/EtOAc, 9:1, v/v). **^{1}H NMR** (600 MHz, $CDCl_3$) δ 7.42 – 7.36 (m, 4H), 7.34 – 7.27 (m, 6H), 7.26 – 7.23 (m, 5H), 7.22 – 7.17 (m, 3H), 7.08 (d, J = 6.5 Hz, 1H), 5.33 (d, J = 2.9 Hz, 1H), 5.01 (d, J = 3.5 Hz, 1H), 4.95 – 4.82 (m, 3H), 4.56 (t, J = 11.6 Hz, 2H), 4.43 (d, J = 12.1 Hz, 1H), 4.21 (d, J = 6.4 Hz, 1H), 3.99 – 3.89 (m, 1H), 3.66 (dd, J = 10.4, 4.8 Hz, 1H), 3.56 (dd, J = 10.4, 3.7 Hz, 1H), 2.31 (s, 3H). **^{13}C NMR** (151 MHz, $CDCl_3$) δ 153.0, 140.6, 138.4, 138.1, 137.8, 136.8, 128.7, 128.6, 128.4, 128.3, 128.2, 128.1, 128.1, 127.8 (127.83, 127.80), 127.5 (127.58, 127.56), 127.3, 125.1, 99.0, 73.6, 73.4, 73.1, 72.3, 71.4, 69.0, 68.8, 21.4. **HRMS** (ESI) m/z: $[M+H]^+$ calcd for $C_{34}H_{35}O_4$ 507.2530; found 507.2531.

(2R,3R,6S)-3,4-bis(benzyloxy)-2-((benzyloxy)methyl)-6-(3,5-dimethylphenyl)-3,6-dihydro-2H-pyran (3i)

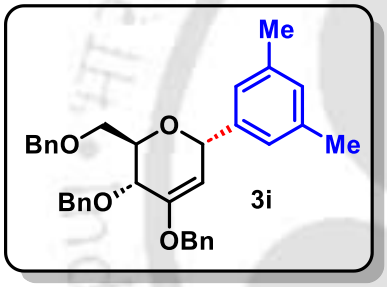

3i was obtained in 83% yield (104 mg) as a yellow oil, R_f = 0.6 (Hexane/EtOAc, 9:1, v/v). **^{1}H NMR** (400 MHz, $CDCl_3$) δ 7.38 (q, J = 8.0 Hz, 4H), 7.34 – 7.28 (m, 5H), 7.28 – 7.22 (m, 6H), 7.01 (s, 2H), 6.90 (s, 1H), 5.29 (d, J = 2.8 Hz, 1H), 4.99 (d, J = 3.5 Hz, 1H), 4.95 – 4.82 (m, 3H), 4.57 (dd, J = 11.7, 7.2 Hz, 2H), 4.44 (d, J = 12.1 Hz, 1H), 4.20 (d, J = 6.4 Hz, 1H), 4.01 – 3.89 (m, 1H), 3.67 (dd, J = 10.4, 4.8 Hz, 1H), 3.56 (dd, J = 10.4, 3.8 Hz, 1H), 2.27 (s, 6H). **^{13}C NMR** (126 MHz, $CDCl_3$) δ 152.8, 140.6, 138.4, 138.1, 137.7, 136.9, 129.5, 128.4, 128.3, 128.2, 128.1, 127.8 (127.85, 127.81), 127.5 (127.59, 127.57), 127.3, 125.9, 99.1, 73.6, 73.4, 73.1, 72.3, 71.4, 69.0, 68.9, 21.2. **HRMS** (ESI) m/z: $[M+H]^+$ calcd for $C_{35}H_{37}O_4$ 521.2686; found 521.2686.

(2R,3R,6S)-3,4-bis(benzyloxy)-2-((benzyloxy)methyl)-6-(naphthalen-1-yl)-3,6-dihydro-2H-pyran (3j)

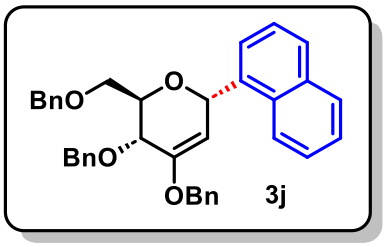

3j was obtained in 92% yield (120 mg), as a colorless oil, R_f = 0.5 (Hexane/EtOAc, 9:1, v/v). **^{1}H NMR** (600 MHz, $CDCl_3$) δ 8.40 (d, J = 8.2 Hz, 1H), 7.84 (d, J = 7.8 Hz, 1H), 7.78 (d, J = 8.1 Hz, 1H), 7.55 – 7.46 (m, 3H), 7.44 (d, J = 7.3 Hz, 2H), 7.39 (t, J = 7.3 Hz, 2H), 7.34 (t, J = 7.5 Hz, 2H), 7.29 – 7.21 (m, 8H), 7.19 (d, J = 7.3 Hz, 2H), 6.12 (s, 1H), 5.10 (d, J = 3.1 Hz, 1H), 4.97 (q, J = 11.9 Hz, 2H), 4.91 (d, J = 11.2 Hz, 1H), 4.58 (d, J = 11.1 Hz, 1H), 4.49 (d, J = 12.1 Hz, 1H), 4.36 (d, J = 12.1 Hz, 1H), 4.31 (d, J = 7.0 Hz, 1H), 3.83 (s, 1H), 3.63 (dd, J = 10.6, 4.5 Hz, 1H), 3.53 – 3.41 (m, 1H). **^{13}C NMR** (151 MHz, $CDCl_3$) δ 154.0, 138.4, 138.1, 136.9, 135.3, 134.0, 132.0,

128.9, 128.5, 128.44, 128.2 (128.26, 128.25, 128.22), 127.8, 127.8, 127.6, 127.5, 127.4, 126.9, 126.2, 125.6, 124.7 (124.75, 124.71), 98.6, 73.8, 73.1, 72.2, 71.5, 70.9, 69.2, 68.7. **HRMS** (ESI) m/z: $[M+H]^+$ calcd for $C_{37}H_{35}O_4$ 543.2530; found 543.2526.

(2R,3R,6S)-3,4-bis(benzyloxy)-2-((benzyloxy)methyl)-6-(4-chloro-3-(4-ethoxybenzyl)phenyl)-3,6-dihydro-2H-pyran (3k)

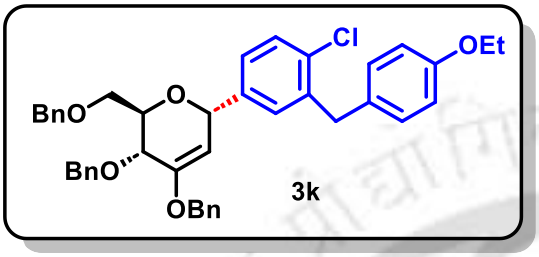

3k was obtained in 85% yield (135 mg), as a colorless oil, R_f = 0.4 (Hexane/EtOAc, 9:1, v/v). **^{1}H NMR** (400 MHz, $CDCl_3$) δ 7.41 – 7.33 (m, 4H), 7.33 – 7.27 (m, 6H), 7.27 – 7.16 (m, 8H), 7.05 (d, J = 8.5 Hz, 2H), 6.76 (d, J = 8.6 Hz, 2H), 5.27 (d, J = 3.1 Hz, 1H), 4.94 (d, J = 3.5 Hz, 1H), 4.89 – 4.78 (m, 3H), 4.53 (dd, J = 11.7, 6.1 Hz, 2H), 4.42 (d, J = 12.1 Hz, 1H), 4.17 (d, J = 6.3 Hz, 1H), 4.03 – 3.89 (m, 4H), 3.88 – 3.81 (m, 1H), 3.62 (dd, J = 10.4, 4.9 Hz, 1H), 3.51 (dd, J = 10.4, 3.6 Hz, 1H), 1.36 (t, J = 7.0 Hz, 3H). **^{13}C NMR** (126 MHz, $CDCl_3$) δ 157.3, 153.3, 139.6, 138.8, 138.3, 138.0, 136.7, 133.5, 131.3, 130.6, 129.8, 129.3, 128.5, 128.3, 128.2, 128.1, 127.8 (127.89, 127.84), 127.6 (127.64, 127.61), 127.3, 127.2, 114.4, 98.5, 73.3, 73.2, 72.9, 72.4, 71.2, 69.1, 68.7, 63.3, 38.3, 14.8. **HRMS** (ESI) m/z: $[M+H]^+$ calcd for $C_{42}H_{42}ClO_5$ 661.2715; found 661.2715.

benzyl 4-((2S,5R,6R)-4,5-bis(benzyloxy)-6-((benzyloxy)methyl)-5,6-dihydro-2H-pyran-2-yl)benzoate (3l)

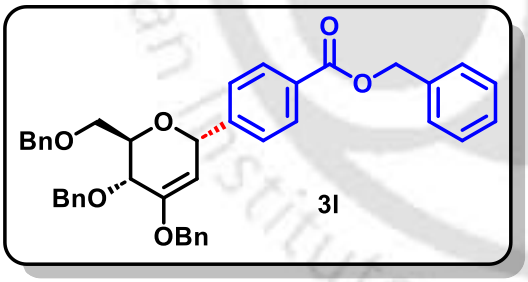

3l was obtained in 79% yield (119 mg), as a white foam, R_f = 0.3 (Hexane/EtOAc, 7:3, v/v). **^{1}H NMR** (600 MHz, $CDCl_3$) δ 8.02 (d, J = 8.2 Hz, 2H), 7.47 (d, J = 8.2 Hz, 2H), 7.44 (d, J = 7.3 Hz, 2H), 7.39 (t, J = 6.7 Hz, 5H), 7.36 – 7.28 (m, 6H), 7.27 – 7.21 (m, 7H), 5.37 (d, J = 14.5 Hz, 3H), 5.01 (d, J = 3.5 Hz, 1H), 4.87 (dt, J = 19.6, 11.5 Hz, 3H), 4.55 (d, J = 12.4 Hz, 2H), 4.44 (d, J = 12.1 Hz, 1H), 4.19 (d, J = 6.3 Hz, 1H), 3.87 (dd, J = 10.1, 4.8 Hz, 1H), 3.64 (dd, J = 10.4, 5.0 Hz, 1H), 3.55 (dd, J = 10.4, 3.6 Hz, 1H). **^{13}C NMR** (151 MHz, $CDCl_3$) δ 166.2, 153.5, 146.2, 138.2, 138.0, 136.6, 136.0, 129.7, 129.5, 128.5 (128.56, 128.50), 128.3, 128.2, 128.1 (128.18, 128.15), 128.0, 127.8 (127.89, 127.83, 127.81), 127.6 (127.63, 127.61), 127.3, 98.2, 73.5, 73.2, 73.0, 72.7, 71.2, 69.2, 68.7, 66.62. **HRMS** (ESI) m/z: $[M+H]^+$ calcd for $C_{41}H_{39}O_6$ 627.2741; found 627.2733.

(2R,3S,6S)-3,4-bis(benzyloxy)-2-((benzyloxy)methyl)-6-(4-methoxyphenyl)-3,6-dihydro-2H-pyran (3m)

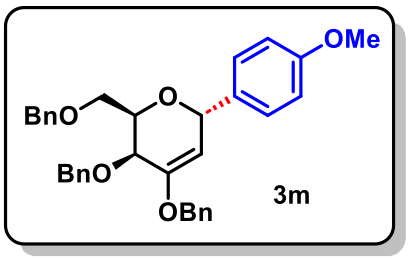

3m was obtained in 78% yield (98 mg), as a slightly yellow oil, R_f= 0.6 (Hexane/EtOAc, 7:3, v/v). **^{1}H NMR** (600 MHz, $CDCl_3$) δ 7.39 (d, J = 3.9 Hz, 4H), 7.36 – 7.30 (m, 4H), 7.28 – 7.27 (m, 3H), 7.26 – 7.23 (m, 4H), 7.20 (d, J = 7.3 Hz, 2H), 6.84 (d, J = 8.4 Hz, 2H), 5.47 (d, J = 3.1 Hz, 1H), 5.14 (d, J = 3.4 Hz, 1H), 4.98 – 4.86 (m, 3H), 4.71 (d, J = 11.7 Hz, 1H), 4.42 (dd, J = 29.7, 11.7 Hz, 2H), 3.89 (d, J = 8.8 Hz, 1H), 3.86 (t, J = 6.2 Hz, 1H), 3.80 (s, 3H), 3.74 (dd, J = 9.5, 6.7 Hz, 1H), 3.63 (dd, J = 9.7, 6.3 Hz, 1H). **^{13}C NMR** (151 MHz, $CDCl_3$) δ 159.2, 153.2, 138.6, 138.2, 136.7, 132.3, 129.3, 128.5, 128.2, 128.1, 128.0, 127.8, 127.6, 127.4 (127.47, 127.42), 113.5, 99.4, 73.2 (73.28, 73.24), 72.9, 71.5, 70.8, 69.3, 69.1, 55.2. **HRMS** (ESI) m/z: $[M+H]^+$ calcd for $C_{34}H_{35}O_5$ 523.2479; found 523.2481.

benzyl 4-((2S,5S,6R)-4,5-bis(benzyloxy)-6-((benzyloxy)methyl)-5,6-dihydro-2H-pyran-2-yl)benzoate (3n)

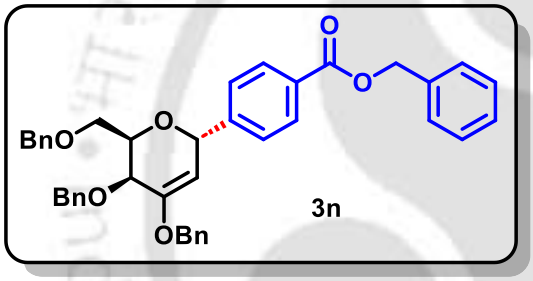

3n was obtained in 73% yield (110 mg), as a white foam, R_f = 0.4 (Hexane/EtOAc, 7:3, v/v). **^{1}H NMR** (600 MHz, $CDCl_3$) δ 8.01 (d, J = 8.3 Hz, 2H), 7.43 (dd, J = 13.8, 7.8 Hz, 4H), 7.41 – 7.37 (m, 6H), 7.36 – 7.33 (m, 2H), 7.31 – 7.27 (m, 5H), 7.24 – 7.20 (m, 5H), 5.53 (d, J = 3.6 Hz, 1H), 5.37 (d, J = 2.3 Hz, 2H), 5.18 (d, J = 3.7 Hz, 1H), 4.97 (d, J = 11.8 Hz, 1H), 4.93 – 4.86 (m, 2H), 4.70 (d, J = 11.7 Hz, 1H), 4.48 (d, J = 11.7 Hz, 1H), 4.42 (d, J = 11.7 Hz, 1H), 3.87 (d, J = 2.1 Hz, 1H), 3.80 (m, 1H), 3.72 (dd, J = 9.9, 5.9 Hz, 1H), 3.67 (dd, J = 9.9, 6.5 Hz, 1H). **^{13}C NMR** (151 MHz, $CDCl_3$) δ 166.2, 153.6, 145.8, 138.4, 138.1, 136.5, 136.0, 129.7, 129.4, 128.6 (128.61, 128.60), 128.2 (128.29, 128.24, 128.20), 128.1, 128.0, 128.0, 127.6, 127.5 (127.57, 127.53, 127.52), 127.4, 98.5, 73.3, 73.1, 73.0, 71.87, 71.4, 69.3, 69.2, 66.6. **HRMS** (ESI) m/z: $[M+H]^+$ calcd for $C_{41}H_{39}O_6$ 627.2741; found 627.2744.

(2S,3S,6R)-3,4-bis(benzyloxy)-2-methyl-6-phenyl-3,6-dihydro-2H-pyran (3o)

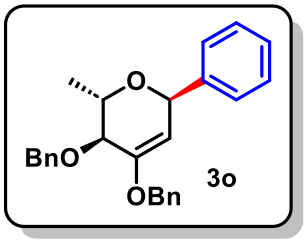

3o was obtained in 89% yield (111 mg), as a colorless oil, R_f= 0.7 (Hexane/EtOAc, 9:1, v/v). **^{1}H NMR** (500 MHz, $CDCl_3$) δ 7.40 (dd, J = 15.6, 7.1 Hz, 5H), 7.34 (dd, J = 15.4, 7.8 Hz, 6H), 7.30 – 7.22 (m, 4H), 5.28 (s, 1H), 5.01 (d, J = 2.9 Hz, 1H), 4.92 – 4.80 (m, 3H), 4.71 (d, J = 11.6 Hz, 1H), 4.11 – 3.98 (m, 1H), 3.78 (d, J = 4.5 Hz, 1H), 1.26 (s, 3H).**^{13}C NMR** (126 MHz, $CDCl_3$) δ 152.2, 141.2, 138.5, 136.8, 128.5, 128.3, 128.2, 128.1, 127.9, 127.8, 127.5, 127.4, 99.6, 76.1, 72.6, 72.5, 70.2, 69.0, 17.3. **HRMS** (ESI) m/z: $[M+H]^+$ calcd for $C_{26}H_{27}O_3$ 387.1955; found 387.1965.

(2S,3S,6R)-3,4-bis(benzyloxy)-6-(4-methoxyphenyl)-2-methyl-3,6-dihydro-2H-pyran (3p)

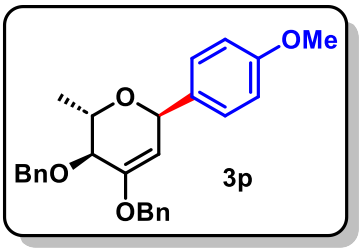

3p was obtained in 87% yield (117 mg), as a slightly yellow oil, R_f = 0.4 (Hexane/EtOAc, 9:1, v/v). **^{1}H NMR** (500 MHz, $CDCl_3$) δ 7.40 – 7.35 (m, 5H), 7.34 – 7.31 (m, 5H), 7.30 – 7.24 (m, 2H), 6.85 (d, J = 8.6 Hz, 2H), 5.24 (s, 1H), 4.97 (d, J = 3.0 Hz, 1H), 4.92 – 4.83 (m, 3H), 4.70 (d, J = 11.6 Hz, 1H), 4.07 – 3.96 (m, 1H), 3.83 – 3.76 (m, 4H), 1.24 (d, J = 6.6 Hz, 3H).**^{13}C NMR** (126 MHz, $CDCl_3$) δ 159.3, 152.3, 138.6, 136.9, 133.4, 129.3, 128.52, 128.3, 128.1, 127.8, 127.5, 127.4, 113.6, 99.8, 76.3, 72.7, 72.2, 69.8, 69.0, 55.3, 17.4. **HRMS** (ESI) m/z: $[M+H]^+$ calcd for $C_{27}H_{29}O_4$ 417.2061; found 417.2068.

(2S,3S,6R)-3,4-bis(benzyloxy)-6-(4-chlorophenyl)-2-methyl-3,6-dihydro-2H-pyran (3q)

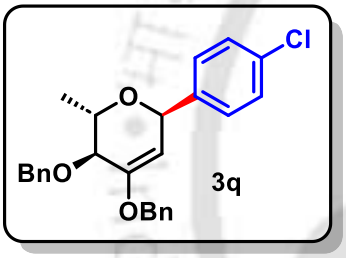

3q was obtained in 88% yield (119.3 mg), as a white solid, R_f = 0.5 (Hexane/EtOAc, 9:1, v/v), mp 128–130 °C. **^{1}H NMR** (400 MHz, $CDCl_3$) δ 7.38 (d, J = 4.6 Hz, 4H), 7.36 – 7.31 (m, 6H), 7.30 – 7.25 (m, 4H), 5.24 (d, J = 2.0 Hz, 1H), 4.93 (d, J = 3.0 Hz, 1H), 4.86 (t, J = 5.8 Hz, 3H), 4.70 (d, J = 11.6 Hz, 1H), 4.07 – 3.94 (m, 1H), 3.76 (d, J = 4.1 Hz, 1H), 1.25 (d, J = 6.5 Hz, 3H).**^{13}C NMR** (126 MHz, $CDCl_3$) δ 152.4, 139.8, 138.4, 136.6, 133.5, 129.2, 128.5, 128.4, 128.3, 128.2, 128.0, 127.8, 127.6, 127.3, 99.1, 76.0, 72.8, 71.8, 70.2, 69.0, 17.2. **HRMS** (ESI) m/z: $[M+H]^+$ calcd for $C_{26}H_{26}ClO_3$ 421.1565; found 421.1577.

1-(4-((2R,5S,6S)-4,5-bis(benzyloxy)-6-methyl-5,6-dihydro-2H-pyran-2-yl)phenyl)ethan-1-one (3r)

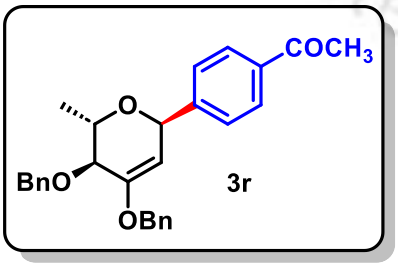

3r was obtained in 87% yield (120 mg), as a white solid, R_f = 0.3 (Hexane/EtOAc, 9:1, v/v), mp 93–95°C. **^{1}H NMR** (600 MHz, $CDCl_3$) δ 7.91 (d, J = 8.3 Hz, 2H), 7.49 (d, J = 8.2 Hz, 2H), 7.40 – 7.36 (m, 4H), 7.36 – 7.32 (m, 3H), 7.31 – 7.24 (m, 3H), 5.32 (d, J = 2.3 Hz, 1H), 4.97 (d, J = 3.1 Hz, 1H), 4.86 (t, J = 5.8 Hz, 3H), 4.70 (d, J = 11.6 Hz, 1H), 4.07 – 3.99 (m, 1H), 3.85 – 3.74 (m, 1H), 2.58 (s, 3H), 1.27 (d, J = 6.6 Hz, 3H).**^{13}C NMR** (151 MHz, $CDCl_3$) δ 197.8, 152.5, 146.7, 138.4, 136.6, 136.6, 128.5, 128.4, 128.3, 128.0, 127.9, 127.8, 127.6, 127.3, 98.8, 76.0, 72.8, 72.0, 70.6, 69.1, 26.6, 17.2. **HRMS** (ESI) m/z: $[M+H]^+$ calcd for $C_{28}H_{29}O_4$ 429.2060; found 429.2067.

(2S,3S,6R)-3,4-bis(benzyloxy)-2-methyl-6-(o-tolyl)-3,6-dihydro-2H-pyran (3s)

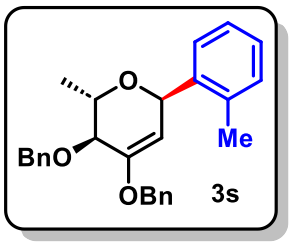

3s was obtained in 85% yield (110 mg), as a colorless oil, R_f = 0.5 (Hexane/EtOAc, 9:1, v/v). **^{1}H NMR** (400 MHz, $CDCl_3$) δ 7.43 – 7.32 (m, 8H), 7.31 – 7.23 (m, 3H), 7.20 – 7.09 (m, 3H), 5.50 (d, J = 2.1 Hz, 1H), 4.96 (d, J = 3.1 Hz, 1H), 4.93 – 4.84 (m, 3H), 4.70 (d, J = 11.6 Hz, 1H), 4.01 – 3.91 (m, 1H), 3.82 – 3.75 (m, 1H), 2.44 (s, 3H), 1.23 (d, J = 6.5 Hz, 3H). **^{13}C NMR** (126 MHz, $CDCl_3$) δ 152.6, 138.6, 138.4, 137.2, 136.9, 130.5, 128.5, 128.4, 128.2, 128.0, 127.9, 127.8, 127.5, 127.4, 125.5, 99.3, 76.4, 72.7, 69.7, 69.6, 69.0, 19.0, 17.4. . **HRMS** (ESI) m/z: $[M+H]^+$ calcd for $C_{27}H_{29}O_3$ 401.2112; found 401.2124.

(2S,3S,6R)-3,4-bis(benzyloxy)-6-(4-chloro-3-(4-ethoxybenzyl)phenyl)-2-methyl-3,6-dihydro-2H-pyran (3t)

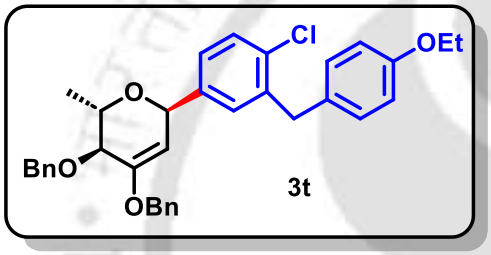

3t was obtained in 83% yield (148 mg), as a colorless oil, R_f = 0.4 (Hexane/EtOAc, 9:1, v/v). **^{1}H NMR** (500 MHz, $CDCl_3$) δ 7.39 – 7.26 (m, 11H), 7.19 (dd, J = 12.7, 4.5 Hz, 2H), 7.07 (d, J = 8.5 Hz, 2H), 6.78 (d, J = 8.5 Hz, 2H), 5.19 (d, J = 1.7 Hz, 1H), 4.91 (d, J = 2.9 Hz, 1H), 4.82 (t, J = 5.7 Hz, 3H), 4.66 (d, J = 11.6 Hz, 1H), 4.01 – 3.92 (m, 5H), 3.76 (d, J = 4.2 Hz, 1H), 1.37 (t, J = 7.0 Hz, 3H), 1.23 (d, J = 6.5 Hz, 3H). **^{13}C NMR** (126 MHz, $CDCl_3$) δ 157.3, 152.3, 140.1, 138.8, 138.5, 136.7, 133.5, 131.3, 130.40, 129.8, 129.4, 128.4, 128.2, 128.0, 127.8, 127.5, 127.3, 127.1, 114.4, 99.2, 76.0, 72.5, 71.8, 70.2, 69.0, 63.34, 38.3, 17.2, 14.8. **HRMS** (ESI) m/z: $[M+H]^+$ calcd for $C_{35}H_{36}ClO_4$ 555.2297; found 555.2296.

(2S,3S,6R)-3,4-bis(benzyloxy)-6-(4-chloro-3-(4-(((R)-tetrahydrofuran-3-yl)oxy)benzyl)phenyl)-2-methyl-3,6-dihydro-2H-pyran (3u)

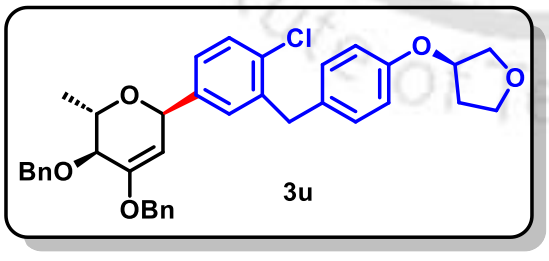

3u was obtained in 81% yield (156 mg), as a colorless oil, R_f = 0.3 (Hexane/EtOAc, 8:2, v/v). **^{1}H NMR** (600 MHz, $CDCl_3$) δ 7.39 – 7.24 (m, 11H), 7.20 (dd, J = 10.4, 2.0 Hz, 2H), 7.07 (d, J = 8.5 Hz, 2H), 6.74 (d, J = 8.6 Hz, 2H), 5.19 (d, J = 2.1 Hz, 1H), 4.91 (d, J = 3.0 Hz, 1H), 4.86 – 4.79 (m, 4H), 4.66 (d, J = 11.6 Hz, 1H), 4.01 – 3.90 (m, 6H), 3.86 (td, J = 8.1, 4.6 Hz, 1H), 3.78 – 3.74 (m, 1H), 2.18 – 2.06 (m, 2H), 1.23 (d, J = 6.5 Hz, 3H). **^{13}C NMR** (151 MHz, $CDCl_3$) δ 155.7, 152.3, 140.2, 138.6, 138.4, 136.6, 133.4, 131.8, 130.3, 129.9, 129.4, 128.4, 128.2, 127.9, 127.8, 127.5, 127.3, 127.1, 115.2, 99.2, 76.0, 73.0, 72.5, 71.8, 70.2, 69.0, 67.1, 38.3, 32.9, 17.2. **HRMS** (ESI) m/z: $[M+H]^+$ calcd for $C_{37}H_{38}ClO_5$ 597.2402; found 597.2401.

4-((2R,5S,6S)-4,5-bis(benzyloxy)-6-methyl-5,6-dihydro-2H-pyran-2-yl)-N-phenylbenzamide (3v)

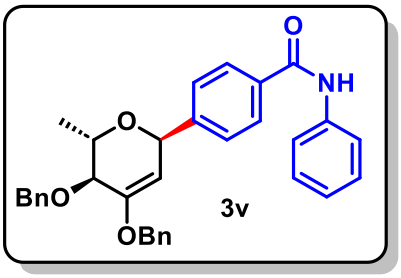

3v was obtained in 88% yield (143 mg), as a white solid, R_f = 0.4 (Hexane/EtOAc, 7:3, v/v), mp 146–148 °C. **^{1}H NMR** (500 MHz, $CDCl_3$) δ 7.81 (d, J = 8.0 Hz, 3H), 7.64 (d, J = 7.9 Hz, 2H), 7.51 (d, J = 8.1 Hz, 2H), 7.43 – 7.26 (m, 12H), 7.15 (t, J = 7.4 Hz, 1H), 5.33 (s, 1H), 4.98 (d, J = 2.8 Hz, 1H), 4.88 (t, J = 5.6 Hz, 3H), 4.71 (d, J = 11.6 Hz, 1H), 4.08 – 3.99 (m, 1H), 3.79 (d, J = 4.1 Hz, 1H), 1.27 (d, J = 6.6 Hz, 3H). **^{13}C NMR** (126 MHz, $CDCl_3$) δ 165.4, 152.5, 145.4, 138.3, 137.9, 136.5, 134.3, 129.0, 128.5, 128.2, 128.1, 128.0, 127.9, 127.6, 127.35, 127.0, 124.5, 120.1, 98.8, 76.0, 72.8, 71.9, 70.5, 69.0, 17.1. **HRMS** (ESI) m/z: $[M+H]^+$ calcd for $C_{33}H_{32}NO_4$ 506.2331; found 506.2326.

4-((2R,5S,6S)-4,5-bis(benzyloxy)-6-methyl-5,6-dihydro-2H-pyran-2-yl)-N-cyclohexylbenzamide (3w)

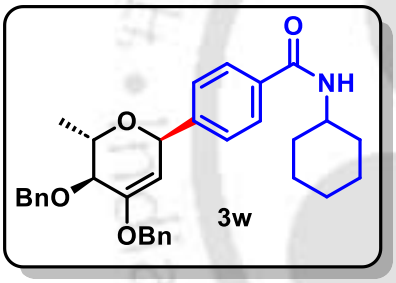

3w was obtained in 86% yield (142 mg), as a slightly yellow solid, R_f = 0.5 (Hexane/EtOAc, 7:3, v/v), mp 139–140 °C. **^{1}H NMR** (500 MHz, $CDCl_3$) δ 7.70 (d, J = 8.1 Hz, 2H), 7.45 (d, J = 8.1 Hz, 2H), 7.40 – 7.24 (m, 10H), 5.94 (d, J = 7.8 Hz, 1H), 5.30 (s, 1H), 4.97 (d, J = 3.0 Hz, 1H), 4.86 (t, J = 5.7 Hz, 3H), 4.70 (d, J = 11.6 Hz, 1H), 4.06 – 3.92 (m, 2H), 3.78 (d, J = 4.7 Hz, 1H), 2.03 (d, J = 12.1 Hz, 2H), 1.81 – 1.71 (m, 2H), 1.43 (dd, J = 24.9, 12.3 Hz, 2H), 1.31 – 1.22 (m, 7H). **^{13}C NMR** (151 MHz, $CDCl_3$) δ 166.3, 152.5, 144.7, 138.46, 136.6, 134.5, 128.5, 128.2, 128.0, 127.9, 127.5, 127.3, 126.8, 99.0, 76.0, 72.8, 72.0, 70.3, 69.0, 48.6, 33.2, 25.5, 24.8, 17.2. **HRMS** (ESI) m/z: $[M+H]^+$ calcd for $C_{33}H_{38}NO_4$ 512.2796; found 512.2796.

methyl (4-((2R,5S,6S)-4,5-bis(benzyloxy)-6-methyl-5,6-dihydro-2H-pyran-2-yl)benzoyl)-L-phenylalaninate (3x)

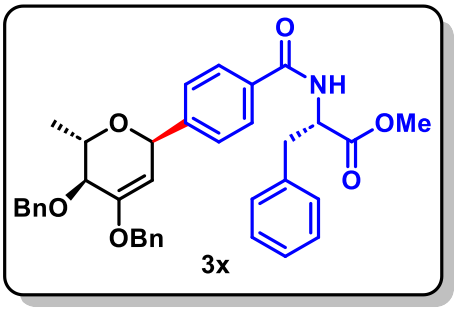

3x was obtained in 79% yield (150 mg), as a colorless oil, R_f = 0.3 (Hexane/EtOAc, 7:3, v/v). **^{1}H NMR** (500 MHz, $CDCl_3$) δ 7.68 (d, J = 8.0 Hz, 2H), 7.45 (d, J = 8.0 Hz, 2H), 7.36 (dd, J = 18.1, 6.3 Hz, 8H), 7.28 (dd, J = 13.1, 6.9 Hz, 5H), 7.12 (d, J = 6.9 Hz, 2H), 6.57 (d, J = 7.4 Hz, 1H), 5.29 (s, 1H), 5.08 (dd, J = 12.7, 5.7 Hz, 1H), 4.96 (d, J = 2.7 Hz, 1H), 4.86 (d, J = 7.8 Hz, 3H), 4.70 (d, J = 11.6 Hz, 1H), 4.04 – 3.98 (m, 1H), 3.81 –

3.72 (m, 4H), 3.28 (dd, J = 13.8, 5.7 Hz, 1H), 3.21 (dd, J = 13.8, 5.3 Hz, 1H), 1.26 (d, J = 6.1 Hz, 3H). **^{13}C NMR** (126 MHz, $CDCl_3$) δ 171.9, 166.5, 152.5, 145.3, 138.3, 136.6, 135.7, 133.2, 129.3, 128.6, 128.4, 128.2, 128.0, 127.9, 127.8, 127.5, 127.3, 127.1, 127.0, 98.8, 75.9, 72.8, 71.9, 70.4, 69.0, 53.4, 52.3, 37.8, 17.1. **HRMS** (ESI) m/z: $[M+H]^+$ calcd for $C_{37}H_{38}NO_6$ 592.2694; found 592.2694.

5-(2,2-dimethyl-1,3-dioxolan-4-yl)-2,2-dimethyltetrahydrofuro[2,3-d][1,3]dioxol-6-yl 4-((2R,5S,6S)-4,5-bis(benzyloxy)-6-methyl-5,6-dihydro-2H-pyran-2-yl)benzoate (3y)

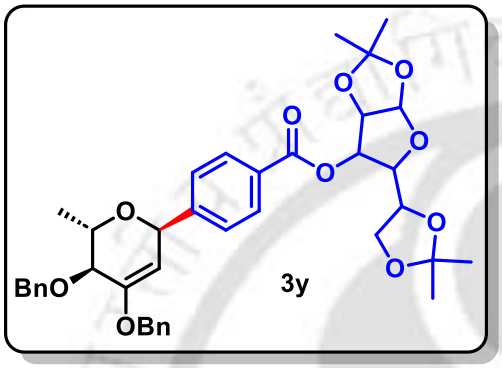

3y was obtained in 80% yield (173 mg), as a colorless oil, R_f = 0.5 (Hexane/EtOAc, 7:3, v/v). **^{1}H NMR** (600 MHz, $CDCl_3$) δ 7.98 (d, J = 8.2 Hz, 2H), 7.49 (d, J = 8.2 Hz, 2H), 7.38 (d, J = 3.8 Hz, 4H), 7.36 – 7.33 (m, 3H), 7.30 (t, J = 7.3 Hz, 2H), 7.28 – 7.25 (m, 1H), 5.94 (d, J = 3.6 Hz, 1H), 5.49 (d, J = 2.5 Hz, 1H), 5.32 (d, J = 2.0 Hz, 1H), 4.97 (d, J = 3.0 Hz, 1H), 4.86 (t, J = 5.6 Hz, 3H), 4.70 (d, J = 11.6 Hz, 1H), 4.62 (d, J = 3.6 Hz, 1H), 4.34 (qd, J = 7.8, 4.1 Hz, 2H), 4.10 (ddd, J = 13.3, 8.5, 5.2 Hz, 2H), 4.05 – 3.99 (m, 1H), 3.78 (d, J = 4.5 Hz, 1H), 1.55 (s, 3H), 1.42 (d, J = 7.4 Hz, 3H), 1.33 (d, J = 9.9 Hz, 3H), 1.27 (d, J = 4.8 Hz, 6H). **^{13}C NMR** (151 MHz, $CDCl_3$) δ 165.0, 152.6, 147.3, 138.4, 136.6, 129.8, 128.93, 128.5, 128.3, 128.1, 127.9, 127.8, 127.6, 127.4, 112.3, 109.4, 105.1, 98.8, 83.4, 80.0, 76.6, 76.0, 72.9, 72.6, 72.0, 70.7, 69.1, 67.2, 26.8 (26.86, 26.80), 26.2, 25.2, 17.2. **HRMS** (ESI) m/z: $[M+H]^+$ calcd for $C_{39}H_{45}O_{10}$ 673.3007; found 673.3005.

(2R,3R,6S)-3,4-dimethoxy-2-(methoxymethyl)-6-(4-methoxyphenyl)-3,6-dihydro-2H-pyran (3z1)

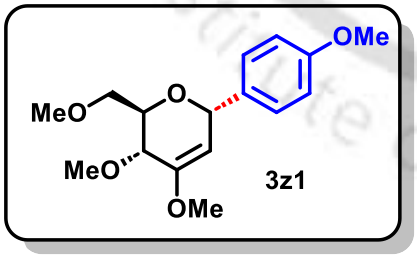

3z1 was obtained in 85% yield (133 mg), as a yellow oil, R_f = 0.4 (Hexane/EtOAc, 8:2, v/v). **^{1}H NMR** (600 MHz, $CDCl_3$) δ 7.30 (d, J = 8.5 Hz, 2H), 6.79 (d, J = 8.5 Hz, 2H), 5.24 (d, J = 2.8 Hz, 1H), 4.82 (d, J = 3.3 Hz, 1H), 3.75 (dt, J = 14.7, 6.2 Hz, 2H), 3.71 (s, 3H), 3.56 (s, 3H), 3.51 (dd, J = 10.3, 4.8 Hz, 1H), 3.45 (s, 3H), 3.40 (dd, J = 10.3, 3.6 Hz, 1H), 3.29 (s, 3H). **^{13}C NMR** (151 MHz, $CDCl_3$) δ 159.4, 153.7, 132.9, 129.5, 113.6, 97.8, 73.2, 73.1, 71.6, 71.4, 59.2, 58.8, 55.3, 54.6. **HRMS** (ESI) m/z: $[M+H]^+$ calcd for $C_{16}H_{23}O_5$ 295.1540; found 295.1540.

(2R,3R,6S)-3,4-diethoxy-2-(ethoxymethyl)-6-(4-methoxyphenyl)-3,6-dihydro-2H-pyran (3z2)

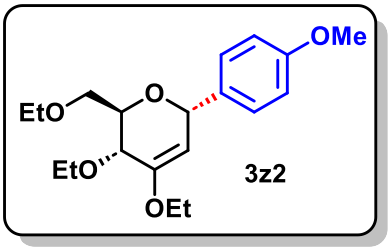

3z2 was obtained in 87% yield (127 mg), as a yellow oil, R_f = 0.5 (Hexane/EtOAc, 9:1, v/v). **^{1}H NMR** (600 MHz, $CDCl_3$) δ 7.31 (d, J = 8.4 Hz, 2H), 6.78 (d, J = 8.4 Hz, 2H), 5.25 (d, J = 2.7 Hz, 1H), 4.78 (d, J = 4.0 Hz, 1H), 3.92 (d, J = 6.9 Hz, 1H), 3.83 – 3.76 (m, 2H), 3.72 (s, 4H), 3.68 – 3.64 (m, 1H), 3.59 – 3.52 (m, 2H), 3.49 – 3.43 (m, 2H), 3.40 (p, J = 7.1, 6.6 Hz, 1H), 1.29 (t, J = 6.9 Hz, 3H), 1.15 – 1.11 (m, 6H). **^{13}C NMR** (151 MHz, $CDCl_3$) δ 153.7, 133.2, 129.6, 113.5, 97.4, 73.4, 71.7, 71.6, 69.4, 66.9, 66.8, 62.6, 55.3, 15.7, 15.2, 14.6. **HRMS** (ESI) m/z: $[M+H]^+$ calcd for $C_{19}H_{29}O_5$ 337.2010; found 337.2012.

(2R,3R,6S)-6-(4-methoxyphenyl)-3,4-bis((4-methylbenzyl)oxy)-2-(((4-methylbenzyl)oxy)methyl)-3,6-dihydro-2H-pyran (3z3)

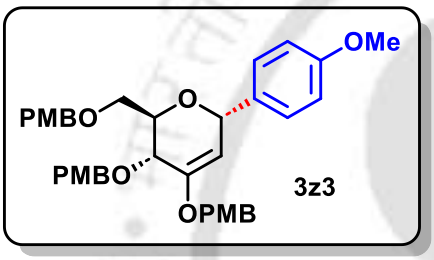

3z3 was obtained in 90% yield (111 mg), as a colorless oil, R_f = 0.4 (Hexane/EtOAc, 9:1, v/v). **^{1}H NMR** (600 MHz, $CDCl_3$) δ 7.24 (dd, J = 24.8, 8.2 Hz, 4H), 7.12 – 7.08 (m, 4H), 7.05 – 6.97 (m, 6H), 6.75 (d, J = 8.6 Hz, 2H), 5.25 (d, J = 2.9 Hz, 1H), 4.89 (d, J = 3.5 Hz, 1H), 4.80 – 4.71 (m, 3H), 4.41 (dd, J = 26.7, 11.5 Hz, 2H), 4.28 (d, J = 12.0 Hz, 1H), 4.10 (d, J = 6.7 Hz, 1H), 3.74 (dt, J = 7.2, 4.1 Hz, 1H), 3.70 (s, 3H), 3.53 (dd, J = 10.4, 4.5 Hz, 1H), 3.41 (dd, J = 10.4, 3.4 Hz, 1H), 2.30 (s, 3H), 2.23 (d, J = 5.6 Hz, 6H). **^{13}C NMR** (151 MHz, $CDCl_3$) δ 159.4, 153.6, 137.6, 137.3 (137.37, 137.32), 135.5, 135.1, 134.0, 133.0, 129.7, 129.2, 129.1, 129.0, 128.4, 128.1, 127.6, 113.6, 98.8, 73.6, 73.4, 73.1, 71.9, 71.2, 69.1, 68.6, 55.3, 21.3, 21.2 (21.29, 21.28). **HRMS** (ESI) m/z: $[M+H]^+$ calcd for $C_{37}H_{41}O_5$ 565.2949; found 565.2941.

(((2R,3R,6S)-3,4-bis(benzyloxy)-6-(4-methoxyphenyl)-3,6-dihydro-2H-pyran-2-yl)methoxy)(tert-butyl)dimethylsilane (3z4)

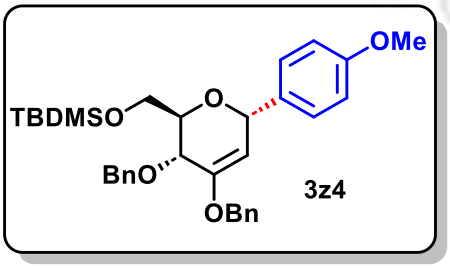

3z4 was obtained in 83% yield (104 mg), as a colorless oil, R_f = 0.5 (Hexane/EtOAc, 9:1, v/v). **^{1}H NMR** (400 MHz, $CDCl_3$) δ 7.37 – 7.24 (m, 12H), 6.83 (d, J = 8.6 Hz, 2H), 5.26 (d, J = 2.3 Hz, 1H), 4.98 (d, J = 3.2 Hz, 1H), 4.88 – 4.81 (m, 3H), 4.67 (d, J = 11.6 Hz, 1H), 4.09 (d, J = 6.4 Hz, 1H), 3.85 (d, J = 5.1 Hz, 1H), 3.80 – 3.73 (m, 5H), 0.84 (s, 9H), 0.05 (s, 6H). **^{13}C NMR** (151 MHz, $CDCl_3$) δ 159.4, 152.6, 138.7, 137.0, 133.4, 129.4, 128.6, 128.4, 128.3, 128.2, 127.9, 127.6, 127.5, 113.7, 113.7, 99.8, 74.6, 73.0, 72.9, 71.4, 69.1, 62.8, 55.4, 26.0, 18.4, -5.1, -5.2. **HRMS** (ESI) m/z: $[M+H]^+$ calcd for $C_{33}H_{43}O_5Si$ 547.2875; found 547.2890.

(2R,3R,6S)-6-(4-methoxyphenyl)-3,4-bis(naphthalen-1-ylmethoxy)-2-((naphthalen-1-ylmethoxy)methyl)-3,6-dihydro-2H-pyran (3z5)

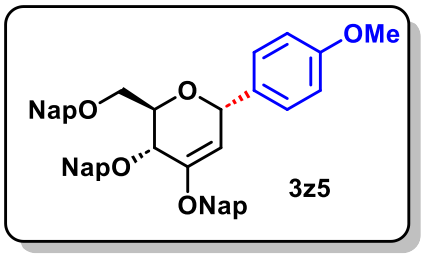

3z5 was obtained in 93% yield (113 mg), as a white solid, mp 120–122 °C R_f = 0.5 (Hexane/EtOAc, 8:2, v/v). **^{1}H NMR** (600 MHz, $CDCl_3$) δ 7.80 – 7.74 (m, 3H), 7.72 – 7.60 (m, 6H), 7.51 – 7.38 (m, 6H), 7.38 – 7.24 (m, 7H), 7.19 – 7.15 (m, 1H), 6.72 (d, J = 8.6 Hz, 2H), 5.29 (d, J = 2.7 Hz, 1H), 5.02 – 4.90 (m, 4H), 4.61 (d, J = 12.6 Hz, 2H), 4.45 (d, J = 12.3 Hz, 1H), 4.25 (d, J = 6.6 Hz, 1H), 3.86 (dt, J = 7.0, 4.2 Hz, 1H), 3.68 (s, 3H), 3.62 (dd, J = 10.4, 4.5 Hz, 1H), 3.50 (dd, J = 10.4, 3.6 Hz, 1H). **^{13}C NMR** (151 MHz, $CDCl_3$) δ 159.4, 153.4, 135.8, 135.6, 134.4, 133.3 (133.39, 133.31), 133.2, 133.1 (133.16, 133.10), 133.0, 132.8, 129.7, 128.4, 128.2, 128.1, 128.0, 127.8 (127.87, 127.82), 127.6, 126.9, 126.8, 126.5, 126.37, 126.3, 126.1, 126.0, 125.9, 125.8, 125.5, 113.6, 99.3, 77.3, 77.1, 76.9, 73.7, 73.4, 73.3, 72.0, 71.4, 69.4, 68.8, 55.3. **HRMS** (ESI) m/z: $[M+H]^+$ calcd for $C_{46}H_{41}O_5$ 673.2949; found 673.2949.

4.5.5. General procedure 1.2: synthesis of 3-oxo-β-aryl-*C*-glycosides

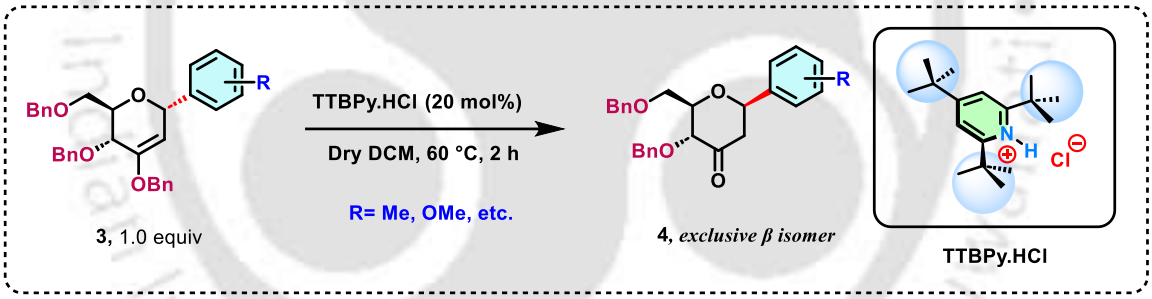

α-*C*-glycoside **3** (0.2 mmol, 1.0 equiv) was dissolved in dry dichloromethane (1 mL) under an argon atmosphere in a screw-capped reaction vial equipped with a magnetic stir bar. To this solution, 2,4,6-tri-*tert*-butylpyridinium hydrochloride catalyst (0.04 mmol, 20 mol%) was added, and the reaction mixture was stirred at 60 °C for 2-3 hours. Upon completion, the reaction was quenched by the addition of triethylamine (NEt_3, 1 mL). The crude mixture was purified by column chromatography (silica gel, EtOAc/hexane) to afford the corresponding anomerized glycoside **4**. The anomerization of α-C-glycosides was confirmed from their **^{1}H NMR** and **^{13}C NMR** data as described in the literature.[1, 29, 30] Also, the β-configuration of the aryl *C*-glycosides was confirmed on the basis of **NOE** experiments and **SC-XRD** data.

4.5.6. Spectroscopic data of 3-oxo-β-aryl-*C*-glycosides (4a-4e)

(2R,3R,6R)-3-(benzyloxy)-2-((benzyloxy)methyl)-6-phenyltetrahydro-4H-pyran-4-one (4a)

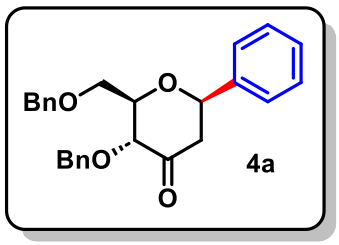

4a was obtained in 74% yield (59.6 mg) as a white foam, R_f= 0.3 (Hexane/EtOAc, 9:1, v/v). **^{1}H NMR** (600 MHz, $CDCl_3$) δ 7.39 – 7.26 (m, 15H), 4.94 (d, J = 11.1 Hz, 1H), 4.68 (dd, J = 17.6, 9.8 Hz, 2H), 4.58 (d, J = 12.2 Hz, 1H), 4.50 (d, J = 11.1 Hz, 1H), 4.28 (d, J = 9.6 Hz, 1H), 3.85 (s, 3H), 2.76 (d, J = 6.9 Hz, 2H).**^{13}C NMR** (101 MHz, $CDCl_3$) δ 205.7, 140.1, 138.27, 137.5, 128.4, 128.4 (128.42, 128.40), 128.2, 128.1, 127.9, 127.7, 127.6, 125.7, 80.9, 79.7, 79.4, 73.61, 73.5, 69.2, 50.0. **HRMS** (ESI) m/z: $[M+Na]^+$ calcd for $C_{26}H_{26}NaO_4$ 425.1723; found 425.1729.

(2R,3R,6R)-3-(benzyloxy)-2-((benzyloxy)methyl)-6-(4-methoxyphenyl)tetrahydro-4H-pyran-4-one (4b)

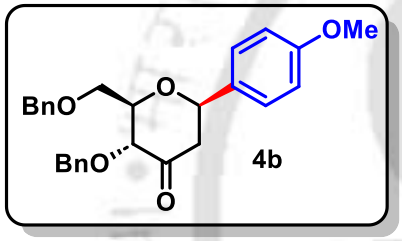

4b was obtained in 76% yield (62 mg) as a reddish foam, R_f= 0.5 (Hexane/EtOAc, 8:2, v/v). **^{1}H NMR** (500 MHz, $CDCl_3$) δ 7.36 – 7.27 (m, 12H), 6.89 (d, J = 8.4 Hz, 2H), 4.93 (d, J = 11.1 Hz, 1H), 4.64 (t, J = 10.0 Hz, 2H), 4.56 (d, J = 12.2 Hz, 1H), 4.49 (d, J = 11.1 Hz, 1H), 4.26 (d, J = 8.7 Hz, 1H), 3.81 (d, J = 12.7 Hz, 6H), 2.83 – 2.66 (m, 2H). **^{13}C NMR** (126 MHz, $CDCl_3$) δ 205.9, 159.5, 138.2, 137.5, 132.2, 128.5, 128.4, 128.3, 128.2, 127.9, 127.7, 127.6, 127.1, 127.0, 114.0, 80.8, 79.7, 79.2, 73.5 (73.58, 73.54), 69.2, 55.3, 49.9. **HRMS** (ESI) m/z: $[M+H]^+$ calcd for $C_{27}H_{29}O_5$ 433.2010; found 433.2007.

(2R,3R,6R)-3-(benzyloxy)-2-((benzyloxy)methyl)-6-(p-tolyl)tetrahydro-4H-pyran-4-one (4c)

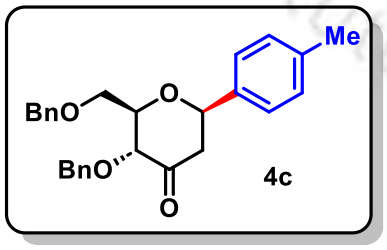

4c was obtained in 76% yield (63 mg) as a reddish oil, R_f = 0.6 (Hexane/EtOAc, 8:2, v/v). **^{1}H NMR** (500 MHz, $CDCl_3$) δ 7.36 – 7.24 (m, 12H), 7.17 (d, J = 7.7 Hz, 2H), 4.94 (d, J = 11.1 Hz, 1H), 4.65 (dd, J = 12.9, 4.8 Hz, 2H), 4.57 (d, J = 12.2 Hz, 1H), 4.50 (d, J = 11.1 Hz, 1H), 4.26 (d, J = 8.8 Hz, 1H), 3.82 (d, J = 10.2 Hz, 3H), 2.81 – 2.68 (m, 2H), 2.34 (s, 3H).**^{13}C NMR** (126 MHz, $CDCl_3$) δ 205.8, 138.2, 137.9, 137.5, 137.1, 129.2, 128.4, 128.3, 128.2, 127.9, 127.7, 127.6 (127.63, 125.68), 80.9, 79.7, 79.4, 73.5 (73.58, 73.54), 69.2, 50.0, 21.1. **HRMS** (ESI) m/z: $[M+H]^+$ calcd for $C_{27}H_{29}O_4$ 417.2060; found 417.2057.

(2R,3R,6R)-3-(benzyloxy)-2-((benzyloxy)methyl)-6-(3-methoxyphenyl)-tetrahydro-4H-pyran-4-one (4d)

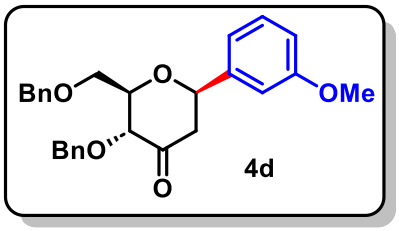

4d was obtained in 71% yield (53 mg) as a slightly yellow foam, R_f = 0.4 (Hexane/EtOAc, 8:2, v/v). **^{1}H NMR** (600 MHz, $CDCl_3$) δ 7.36 – 7.25 (m, 11H), 6.95 (d, J = 7.3 Hz, 2H), 6.85 (d, J = 7.6 Hz, 1H), 4.94 (d, J = 11.1 Hz, 1H), 4.70 – 4.64 (m, 2H), 4.58 (d, J = 12.2 Hz, 1H), 4.50 (d, J = 11.1 Hz, 1H), 4.27 (d, J = 8.8 Hz, 1H), 3.86 – 3.80 (m, 6H), 2.75 (d, J = 6.7 Hz, 2H).**^{13}C NMR** (126 MHz, $CDCl_3$) δ 205.7, 159.8, 141.6, 129.6, 128.4 (128.41, 128.40), 128.2, 127.9, 127.7, 127.6, 117.9, 113.6, 111.3, 80.8, 79.7, 79.2, 73.5, 69.2, 55.2, 50.0. **HRMS** (ESI) m/z: $[M+Na]^+$ calcd for $C_{27}H_{28}NaO_5$ 455.1829; found 455.1832.

(2R,3R,6R)-3-(benzyloxy)-2-((benzyloxy)methyl)-6-(3,5-dimethylphenyl)tetrahydro-4H-pyran-4-one (4e)

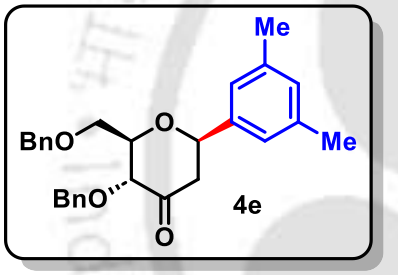

4e was obtained in 73% yield (60 mg) as a reddish foam, R_f = 0.5 (Hexane/EtOAc, 8:2, v/v). **^{1}H NMR** (600 MHz, $CDCl_3$) δ 7.37 – 7.25 (m, 10H), 6.99 (s, 2H), 6.94 (s, 1H), 4.94 (d, J = 11.1 Hz, 1H), 4.66 (d, J = 12.3 Hz, 1H), 4.58 (t, J = 9.1 Hz, 2H), 4.50 (d, J = 11.1 Hz, 1H), 4.27 (d, J = 9.7 Hz, 1H), 3.82 (dd, J = 10.5, 7.7 Hz, 3H), 2.82 – 2.68 (m, 2H), 2.32 (s, 6H).**^{13}C NMR** (151 MHz, $CDCl_3$) δ 205.9, 139.8, 138.1 (138.18, 138.17), 129.7, 128.3 (128.35, 128.33), 128.2, 127.9, 127.6, 127.5, 123.4, 80.8, 79.6, 79.5, 73.4, 73.4, 69.1, 49.9, 21.2. **HRMS** (ESI) m/z: $[M+Na]^+$ calcd for $C_{28}H_{30}NaO_4$ 453.2036; found 453.2027.

4.5.7. Procedure for the Synthesis of 5b

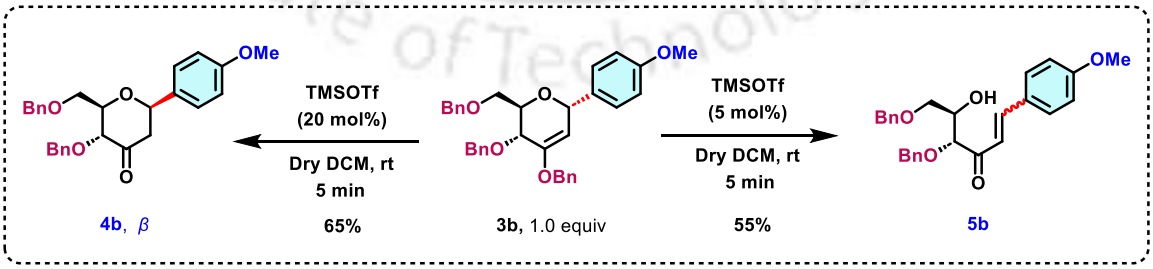

Treatment of glycoside **3b** (100 mg, 0.19 mmol) with TMSOTf (20 mol%, 7 µL, 0.04 mmol) in anhydrous dichloromethane (1 mL) at room temperature for 5 minutes afforded product **4b** in 65% yield (53 mg). Furthermore, treatment with 5 mol% TMSOTf (1.7 µL, 0.0095 mmol) in anhydrous dichloromethane (1 mL) at rt for 5 minutes afforded the ring-

opened alcohol **5b** in 55% yield (45 mg). After completion of the reaction, the reaction mixture was quenched by adding NEt_3 (1 ml). The reaction mixture was purified by using column chromatography (SiO_2, EtOAc/Hexane) to acquire the products (**4b**, **5b**). The configuration of the aryl *C*-glycoside (**5b**) was confirmed on its **^{1}H NMR** and **^{13}C NMR** data as described in the literature.[1]

(4R,5R)-4,6-bis(benzyloxy)-5-hydroxy-1-(4methoxyphenyl)hex-1-en-3-one (E:Z, 1:1) (5b)

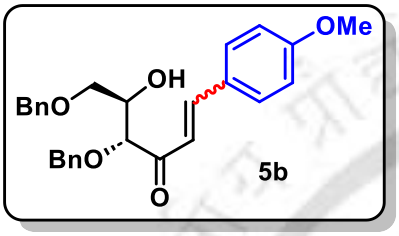

5b was obtained in 55% yield (45 mg) (E:Z, 1:1) as a colorless oil, R_f = 0.3 (Hexane/EtOAc, 7:3, v/v). **E:Z, 1:1. ^{1}H NMR** (600 MHz, $CDCl_3$) δ 7.69 (dd, J = 15.9, 11.4 Hz, 2H), 7.50 (dd, J = 8.6, 5.4 Hz, 4H), 7.37 – 7.25 (m, 20H), 7.04 (dd, J = 17.6, 16.0 Hz, 2H), 6.90 (d, J = 8.6 Hz, 4H), 4.73 (d, J = 11.6 Hz, 1H), 4.66 (d, J = 11.6 Hz, 1H), 4.57 – 4.45 (m, 6H), 4.16 (dd, J = 38.7, 5.2 Hz, 4H), 3.85 (d, J = 0.7 Hz, 6H), 3.66 (d, J = 4.1 Hz, 2H), 3.58 (d, J = 5.6 Hz, 2H), 2.67 (s, 2H). **^{13}C NMR** (151 MHz, $CDCl_3$) δ 199.6, 199.5, 161.9, 161.8, 143.9, 137.8, 137.1, 137.0, 130.5, 130.4, 128.5 (128.52, 128.51), 128.3 (128.39, 128.36, 128.30), 128.1 (128.16, 128.14), 128.0, 127.7 (127.79, 127.77, 127.75, 127.70), 127.2, 127.1, 119.3, 119.2, 114.3 (114.39, 114.38), 83.9, 83.5, 73.4, 73.0, 72.9, 71.4, 71.3, 70.4, 70.3, 55.4. **HRMS** (ESI) m/z: $[M+H]^+$ calcd for $C_{27}H_{29}O_5$ 433.2010; found 433.2013.

4.6. References

1. Liu, C.-F.; Xiong, D.-C.; Ye, X.-S., "Ring Opening–Ring Closure" Strategy for the Synthesis of Aryl-C-glycosides. *J. Org. Chem.* **2014,** *79* (10), 4676-4686.
2. Štambaský, J.; Hocek, M.; Kočovský, P., C-Nucleosides: Synthetic Strategies and Biological Applications. *Chem. Rev.* **2009,** *109* (12), 6729-6764.
3. Lopez, J.; Lagunas-Rivera, S.; Vargas-Diaz, M. E.; Alcaraz-Contreras, Y.; Vazquez, M. A., Chapter 1 - Recent advances in pluramycins, biological activity, and synthetic strategies. In *Stud. Nat. Prod. Chem.*, Atta ur, R., Ed. Elsevier: 2022; Vol. 73, pp 1-44.
4. Bililign, T.; Griffith, B. R.; Thorson, J. S., Structure, activity, synthesis and biosynthesis of aryl-C-glycosides. *Nat. Prod. Rep.* **2005,** *22* (6), 742-760.
5. Hultin, P. G., Bioactive C-glycosides from bacterial secondary metabolism. *Curr. Top. Med. Chem.* **2005,** *5* (14), 1299-1331.
6. Chao, E. C.; Henry, R. R., SGLT2 inhibition — a novel strategy for diabetes treatment. *Nat. Rev. Drug Discov.* **2010,** *9* (7), 551-559.
7. Singh, A. K.; Kanaujiya, V. K.; Tiwari, V.; Sabiah, S.; Kandasamy, J., Development of Routes for the Stereoselective Preparation of β-Aryl-C-glycosides via C-1 Aryl Enones. *Org. Lett.* **2020,** *22* (19), 7650-7655.
8. Schmidt, R. R.; Hoffmann, M., C-glycosides from O-glycosyl trichloroacetimidates. *Tetrahedron Lett.* **1982,** *23* (4), 409-412.
9. Casiraghi, G.; Cornia, M.; Rassu, G.; Zetta, L.; Fava, G. G.; Belicchi, M. F., A simple diastereoselective synthesis of 2',3'-unsaturated aryl c-glucopyranosides. *Tetrahedron Lett.* **1988,** *29* (27), 3323-3326.

10. Friesen, R. W.; Loo, R. W., Preparation of C-aryl glucals via the palladium catalyzed coupling of metalated aromatics with 1-iodo-3,4,6-tri-O-(triisopropylsilyl)-D-glucal. *J. Org. Chem.* **1991,** *56* (16), 4821-4823.
11. Bai, Y.; Kim, L. M. H.; Liao, H.; Liu, X.-W., Oxidative Heck Reaction of Glycals and Aryl Hydrazines: A Palladium-Catalyzed C-Glycosylation. *J. Org. Chem.* **2013,** *78* (17), 8821-8825.
12. Schmidt, B., A de Novo Synthesis of 2,6-Dideoxy-C-aryl Glycosides Based on Ring Closing Metathesis and Diastereoselective Epoxide Cleavage/Anomerization Reactions. *Org. Lett.* **2000,** *2* (6), 791-794.
13. Vu, N. Q.; Leconte, S.; Brown, E.; Grée, D.; Grée, R.; Dujardin, G., A Straightforward and Flexible [4 + 2] Route to β-C-Naphthyl-2-deoxy-glycosides through Tandem Hydroboration-Ketal Reduction: De Novo Access to C-Naphthyl-6-fluoro and 6,6-Difluoro 2-Deoxyglycosides. *J. Org. Chem.* **2005,** *70* (7), 2641-2650.
14. Price, S.; Edwards, S.; Wu, T.; Minehan, T., Synthesis of C-aryl-Δ2,3-glycopyranosides via uncatalyzed addition of triarylindium reagents to glycals. *Tetrahedron Lett.* **2004,** *45* (27), 5197-5201.
15. Xiong, D.-C.; Zhang, L.-H.; Ye, X.-S., Oxidant-Controlled Heck-Type C-Glycosylation of Glycals with Arylboronic Acids: Stereoselective Synthesis of Aryl 2-Deoxy-C-glycosides. *Org. Lett.* **2009,** *11* (8), 1709-1712.
16. Steinhuebel, D. P.; Fleming, J. J.; Du Bois, J., Stereoselective Organozinc Addition Reactions to 1,2-Dihydropyrans for the Assembly of Complex Pyran Structures. *Org. Lett.* **2002,** *4* (2), 293-295.
17. Li, H.-H.; Ye, X.-S., Regio- and stereo-selective synthesis of aryl 2-deoxy-C-glycopyranosides by palladium-catalyzed Heck coupling reactions of glycals and aryl iodides. *Org. Biomol. Chem.* **2009,** *7* (18), 3855-3861.
18. Lei, M.; Gao, L.; Yang, J.-S., Microwave-assisted palladium-catalyzed cross-coupling reactions between pyranoid glycals and aryl bromides. Synthesis of 2′-deoxy C-aryl-β-glycopyranosides. *Tetrahedron Lett.* **2009,** *50* (36), 5135-5138.
19. de la Figuera, N.; Forns, P.; Fernàndez, J.-C.; Fiol, S.; Fernández-Forner, D.; Albericio, F., Avoiding pyran ring opening during palladium acetate catalyzed C-glycosidation of peracetylated glycals. *Tetrahedron Lett.* **2005,** *46* (42), 7271-7274.
20. Ramnauth, J.; Poulin, O.; Rakhit, S.; Maddaford, S. P., Palladium(II) Acetate Catalyzed Stereoselective C-Glycosidation of Peracetylated Glycals with Arylboronic Acids. *Org. Lett.* **2001,** *3* (13), 2013-2015.
21. Kusunuru, A. K.; Yousuf, S. K.; Tatina, M.; Mukherjee, D., Desulfitative C-Arylation of Glycals by Using Benzenesulfonyl Chlorides. *Eur. J. Org. Chem.* **2015,** *2015* (3), 459-462.
22. Amatore, C.; Jutand, A.; M'Barki, M. A., Evidence of the formation of zerovalent palladium from Pd(OAc)2 and triphenylphosphine. *Organometallics* **1992,** *11* (9), 3009-3013.
23. de Kleijne, F. F. J.; Moons, S. J.; White, P. B.; Boltje, T. J., C-2 auxiliaries for stereoselective glycosylation based on common additive functional groups. *Org. Biomol. Chem.* **2020,** *18* (6), 1165-1184.
24. Liu, M.; Luo, Z. X.; Li, T.; Xiong, D. C.; Ye, X. S., Electrochemical Trifluoromethylation of Glycals. *J. Org. Chem.* **2021,** *86* (22), 16187-16194.
25. Ghosh, T.; Mukherji, A.; Kancharla, P. K., Sterically Hindered 2,4,6-Tri-tert-butylpyridinium Salts as Single Hydrogen Bond Donors for Highly Stereoselective Glycosylation Reactions of Glycals. *Org. Lett.* **2019,** *21* (10), 3490-3495.
26. Bi, J.; Tan, Q.; Wu, H.; Liu, Q.; Zhang, G., Rhodium-Catalyzed Denitrogenative Transannulation of N-Sulfonyl-1,2,3-triazoles with Glycals Giving Pyrroline-Fused N-Glycosides. *Org. Lett.* **2021,** *23* (16), 6357-6361.
27. Lellouche, J.-P.; Koeller, S., The Particular Sensitivity of Silyl Ethers of d-Glucal toward Two Vilsmeier−Haack Reagents POCl3·DMF and (CF3SO2)2O·DMF. Their Unique and Selective Conversion to the Corresponding C(6)-O-Formates. *J. Org. Chem.* **2001,** *66* (3), 693-696.
28. Dev, D.; Palakurthy, N. B.; Thalluri, K.; Chandra, J.; Mandal, B., Ethyl 2-Cyano-2-(2-nitrobenzenesulfonyloxyimino)acetate (o-NosylOXY): A Recyclable Coupling Reagent for Racemization-Free Synthesis of Peptide, Amide, Hydroxamate, and Ester. *J. Org. Chem.* **2014,** *79* (12), 5420-5431.
29. Tang, S.; Zheng, Q.; Xiong, D.-C.; Jiang, S.; Li, Q.; Ye, X.-S., Stereocontrolled Synthesis of 2-Deoxy-C-glycopyranosyl Arenes Using Glycals and Aromatic Amines. *Org. Lett.* **2018,** *20* (10), 3079-3082.
30. Singh, A. K.; Venkatesh, R.; Kandasamy, J., Palladium-Catalyzed One-Pot Stereospecific Synthesis of 2-Deoxy Aryl C-Glycosides from Glycals and Anilines in the Presence of tert-Butyl Nitrite. *Synthesis* **2019,** *51* (22), 4215-4230.

4.7. Selected spectra

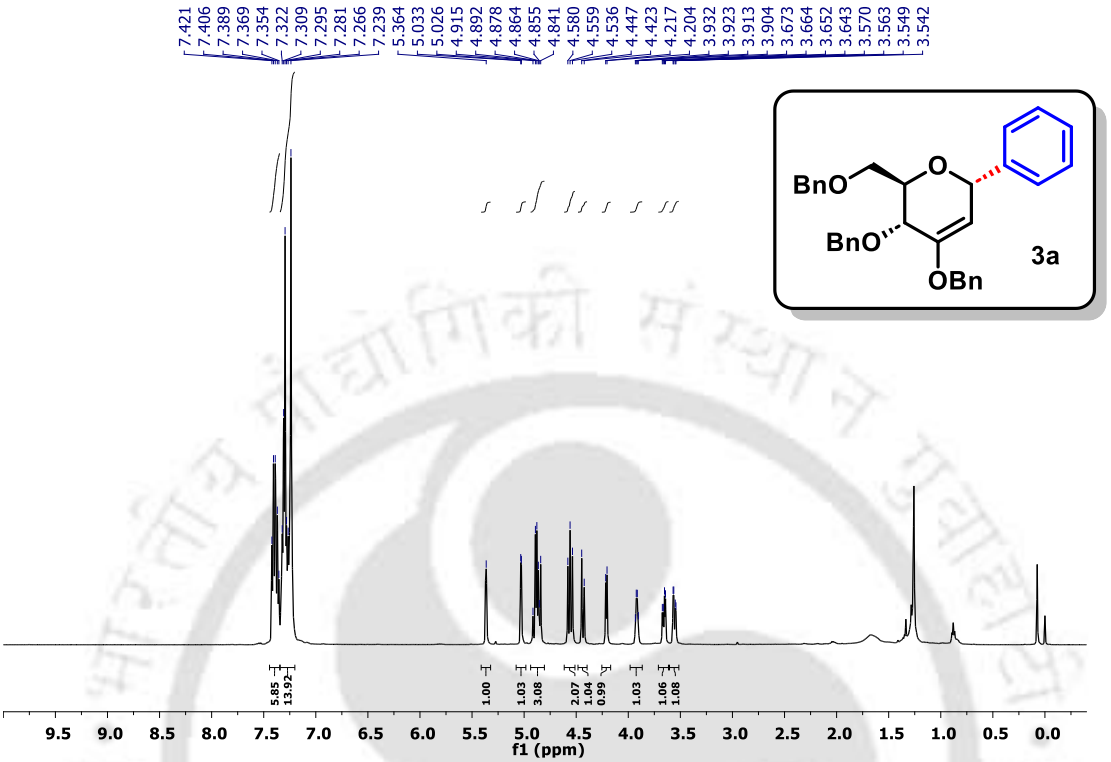

Figure 4.10. *[1]H NMR of compound **3a** (500 MHz, $CDCl_3$).*

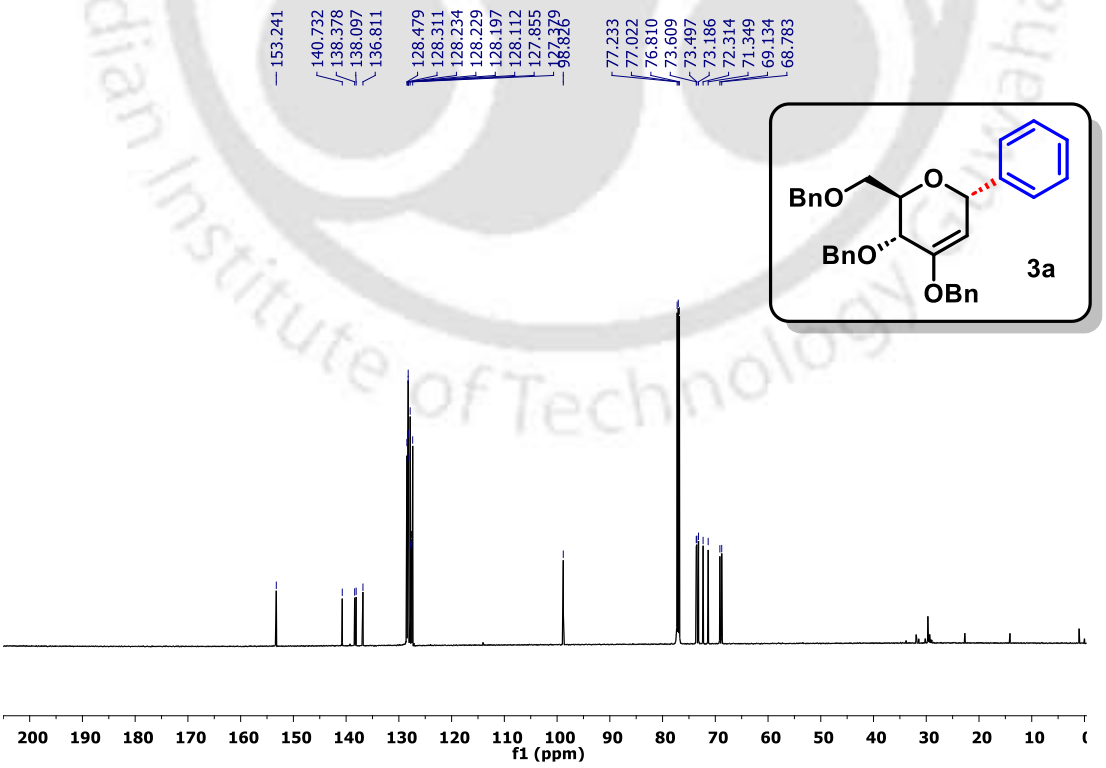

Figure 4.11. *[13]C NMR of compound **3a** (151 MHz, $CDCl_3$).*

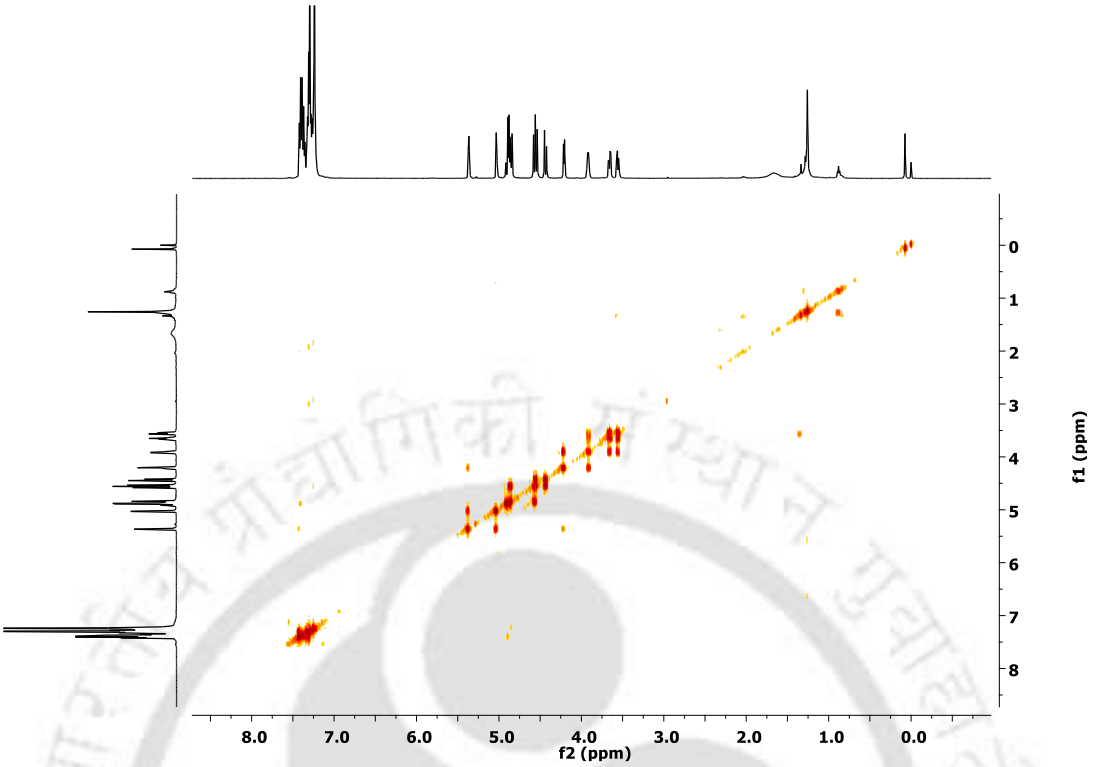

Figure 4.12. *COSY NMR of compound **3a** (500 MHz, $CDCl_3$).*

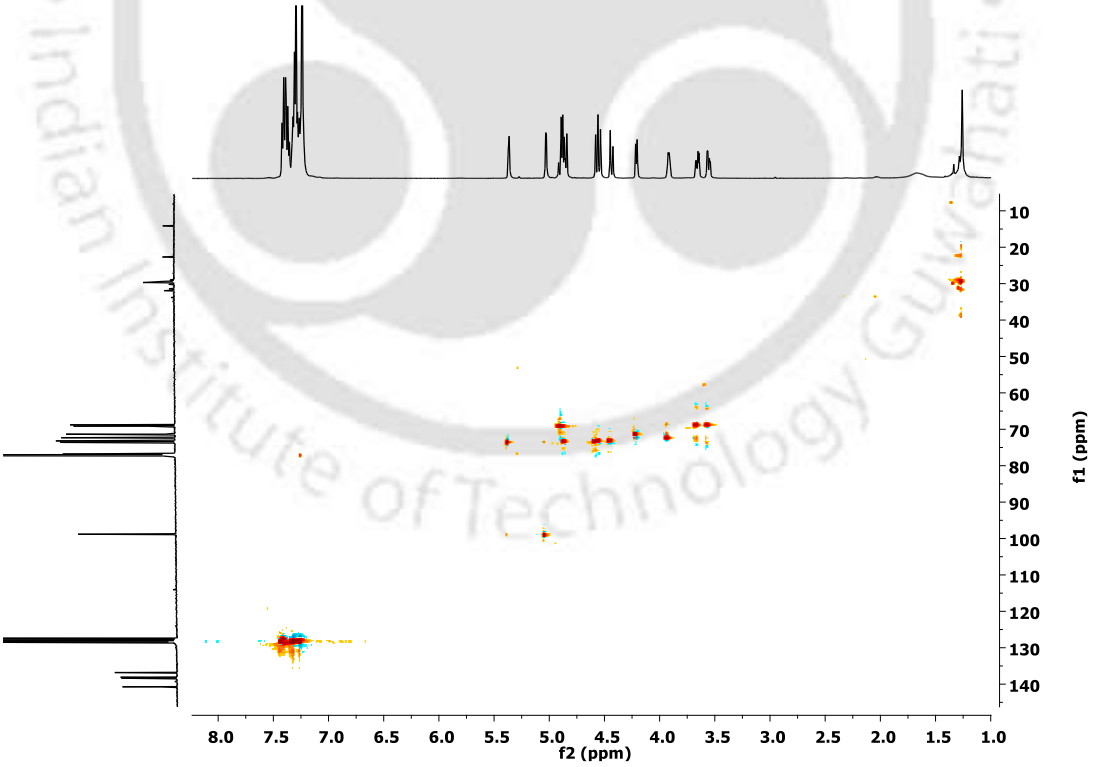

Figure 4.13. *HSQC-GP NMR of compound **3a** (500 MHz, $CDCl_3$).*

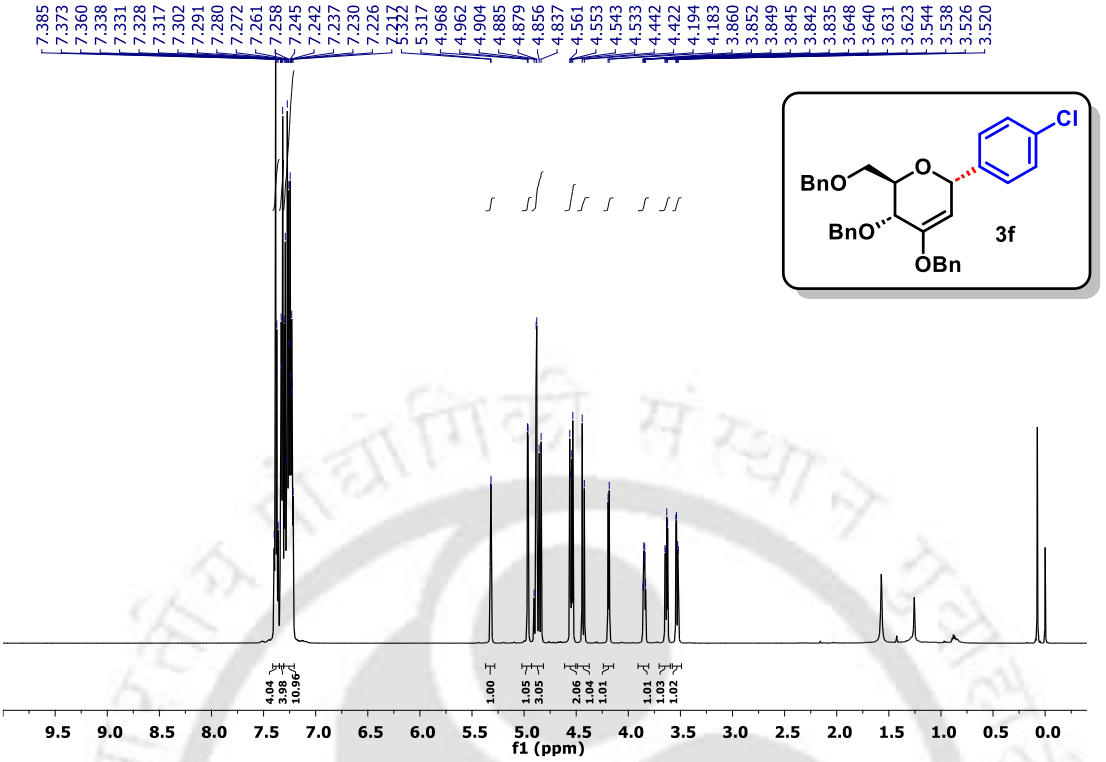

Figure 4.14. *^{1}H NMR of compound **3f** (600 MHz, $CDCl_3$).*

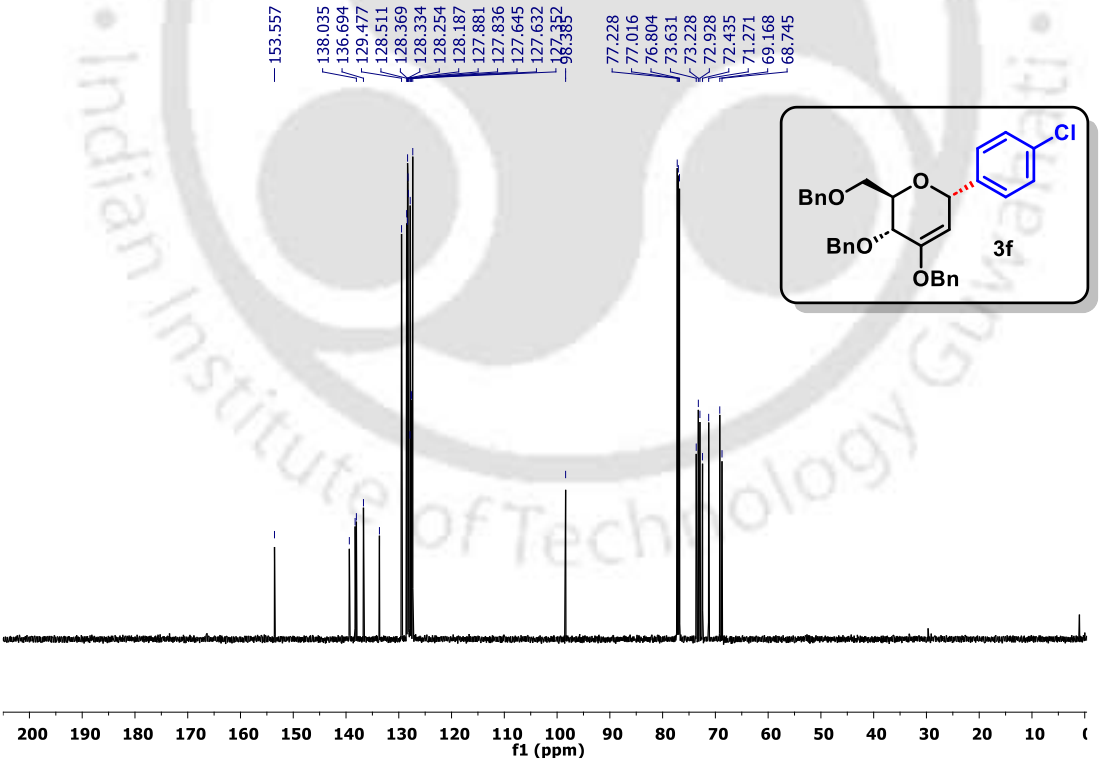

Figure 4.15. *^{13}C NMR of compound **3f** (151 MHz, $CDCl_3$).*

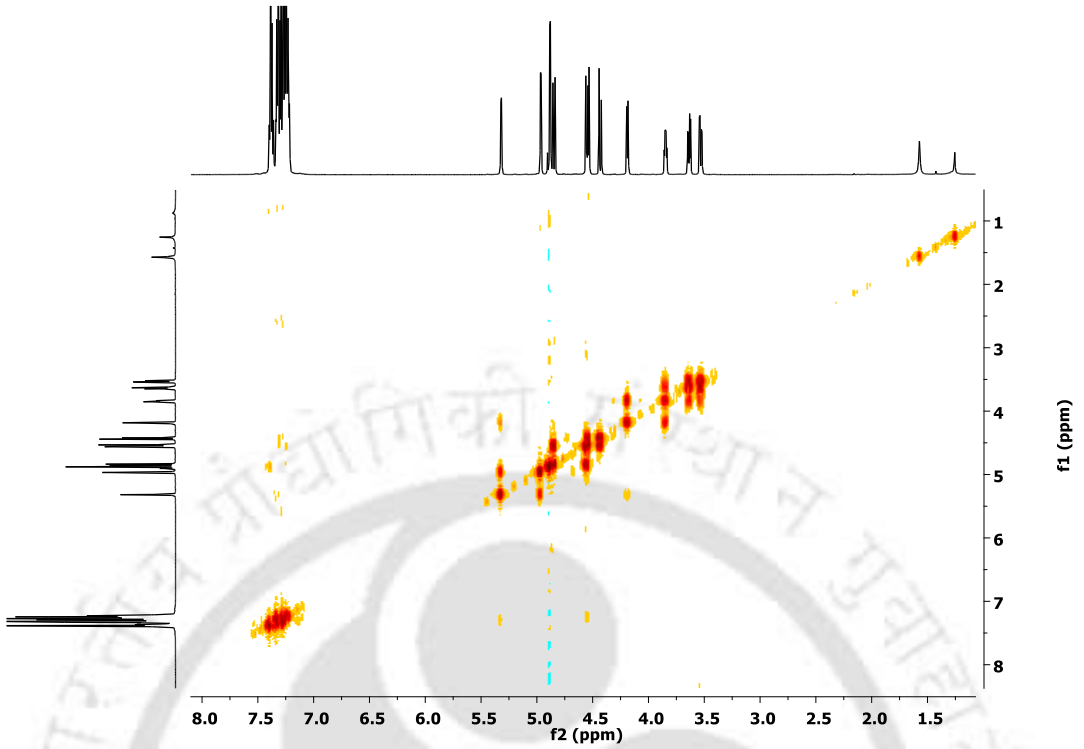

Figure 4.16. *COSY NMR of compound* ***3f*** *(600 MHz, $CDCl_3$).*

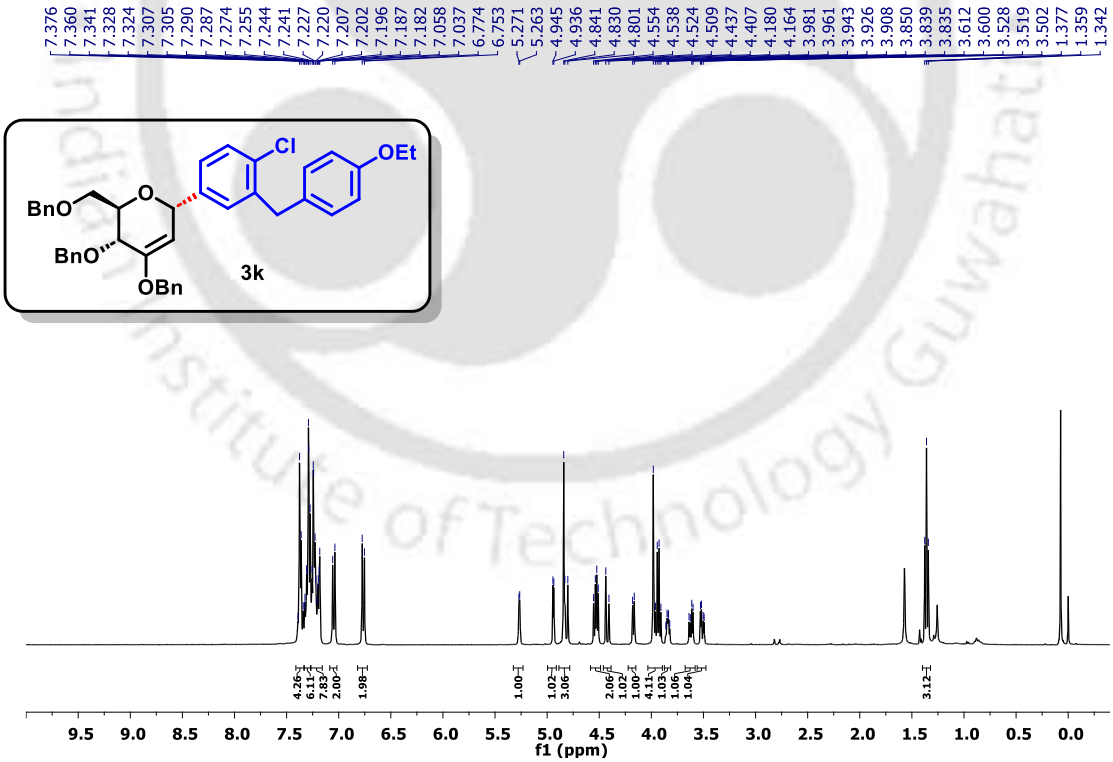

Figure 4.17. *^{1}H NMR of compound* ***3k*** *(400 MHz, $CDCl_3$).*

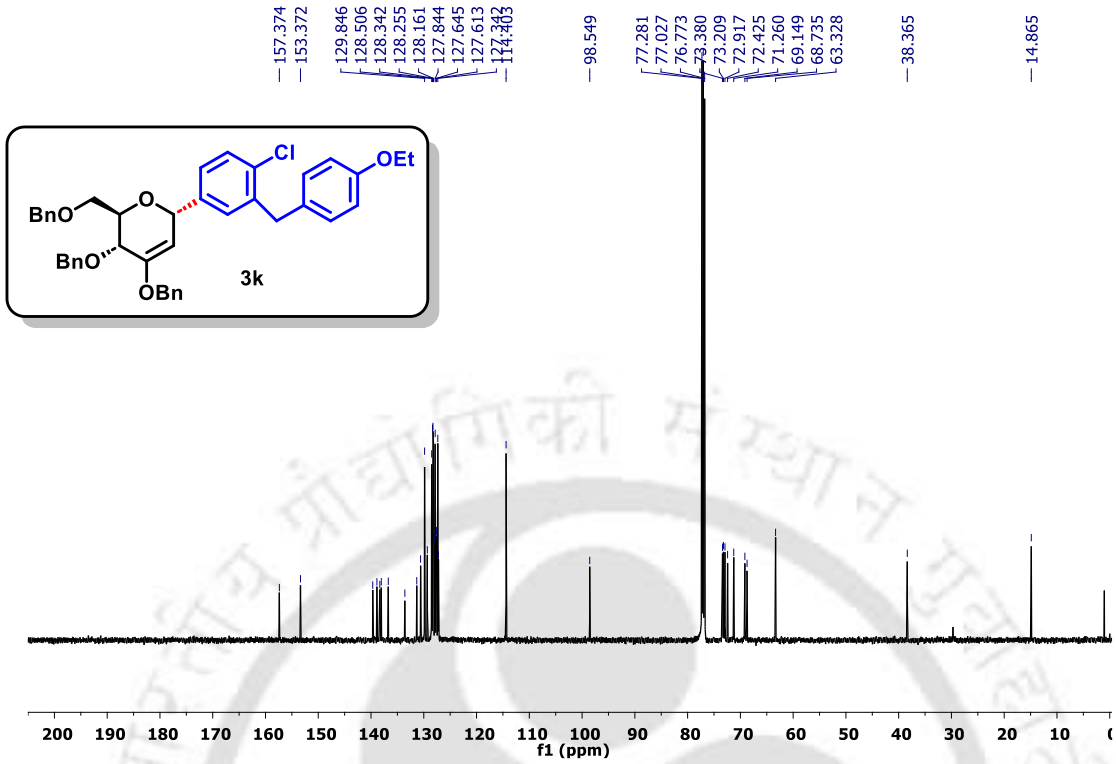

Figure 4.18. *^{13}C NMR of compound **3k** (126 MHz, $CDCl_3$).*

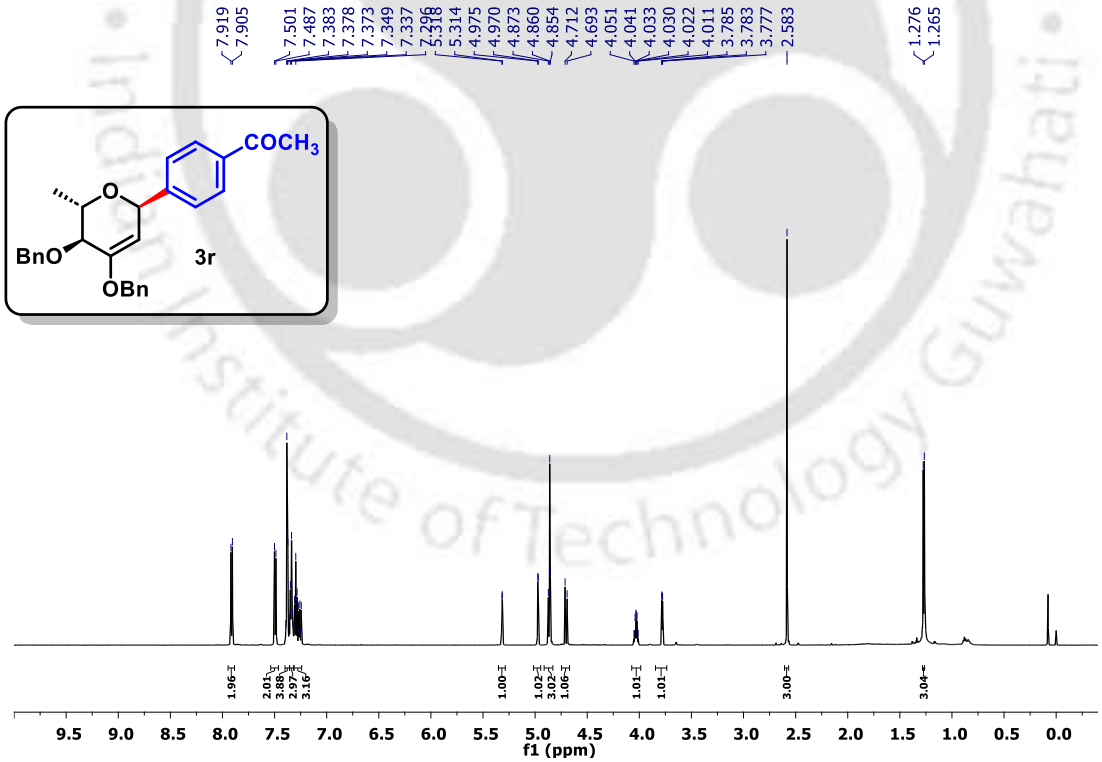

Figure 4.19. *^{1}H NMR of compound **3r** (600 MHz, $CDCl_3$).*

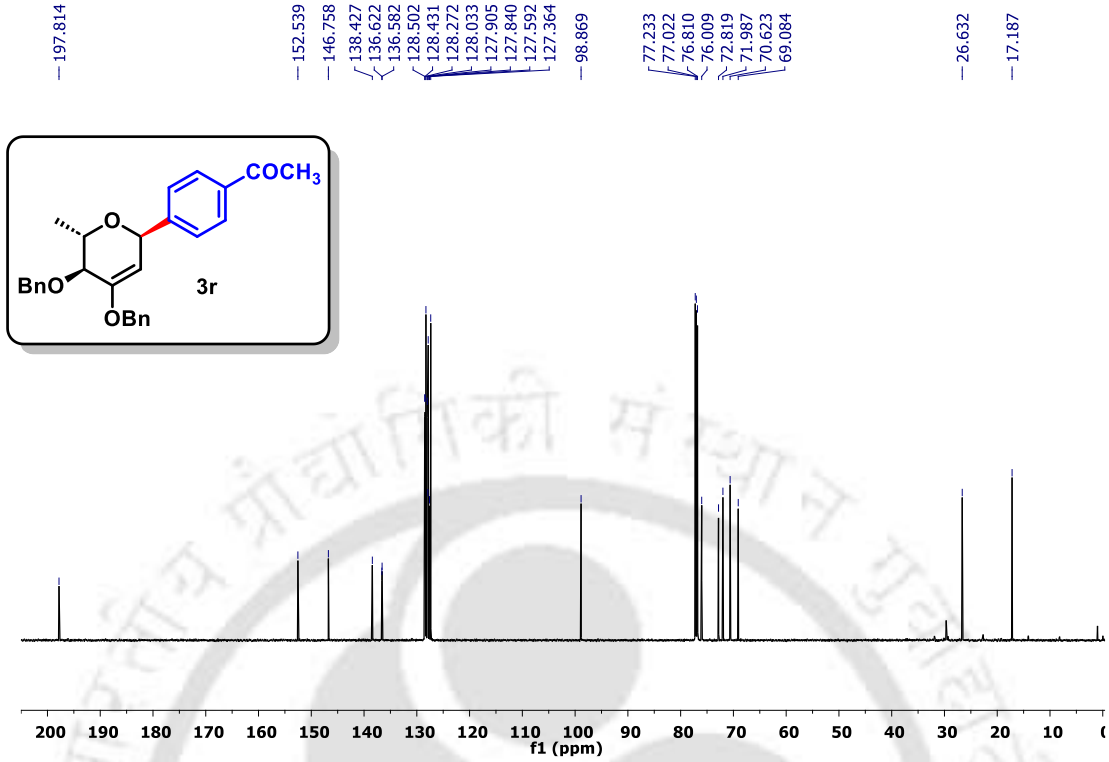

Figure 4.20. *^{13}C NMR of compound **3r** (151 MHz, $CDCl_3$).*

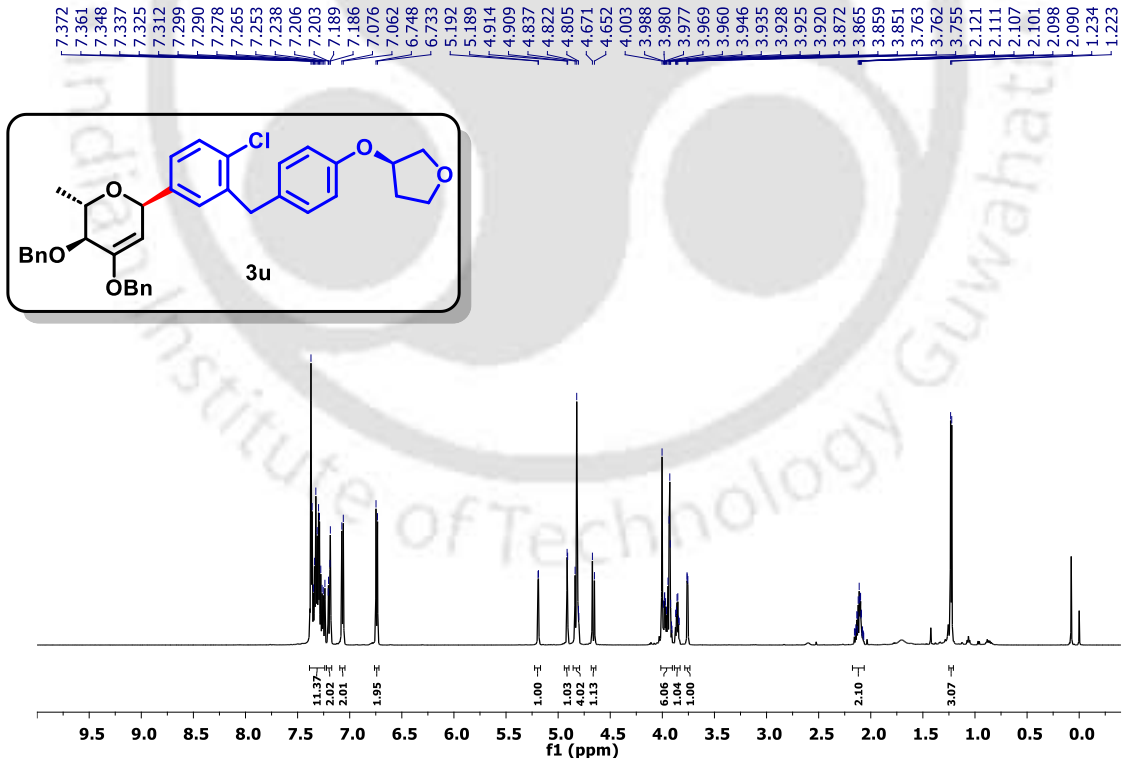

Figure 4.21. *^{1}H NMR of compound **3u** (600 MHz, $CDCl_3$).*

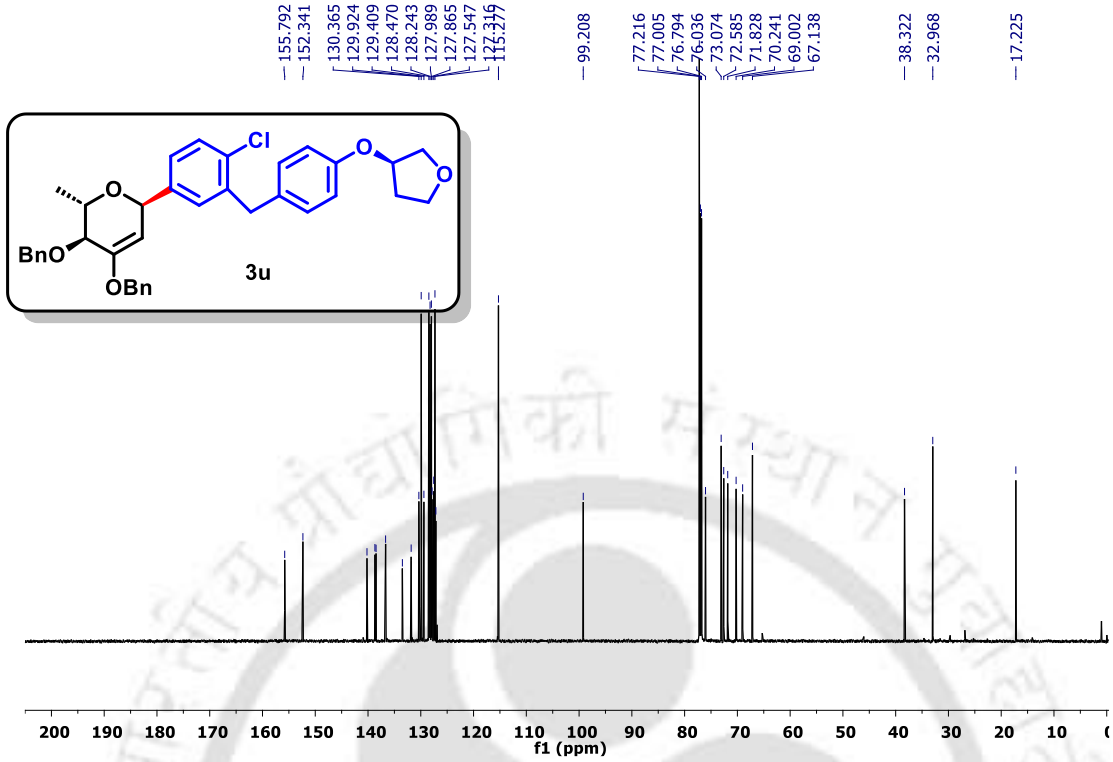

Figure 4.22. *^{13}C NMR of compound **3u** (151 MHz, $CDCl_3$).*

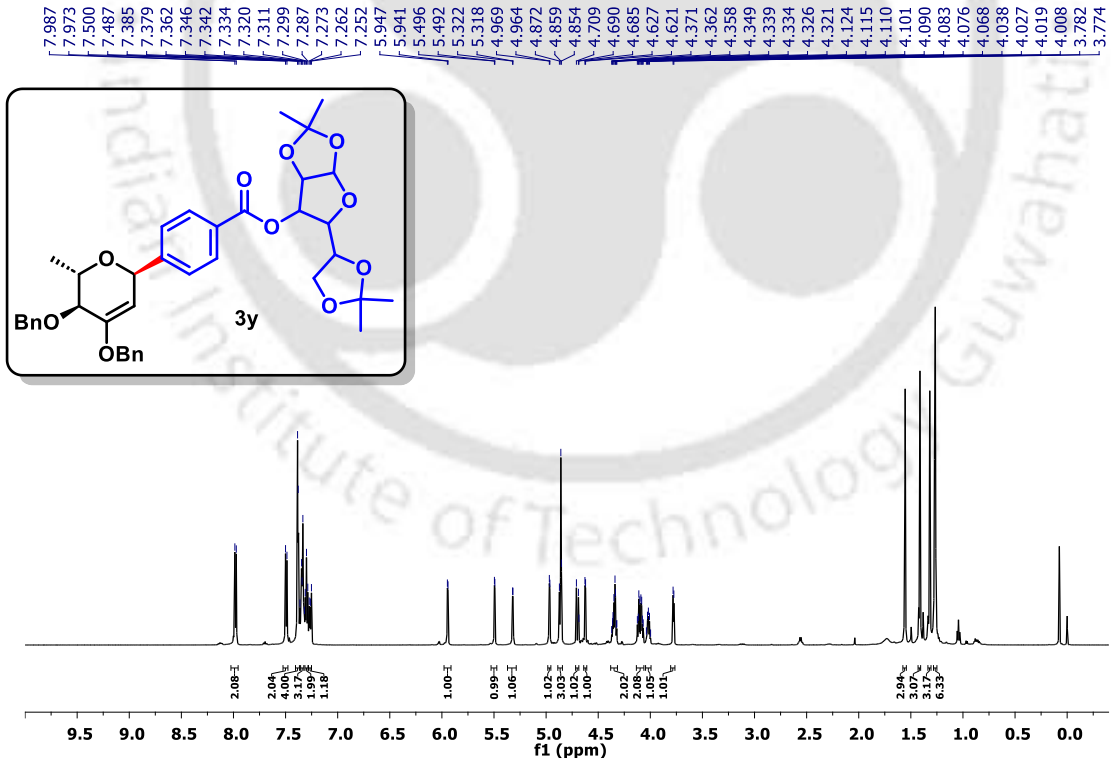

Figure 4.23. *^{1}H NMR of compound **3y** (600 MHz, $CDCl_3$).*

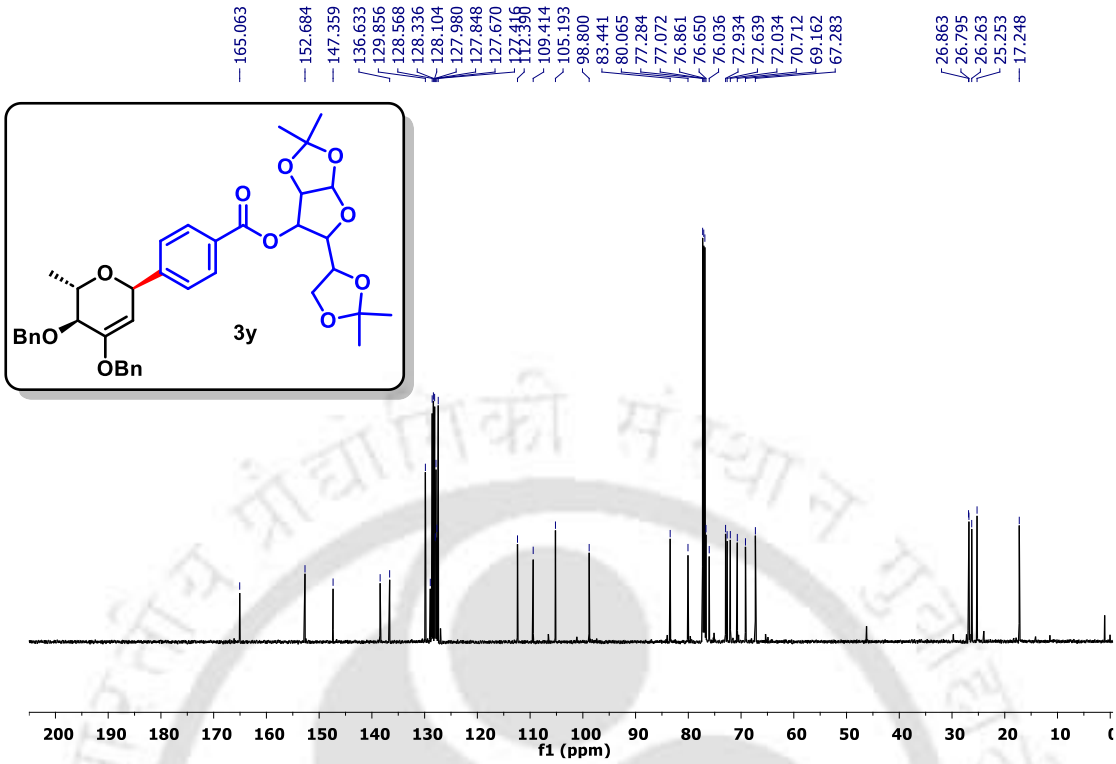

Figure 4.24. *^{13}C NMR of compound **3y** (151 MHz, $CDCl_3$).*

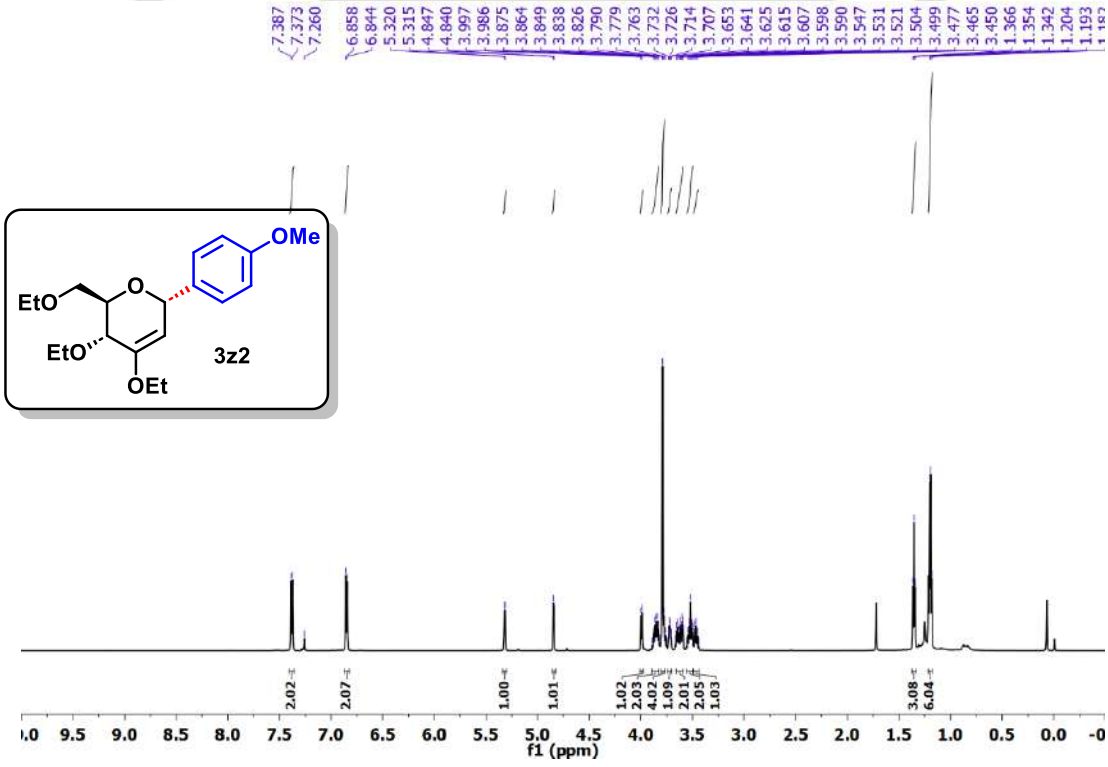

Figure 4.25. *^{1}H NMR of compound **3z2** (600 MHz, $CDCl_3$).*

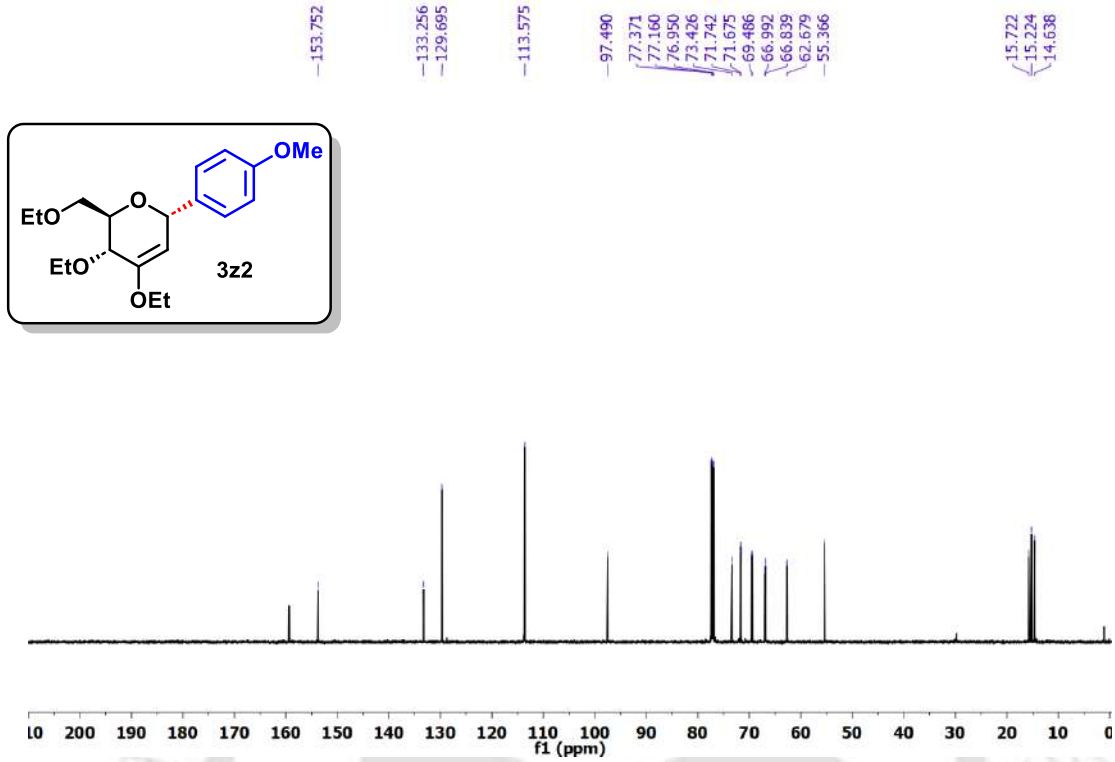

Figure 4.26. *^{13}C NMR of compound **3z2** (151 MHz, $CDCl_3$).*

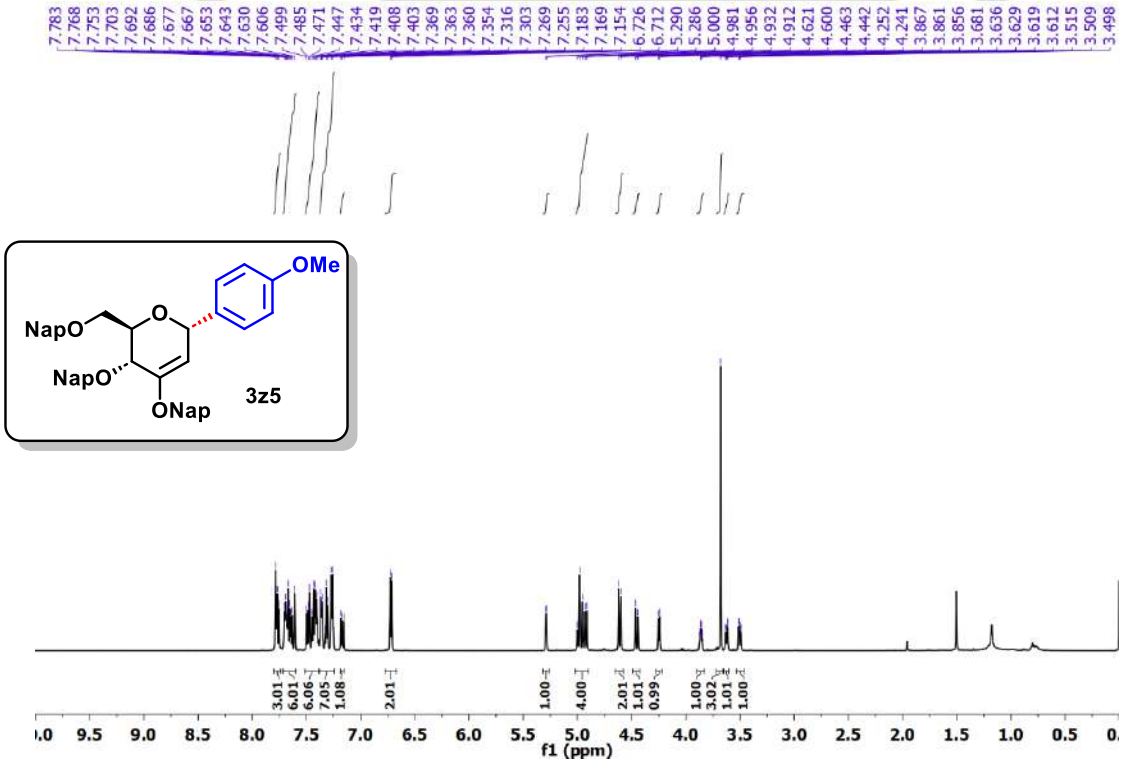

Figure 4.27. *^{1}H NMR of compound **3z5** (600 MHz, $CDCl_3$).*

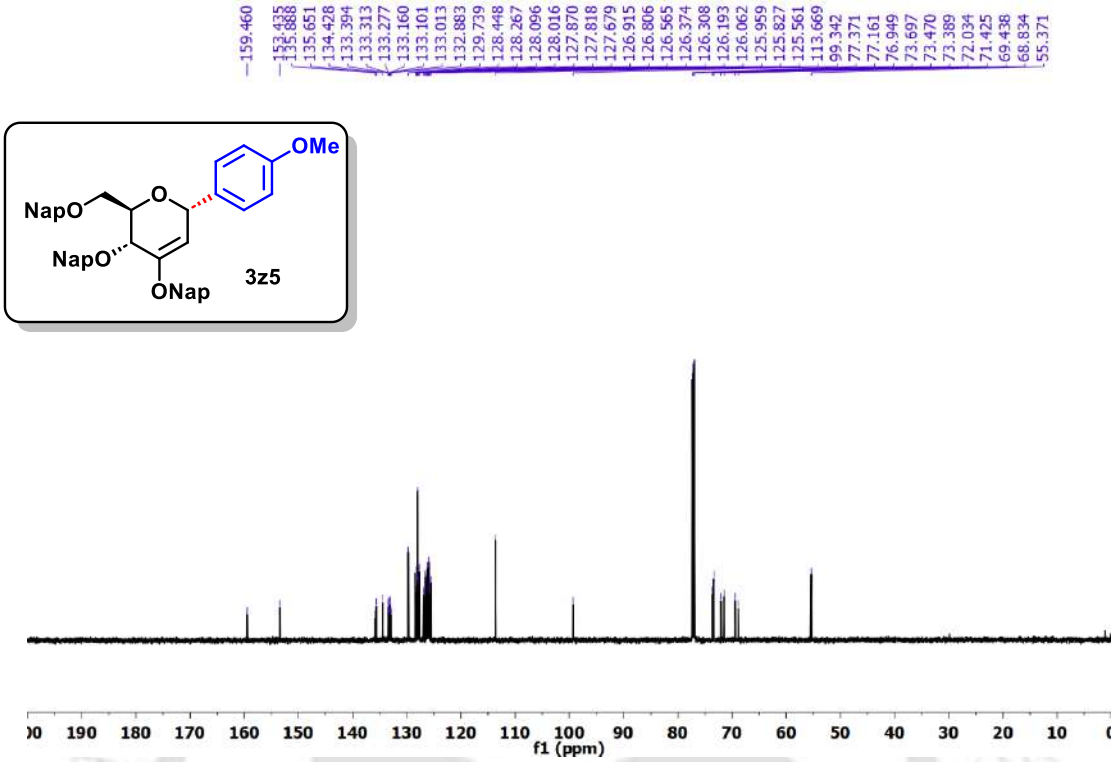

Figure 4.28. *^{13}C NMR of compound **3z5** (151 MHz, $CDCl_3$).*

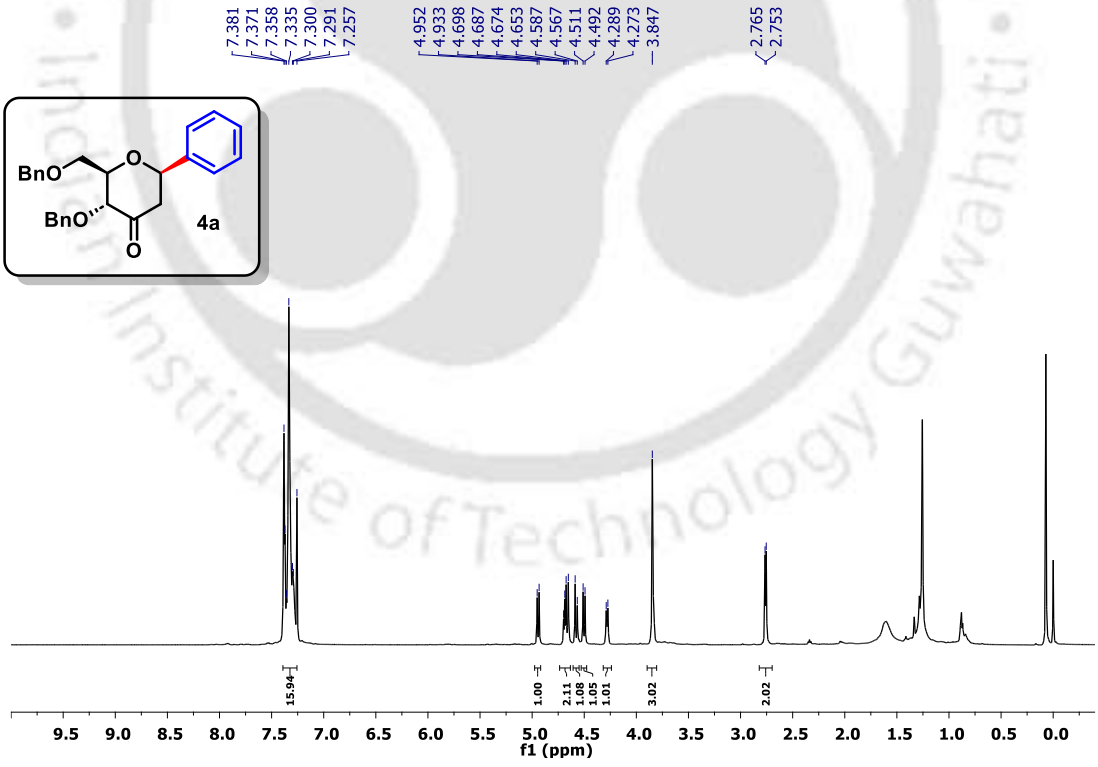

Figure 4.29. *^{1}H NMR of compound **4a** (600 MHz, $CDCl_3$).*

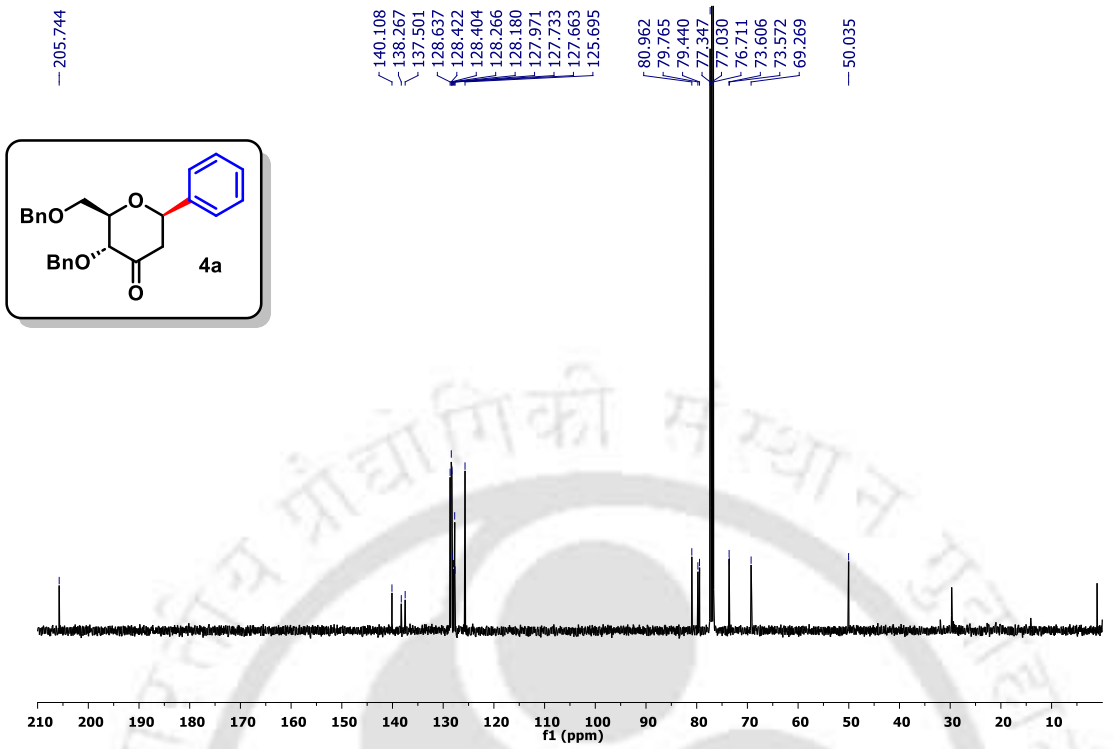

Figure 4.30. *^{13}C NMR of compound **4a** (101 MHz, $CDCl_3$).*

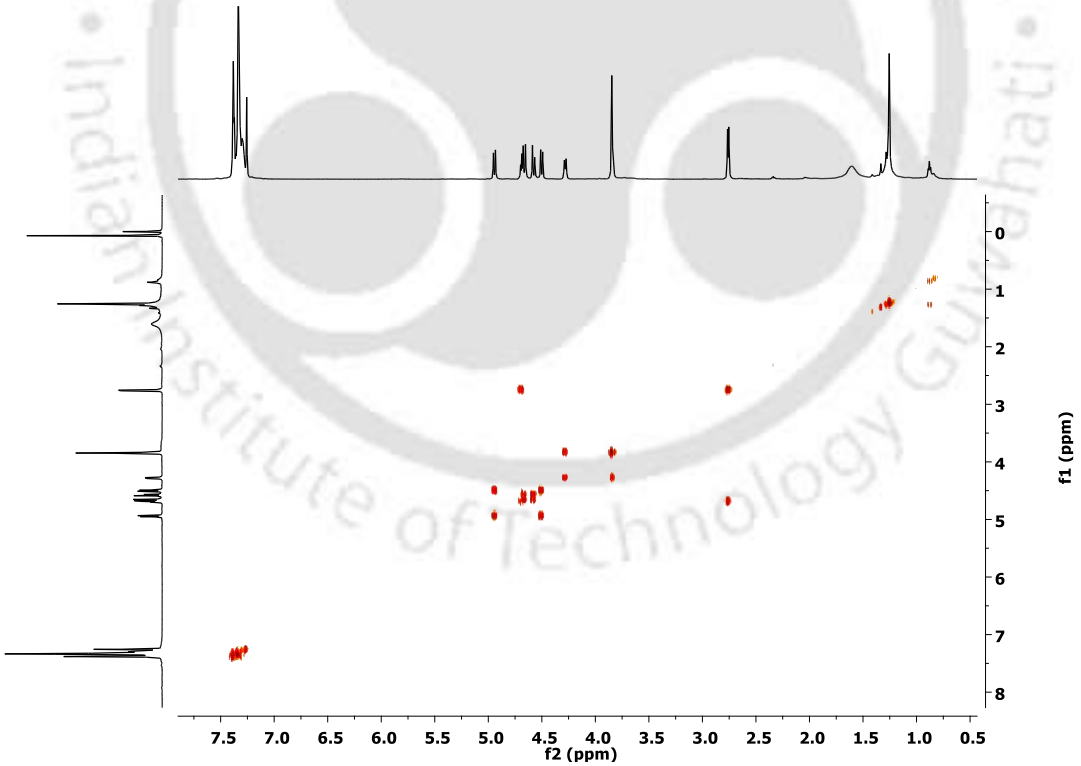

Figure 4.31. *COSY NMR of compound **4a** (600 MHz, $CDCl_3$).*

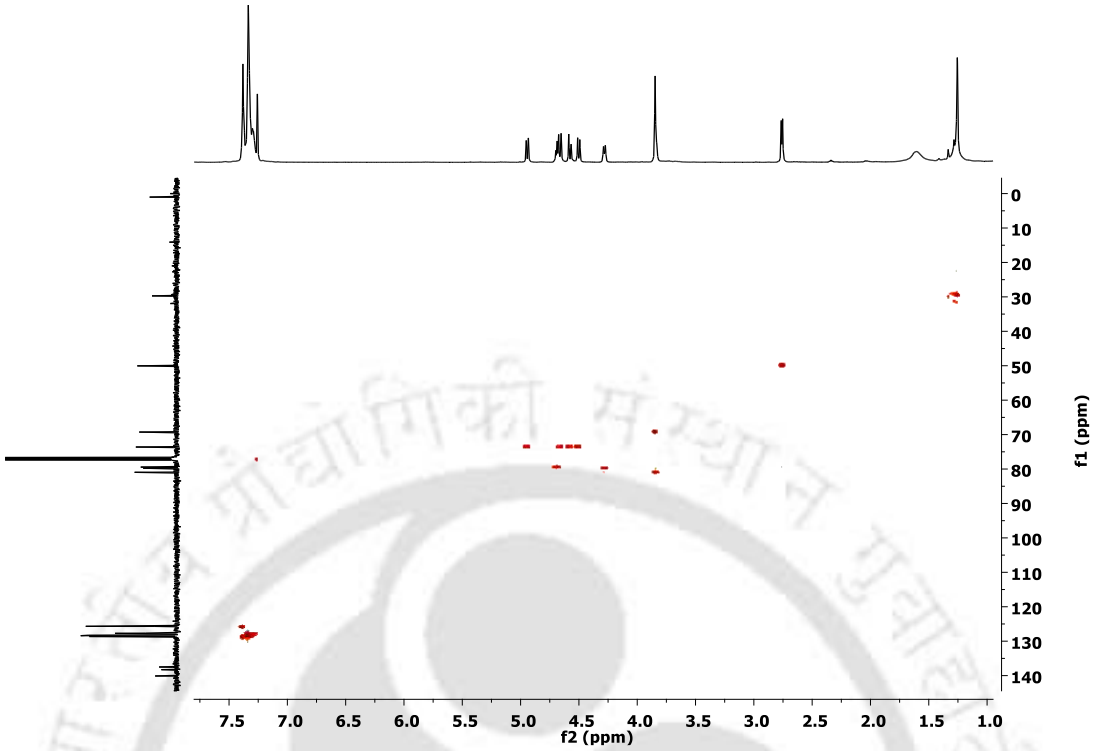

Figure 4.32. *HSQC-GP NMR of compound* ***4a*** *(600 MHz, $CDCl_3$).*

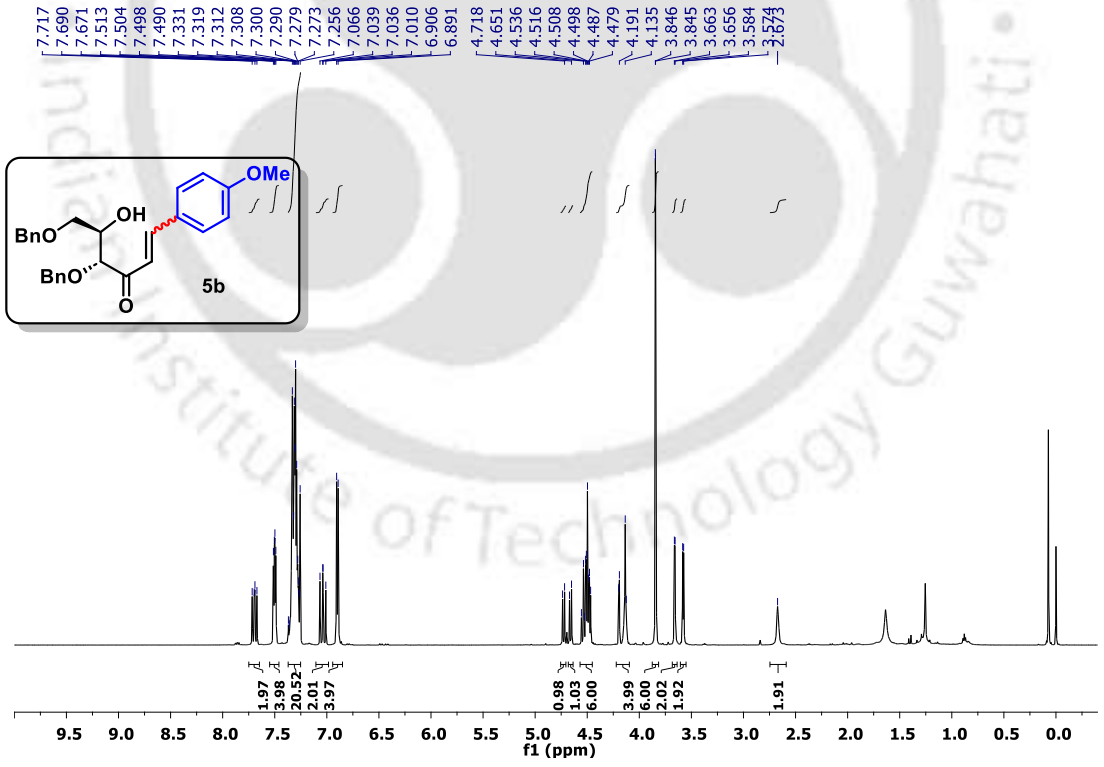

Figure 4.33. *^{1}H NMR of compound* ***5b*** *(600 MHz, $CDCl_3$).*

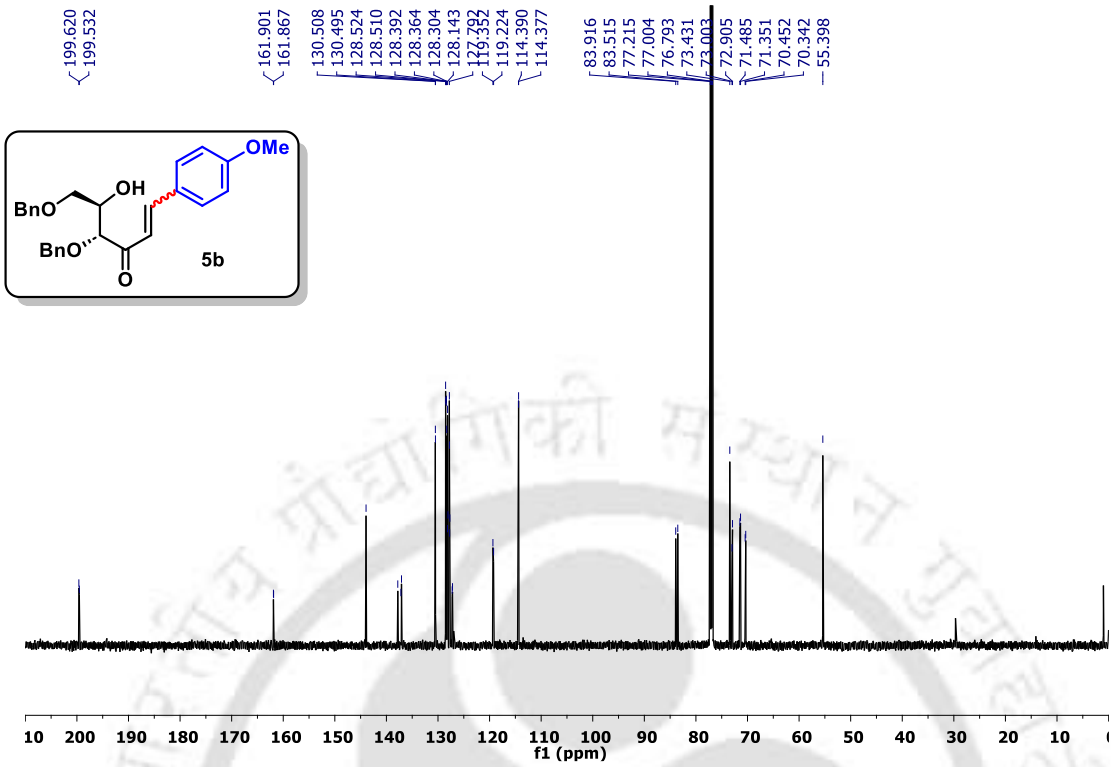

Figure 4.34. *^{13}C NMR of compound **5b** (151 MHz, $CDCl_3$).*

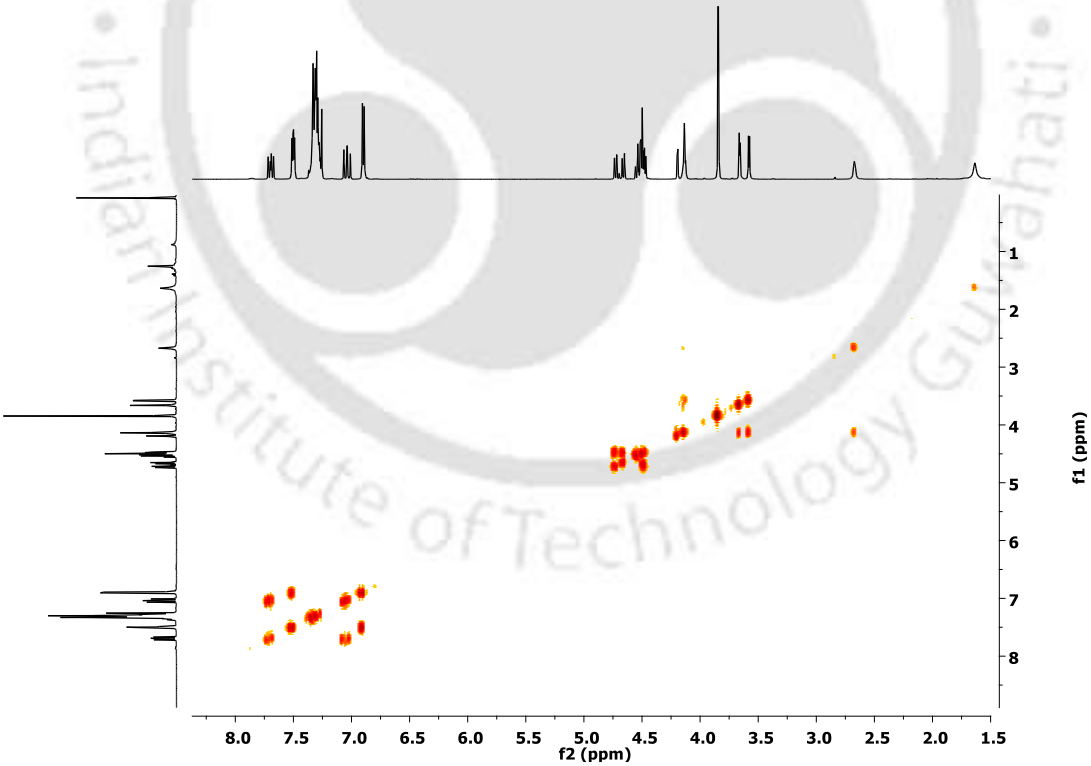

Figure 4.35. *COSY NMR of compound **5b** (600 MHz, $CDCl_3$).*

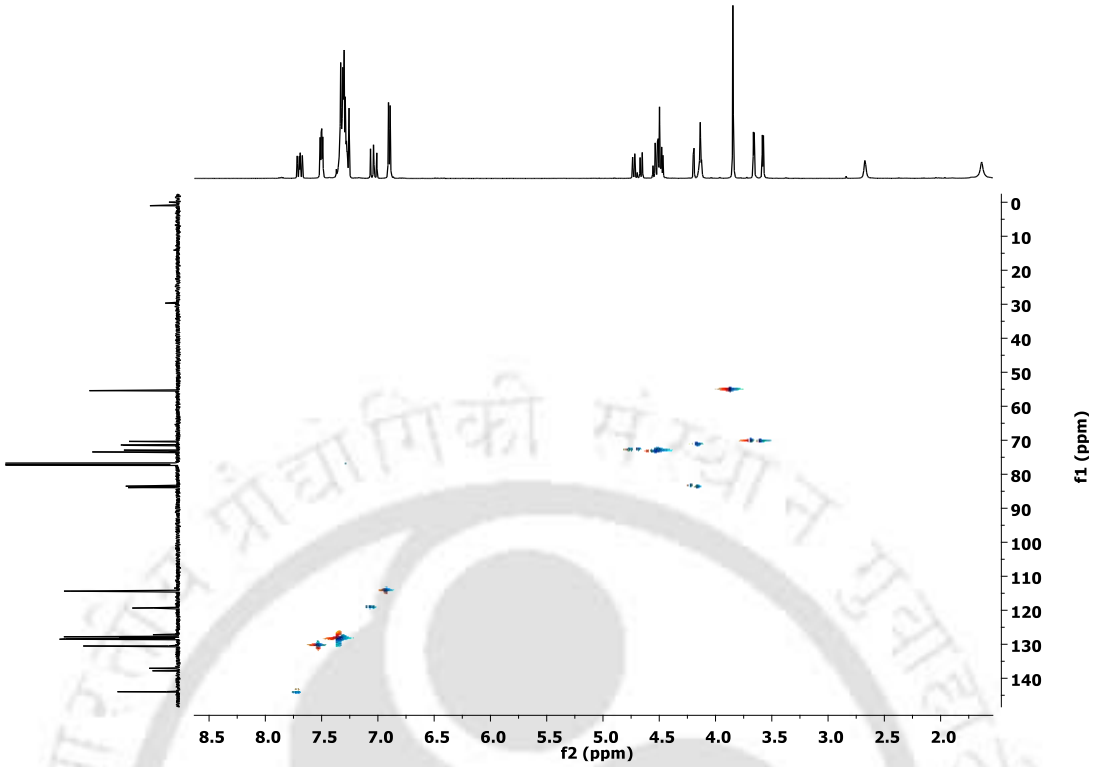

Figure 4.36. *HSQC-GP NMR of compound* ***5b*** *(600 MHz, $CDCl_3$).*

4.8. SC-XRD Data

XRD Data of 3q

The ORTEP diagram with an ellipsoid of 30% probability.

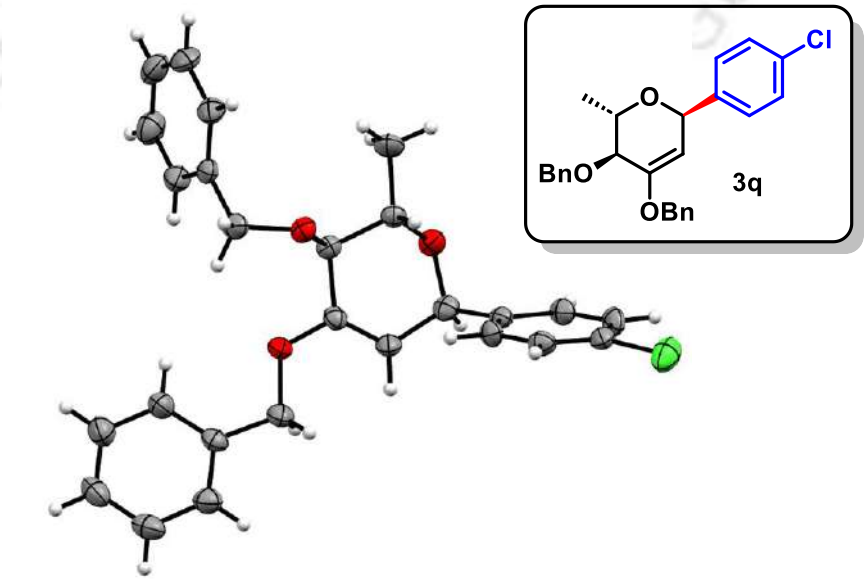

XRD Data of 4b

The ORTEP diagram with an ellipsoid of 30% probability.

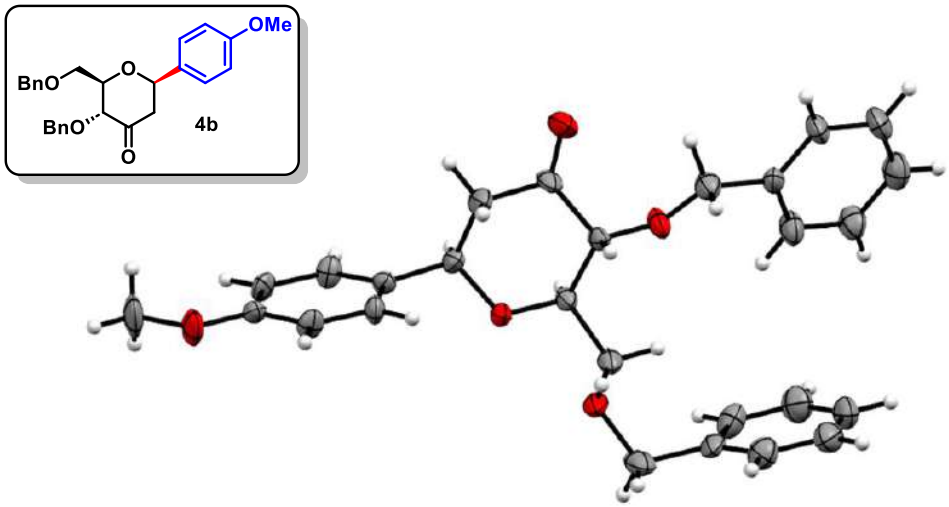

XRD Data of 3z5

The ORTEP diagram with an ellipsoid of 30% probability.

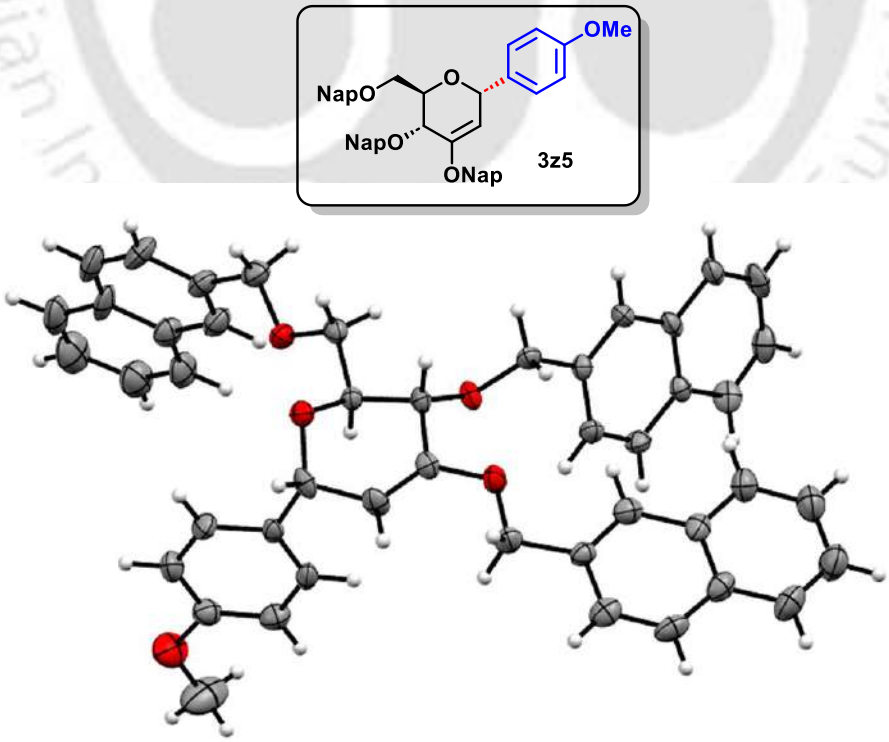

Table 4.4: Crystal parameters and refinement data of **3q, 4b and 3z5**

Parameters	Substrate 3q	Substrate 4b	Substrate 3z5
Formula	$C_{26}H_{25}ClO_3$	$C_{27}H_{28}O_5$	$C_{46}H_{40}O_5$
Fw	420.91	432.49	672.78
Crystal system	monoclinic	monoclinic	monoclinic
Space group	*P 21*	*P 21*	*P 21*
a/Å	10.518(2)	5.509(4)	15.3551(12)
b/Å	5.8267(14)	7.990(6)	6.1872(5)
c/Å	17.830(4)	26.430(19)	19.4490(16)
α/°	90.00	90.00	90
β/°	93.951(8)	93.290(19)	107.898(2)
γ/°	90.00	90.00	90
V/Å^3	1090.1(4)	1161.5(15)	1758.3(2)
Z	2	2	2
D_c/g cm^{-3}	1.282	1.237	1.271
μ Mo K_α/mm^{-1}	0.200	0.084	0.081
F000	444	460	712
T/K	298(2)	297(2)	301(2)
θ max.	23.85	25.03	26.31
Total no. of reflections	14297	23174	32980
Independent reflections	3828	4001	6061
Observed reflections	2983	2181	3597
Parameters refined	272	290	461
R_1, I > 2σ(I)	0.0402	0.1389	0.1652
wR_2, I > 2σ(I)	0.0842	0.2448	0.3054
GOF (F^2)	0.897	1.304	1.483
CCDC No.	2341010	2341011	2347397

Chapter 5

Influence of Sterics vs Inductive vs Through Space Stabilization Effects on the Basicity and Reactivity of the Pyridinium Cation

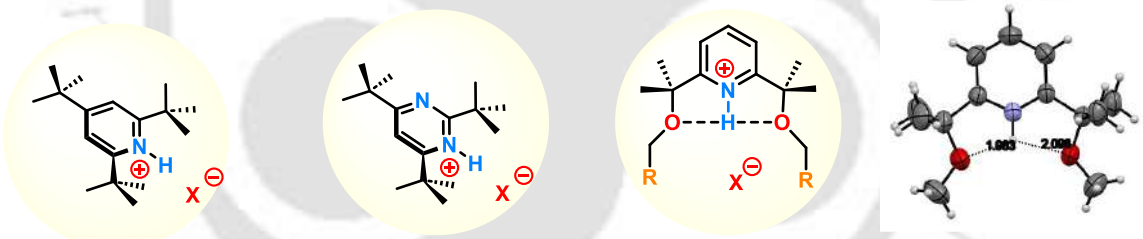

Sterics vs Inductive Effect vs H-bonding

5.1. Introduction

5.1.1. Importance of sterically hindered pyridine derivatives

Pyridine is a highly versatile compound with significant importance in organic synthesis, agriculture, pharmaceuticals, and industrial applications. Its nitrogen atom imparts distinctive properties, making it an essential heterocyclic compound in both organic and medicinal chemistry.[1] Its derivatives, particularly sterically hindered ones, further enhance its utility by improving selectivity, stability, and overall efficiency in modern chemical processes.[2] Bulky pyridine derivatives such as 2,6-di-*tert*-butylpyridine (DTBP), 2,6-di-*tert*-butyl-4-methylpyridine (DTBMP), 2,4,6-tri-*tert*-butylpyridine (TTBPy), and 2,4,6-tri-*tert*-butylpyrimidine (TTBP) are among the most extensively studied, holding a distinctive place in organic chemistry. Since Brown's discovery that DTBP is unable to form the typical Lewis acid-base adduct with strong Lewis acids such as BF_3 or CH_3^+, except with H^+, unlike simple pyridine derivatives, organic chemists have recognized the utility of this class of compounds as non-nucleophilic bases that can differentiate Brønsted acids from Lewis acids.[3] These bulky pyridines are now routinely used as proton-trapping agents in reactions that generate strong Brønsted acids and have long been employed as traditional acid scavengers.[4, 5]

Interestingly, the aqueous pK_a values of sterically hindered pyridines are lower than anticipated. The alkyl-substituted pyridines are usually more basic than the unsubstituted pyridines; however, a trend reversal is observed when the two ortho positions are flanked with sterically hindered tertiary butyl groups.[6] The diminished basicity arises from poor solvation of their protonated forms due to steric hindrance, resulting in weak basicity (e.g., $TTBPyH^+$, pK_a = 3.54) (Figure 5.1).[7]

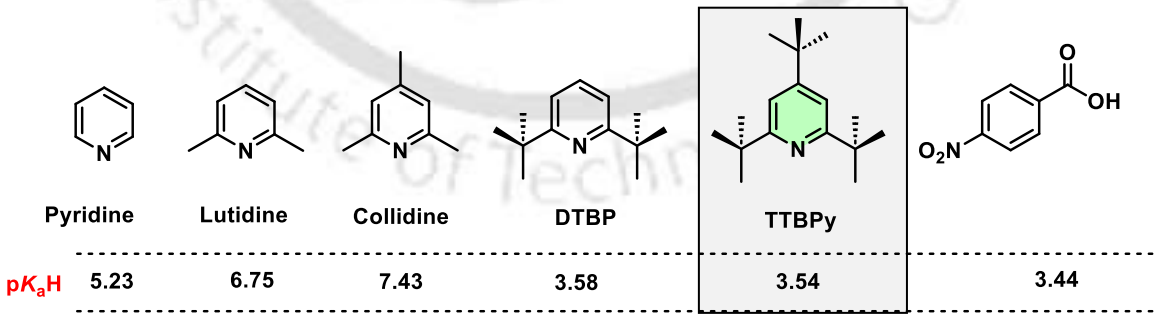

Figure 5.1. Substituent effects on pyridine basicity.

Shenderovich and co-workers demonstrated that even the strongest coordinating ligand, such as fluoride, fails to form an H-bond with the cationic N-H of protonated DTBP, highlighting the strong influence of steric hindrance around the nitrogen center.[8] Despite the widespread use of bulky pyridine derivatives as proton-trapping agents in organic

reactions, our laboratory has developed structurally strained Brønsted salts that, owing to weak ion-pair interactions arising from steric bulk around the positively charged nitrogen center, exhibit frustrated ion-pair reactivity and can catalyze various stereoselective glycosylation reactions easily.[7, 9-11]

5.1.2. Knowledge gap

Although bulky pyridines such as 2,4,6-tri-*tert*-butylpyridine (TTBPy), 2,6-di-*tert*-butyl-4-methylpyridine (DTBMP), and 2,6-di-*tert*-butylpyridine (DTBP) are widely used for their utility as proton-trapping agents, their high cost and lengthy synthetic routes (often requiring 5-6 steps) highlight the need for more accessible, cost-effective alternatives that can not only serve as proton scavengers but also function as versatile organocatalysts for promoting new classes of organic transformations.

5.1.3. Purpose and objectives of the chapter

These bulky pyridines are routinely employed by organic chemists as proton-trapping agents. Despite their widespread use, these bulky pyridines display unusually low basicity in aqueous solution, as evidenced by their unexpectedly low pK_a values. This diminished basicity has been attributed to their poor solvation in polar solvents, arising from steric shielding of the cationic $[N\text{-}H]^+$ site by the surrounding *tert*-butyl groups.

In this thesis, we present the synthesis of a series of 2,6-disubstituted pyridine derivatives in which one methyl group of the *tert*-butyl substituent has been replaced with methoxy, ethoxy, or benzyloxy groups. These derivatives act as molecular balances to disentangle the relative contributions of steric hindrance, inductive effects, and through-space stabilization by heteroatoms to the basicity and reactivity of bulky pyridinium species. The study further reveals how the Thorpe-Ingold effect shapes the accessible conformational landscape of this new class of alkoxy-substituted pyridinium salts. Importantly, we demonstrate that these cost-effective hindered pyridines retain the properties of non-nucleophilic bases and represent promising alternatives to established proton sponges such as TTBPy, DTBMP, DTBP, and TTBP.

5.2. Results and discussion

5.2.1. Design and synthesis of pyridinium triflate salts

Our study commenced with the synthesis of a variety of heteroatom-containing bulky pyridines (Scheme 5.1). The protection of 2,6-pyridine dicarboxylic acid as a methyl ester, followed by the addition of excess methyllithium, afforded 2,6-disubstituted

pyridine-derived tertiary alcohols, which were functionalized with various alkyl groups by treatment with appropriate alkyl halides (Scheme 5.1). We restricted our study to the synthesis of methyl, ethyl, and benzyl derivatives to understand the influence of the heteroatom and steric effects on the protonation/basicity of the pyridine nitrogen. All the desired compounds (**4a-4c** and **6c**) were obtained in good yields (Scheme 5.1). Subsequently, all these compounds were converted into their respective triflate salts (**7a-7c** and **7e**) by simply treating the substituted pyridines with 1 equivalent of triflic acid in ether (Scheme 5.1). NMR and X-ray crystallography were used to characterize all newly synthesized salts.

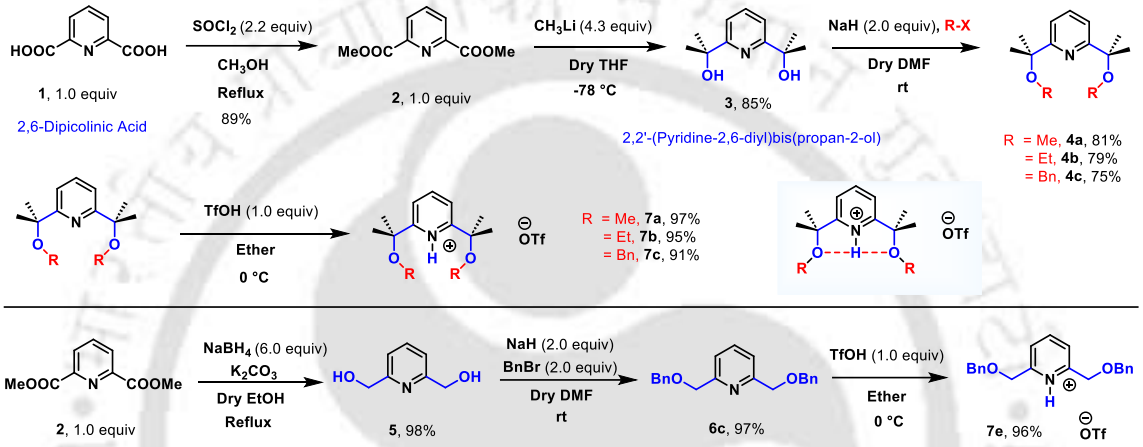

Scheme 5.1. Synthetic approaches to pyridinium triflate salts.

5.2.2. Crystal structure insights into alkoxy-substituted pyridinium salts: Thorpe-Ingold effects and ion-pair destabilization

The crystal structures of the newly synthesized salts provide vital information on the influence of the alkoxy groups on the pyridinium cation. In all cases (**7a-7c**), the alkoxy oxygens appear to be hydrogen-bonded to the $[N\text{-}H]^+$. Strikingly, there is a significant deviation in the anion-H-N bond angle from the usual near-linear (∠180°) orientation (Figure 5.2). While the angle in the OMe derivative **7a** is ∠100.8°, it is ∠66.6° and ∠64.2° in the case of **7b** and **7c**, respectively. Also, the N–H···anion distance in all these substrates is much longer than the usual range of 1.9 Å (Figure 5.2). These deviations reflect poor ion-pair stabilization in these hindered salts, like those observed in the TTBPy salts.

To understand the influence of the Thorpe-Ingold effect on the conformational landscape of these oxygen analogues of the hindered pyridinium salts, we also synthesized a simple dibenzyl pyridinium salt, **7e**, which is devoid of the gem-dimethyl groups. Interestingly, the N–H···anion distance in **7e** is 1.9 Å, and with the N-H-anion bond angle of ∠166.3°, as expected for pyridinium salts (Figure 5.2). In addition, only

one of the benzyloxy oxygens provides some through-space stabilization, with a dihedral angle of ∠72.2°, while the other C-O bond adopts an anti-periplanar orientation with the C-N bond, with a dihedral angle of ∠164.7°. This indicates the influence of the Thorpe-Ingold effect in restricting the possible conformations of the oxygen analogues, thereby imparting poor ion-pair interactions (Figure 5.2). Despite other possible conformations of these oxygen analogues (Figure 5.2), these compounds appear to retain the same conformations in solution, as determined by ^{1}H NMR spectral data. This shows that while methyl groups are associated with steric hindrance, the oxygen atoms do provide some through-space stabilization (H-bonding) to the proton.

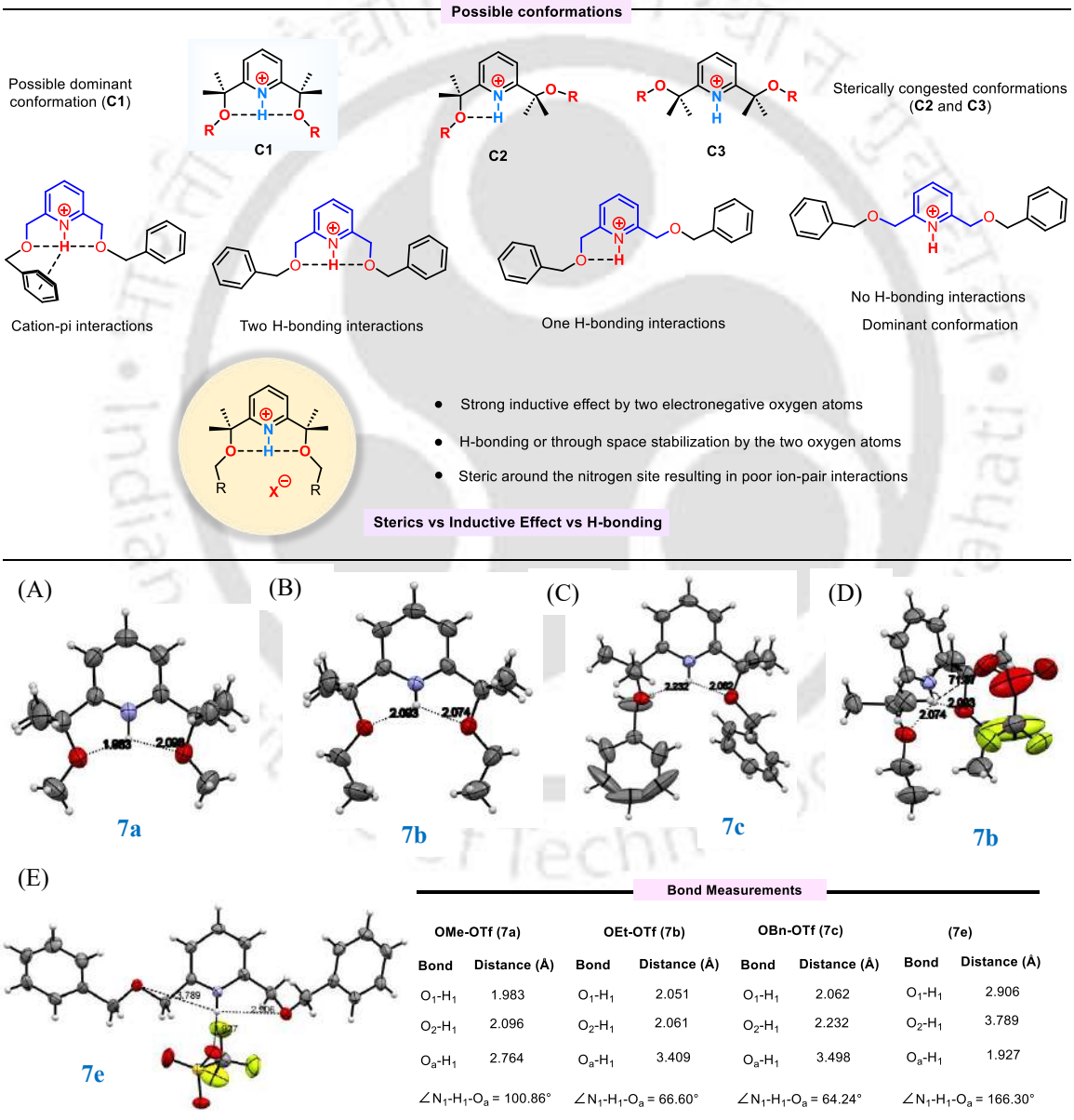

Figure 5.2. Steric effects on pyridinium conformation and ORTEP diagram with an ellipsoid of 30% probability (A) **7a** (B) **7b** (C) **7c** (D) **7b** (D) **7e**.

5.2.3. NMR titration studies of proton transfer and basicity in sterically hindered pyridines

Later, we decided to study the basicity of this new class of pyridine derivatives against TTBPy and TTBP using ^{1}H NMR spectroscopy. A series of NMR experiments was performed to investigate the basicity of the pyridine nitrogen in *O*-analogues of 2,2′-(pyridine-2,6-diyl)bis(propan-2-ol).

NMR titration experiment-1: with TTBPy and OMe-OTf salt (7a)

Our experiments commenced by mixing 0.032 mmol of the triflate salt **7a** and 0.032 mmol of neutral TTBPy in a 1:1 ratio in 0.5 mL of $CDCl_3$, and the ^{1}H NMR spectrum of the solution was recorded. The spectra revealed a significant upfield shift of the protons of compound **7a** (**H$_a$**, from δ 8.729 to 7.652 ppm; **H$_b$**, from δ 8.112 to 7.375 ppm; and **H$_c$**, from δ 3.509 to 3.179 ppm). These chemical shift values match those of the neutral OMe compound **4a**. Furthermore, the chemical shift of **H$_y$** (δ 7.619 ppm) corresponds to the **H$_y$** proton value in the TTBPyH·OTf salt. This clearly suggests that, despite the sterically hindered nature of both TTBPy and compound **7a**, there is an instantaneous transfer of the N-H proton from the OMe-OTf salt **7a** to TTBPy (Figure 5.3).

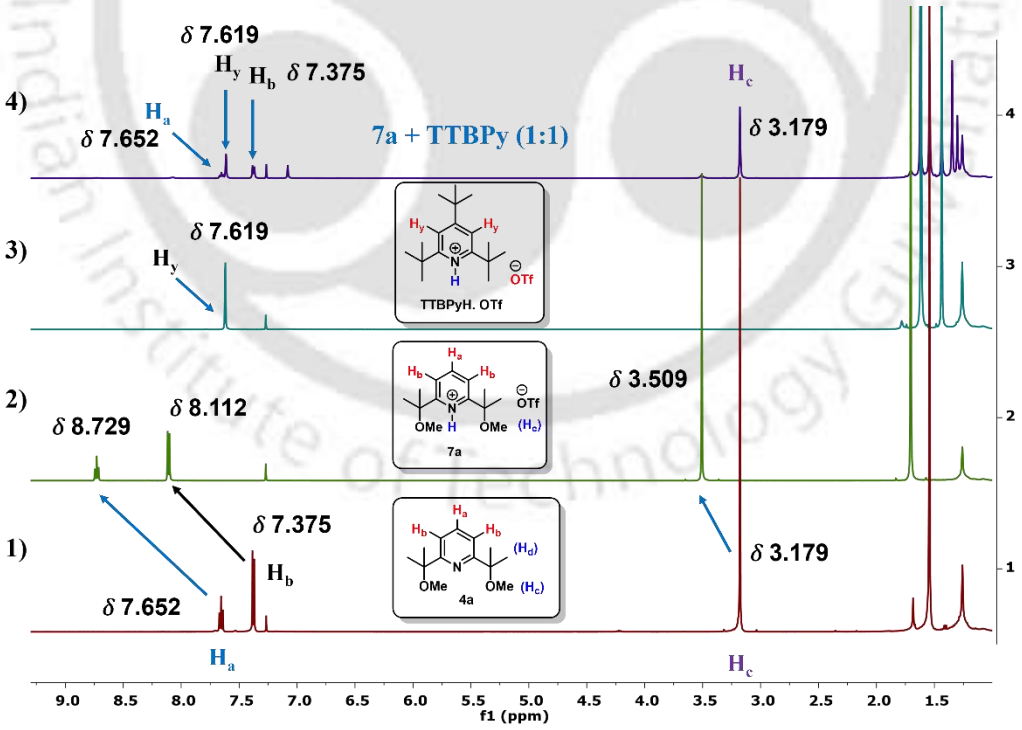

Figure 5.3. ^{1}H NMR titration of the catalyst **7a** with 2,4,6-tri-*tert*-butylpyridine (TTBPy) in 0.5 mL solution of $CDCl_3$. 1) 0.032 mmol of **4a** 2) 0.032 mmol of **7a** 3) 0.032 mmol of TTBPy-OTf salt 4) 0.032 mmol of **7a** and 0.032 mmol of TTBPy (1:1 ratio).

This raises the critical question of whether proton transfer between sterically hindered bases proceeds predominantly through conventional molecular collisions, as typically anticipated, or whether quantum-mechanical proton tunneling plays a significant role in facilitating the process. These observations, however, demonstrate that 2,4,6-tri-*tert*-butylpyridine (TTBPy) is more basic than 2,6-bis(2-methoxypropan-2-yl)pyridine (**4a**) (Figure 5.3).

In other words, this simple experiment also demonstrates the superior influence of the through-bond inductive effect of the two oxygens, making the pyridine nitrogen less basic than the through-space stabilization of $[N\text{-}H]^+$ by the oxygen lone pairs. Alternatively, the poor basicity of the methoxy derivative could be due to a perceived increase in steric bulk around the protonated site. However, careful analysis is needed to determine the steric influence on the increased basicity. While the 2-methoxypropyl group seems to be bulkier than the *tert*-butyl group, the steric influence depends on the orientation of the O-CH_3 bond.

NMR titration experiment-2: with TTBP and OMe-OTf salt (7a)

When an equimolar amount of compound **7a** and the more electron-deficient 2,4,6-tri-*tert*-butylpyrimidine (TTBP) was mixed, no shift of the protons (**H_a**, **H_b**, **H_c**) of catalyst **7a** was observed, indicating that no transfer of the N-H proton from the OMe-OTf salt **7a** to TTBP occurred. These observations strongly indicate that 2,4,6-tri-*tert*-butylpyrimidine (TTBP) is less basic than 2,6-bis(2-methoxypropan-2-yl)pyridine **4a** (Figure 5.4). Increasing electron deficiency within the aromatic ring has a greater influence than the inductive effect of the two oxygens outside the ring.

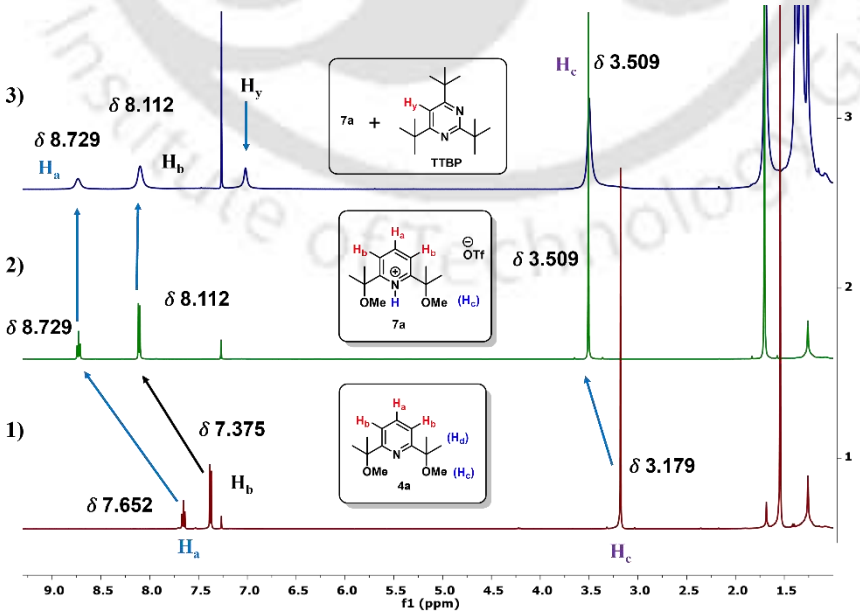

Figure 5.4. ^1H NMR titration of the catalyst **7a** with 2,4,6-tri-*tert*-butylpyridine (TTBP) in 0.5 mL solution of $CDCl_3$. 1) 0.032 mmol of **4a** 2) 0.032 mmol of **7a** 3) 0.032 mmol of **7a** and 0.032 mmol of TTBP.

NMR titration experiment-3: with TTBPyH.OTf salt with 4b

Interestingly, contrary to the methoxy compound **7a**, mixing the catalyst TTBPyH·OTf with the neutral ethoxy compound **4b** in a 1:1 ratio resulted in an instantaneous proton transfer to the ethoxy compound. A significant downfield shift of the protons of compound **4b** (**H_a**, from δ 7.635 to 8.715 ppm; **H_b**, from δ 7.373 to 8.087 ppm; and the other protons, from δ 3.319 to 3.689 ppm), indicating the transfer of the N-H proton from the TTBPyH·OTf salt to **4b**, is observed. These observations indicate that 2,4,6-tri-*tert*-butylpyridine (TTBPy) is less basic than 2,6-bis(2-ethoxypropan-2-yl)pyridine **4b** (Figure 5.5), whereas it is a stronger base relative to the OMe derivative **4a**. The expected electronic influence of an extra methyl group is insignificant and presumably not sufficient to explain the stronger basic character of the OEt derivative. However, the crystal structure of the OEt salt shows that the proton is sterically much more shielded than in both TTBPy and the OMe derivative. The conformation of the ethyl groups facing each other could result from London dispersion forces.

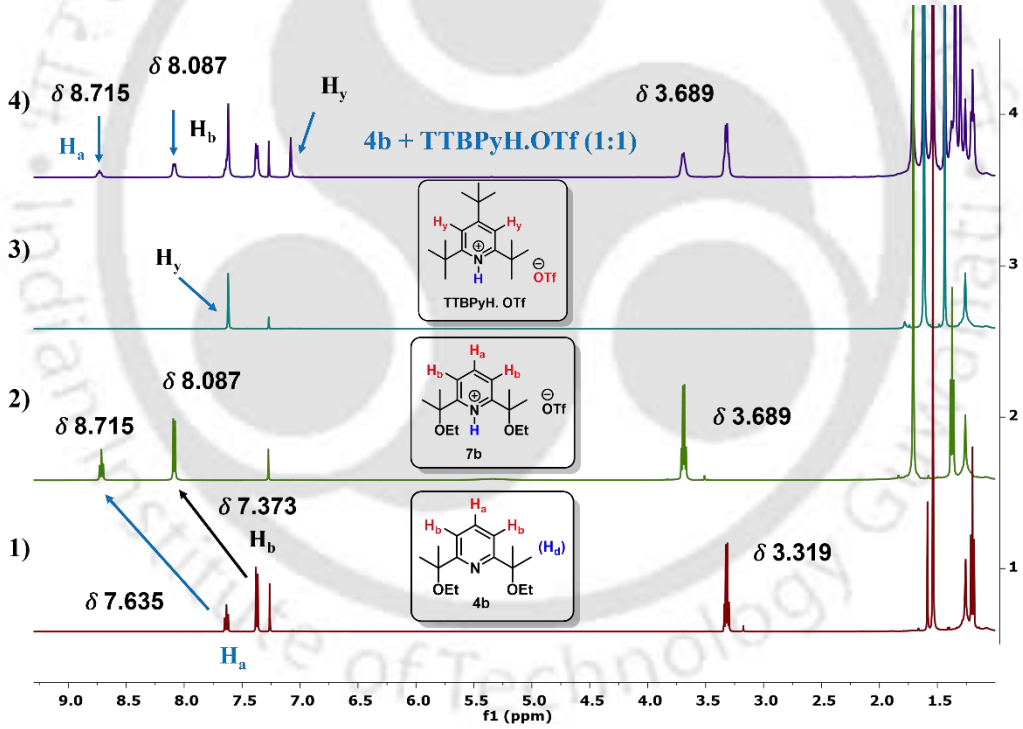

Figure 5.5. ^{1}H NMR titration of the 2,4,6-tri-*tert*-butylpyridinium triflate salt (TTBPyH.OTf) with **4b** in 0.5 mL solution of $CDCl_3$. 1) 0.032 mmol of **4b** 2) 0.032 mmol of **7b** 3) 0.032 mmol of TTBPy-OTf salt 4) 0.032 mmol of **4b** and 0.032 mmol of TTBPyH.OTf (1:1 ratio).

NMR titration experiment-4: with TTBPy and OBn-OTf salt (7c)

Intriguingly, when the same experiment is performed between the benzyl derivative **7c** and TTBPy, proton transfer has occurred again to TTBPy, similar to the case of the OMe derivative **7a** (an upfield shift of the protons of catalyst **7c** was observed: **H_a**, from δ

8.741 to 7.660 ppm; **H_b**, from δ 8.109 to 7.489 ppm; and the benzylic protons, from δ 4.582 to 4.379 ppm (Figure 5.6). This result also underscores the benzyl derivative's weaker basicity relative to TTBPy. The benzylic groups do not adopt a symmetric orientation in the salt; instead, they orient to exploit C-H···π interactions, thereby reducing the steric shielding effect on the N-H proton. This proton transfer leads to the formation of the neutral OBn compound **4c** along with the TTBPyH·OTf salt. Overall, the relative basicity order of the newly synthesized pyridines relative to TTBPy and TTBP is shown in Figure 5.7.

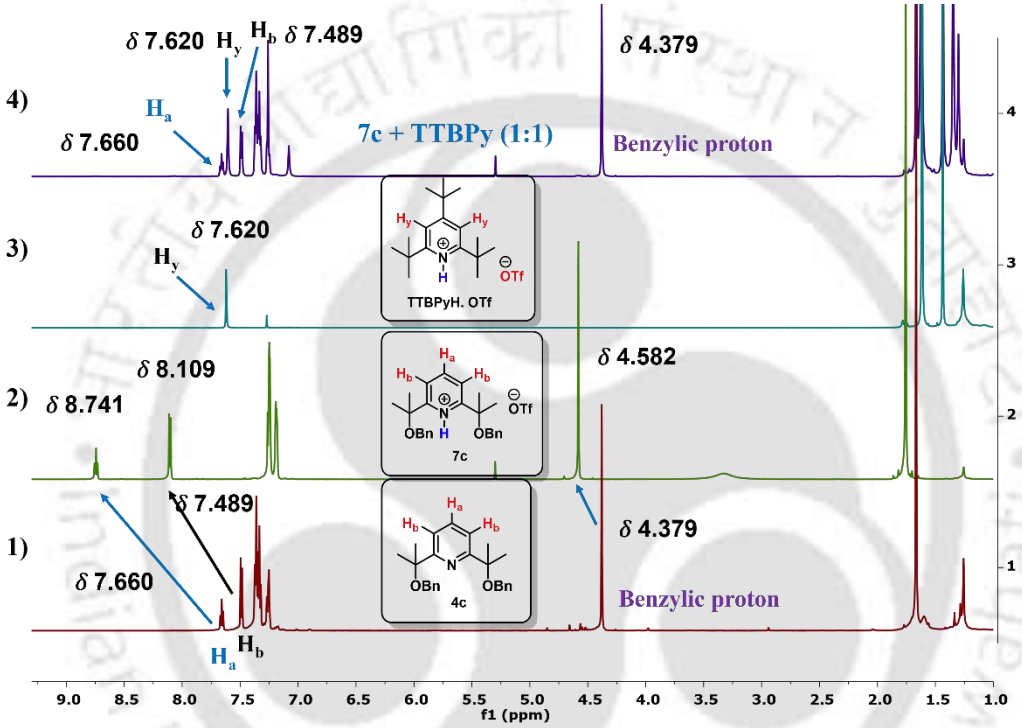

Figure 5.6. ^{1}H NMR titration of the catalyst **7c** with 2,4,6-tri-*tert*-butylpyridine (TTBPy) in 0.5 mL solution of $CDCl_3$. 1) 0.032 mmol of **4c** 2) 0.032 mmol of **7c** 3) 0.032 mmol of TTBPy-OTf salt 4) 0.032 mmol of **7c** and 0.032 mmol of TTBPy (1:1 ratio).

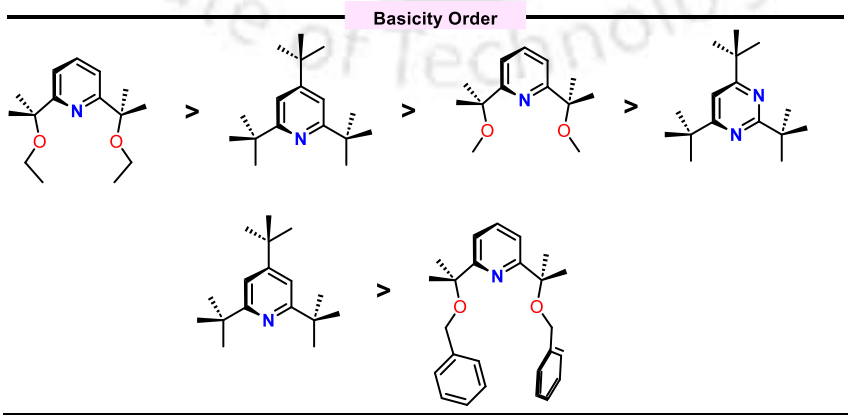

Figure 5.7. Relative basicity of sterically hindered pyridines.

5.2.4. Comparison with established bulky pyridines (TTBPy, TTBP)

5.2.4.1. Evaluation of Lewis vs. Brønsted acid interactions

To understand the ability of these new sterically hindered pyridines to differentiate between Lewis and Brønsted acids, we reacted the OMe derivative **4a** with 1 equiv of $BF_3{\cdot}OEt_2$ to observe the formation of a Lewis acid-base adduct. However, akin to TTBPy, **4a** also failed to form the Lewis acid-base adduct due to steric congestion and instead led only to the formation of the HBF_4 salt via a disproportionation reaction, rather than stable BF_3 adducts (Scheme 5.2).[12, 13]

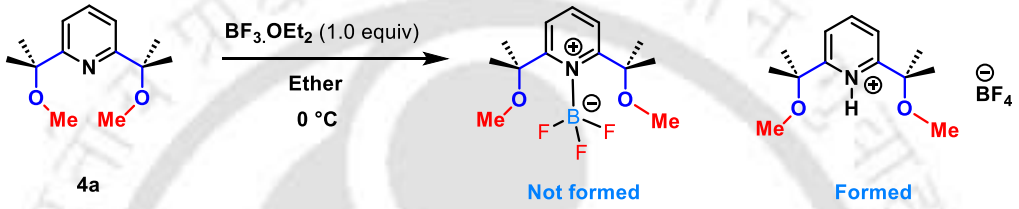

Scheme 5.2. Reaction of OMe Derivative **4a** with $BF_3{\cdot}OEt_2$.

5.2.4.2. Proton-trapping efficiency of 4b in *β*-mannosylation reaction

Also, we tested the OEt derivative **4b** as a proton-trapping agent in the stereoselective *β*-mannosylation reaction, like TTBPy, DTBMP, and TTBP. Interestingly, compound **4b** exhibited comparable efficiency, and the *β*-adamantyl mannoside product was obtained with yields and anomeric selectivity similar to those observed with other routinely used proton-trapping agents (Scheme 5.3).[14] These experiments establish that this new class of compounds possesses all the properties of standard bulky pyridine derivatives and can serve as potential cost-effective alternatives to expensive TTBPy and other hindered pyridines and pyrimidines.

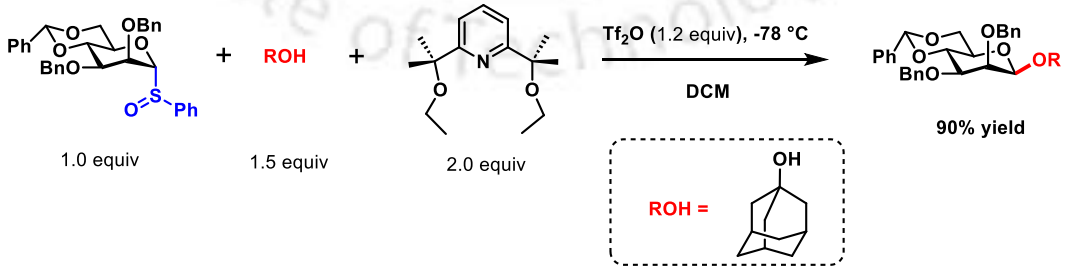

Scheme 5.3. Stereoselective *β*-mannosylation using **4b**.

5.3. Conclusion

In conclusion, we have developed a new class of cost-effective, heteroatom-containing, sterically hindered pyridine derivatives. This new class of pyridine derivatives retains the properties of proton sponges and can be used as alternatives to the expensive TTBPy, DTBMP, DTBP, and tri-*tert*-butylpyrimidine (TTBP). The X-ray crystal structures of the pyridinium salts provide valuable insights into the influence of heteroatoms and the conformational landscape of such species on the overall basicity of bulky pyridines. The study also dissects the influence of the Thorpe-Ingold effect on the accessible conformations of the oxygen analogues, making them resemble proton-pincer complexes. ^{1}H NMR studies reveal that subtle structural variations, such as changing methoxy to ethoxy (**7a** and **7b**), lead to substantial differences in relative basicity compared to TTBPy. Given the rising importance of bulky and simple pyridinium salts as organocatalysts, this new class of pyridinium salts holds great potential for catalyzing various organic reactions, and exploration of this potential is currently in progress in our laboratory.

5.4. Experimental section

5.4.1. Synthesis of *O*-analogues of 2,2′-(Pyridine-2,6-diyl)bis(propan-2-ol)

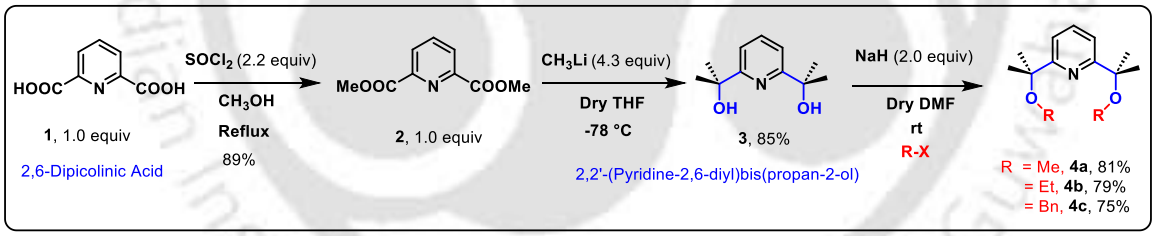

In a 500 mL round-bottom flask, thionyl chloride ($SOCl_2$, 9.6 mL, 131.6 mmol) was added dropwise to the stirred solution of 2,6-Dipicolinic acid (10 g, 59.8 mmol) in methanol (250 mL) at 0 °C. After stirring at reflux for 12 h and monitoring via TLC, the solvent was removed by evaporation in vacuo. The reaction mixture was reduced to dryness by azeotropic with toluene (300 mL) to give **2** as a white powder with 89% yield (10.4 g). **^{1}H NMR** (500 MHz, $CDCl_3$) δ 8.30 (d, J = 7.8 Hz, 2H), 8.02 (t, J = 7.8 Hz, 1H), 4.01 (s, 6H). **^{13}C NMR** (126 MHz, $CDCl_3$) δ 165.2, 148.3, 138.5, 128.2, 53.3. **HRMS** (ESI) m/z: $[M+H]^+$ calcd for $C_9H_9NO_4$ 196.0605; found 196.0607.

An oven-dried 250 mL two-necked round-bottom flask was equipped with a magnetic stir bar and fitted with two rubber septa to introduce an inert atmosphere. MeLi (54 mL of a 1.6 M solution, 86 mmol) was added dropwise to dimethyl pyridine-2,6-dicarboxylate (**2**, 4 g, 20.05 mmol) in the 100 mL dry THF at -78 °C. After stirring the reaction mixture at room temperature for 2 hours, quench it with an aqueous saturated NH_4Cl solution (100

mL). The crude product was extracted with CH_2Cl_2 (30 mL) after evaporation of the solvent. The organic layer was dried over anhydrous Na_2SO_4, filtered, concentrated, and purified by column chromatography on silica gel using hexane/ethyl acetate (8:2) to give **3** as a white solid with 85% yield (3.3 g). R_f = 0.5 (ethyl acetate/petroleum ether: 3/7). **^{1}H NMR** (500 MHz, $CDCl_3$) δ 7.71 (t, J = 7.8 Hz, 1H), 7.31 (d, J = 7.7 Hz, 2H), 4.28 (s, 2H), 1.56 (s, 12H). **^{13}C NMR** (126 MHz, $CDCl_3$) δ 164.7, 138.2, 116.9, 72.4, 30.7. **HRMS** (ESI) m/z: $[M+H]^+$ calcd for $C_{11}H_{17}NO_2$ 196.1333; found 196.1334.

2,6-bis(2-methoxypropan-2-yl)pyridine (4a)

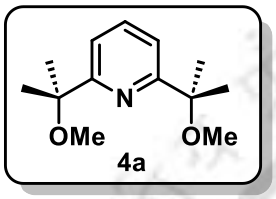

4a

To a solution of 2,2'-(pyridine-2,6-diyl)bis(propan-2-ol) (**3**, 500 mg, 2.56 mmol) in DMF (30.0 mL) at 0 °C was added NaH (60% in mineral oil, 359 mg, 8.96 mmol, 3.5 equiv), and the mixture was stirred at 0 °C for 50 min. Iodomethane (0.6 mL, 8.96 mmol, 3.5 equiv) was added to the solution and stirred at rt for 24 h. The reaction mixture was quenched with methanol and evaporated under reduced pressure. CH_2Cl_2 was added to the cold solution of the reaction mixture, and the organic phase was separated. The aqueous layer was extracted a second time with CH_2Cl_2. The combined organic layers were washed with brine, dried over anhydrous Na_2SO_4, filtered, and concentrated. The obtained crude residue was purified by column chromatography on silica gel (hexane/ethyl acetate (95:5)) to afford **4a** with 81% (463 mg) yield as a pale-yellow oil. R_f = 0.6 (ethyl acetate/petroleum ether: 2/8). **^{1}H NMR** (500 MHz, $CDCl_3$) δ 7.65 (t, J = 7.8 Hz, 1H), 7.37 (d, J = 7.8 Hz, 2H), 3.17 (s, 6H), 1.54 (s, 12H). **^{13}C NMR** (101 MHz, $CDCl_3$) δ 163.7, 136.7, 117.6, 79.2, 50.9, 26.6. **HRMS** (ESI) m/z: $[M+H]^+$ calcd for $C_{13}H_{21}NO_2$ 224.1646; found 224.1645.

2,6-bis(2-ethoxypropan-2-yl)pyridine (4b)

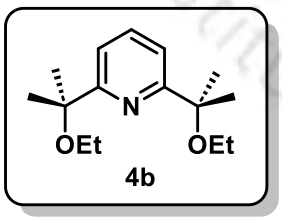

4b

To a solution of 2,2'-(pyridine-2,6-diyl)bis(propan-2-ol) (**3**, 500 mg, 2.56 mmol) in DMF (30.0 mL) at 0 °C was added NaH (60% in mineral oil, 359 mg, 8.96 mmol, 3.5 equiv), and the mixture was stirred at 0 °C for 50 min. Iodoethane (1.1 mL, 12.8 mmol, 5 equiv) was added to the solution and stirred at rt for 48 to 72 h. The reaction mixture was quenched with methanol and evaporated under reduced pressure. CH_2Cl_2 was added to the cold solution of the reaction mixture, and the organic phase was separated. The aqueous layer was extracted a second time with CH_2Cl_2. The combined organic layers were washed with brine, dried over anhydrous Na_2SO_4, filtered, and concentrated. The crude residue was purified by column chromatography on silica gel (hexane/ethyl acetate (95:5)) to afford **4b** with 79% yield (508 mg) as a yellow oil. R_f = 0.7 (ethyl acetate/petroleum ether: 2/8). **^{1}H NMR** (500 MHz, $CDCl_3$) δ 7.63 (t, J = 7.8 Hz, 1H), 7.37 (d, J = 7.8 Hz, 2H), 3.32 (q, J = 7.0 Hz, 4H), 1.54 (s, 12H), 1.20 (t, J = 7.0

Hz, 6H). **^{13}C NMR** (126 MHz, $CDCl_3$) δ 164.4, 136.6, 117.4, 78.9, 58.5, 27.3, 16.1. **HRMS** (ESI) m/z: $[M+H]^+$ calcd for $C_{15}H_{25}NO_2$ 252.1959; found 252.1971.

2,6-bis(2-(benzyloxy)propan-2-yl)pyridine (4c)

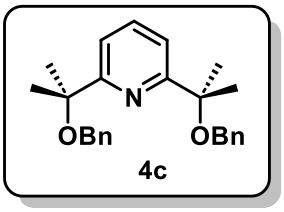

To a solution of 2,2'-(pyridine-2,6-diyl)bis(propan-2-ol) (**3**, 500 mg, 2.56 mmol) in DMF (30.0 mL) at 0 °C was added NaH (60% in mineral oil, 359 mg, 8.96 mmol, 3.5 equiv), and the mixture was stirred at 0 °C for 50 min. Benzyl bromide (1.6 mL, 12.8 mmol, 5 equiv) was added to the solution and stirred at rt for 48 h. The reaction mixture was quenched with methanol and evaporated under reduced pressure. CH_2Cl_2 was added to the cold solution of the reaction mixture, and the organic phase was separated. The aqueous layer was extracted a second time with CH_2Cl_2. The combined organic layers were washed with brine, dried over anhydrous Na_2SO_4, filtered, and concentrated. The crude residue was purified by column chromatography on silica gel (hexane) to afford **4c** with 75% yield (720 mg) as a colorless oil. R_f = 0.8 (ethyl acetate/petroleum ether: 1/9). **^{1}H NMR** (600 MHz, $CDCl_3$) δ 7.66 (t, J = 7.7 Hz, 1H), 7.49 (d, J = 7.8 Hz, 2H), 7.35 (dt, J = 14.9, 7.6 Hz, 8H), 7.27-7.25 (m, 2H), 4.38 (s, 4H), 1.67 (s, 12H). **^{13}C NMR** (151 MHz, $CDCl_3$) δ 163.9, 139.6, 136.8, 128.5, 127.45, 127.45, 127.3, 117.9, 79.5, 65.4, 27.3. **HRMS** (ESI) m/z: $[M+H]^+$ calcd for $C_{25}H_{29}NO_2$ 376.2272; found 376.2285.

5.4.2. Synthesis of 2,6-bis((benzyloxy)methyl)pyridine (6c)

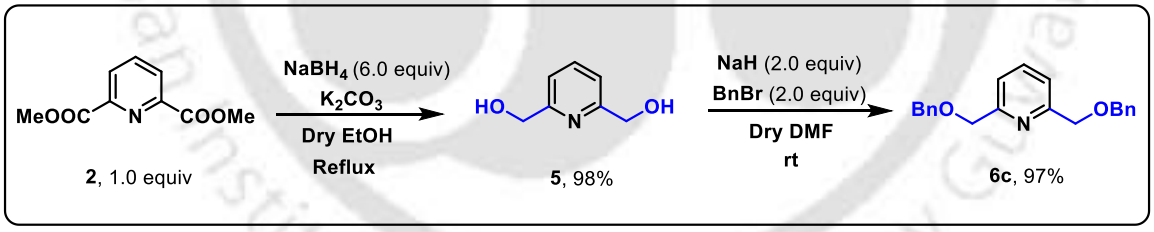

Pyridine-2,6-dicarboxylate (**2**, 2.00 g, 10.24 mmol) was dissolved in dry ethanol (40 mL) under an inert atmosphere. After that, $NaBH_4$ (2.42 g, 63.96 mmol) was slowly added to the reaction mixture at 0°C. The solution was stirred for 4 h at rt followed by reflux for 8 h. The reaction mixture was concentrated under vacuum, followed by the addition of a saturated solution of K_2CO_3 (40 mL). The mixture was stirred for an extra 3 h at 60 °C. The product was extracted into CH_2Cl_2 (30 mL×3), and the organic layer was dried over anhydrous Na_2SO_4. Removal of volatiles under reduced pressure yielded pyridine-2,6-diyldimethanol 5 as a white solid in 98% yield (1.4 g). **^{1}H NMR** (600 MHz, $CDCl_3$) δ 7.70 (t, J = 7.7 Hz, 1H), 7.19 (d, J = 7.7 Hz, 2H), 4.78 (s, 4H), 3.35 (s, 2H). **^{13}C NMR** (151 MHz, $CDCl_3$) δ 158.6, 137.6, 119.3, 64.6. **HRMS** (ESI) m/z: $[M+H]^+$ calcd for $C_7H_9NO_2$ 140.0707; found 140.0709.

To a solution of pyridine-2,6-diyldimethanol (**5**, 500 mg, 3.6 mmol, 1 equiv) in DMF (30.0 mL) at 0 °C was added NaH (60% in mineral oil, 3.5 equiv), and the mixture was stirred at 0 °C for 50 min. Benzyl bromide (4.0 equiv) was added to the solution and stirred at rt for 24 h. The reaction mixture was quenched with methanol and evaporated under reduced pressure. CH_2Cl_2 was added to the cold solution of the reaction mixture, and the organic phase was separated. The aqueous layer was extracted a second time with CH_2Cl_2. The combined organic layers were washed with brine, dried over anhydrous Na_2SO_4, filtered, and concentrated. The crude residue was purified by column chromatography on silica gel (hexane/ethyl acetate) to afford the desired product **6c** in 97% yield (1.1 g) as a white solid, R_f = 0.5 (Hexane/EtOAc, 8:2, v/v). **^{1}H NMR** (600 MHz, $CDCl_3$) δ 7.73 (t, J = 7.7 Hz, 1H), 7.44 – 7.39 (m, 6H), 7.37 (t, J = 7.5 Hz, 4H), 7.31 (t, J = 7.3 Hz, 2H), 4.69 (s, 4H), 4.66 (s, 4H). **^{13}C NMR** (151 MHz, $CDCl_3$) δ 158.0, 138.1, 137.4, 128.6, 127.94, 127.94, 127.86, 120.1, 73.6, 73.1. **HRMS** (ESI) m/z: $[M+H]^+$ calcd for $C_{21}H_{21}NO_2$ 320.1646; found 320.1660.

5.4.3. Synthesis of pyridinium triflate salt

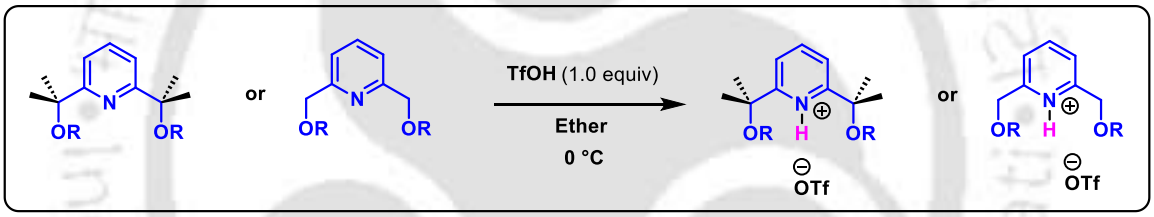

To a solution of alkyl or benzyl group protected 2,2'-(pyridine-2,6-diyl)bis(propan-2-ol) (200 mg, 1 equiv) in ether (3 mL) at 0 °C was added triflic acid (1 equiv). After that, it was stirred at 0 °C for 10 minutes, and a white precipitate was immediately observed. Then, the solution was allowed to settle down for a few min, and after decanting the solution, the solid was washed with ether (5x5 ml) to afford the triflate salts.

2,6-bis(2-methoxypropan-2-yl)pyridinium triflate salt (7a)

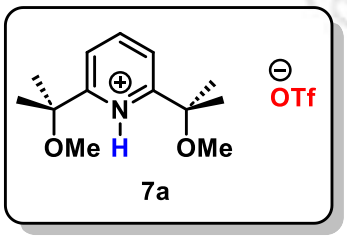

7a was obtained in 97% yield as a white solid. **^{1}H NMR** (500 MHz, $CDCl_3$) δ 8.73 (t, J = 8.3 Hz, 1H), 8.10 (d, J = 8.2 Hz, 2H), 3.50 (s, 6H), 1.70 (s, 12H). **^{13}C NMR** (151 MHz, $CDCl_3$) δ 158.8, 148.9, 123.3, 76.1, 50.8, 25.5. **HRMS** (ESI) m/z: $[M+H]^+$ calcd for $C_{13}H_{22}NO_2$ (positive mode only) 224.1646; found 224.1649.

2,6-bis(2-ethoxypropan-2-yl)pyridinium triflate salt (7b)

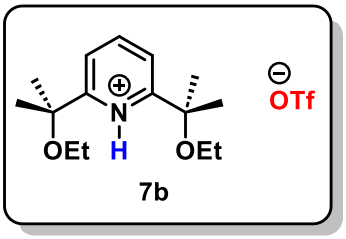

7b was obtained in 95% yield as a white solid. **^{1}H NMR** (500 MHz, $CDCl_3$) δ 13.06 (br s, 1H), 8.70 (t, J = 8.0 Hz, 1H), 8.07 (d, J = 8.1 Hz, 2H), 3.68 (q, J = 7.0 Hz, 4H), 1.69 (s, 12H), 1.36 (t, J = 6.9 Hz, 6H). **^{13}C NMR** (151 MHz, $CDCl_3$) δ 158.9, 148.7, 122.9, 75.7, 58.5, 25.9, 15.6. **HRMS** (ESI) m/z: $[M+H]^+$ calcd for $C_{15}H_{26}NO_2$ (positive mode only) 252.1959; found 252.1963.

2,6-bis(2-(benzyloxy)propan-2-yl)pyridinium triflate salt (7c)

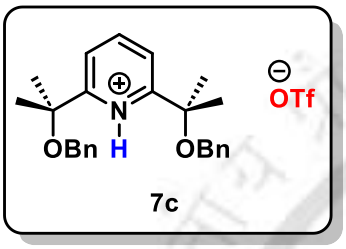

7c was obtained in 91% yield as a white solid. **^{1}H NMR** (500 MHz, $CDCl_3$) δ 12.96 (br s, 1H), 8.75 (t, J = 8.1 Hz, 1H), 8.12 (d, J = 8.0 Hz, 2H), 7.27 – 7.18 (m, 10H), 4.58 (s, 4H), 1.76 (s, 12H). **^{13}C NMR** (151 MHz, $CDCl_3$) δ 158.8, 149.3, 137.0, 128.8, 128.3, 127.5, 123.4, 76.8, 65.8, 26.5. **HRMS** (ESI) m/z: $[M+H]^+$ calcd for $C_{25}H_{29}NO_2$ (positive mode only) 376.2272; found 376.2271.

2,6-bis(2-methoxypropan-2-yl)pyridinium tetrafluoroborate salt (7d)

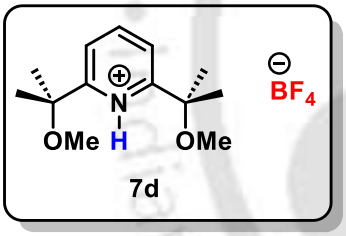

To a solution of 2,6-bis(2-methoxypropan-2-yl)pyridine (200 mg, 1 equiv) in ether (3 mL) at 0 °C was added boron trifluoride diethyl etherate (1 equiv). After that, it was stirred at 0 °C for 10 minutes, and a white precipitate was immediately observed. Then, the solution was allowed to settle down for a few min, and after decanting the solution, the solid was washed with ether (5x5 ml) to afford the desired salt **7d** as a white solid with 98% of yield. **^{1}H NMR** (600 MHz, $CDCl_3$) δ 12.81 (br s, 1H), 8.66 (t, J = 8.0 Hz, 1H), 8.04 (d, J = 7.9 Hz, 2H), 3.48 (s, 6H), 1.67 (s, 12H). **^{13}C NMR** (151 MHz, $CDCl_3$) δ 158.6, 148.9, 123.2, 76.1, 50.9, 25.4. **HRMS** (ESI) m/z: $[M+H]^+$ calcd for $C_{13}H_{22}NO_2$ (positive mode only) 224.1646; found 224.1646.

2,6-bis((benzyloxy)methyl)pyridinium triflate salt (7e)

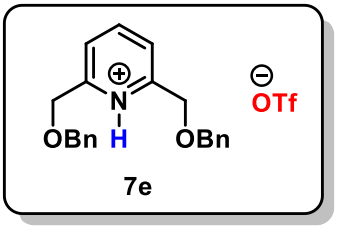

7e was obtained in 96% yield as a colorless oil. **^{1}H NMR** (400 MHz, $CDCl_3$) δ 8.24 (t, J = 8.0 Hz, 1H), 7.82 (d, J = 8.0 Hz, 2H), 7.44 – 7.27 (m, 10H), 4.95 (s, 4H), 4.74 (s, 4H). **^{13}C NMR** (126 MHz, $CDCl_3$) δ 156.5, 141.4, 137.4, 128.7, 128.24, 128.22, 121.8, 73.7, 70.4. **HRMS** (ESI) m/z: $[M+H]^+$ calcd for $C_{21}H_{22}NO_2$ (positive mode only) 320.1646; found 320.1646.

5.4.4. Synthesis of (2R,4aR,6S,7S,8S,8aR)-6-(((3R,5R,7R)-adamantan-1-yl)oxy)-7,8-bis(benzyloxy)-2-phenylhexahydropyrano[3,2-d][1,3]dioxine (7f)

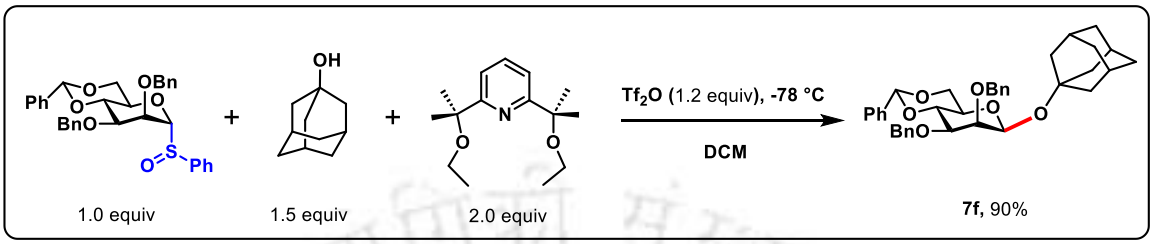

To a stirred solution of sulfoxide donor (0.1 mmol) and OEt-compound **4b** (0.2 mmol) in dry DCM at −78 °C under an inert condition, Tf_2O (0.12 mmol) was added. After 5 min, a solution of the glycosyl acceptor (0.15 mmol) in dry DCM (1 mL) was added dropwise. The reaction mixture was stirred at −78 °C for 1 h, then warmed to 0 °C. The reaction was quenched with aqueous $NaHCO_3$, and the organic phase was separated. The aqueous layer was extracted again with CH_2Cl_2. The combined organic layers were washed with brine, dried over anhydrous Na_2SO_4, filtered, and concentrated under reduced pressure. The crude residue was purified by column chromatography on silica gel (hexane/ethyl acetate) to afford the desired product **7f** in 90% yield (52 mg) as a colorless oil (R_f = 0.5, hexane/EtOAc 9:1, v/v). **^{1}H NMR** (600 MHz, $CDCl_3$) δ 7.43 (d, J = 7.2 Hz, 4H), 7.33 – 7.17 (m, 11H), 5.54 (s, 1H), 4.95 (d, J = 12.7 Hz, 1H), 4.86 (d, J = 12.5 Hz, 1H), 4.68 (s, 1H), 4.59 (d, J = 12.7 Hz, 1H), 4.51 (d, J = 12.5 Hz, 1H), 4.23 – 4.10 (m, 2H), 3.86 (t, J = 10.4 Hz, 1H), 3.70 (d, J = 2.9 Hz, 1H), 3.52 (dd, J = 9.9, 3.1 Hz, 1H), 3.24 (td, J = 9.9, 5.0 Hz, 1H), 2.09 (d, J = 5.5 Hz, 4H), 1.77 (d, J = 10.6 Hz, 3H), 1.68 (d, J = 11.2 Hz, 3H), 1.64 (d, J = 2.4 Hz, 2H), 1.56 – 1.53 (m, 3H). **^{13}C NMR** (151 MHz, $CDCl_3$) δ 137.6, 137.5, 136.7, 127.84, 127.79, 127.3, 127.2, 127.0, 126.47, 126.45, 126.4, 125.1, 100.4, 93.9, 77.6, 77.4, 75.9, 74.2, 73.6, 71.3, 67.8, 66.3, 44.3, 41.4, 35.2, 35.1, 29.7, 29.6. **HRMS** (ESI) m/z: $[M+H]^+$ calcd for $C_{37}H_{43}O_6$ 583.3055; found 583.3063.

5.5. References

1. De, S.; Kumar S K, A.; Shah, S. K.; Kazi, S.; Sarkar, N.; Banerjee, S.; Dey, S., Pyridine: the scaffolds with significant clinical diversity. *RSC Adv.* **2022,** *12* (24), 15385-15406.
2. Dimroth, K.; Mach, W., Preparation of 2,4,6-Tri-tert-butylpyrylium Tetrafluoroborate, 2,4,6-Tri-tert-butylpyridine, and 2,4,6-Tri-tert-butylphosphorin. *Angew. Chem. Int. Ed. Engl.* **1968,** *7* (6), 460-461.
3. Brown, H. C.; Kanner, B., Preparation and Reactions of 2,6-Di-t-butylpyridine and Related Hindered Bases. A Case of Steric Hindrance toward the Proton1,2. *J. Am. Chem. Soc.* **1966,** *88* (5), 986-992.
4. Crich, D.; Dudkin, V., An unusual example of steric buttressing in glycosylation. *Tetrahedron Lett.* **2000,** *41* (30), 5643-5646.
5. Xu, X.-H.; Liu, G.-K.; Azuma, A.; Tokunaga, E.; Shibata, N., Synthesis of Indole and Biindolyl Triflones: Trifluoromethanesulfonylation of Indoles with Tf_2O/TTBP (2,4,6-tri-tert-butylpyridine) System. *Org. Lett.* **2011,** *13* (18), 4854-4857.
6. van der Plas, H. C.; Koudijs, A., Steric effects in alkylpyrimidines. *Recl. Trav. Chim. Pays-Bas* **1978,** *97* (6), 159-161.
7. Ghosh, T.; Mukherji, A.; Kancharla, P. K., Sterically Hindered 2,4,6-Tri-tert-butylpyridinium Salts as Single Hydrogen Bond Donors for Highly Stereoselective Glycosylation Reactions of Glycals. *Org. Lett.* **2019,** *21* (10), 3490-3495.
8. Andreeva, D. V.; Ip, B.; Gurinov, A. A.; Tolstoy, P. M.; Denisov, G. S.; Shenderovich, I. G.; Limbach, H.-H., Geometrical Features of Hydrogen Bonded Complexes Involving Sterically Hindered Pyridines. *J. Phys. Chem. A.* **2006,** *110* (37), 10872-10879.
9. Addanki, R. B.; Halder, S.; Kancharla, P. K., TfO–···H–O–H Interaction-Assisted Generation of a Silicon Cation from Allylsilanes: Access to Phenylallyl Ferrier Glycosides from Glycals. *Org. Lett.* **2022,** *24* (7), 1465-1470.
10. Mukherji, A.; Kancharla, P. K., C–H···Anion Interactions Assisted Addition of Water to Glycals by Sterically Hindered 2,4,6-Tri-tert-butylpyridinium Hydrochloride. *Org. Lett.* **2020,** *22* (6), 2191-2195.
11. Pradhan, P.; Biswas, A.; Rotta, M. K. V.; Kancharla, P. K., Strained Ion Pair Interactions-Driven Anion-Assisted Concerted Addition of Ketoximes/Aldoximes and Hydroxamic Acids to Glycals. *Org. Lett.* **2024,** *26* (48), 10382-10387.
12. Addanki, R. B.; Moktan, S.; Halder, S.; Sharma, M.; Sarmah, B. K.; Bhattacharyya, K.; Kancharla, P. K., Exploiting the Strained Ion-Pair Interactions of Sterically Hindered Pyridinium Salts Toward SN2 Glycosylation of Glycosyl Trichloroacetimidates. *J. Org. Chem.* **2024,** *89* (6), 3713-3725.
13. Jiang, C.; Blacque, O.; Fox, T.; Berke, H., Heterolytic Cleavage of H2 by Frustrated B/N Lewis Pairs. *Organometallics* **2011,** *30* (8), 2117-2124.
14. Crich, D.; Sun, S., Direct chemical synthesis of β-mannopyranosides and other glycosides via glycosyl triflates. *Tetrahedron* **1998,** *54* (29), 8321-8348.

5.6. Selected spectra

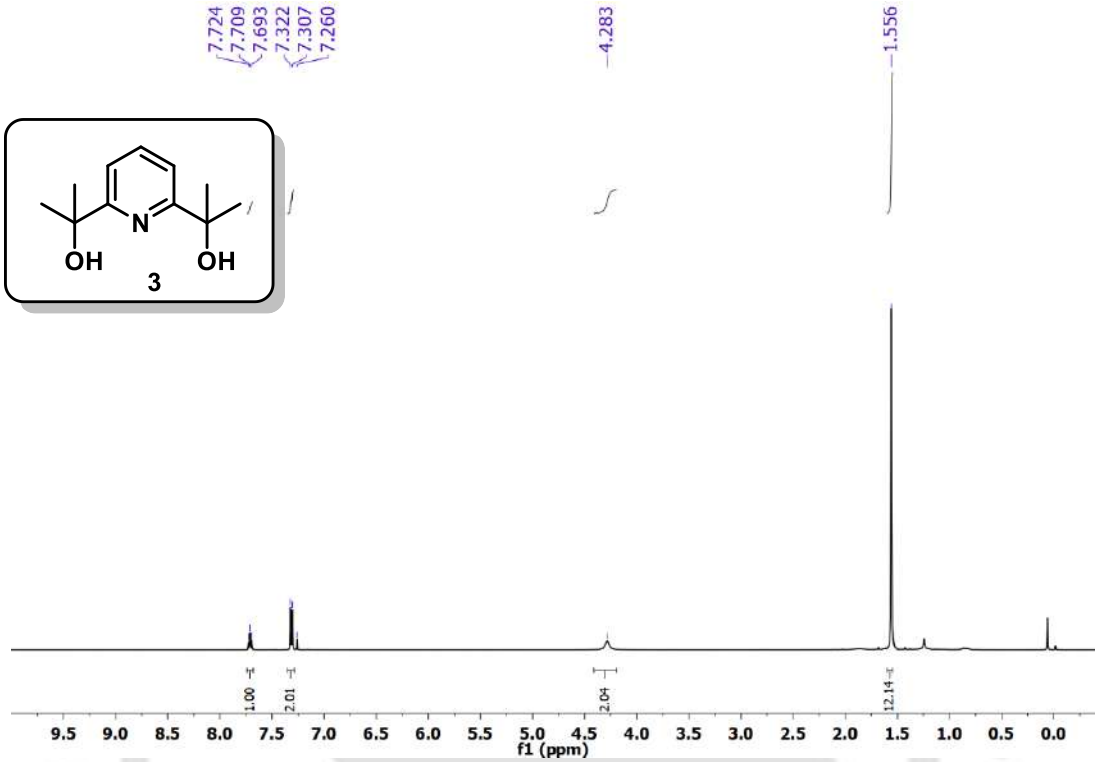

Figure 5.8. *^{1}H NMR of compound **3** (500 MHz, $CDCl_3$).*

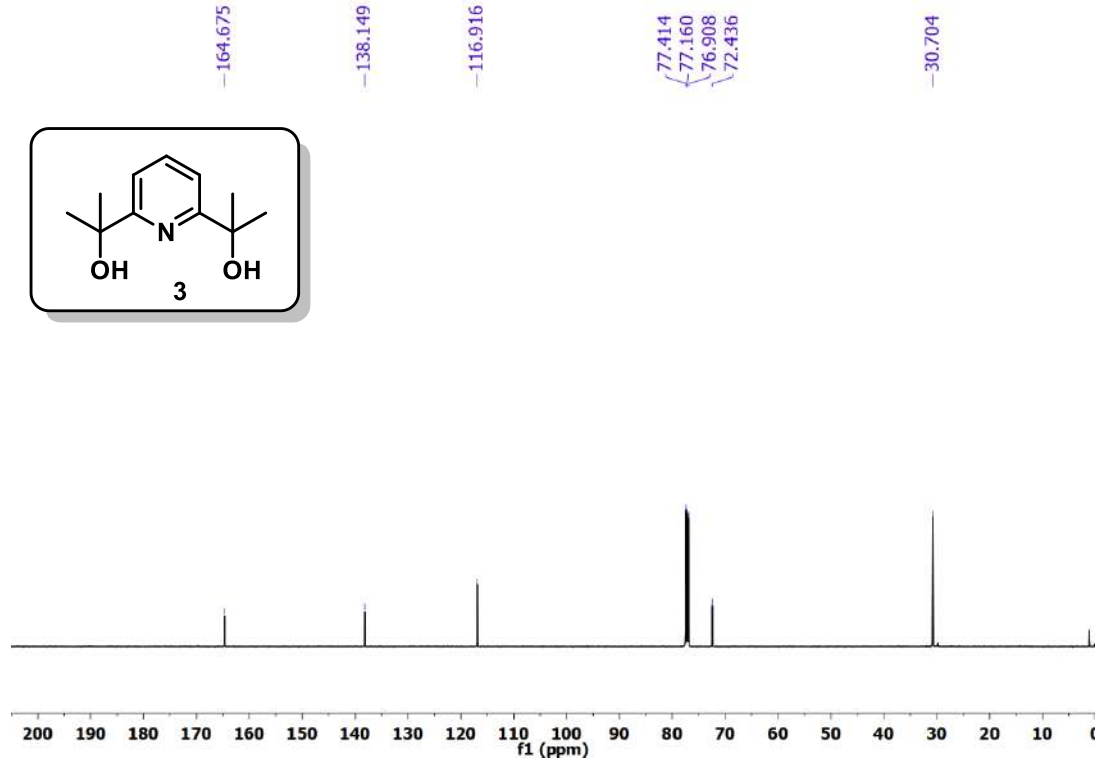

Figure 5.9. *^{13}C NMR of compound **3** (126 MHz, $CDCl_3$).*

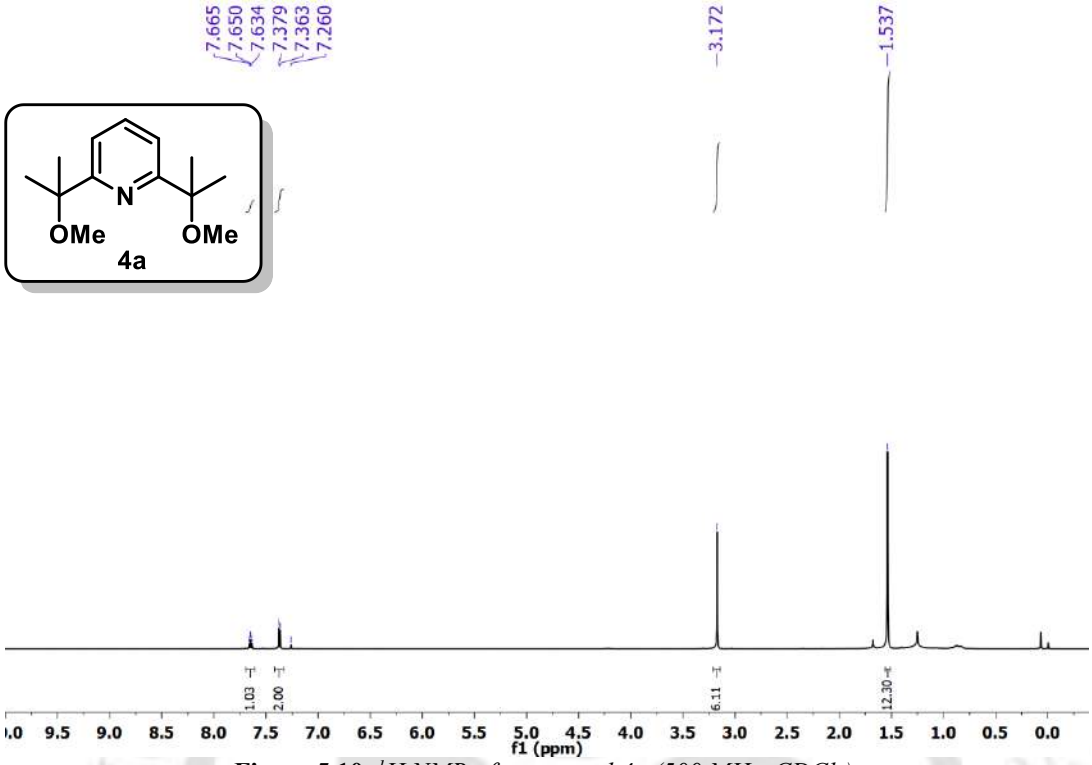

Figure 5.10. *^{1}H NMR of compound **4a** (500 MHz, $CDCl_3$).*

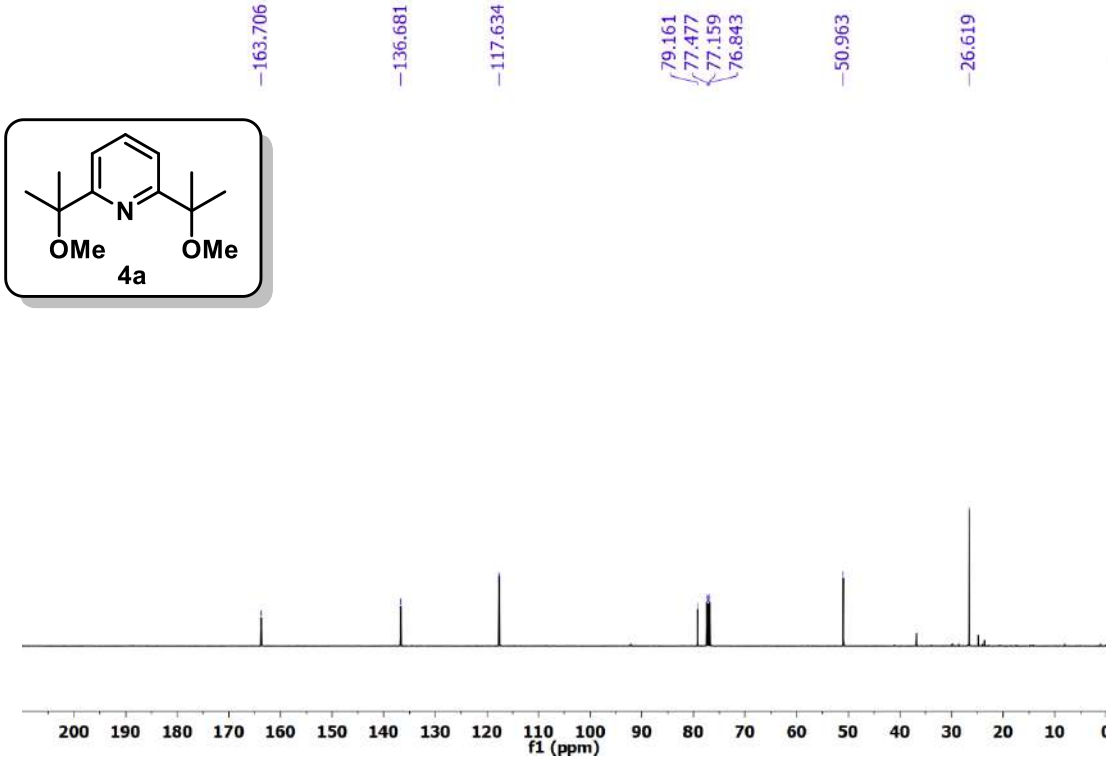

Figure 5.11. ^{13}C NMR of compound **4a** (101 MHz, $CDCl_3$).

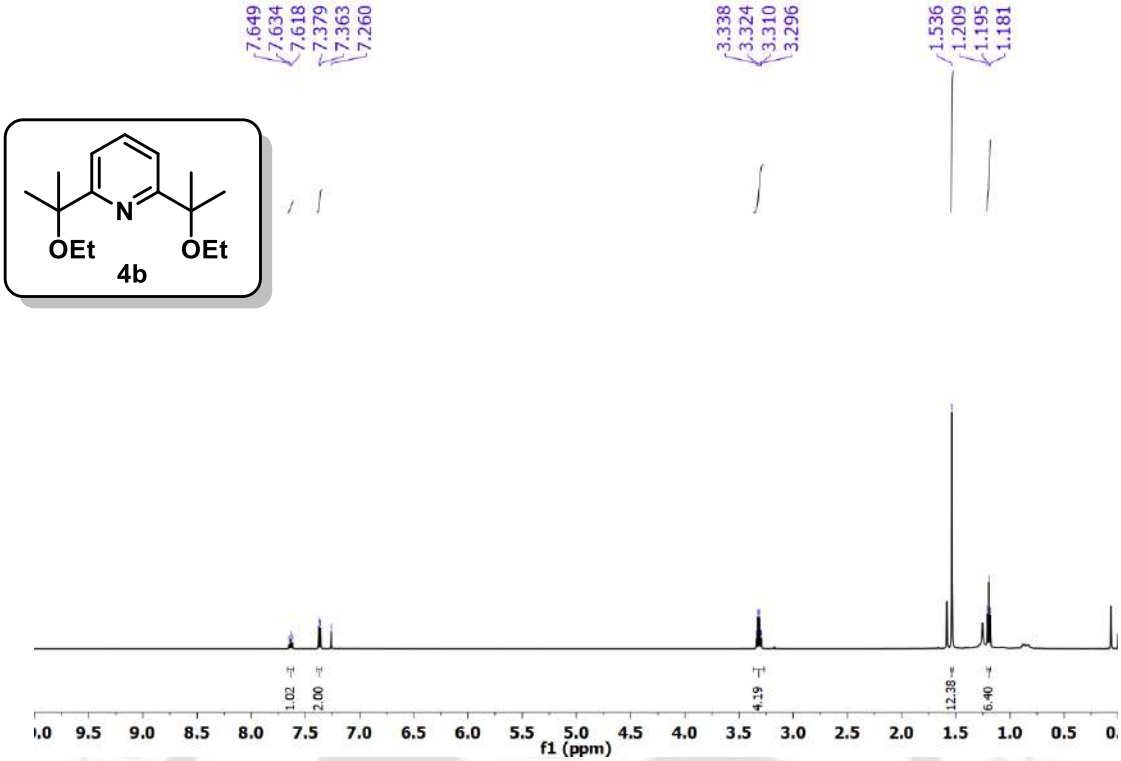

Figure 5.12. ^{1}H NMR of compound **4b** (500 MHz, $CDCl_3$).

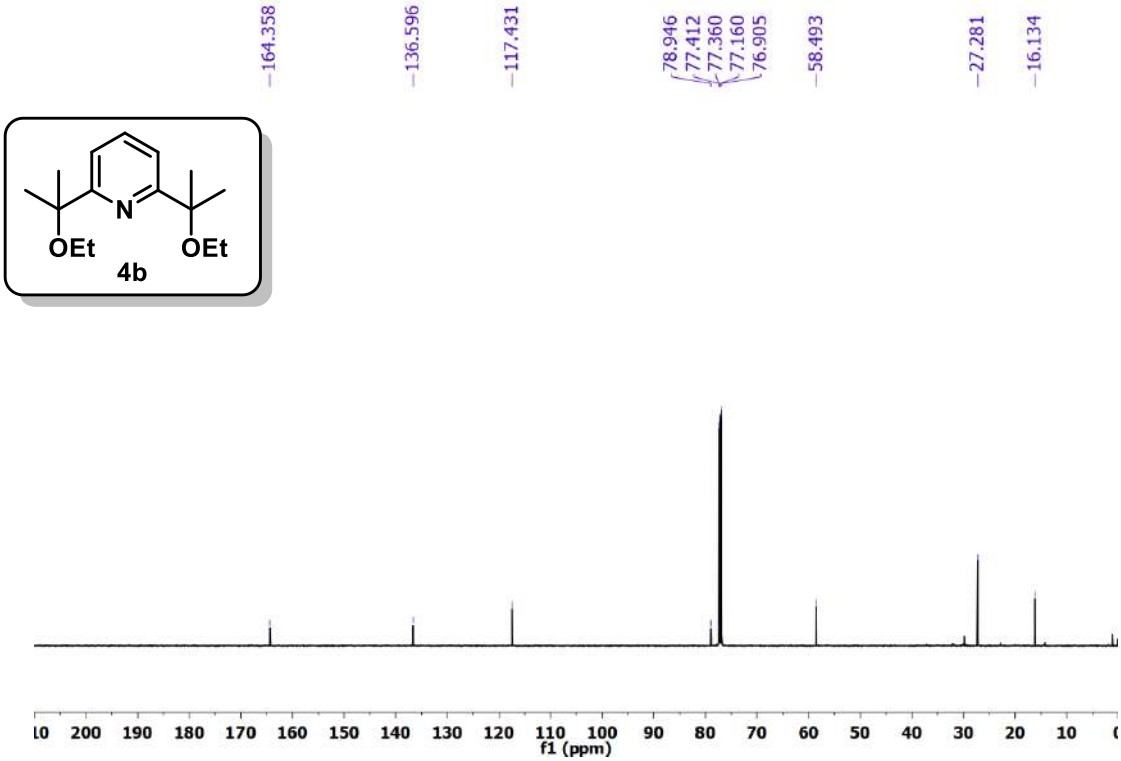

Figure 5.13. ^{13}C NMR of compound **4b** (126 MHz, $CDCl_3$).

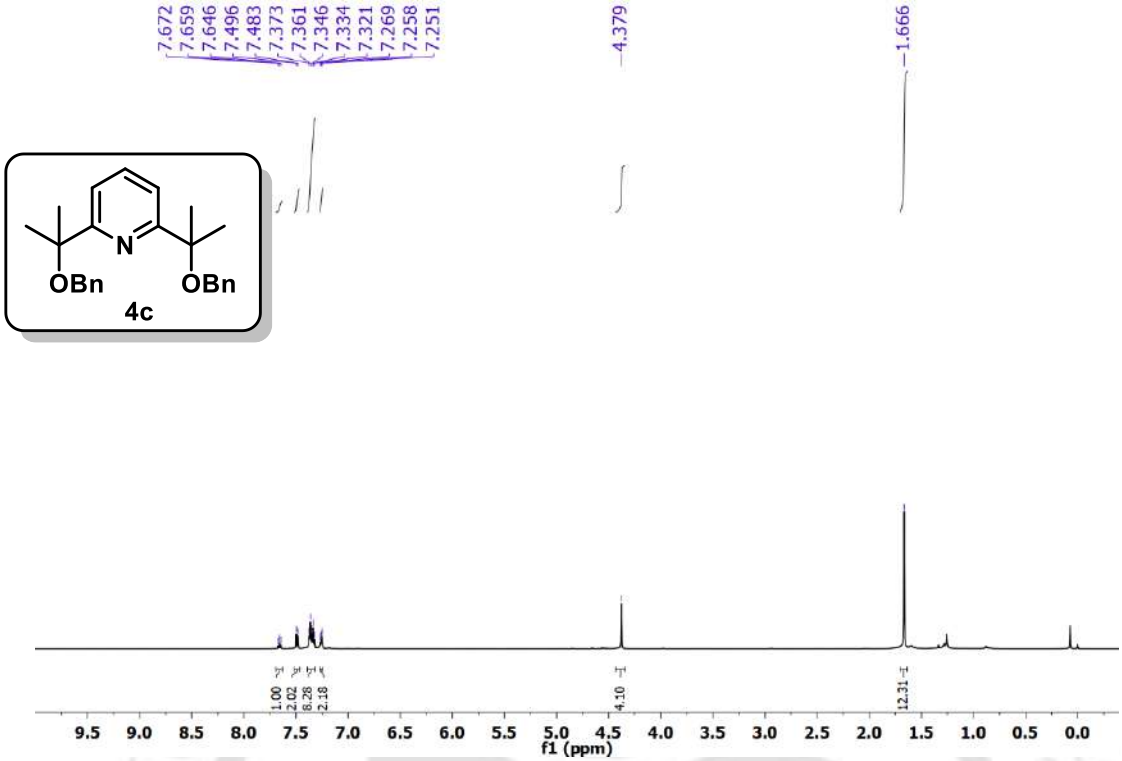

Figure 5.14. ^{1}H NMR of compound **4c** (600 MHz, $CDCl_3$).

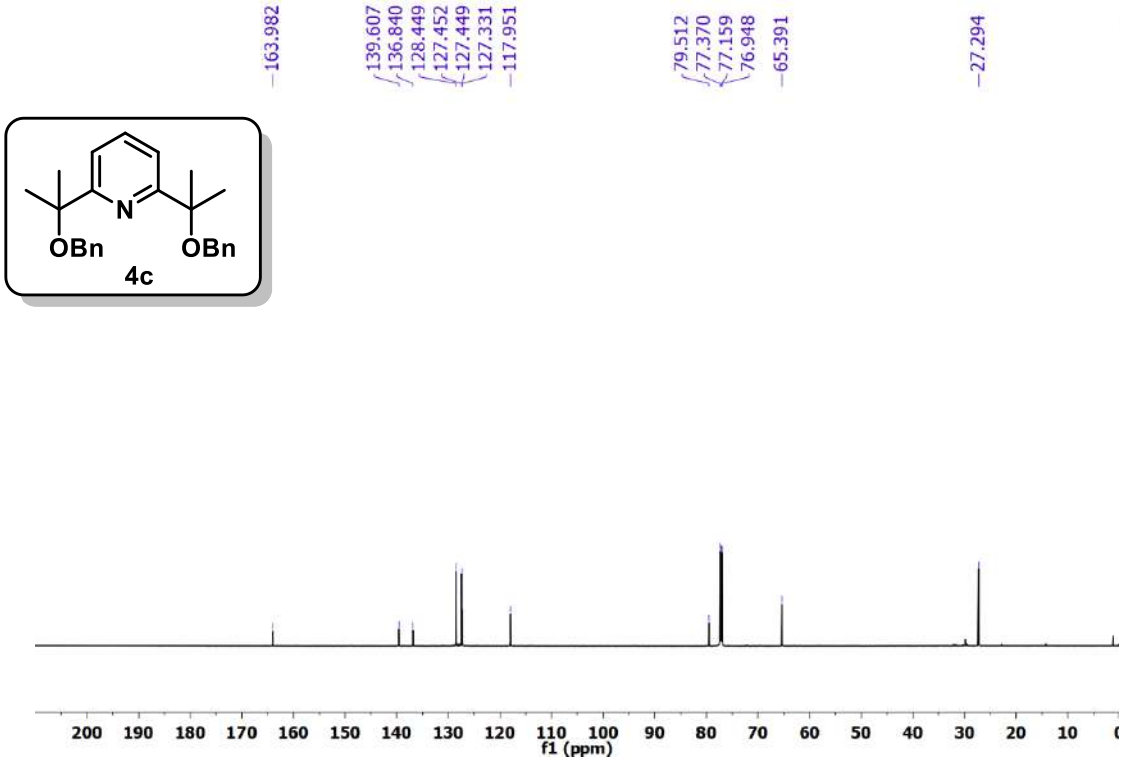

Figure 5.15. ^{13}C NMR of compound **4c** (151 MHz, $CDCl_3$).

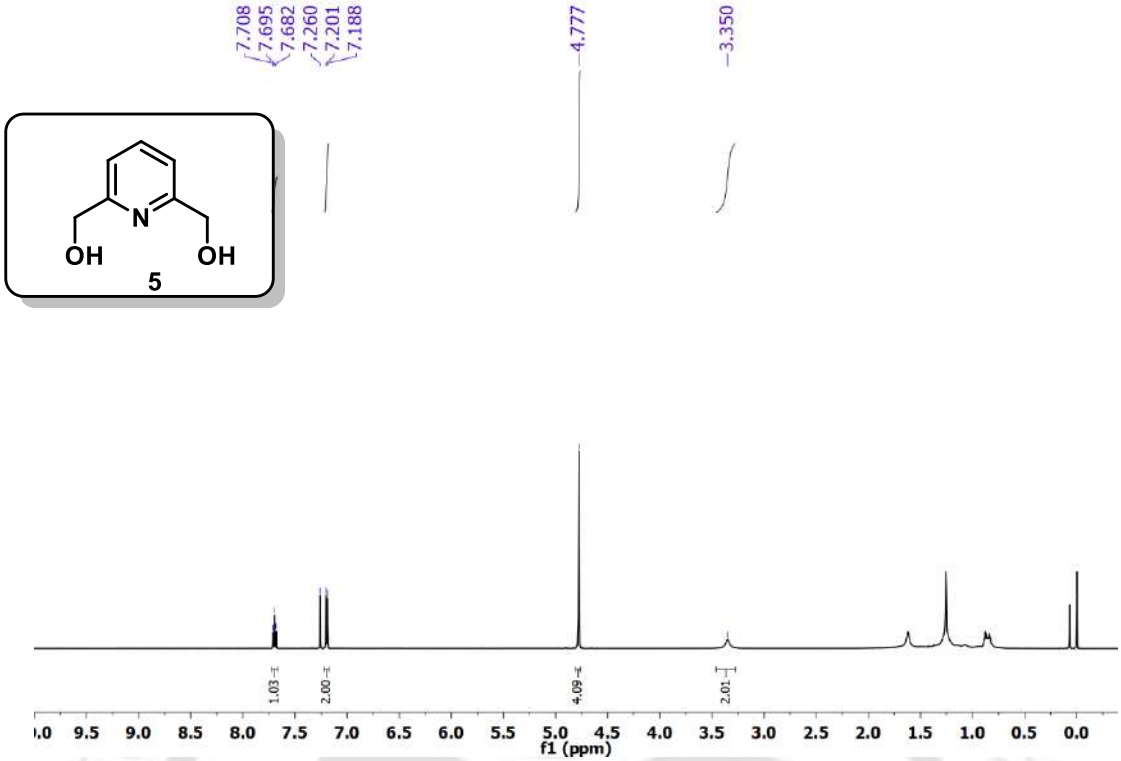

Figure 5.16. ^{1}H NMR of compound **5** (600 MHz, $CDCl_3$).

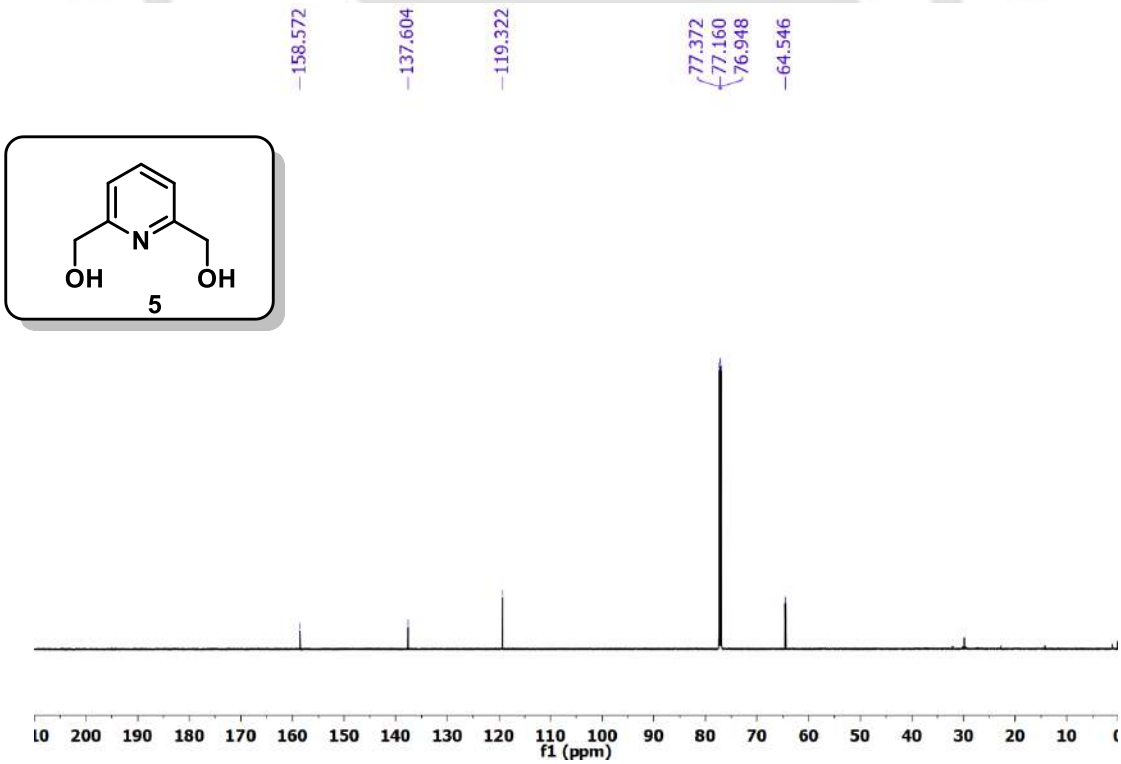

Figure 5.17. ^{13}C NMR of compound **5** (151 MHz, $CDCl_3$).

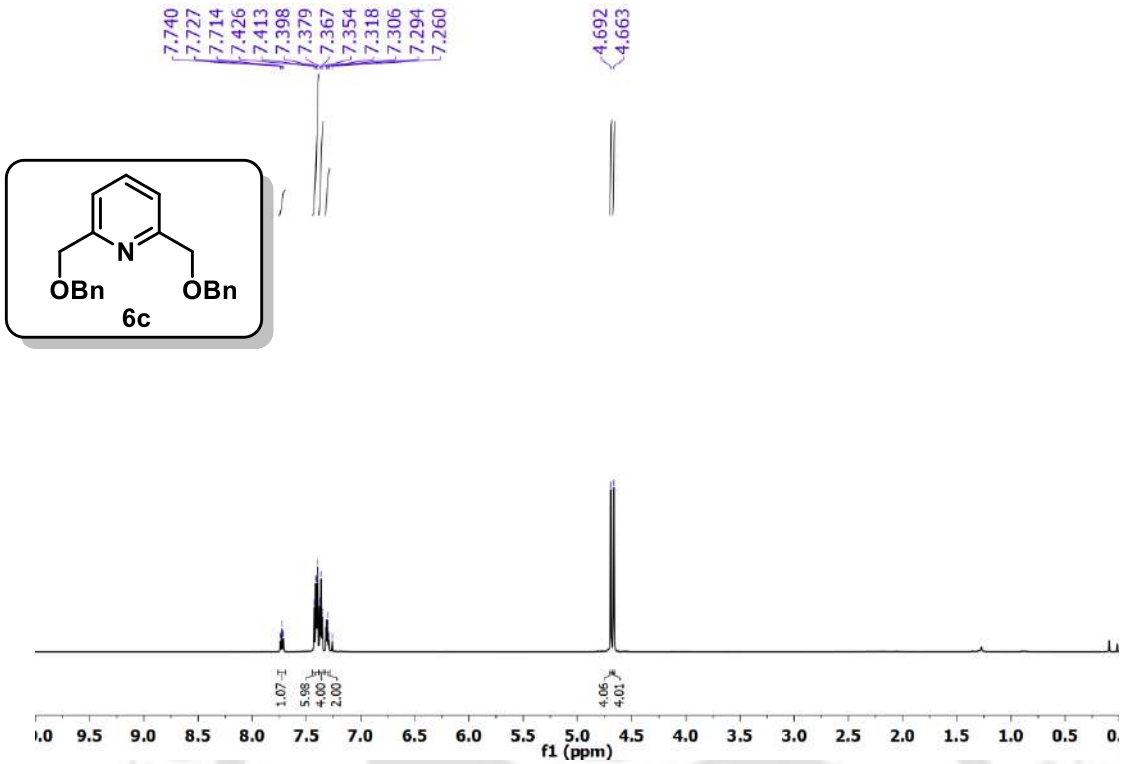

Figure 5.18. ^{1}H NMR of compound **6c** (600 MHz, $CDCl_3$).

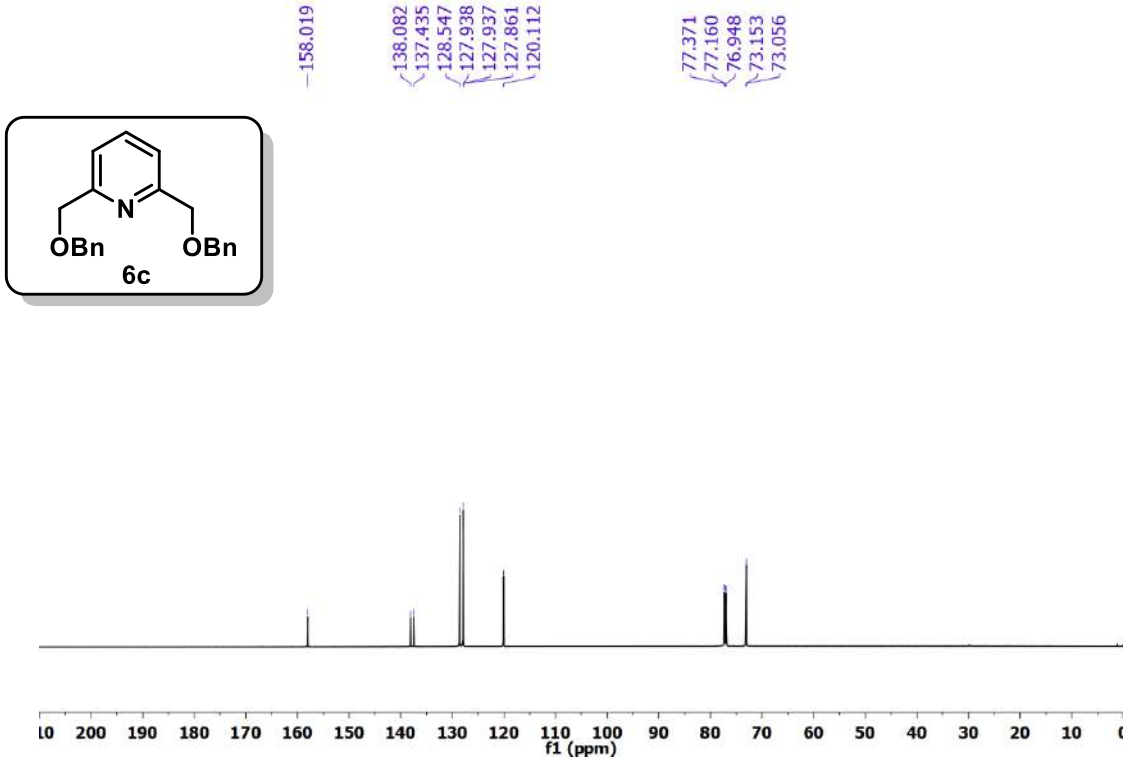

Figure 5.19. ^{13}C NMR of compound **6c** (151 MHz, $CDCl_3$).

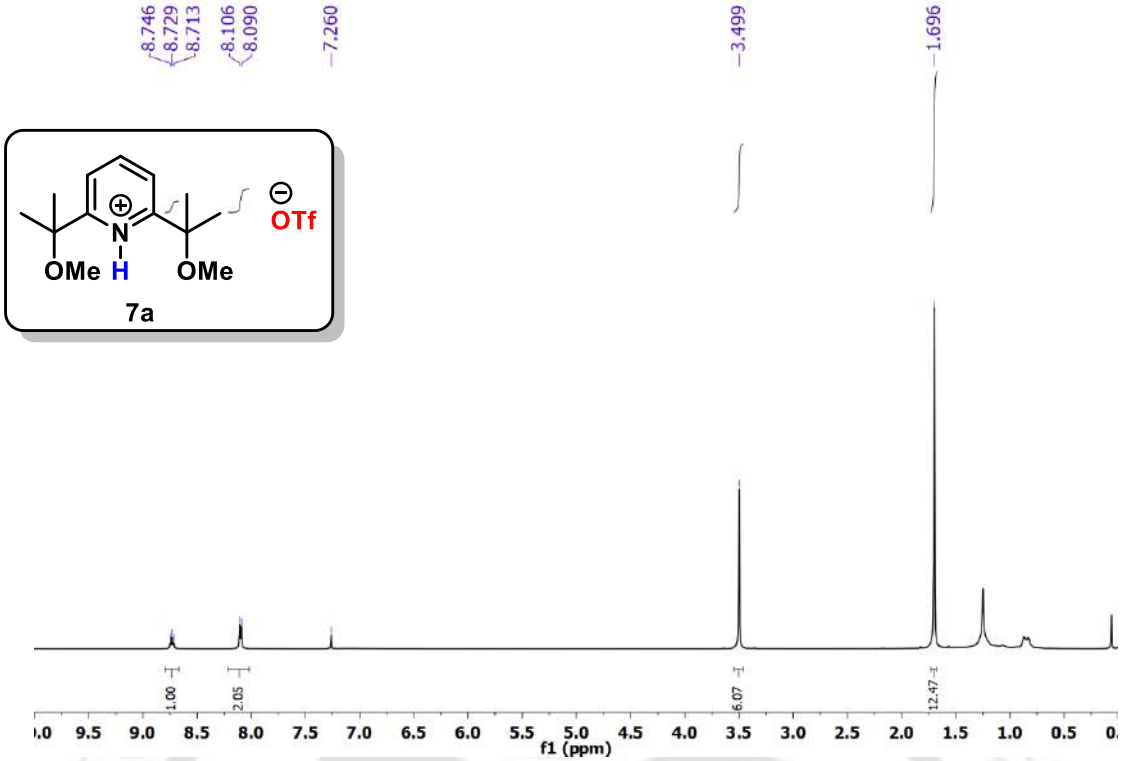

Figure 5.20. ^{1}H NMR of compound **7a** (500 MHz, $CDCl_3$).

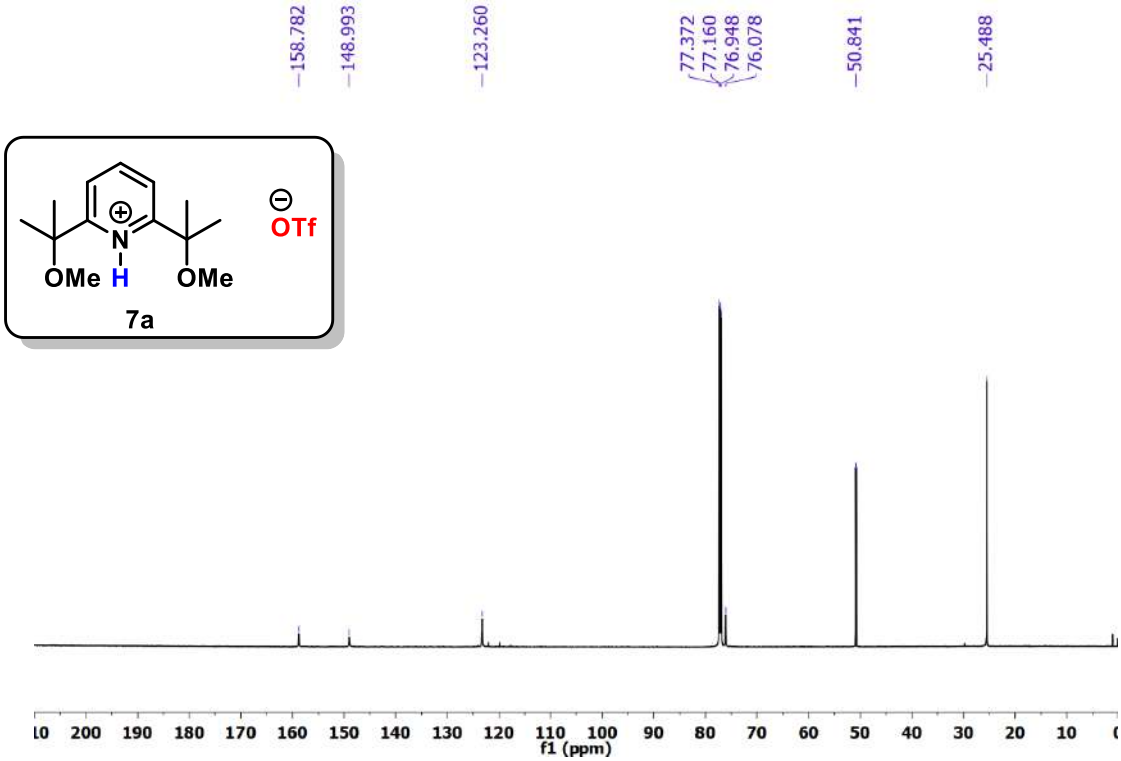

Figure 5.21. ^{13}C NMR of compound **7a** (151 MHz, $CDCl_3$).

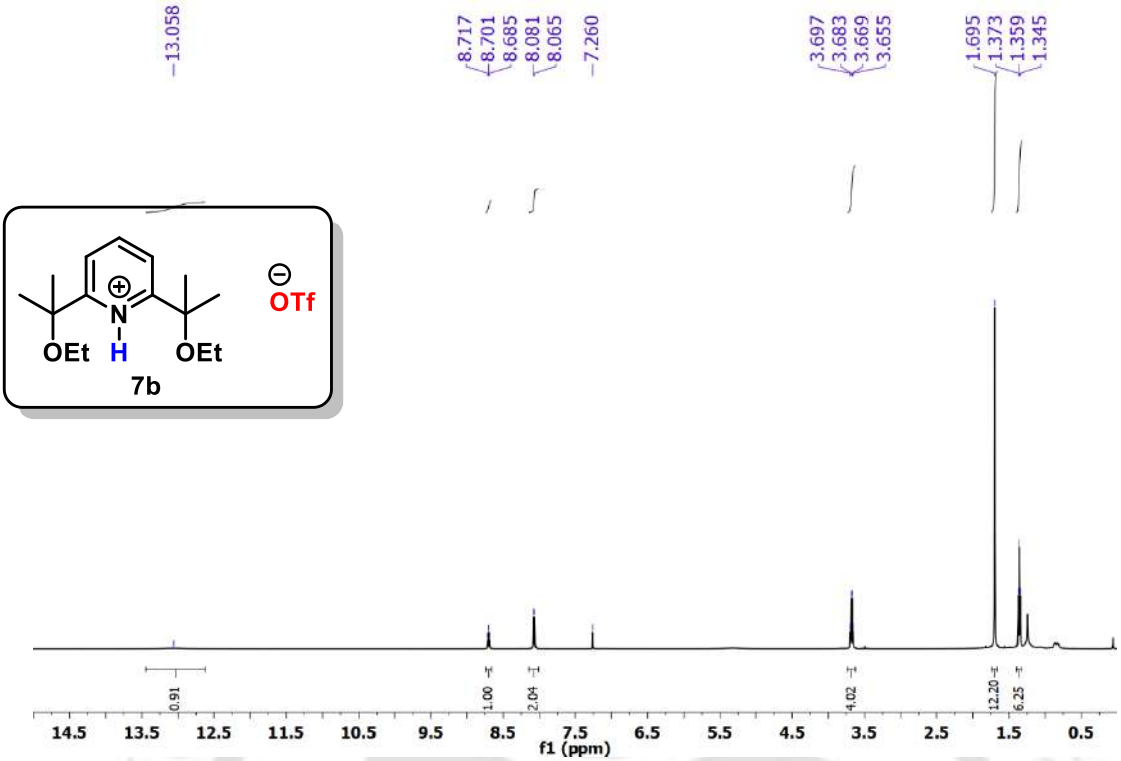

Figure 5.22. ^{1}H NMR of compound **7b** (500 MHz, $CDCl_3$).

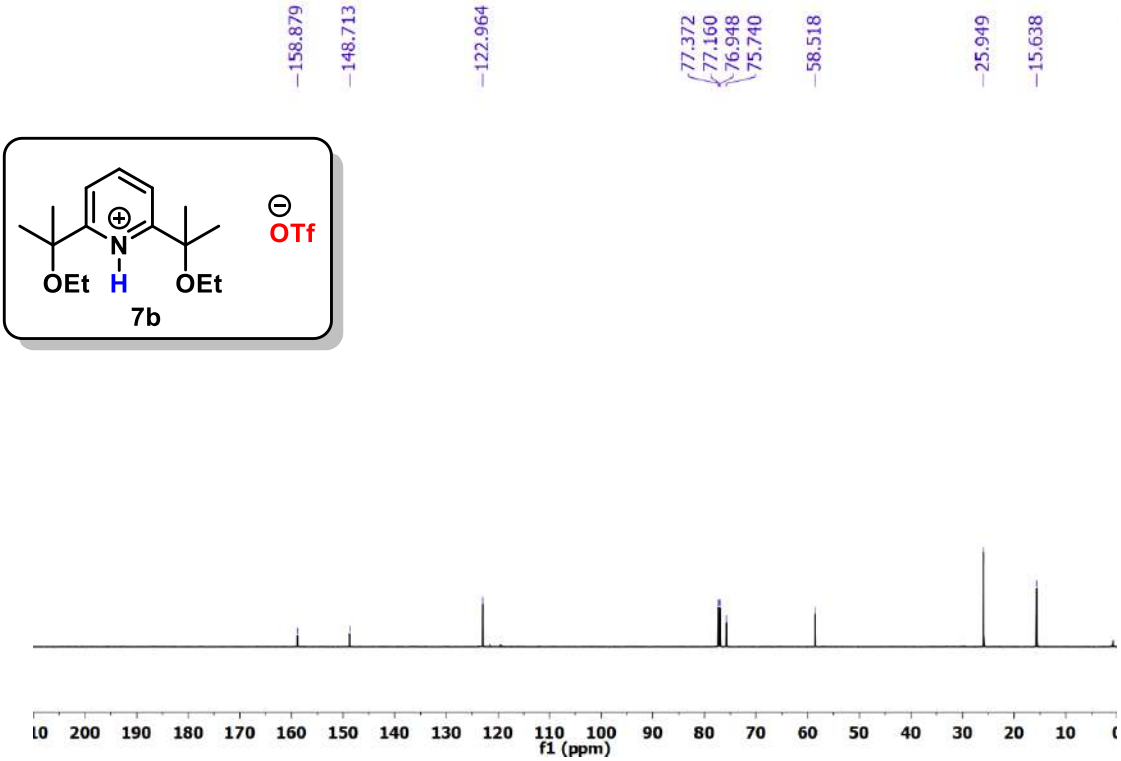

Figure 5.23. ^{13}C NMR of compound **7b** (151 MHz, $CDCl_3$).

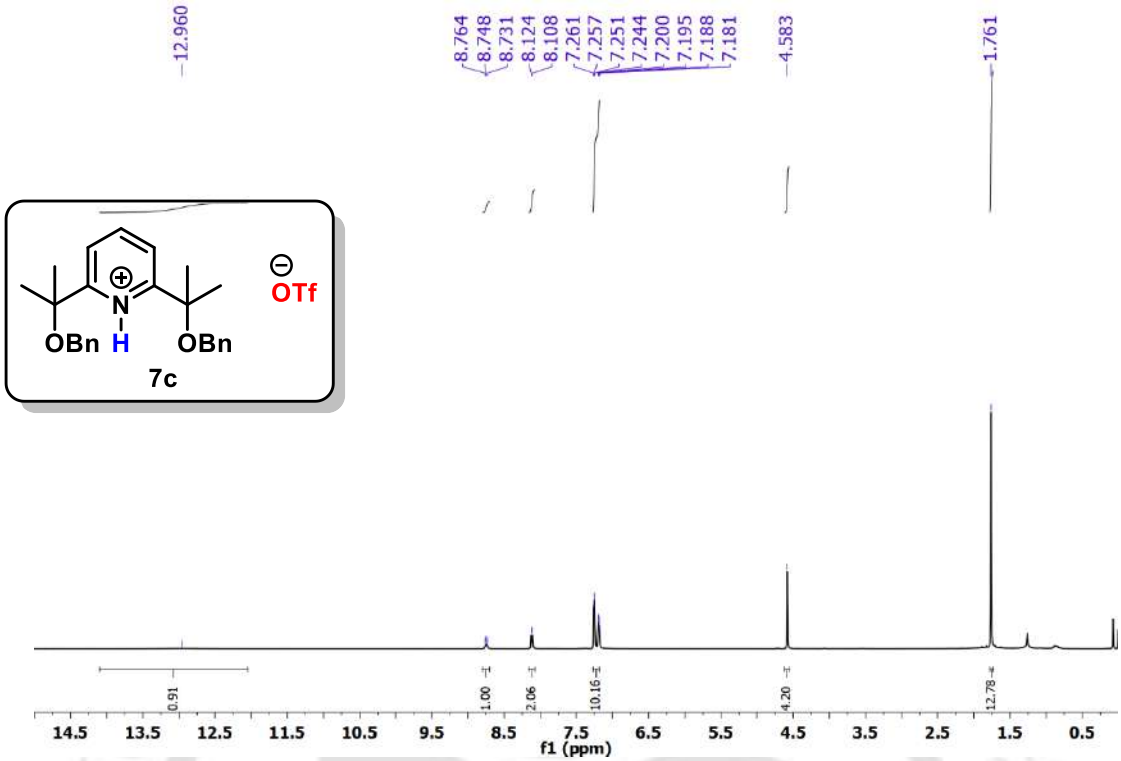

Figure 5.24. ^{1}H NMR of compound **7c** (500 MHz, $CDCl_3$).

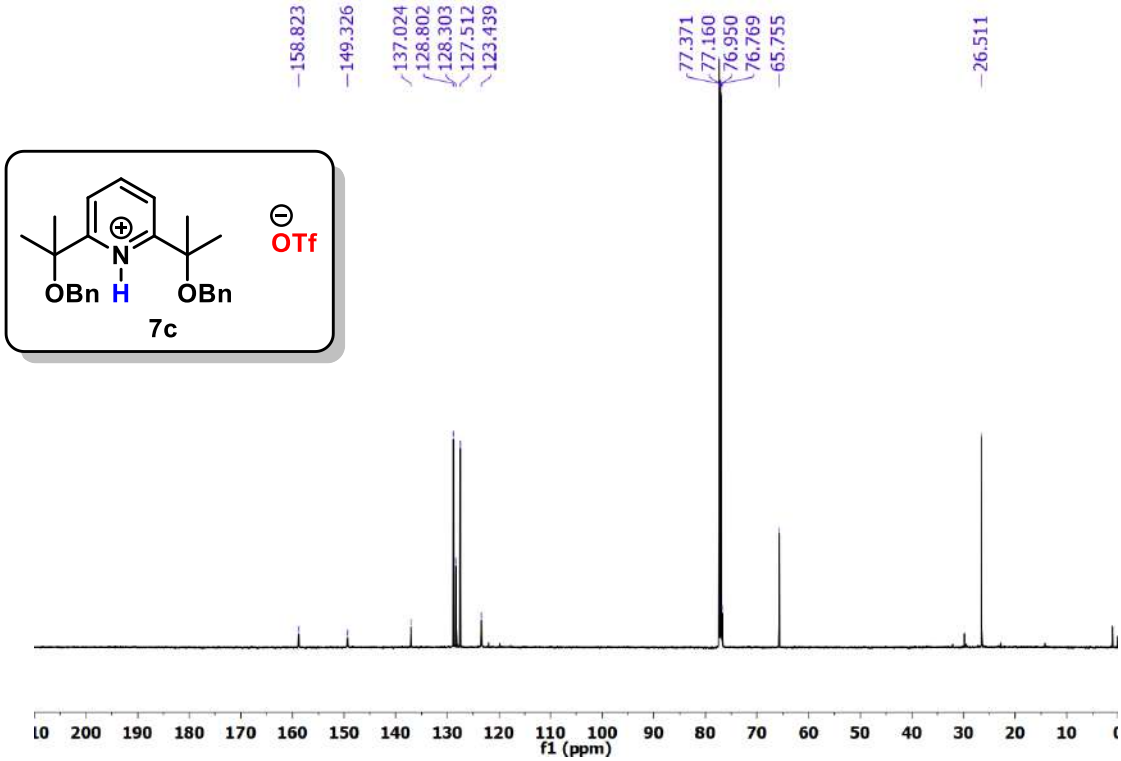

Figure 5.25. ^{13}C NMR of compound **7c** (151 MHz, $CDCl_3$).

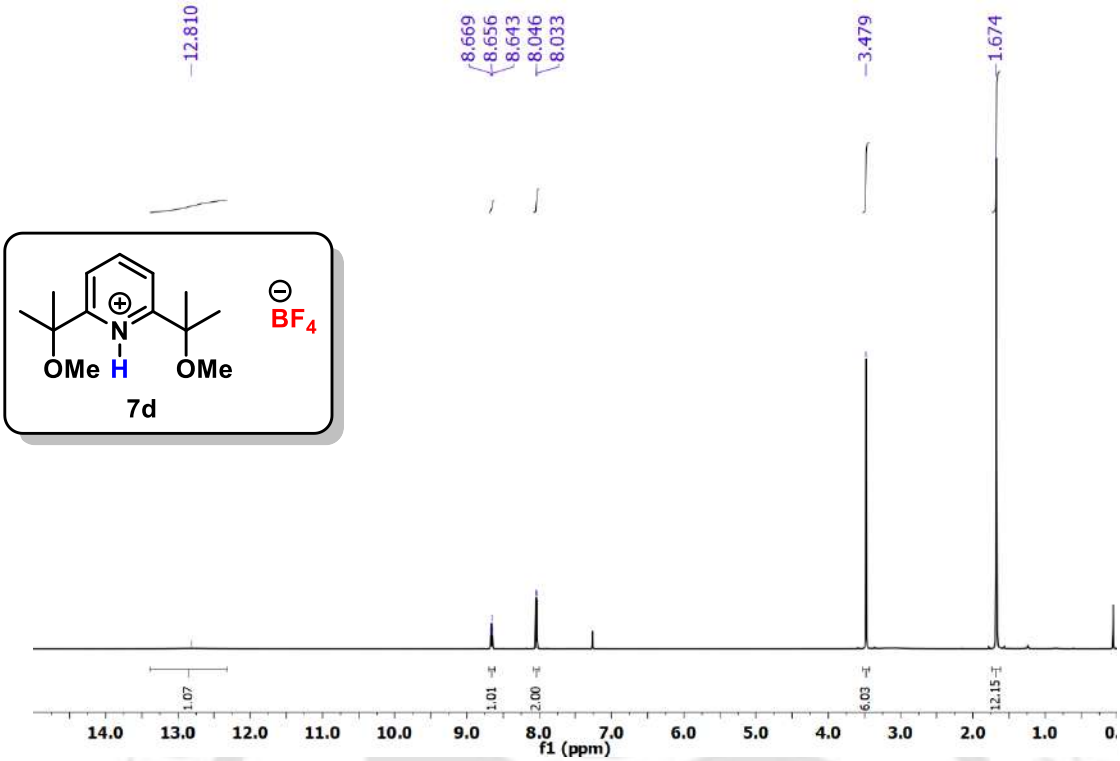

Figure 5.26. ^{1}H NMR of compound **7d** (600 MHz, $CDCl_3$).

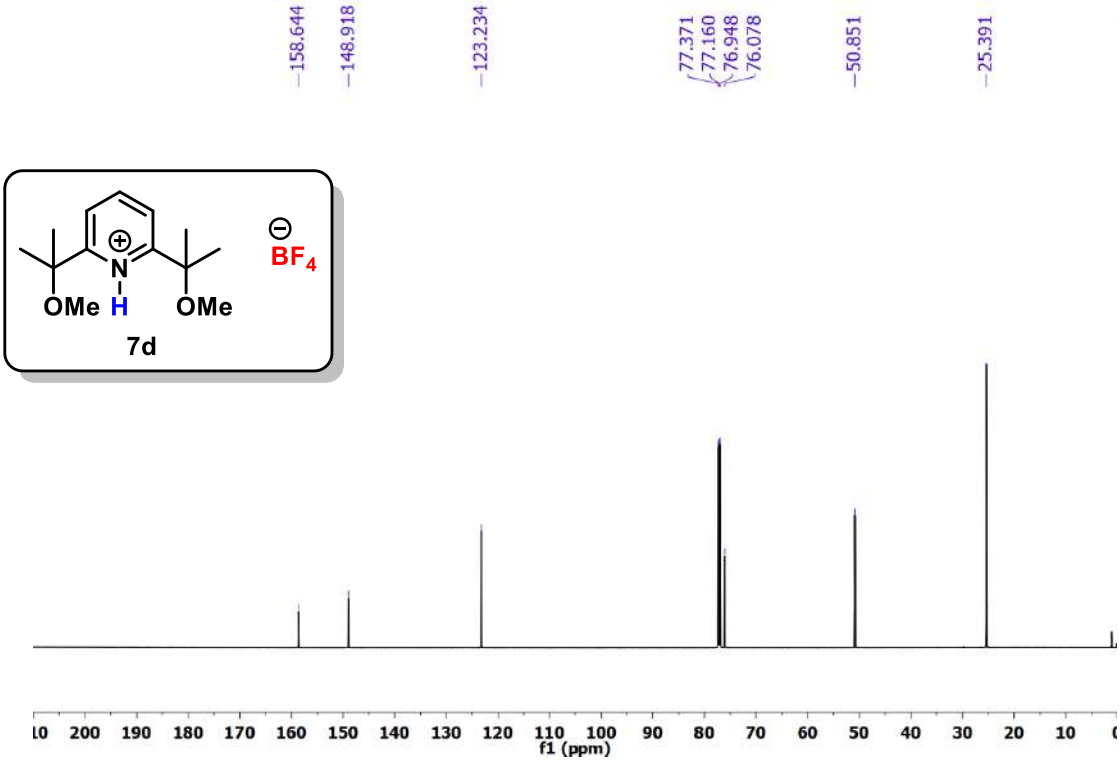

Figure 5.27. ^{13}C NMR of compound **7d** (151 MHz, $CDCl_3$).

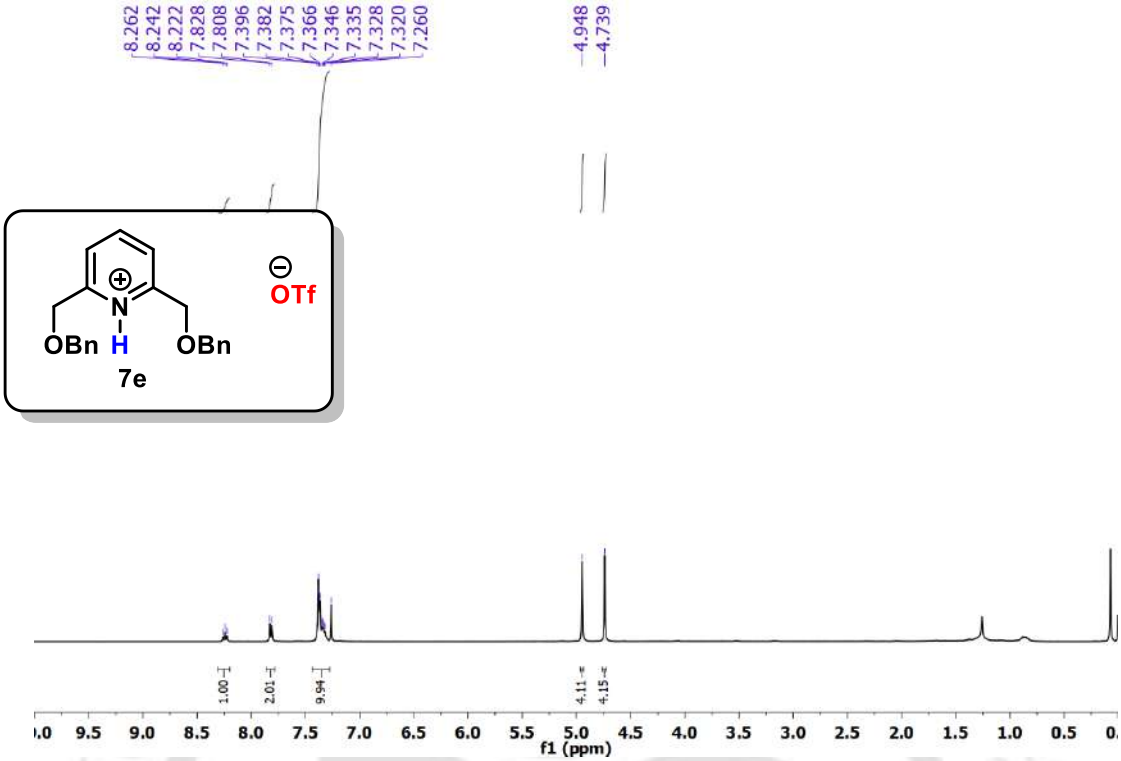

Figure 5.28. ^{1}H NMR of compound **7e** (400 MHz, $CDCl_3$).

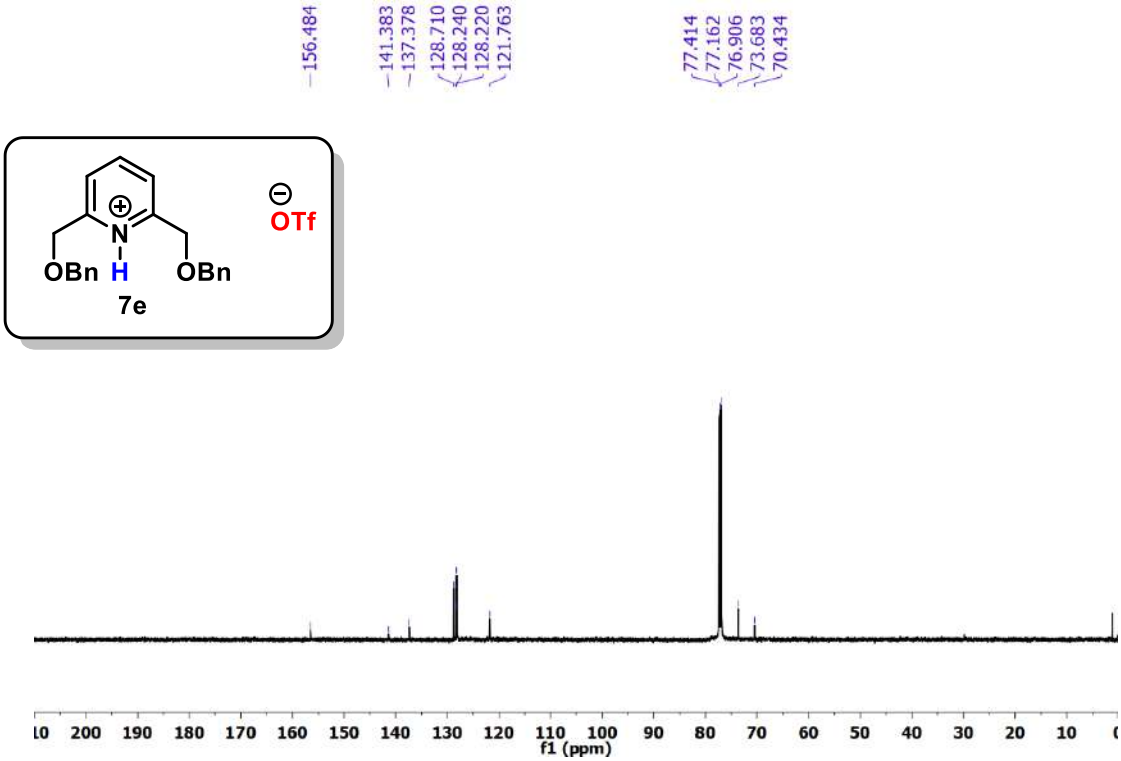

Figure 5.29. ^{13}C NMR of compound **7e** (126 MHz, $CDCl_3$).

5.7. SC-XRD data

SC-XRD Data of 7a: The ORTEP diagram with an ellipsoid of 30% probability.

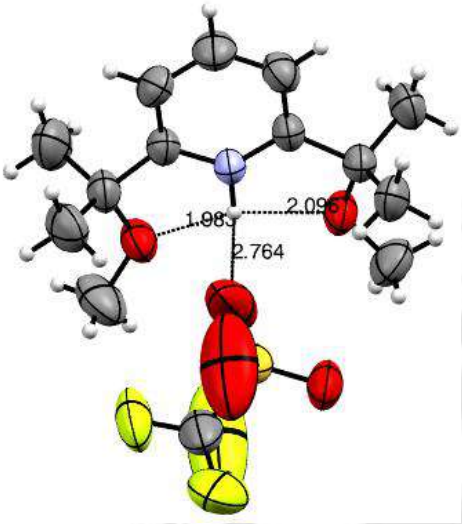

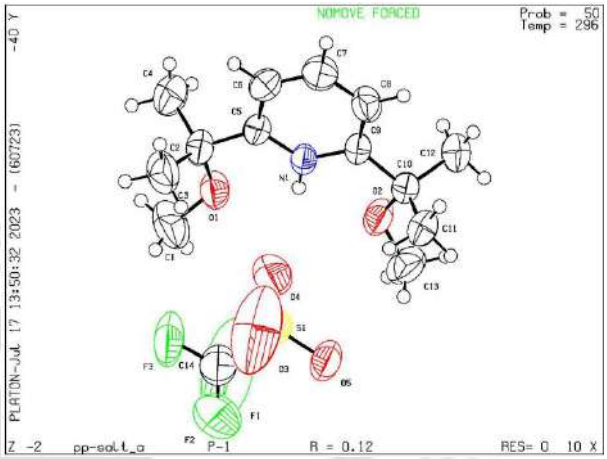

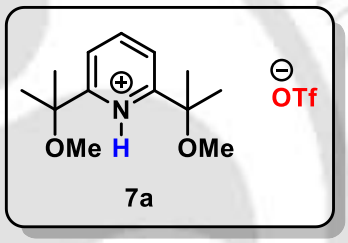

7a

SC-XRD Data of 7b: The ORTEP diagram with an ellipsoid of 30% probability.

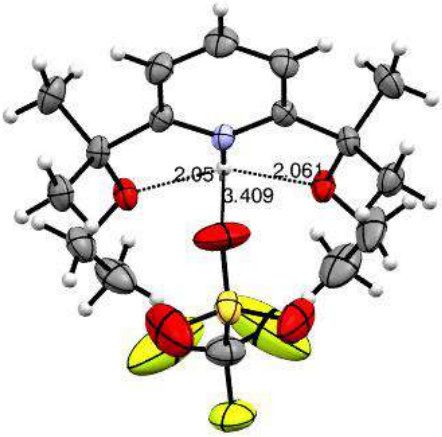

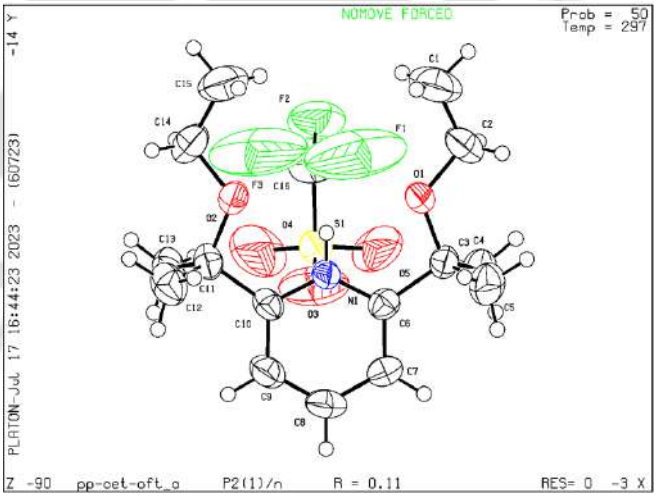

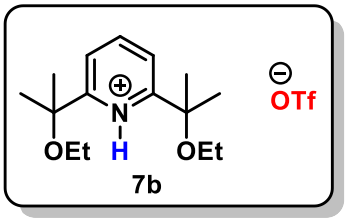

7b

SC-XRD Data of 7c: The ORTEP diagram with an ellipsoid of 30% probability.

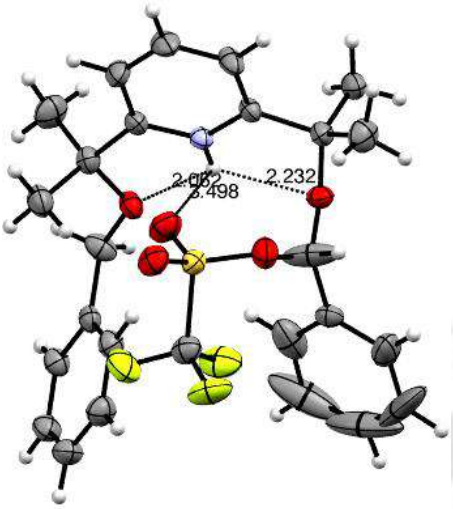

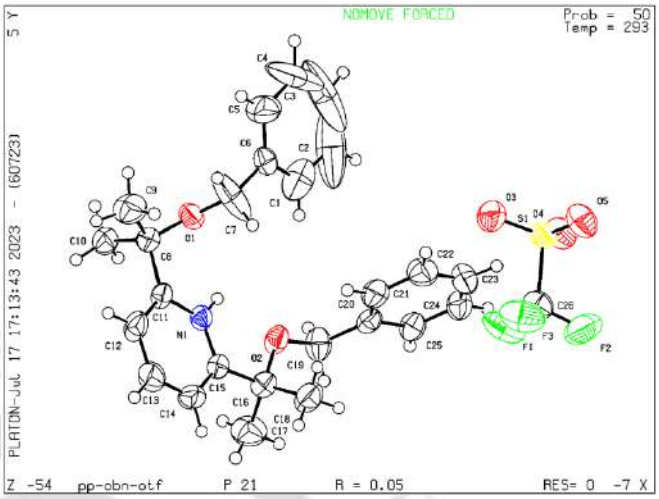

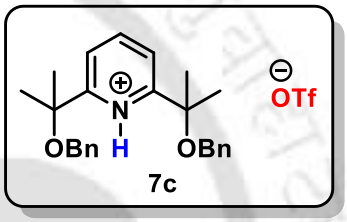

SC-XRD Data of 7d: The ORTEP diagram with an ellipsoid of 30% probability.

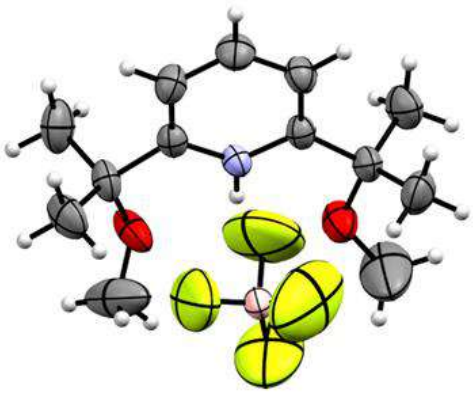

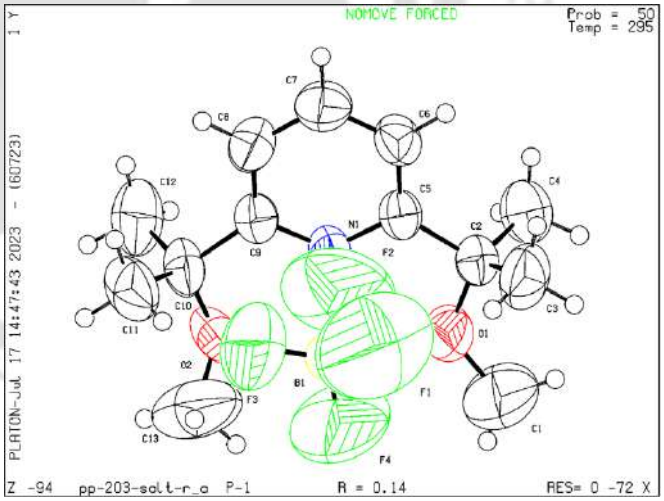

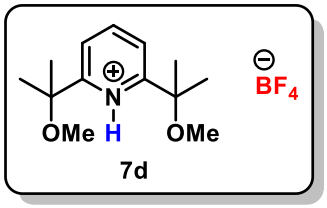

SC-XRD Data of 7e: The ORTEP diagram with an ellipsoid of 30% probability.

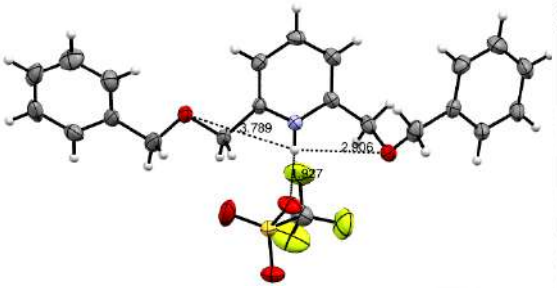

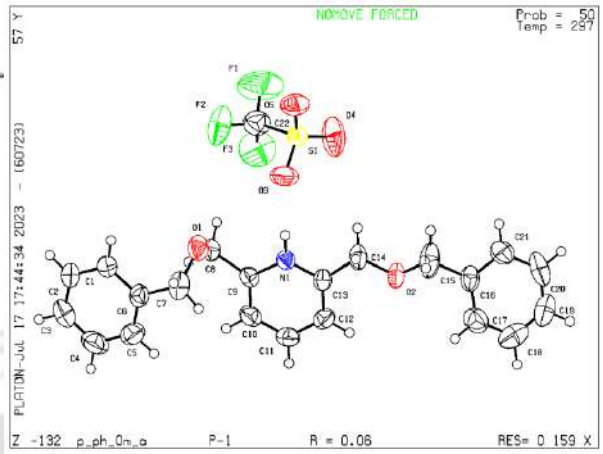

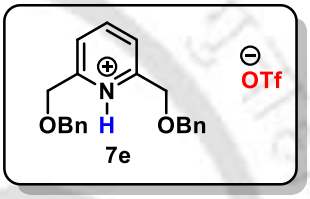

SC-XRD Data of 7f: The ORTEP diagram with an ellipsoid of 30% probability.

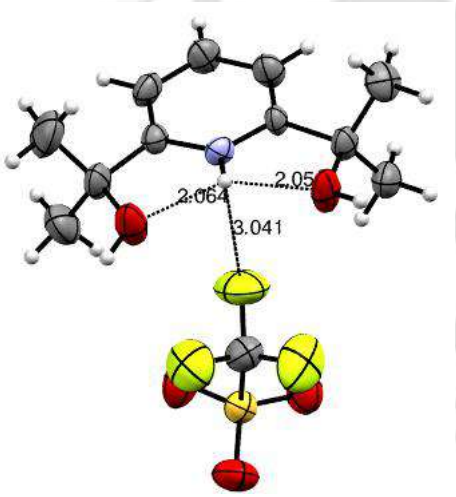

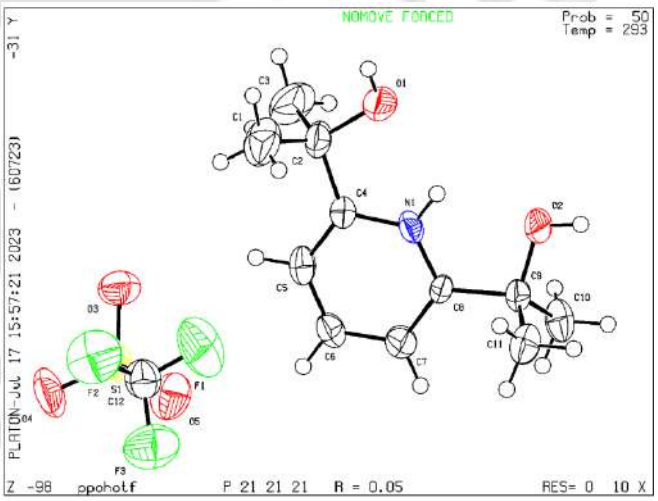

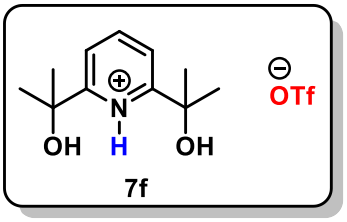

Table 1: Crystal parameters and refinement data of **7a, 7b, 7c and 7d**

Parameters	Substrate 7a	Substrate 7b	Substrate 7c	Substrate 7d
Formula	$C_{14}H_{22}F_3NO_5S$	$C_{16}H_{26}F_3NO_5S$	$C_{26}H_{30}F_3NO_5S$	$C_{13}H_{22}BF_4NO_2$
Fw	373.38	401.44	525.57	311.12
Crystal system	Triclinic	Monoclinic	Monoclinic	Triclinic
Space group	*P-1*	*P2(1)/n*	*P 21*	*P-1*
a/Å	8.645(2)	9.0346(13)	9.7881(7)	7.6631(9)
b/Å	8.726(2)	10.7077(16)	10.5092(7)	10.3785(9)
c/Å	13.631(3)	21.484(3)	12.8609(12)	10.7839(10)
α/°	95.465(6)	90.00	90.00	105.633(3)
β/°	98.183(6)	100.554(4)	106.405(9)	90.511(3)
γ/°	115.603(6)	90.00	90.00	97.875(2)
V/Å^3	903.6(4)	2043.2(5)	1269.08(17)	817.20(14)
Z	2	4	2	2
D_c/g cm^{-3}	1.372	1.305	1.375	1.264
μ Mo K_α/mm^{-1}	0.231	0.209	0.187	0.113
F000	392	848	552	328
T/K	296(2)	297(2)	293(2)	295(2)
θ max.	24.85	24.97	23.8850	25.04
Total no. of reflections	28802	54517	4880	21276
Independent reflections	2994	3391	3104	2668
Observed reflections	2163	2710	2452	2039
Parameters refined	227	241	329	196
R_1, I > 2σ(I)	0.1221	0.1085	0.0539	0.1471
wR_2, I > 2σ(I)	0.3410	0.3247	0.1387	0.3723
GOF (F^2)	2.201	2.301	0.940	2.061
CCDC No.	2540282	2540276	2540311	2540312

Table 2: Crystal parameters and refinement data of **7e and 7f**

Parameters	Substrate 7e	Substrate 7f
Formula	$C_{22}H_{22}F_3NO_5S$	$C_{12}H_{18}F_3NO_5S$
Fw	469.46	345.33
Crystal system	Triclinic	orthorhombic
Space group	*P-1*	*P 21 21 21*
a/Å	8.7821(11)	7.3143(6)
b/Å	10.3538(13)	12.5730(8)
c/Å	13.4931(16)	17.5208(13)
α/°	95.161(3)	90.00
β/°	95.951(3)	90.00
γ/°	114.634(3)	90.00
V/Å^3	1097.1(2)	1611.3(2)
Z	2	4
D_c/g cm^{-3}	1.421	1.424
μ Mo K_α/mm^{-1}	0.207	0.253
F000	488	720
T/K	297(2)	293(2)
θ max.	25.66	25.7500
Total no. of reflections	29583	3709
Independent reflections	3844	2440
Observed reflections	3256	1858
Parameters refined	289	205
R_1, I > 2σ(I)	0.0537	0.0527
wR_2, I > 2σ(I)	0.1455	0.1143
GOF (F^2)	1.156	0.928
CCDC No.	2540176	2540283

Research Outcome

Publications:

1. Biswas, A.; **Pradhan, P.**; Nayak, S.; Kancharla, P. K. Sulfonium-Stabilized Phenols as Organocatalysts toward Divergent Stereoselective 2-Deoxy and Ferrier Glycosylation of Glycals. *Org. Lett.* **2026**, *28*, 5847-5852.
2. **Pradhan, P.**; Biswas, A.; Kancharla, P. K. Sulfonium Stabilized Phenols as Hydrogen Bonding Catalysts toward Diastereoselective Glycosylation of Cyclopropanated Sugars. *Org. Lett.* **2025**, *27*, 11650-11655.
3. Biswas, A.; **Pradhan, P.**; Wakpanjar, S. A.; Kancharla, P. K. Direct organocatalytic esterification of carboxylic acids and alcohols by redox neutral sulfur(iv) catalysis via intramolecularly interrupted Pummerrer intermediates. *Chem. Commun.* **2025**, *61*, 5746-5749.
4. Rotta, M. K. V.; Moktan, S.; **Pradhan, P.**; Kancharla, P. K., Direct Stereoselective Synthesis of 2-Deoxyglycosides via Visible-Light-Induced Photoacid-Catalyzed Activation of Glycosyl o-[1-(p-MeO-Phenyl)vinyl]benzoates (PMPVBs) as Donors. *J. Org. Chem.* **2025**, *90*, 1196-1208.
5. **Pradhan, P.**; Biswas, A.; Rotta, M. K. V.; Kancharla, P. K. Strained Ion Pair Interactions-Driven Anion-Assisted Concerted Addition of Ketoximes/Aldoximes and Hydroxamic Acids to Glycals. *Org. Lett.* **2024,** *26*, 10382-10387.
6. **Pradhan, P.**; Moktan, S.; Biswas, A.; Das, A.; Lenka, R.; Kancharla, P. K. Triple Role of Proton Sponge (DMAN) in the Palladium-Catalyzed Direct Stereoselective Synthesis of C-Aryl Glycosides from Glycals. *Org. Lett.* **2024**, *26*, 3563-3568.
7. Moktan, S.; Rotta, M. K. V.; Halder, S.; **Pradhan, P.**; Kancharla, P. K. ortho-[1-(p-MeOPhenyl)vinyl]benzoate PMPVB as a recyclable auxiliary for C–O and C–S bond formation reactions under Brønsted acid catalysis. *Org. Biomol. Chem.* **2023**, *21*, 5929-5934.
8. Sahoo, K.; **Pradhan, P.**; Panda, N. Access to C4-arylated benzoxazoles from 2-amidophenol through C–H activation. *Org. Biomol. Chem.* **2020**, *18*, 1820–1832.

Conferences:

Poster presentation:

1. International Carbohydrate Conference (ETGG-2025) held at Banaras Hindu University (BHU), India, 21-23rd November **(Best Poster Presentation)**.
2. International Conference on Recent Advances in Glycoscience and Glycotechnology (CARBO-XXXVIII-2024) held at Guwahati University, India, 4-6th December.
3. 7th International Conference on Frontiers in Chemical Sciences (FICS-2024) held at IIT Guwahati, India, 2-4th December.
4. Research & Industrial Conclave (RIC-2023) held at IIT Guwahati, India, 14-16th May.
5. International Conference on Emerging Trends in Chemistry (ICETC-2023) held at Assam Don Bosco University, India, 16-17th March.

Oral presentation:

1. Research & Industrial Conclave (RIC-2025) held at IIT Guwahati, India, 10-12th October **(Best Oral Presentation)**.
2. International Conference on "Frontiers in Chemistry for a Sustainable Future (FCSF 2025) held at ICFAI University Tripura, India, 2-4th July **(Best Oral Presentation)**.
3. ACS Spring 2025 symposium held online, March 23-27th .

Priyanka Pradhan

Personal Information:

Date of Birth: 24th July 1997
Father's Name: Tapas Kumar Pradhan
Nationality: Indian
Religion: Hindu
Gender: Female
Tel no. +91-9002142968
Email: priyankapradhan3507@gmail.com/ p.priyanka@iitg.ac.in

Present Address:

Research Fellow, Organocatalysis and Carbohydrate chemistry laboratory, Department of Chemistry, IIT Guwahati, Guwahati, Assam-781039, India.

Permanent Address:

Medinipur, Paya Medinipur, Digha, West Bengal-721428, India.

Academic Qualifications

01/2021–Present	**Ph.D. in Chemistry (CPI 8.75 out of 10)** Indian Institute of Technology Guwahati, Assam-781039, India. Thesis: **Design and Development of Stereoselective Methods for *C*-, *O*-, and *S*-Glycoside Synthesis Utilizing Sterically Strained Nitrogen Bases and Cyclic Sulfonium Salts** Thesis advisor: Dr. Pavan Kumar Kancharla
07/2018–07/2020	**M.Sc. in Chemistry (CPI 8.88 out of 10)** National Institute of Technology Rourkela, Rourkela, Odisha-769008, India. Thesis: **Synthetic approach to 8-hydroxy carbostyrils** Thesis advisor: Prof. Niranjan Panda
07/2015–05/2018	**B.Sc. in Chemistry Honours (63%, First Class) with Physics and Mathematics** St. Paul's C. M. College, Calcutta University, West Bengal-700009, India.
2013–2015	**Higher Secondary Examination (WBCHSE) (87%, First Division) with Physics, Chemistry, Mathematics, Biology, English, and Bengali** Gobra I. N. K. M. High School, West Bengal-721428, India.

Achievements and Awards

- Awarded the Prime Minister's Research Fellowship (PMRF 2022-2025), Govt. of India.
- Qualified Joint CSIR-UGC NET 2020 in Chemical Science, India (AIR- 100, JRF, UGC).
- Qualified Graduate Aptitude Test in Engineering (GATE) 2020, organized by the Ministry of Human Resource Development, Government of India.
- Qualified "Joint Admission Test for Master's (JAM 2018)" examination, India (AIR-910).
- Awarded Swami Vivekananda Merit-cum-Means Scholarship 2013, 2015.

Research Experience

- Design and development of sterically hindered salts as organocatalysts.
- Sulfonium salt-catalyzed stereocontrolled glycosylation: a new synthetic avenue.
- Expertise in transition metal-catalyzed C-C bond-forming reactions.
- Synthetic explorations of 2-Deoxysugars from Glycals and studying reaction mechanisms.
- Expertise in the synthesis of glycosyl donors and acceptors.
- Skilled in spectroscopic/chromatographic methods such as NMR (1D/2D), MS, FT-IR, UV, Fluorescence, Flash chromatography, and HPLC.
- Strong English communication, presentation, and scientific writing skills.

Academic and Professional Skills

- **Laboratory and Instrumentation:** I possess extensive experience in organic synthesis, particularly in glycosylation. I am proficient in forming C-C bonds via cross-coupling processes and have substantial experience in the crystallization of small molecules. I have hands-on experience with various analytical instrumentation techniques, including NMR (1D and 2D), FT-IR, ESI-MS, HPLC, UV–Vis spectroscopy, and Fluorescence spectroscopy.
- **Software:** MS Office, ChemDraw, MestreNova, MassHunter, Origin, Adobe Illustrator, SHELXL, Mercury, EndNote, and Topspin.
- **Language:** Bengali, Hindi, and English.

Research Interests

- Organic Synthesis (Carbohydrate Chemistry, Organocatalysis, New Synthetic Methodology, Asymmetric Synthesis, Natural Product Synthesis, Medicinal Chemistry).